Proceedings of the
Fourteenth ERDA Air Cleaning
Conference

Editor Melvin W. First	Volume 2 February 1977	Held at **Sun Valley, Idaho** 2-4 August, 1976

Sponsors

Energy Research & Development Administration

Harvard Air Cleaning Laboratory

PROGRAM COMMITTEE:

W. L. ANDERSON

R. R. BELLAMY

C. A. BURCHSTED

J. T. COLLINS

J. C. DEMPSEY

D. C. DREHMEL

H. L. ETTINGER

H. GILBERT

J. L. KOVACH

D. W. MOELLER

D. PENCE

R. D. RIVERS

C. E. STEVENSON

M. W. FIRST, CHAIRMAN

LOCAL ARRANGEMENTS

GEORGE WEHMANN

SHARLEEN WHITE, ASSISTANT

IDAHO OPERATIONS OFFICE

U.S. ENERGY RESEARCH AND DEVELOPMENT

ADMINISTRATION

TABLE OF CONTENTS

VOLUME I

SYSTEM PROTECTION FROM FIRE, EXPLOSION, AND NATURAL DISASTERS
Session III - Monday, August 2, 1976
CHAIRMAN: B. P. Brown
ERDA

RADIOIODINE REMOVAL AND RETENTION
Session IV - Monday, August 2, 1976
CO-CHAIRMEN: R. D. Rivers,
American Air Filter Co.,
J. G. Wilhelm,
Laboratorium fur Aerosolphysik and
und Filtertechnik, Karlsruhe

<u>SAMPLING AND MONITORING</u>
Session V - Tuesday, August 3, 1976
CHAIRMAN: H. Ettinger,
Los Alamos Scientific Laboratory

VOLUME II

LUNCHEON MEETING
Session VII - Tuesday, August 3, 1976
CHAIRMAN: G. Wehmann,
                    Idaho Operations Office, USERDA

SYSTEM DESIGN FOR NUCLEAR FACILITIES
Session VIII - Tuesday, August 3, 1976
CHAIRMAN: J. Murrow,
                    Bechtel Corporation

OPEN END
Session IX - Tuesday, August 3, 1976
CHAIRMAN: M. W. First,
Harvard Air Cleaning Laboratory

LMFBR AIR CLEANING SYSTEMS
Session X - Wednesday, August 4, 1976
CHAIRMAN: C. Newton,
USERDA

REMOVAL OF NOBLE GASES, TRITIUM, AND ^{14}CARBON
Session XI – Wednesday, August 4, 1976
CHAIRMAN: J. A. Buckham,
Allied Chemical Corporation

REGULATION
Session XII - Wednesday, August 4, 1976
CHAIRMAN: J. T. Collins,
Nuclear Regulatory Commission

INTERNATIONAL SYMPOSIUM ON THE MANAGEMENT OF WASTES
FROM THE NUCLEAR FUEL CYCLE
Session XIII - Wednesday, August 4, 1976
CHAIRMAN: R. W. Ramsey,
USERDA

SESSION VI

PARTICLE COLLECTION

Tuesday, August 3, 1976
CO-CHAIRMEN: H. Gilbert, C. A. Burchsted

THE SRP SAND FILTER: MORE THAN A PILE OF SAND

D. A. Orth and G. H. Sykes
E. I. du Pont de Nemours and Co., Inc.
Savannah River Plant
Aiken, South Carolina
and
G. A. Schurr
Engineering Service Division
E. I. du Pont de Nemours and Co., Inc.
Newark, Delaware

Abstract

Sand filters at the two SRP separations plants have operated well for over twenty years, displaying steadily increasing efficiency for removal of activity. Pressure drop remained low on one filter although some sand was removed from the other to counteract rising pressure drop due to salts in the bed. Activity is not migrating through the beds and such breakthrough does not appear to be a life-limiting phenomenon. The underbed supports and air distribution systems were weakened by acid attack and erosion, with localized failure, prompting construction of new filters. Design studies and tests defined relations between sand characteristics, airflow resistance, and filtration efficiency. Appropriate sands were selected and monitored during construction to ensure that the new filters would have satisfactory efficiency, airflow, and pressure drop at startup.

I. Introduction

The two fuel processing buildings at the Savannah River Plant each have a deep bed sand filter on the exhaust air from the high level radioactive operations. Both the original plant units and a recent addition to the Savannah River Laboratory ventilation exhaust system have been described[1,2]. The general configuration and operating conditions are given in Table 1. During the first fifteen years of operation, both of the original plant units had suffered from severe acid attack and erosion of the concrete support structure, which became apparent when there was a localized loss of filter medium and resultant short release of activity from each bed (one 1969, and 1971). The holes were blocked and normal performance was restored almost immediately. The bottom support systems on both were modified to prevent further breakthrough. The failures also prompted consideration of new filters as ultimate replacements for the original units and resulted in extensive test work for both the plant filters and the Savannah River Laboratory filter[3,4]. Two new plant filters were designed and constructed; one was put into service in December, 1975, and the other is in final stages of completion.

The twenty-odd years of plant experience on the original filters, plus the continuing test work as the new filters were constructed, provide much useful performance information, which can be extended to give design and operating criteria for sand filters. The first of the sections below presents the history of the plant units and analyzes the performance data. The second section discusses the test work aimed at insuring that the replacement filters started up with

an efficiency comparable to the old filters so that there would be no increase in activity releases.

II. Plant Experience

SRP Separations Plants

The two separations plants are large, versatile facilities, in which irradiated reactor fuels and targets are processed to recover desired materials. The feed materials are dissolved, then processed primarily by solvent extraction, with some auxiliary ion exchange processes. A wide variety of materials have been irradiated or formed by irradiation, and subsequently processed in these plants, including uranium-233, -235, and -238, plutonium-238, and -239, various mixtures of higher plutonium isotopes, neptunium-237, americium and curium (various isotopes), and thorium. All of these have been associated with large amounts of fission products formed in the reactors. Some ventilation streams are treated separately and some are prefiltered with HEPA filters or packed glass fiber filters, but basically the sand filters provide the final barrier between the radioactive materials in process and the environment, and obviously are required to handle a large variety and amount of radioactive material.

Efficiency

The two plant filters originally had efficiencies of 99.7 to 99.8% as measured by input-output activity measurements, similar to other units that have been reviewed[5]. This apparent efficiency increased steadily over the years, with one filter also becoming markedly better than the other, concurrently with increasing pressure drop on that filter. The more efficient filter finally reached a limiting efficiency for activity removal approaching 99.995%, but pressure drop also became excessive and one foot of the fine sand layer was removed in 1972. Subsequent DOP tests gave an efficiency of 99.96% for this filter and 99.98% for the other, unaltered filter. Activity input-output measurements confirmed limiting efficiencies of 99.97 to 99.98% for both filters for fission product and alpha activity.

The two failures of the support structures referred to previously allowed rock and sand to run through, forming craters with a small hole in the apex. The activity releases increased for a short time until the holes were blocked and the craters filled with sand, then releases returned to normal. The supports were shored in such a way that no more complete penetrations of the beds could occur. However, some of the far reaches of the air distribution trenches could not be protected, and failures there occasionally give small depressions that thin the effective sand layer and decrease efficiency measurably without being serious. These are filled with more sand when detected, with no long-term effect on efficiency.

The term "limiting efficiency" as used above represents the efficiency that can be expected with very large inputs; it is the justifiable value to use in accident analyses and does agree with the DOP tests. The relation between apparent efficiency and input

activity is illustrated in Figure 1, where input beta-gamma activity for three different years is plotted against penetration (1-efficiency). The graph shows both the pattern of increasing efficiency with time and the increasing apparent efficiency (toward limiting values) as the input activity increased. This behavior is indicative of two mechanisms for the penetration of activity through the filter, with some re-entrainment of activity from the large inventory present as well as some fraction of input that escapes filtration in accordance with the true efficiency. The small "inventory release" gives a low background emission even when the input air is relatively clean. This background release and the proportion of long-lived activities such as ^{137}Cs and ^{90}Sr in it have not increased as the total inventory of activity on the filters has built up; indeed, it has decreased, which argues for deposited activity being at risk of re-entrainment for only some limited period.

Alpha activity has shown the same general pattern as beta-gamma activity with lower apparent efficiency at low inputs and the same limiting efficiency at high input, although the amount of alpha activity input has not been high enough to really define the limiting value. Input and output activity can be plotted as on Figure 2 to show the low level background that is independent of input and an apparent limiting efficiency of 99.98%. On such a graph, abnormal conditions in the filter, such as the small craters, are discernible above the envelope of normal conditions.

Finally, the limiting efficiencies also apply to ruthenium that initially may be evolved from the process as gaseous ruthenium tetroxide. This material can be produced in evaporators at very high nitrate concentrations and from process solutions with excess oxidizing agents such as potassium permanganate. The highest beta-gamma inputs to the filters have been associated with evolution of ruthenium in the process; hence, in these cases the high limiting efficiencies basically measured the efficiency for retention of ruthenium. The sand filter may be efficient because it offers a large surface for the ruthenium compound to decompose on, or it may be filtering particles on which the ruthenium has condensed after hydrolyzing in the generally humid off-gas streams. The mechanism is not as important as the fact that the ruthenium is collected.

Pressure Drop and Water Effects

As noted previously, the pressure drop on one filter became excessive and one foot of the fine sand was removed. The increasing pressure drop probably had several causes: a concrete dust loading from some in-building construction activity; concrete and sand fines from the severe acid erosion found later in the entrance tunnel and bed support structure; nonsilica minerals present in the sand in greater abundance in this filter than the other. Superimposed on the steady increase were a marked semiannual variation (Figure 3). This variation may result from moisture; samples of sand from deep in the bed appear damp in moist air and now contain appreciable chemicals, primarily calcium and magnesium salts. The annual changes in humidity and temperature in the humid southeastern environment, plus hygroscopic salts, provide a reasonable explanation of the cyclic effect. Additionally, there were specific episodes where external

ground water and rain reached the bed; these events were eliminated by appropriate repairs. Most noteworthy, the free water reaching the bed gave high pressure drop but did not hurt filtration efficiency. At the low air velocity, water apparently did not aspirate up through the bed and carry activity through to the outlet side.

Life of Sand Filters

The limiting useful life of a sand filter is not known and a filter without structural defects may last the life of the processing plant judging from the SRP experience. The limiting factors would be breakthrough of activity and pressure drop. SRP data show that activity is not moving through the filter and that pressure drop can remain stable if the sand is not reactive and dust loadings are not excessive. Radiation profiles through the filters have been monitored since startup with a network of bore tubes. Activity peaks are found at interfaces between the coarse sand layers below the thick bed of fine sand, which in effect acts as a polishing filter. Successive profiles over the years show the activity peaks moving lower (Figure 6). The radiation profiles basically measure recently deposited fission products and do not preclude a slow migration of old material; the lack of increase in the background release is the best evidence against migration.

Pressure drop does not have to be a life-limiting factor either, according to SRP experience. Although the pressure drop on one filter increased markedly, pressure drop on the other increased only a small amount, as noted previously. Measurements through the bed with lower pressure drop do not show any specific interfaces responsible for the bulk of the pressure drop (Figure 4). The data dispelled fears that some specific zone might be gradually plugging and offer potential for a large increase in pressure drop with the addition of only a small amount of additional dust. In essence, pressure drop on this filter could be projected to be tolerable for the foreseeable future.

The filter with high pressure drop and from which sand was removed, also had no sharp pressure drops at interfaces, with the flow resistance basically spread through the entire fine sand layer (Figure 5). As noted previously, nonsilica minerals and calcium and magnesium salts are in this bed. Again, the data imply that pressure drop would not be a problem if foreign materials were excluded during construction and operation. Finally, the success in removing a foot of sand from this filter, though at some sacrifice in efficiency, shows that maintenance is possible and that sand probably could be removed and replaced whenever necessary to maintain both satisfactory pressure drop and efficiency.

New Filters, Initial Operation

The deterioration of the structures prompted work on new filters and resulted in the extensive test work discussed previously. Sands were selected on the basis of the experimental work and ordered for the new filters. Continuing test work, covered in Section III of this report, showed the sand as supplied had lower efficiency than the test batches and a thin layer of different sand was added to

attain better performance. The first new unit, 30.5 by 110 meters, was put into operation in December 1975, in parallel with the original filter. Initial flow velocity through the new unit, 1.2 cm/sec, is lower than ultimate design basis of 3 cm/sec. The old filter that is being operated in parallel has a resultant flow velocity of .75 cm/sec versus the former 2.5 cm/sec on that unit. DOP tests on the combined, parallel system gave an efficiency of 99.99+%, as would be expected at the low velocity, according to the design tests. The old unit will be operated in parallel for as long as it can be maintained, because of the benefits of low flow. The average releases of radioactivity from the combined filter units did decrease by a factor of about two for the first four months of combined operation as compared to the last four months with just the old filter.

III. Design Work for New Filters

Design Bases

The original sand filter installation at Hanford provided the filter model for those designed for the Savannah River Plant[6]. In this design, a relatively deep prefilter section of graded coarse aggregate, characterized by a large void volume, high air permeability (low pressure drop for a given flow), and modest filtration efficiency, is followed by layers of finer sands which provide high efficiency filtration with an attendant lowering of air permeability. Reports on the characteristics of this design for specific sand types show the prefilter acts as a storehouse for all but the finest dust and aerosols, protecting the finer layers and prolonging useful filter life[3]. In these filters, sands falling in the size range from 20 to 50 mesh have been critical in controlling both overall efficiency and permeability. Data have also been presented in performance, dependent upon sand grain shape characteristic of the deposit from which it was taken[4]. The variability in naturally occurring sands makes the design of a filter more complex than simply creating a pile of sand. Design criteria used for the construction of new filters at the Savannah River Plant are presented to illustrate the importance of testing and quality control in meeting performance criteria.

Long life, high efficiency, and high air permeability are the goals in sand filter design. The optimization of these is limited by physical and economic restraints which make compromise essential. A superficial flow velocity in the range of 2.5 to 3.0 cm/sec has been found to provide a suitable compromise for efficiency and permeability and still provide a manageable size filter. Prefilter sections built to specifications given in Table 2 have been demonstrated effective in over twenty years of service in existing filters at Savannah River. A 30.5 cm (12 in.) layer of sand in the size range from 8 to 20 mesh (F grade) provides a transition between coarse gravels and the finer sands. It is the sand finer than 20 mesh which becomes limiting for both filter efficiency and air permeability. Its selection and placement control the ultimate performance of the filter. Work reported here is concentrated on this area of filter design.

Sand Selection

Ten sources of sand with size distributions falling within the 20 to 50 mesh range were evaluated as filter media[4]. Characteristics varied widely according to size distribution and surface texture. Some good sands were eliminated due to inadequate source or vendor capability. One of the best sources available from a vendor with adequate facilities at a competitive price was selected. A test program was initiated to verify the properties and uniformity of the sands taken from this deposit and provide ongoing design assistance throughout the construction phase of the project.

Sands with two different size specifications, subsequently called types G and H, taken from the single deposit, were carefully evaluated for suitability as sand filter media. The Photoscan technique for measuring surface texture was used to check shape uniformity throughout the sample. All samples had a surface texture of 17.5 ± 0.5 units. This is considered sand of good surface uniformity. An acid leachability test using a 10% boiling HNO_3 acid solution was devised. Sands from this deposit were found not to lose weight after 48 hours of exposure.

Test Work

The type G sand was used in the previously constructed Savannah River Plant filters for the high efficiency section, and as noted previously, efficiency was only moderate at startup. For the new filters, the sand had to provide a higher efficiency, comparable to the final efficiency reached by the old filter, and a test program was initiated to assure adequate performance. Samples of the type G sand were taken from each car loaded at the mine, and size and permeability were measured to determine uniformity. Composite samples of sand were taken at the filter site and tested for size distribution, permeability, and relative filtration efficiency as determined by DOP aerosol test criteria.

Laboratory test work was performed in a 20-cm square filter column, 150 cm deep. The relative effect of the fine sands measured alone was found to correlate well with results obtained in the 61-cm square filter column used for earlier test work in which the coarser prefilter sand and gravel were included. Permeability and efficiency of the sand were determined. Variations were found among the composite samples. Typical results are shown in Table 3 where the size distributions, pressure drops, and filtration efficiency using a 0.8 micron average polydisperse DOP aerosol are reported. It is noted that the size distribution of sand varies among the samples. The finer distributions tend to have lower permeability (higher pressure drop) and better efficiency.

The effect of depth of "G" sand on collection efficiency is illustrated in Figure 7. Here, "G" sand depths ranging from 90 to 140 cm were tested at superficial velocities between 2.5 and 3.5 cm/sec. The pressure drops at respective test points are shown. Here it is seen that substantial improvements in efficiency can be obtained by increasing the depth of the fine sand at a subsequent

penalty in terms of higher pressure drop.

As "G" sand was shipped, a running composite was obtained that projected the average sand size distribution for the "G" sand. It was determined that it was best approximated by sample C given in Table 3. The performance of this sand was evaluated and results are shown in Figure 8.

An alternate to a greater depth of "G" sand was also evaluated. A type H sand with the size specification shown in Table 4 was tested as an "add-on" to type G. Its effectiveness is shown by the efficiencies and pressure drops illustrated in Figure 9. A bed with 91 cm of "G" plus 20 cm of "H" is seen to give a measured efficiency of 99.98% at a flow of 2.5 cm/sec with a pressure drop of 150 mm WG.

Conclusions

Data presented here show the importance of sand selection in filter design. Furthermore, careful monitoring of the fine sands at delivery is needed to assess the effect of variations throughout the natural deposit. These can make the final composite different than would be anticipated from only surface samples taken at the mine. In the case discussed, it was found that a shift in the size distribution between rather narrow limits was sufficient to affect filter performance while shape and texture remained constant. The test program showed performance fluctuations could be handled by varying bed depth in a single grade, "G", or adding another grade, "H", to a "G" sublayer. The newest filter at the Savannah River Plant has 91 cm of "G" sand topped by 20 cm of "H" grade. This filter was started up with an old filter in parallel so that its performance with regard to the specifications has not been determined independently. However, past experience indicates its performance will closely match that predicted from small scale model testing.

Table I.   Original sand filters.

Dimensions, meters
Length	73.15
Width	30.48
Depth	2.44
Superficial velocity, cm/min	152.40
Initial ΔP, cm WG	19.30
Total air flow, m^3/min	3000-3500

Table II.   Sand prefilter materials.

Gravel Type	Depth	Specification
A	12 in.	0% retained in 3" screen; less than 2% passing 1-1/4" screen.
B	12 in.	0% retained on 1-1/2" screen; less than 2% passing 5/8" screen.
C	12 in.	0% retained on 5/8" screen; less than 5% passing 1/4" screen.
E	6 in.	Less than 1% retained on 1/4" screen; less than 5% passing 8 mesh screen.

Table III.   Type G sand characteristics.

Size Analysis

Mesh	Sample A, %	Sample B, %	Sample C, %
+20	0.3	0.2	0.1
+30 -20	47.6	40.7	48.3
+40 -30	41.2	42.6	46.2
+50 -40	9.1	12.8	4.8
-50	1.8	3.7	0.6

Performance in 20-cm Square Filter Column (91-cm Sand Depth)

Sample →	A	B	C
Velocity, cm/sec	2.6	2.6	2.6
ΔP, mm WG	153	157	127
Efficiency, % DOP	99.96	99.94	99.88

Table IV.   Size specification for type H sand.

Mesh	Percent
+30	1.0
-30 +40	65.0
-40 +50	30.0
-50 +70	3.5
-70	0.5

DISCHARGE (PENETRATION),
% OF INPUT

INPUT β, γ ACTIVITY, m Ci/MONTH
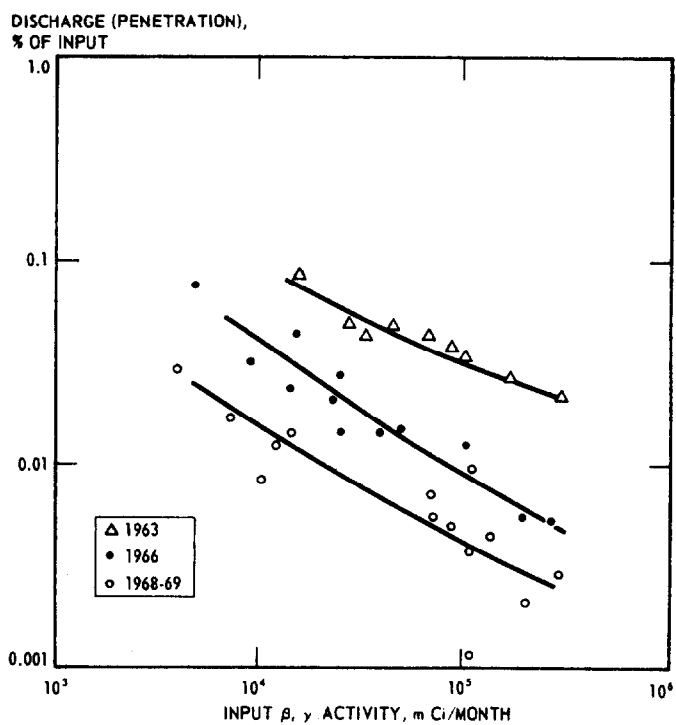
FIGURE 1.   FILTER PERFORMANCE

RELATIVE ALPHA OUTPUT, PER MONTH
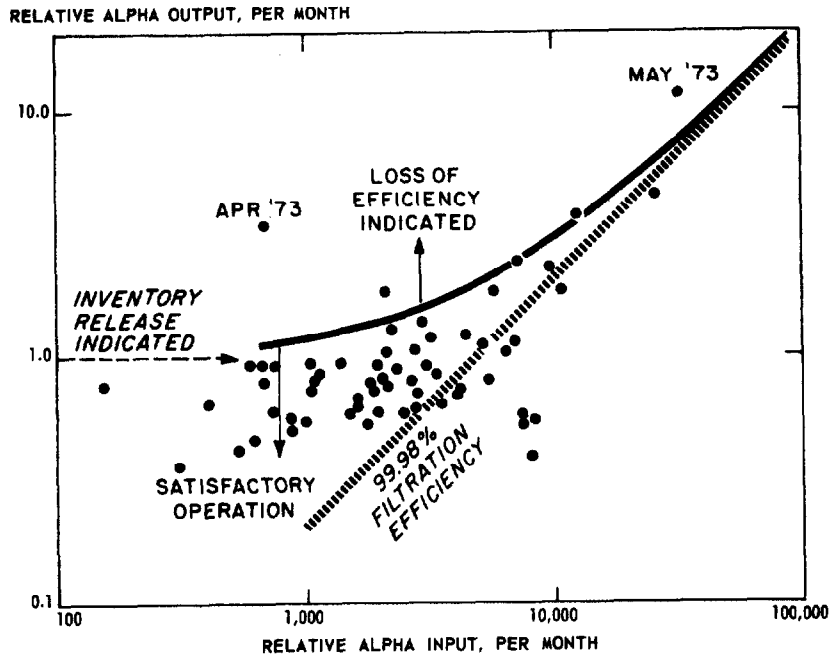
FIGURE 2. H-AREA SAND FILTER PERFORMANCE
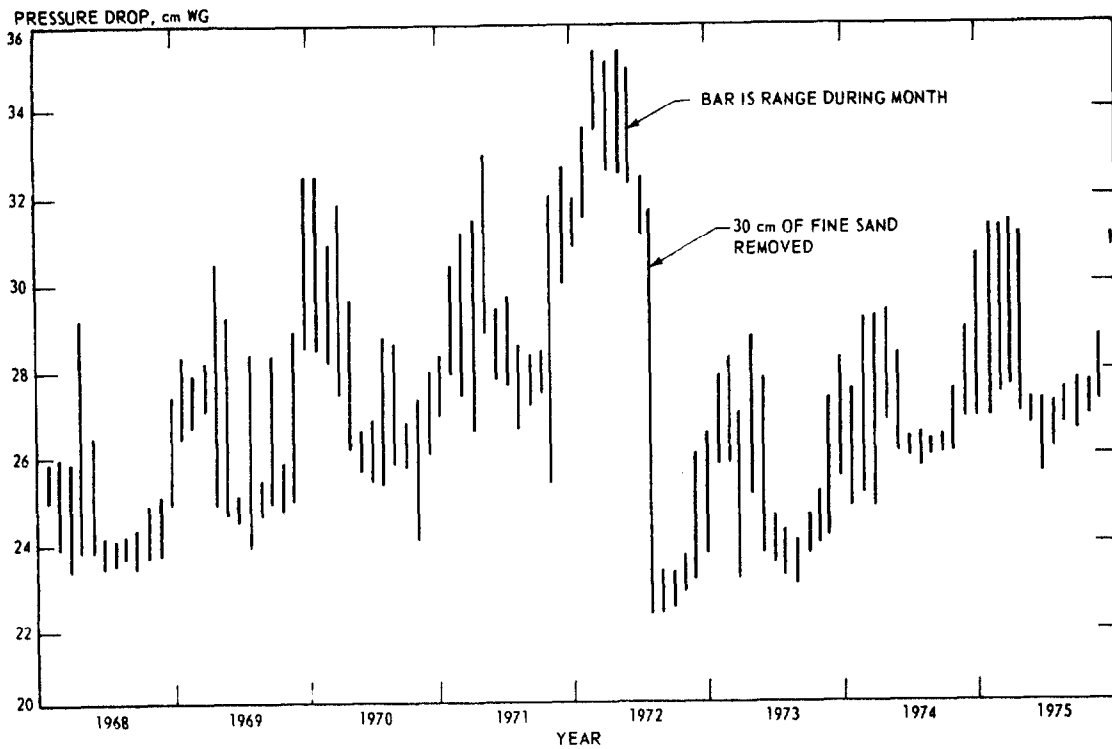
PRESSURE DROP, cm WG

FIGURE 3. PRESSURE DROP HISTORY

DISTANCE FROM BOTTOM, cm
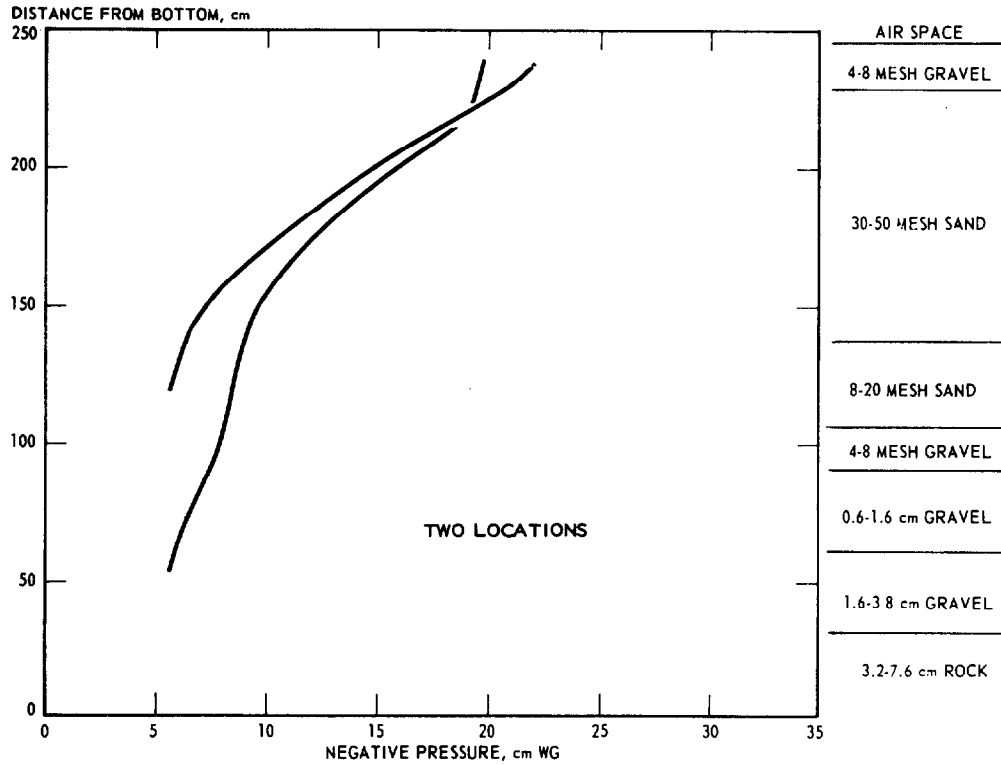
FIGURE 4. DISTANCE FROM BOTTOM VERSUS NEGATIVE PRESSURE

DISTANCE FROM BOTTOM, cm
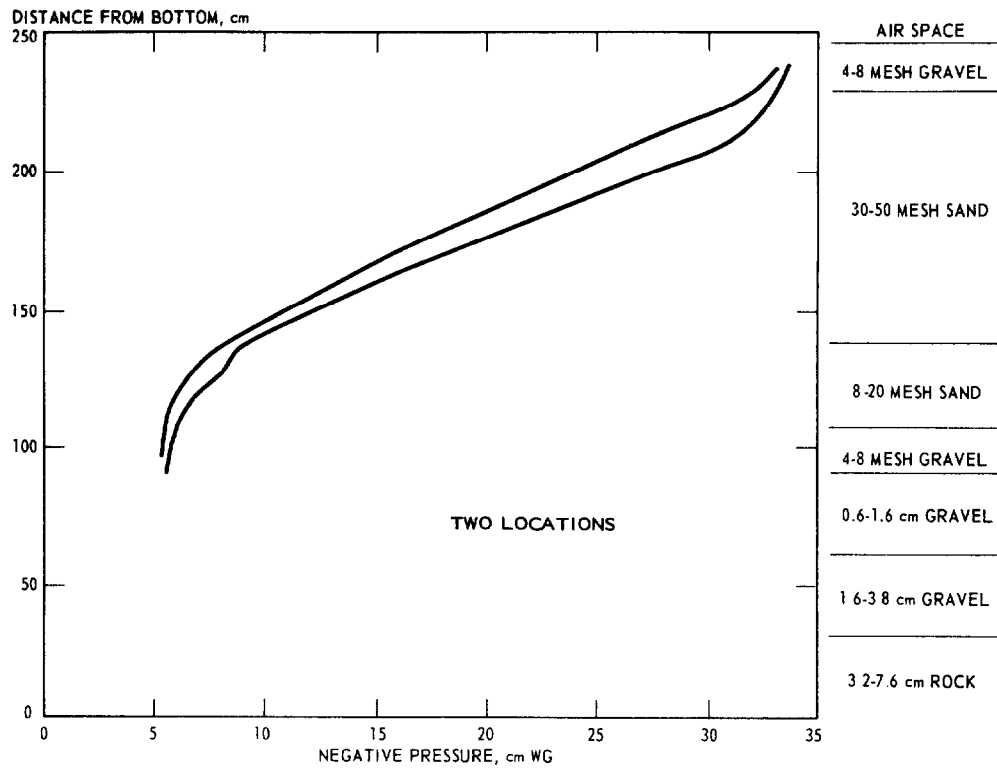
FIGURE 5. DISTANCE FROM BOTTOM VERSUS NEGATIVE PRESSURE

552

THICKNESS OF LAYER, cm

15.2	.64-1.6 cm GRAVEL	
15.2	4-8 MESH GRAVEL	
91.5	30-50 MESH SAND	
30.5	8-20 MESH SAND	
15.2	4-8 MESH GRAVEL	
30.5	.64-1.6 cm GRAVEL	
30.5	1.6-3.9 cm GRAVEL	
30.5	3.2-7.6 cm ROCK	

1957   1960   1963
1966
1975

RADIATION MOVING BASE
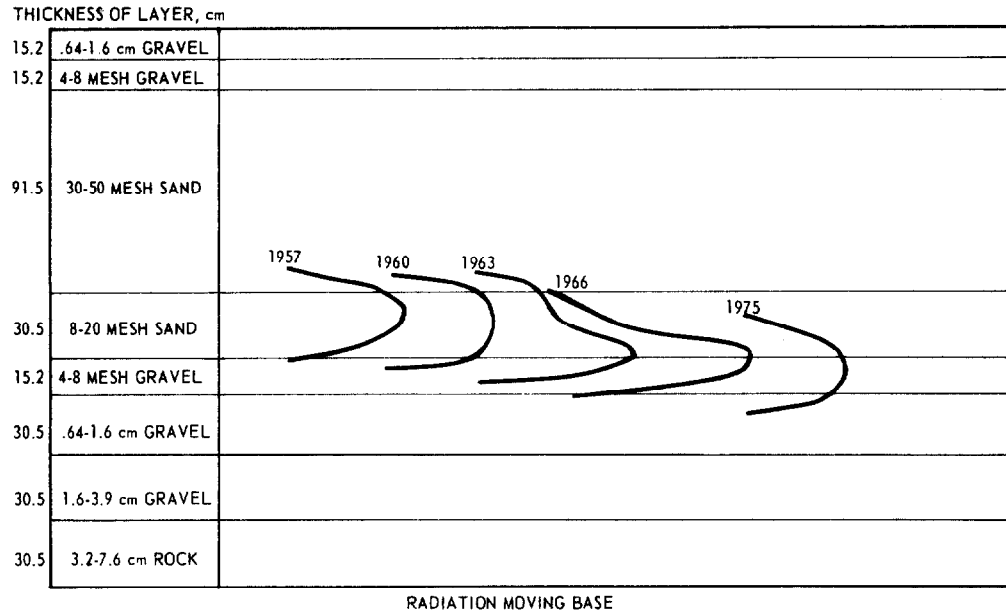
FIGURE 6.   RELATIVE DEPTHS OF RADIATION PEAKS

FILTRATION EFFICIENCY,
PERCENT (DOP)

(PRESSURE DROP)

100.00 (226 mm WG) 140 cm SAND
(198 mm WG) (270 mm WG)
(234 mm WG)
99.98 (163 mm WG) 127 cm SAND
(279 mm WG)
99.96
(190 mm WG)
99.94 (155 mm WG) 107 cm SAND
99.92 (224 mm WG)
(185 mm WG)
99.90 91 cm SAND
99.88 (206 mm WG)

2.0   3.0   4.0
SUPERFICIAL VELOCITY, cm/sec
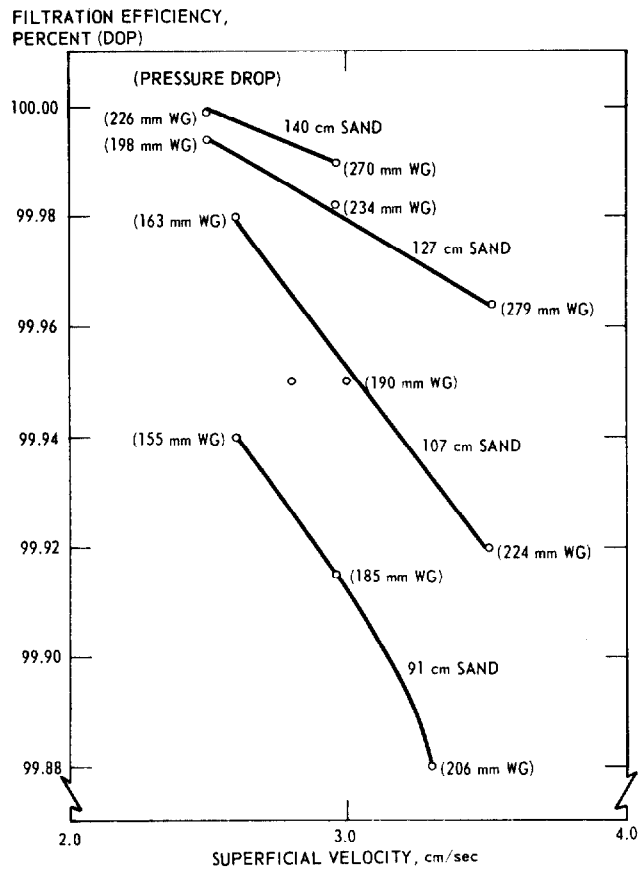
FIGURE 7.   FILTRATION EFFICIENCY VERSUS
VELOCITY SAMPLE B "G" SAND

FILTRATION EFFICIENCY,
PERCENT (DOP)
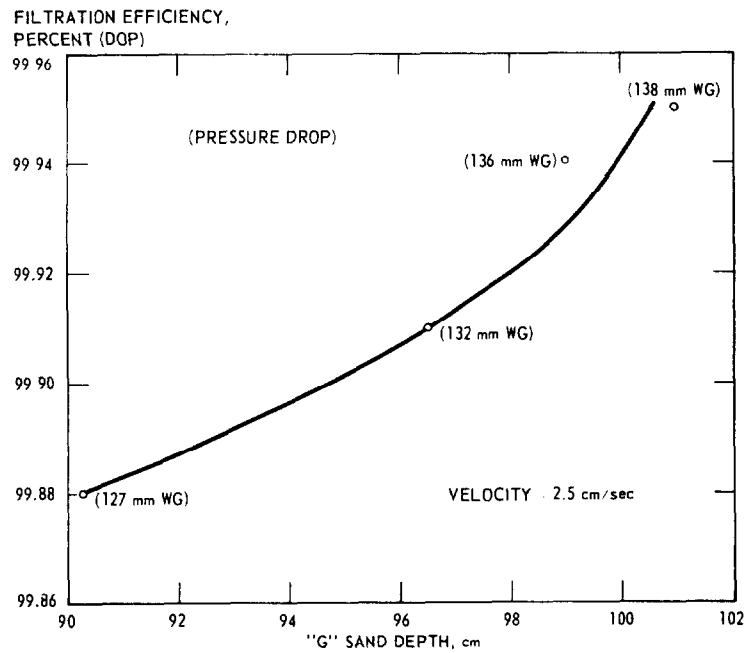
FIGURE 8.   FILTRATION EFFICIENCY VERSUS
DEPTH SAMPLE C "G" SAND

FILTRATION EFFICIENCY,
PERCENT (DOP)
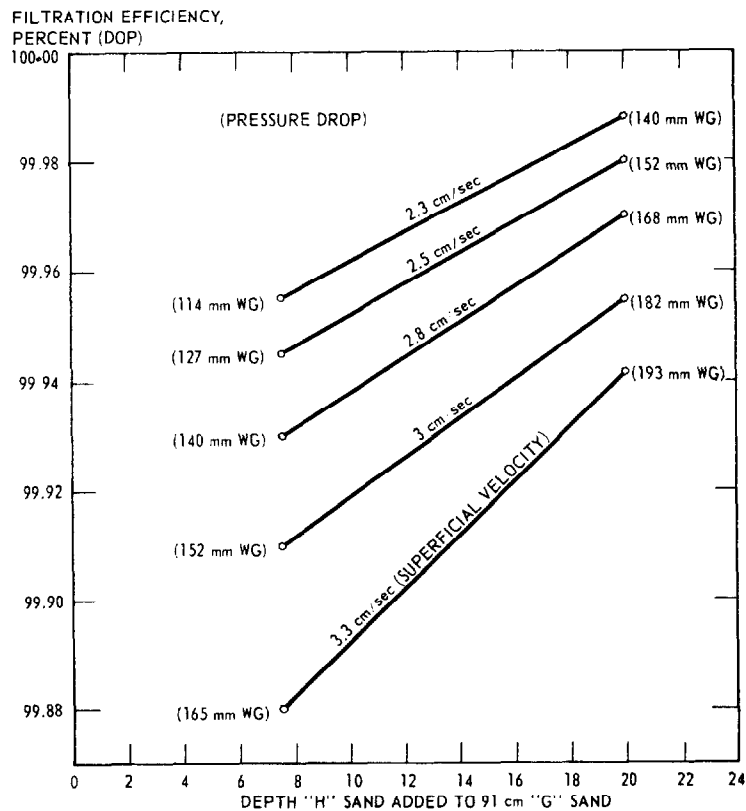
FIGURE 9.   EFFECT OF "H" SAND ADDITION ON EFFICIENCY

554

References

1. Sykes, G. H., and J. A. Harper, "Design and operation of a large sand bed for air filtration," Treatment of Air Borne Radioactive Wastes (IAEA Symposium), CONF 680811-13 (1968).

2. Moyer, R. A., J. H. Crawford, and R. E. Tatum, "Deep-bed sand filter at Savannah River Laboratory," 13th USAEC Air Cleaning Conference (1974).

3. Schurr, G. A., D. B. Zippler, and D. C. Guyton, "Deep-bed filter performance tests," 12th AEC Air Cleaning Conference (1972).

4. Schurr, G. A., and J. E. Johnston, "Characterizing sand grains to optimize filter performance," 13th USAEC Air Cleaning Conference (1974).

5. Juvinall, R. A., R. W. Kessie, and M. J. Steindler, "Sand-bed filtration of aerosols: a review of published information of their use in industrial and atomic energy facilities," ANL-7683 (1970).

6. Lapple, C. E., "Deep-bed sand and glass-fiber filters," Second Air Cleaning Seminar, WASH-149 (1954).

DISCUSSION

SCHIKARSKI   One disadvantage of sand filters is the large amount of contaminated sand. As we reported at the San Francisco Air Cleaning Conference you can optimize the mass without losing efficiency by special arrangement of layers of different mesh size sand. Have you optimized your filter in that respect and thus avoided the large amount of sand used in earlier installations?

ORTH: I'm not sure I completely understand the question. If you're talking about optimizing to obtain the minimum depth of sand, just to minimize the amount of final waste, I think the answer is yes, we could do that, but at higher pressure drop. Our system is a compromise within our engineering constraints.

SCHIKARSKI: Usually, the sand filter designs have too much sand in them. We optimize for just sufficient mass to give the result we want.

ORTH: What you say is correct. We could optimize and just arrive at a certain efficiency. We're trying to do the best we can within the limits of the pressure drop we can tolerate. Minimizing waste was not a consideration.

SCHURR: I might also answer that question. We did optimize the designed sand depth on the criteria of life expectancy, efficiency, and pressure drop. The problems of commercial availability and quality control make us have more sand than would be required, ideally.

DUST FILTRATION ON A PANEL BED OF SAND

W.R.A. Goossens, A. Francesconi, G. Dumont, R. Harnie

S.C.K./C.E.N.

Mol (Belgium)

Abstract

The development of a panel bed of sand as dust filter is described. The results obtained in a technical set-up with a filtering area of 1 m^2 are given. The data of a 2^4 factorial design experimental campaign are presented in the form of the resulting statistical equation.

I. Introduction

Dust filtration with the help of granular materials has been applied since many years [1]. For example at the Hanford site, deep beds of graded sand and gravel are in use to remove dust and aerosols from nuclear off-gases [2].

Recently, attention has been drawn again on the possible use of a tall and narrow vertical layer of granular solids in order to filter a gas stream passing this layer in cross-flow [3]. Such a set-up, called panel bed, has been investigated at S.C.K/C.E.N. too. The main objective was to gather information on performance of such a panel bed for the filtration of hot outlet gases released by a radioactive waste incinerator.

This paper describes the results obtained in a technical set-up in which the trapping of fly ash by a panel bed of sand was investigated in order to allow proper design of the panel bed for the waste incinerator. Preliminary, the panel bed concept was tested in a laboratory unit.

II. Preliminary experiments in a laboratory unit

The filtration possibilities of a vertical layer of granular solids were investigated in a laboratory unit made of perspex. The 5 cm thick layer of 350 μm sand grains was kept in place by a louvered wall at the gas inlet side and a special low resistant perforated plate "Conidur" at the gas outlet side as shown schematically in Fig. 1. The gas crossing this vertical layer in the

horizontal direction was artificially loaded with fly ash at a concentration of 300 mg per m^3. The effective filtration area was 90 cm^2.
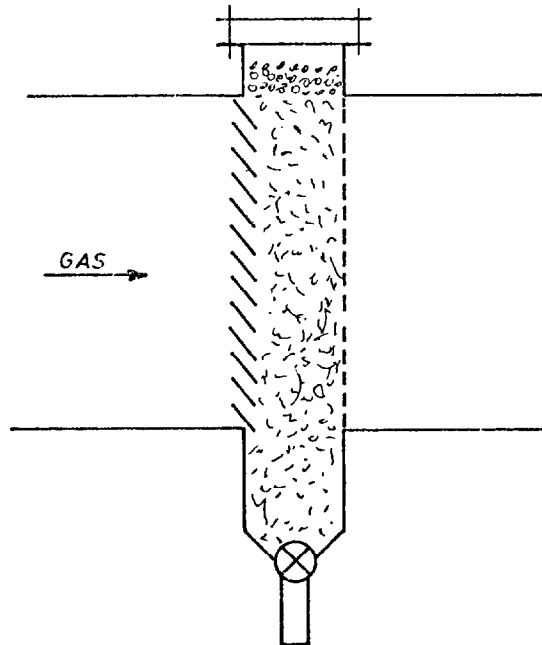
FIG. I   CROSS -SECTION OF THE BENCH SCALE PANEL-BED FILTER

The dust trapping efficiency reached 99.5 % at a face velocity of 40 cm s^{-1}. The dust appeared to get trapped in the front layer of the filter. The resulting pressure drop increase is shown on Fig. 2. The pressure drop increase offered only a limited operation time to this batch type operation of the granular layer, so that a layer renewal system had to be developed for long operation times.
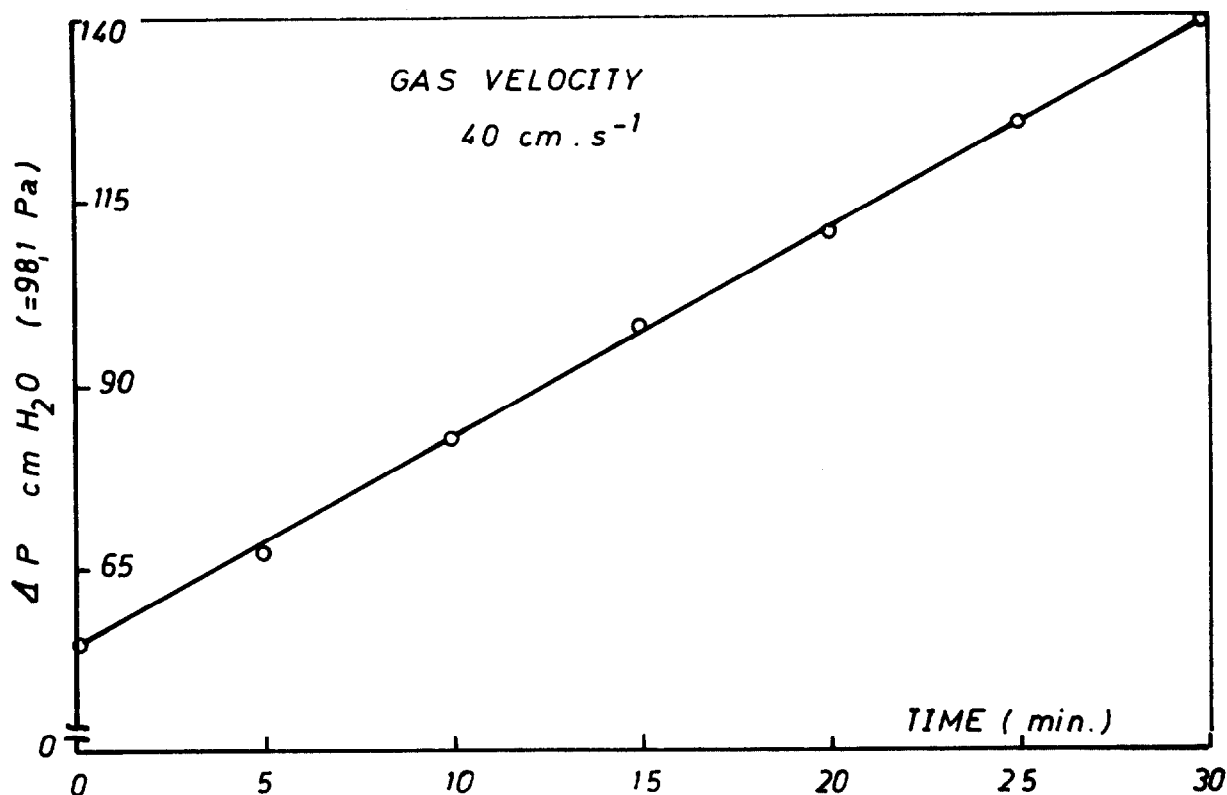
FIG. 2   PRESSURE DROP AS A FUNCTION OF FILTRATION TIME

III. Experimental procedure in the technical set-up

In the technical set-up with an effective flow area of 1 m^2 the solids recycling was performed with an air lift and a vibrating screen was applied for the necessary dust sand separation. As schematically indicated on Fig. 3, two louvered walls were now applied to keep the vertical sand layer in place. The distance between both walls was variable so that a sand layer tickness between 3.9 cm and 18.9 cm was obtainable. A standard sieve ASTM No. 35 (sieve opening 0.5 mm) was used to separate the sand and the dust in a vibrating device. The dust collected was reloaded to the inlet gas with the help of a home-made dust feeder. A view of the

installation is given in Fig. 4.
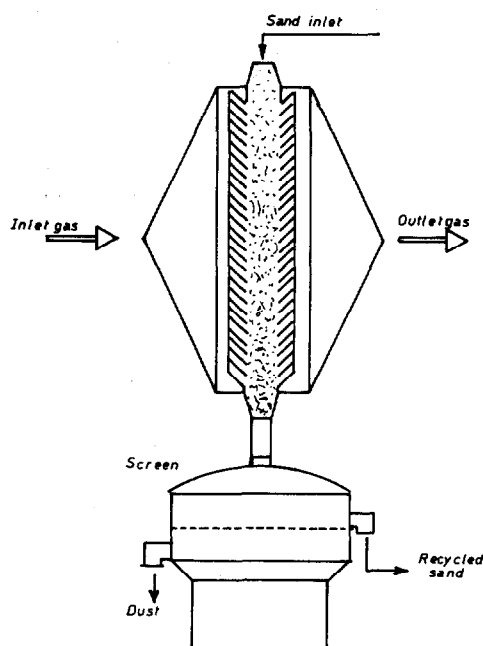
FIG. 3   SCHEME OF A PANEL BED FILTER
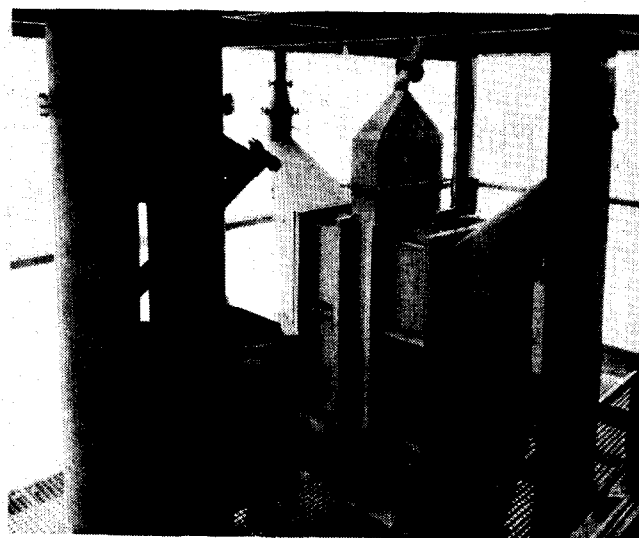
FIG. 4   VIEW ON THE INSTALLATION

The carrier gas was compressed air at a maximum flow rate of 450 $m^3.h^{-1}$. The dust used was fly ash from a coal power station with a maximum size of 110 μm. The carrier gas was artificially loaded with this fly ash at a mass flow rate between 176 and 1580 $g.h^{-1}$.

Dust samples were taken isokinetically in the 9.5 cm diameter inlet or outlet tube. The inner diameter of the sampling line was 5 mm. The dust present in the sampled gas was quantitatively trapped on a millipore membrane filter with a diameter of 47 mm and an average pore size of 0.6 μm. The quantity of dust collected during a definite time was determined by differential weighing.

IV Results

In a first experimental campaign, 1.5 mm sand particles were kept at rest in the 4.5 cm thick panel bed. A filtration efficiency higher than 99 % was thus obtained at an air flow rate of 400 m^3h^{-1} and a dust load rate of 430 $g.h^{-1}$. When the sand circulation was

installed at a mass flow rate of 1700 kg.h^{-1}, the filtration efficiency became slightly smaller. However, gas leaks from the air lift to the panel bed were observed so that various adaptations on the circulating line were necessary. To increase the linear gas velocity the filtering area was decreased by obstructing part of the panel bed. In this way, it was shown that a maximum linear gas velocity of 90 cm.s^{-1} could be allowed in the panel bed without any sand entrainment while the dust trapping efficiency remained above 99 %.

To complete the technical data, a 2^4 factorial design experimental campaign was performed with the sand at rest during the runs, each three hours long. This way of operation was possible since the average pressure drop increase during the filtration was only 25 Pa ($\simeq$ 2.5 mm H$_2$O) per hour. Further, the dust trapped during a run was removed by screening the panel bed load during 1 h and 1 1/2 h with a distance between the louvered walls of 3.9 and 8.9 cm respectively.

The following parameter levels were used : 150 and 200 m^3 h^{-1} for the gas flow rate ; 0.32 and 0.48 g m^{-3} for the inlet dust concentration ; 0.9 and 1.5 mm for the average size of the sand ; 3.9 and 8.9 cm for the tickness of the vertical sand layer. The conditions of the various runs are enumerated in Table I on the basis of the factorial design principle.

TABLE I
Symbols for the set of combinations

Symbol of the combination	Level of parameters			
	G	c	Dp	d
(1)	−	−	−	−
a	+	−	−	−
b	−	+	−	−
a b	+	+	−	−
c	−	−	+	−
a c	+	−	+	−
b c	−	+	+	−
a b c	+	+	+	−
d	−	−	−	+
a d	+	−	−	+
b d	−	+	−	+
a b d	+	+	−	+
c d	−	−	+	+
a c d	+	−	+	+
b c d	−	+	+	+
a b c d	+	+	+	+

The statistical analysis of the experiments gave the best independent results when the outlet dust concentration was taken as the dependent variable. This leads to the following regression equation for this outlet dust concentration, c_o, in mg m^{-3} :

$$c_o = 3.124 + 3.422 \, D_p - 0,660 \, L \pm 1.11$$

where : D_p is the average diameter of the sand in cm and L is the bed tickness in cm. The confidence level of both effects was higher than 99 %

The flow rate and the inlet dust concentration dit not show a significant effect under these operating conditions, while also the interactions between the various parameters were negligable.

The value of the standard deviation was estimated on the basis of the mean square value of all interactions observed during these non-repetitive runs.

A similar statistical analysis of the data obtained for the pressure drop increase per hour resulted in the following expression:

$$\Delta P = 0.8537 + 0.0176 \, G - 2.233 \, D_p \pm 0.63$$

where : ΔP is the hourly pressure drop increase in mm H$_2$O (=9.8 Pa) per hour and G is the gas flow rate in m^{3}h^{-1}.
Hence, the gas flow rate and the grain size of the sand have an important effect on the pressure drop.

V. Conclusions

The practical results obtained in the technical set-up gave sufficient information for an engineered design of a panel bed of sand as a dust filter for incinerator gases. This pilot unit working at 2.800 m^{3}h^{-1} (STP) and at 600°C will have a guaranteed outlet dust concentration of less thant 50 mg m^{-3}. Its mechanical reception is in progress.

Notations

d	: tickness of sand layer	L	
d_p	: sand particle average diameter	L	
G	: carrier gas flow rate	$L^3 \, T^{-1}$	
c	: inlet dust concentration	$M \, L^{-3}$	
c_o	: outlet dust concentration	$M \, L^{-3}$	
ΔP	: pressure drop in filter bed	$F \, L^{-2}$	
μ	: filtration efficiency	%	

REFERENCES

(1) R.H. PERRY, C.H. CHILTON, Chemical Engineers Handbook
5th ed., Mc. Graw-Hill, N.Y., 1973, p. 20/87 - 89

(2) H.A. LEO, Guide to Fire Protection in Caves Canyons
and Hot Cells, ARH-3020 (1974)

(3) A.M. SQUIRES, R. PFEFFER, Panel bed filters for
simultaneous removal of fly ash and sulfur dioxide,
APCA Journal, 20, 534-538 (1970)

DISCUSSION

MICHELS: Would you please comment on the ability of the panel filter to withstand pressure surges? Also, does the sand remain free-flowing and does it discharge readily from the panel after service?

GOOSSENS: The ability of the panel filter to withstand pressure surges depends on the geometrical characteristics of the panel filter assembly. The filter described in our paper shows only a limited resistance against pressure surges since the grains can get entrained fairly easily. During our experimental investigation we have never had discharge difficulties after service. The sand remained free-flowing, as you call it. Nevertheless, the angle of repose and the flow properties of the sand plus dust mixture differ slightly from the flow properties shown by new sand. Furthermore, it must be stressed that our investigation was performed at ambient temperature.

INHOMOGENEOUS ELECTRIC FIELD AIR CLEANER*

B.G. Schuster
Los Alamos Scientific Laboratory
University of California
Los Alamos, New Mexico 87545

Abstract

For applications requiring the filtration of air contaminated with enriched uranium, plutonium or other transuranium compounds, it appears desirable to collect the material in a fashion more amenable to recovery than is now practical when material is collected on HEPA filters. In some instances, it may also be desirable to use an air cleaner of this type to substantially reduce the loading to which HEPA filters are subjected.

A theoretical evaluation of such an air cleaner considers the interaction between an electrically neutral particle, dielectric or conducting, with an inhomogeneous electric field. An expression is derived for the force exerted on a particle in an electrode configuration of two concentric cylinders. Equations of motion are obtained for a particle suspended in a laminar flow of air passing through this geometry. An electrical quadrupole geometry is also examined and shown to be inferior to the cylindrical one. The results of two separate configurations of the single cell prototypes of the proposed air cleaner are described. These tests were designed to evaluate collection efficiencies using mono-disperse polystyrene latex and poly-disperse NaCl aerosols. The advantages and problems of such systems in terms of a large scale air cleaning facility will be discussed.

I. Introduction

In many cases, particularly for recovery and/or simplified solid waste disposal purposes, it is desirable to have an air cleaning system in which the particulate material collection may be concentrated. This goal may possibly be attained by flowing the aerosol laden air through a matrix of coaxial cylinders with a high electric field across each coaxial pair. The electric field will induce a dipole moment on the aerosol particles which will then be subject to a force in the direction of the central cylinder due to the field gradient produced by the coaxial configuration. Calculations based on such a system indicate the possibility of 100% collection for 1.0 μm particles in slow laminar flow, providing the particles stick to the collector surface. Power requirements are not expected to be high since the only work to be done is that required to overcome viscous drag forces acting to resist the particle motion, permitting operation of this air cleaner during emergency conditions with use of a capacitor bank. The interaction of the carrier gas (air) with the electric field is considered negligible.

II.   Trajectory Analysis, Coaxial Cylinder System Radial Motion

We consider a flow of particulates in air, with the particulates assumed to be electrically neutral. The principle to be invoked for the transport of the uncharged particles to a collection surface is that of an induced dipole interaction between the particle and an applied inhomogeneous electric field.

The induced dipole moment of a spherical particle in a locally uniform field approximation is given by

$$\vec{p} = 4\pi R^3 \epsilon_0 \frac{k-1}{k+2} \vec{E} \tag{1}$$

where $\vec{p}$ = induced dipole moment
$\vec{E}$ = electric field strength
R = particle radius
ϵ_0 = permittivity of vacuum
k = dielectric constant

A typical value of k is 10. For conductors, $(k-1)/(k+2)$ approaches unity.

The field at a radial distance r produced by a potential, V, applied between two coaxial cylinders is given by

$$\vec{E} = \frac{-\hat{r}}{r} \frac{V}{\ln b/a} \tag{2}$$

where b = radius of outer cylinder
a = radius of inner cylinder
$\hat{r}$ = unit radius vector.
The force on the particle is given by

$$\vec{F} = (\vec{p} \cdot \nabla)\vec{E} = -4\pi R^3 \epsilon_0 \frac{k-1}{k+2} \frac{V^2}{\ln^2 b/a} \frac{\hat{r}}{r^3} = \frac{-\alpha \hat{r}}{r^3} \tag{3}$$

Besides the electrical driving force on the particle, a viscous velocity-dependent force will exist. This is given, for small particles, by the product of the Stokes force and the slip correction factor, i.e.,

$$\vec{F}_d = \frac{6\pi \eta R}{1+A \lambda/R} \vec{v} = \beta \vec{v} \tag{4}$$

where η is the viscosity [which must be transformed to the mks units used in Eq. (3)], v is the velocity, λ the molecular mean free path, and A is a constant.

Combining Eq. 3 and 4 with the particle inertial term yields radial and tangential equations of motion. The tangential motion immediately damps out because of the lack of a driving force, leaving the radial equation of motion in the form.

$$m\ddot{r} + \frac{6\pi\eta R}{1+A\lambda/R}\,\dot{r} + 4\pi R^3 \epsilon_0\left(\frac{K-1}{K+2}\right)\frac{V^2}{\ln^2 b/a}\,\frac{1}{r^3} = 0 \quad , \tag{5}$$

where m is the particle mass and r the radial distance.

This equation is not amenable to analytic solution, however, the inertial term is negligible, i.e., the relaxation time is very small, and so $\ddot{r}$ can be set equal to zero. The resulting equation may now be integrated from the outer cylinder at radius b, to some other position at radius r to yield

$$r^4 = b^4 - \frac{8R^2\epsilon_0 V^2}{3\eta\,\ln^2 b/a}\left(\frac{K-1}{K+2}\right)t \quad , \tag{6}$$

where t = time. Defining

$$\frac{8R^2\epsilon_0 V^2}{3\eta\,\ln^2 b/a}\left(\frac{K-1}{K+2}\right) \equiv \alpha \quad , \tag{7}$$

Eq. 6 may be written as

$$r^4 = b^4 - \alpha t \tag{8}$$

Axial Motion

The longitudinal equation of motion is obtained from the laminar flow profile of air moving in the annular region under consideration. Following Joos', the differential equation for the velocity profile may be written as

$$\frac{d}{dr}\left(r\frac{dv}{dr}\right) = -\frac{(P_1-P_2)}{\eta l}\,r \quad , \tag{9}$$

where P_1-P_2 is the pressure drop along a length, l, of the system. Performing two integrations results in

$$v = -\frac{(P_1-P_2)}{4\eta l}\,r^2 + c_1\,\ln r + c_2 \quad . \tag{10}$$

The integration constants C_1 and C_2 may be evaluated from the boundary condition at the walls, which are

$$v = o \text{ when } r = a, \ r = b.$$

Substituting the values of C_1 and C_2 thus obtained into Eq. 1 yields the final form of the velocity profile for laminar flow in an annular region.

$$v(r) = \frac{P_1 - P_2}{4\eta l}\left[a^2 - r^2 + (b^2 - a^2)\frac{\ln r/a}{\ln b/a}\right], \tag{11}$$

This velocity profile is plotted in Fig. 1.

The flow rate, Q, for this system may be obtained by integrating the velocity profile over the cross section to yield, for $b \gg a$,

$$Q = \frac{\pi}{2}b^4\left(\frac{P_1 - P_2}{4\eta l}\right)\left(1 - \frac{1}{\ln b/a}\right) \tag{12}$$

The average velocity, $\bar{v}$, is given by the flow rate divided by the cross sectional area:

$$\bar{v} = \frac{1}{2}b^2\left(\frac{P_1 - P_2}{4\eta l}\right)\left(1 - \frac{1}{\ln b/a}\right) \tag{13}$$

The maximum velocity can be obtained by differentiating Eq. 11 and setting the result to zero. Letting $\gamma = \frac{P_1 - P_2}{4\eta l}$,

$$\frac{dv}{d} = \gamma\left[\frac{b^2 - a^2}{\ln b/a} \times 1/r - 2r\right] = 0 \tag{14}$$

Solving for r results in

$$r_{max} = \sqrt{\frac{b^2 - a^2}{2\ln b/a}} \doteq \frac{b}{\sqrt{2\ln b/a}} \tag{15}$$

Substituting this value of r_{max} into Eq. 11 yields

$$v_{max} \doteq \gamma\left[\frac{b^2}{\ln b/a}\left\{\ln\left(\frac{b}{a\sqrt{2\ln b/a}}\right) - 1/2\right\} + a^2\right] \tag{16}$$

The trajectory of a particle introduced into the airflow at radius b may now be computed from Eqs. 8 and 11. Letting $dz/dt = v(r)$ where z defines the axial coordinate and substituting Eq. 8 into Eq. 11 wherever r occurs results in

$$\frac{dz}{dt} = \gamma\left[a^2 - (b^4 - \alpha t)^{1/2} + \left(\frac{b^2 - a^2}{\ln b/a}\right)\left(\frac{1}{4}\ln\,[b^4 - \alpha t] - \ln a\right)\right], \tag{17}$$

Integrating this expression between the limits z_o to z and o to t results in

$$z-z_o = \gamma \left\{ a^2 t + 2/3 \frac{(b^4-\alpha t)^{3/2}}{\alpha} - \left(\frac{b^2-a^2}{\ln b/a}\right)\left(\frac{b^4-\alpha t}{4\alpha}\left[\ln(b^4-\alpha t)-1\right]+t\ln a\right) -2/3 \frac{b^6}{\alpha} + \left(\frac{b^2-a^2}{\ln b/a}\right)\left(\frac{b^4}{4\alpha}(\ln b^4-1)\right) \right\}$$ (18)

Substituting for t from Eq. 8, Eq. 18 becomes

$$z-z_o = \frac{\gamma}{\alpha} \left\{ a^2(b^4-r^4) + \frac{2r^6}{3} - \left(\frac{b^2-a^2}{\ln b/a}\right)\left(r^4[\ln r-\tfrac{1}{4}] + [b^4-r^4]\ln a\right) -2/3\,b^6 + \left(\frac{b^2-a^2}{\ln b/a}\right)\left(b^4[\ln b-\tfrac{1}{4}]\right) \right\}$$ (19)

The maximum downstream displacement of the particle occurs when it hits the inner cylinder, i.e., when $r = a$. For this condition, and $b >> a$ such that $b^n-a^n = b^n$, Eq. 19 can be evaluated as

$$(z-z_o)_{max} \doteq \frac{\gamma}{\alpha} \left\{ a^2 b^4 - b^6 \frac{\ln a}{\ln b/a} - 2/3\,b^6 + \frac{b^6}{\ln b/a}(\ln b - \tfrac{1}{4}) \right\}$$ (20)

As an example of the values to be expected from such a system, consider the design parameters of b = .0102 m, a. = .0016 m, v = 10^4 volts, average flow velocity of .05 m/s and a 5.0 μm particle. Using Eq. 13 with v equal .05 m/s, a value of γ = 1.98×10^3 is obtained. Using this figure in evaluating Eq. 20, a value of 2.0 m is obtained as a minimum collector length for 5.0 μm conducting particles entering the system at the outer perimeter. Smaller particles which enter the system closer to the collector electrode will also be captured.

III. Trajectory Analysis, Quadrupole System

The translation and subsequent collection of uncharged particles in an electric field requires that the field be inhomogeneous, i.e., that there exist a strong field gradient in the direction of the field. The coaxial cylinder geometry is one configuration that will perform this task, and is amenable to analysis. A simpler configuration, from the viewpoint of engineering and construction, would be more desirable. One such system might consist of an array of oppositely charged rods or wires aligned with the airflow.

In order to analyze such a system, a sub-set of this array, consisting of four elements was chosen. A system such as this is often referred to as a quadrupole (Fig. 2). The calculations of field and field gradient for this system are readily accomplished in rectangular coordinates. Unfortunately, the resulting differential equations of motion for this system are very complex and coupled, even with the omission of the acceleration (inertial) term.

From the symmetry of the system and the lines of zero potential, one quadrant of this configuration can be isolated for analysis in a circular cylinder coordinate system. However, the resultant equations of motion are expressed in terms of an infinite series in two variables, which are again coupled and would require a numerical rather than an analytical solution.

In order to obtain an analytical solution, the equipotentials in each quadrant are approximated as cylindrical hyperbolas (Fig. 3). The electrostatic potential of such a system may be represented by

$$\Phi_1 = \frac{\Omega}{2}(x^2 - y^2) \tag{21}$$

where Ω represents the strength of the potential, ϕ_1. This equation represents a family of hyperbolas, e.g., for $\Phi = 0$, Eq. 30 may be solved to yield $y = \pm x$, which are the equations of the planes intersecting at the origin. The electric field, E_1, is given by

$$\vec{E}_1 = -\vec{\nabla}\Phi_1 = -\Omega(\hat{i}x - \hat{j}y) \tag{22}$$

where $\hat{i}$ and $\hat{j}$ are unit vectors. The dipole moment of a spherical particle is given by

$$\vec{P} = 4\pi\epsilon_0 \left(\frac{K-1}{K+2}\right) R^3 \vec{E} \doteq 4\pi\epsilon_0 R^3 \vec{E} \tag{23}$$

The approximate expression above is valid for large values of K and for conductors. The force term is now given by

$$\vec{F} = (\vec{P}\cdot\vec{\nabla})\vec{E}_1 = 4\pi\epsilon_0 R^3 \Omega^2 (\hat{i}x + \hat{j}y) \tag{24}$$

which may be summed with the acceleration term and the viscous (Stokes) term to yield

$$4\pi\epsilon_0 R^3\Omega^2(\hat{i}x+\hat{j}y) = 4/3\,\pi\rho R^3(\hat{i}\ddot{x}+\hat{j}\ddot{y}) + \frac{6\pi\eta R}{F}(\hat{i}\dot{x}+\hat{j}\dot{y}) \tag{25}$$

where ρ is the density of the particle, η is the viscosity of the medium (air) and F is the slip correction factor. The single and double dotted variables may be recognized as velocity and acceleration components, respectively. For convenience, let $4\,\pi\epsilon_0 R^3\Omega^2 = C$, $4/3\,\pi\rho R^3 = A$, and $6\,\pi R\,\eta/F = B$. If it is assumed, as for the coaxial cylinder case, that the inertial term is negligible, then

$$C(\hat{i}x+\hat{j}y) = B(\hat{i}\dot{x}+\hat{j}\dot{y}) \tag{26}$$

Solving this differential equation for the appropriate components yield the solutions

$$x = x_0 \, e^{C/B \, t}, y = y_0 \, e^{C/B \, t}$$

(27)

where x_0 and y_0 are the initial coordinates of a particle in the system. Elimination of the time parameter in Eq. (27) results in

$$y = \frac{y_0}{x_0} \, x$$

(28)

where, because of the systems geometry, $0 \leq y_0/x_0 \leq 1$. For a particle initially at the origin i.e., $x_0 = 0$, $y_0 = 0$, no motion will exist, according to Eq. 27. Physically this is because the electric field is zero at this position. Referring back to Eq. 26. the vector $\hat{i}x + \hat{j}y$ and its time derivatives are equal, respectively, to the vector r and its time derivatives. Hence, the general solution to Eq. 26, analogous to Eq. 27, is

$$\vec{r} = \vec{r}_0 \, e^{C/B \, t}$$

(29)

Now, return to the complete equation of radial motion, Eq. 25 which may be written as

$$\ddot{\vec{r}} + B/A \, \dot{\vec{r}} - C/A \, \vec{r} = 0$$

(30)

This may be solved exactly to yield

$$\vec{r} = \vec{r}_{01} \exp\left[-\tfrac{1}{2}\left(B/A - \sqrt{\frac{B^2}{A^2} + \frac{4C}{A}}\right)t\right] + \vec{r}_{02} \exp\left[-\tfrac{1}{2}\left(B/A + \sqrt{\frac{B^2}{A^2} + \frac{4C}{A}}\right)t\right]$$

(31)

It will now be shcwn that for typical values of particle size and density, and a realistic value of potential, that the solution, Eq. 29 is an extremely good approximation, i.e. the contribution of the inertial term is negligible. Letting the potential Φ, be 5 x 10^3 V and the distance from the origin to the vertex of the hyperbolic surface be .01 m, the value of Ω becomes 10^8. For a 1.0 μm particle, the slip correction factor is 1.16. The values of A, B, and C are A = .52x 10^{-15}, B = 14.71 x 10^{-11}, C = 13.90 x 10^{-14}. Referring to the exponentials in Eq. 31, it can be seen that $B^2/A^2 \gg$ 4 C/A, hence, the expansion to first order,

$$\sqrt{\frac{B^2}{A^2} + \frac{4C}{A}} = B/A\sqrt{1 + \frac{4CA}{B^2}} \doteq B/A \left(1 + \frac{2CA}{B}\right)$$

(32)

570

is essentially exact. Substituting this last expression into Eq. 31 results in

$$\dot{r} = \dot{r}_{01} e^{+C/B \, t} + \dot{r}_{02} e^{-(C/B + B/A) \, t} =$$

$$\dot{r}_{01} e^{.00095 \, t} + \dot{r}_{02} e^{-(.00095 + 2.8 \times 10^5) t} \tag{33}$$

The second term in the above damps out almost instantaneously. The factor 2.8×10^5 is the reciprocal of the relaxation time for a 1.0 μm particle. The first term of Eq. 33 is identical to Eq. 29, hence, steady state motion may be described by an abridged differential equation of motion such as Eq. 26.

The trajectory calculation is now continued from the hyperbolic surface to a physical rod of radius a which is the actual element of the quadrupole field. In order to locate the position of this rod, the radius of curvature of the hyperbola, at its vertex, must be calculated. The radius of curvature, G, is defined by[2]

$$G = \frac{[1 + (dy/dx)^2]^{3/2}}{|d^2y/dx^2|} \tag{34}$$

Solving Eq. 21 for y^2 yields

$$y^2 = x^2 - \frac{2\Phi_1}{\Omega} \tag{35}$$

The required derivatives are

$$\left(\frac{dy}{dx}\right)^2 = \frac{x^2}{x^2 - \frac{2\Phi_1}{\Omega}} \quad \text{and} \quad \frac{d^2y}{dx^2} = \left(x^2 - \frac{2\Phi_1}{\Omega}\right)^{-1/2} - x^2 \left(x^2 - \frac{2\Phi_1}{\Omega}\right)^{-3/2} \tag{36}$$

Substitution of these expressions in Eq. 34 result in

$$G = \frac{[y^2 + x^2]^{3/2}}{|y^2 - x^2|} \tag{37}$$

which evaluated at x = b, y = 0, yields

$$G(b,o) = b \tag{38}$$

hence locating the cylindrical electrode at a distance 2b from the origin.

For the remainder of the trajectory calculation it is assumed that the electrostatic field between the rod at 2b and the hyperbolic

potential surface at b can be described by a field produced by coaxial cylinders. If Φ_1 is the potential of the outer cylinder (hyperbolic surface) of radius b, and Φ_2 is the potential of the rod of radius a, then the electric field, E_c between them is given by

$$\vec{E}_c = \frac{-(\Phi_2 - \Phi_1)}{\ln b/a} \frac{\hat{r}_c}{r_c}$$

(39)

where r_c is the radial distance between the two cylinders and $\hat{r}_c$ is the corresponding unit radius vector. Invoking continuity of the normal components of the displacement vector, $\varepsilon_0 E$, between the two regions separated by the hyperbolic surface requires that

$$|\vec{E}|_{x=b,y=0} = |E_c|_{r_c = b}$$

(40)

Evaluating Eqs. 22 and 39 in this fashion leads to

$$-\Omega b = \frac{-(\Phi_2 - \Phi_1)}{b \ln b/a}$$

(41)

or

$$\Phi_2 = \Phi_1 + \Omega b^2 \ln b/a$$

(42)

which determines the potential at the rod. The calculation for the radial component of this part of the trajectory is essentially that given in Eq. 6 with $r^4 = 0$, i.e.,

$$\tau_2 = \frac{3\eta \ln^2 b/a}{8 f R \varepsilon_0 (\Phi_2 - \Phi_1)^2} b^4$$

(43)

where τ_2 is the time required for the particle to go from the hyperbolic surface to the collector rod. Using Eq. 42 to substitute for $\Phi_2 - \Phi_1$ yields

$$\tau_2 = \frac{3\eta}{8 F R^2 \varepsilon_0 \Omega^2}$$

(44)

The time required to traverse the first portion of the trajectory is, from Eq. 29 or 33 ,

$$\tau_1 = B/C \ln r/r_c$$

(45)

For a hypothetical case of the quadrupoles arranged on a 2-cm radius bolt circle, opposite poles charged to plus and minus 10KV, the sum of T_1 and T_2 yields a radial transit time, for an initial position 1mm from the center of the bolt circle, which is comparable to the concentric cylinder configuration of radii 2 cm and .1 cm. The deciding factors which favor the cylindrical configuration are the absence of a null interaction region and a voltage difference only half that of the quadrupole case. The airflow profile is also much less favorable for the quadrupole case in that the highest velocity occurs in the weakest interaction region, hence requiring a longer flow distance, i.e., a longer collecting configuration.

Consideration of the relative merits of the two types of electrode configurations leads to the conclusion that the coaxial cylinder geometry is more efficient.

IV. Preliminary Experimental Results

Figure 4 schematically displays the very low velocity laboratory scale coaxial inhomogeneous electric field apparatus initially designed to confirm the theoretical development of part II. Monodisperse PSL aerosol dispersed by a Lovelace generator is sent through a Kr^{85} aerosol charge neutralizer. A charged particle precollector composed of two parallel plates .30 m x .06 m with .015 m spacing was constructed to filter out charged particles not neutralized by the Kr^{85} neutralizer. A coating of silicon oil was used on these plates to enhance their retentivity. After leaving the precollector, the aerosol is introduced into a second, smaller precollector (.19 x .13 x .015 m) housed in a box which has as one of its sides a HEPA filter to allow pressure within the box to stay at the ambient value. The aerosol within the box is drawn in through the outer annular region of the inhomogeneous field collector. This outer annulus serves to define the initial conditions so that a monodisperse aerosol will be localized on the .63m collector rod. Detection of particles was with a single particle laser spectrometer.

The design airflow turned out to be too low to introduce a significant amount of aerosol into the system, so the average flow velocity was increased to .05 m/s. This, coupled with the fact that the spectrometer was limited to an upper size of 2.9 μm restricted particle size to standard 2.01 μm PSL particles. Although very little loss in transmission was anticipated, 100% collection was obtained at 8KV, as shown in Fig. 5. In order to determine if a large population of charged particles still existed, the precollectors were deactivated. This resulted in only a 25% increase in total population but resulted in an almost identical penetration curve as illustrated in Fig. 5.

If a Boltzman distribution for the charge is assumed, 10% of the particles have zero charge, and 9% have one charge of + 1 and -1. Singly charged particles should still be capable of getting through the collector. The results of an approximate calculation of the collection efficiency, pre-supposing this distribution, is shown by the solid line in Fig. 5.

A calculation was performed assuming that the particles drawn into the drift tube immediately migrated to a position midway between

the tube and collector. These results also indicated that the uncharged particles would not be collected. The possibility of corona charging from the collector was discarded by using a radio to detect corona discharge. The current flow was also monitored with a microammeter.

Various coatings were applied to the collector to enhance the sticking of particles. Substances used were silicon oil, silicon grease, apiezon grease, glycol, and water. All but the latter two had no effect on the transmission curve. Water and glycol produced zero penetration at 6 to 7 KV not only for 2 μm particles but all the way down the spectrum to .1 μm particles (penetration <1%). The collection was accompanied by corona. Visual examination of the apparatus disclosed aerosol on the interior of the drift tube. In the case of glycol, the glycol was also found in the drift tube. The mechanism appears to be that of electrostatic spraying of the medium coating the collector electrode. The droplets thus formed would be expected to be highly charged and thus attracted to the drift tube. During their traverse, they inter-act with the aerosol particle so that the system of particle and droplet are deposited on the surface of the drift tube.

A typical transmission plot for a mixture of 2.0, 1.0 and .53 μm particles, collector coated with glycol, is shown in Fig. 6.

V. Future Work

A two meter precollector and 3 meter drift tube have been constructed for further investigation of both neutral particle collection and the electrostatic spraying phenomenon. At present, the latter method appears to be a much more efficient air cleaner but suffers from collection taking place on the drift tube rather than being localized on a small center electrode which can be more readily cleaned.
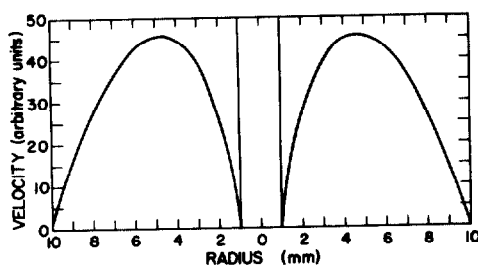
Fig. 1.

Coaxial Cylinder Flow Profile.
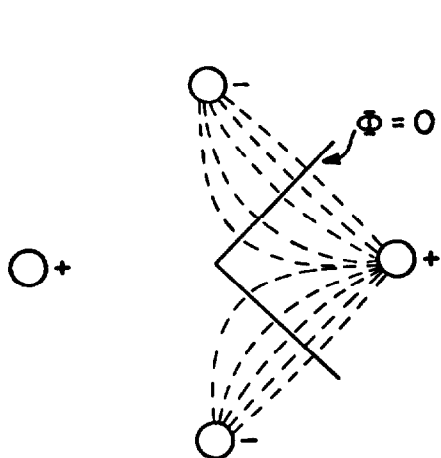
Fig. 2.

Electric Quadrupole Showing
Equipotentials and Field Lines.
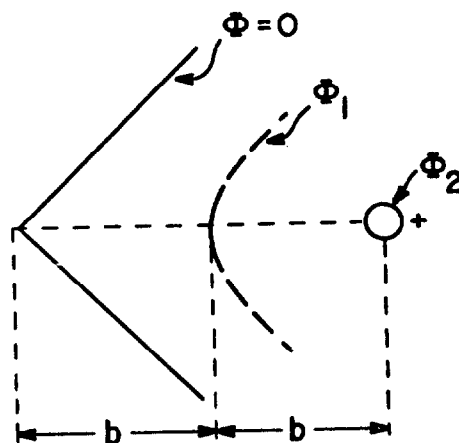
Fig. 3.

Approximate Quadrupole.

INHOMOGENEOUS ELECTRIC FIELD AIR CLEANER
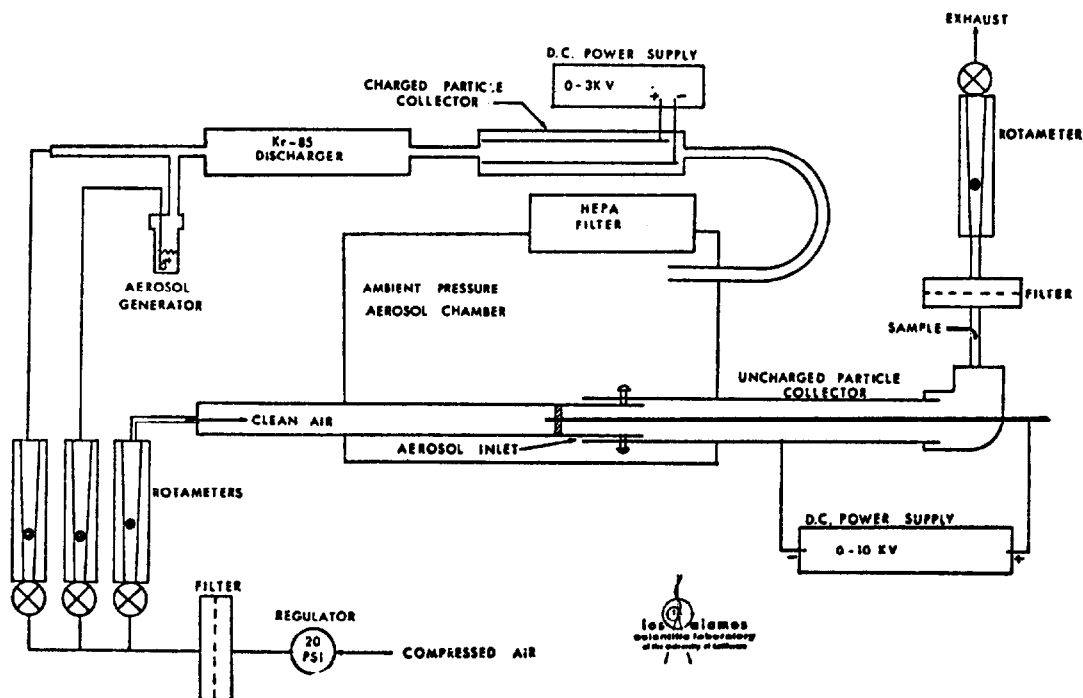
Fig. 4.

Inhomogeneous Field Apparatus.
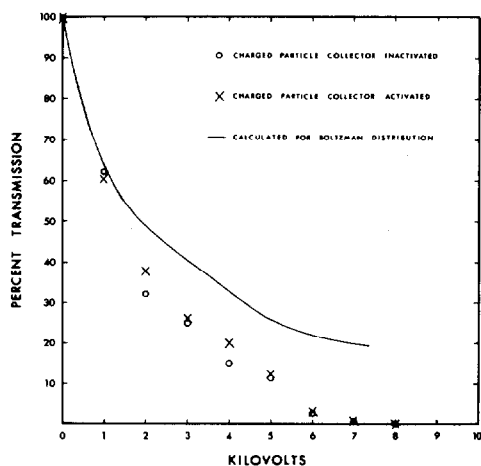
Fig. 5.

Aerosol Transmission as a
Function of Applied Voltage.
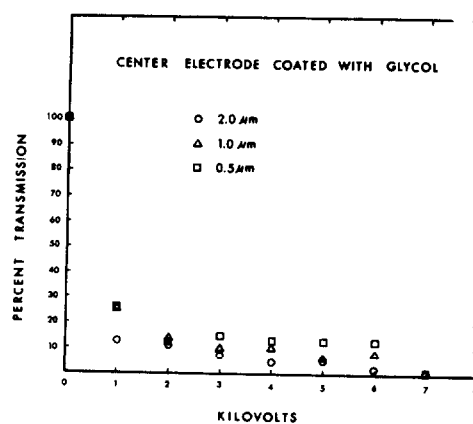
Fig. 6.

Aerosol Transmission as a
Function of Applied Voltage.

References – Inhomogeneous Field

1. Georg Joos, <u>Theoretical Physics</u>, 2nd edition, Hafner Publishing Co., New York, 1950, P.P. 212-213.

2. R.R. Middlemiss, <u>Differential and Integral Calculus</u>, McGraw-Hill Book Company, Inc., New York and London, 1946, P.129.

DISCUSSION

<u>HINDS:</u>   Would you comment on how this system would perform with dielectric particles and conductive particles?

<u>SCHUSTER:</u>   The dielectric particles will need a longer path length. The force is maximized when we have a conducting particle. The force on the particle decreases by the ratio of K-1/K+2. Typically, very small particles have some reasonable conductivity and I think that the ratio of K-1/K+2 will always be greater than one half.

<u>RIVERS:</u>   I can't discover in your paper what your efficiency determination method is.

<u>SCHUSTER:</u>   The velocity for that particular device is 300 centimeters per minute. It's not particularly fast. The particle sizes used were two μm polystyrene latex. Although my calculation isn't really an efficiency calculation, it can easily be transformed into one. I have taken the worst case, where the particle enters at the very outer boundary. The closer the particles enter to the central collector, the more efficiently they will be collected. If you get very close to the central collector, you can collect a tenth of a micron particle in the same length of system.

<u>RIVERS:</u>   What was your experimental method of measuring efficiencies?

<u>SCHUSTER:</u>   We measured efficiency by transmission, as we use the single particle detector that I described earlier to look at the particles going through, initially, without any potential, and then we vary the potential difference or velocity, as the case might be, and look at the transmission. We have all of the particles going through the single particle counter, which provides the flow for the system.

<u>RIVERS:</u>   I would be interested in some sort of weight measurement, such as using membrane filters, to determine the overall efficiency of this unit by an alternate technique. Our experience would indicate the efficiencies you obtained are very high for operating conditions given.

<u>SCHUSTER:</u>   Have you tried the configuration in your laboratory?

<u>RIVERS:</u>   Very similar things.

THE ELECTROSTATIC CAPTURE OF SUBMICRON PARTICLES

IN FIBER BEDS*

D. L. Reid and L. M. Browne
Battelle
Pacific Northwest Laboratories
Richland, Washington

Abstract

The emission of submicron sized particles is the most difficult to effectively control with current state-of-the-art technology. Experiments at Battelle-Northwest led to the discovery that charged particles could be efficiently captured by a thick fiber bed having a high bed-volume to fiber-volume ratio and a very low pressure drop. Interim results are presented for the removal efficiency as a function of particle resistivity, superficial gas velocity, bed depth and aerosol concentration. In general, for bed pressure drops less than 0.5 in H_2O efficiencies greater than 90 percent were obtained at 300 ft/min ($\sim$152 cms/sec) face velocity over the particle size range of 0.06-0.7 μm AMD and a particle resistivity range of 10^8 – 10^{12} ohm-cm. The most important variable was the bed face velocity with the collection efficiency varying inversely with velocity. The bed depth and volume void fraction were other significant variables bearing on the efficiency of the system.

Emperical equations indicate a 100 percent collection efficiency might be attainable near or somewhat below a bed face velocity of 50 ft/min ($\sim$25 cms/sec). However, a more sensitive measurement method would be required for experimental confirmation.

Introduction

The cost/benefit ratio for the control of particulate emissions has increased significantly with the decreasing control limits and for the more resistant submicron particulates there is a large imbalance which will probably increase as attention becomes focused on the submicron species once the "boulders" are under control. Consequently, there is a great need for control technology that will meet the atmospheric disposal limits and yet have a marked influence on lowering both the capital investment and operating expense. It is recognized by all that as the particle resistivity increases and the size decreases, the efficiency of the electrostatic precipitator (ESP) is significantly degraded. The trend to burn Western low sulfur coal to reduce the sulfur emission has initiated a large effort in gas-particle conditioning in an effort to offset the ESP loss of

-----

efficiency due to the higher particle resistivity. Present-day mechanical devices control the "rocks" reasonably well but are found wanting for the smaller submicron particulates. Bag filters are the most effective present technology for filtration of submicron particulates, but have a very significant drawback in the limited face velocity and high pressure drop. Consequently, for high volume discharge gases the filter area required is extremely large producing high capital and operating costs. The problem initiated a myriad of research programs aimed at improving or developing a system or device to meet the emission standards and somewhat secondarily for more economically controlling emissions. A significant portion of the work was oriented toward the use of electrical charges or electrical properties for enhancement of filtration efficiencies. The novel concept described utilizes the electrostatic properties of particles and fibers of high dielectric strength to effectively remove submicron and other particulates from waste or process gas streams.

Background

During the course of experiments based on charged water spray-droplet scrubbing, it was discovered that a dry demister pad of a non-conducting fiber was acting as an effective filter for submicron particulates of unipolar charge and produced significantly greater efficiencies than observed for the charged particle-charged spray drop tests. This observation, by A. K. Postma and W. K. Winegardner,* initiated a few confirmatory tests that reduced the phenomenon to practice and led to an Environmental Protection Agency (EPA)** grant to explore the boundary conditions of the variables thought to be of importance. Funding was later obtained from the Battelle Energy Program office (BEP) for a phase of the work specifically directed toward fly ash and for continued mathematical modeling of the observed phenomenon.

Availability and cost of a new system dictated the use of the spray-drop system for the initial parametric tests. The variability of the data and unexplained observations highlighted the inadequacies of the system for the more refined tests addressing parametric boundary conditions. However, the data were sufficiently encouraging to warrant a new wind tunnel that would provide a unidirectional, constant velocity flow between the principal sampling points. This discussion of interim information relates, principally, to the experimental data obtained with the new wind tunnel and addresses only the interim experimental tests assigned to the EPA grant program.

The mathematical modeling of the phenomenon by D. L. Lessor (BNW) is too extensive for this discussion and will be issued in detail at a later date. At this point in time, a logical equation-of-state has been developed but an equation providing apriori predictions is not yet completed.

-----

* Patent pending.

** Work performed under EPA Grant No. R-801581-02-2.

Methods of Approach

The collection mechanism involves the deposition of charged particles by self-induced electric fields within a bed of electrically non-conducting fibers. Since the electrical field in the bed is induced by molecular ion or charged particle deposition, efficient operation of the system depends on the development of electrical fields of the same polarity sufficient to overcome the coulombic repulsion of the fiber within times smaller than the residence time of the particle within the bed. From this criteria, the following variables might be expected to play an important role:

Particle Size –   influences mobility

Air Velocity –   residence time of particles in the vicinity of a fiber

Pad Resistivity –   charge leakage rate and field strengths and distribution

Pad Thickness –   target area residence time

Dust Surface Coverage –   flow geometry, charge leakage rate

Particle Resistivity –   charge leakage for continuous coating and particle charge level

Charge Level of Particles –   mobility of particles in field

Total Charge Interception Rate –   maximum field in bed due to particle deposition

Fiber Density –   mean free path between particle and fiber -- localized residence time

Humidity –   influence on bed conductivity for hygroscopic particles

A complete block experimental plan involving the ten parameters listed would require more than a practical number of tests for proof of the concept. Therefore the program was designed to explore ranges of most of the variables listed. The boundary conditions of the parameters to be explored included the following:

Particle Size – not to be considered a prime variable. All tests will involve submicron particles near the 0.1 to 0.3 μm size range, which corresponds to minimum mobility and maximum challenge to the system. The removal efficiency would be expected to be higher for particles above 1 μm.

Air Velocity – to be varied from 50 to 400 ft/min (∿25 to 200 cms/sec) superficial bed velocity.

Pad Resistivity – Available demisters of stainless steel, polypropylene and teflon will be used. The stainless steel will show the effect of pad conductivity. Teflon fibers would allow operation at temperatures near 300°F and should be examined for application.

Pad Thickness - Thickness of 3, 6 and 12 in. beds will be tested for comparative efficiencies.

Particle Resistivity - Highly important, generation of particles having resistivities of 10^7, 10^9, 10^{11} ohm-cm will be sought -- the highest resistivity reflecting a severe challenge to electrostatic precipitators.

Particle Charge Level - not considered as a primary parameter for study at this time. Saturation or near saturation charge appears advantageous and the charger will be operated at a voltage to produce same.

Dust Loading - Particle concentrations will be varied from 10 to 100 milligrams per cubic meter.

The data for each experiment included the removal efficiency, pressure drop, relative humidity, air flow rate, and dust loading. The particle size and particle resistivity was determined for each generating condition thought to alter these characteristic properties of the particle. The electrical properties of the bed, e.g. field charge level, would be dependent primarily on charge deposition and leakage rate through some finite resistance for the ungrounded bed. Consequently, some indication of the relative field charge level and distribution within the bed was obtained during "steady state" conditions by inference from current measurements. These measurements were considered as important input for support of a mathematical model and possibly desirable for scaleup with a design engineering model.

Experimental Equipment

The initial investigation of the observed phenomenon was conducted in the available charged spray-drop test apparatus which experimentally left much to be desired for the more definitive parametric study attempting to define the influencing variables and the related boundary conditions. A new wind tunnel system was designed to provide a unidirectional uniform velocity from particle generation point to the last downstream sampling point.

Test System

Figure 1 is a schematic drawing of the system which consists of a 7 foot long 24 in. diameter pipe, a short corona charging section with an effective cross-sectional charging area equal to that of the duct, a 3 foot long section between the charger and fiber bed to preclude any direct field charge effects from the charge section, and a bed frame for the knitted fiber mats. The inlets and outlets to the bed were 24 in. diameter. The bed dimension was made 28 in. x 28 in. to extend the experimental run time before edge leakage became the predominant source of downstream particles. The frame was made with lucite and was electrically isolated from the rest of the system as was the charging section. The system was built in sections for future alteration of configurations and distances between principal components and was held together with electrically
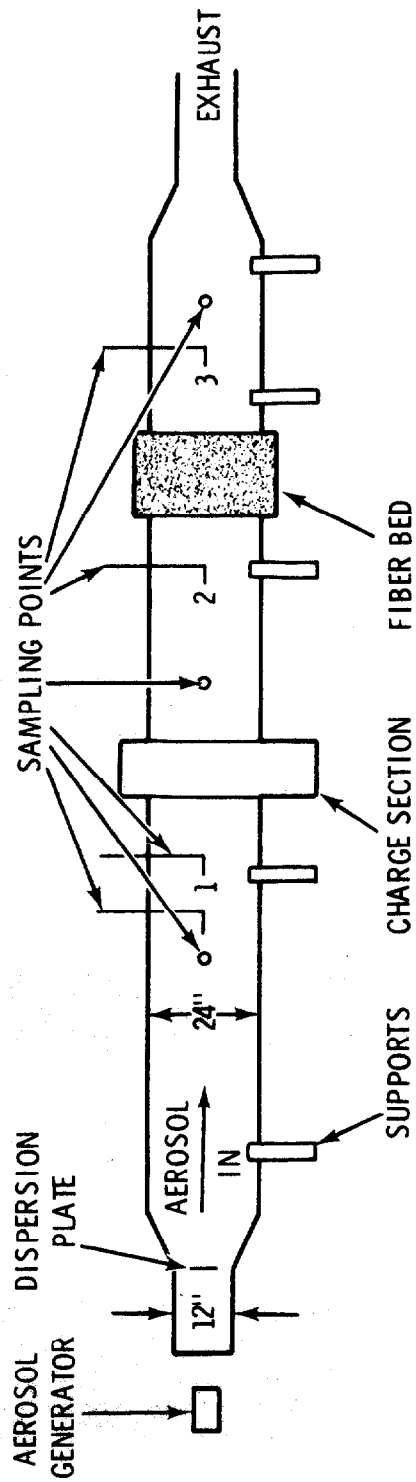
FIGURE 1 Wind Tunnel Schematic

insulated external straps. A dispersion plate was placed in the 12 in. diameter inlet at the transition point to produce the required uniform velocity profile at the three principal sampling points at positions 1, 2 and 3.

Corona Charging Section

The charging section was designed for rather easy alteration of the electrode-to-ground spacing to vary the particle deposition on the ground rods. Half-inch diameter rods rather than plates were used for the ground in an effort to reduce deposition, to minimize the sparkover rate late in the runs and to extend run time without particle charging degradation. The effective field depth of about 15 cms gave a particle residence time of about 100 milliseconds at 300 ft/min (∿150 cms/sec) face velocity - more than adequate to reach near saturation charge.

Fiber Bed Section

The frame holding the fiber bed was made of 1/2 in. thick lucite for visibility and for its high dielectric properties. The bed surface area extended 2 in. beyond the duct diameter to eliminate early edge leakage along the framing where the fiber density is at a minimum as was observed in experiments using the spray-drop test system. This apparently delayed leakage until a significant load had accumulated on the front face and the increase in the pressure drop diverted some particles to the region of a lower pressure drop. From visual observation this edge leakage, which was accentuated by the support wires, appeared to lower the efficiencies for some of the last tests in a run series just prior to bed cleaning. The observed "frame" leakage is strictly a function of the experimental bed construction and could be designed out of a bed made specifically for electrostatic filtration. Also, under industrial applications the bed would normally be cleaned before the pressure drop increased sufficiently to alter the flow pattern and increase the velocity through a much smaller bed fraction.

The bed was supported within the frame by a teflon coated wire grid with about a 4 in. wire spacing. The used demister pads were disassembled and the individual knitted mats layered into the supporting frame. Since the maximum width of the mats was about 14 in., alternate layers were juxtapositioned at 90° angles to each other to preclude gaps or any major lower density regions that might "short circuit" the bed. This method of forming the bed also provided a means for varying the void volume fraction -- that space unoccupied by fibers.

Experimental Conditions

Fiber Bed Void Fraction

The void fraction of the fiber bed was defined as that volume of the bed not occupied by the fiber volume and was determined from the bulk weight of the fiber mats, density of the fiber per unit length and the fiber diameter. For this series of tests the 6 in.

bed was packed to a void fraction (VF) of ~0.96. For the 12 in. bed, the flow direction of the frame was reversed and the first 6 in. then packed to a VF of ~0.975. The lower fiber density was used in the first 6 in. to increase particle penetration depth and increase the load to bed-pressure-drop ratio. The lower density in the first 6 in. accomplished both goals, but appeared to be detrimental with respect to efficiencies in the later stages of a continuous run series and to the length of operating time before breakthrough. This was true particularly for MgO which normally showed a greater penetration depth than NH_4Cl or Na_2O. Breakthrough of the bed is defined as the appearance of agglomerates on the sample downstream from the fiber bed which were not observed in the previous samples. A conducting copper wire surrounded the fiber bed and small screens were placed on the front and back faces to intermittently measure the current to ground as an indication of the bed electrical conditions during operation.

Particle Generation and Characteristics

Three particles were used in this series of experiments to highlight any change in efficiency with particle resistivity -- namely ammonium chloride, magnesium oxide and sodium oxide. The NH_4Cl particle was generated by air sparging of HCl and NH_4OH solutions with interception of the gas streams at the inlet to the system. The particle generation rate was controlled by varying both the concentration of the solutions and the sparge air flowrate. The MgO and Na_2O particles were generated by metal vaporization and oxidation. The metal was heated inductively in an enclosed boat. An inert gas forced the metal vapors out the end of the tube where ignition to the oxide occurred. The generation rate was controlled principally by the temperature but also to a small degree by the inert gas flow. It was found that the aerodynamic mean diameter (AMD) was rather simply altered by varying the flow rate of the inert carrier gas. No special attempts were made to obtain a specific particle size or develop a technique for generating a monodisperse aerosol since this was not a specific part of the program. Since the technique was available for varying the particle size, some tests were made with MgO particles having an AMD of less than 0.1 µm.

An eight-stage Anderson sampler was inserted upstream of the charge section to obtain the aerodynamic mean diameter for each generation in which the conditions were altered. It should be recognized that the last stage of the available sampler had an effective cutoff diameter of about 0.4 µm for the isokinetic flow conditions. Since about 90 percent of the particle mass was collected on the filter, extrapolation of a log normal plot to obtain the AMD was a questionable practice although it was the only approach available at the time. Consequently, the stated AMD's are thought to be high. The apparent particle sizes and particle properties, shown in Table I, are the predominant observations for all generations. The mass median diameter (MMD) was calculated assuming a unit particle density and is related to the AMD by $MMD = \dfrac{AMD}{\sqrt{\rho}}$ where ρ is the particle density.

TABLE I
PARTICLE PROPERTIES OF GENERATED AEROSOLS

Particle	AMD in Microns	MMD in Microns	Resistivity in Ohm-Cm
NH_4Cl	0.25, 0.38	0.16-0.24	$\sim 10^8$
Na_2O	0.25, 0.3, 0.4, 0.6, 0.7	0.17-0.56	$\sim 10^{10}$
MgO	0.06, 0.1, 0.15, 0.25	0.03-0.13	$\sim 10^{12}$

Sampling

Mass samples were collected upstream of the corona charger and upstream and downstream of the fiber bed with the time increased as the rate of generation decreased. Millipore filters (0.65 μ pore size) were satisfactory for NH_4Cl and lower mass/unit-of-time generations for Na_2O and MgO. Fiber glass filters were required for the higher particle concentration tests of Na_2O and MgO to avoid changing the pressure drop across the calibrated flowmeters and to prevent sampling flow reduction or premature plugging of the filter.

The weight increase of the filter without particle generation, balance sensitivity (±0.02 mg) and high filtration efficiency of the fiber bed prevented efficiency measurements at 50 ft/min face velocity and limited the maximum efficiency that could be determined at 100 ft/min to ~ 99.9 and ~ 99.6 percent for 100 mg/M^3 and 25 mg/M^3 concentrations without extensively increasing each test period. The weight gain of the filter was determined by sampling the tunnel air with charger on using double millipore filters. The top filter was tossed and the bottom filter weighed before and after desiccation at room temperature for up to four hours. The average weight gain was 0.02 mg and was not altered by drying in the desiccator. This suggested that bound moisture was creating the weight bias. The fiber glass filters created an opposite problem since some sloughing off or loss of fibers generally resulted when removing the paper from the holder. This weight loss was reduced from about 0.15 mg to 0.04 mg by carefully brushing off the edges of the paper before weighing and inserting into the sampler. However, since these were used only for the higher flow rates at high air loadings, the fractional influence on the efficiency was around .002.

Test Procedure

The aerosol generator was started along with the elapsed generation timer and brought up to the desired generation rate as quickly as possible, the conditions for which had been previously, roughly established. Samples were collected at three points; namely, (1) upstream of the charger, (2) between the charger and bed and (3) downstream of the bed. The average volume flow rates and superficial bed velocities for any setting were based on pitot tube profiles of the duct at the flow rates of interest. Velocity profiles

at the three sampling points were not significantly different. Consequently, the same sampling flow rate was used for the three mass sampling points. The high particle and field charges at the second sampling point produced some odd results that defied interpretation and precluded the use of the data for determining the bed efficiency. For example, indicated bed efficiencies were 10 and 92 percent for two successive runs under identical conditions with both showing about 98 percent total efficiency. Consequently, the results reported are for the total efficiency of the system. More recent tests have shown a marked improvement in the comparative bed and system efficiencies -- within 1 to 2 percent with some being identical. The only change made to the system for these tests was an increase in the distance between the electrodes and ground rods of the charger which reduced the current to one-half of that observed with the original configuration. This further indicated the problem was associated with sampling in a high electrical field since a major reduction in the field downstream of the charger ameliorated the discrepancies markedly.

Generally, sampling was continuous until the end of the day or until apparent breakthrough (whichever came first) except during adjustment of generation rate and flow. Low aerosol concentration runs generally required two days of operation. When this occurred, the system was shut down over night. Prior to particle generation the second day, the charger was turned on to impose a field charge on the bed and a reentrainment test made at 300 ft/min flow ($\sim$150 cms/sec). There were no apparent degrading effects even though the bed charge was at zero over night. For a series of measurements, the flow rate was varied from low to high and back to low or in the reverse order. Generally, two consecutive measurements were made before changing the flow and/or concentration.

It should be recognized that the collection efficiencies noted were based on mass measurements for submicron particles and comparative efficiencies would be expected to be higher for aerosols having a mass median diameter greater than 1 μm.

Results and Discussion

Six Inch Thick Polypropylene Bed- NH_4Cl and Na_2O

The void fraction for this bed was approximately 0.96. Figure 2 shows the average efficiency as a function of velocity as well as the sample 2σ limits. For both, the efficiency up to 200 ft/min ($\sim$100 cms/sec) filter face velocity is approximately linear and then appears to change to some other function or to a linear function with a different slope. Sufficient data are not available to describe the point of change and relationship between 200-300 ft/min ($\sim$100-150 cms/sec). The single NH_4Cl measurement at 250 ft/min (125 cms/sec) was the last measurement taken before bed cleaning and is thought to be low due to observed breakthrough which, from visual observation, was assigned to migration of the particles along the lucite frame. This short circuiting was observed only after the pressure drop increase in the original flow regime of the bed diverted some of the flow to the outer edges. The supporting wire grid

work appeared to accentuate the diversion of particles to the bed fringes as evidenced by the predominant earlier particle migration along the wires. This leakage along the bed frame would be eliminated with a fiber bed designed for this specific application. The equations developed from a linear regression fit of the data, 200 ft/min (∿100 cms/sec) velocity and below, are shown in Table II and represented by the solid line in Figure 2. These equations also indicate an efficiency of 100 percent might be expected at a face velocity below 50 ft/min (∿25 cms/sec).

The total efficiency measured for Na_2O was significantly lower than that for NH_4Cl which has a lower resistivity than Na_2O. Since this was contradictory to the developed theory which predicts a decreasing efficiency with decreasing particle resistivity due to a lower space charge, an investigation was initiated to shed some light on the observation. During examination of all operating data it was noted that the current flow in the charger during this series of measurements increased with time and was uncharacteristically very high during the last few measurements at 200 and 300 ft/min (∿100 and 150 cms/sec). Examination of the charging section showed that a buildup of Na_2O on the terminal weights of the electrodes, which were nearly touching the ground rods, created a more conductive path to ground through absorption of moisture and subsequent formation of the more conducting NaOH. Thus this effectively reduced the corona field and apparently the particle charging efficiency resulting in an anomalous low system efficiency at least near the end of the series. Another indicator of this problem was the necessity to reduce the power supply voltage gradually with time to prevent automatic cutoff by the power supply current limit switch. The moral of this sequel is to never use Na_2O particles at high air humidity (>40 percent) when the electrode weights are in close proximity to an electrical ground that produces a direct short -- principally a geometric design problem.

Twelve-Inch Thick Polypropylene Filters

The first 6 in. of this bed were packed to a void fraction of 0.975 with the last 6 in. at ∿0.96 principally to extend the run time for NH_4Cl aerosols of the higher concentrations. Since there was no discernable effect of particle concentration on system efficiency over the range of 6-148 mg/M^3, only higher concentrations were used in this series of tests in an effort to reduce the run time and maintain reasonable reproducibility. This was accomplished to some degree but again sensitivity of the measurements produced a higher variability than desired. However, the frequency of unexplained "fliers" was significantly lower.

The efficiency for NH_4Cl, MgO and Na_2O is plotted against flow rate in Figure 3. As shown by the least squares fit curves, the efficiency decreased linearly with increasing velocity at least up to 300 ft/min (∿150 cms/sec) rate -- the maximum flow attainable with the present system. The Na_2O data points are the average of all measurements at a single velocity. The 95 percent confidence limits are also shown. The MgO and NH_4Cl data are duplicate measurements. Consequently, all data are plotted and no limits shown.

FIGURE 2
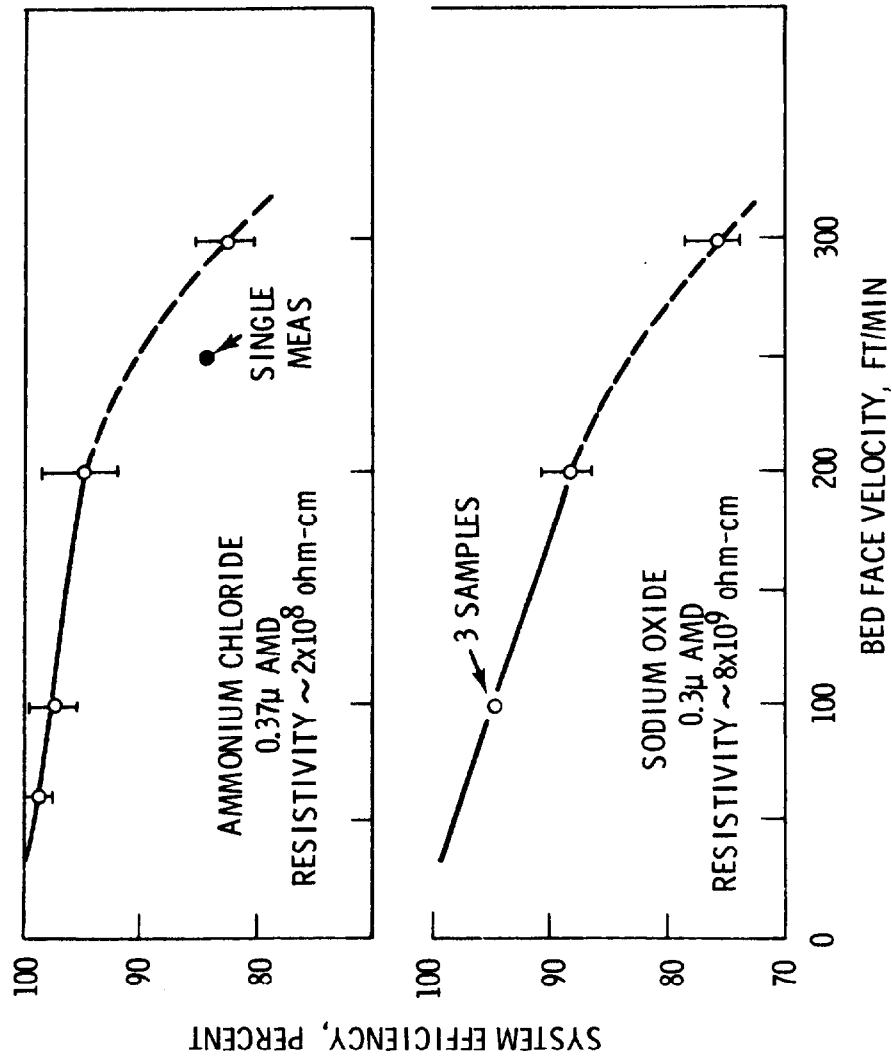
SYSTEM EFFICIENCY VS FLOWRATE
6" POLYPROPYLENE BED
0.96 VOID FRACTION
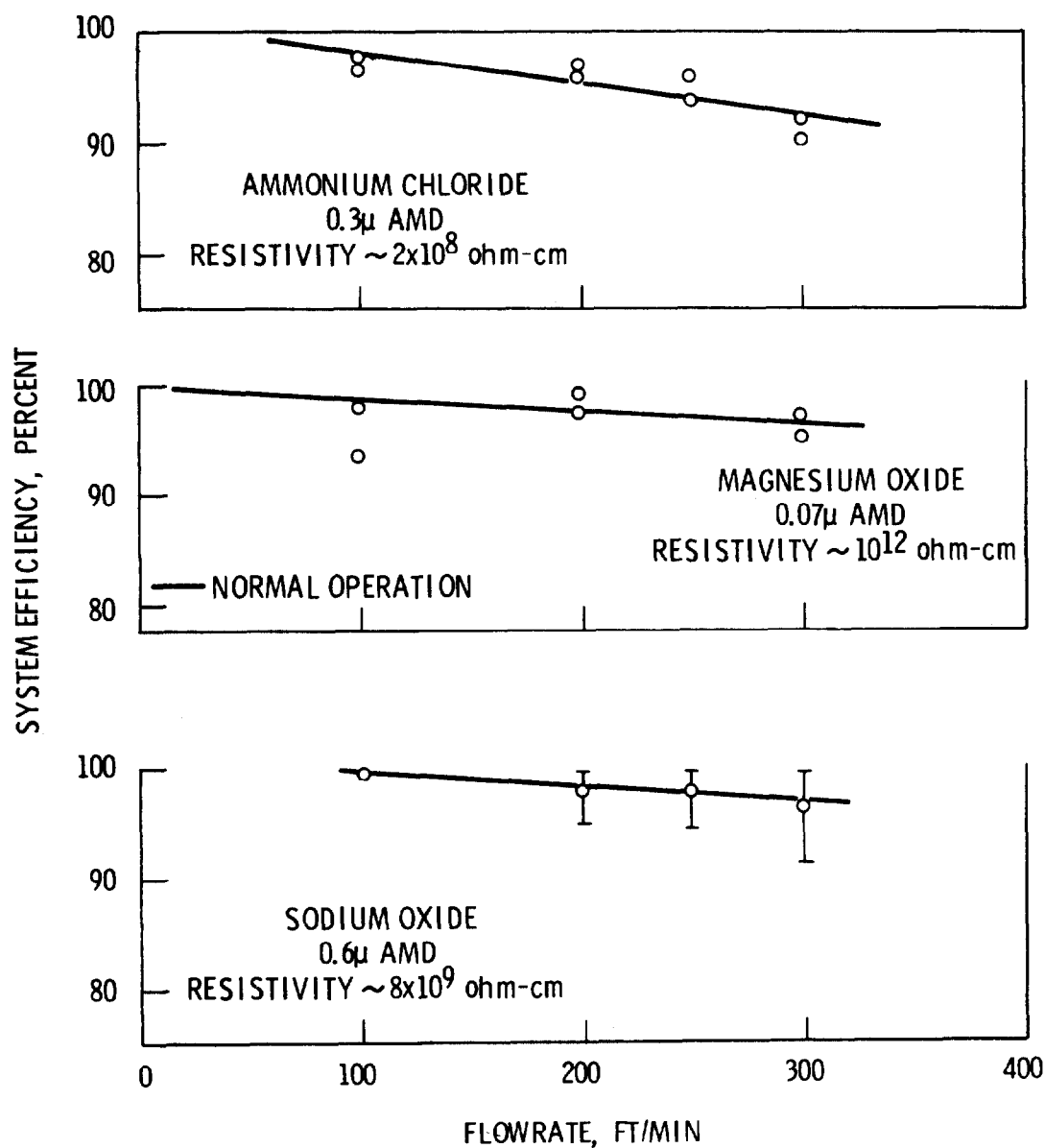
SYSTEM EFFICIENCY VS FLOWRATE
12" THICK POLYPROPYLENE
GRADED BED VOID FRACTION

FIGURE 3

The low point at 100 ft/min ($\sim$50 cms/sec) for MgO appears to be one of those "fliers" that occur now and then without any apparent explainable reason. However, with a statistically significant number of tests, these generally fall out as "outliers". Consequently, it was not used in the linear regression analysis. Although this value was not used, the data indicate an efficiency less than 100 percent at zero flow -- not very probable. This suggested that these last two measurements in the run series at 100 ft/min ($\sim$50 cms/sec) flow were probably on the low side.

The average efficiency for NH_4Cl was lower than that of MgO or Na_2O by about 2 to 5 percent over the range of 100-300 ft/min ($\sim$50-150 cms/sec) face velocity. This is the first data that might confirm the model's prediction that efficiency should decrease with decreasing resistivity. Since the bulk of the data does not indicate a like trend, final judgment is reserved until a statistically significant number of measurements are completed. Also bearing on the reservation is the lack of any discernable difference in the bed field charge, inferred from current measurements, between the three aerosols used. Thus, it is not unlikely that significantly lower efficiencies would be observed only for a much more conducting particle and the threshold for this effect would occur at a lower resistivity than the 10^8 ohm-cm of NH_4Cl. The linear equations for the lines, Figure 3, are shown in Table II. All equations, except that for MgO, indicate 100 percent efficiency will be attained at some velocity lower than 50 ft/min ($\sim$25 cms/sec).

TABLE II

EMPERICAL EQUATIONS OF EFFICIENCY

Particle	6" Bed – <200 ft/min	12" Bed – <300 ft/min
Na_2O	$E = 101.5 - 0.065V$	$E = 100.91 - 0.0116V$
MgO		$E = 99.8 - 0.0116V$
NH_4Cl	$E = 100.513 - 0.028V$	$E = 101.286 - 0.0283V$

Where E = Efficiency in Percent and,
       V = Superficial Bed Velocity – ft/min.

Aerosol Decontamination Factor

The calculated decontamination factors for both the 6 in. and 12 in. beds are plotted as a function of velocity in Figure 4. The data approximate the expected relationship with the log of the decontamination factor varying linearly with the power of the velocity. For the 6 in. bed, all data were considered to be from the same population for the least squares fit which is represented by the solid line. This appears to be a reasonable assumption since the coefficient of determination was 0.9 and all data fell within the 2σ limits of sampling and measurement errors. Consequently, the fitted equation probably represents a reasonable average for the experimental conditions.
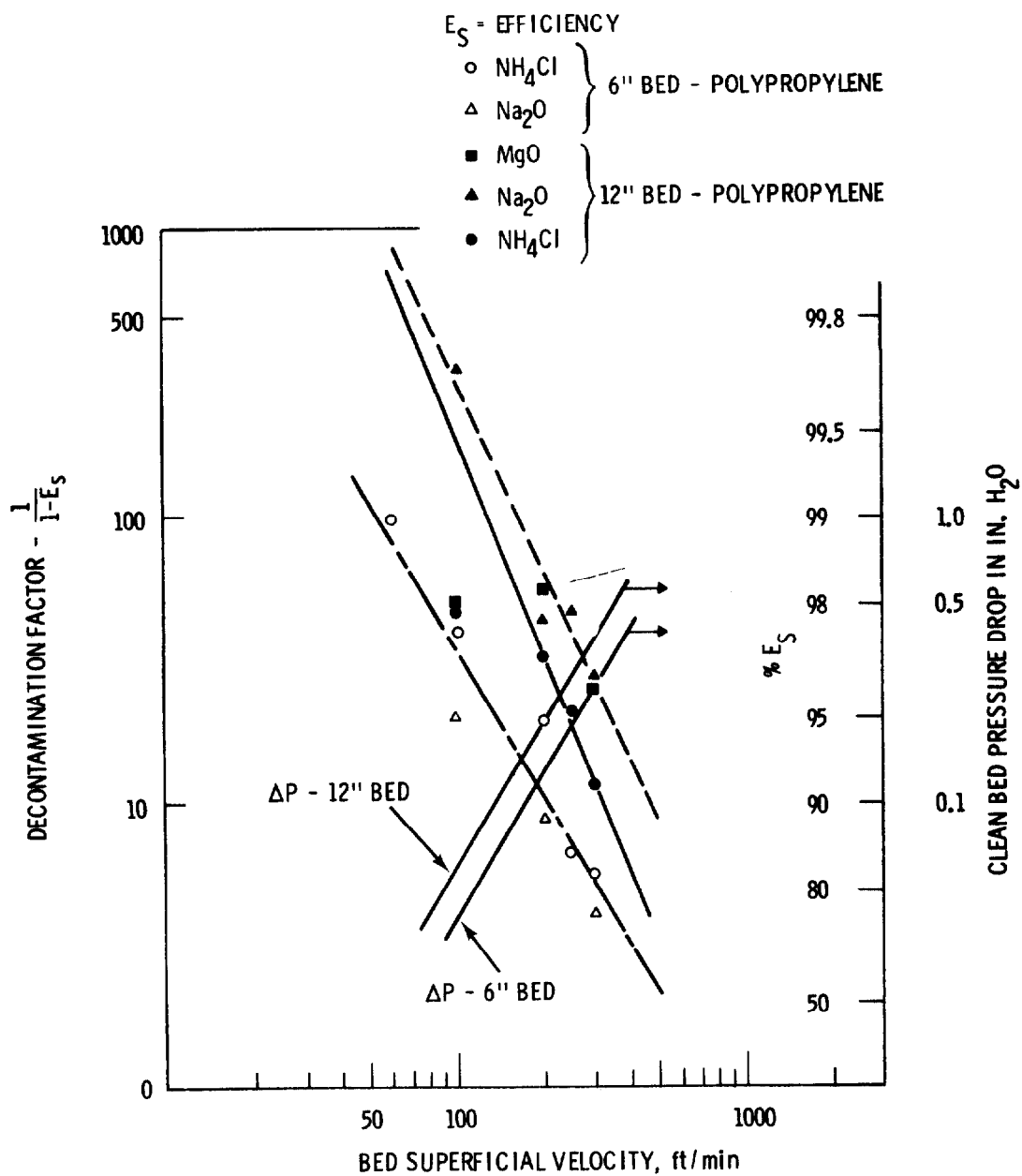
FIBER BED DECONTAMINATION FACTORS

FIGURE 4

For the 12 in. bed, the log-log plot of the data suggests a real, although small, difference in the bed efficiency for NH_4Cl particles compared to that for Na_2O and MgO and were segregated for calculation of the linear regression fit of the data while the Na_2O and MgO data were lumped together. The apparently anomalously low values for NH_4Cl and MgO (100 ft/min - 50 cms/sec) were the last samples taken in each series when the operating log noted leakage along the bed edges. Since it is unrealistic, based on the preponderance of data, that the efficiency should decrease with decreasing velocity, the bed leakage was assigned as the major cause for the low values which were not included in the curve fitting process. The pressure drop curves shown in Figure 4 are for the previously described void fractions in a clean state. The equations for the fitted curves are contained in Table III.

TABLE III

DECONTAMINATION FACTOR EMPIRICAL EQUATIONS
(New Wind Tunnel)

Fiber Bed			Partical			
			Type	Size		
6 in. V.F. - 0.956			NH_4Cl	~ 0.3		$D_f \cong (9.5 \times 10^4) V^{-1.72}$
			Na_2O	~ 0.25		$r^2 = 0.9$
12 in. V.F. - 6 in. at 0.975			NH_4Cl	~ 0.25		$D_f \cong (2.12 \times 10^7) V^{-2.52}$ $r^2 = 0.99$
and 6 in. at 0.956			MgO	~ 0.06		$D_f \cong (7.8 \times 10^6) V^{-2.21}$
			Na_2O	~ 0.25		$r^2 = 0.97$

Three Inch Thick Fiber Bed

Since the efficiency appeared to be dependent upon fiber density as well as the demonstrated dependence on thickness, a run series was made with the NH_4Cl aerosol using a 3 in. thick bed packed to a void fraction of 0.946 -- the maximum packing density that could be restrained by the grid wires to a 3 in. dimension. Also, a folded fiber mat was placed along each bed edge in an effort to reduce the leakage along the frame and extend run time to edge breakthrough. In this test series a minimum of four successive measurements were taken at one system flow rate before altering the conditions and at 100 ft/min (~ 50 cms/sec) face velocity and about 75 mg/M^3 aerosol particle load, twenty, thirty-minute samples were taken over a thirteen hour period.

The equation developed from the least squares fit of the efficiency versus velocity was

$$E_S = 102.8 - 0.0514\ V$$

where E_S = system efficiency in percent and,

$\quad\quad V$ = bed face velocity in ft/min and,

$\quad\quad r^2 = 0.986.$

The plot of the decontamination factor vs. velocity (Figure 5) again shows the expected relationship with relatively good agreement as indicated by the 0.94 coefficient for the lease squares fit. The average values for each velocity are plotted along with the 95 percent confidence levels. The equation developed from the least squares fit was

$$D_f \cong (3.87 \times 10^7) V^{-2.74}$$

where $D_f = \dfrac{1}{1-E_S}$, dimensionless and

$\quad\quad V$ = bed face velocity in ft/min.

Comparatively, this thinner bed with a lower void fraction exhibited an efficiency about equal to the 6 and 12 in. beds at 100 ft/min ($\sim$50 cms/sec) flow rate and was about 5 percent higher and lower than the 6 and 12 in. beds at 300 ft/min ($\sim$152 cms/sec) flow rate. The initial pressure drop across this bed was slightly higher and lower than the 6 and 12 in. beds.

This test illustrates that for low flow rates and low aerosol load the thinner bed would have a practical application. The dependency of efficiency on both the fiber bed thickness and density was demonstrated but not in sufficient detail to develop a mathematical relationship.

Six Inch Thick Stainless Steel Bed

The series of experiments leading to the discovery of this concept suggested that an electrically non-conducting fiber bed was required to obtain the observed high collection efficiencies. To support this idea, a conducting bed of stainless steel was tested under equivalent conditions. As suspected, the efficiencies obtained were very low, between 35 and 43 percent at 350 and 50 ft/min ($\sim$175 and 25 cms/sec), and approximated that calculated for collection due to image forces under the test conditions.

Bed Loading Runs

Data collected during two NH_4Cl loading runs at 100 ft/min ($\sim$50 cms/sec) face velocity are shown in Figure 6A for a clean bed at the start of the run and Figure 6B which started with a partially loaded bed from the previous day's tests. Obviously, the scatter in the data was greater at 50 mg/M^3 aerosol concentration than at twice that concentration. As discussed previously, this scatter in the data was ascribed to the sensitivity of the mass measurement for the downstream sampling position which was hovering around the
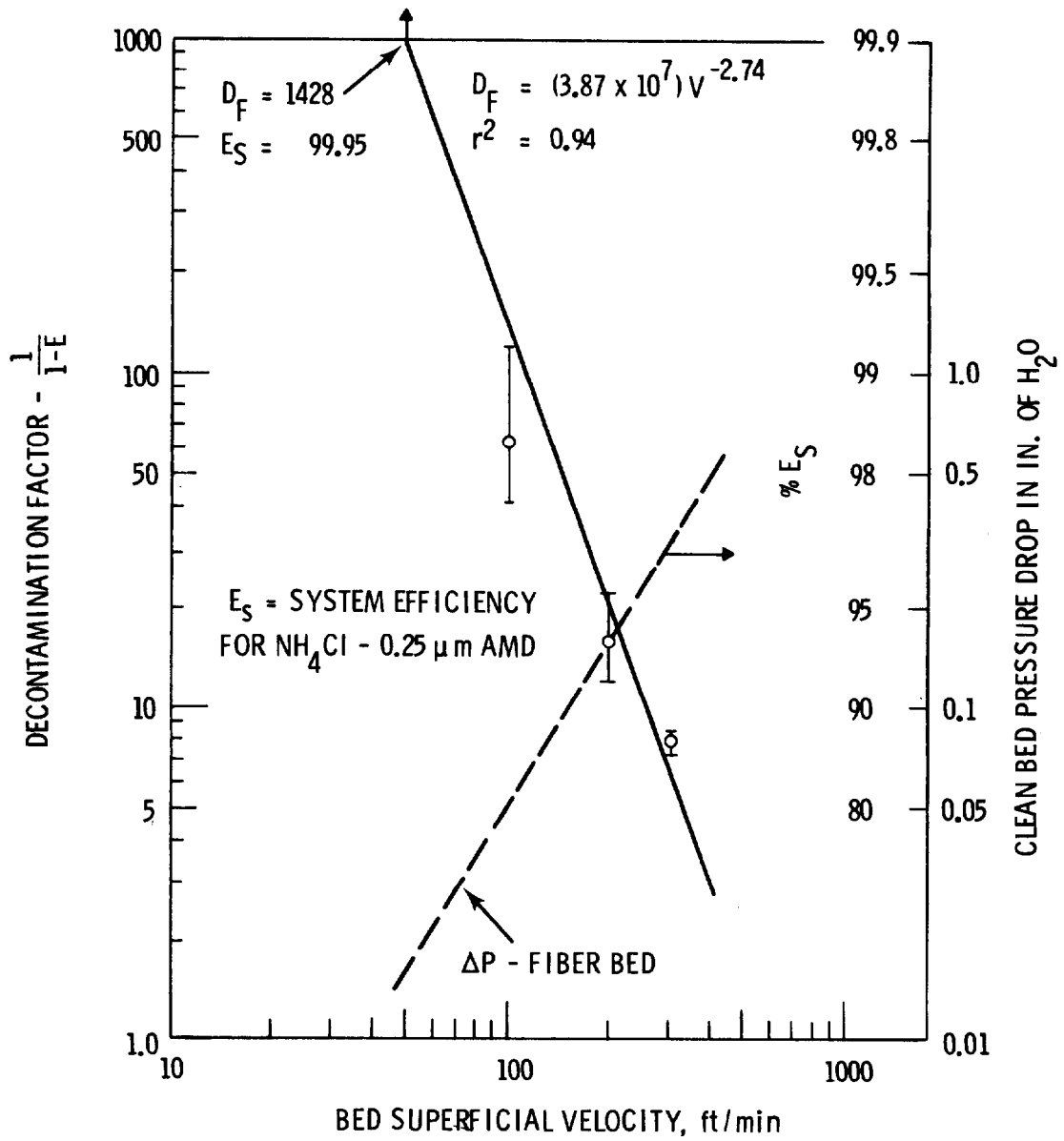
DECONTAMINATION FACTOR FOR FIBER BED
3 INCH POLYPROPYLENE - 0.946 VOID FRACTION

FIGURE 5
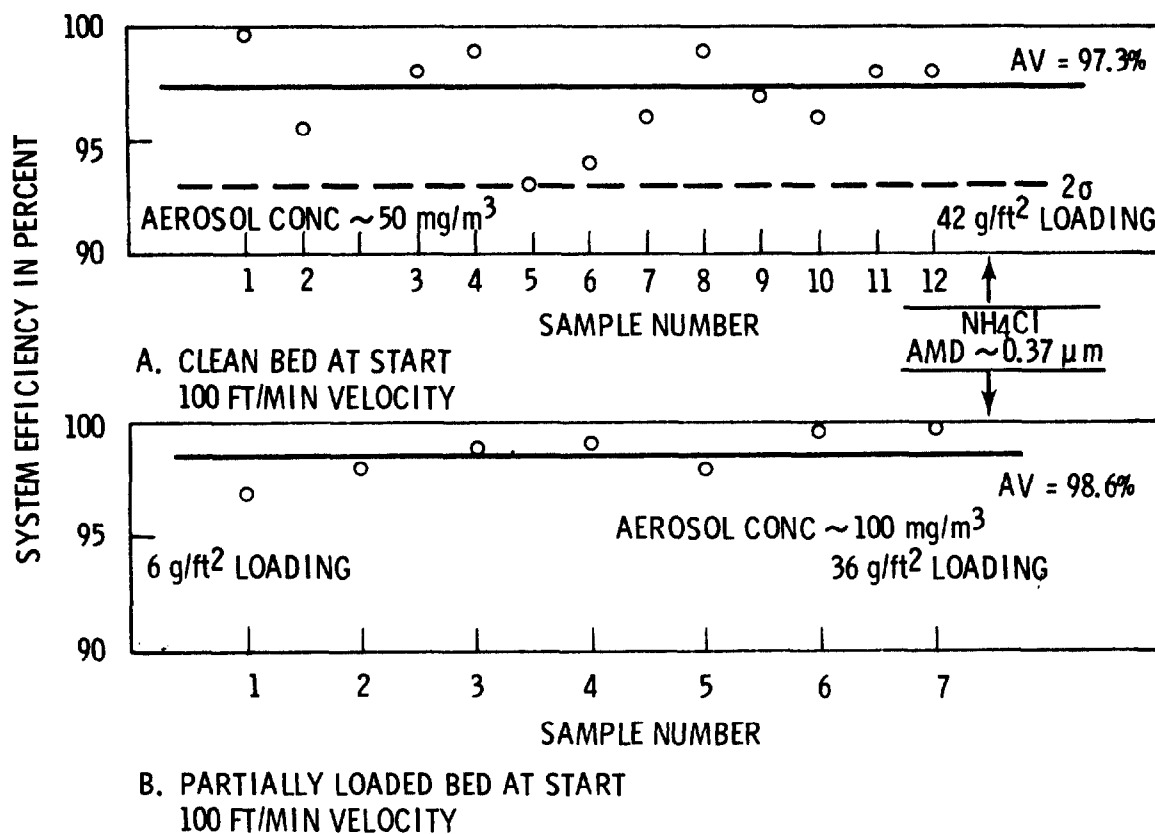
EFFICIENCY VS LOADING - 6'' BED
0.96 VOID FRACTION

FIGURE 6

balance sensitivity at these high efficiencies and aerosol concentrations. Although the averages appear to be different, it is thought to be principally an artifact of the sensitivity rather than a real difference since differences in the efficiency due to aerosol concentration over the range tested were not discernable. There appears to be a slight trend for the efficiency to increase with bed loading, Figure 6B, which was also observed with other loading runs made at a constant velocity.

Pressure Drop Increase

The increase in pressure drop with bed loading appears to be predominantly a function of both the bed void fraction and particle characteristics which apparently influence the predominant plane of deposition perpendicular to the flow, at least for the submicron size range. The aerosols of 2 μm AMD size and above may also influence depth of penetration into the bed. The velocity of air flow might also be a factor in directing the depth of penetration but cursory visual observations indicate that it would be of a second order magnitude. This later impression was obtained from the NH_4Cl aerosols over a flow range of 50-300 ft/min ($\sim$25-152 cms/sec). For these tests, visual inspection did not reveal any dramatic change in the plane of principal deposition which would have been required to be discernable. This is also supported to a degree by the much faster pressure drop increase for the higher flow rates under equal aerosol concentrations. Specific tests to define the effect of velocity on the pressure drop-bed load relationship have not been made. Relative comparisons, for a bed void fraction of 0.96, 100 ft/min ($\sim$50 cms/sec) face velocity and an approximately equal pressure drop increase from 0.08 to 0.3 in. of H_2O, gave bed loadings of about 540, 650 and 970 g/M^2 for approximately 10^8, 10^{10} and 10^{12} ohm-cm particle resistivities having nearly equal AMD's.

For non-characteristic aerosols, like the ones used, any tests defining the load - ΔP - VF relationship would be of academic interest only. The information obtained to date suggests that for industrial applications, particle characteristics, principally resistivity and concentration and secondarily size, as well as the control system operating conditions are necessary to optimize the efficiency, cleaning frequency and area of the fiber bed.

Pictures of a loaded bed, Figure 7, show the upstream and downstream faces of a fiber bed loaded with NH_4Cl particles. The pictures are somewhat deceiving since the front face gives the appearance of being plugged. However, the pressure drop across this 12 in. thick bed under this particle load of $\sim$80 g/ft^2 (860 g/M^2) was about 0.6 in. of water at 300 ft/min ($\sim$150 cms/sec) face velocity. Although not readily visible, there was a very slight deposit on the rear face fibers and support wires which demonstrates the effectiveness of this filtration concept.

Electrical Properties of Bed

The electrical properties of the bed could only be inferred from the leakage current of the bed and from the screens positioned on the upstream and downstream bed faces. The bed leakage current
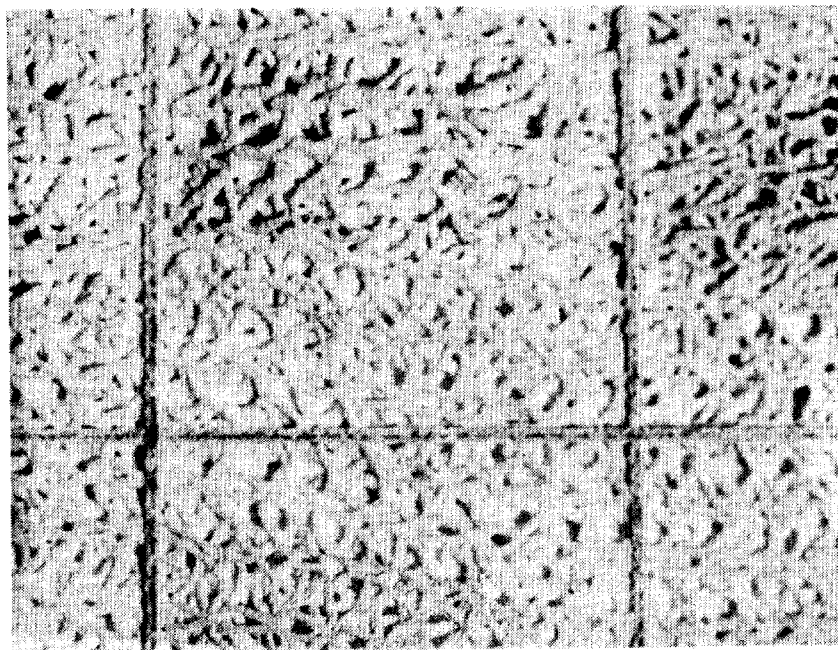
UPSTREAM FACE
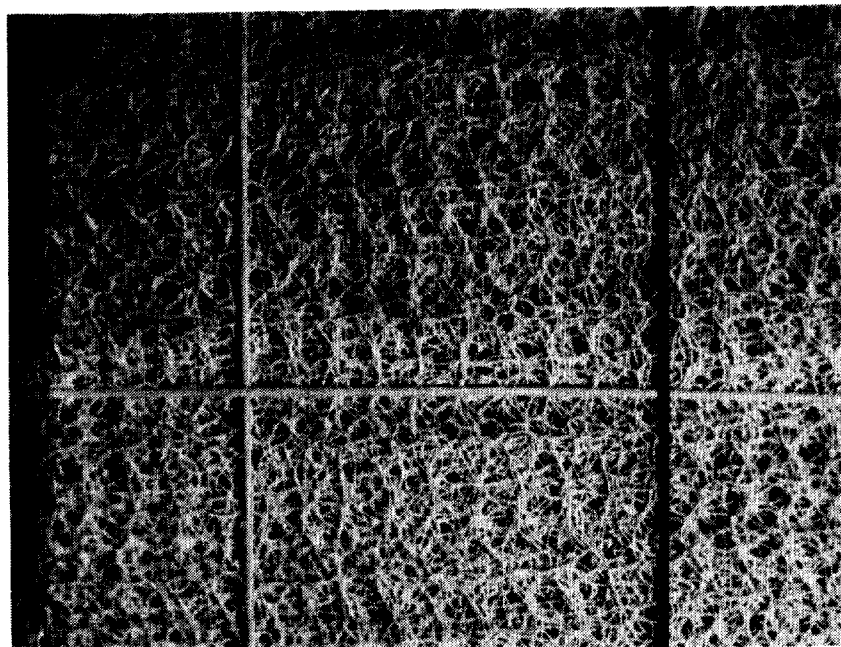
DOWNSTREAM FACE

FIGURE 7   12" Polypropylene Fiber Bed - NH_4Cl Load ~ 80 g/ft^2

was obtained from a bare wire encompassing the bed at the frame-bed interface. A single wire was found to produce the same leakage current as a full width aluminum foil. From the measured leakage current of the bed and the four screens, the space charge of the bed built instantaneously upon activation of the charger to about a factor of ten less than that observed during particle generation and deposition and increased proportionally with flow rate. This suggests that molecular ion or charged Aitken nuclei deposition produces a significant contribution to the bed field charge and impaction of charged particles is not required to initiate the action. The charge varied with mass per unit time depositing on the filter but only by about a factor of five over the range tested (10-150 mg/M^3). At any one particle deposition rate the space charge increased immediately by an order of magnitude and then remained constant indicating that charge leakage from the bed was equal to that being deposited with the particles.

By assuming that the charge distribution in the bed is directly proportional to current measurement, some inferences relative to its shape can be made from the current measurements of the planted screens. For the 6 in. bed, there is an order of magnitude decrease between the front and rear face which prevailed throughout the run and was present with or without particle deposition. This suggests essentially an instantaneous equalization of the charge deposited by the particles. The field charge distribution transverse to the flow appeared to be uniform within the rather approximate measurements resulting from the fluctuating meter. The above observations prevailed also for the 12 in. thick bed except the average reduction in the inferred field charge front to rear was about 20 and was more variable than for the 6 in. bed.

It was observed from the runs where electrode shunting occurred and the charger current increased continuously throughout the test from 18 to 21 ma that the inferred field charge decreased to about one fourth of the initial charge in addition to that expected from particle concentration variations. Although not a sensitive indicator, it confirmed the suspected reduced particle charging efficiency from electrical shunting in the charger and the related lower system efficiencies discussed previously.

Summary and Conclusions

The efficient removal of charged submicron particles from flowing gas streams with a bed consisting of fibers having a high dielectric constant was demonstrated experimentally. Although not all of the facets of operation for optimization of the concept have been explored in detail, the tests conducted to date suggest many practical applications for relatively economical particle control not attainable with presently available concepts. Based on mass measurements, the emperical equations developed from the data collected to date indicate a 100 percent collection efficiency at some face velocity below 50 ft/min ($\sim$25 cms/sec). Other observations from the information accumulated to date were as follows:

1. <u>Velocity</u> was the prime variable with respect to efficiency. For the 6 in. thick bed, the efficiency decreased linearly with increasing velocity up to about 200 ft/min ($\sim$100 cms/sec) bed face velocity. The minimal data beyond this velocity are suspect and need redefinition. For the 12 in. thick bed the linear relationship existed up to the highest flow rate tested of 320 ft/min ($\sim$160 cms/sec). Both produced efficiencies above 90 percent at the above-stated flow rates for the submicron particles used.

2. <u>Bed thickness</u> apparently had a pronounced effect on collection efficiency. However, bed thickness and fiber volume density are dependent variables as evidenced by the compressed 3 in. bed which showed a higher efficiency than the 6 in. bed having a slightly higher void fraction. Although not directly comparable due to void fraction differences the 12 in. filter showed about a 10 and 2 percent higher efficiency than the 6 in. bed at 300 and 100 ft/min ($\sim$150 and 50 cms/sec) face velocity. This difference in the slope of the curves suggests a deeper penetration with increasing velocity which appears reasonable providing all other conditions are equal. Thus the ratio of the efficiencies (12 in./6 in.) should increase with velocity for equivalent particle characteristics.

3. <u>Particle Size</u>. Although not a prime variable, there was no detectable influence on efficiency over the range tested -- $\sim$0.06 to 0.83 μm AMD. The stated AMD's are thought to be high due to the uncertainty of extrapolation from about 90 to 50 percent of the log normal plot.

4. <u>Pad Resistivity</u>. There was no discernable difference between polypropylene or teflon fibers with respect to efficiency and apparent field charge strength and shape. The principal criteria for a fiber are that it be electrically non-conducting and have a significantly larger diameter than the submicron particles. A 6 in. thick stainless steel demister pad produced very low collection efficiencies -- about equal to that expected for image force collection.

5. <u>Particle Resistivity</u>. The majority of the data indicated there was no significant trend in collection efficiency over the range of approximately 10^8 - 10^{12} ohm-cm particle resistivity. Since one test series showed a slightly lower efficiency for the 10^8 ohm-cm NH_4Cl and the model suggests that efficiency should decrease with decreasing particle resistivity, particles with a much lower resistivity should be studied to better describe any differences and establish the lower boundary limit, if one exists. The depth of particle penetration into the bed was directly related to particle resistivity.

6. <u>Dust Concentrations</u>. Particle concentrations ranging from 10 to 250 mg/M^3 were used without any significant differences except for the apparent higher field charge for the higher concentrations. Since measurement reproducibility increased and length of test time varied inversely with concentration, most of the new wind tunnel tests were made at 50-100 mg/M^3 dust loading.

7. Particle Charge Level. The fraction of uncharged particles
    challenging the filter is apparently more pertinent to the suc-
    cess of the concept than the charge level of the particles at
    least if near saturation charge is obtained. As would be
    expected, the bed had no affinity for uncharged particles at
    the higher velocities and showed about 8 percent retention at
    50 ft/min ($\sim$25 cms/sec). The instrumentation used was not sen-
    sitive enough to provide the refinement required to accurately
    define the fraction of uncharged particles downstream of the
    charge section. Consequently, valid information is not avail-
    able on the ratio of charged to uncharged particles reaching
    the filters. However, the efficiencies obtained indicate that
    the uncharged particles must have been a very small fraction of
    the total particle load. Faraday cage measurements indicated
    both near and supersaturation charge of the particles. The
    variability of the data is believed to be a function of the
    measurement of small currents in the presence of relatively high
    electrical fields and very little credence is given to the data.

8. Humidity. No attempts were made to study humidity of the aerosol
    as a variable. The maximum relative humidity observed during the
    experiments was 50 percent and generally hovered between 30-40
    percent. Consequently, no generally applicable effects of
    humidity were discernable. For the special case with Na_2O par-
    ticles, humidity in excess of about 45 percent produced a
    degraded operation. The principal cause for the loss of effi-
    ciency, particle charging or bed collection or a combination of
    both, was indeterminant.

Acknowledgments

The authors wish to acknowledge the assistance of co-workers
D. A. Nelson for his experimental work and D. L. Lessor for dis-
cussions on the mathematical modeling of the phenomenon.

DISCUSSION

ETTINGER: Did you perform, or do you plan to perform any tests
to indicate what the effect of high humidity air will be on the col-
lection efficiency?

REID: We feel that this should be done. We have not been
able to do it up to this point. We had one test in which we were
using sodium oxide and the humidity in the room increased to about
47 per cent. We created sodium hydroxide from this and quite a mess
internally. The efficiency under that condition decreased from about
85 per cent down to 72 per cent over a period of about seven hours.
We feel humidity needs to be investigated. However, if the humidity
is not sufficient to give us a conducting fiber, we do not feel it will
have any significant effect. Another important part of this system
is that it can be cleaned easily. You don't have to remove it to
clean it.

UNDERHILL: The previous question almost answered the question I had. How much moisture pickup was there during the course of your experiments and was the aerosol basically oxide or was it sodium hydroxide? Thermodynamic equations lead me to believe that it was NaOH or Na_2CO_3.

REID: It's pretty dry at Hanford. Most of the time, humidity was running about 35 to 40 per cent during the test. We're not certain whether we had sodium oxide or sodium carbonate. We did not have sodium hydroxide until we reached a humidity above 45 per cent, then we developed sodium hydroxide. This we were certain of from resistivity measurements.

UNDERHILL: Phase diagrams of sodium hydroxide and sodium carbonate as a function of relative humidity might be of interest to you.

FIRST: We've been doing experiments with sodium aerosols, also, and we find particle sizes almost on order of magnitude larger than you are reporting for the concentrations that we are dealing with. Our relative humidity for these experiments was 20 per cent. This certainly corresponds with yours. Could you tell us how you determined the size?

REID: It was with an Anderson Cascade impactor sampler. Possibly, the way we generated the particle would account for the different sized particles. We don't believe that particle size is normally distributed by the method in which we generated the particles because we were getting about 90 per cent of the particles on the filter paper downstream in the last stage. So, the particle sizes stated in the paper are probably larger than what we actually had. We saw no relationship between efficiency and particle size over the particle size range from .06 to about .7 μm AMD. We need a better method of measuring particle size when you get down into this range.

RIVERS: An earlier question suggested that the conductivity of the fiber bed might be a significant factor in the performance of the filter. It may be, but I would guess that a conductive fiber bed would be better than a dielectric fiber bed. The reason is that if particles captured in the bed retain their charge, they would tend to repel similarly charged particles later. Fields within the fiber bed voids can be produced by the space charge of uncaptured particles – and dielectrophoretic forces exist between a charged particle and a grounded fiber. A conductive fiber bed could be considerably less flammable than a plastic fiber.

AIR FILTRATION ENHANCEMENT USING ELECTRONIC TECHNIQUES*

G. O. Nelson, C. P. Richards, A. H. Biermann,
R. D. Taylor, and H. H. Miller
University of California, Lawrence Livermore Laboratory
Livermore, California 94550

Abstract

Dielectrophoretic filtration experiments were conducted on glass, polyester, dacron, Teflon, wool, acrylic and polypropylene filter media. A polydispersed (σg = 2.0, ammd = 0.95 μm) sodium chloride particle was used as a test aerosol. All materials exhibited significant increases in efficiency with increasing field strengths. Efficiencies of >99% could be obtained from glass fiber mats using a 13 kV/cm electric field at 16.3 cm/s face velocity.

I.   Introduction

High-efficiency particulate air (HEPA) filters are commonly used at radioactive handling facilities to remove airborne contaminants. A survey by Cooley indicated that approximately 16 000 HEPA filters were used in the United States in 1973[1]. Although the original cost averages $150/filter, the total expense to buy, install, test, remove, decontaminate and dispose of the filter has been estimated to be three to ten times the initial filter cost[2],[3]. Hence, a significant savings could be realized if filter service life could be extended.

A number of approaches were considered. Most of these were focused on the design of an adequate prefilter rather than some modification of the HEPA filter. Inertial devices such as cyclones or impaction plates would probably be inappropriate because of the small particle size usually encountered (typically 0.05-5 μm)[4],[5]. Wet- and foam-type scrubbers, although efficient for submicron particles, generate too excessive liquid wastes to be practical.

The direction which appears to show the most promise is the dielectrophoretic or non-ionizing electrostatic air filter[6],[7],[8]. This involves placing a non-conducting filter media between two perforated metal plates maintained at a potential difference of 5-10 kV/cm. The media distorts the electric field and creates higher field intensities near the individual fibers. When a particle enters the electric field, it is polarized and attracted more effectively toward the locations of highest field intensities. Power requirements are generally quite low (typically less than 1 μA) when compared to conventional electrostatic precipitation techniques since particle charging is not required. However, any net charge present on the particle or filter media which occurs naturally or is induced from small current leakages only serves to enhance an already powerful particle-fiber interaction.

The purpose of this investigation is to present the results from our dielectrophoretic filtration experiments using glass, carbon and polymeric filters tested with a polydisperse sodium chloride aerosol. This report is intended to be interim in nature since several crucial experiments involving filter configuration and particle charging as well as theoretical modeling calculations have yet to be completed.

II. Experimental

Aerosol Generator

Filters were tested using the apparatus shown in Fig. 1. The system consists of an air mover, a sodium chloride aerosol generation system, prefilter test section, and experimental diagnostic equipment.

Filtered air is drawn into the system by a high-volume air sampler, and the flow is measured using a mass flowmeter. A variable transformer between the sampler and the power source maintains the flow between 5 and 25 litres/s.

The aerosol is produced by using four air-driven modified Wright-type nebulizers, shown in Fig. 2. The nebulizer screws into a 500-ml polyethylene bottle containing a solution of dissolved salt. Air pressure supplied to the nebulizer aspirates the solution from the reservoir to the nebulizer where it is atomized into small droplets.

The droplets mix with air in the aging chamber, evaporate, and subsequently form a test mixture of cubical salt particles in a moving air stream. The resultant aerosol characteristics are a function of the airflow, nebulizer air pressure, solution concentration, and the number of nebulizers used.

Particle size characteristics using a 1% sodium chloride solution at a nebulizer pressure of 340 kPa show the aerodynamic mass
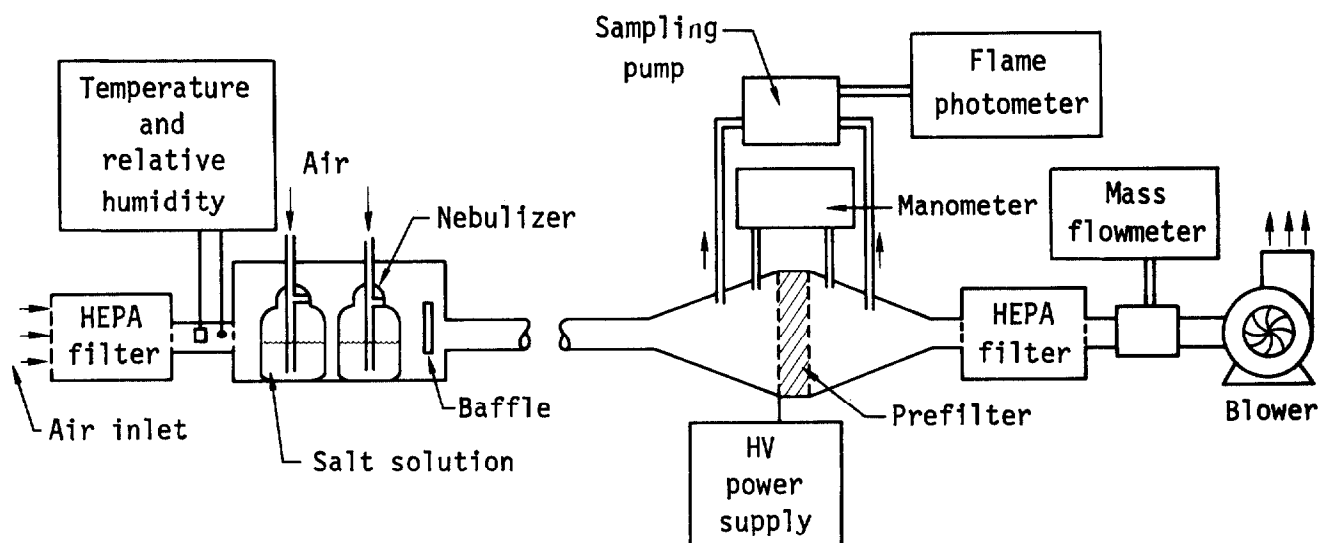
Fig. 1. Schematic Diagram of Aerosol generation system.
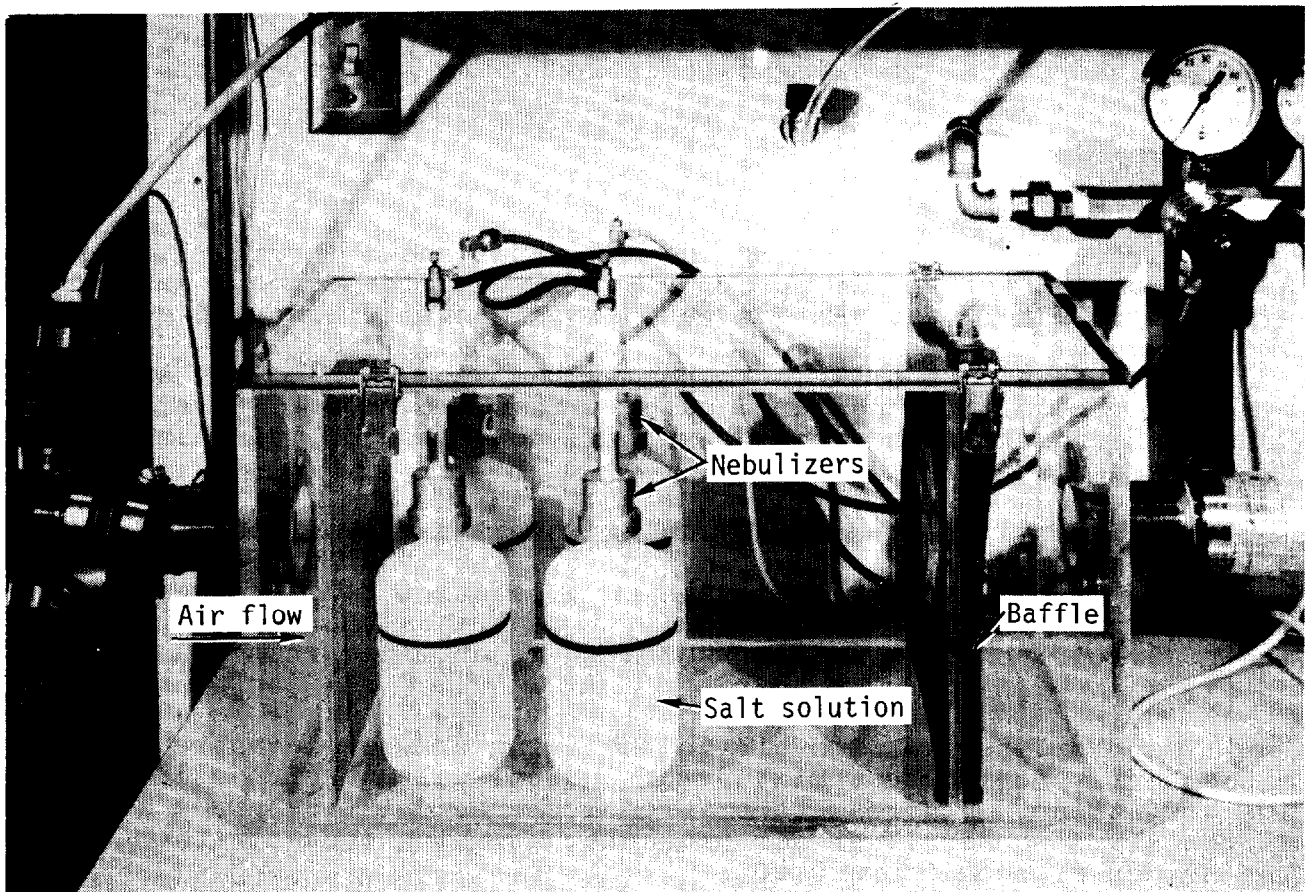
Fig. 2. Sodium chloride aerosol generation system. Four Wright-type
nebulizers situated inside the aging chamber.

median diameter to be 0.95 μm with a geometric standard deviation of
2.0. The mass concentration using all four nebulizers at
23.6 litres/s is 4.5 mg/m^3.

System diagnostic equipment includes a flame photometer to
determine filter efficiency and an electronic manometer to record
pressure differential as a function of time. Relative humidity, tem-
perature and air flowrate are monitored throughout the experiment.

Filter Testing Assembly

The dielectrophoretic filtration experiments were conducted in
the test section located just in front of the HEPA filter. The dis-
assembled test assembly is shown in Fig. 3. The 5-cm-diam duct
expands to accommodate a 19.1- × 19.1-cm-square filter. The filter
is held between two 0.5-mm-thick perforated stainless steel plates
(29% open) spaced 13 mm apart by two polyethylene spacers. A nega-
tive d.c. high-voltage lead is connected to the front screen, and
the rear screen is grounded.
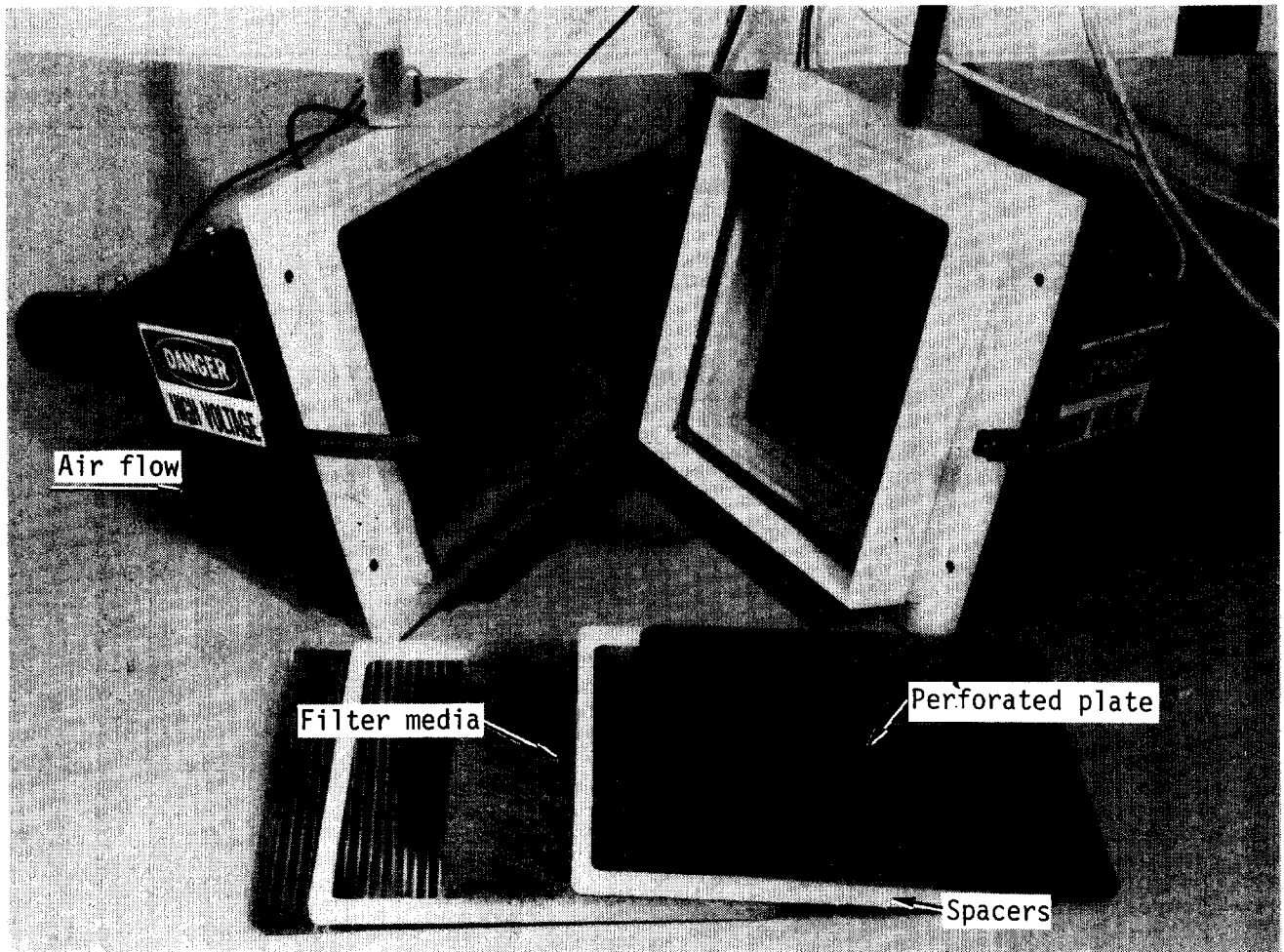
Fig. 3. Disassembled filter test section.

The 33 filtering media shown in Table 1 were tested between the electrified perforated plates. Testing was normally conducted at face velocities of 65 cm/s. However, a glass and a polyester filter were tested at face velocities of 16.3, 32.5, 48.8 and 65 cm/s.

The efficiency was measured at voltages ranging from 0-15 kV, and the pressure differential was monitored throughout the testing period. The enhancement coefficient (the ratio of the dielectrophoretic-to-initial efficiency) was then calculated.

Table I. Characteristics of filter media.

Run No.	Fiber Material	Designation	Source	Uncompressed Thickness (mm)
5A	Glass Mat	Aeroglass	Alfco Products[b]	16
9	Glass Mat	High density	Dow Corning	7
13	Glass Mat	FM 004	Owens Corning	7
14	Glass Mat	Type C	Owens Corning	18
15	Wood-Polypropylene Mat	50%/50%	Globe Albany	4
17	Wool-Acrylic Mat	50%/50%	GAF	4.8
18	Glass Mat	AU-300	Owens Corning	12.5
20	Teflon Mat	Armalon XT 2663	Dupont	2
21	Polyester Mat	#5/8-in.	Filpaco	16
22	Glass Mat	Packing material	Owens Corning	12
23	Glass Batting	Basic filtration fiber	Owens Corning	70-90
24	Glass Mat	High density	Dow Corning	6-8
25	Glass Mat	Commercial filter media	Owens Corning	20
26	Glass Mat	Dust stop filter media	Owens Corning	16
27	Glass Mat	Microlite Insulation	Johns Manville	28
28	Glass Mat	Microlite Insulation	Johns Manville	14
29	Glass Mat	Type A	Owens Corning	20
30	Glass Mat	FM 060	Owens Corning	1-2
31	Teflon Mat	XT 2363	Dupont	2
32	Glass Mat	U-trim-it	Owens Corning	4-5
33	Carbon[a]Mat	1/8-in	Fiber Materials Inc.	4
34	Polyester Batting	—	Fabco	4-4
35	Dacron Batting	DA CH-101	Filpaco	4
36	Teflon Mat	XT 7600	Dupont	2-3
37	Glass Mat	Prefilter mat	Owens Corning	1
38	Polypropylene Fabric	222-013-17	National Filter Media	0.5-1
39	Glass Mat	B-100	Hitco	3
40	Glass Mat	Duct insulation	Owens Corning	14
41	Polyester Fabric	192-014-03	National Filter Media	1
42	Wool/Acrylic	50%/50%	J. C. Penny	1-2
43	Polypropylene Fabric	222-018-03	National Filter Media	1.5
44	Polyester Batting	—	J. C. Penny	15
45	Polyester Fabric	190-010-06	National Filter Media	0.3

[a]Glass fiber filter (Lennox, #30024, 40-mm uncompressed thickness) added to prevent shorting of carbon filter.

[b]Reference to a company or product name does not imply approval or recommendation of the product by the University of California or the U.S. Energy Research & Development Administration to the exclusion of others that may be suitable.

III. Results and Discussions

Effect of Filter Media

The ideal filter should have a relatively high initial efficiency and enhancement coefficient, but a low initial pressure and pressure drop growth. The results shown in Table 2 indicate that no filter media is outstanding in all four categories. However, glass (runs 14, 22, 23, 25, 26, 27, 28, 30, and 40), polyester (run 21) and dacron fibers (run 35) are all strong candidates. Woven fibers and teflon mats have high initial efficiencies, but their pressure drop growth is so rapid that they are unsuitable in this type of application. The polypropylene and polyester weaves used in runs 43 and 45 experienced such a rapid pressure drop growth that there was no time to ascertain its efficiency enhancement using the electric field.

Table II. Results of filter efficiency tests.

Run No.	Fiber Material	Initial ΔP (in. H₂O)	Rate of ΔP change (in. H₂O/hr)	Filter Efficiency - % (E_t) 0(E_0)	2 kV	4 kV	6 kV	8 kV	10 kV	12 kV	Enhancement Coefficient [(E_t-E_0)/E_0] 2 kV	4 kV	6 kV	8 kV	10 kV	12 kV
5A	Glass	0.45	—	1.9	3.8	5.7	9.5	11.3	15.1	17.0	1.0	2.0	4.0	5.0	7.0	7.9
9	Glass	3.76	2.07	25.0	27.5	35.0	38.0	40.0	—	—	0.91	1.40	1.52	1.60	—	—
13	Glass	1.35	1.51	94.4	94.6	94.6	94.7	94.9	95.0	—	0.002	0.003	0.003	0.005	0.008	—
14	Glass	0.055	0.01	14.4	17.6	19.7	22.0	26.5	27.2	30.5	0.22	0.37	0.53	0.84	0.89	1.16
15	Wool/Polypropylene	0.98	0.66	68.7	72.7	76.6	78.7	80.8	80.8	80.3	0.06	0.12	0.16	0.18	0.18	0.17
17	Wool/Acrylic	0.80	0.78	85.0	86.3	86.9	87.5	87.8	88.1	89.1	0.015	0.022	0.029	0.033	0.036	0.048
18	Glass	0.40	0.15	28.7	34.7	—	—	—	—	—	0.21	—	—	—	—	—
20	Teflon	2.85	4.6	80.4	81.9	—	83.0[a]	83.5	—	—	0.019	—	0.031[a]	0.039	—	—
21	Polyester	0.092	0.012	12.3	17.2	21.4	25.6	29.0	33.1	36.8	0.40	0.74	1.08	1.36	1.69	1.99
22	Glass	0.502	0.144	37.1	42.5	51.5	59.4	64.8	68.7	70.8	0.15	0.39	0.60	0.75	0.85	0.91
23	Glass	0.165	0.0084	19.0	23.5	26.8	29.5	34.8	41.5	45.7	0.24	0.41	0.55	0.90	1.18	1.41
24	Glass	2.25	1.86	91.4	92.5	93.5	94.0	94.2	94.4	94.0	0.013	0.023	0.029	0.030	0.033	0.028
25	Glass	0.065	0.0045	13.6	14.5	15.9	17.9	19.7	21.1	22.6	0.10	0.20	0.36	0.49	0.60	0.71
26	Glass	0.069	0.005	9.6	11.5	15.2	17.2	19.4	22.5	24.7	0.20	0.55	0.79	1.02	1.3	1.6
27	Glass	0.49	0.13	45.6	51.9	62.1	70.2	75.6	78.8	81.3	0.14	0.36	0.54	0.66	0.73	0.78
28	Glass	0.23	0.070	27.6	30.7	39.1	44.9	51.5	58.1	62.2	0.11	0.43	0.63	0.87	1.1	1.39
29	Glass	0.070	0.010	9.6	10.6	12.4	13.7	15.3	15.7	17.3	0.10	0.29	0.43	0.59	0.64	0.80
30	Glass	0.10	0.046	14.8	14.8	17.4	18.7	21.0	21.1	—	0	0.18	0.26	0.42	0.43	—
31	Teflon	4.0	24	90.2	—	91	—	91	—	—	—	0.008	—	0.008	—	—
32	Glass	0.075	0.003	5.5	7.8	8.8	11.9	12.7	14.5	15.4	0.42	0.60	1.20	1.31	1.64	1.80
33	Glass/carbon	1.32	1.1	46.1	47.2	48.4	—	—	—	—	0.024	0.049	—	—	—	—
34	Polyester	0.075	0.004	14.1	14.6	15.4	16.8	16.8	19.1	—	0.006	0.015	0.031	0.031	0.058	—
35	Dacron	0.42	0.05	27.5	29.3	28.8	31.3	31.6	34.4	—	0.07	0.05	0.14	0.15	0.25	—
36	Teflon	9.55	12.3	89.6	—	—	—	—	—	—	—	—	—	—	—	—
37	Glass	0.11	0.02	7.4	8.7	10.2	10.7	11.1	—	—	0.18	0.38	0.47	0.50	—	—
38	Polypropylene	1.35	2.6	62.0	62.7	62.9	64.0	64.6	—	—	0.01	0.01	0.03	0.04	—	—
39	Glass	0.58	0.074	40.3	41.4	43.0	44.4	46.1	49.9	—	0.03	0.07	0.10	0.15	0.24	—
40	Glass	0.23	0.04	30.6	41.0	54.0[b]	63.7	70.9	75.0	79	0.34	0.76	1.08	1.32	1.45	1.58
41	Polyester	2.08	7.7	71.0	—	72.3	72.8	73.2[c]	—	—	—	0.018[b]	0.025	0.031[c]	—	—
42	Wool/Acrylic	0.42	0.08	34.0	35.3	35.0	39.9	42.4	—	—	0.04	0.03	0.17	0.25	—	—
43	Polypropylene	2.46	>10	—	—	—	—	—	—	—	—	—	—	—	—	—
44	Polyester	0.08	0.01	8.1	10.1	12.1	14.1	17.1	18.3	—	0.25	0.49	0.74	1.11	1.27	—
45	Polyester	2.11	>20	—	—	—	—	—	—	—	—	—	—	—	—	—

[a] 5 kV
[b] 3 kV
[c] 9 kV
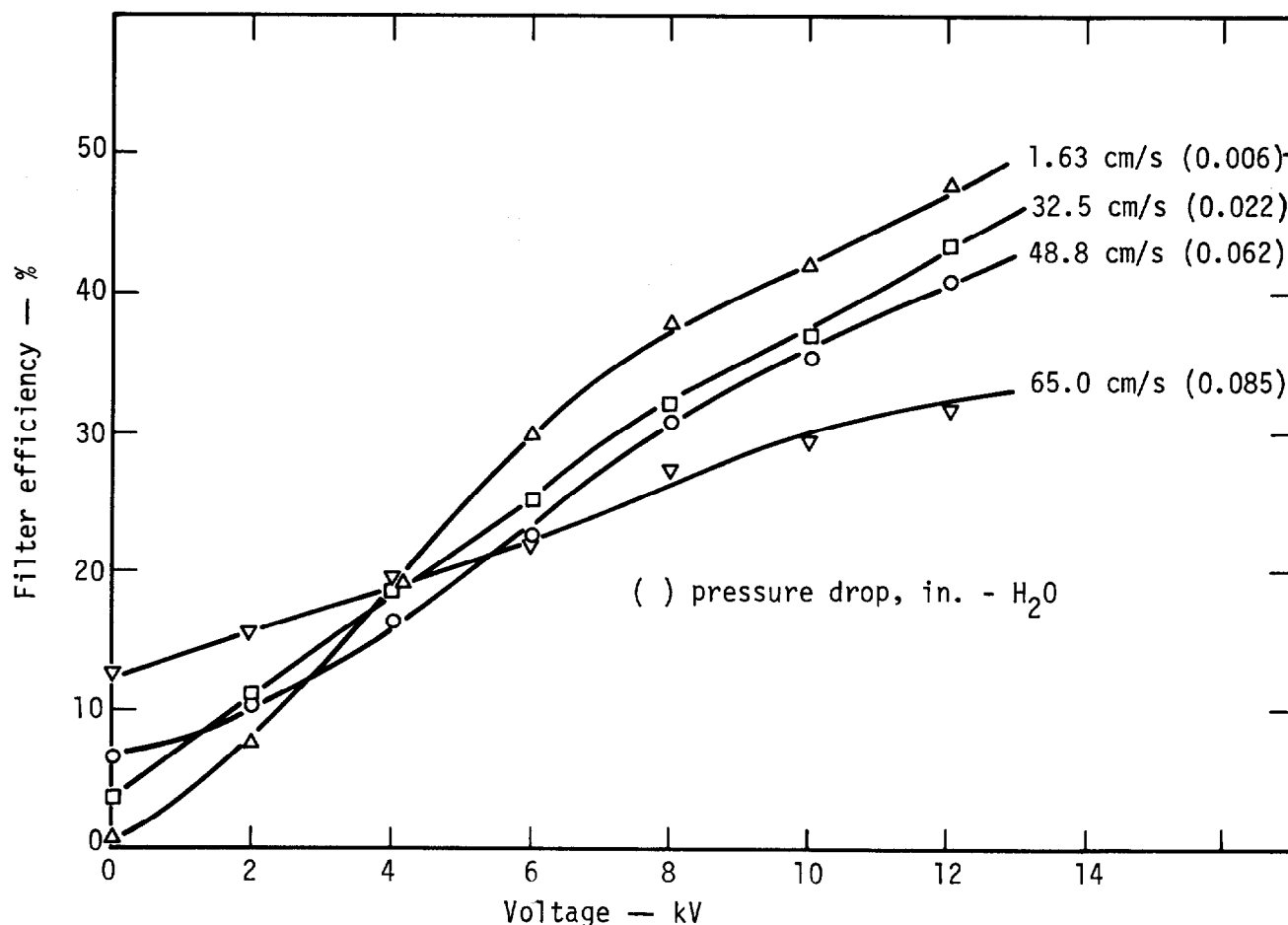
Fig. 4. Efficiency of polyester loft (Filpaco Ind #5/8-in.) as a function of voltage and face velocity.

Effect of Flowrate

Figures 4 and 5 show the efficiencies for polyester and glass fiber materials. Here the efficiency is shown as a function of applied voltage at various face velocities. With no voltage applied, the efficiency, as one might suspect, is greater with increasing face velocities. However, as the voltage between the plates is increased, the inertial component of the efficiency becomes less important and the electrical effects begin to dominate. At 16.3 cm/s, the efficiency of the polyester fiber is increased by a factor of 100 and the glass fiber increases from 29% to >99% when the voltage is increased from 0 to 12 kV. This behavior has also been observed by Fielding[6] and Borgardus[7] using a 0.3- and 1.0-μm DOP aerosol.
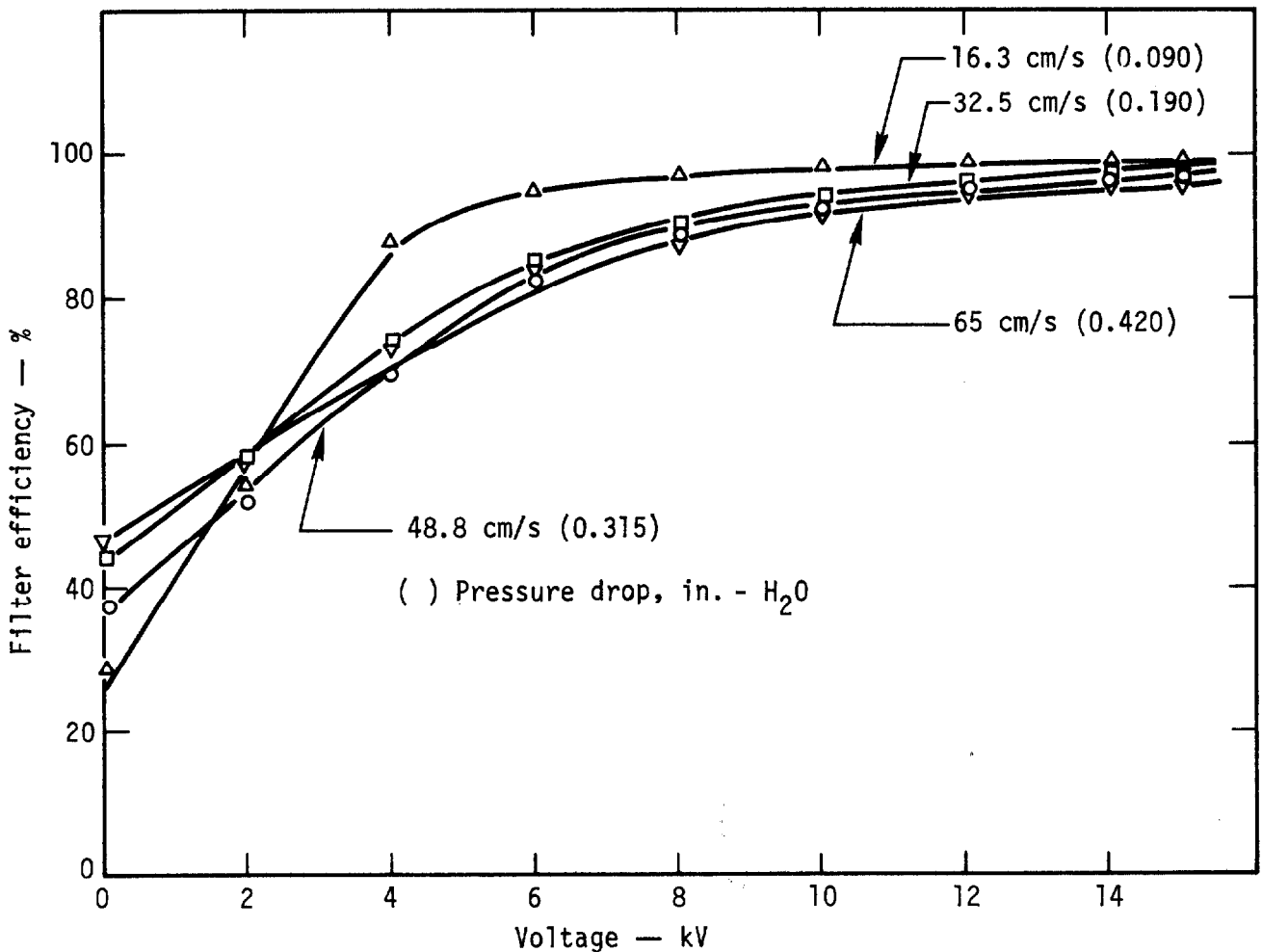
Fig. 5. Efficiency of fiberglass media (Johns Manville 1/2-in. Micro-lite Insulation) as a function of voltage and face velocity.

IV.   Conclusions

All filter media tested with a polydispersed sodium chloride aerosol exhibited increased efficiency when placed in an electric field between two perforated plates. Glass fiber beds achieved the highest efficiency (>99% at a face velocity of 16.3 cm/s) and appear to·be the best media based on initial efficiency, pressure differential, enhancement coefficient, and fire resistance. Future experimental work will include determining the effect of plate design, filter configuration and particle charge on filter media efficiency.

References

1. Cooley, C. R., "Commercial Alpha Waste Program Quarterly Progress Report," July-September 1974 HEDL TME 74-61, UC-70 (Nov 1974).

2. Lipera, J., Lawrence Livermore Laboratory, private communication.

3. Bolton, N. E., Oak Ridge National Laboratory, private communication.

4. Ettinger, H. J., Elder, J. C., Gonzales, M. "Performance of Multiple HEPA Filters Against Plutonium Aerosols," Los Alamos Scientific Laboratory, Report LA-5349-Pk, July 1973.

5. Newton, G., Lovelace Foundation, private communication.

6. Fielding, G. H., Borgardus, H. F., Clark, R. C., and Thompson, J. K., "Electrically Augmented Filtration of Aerosols," Naval Research Laboratory Rept. (1974).

7. Borgardus, H. F., Clark, R. C., Thompson, J. K., and Fielding, G. H., "Enhancement of Filter Media Performance by Corona-Face Electric Fields," Proceedings of the Thirteenth AEC Air Cleaning Conference, San Francisco, Calif., August 1974.

8. Rivers, R. D., "Operating Principles of Non-Ionizing Electrostatic Air Filters," ASHRAEJ p. 37 (Feb 1962).

DISCUSSION

GILBERT: I want to ask what the pressure drop was with a double layer of Johns-Manville's duct insulation at 99%.

NELSON: The pressure drop was about six-tenth of an inch. That includes two metal perforated plates and the filter medium itself. It was in that range. It was less than an inch. Bear in mind that we didn't do anything to maximize the surface area of the filter. It was just the flat filter right in front of the HEPA filter.

ORTH: Since the goal of your work is to reduce the volume of HEPA filter waste, 1) do you plan to work on self-cleaning electrostatic pre-filters and 2) how does the volume of waste from the pre-filters you are testing now compare with the HEPA filter waste volume that is saved?

NELSON: That question comes up. We alleviated one problem and created another. We are hoping this type of filter will have a little higher loading capacity than the HEPA. Also, being glass media, they can be removed and washed with acid and that sort of thing. There isn't an organic material to break down, such as in the HEPA filter. We hope it will be possible to leach out the contaminants and have them in a form where they can be readily recovered.

BURCHSTED: I have two points. Are the efficiencies shown in your slides count efficiency or mass efficiency? The distinction is important.

NELSON: The efficiencies are based on mass efficiencies. We use a flame photometer.

BURCHSTED: The second point is that I noted teflon, wool, and polypropylene in your slides. These are all adversely affected by heat. We would recommend the use of fire resistive media.

NELSON: Right. That is why I think eventually we will use glass fibers. None of these fibers will be suitable in a fire situation. I might mention, too, that a similar type of work was presented at the last air cleaning conference. This concept is not new. The Naval Research Laboratory has been working on it for some time. They used different media and they observed this same effect.

TESTING OF AIR FILTERS UNDER
QUALITY CONTROL SAFETY PROGRAM

Charles D. Skaats
Filter Certification Laboratory
Rocky Flats Plant
Rockwell International
P.O. Box 464
Golden, Colorado 80401

Abstract:

Testing and inspection of filters used in air filtration systems
are conducted at Rocky Flats Plant under the Energy Research and
Development Administration and Rockwell quality control program.
Some 8,000 high efficiency particulate air (HEPA) filters purchased
from three principal suppliers were examined over the year by the
Filter Certification group. In facilities handling radioactive
materials, filters must function efficiently to provide accurate
data on air contamination to safeguard personnel and the environ-
ment. Data are given on filter rejects under established criteria
and on recommendations for action to the suppliers.

INTRODUCTION

Under the air-cleaning program at Rocky Flats Plant, testing and
inspection of components used in air filtration systems are under-
taken to certify conformance with Standards Laboratory requirements.
Although programs are of interest to other plant sites under Energy
Research and Development Administration contracts,* limited data
are available. The function of filters in air systems must be
fully effective to provide data on air contamination to assure
personnel and environmental safety. Filters purchased from
suppliers are inspected to assure compliance with criteria estab-
lished. During the past year, filters from three principal
suppliers, X, Y, and Z, were examined.

DISCUSSION

Test Procedures

Some 8,000 filters classified as Size 5 (2 by 2 by 1-foot), high
efficiency particulate air (HEPA) components were tested. The
tests are performed on a modified penetrometer, Q-107, manufactured
by Air Techniques, Baltimore, Maryland. All HEPA filters are
tested by their rated flows of 1000 cubic feet per minute (cfm)
using a dioctylphthalate (DOP) aerosol. The DOP is controlled at

---

*Humphrey Gilbert. "The Filter Test Program, and Installation
Manual, and Filter Research." Paper presented at the Seventh Atomic
Energy Commission Conference, Brookhaven National Laboratory, New
York. October 10-12, 1961.

a particle size of 0.3 micrometres (μm). At the same time, the resistance or pressure drop is noted. Classified as rejects are: (1) filters that exceed a penetration of 0.03 percent of the 0.3 μm particle; (2) those that exceed a one-inch pressure drop; (3) those that are damaged out of square or for other mechanical defects; and (4) those that do not meet filter media specifications. Reject filters are destroyed and replaced by the manufacturer as advised.

To indicate the various phases of testing, categories of rejects have been established. The bar graph of Figure 1 shows the percentage of filters rejected every six months, excluding carrier damage. In Figure 2, data are given on the percentage of rejects on a 6-month basis of filters supplied by Manufacturer X. Table I shows the rejects by category.

TABLE I. Number of Manufacturer X Rejects by Category.

Category	1974 Sep-Dec	1975 Jan-June	1975 June-December	1975 January-June
High Penetration	14	29	95	*7
Hole in Media	6	4	5	
Unusual Damage	2	9	6	
Handling Damage			3	

*Decline relates to manufacturer cooperation to improve filters.

Figure 3, shows the percentage of rejects on a six-month basis of filters supplied by Manufacturer Y. Table II shows the rejects by category.

TABLE II. Number of Manufacturer Y Rejects by Category.

Category	1975 July-December	1976 January-June
High Penetration	61	10
Hole in Media	5	0
Unusual Damage	1	0
Handling Damage	2	
Loose Pack	1	3
Banding Damage		6
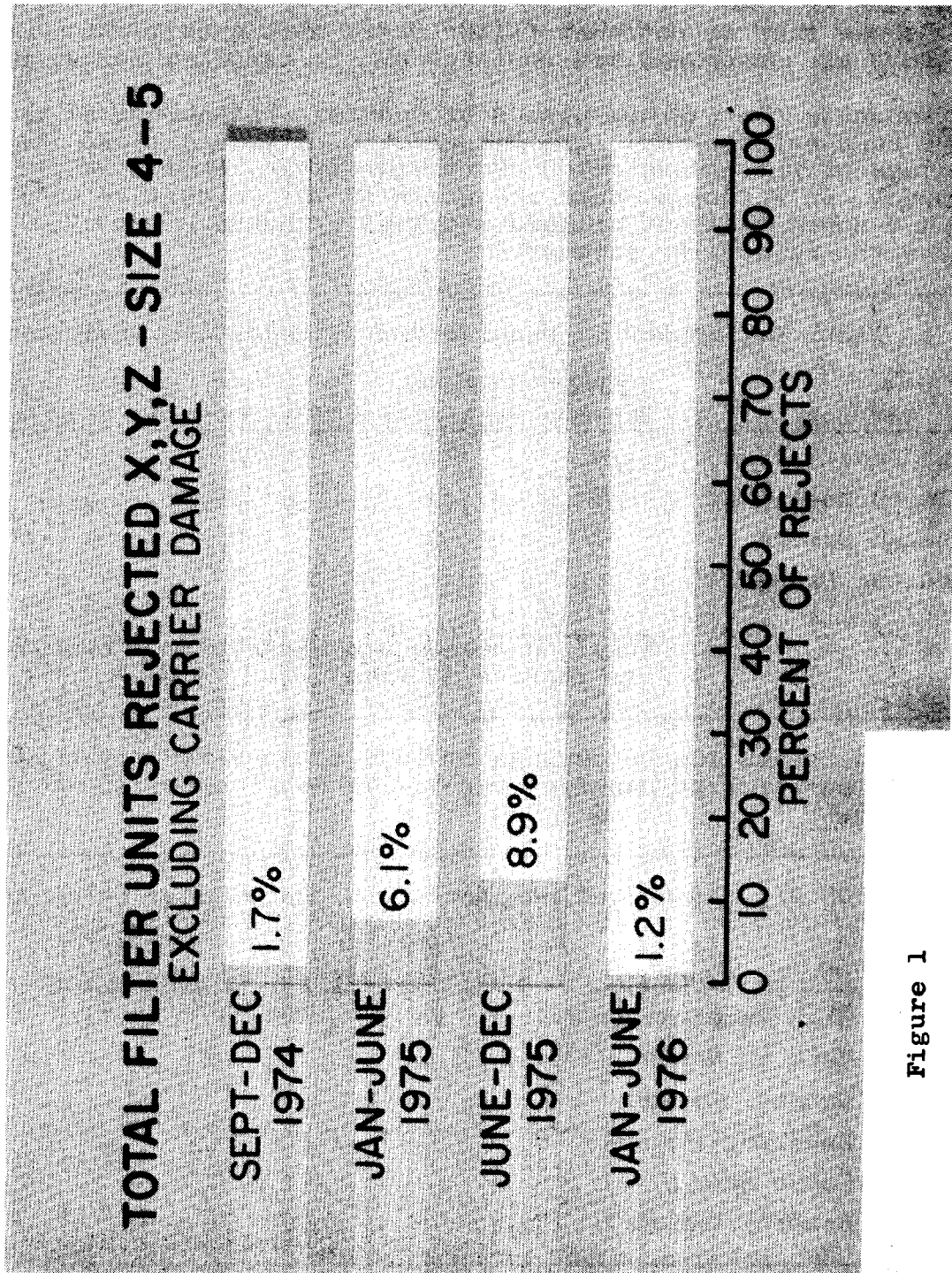
Figure 1

REJECTIONS OF MANUFACTURER X-SIZE 5
ALL CAUSES

SEPT-DEC
1974   1.7%

JAN-JUNE
1975   3.9%

JULY-DEC
1975   6%

JAN-JUNE
1976   .003%

0   10   20   30   40   50   60   70   80   90   100
PERCENT OF REJECTS
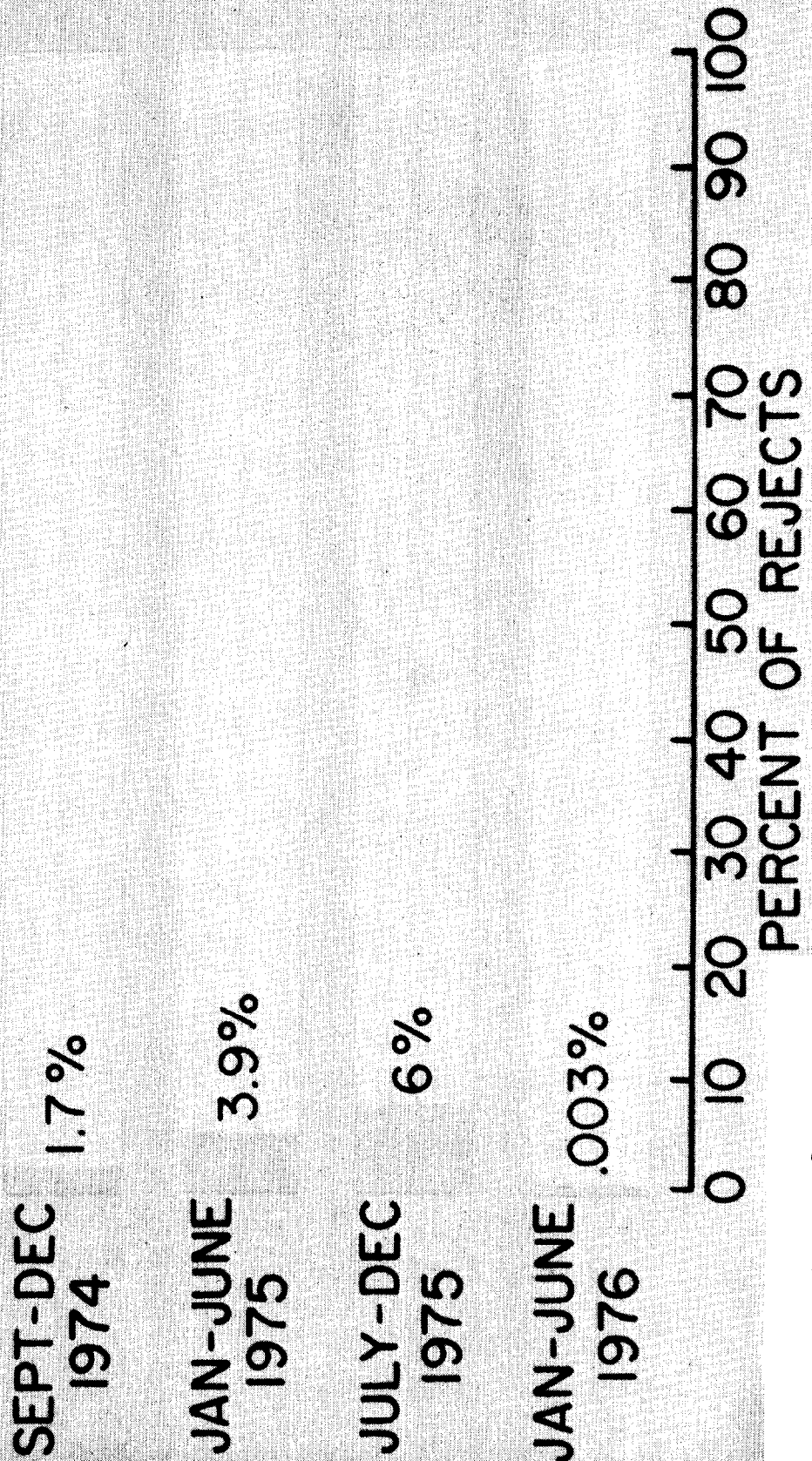
Figure 2

REJECTS BY CATEGORY - MANUFACTURER X

	HIGH PENETRATION	HOLE IN MEDIA	HANDLING DAMAGE	UNUSUAL DAMAGE	UNITS SHIPPED	PERCENT REJECTS
SEPT - DEC 1974	14	6		2	1292	1.7
JAN - JUNE 1975	29	4		9*	1060	3.9
JULY - DEC 1975	95	5	3	6*	1810	6
JAN - JUNE 1976	7				1838	.003

*SLITS IN MEDIA

Table I

REJECTIONS BY MANUFACTURER Y
ALL CAUSES

JULY-DEC 1975 — 10%

JAN-JUNE 1976 — 5%

PERCENT OF REJECTS

0 10 20 30 40 50 60 70 80 90 100
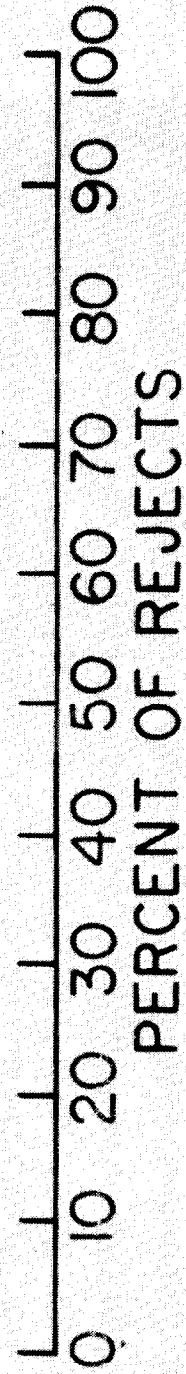
Figure 3

REJECTS BY CATEGORY - MANUFACTUER Y

	HIGH PENETRATION	HOLE IN MEDIA	HANDLING DAMAGE	LOOSE PACK	UNUSUAL DAMAGE	UNITS SHIPPED	PERCENT REJECTS
JULY - DEC 1975	61	5	2	1	1	737	9%
JAN - JUNE 1976	10			3	6*	378	5%

*BANDING DAMAGE

Table II

Figure 4 shows the percentage of rejects on a 6-month basis of filters supplied by Manufacturer Z. Table III gives the rejects by category.

TABLE III. Number of Manufacturer Z Rejects by Category.

Category	1975 January-June	1976 January-June
High Penetration	3	4
Hole in Media	4	2
Unusual Damage	1	0
Handling Damage	0	0
Loose Pack	8	2
Out-of-Square	9	2

Of the manufacturers, X, Y, and Z, one has given continuous authorization to destroy all filter units which were rejected for high penetration. The other manufacturers usually give permission after being notified of rejections.

Manufacturer X

The percentage of rejects from Manufacturer X from September 1974 to December 1974 was 1.7 percent. Examination of the reject usually pinpointed the problem, and little or no action was required.

It was not until the July-December 1975 reporting period that the reject rate increased by 20 percent over the September-December 1975 reject rate. Manufacturer X was notified of the finding. One rejected filter was then destroyed and the media tested to specification MIL-F-51079B. Findings were as follows:

1. High penetration
2. Cross machine tensile below specifications
3. Low pressure drop

Random samples of media were tested from other rejected filters. Manufacturer X was notified and corrective action was taken. Since that particular time period, Manufacturer X has had several shipments with zero rejects.

Manufacturer X later produced a special filter for use at Rocky Flats, but the reject rate was high. By cooperation between the manufacturer and user, the cause for the reject was isolated. The method of sealing the pack to the frame was such that any small deflection in the frame would cause the seal to crack. The manufacturer suggested a new sealant be used, since this was a special use filter. It was required that a complete test be made on the sealant. The sealant was approved, and the reject rate has since dropped to zero.

REJECTIONS BY MANUFACTURER-SIZE 5
ALL CAUSES

JAN-JUNE
1975   75%

JAN-JUNE
1976   5.7%
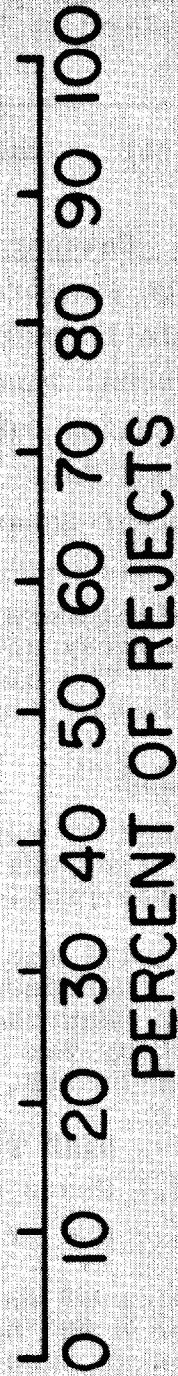
PERCENT OF REJECTS

Figure 4

REJECTS BY CATEGORY / MANUFACTURER Z

	HIGH PENETRATION	HOLE IN MEDIA	LOOSE PACK	OUT OF SQUARE	UNUSUAL DAMAGE	UNITS SHIPPED	PERCENT REJECTS
JAN - JUNE 1975	3	4	8	9	1	33	75%
JAN - JUNE 1976	4	2	2	2		175	5%

Table III

Manufacturer Y

Manufacturer-Y rejects were directly related to two causes, media and shipping damage. For the six-month period, July-December 1975, Manufacturer-Y rejects were directly traceable to defective media. Proceeding in the same manner as with those of Manufacturer X, tests were made on media samples. Although the media were marginal, they alone did not account for the high percentage of rejects. (See Figure 5.)

Not until the entire pack was removed from a filter, was a crease observed randomly which went along the length of the media. Samples were tested at the creased area and a high penetration was observed. Also at the crease was a thin detachment or delamination of the media. Samples of this media were sent to the Rocky Flats Service Laboratory. The samples were examined by 2000X magnification in the same general area. (See Figures 6 and 7.)

The detached film of Manufacturer Y had no binder present although the main section showed evidence of binder. Other rejected filters were disassembled and the same crease was found. The manufacturer's Quality Control Group was notified of the findings. They were unaware of the crease and could not determine how the defect could have occurred.

The question was: How many filters or rolls of media were affected? Through the use of lot numbers, the manufacturer was able to determine that all the media which could have the defects were used. The Plant was informed as to the serial numbers of the filters using that particular media lot, and was able to locate those filters and verify further that they had been tested and were rejects. These filters had been tested previously by the manufacturer and determined to be acceptable. Either through handling or shipping, a strain had been placed on the creased area causing the filter to fail.

Further discussions with the Quality Control Group of the Manufacturer revealed the following:

1. It was established that the media had been on hand for a long period of time.

2. The defective media had not been observed when the filters were manufactured.

This defect in the media was evaluated by two known filtration experts, and it was determined that the crease had occurred when the manufacturer produced the media.

For the six-month period, January-June 1976, Manufacturer Y shipped several loads. Each load of filters in individual cartons was banded and palletized. Rocky Flats normally receives loads in a nonbanded condition whether it be a full load or short load. In this instance, the banding of the load created the majority of the rejects consisting of broken frames, scraped media, out of square, and loose packs.
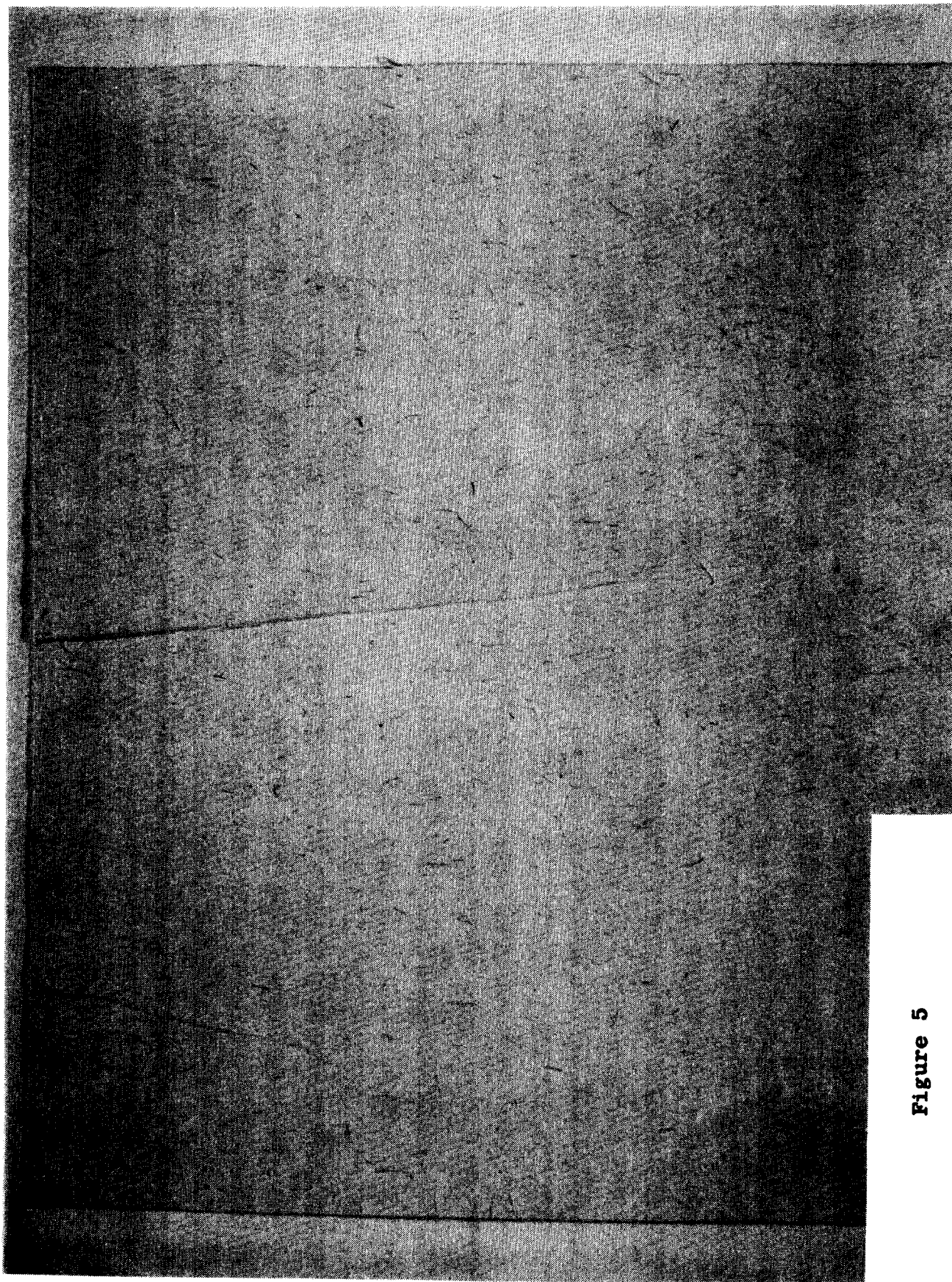
Figure 5
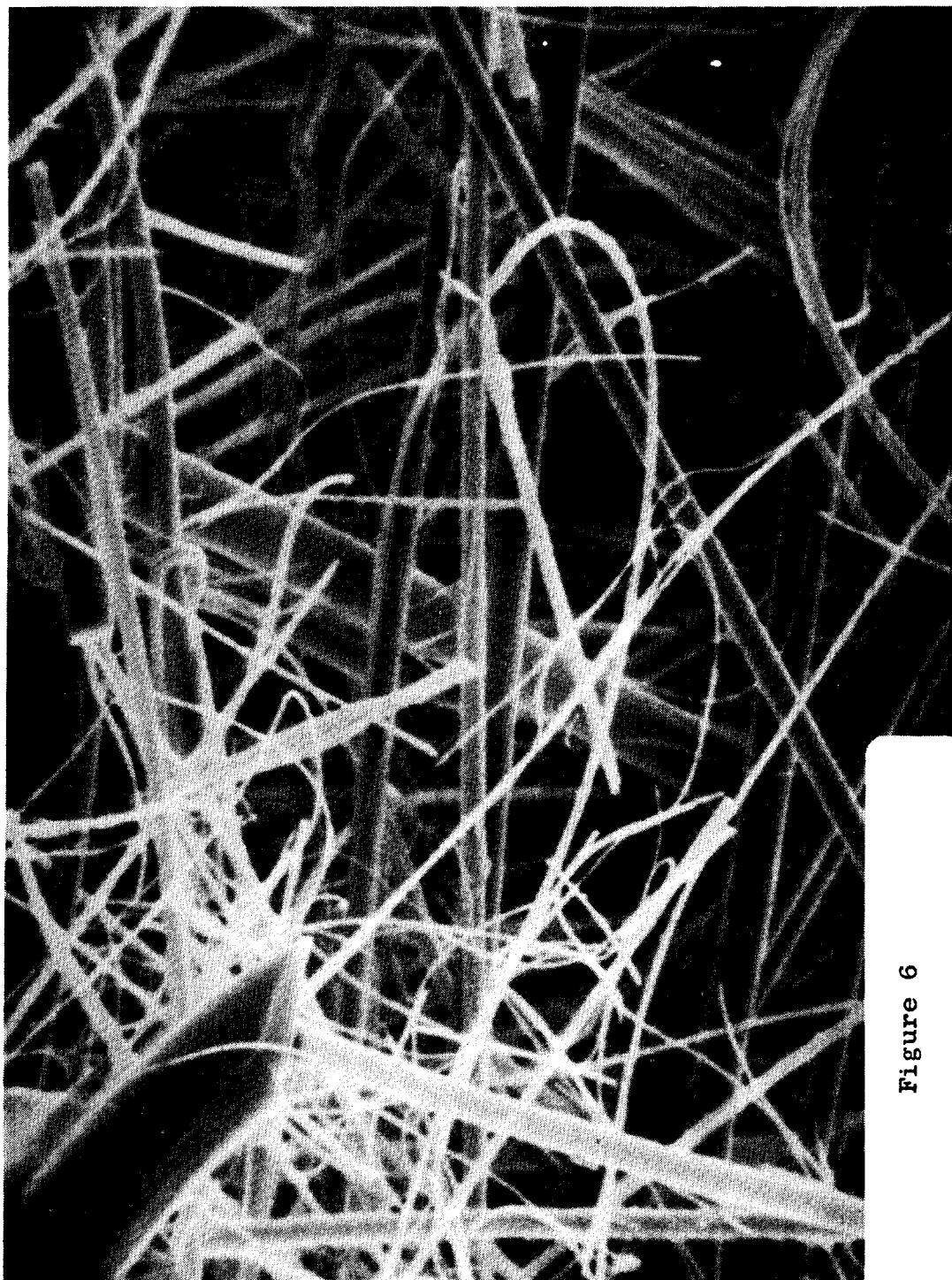
Figure 6

Figure 7

The Rocky Flats shipping procedure is as follows:

1. Full loads (320 to 340 filters) are shipped in an exclusive use trailer which is sealed by the manufacturer and routed directly to Rocky Flats. Once the trailer is on its way, it will arrive at Rocky Flats four to five days later.

2. Partial loads are loaded into a trailer and shored to prevent shifting or damage.

For over a year, the other Manufacturer, X, has shipped in this manner, with no shipping damage.

Manufacturer Z

Manufacturer Z has supplied Rocky Flats with only a token shipment of Size 4 and 5 filters during the reporting periods. From this amount, a trend was noted that could prevent future problems. Investigations into the cause for rejects by Manufacturer Z were conducted on the filter media. Differences arose between manufacturer and user on requirements for media to meet on test experiments. Basically, the disagreement was over tensile and penetration values. In addition, the media from Manufacturer Z was also found thinner than the 0.015-inch thickness in a predominance of cases.

Other than media quality, Manufacturer-Z rejects fell into three categories:

1. Filter being out of square

2. Loose packs

3. Gasket problems, either missing or not glued properly

The manufacturer and user have been cooperating to correct the deficiencies as soon as feasible.

Because of chemical contamination of some air streams, asbestos separators are required in filters for Rocky Flats plant. Better asbestos separators have been needed in the ERDA program for many years. The Plant derives much satisfaction in the report that two of the filter manufacturers are producing satisfactory asbestos separators for filters. There is also some optimism for further improvement in separators to resist chemical exposure. (See Figure 8.)

CONCLUSIONS

Referring to the paper by Humphrey Gilbert (see our Introduction Footnote), his data on percentage of rejects to the current percentages were compared by averaging his percentage from January 1960 to June 1961. The reject rate showed a decrease from 10.5 to 4 percent. The trend currently reflects on the continued cooperation being made to improve the HEPA filter.
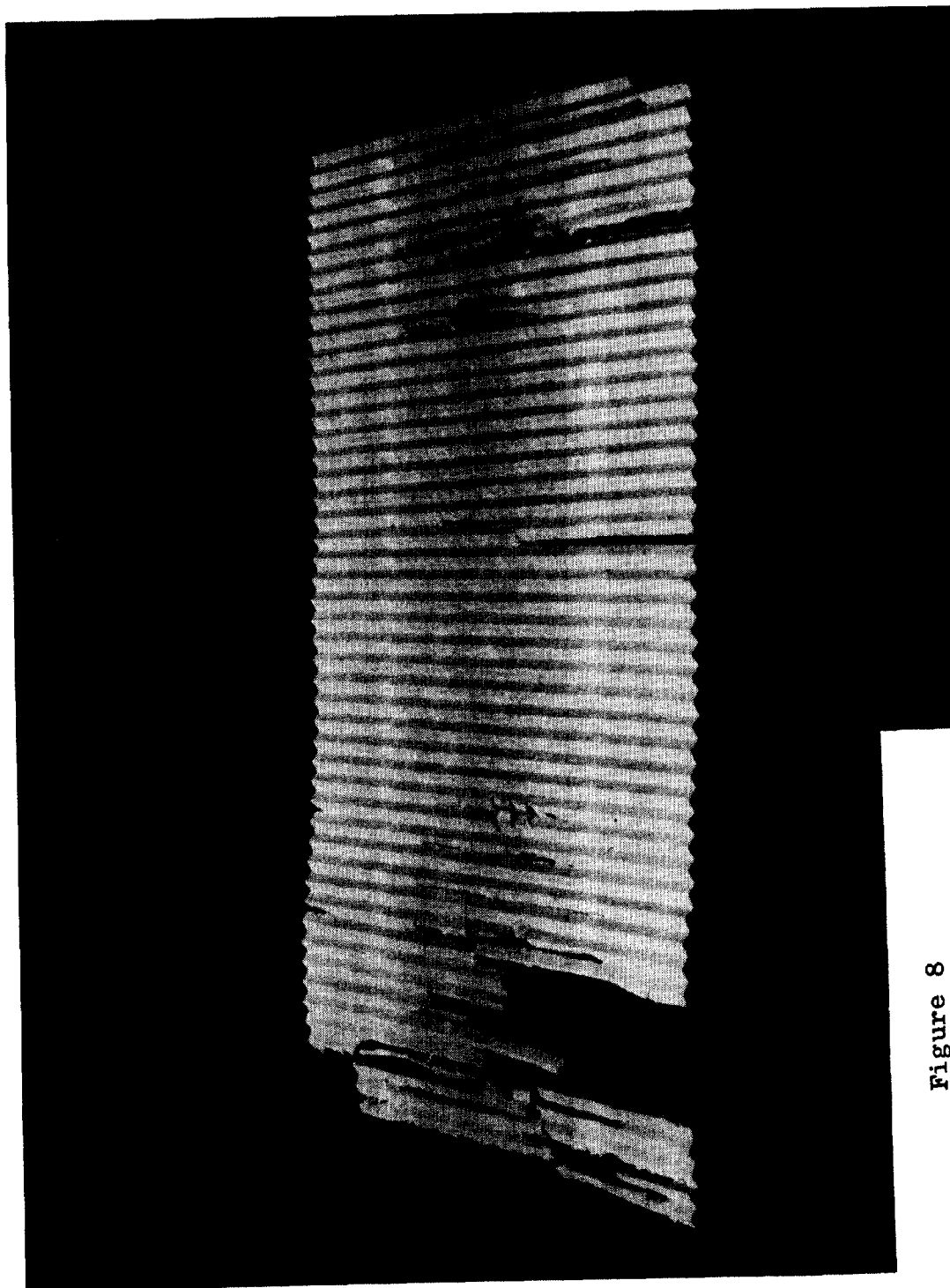
Figure 8

The decline in rejects for the period January-June 1976 (see TableI) indicated that manufacturers can produce an improved quality filter. Rocky Flats will continue to examine reject filters and data from those rejects will be relayed to respective manufacturers toward development of even better quality in filters.

Rocky Flats Plant does not wish to become a quality control unit for a manufacturer. However, since a reject at Rocky Flats can prove costly at the place of manufacture, the intent is to assist the manufacturer in resolving any problems as expeditiously as possible. This will assure a continued supply of inexpensive high quality filters for plant use.

Representatives from the three manufacturers (X, Y, and Z) have visited the test facility on several occasions to review defects or discuss problems that have occurred with their products. In most cases, the representatives have been appreciative of the test methods and the thoroughness of the filter testing program. With the ever-increasing cost of the filter, the enlarging demand for protection of the environment, and the pressing need to assure a quality product to provide protection, the certification group considers that continued investigations have merit for both supplier and user.

DISCUSSION

EDWARDS: First time I ever wanted to be Brand X. Do you have any information to indicate that the other test facilities are having the same kind of trends that you're having now, Mr. Skaats, at Rocky Flats?

SKAATS: I have seen some of the reports from some of the other test stations. They indicate reject rates similar to ours. We have found this out by talking with the Hanford or Oak Ridge test stations and from reports that Mr. Dempsey sends me.

DEMPSEY: I wonder if you have determined what percentage might be from shipment and what percentage from inherent defects?

SKAATS: In most of the shipments, we find the defect. Manufacturer X has had no problems with shipment. Manufacturer Y's problem was with banding. Their bands were too tight. I think this is very important as they crush the frames. With Z, we have not had enough experience. Their shipments have only been small filters which were packed very nicely. We've had no shipping damage. If handled properly and if the manufacturer bands them properly, the filters should come through in good shape.

DEMPSEY: I would like to thank you for the excellent paper you presented and I want the audience to know what Mr. Skaats was requested by the Program Committee to present this particular topic.

HEPA FILTER PERFORMANCE COMPARATIVE STUDY

C. A. Gunn and D. M. Eaton
Filter Applications Engineering
Mine Safety Appliances Company
Evans City, Pennsylvania 16033

Abstract

Current products such as HEPA filters made without separators, with tapered separators and with mini separators have raised many questions for the Nuclear Ventilation System Design Engineer and/or the end user. The principal objective of this investigation is to report HEPA filter performance data and to compare the effectiveness of the various type HEPA filters for use in Nuclear Ventilation Systems with all tests run on the same equipment and under the same controlled conditions.

I. Introduction

As nuclear plants become larger and more numerous, great emphasis is being placed on improved, high performance ventilating systems. Under either accident situations or during routine operation, efficient and dependable air cleaning systems are required if nuclear release limits are to be met. As a result of the California referendum, increasing public awareness, and low as practical release limits, it is essential today to have a complete knowledge of HEPA performance to design a safe and reliable system.

The ability of HEPA filters to remove radioactive contamination in the form of particulates has been investigated by others. However these past studies have been limited to either specific removal systems using standard HEPA filters or have been conducted on well controlled manufactured units. This investigation was conducted on production models in which the tests were all conducted under essentially the same conditions.

The Nuclear Ventilating System Design Engineer needs to know if the type of HEPA filter he is going to use will function after exposure to postulated conditions which could occur in his particular system. The filter can be exposed to steam-air atmospheres for extended periods of time during a design basis accident; to heavy entrained water loadings as a result of spray activation; to excessive overpressures resulting from local tornadoes or inadvertent damper closing; to excessive heat due to fires, and to a possible seismic event. Based on this background and the many questions from designers and end users about filter performance, comparative tests were conducted on various types of filters to determine:

1. HEPA Filter integrity after exposure to abnormal conditions
2. HEPA Filter service life
3. Particle size penetration

HEPA filters were obtained at random from various vendors. The types of filters tested are shown in Figures 1.A through 1.E and can be described as follows:

1.A The Type A Separatorless Filter is formed from glass filter medium molded and formed into a corrugated shape and then folded back and forth on itself so that it becomes self-supporting. No separators are used. Estimated medium area is about 250 square feet. Manufacturer's rating is 1500 CFM @ 1" W. G. resistance.

1.B The Type B Separatorless Filter contains sixteen individual filter panels arranged in a vee shaped pattern and sealed into an outer metal retaining frame. The individual filter panels consist of a sheet metal frame containing pleated filter medium. Pleat depth is about 3/4 of an inch. Folds are spaced and retained in position by glass thread attached to the media surfaces in accurately located lines normal to the pleats so that when folded only string contacts string. Estimated filter media area is about 320 square feet. Manufacturer's rating is 1765 CFM @ 1" W. G. resistance.

1.C The Type C Tapered Separator Filter is constructed by folding glass filter medium over tapered aluminum separators. The separator is tapered from the front face of the filter to the rear of the fold. Net result is a filter medium pleat which is vee shaped. Estimated filter media area is about 250 square feet. Manufacturer's rating is 1320 CFM @ 1" W. G. resistance.

1.D The Type D Mini Separator Filter rated 1500 CFM is constructed by folding glass filter medium over standard design corrugated aluminum separators whose height has been decreased to permit the use of about 300 square feet of filter medium. Manufacturer's rating is 1500 CFM @ 1.2" W. G. resistance.

1.E The Type E Standard Separator Filter is constructed by folding glass filter medium over standard design and standard height separators. Filter media area is about 240 to 250 square feet. Manufacturer's rating is 1000 CFM @ 1.0" W. G. resistance.

II. HEPA Filter Integrity After Exposure to Postulated Abnormal Conditions

Heavy Entrained Water Loading Tests

Test conditions were maintained as follows:

Test Conditions	Test Requirements
1. Temperature	$95° \pm 5°F$
2. Relative Humidity	95% Minimum
3. Rate of Air Borne Water Droplets Flowing Toward the Filter	1-1/4 pounds per minute per 1000 CFM of nominal rated filter capacity
4. Pressure Differential across filter	$10.0 \pm .02$ inch water gage

5.	Time to Reach Maximum Pressure Differential	1-1/2 minute maximum
6.	Air Flow	That required to produce 10.0 ± .02 inch water gage differential

Figure 2 is a drawing of the test apparatus and test results are summarized in Table I.* The test duct is approximately 24" wide x 26" high by 48" long. Air flow is once thru. The required air flow is provided by a high pressure blower. Steam is fed into the blower intake to maintain temperature and RH requirements. Water is fed into the system through spray nozzles located an average distance of approximately 18" from the face of the filter under test. As a result, there is direct impingement of water droplets on the HEPA filter, an arrangement which allows for the most vigorous conditions which could be encountered.

The data shows that for heavy entrained moisture loadings, HEPA filters made with separators are structurally capable of performing under these conditions. These results are in agreement with others that corrugated separators add strength to the filter core.[1] Conversely both type separatorless filters failed. Type B failure was marginal or questionable because the initial penetration was .03% or borderline at the start. However, Type A was a definite failure and the results were the same on subsequent tests.

Pictures of the exposed filters are shown in Figures 3A through 3E. Figures 3C, 3D, and 3E show the corrugated separator styles in which there was no visible damage evident. Figure 3B shows the Type B separatorless filter. The circled area is where pin holes developed during the test. Figure 3A shows the Type "A" separatorless filters with heavy structural damage.

Excessive Pressure Tests

These tests were conducted on filters which had first been dust loaded to 4" water gage resistance with ASHRAE test dust** per ASHRAE Standard 52-68. Tests were then conducted in the high pressure test duct shown in Figure 4.

Cottrell precipitate was fed into the system at the rate of 454 grams per minute while maintaining air flow through the filter of 1000 CFM or 1500 CFM. Increase of resistance was noted and an insitu cold generated DOP penetration test was conducted after each 454 grams of dust was fed.[2] Dust loading was discontinued when visible rupture took place at which time a final DOP penetration was measured. Test results are summarized in Table II.

---

* All DOP penetrations reported in the heavy entrained water loading tests were obtained on the Q107 Penetrometer (136-300-175A).
** ASHRAE Standard 52-68 test dust is a specially compounded dust which is 72% by weight Standardized Air Cleaner Test Dust Fine, 23% Molocco Black and 5% ground linters.

An analysis of the data shows that a HEPA filter made with standard configuration separators will give the most reliable performance at pressure drops exceeding 10" water gage. The Type D Mini Separator Filter was dust loaded at 1500 CFM to 30.25" water gage with no sign of visible rupture and with only a small increase of .003 percent in DOP penetration. The Type E Standard Separator Filter was dust loaded at 1000 CFM to 31.25 inches water gage resistance before visible rupture was noted. Final DOP penetration was 6.0 percent; however, the last DOP penetration prior to rupture was .001%. Filter resistance when this measurement was taken was 29 inches water gage. The Type A Separatorless Filter dust loaded at 1000 CFM showed visible rupture at 20" W.G. resistance. DOP penetration was 1.5%. The Type A Separatorless Filter dust loaded at 1500 CFM showed visible rupture at 13.25" W.G. and DOP penetration was 0.06%.

Steam-Air Exposure Tests

These tests were conducted on a separator type filter and a separatorless type filter. Tests were conducted in the MSA Environmental Test Facility described in MSAR 71-45 and shown in Figure 5. (3)

Tests were conducted per the following parameters:

1. Steam Air Volume Flow   1000 CFM
2. Steam Air Temperature   270°F
3. Steam Air Pressure   47 PSIG

The Type D separator type filter was subjected to the above conditions for 24 hours. The filter had an initial resistance of 0.90 inches water gage and an initial DOP penetration* of .001%. After 24 hours exposure the filter had a DOP penetration of .017% and a resistance of .91 inches water gage when tested at 1000 CFM.

The Type A separatorless filter was exposed to the same steam air conditions for 12 hours when visible rupture was noted. The filter had an initial DOP penetration of .006 and an initial resistance of .72 inches water gage at 1000 CFM. After exposure, the filter had a DOP penetration of 24 percent.

III. HEPA Filter Service Life

Filter life was evaluated utilizing the following dust loading tests:

1. ASHRAE 52-68
2. Sodium Oxide Collection

Curves were obtained relating clean filter pressure drop to air flow volumes. All data was obtained on ASHRAE 52-68 test duct. Results are shown in Figure 6.

---

*All DOP penetrations reported in the Steam Air Exposure Tests were obtained on the Q107 Penetrometer (136-300-175A).

Pressure drops at 1000 CFM ranged from .42 inches water gage for the Type B Separatorless Filter to .80 inches water gage for the Type A Separatorless Filter. Pressure drops at 1500 CFM ranged from .70 inches water gage for the Type B Separatorless Filter to 1.20 inches water gage for the Type D Mini Separator Filter and the Type A Separatorless Filter.

ASHRAE 52-68 Dust Loading

ASHRAE 52-68 dust loading curves are shown in Figures 7 and 8. The ASHRAE 52-68 Test Duct is shown in Figure 9. Test air flow is measured using a calibrated, long radius flow nozzle. Test air is brought in from the outside into a large mixing plenum. Dust is fed into the entrance between the large mixing plenum and the main test duct. A dust mixing baffle coupled with high air velocity between the mixing plenum and the test duct insures uniform air dust concentration. This test duct is designed on sound aero dynamic principals which insures accurate air volume measurement and consequent accurate filter resistance measurements.

An analysis of the curves reveals that filter dust holding capacity is determined by initial pressure drop, filter media area and the design configuration of the air passages. Considering those tests conducted at 1500 CFM, the Type B Separatorless Filter had the largest filter media area and the lowest initial pressure drop. However, because of the design of the air passage, its dust holding capacity was essentially the same as the Type D Mini Separator Filter and the Type A Separatorless Filter, both of which had higher initial pressure drops and less filter media area but had a better air passage design.

Sodium Oxide Tests

These tests were conducted to compare dust loadings on finer particulate because this type particulate can be encountered in Nuclear Power Plant Ventilating Systems. Sodium Oxide particles range in size from 1.4 to 2.5 microns mass median diameter as compared to the 4.2 microns mass median diameter of the ASHRAE test dust.[4] The tests were conducted on full size filters in the test duct shown in Figure 10.

A weighed amount of sodium* was placed in a stainless steel pan where burning was initiated by an acetylene torch in the presence of excess air such that the air and all of the resulting smoke was sucked from the pan and discharged through the filter into the atmosphere. Air flow was measured with a standard pitot tube and controlled with a butterfly damper during the test.

Test air volume rate was 1500 CFM. Filters were weighed before and after the test. All filters were loaded to a final resistance of 6 inches water gage. Results are summarized in Table III. The

---

*Sodium in the brick form (as shipped condition) with no attempt made to remove the oxide layer.

results confirm that dust holding capacity depends on initial pressure drop, filter media area and the design configuration of the air passage.

IV. Particle Size Penetration

Particle size penetration measurements were conducted at filter media flow rates ranging from 3 FPM to 28 FPM using homogeneous 0.56, 0.40, 0.30 and 0.16 micron diameter DOP particles. No comparative tests were conducted on the various filter medium because virtually all filter paper is manufactured with glass fibers which have the same spectrum of fiber diameters and lengths. Consequently most filter medium should show the same general particle penetration characteristics.

For the most part, the aerosols of importance to the design engineer are particles <10μ in size and perhaps the major portion are in the sub-micron range. For example, Whitby et al reported that in general 99% by count of atmospheric air particles are ≤1μ with the majority in the sub-micron range.[5] In addition to naturally occurring atmospheric particles, particles in the .005 to 0.1μ size can be present in nuclear ventilating systems due to the oxidation of plutonium, sodium, uranium, zirconium, etc. Langmiur and others have shown the most difficult particles to capture are in the general range of 0.1 to 0.3μ in size.[6]

Test aerosols were formed by the method outlined in the Hand-book of Aerosols, AEC, 1950.[7] Figure 11 shows the apparatus used. Condensation nuclei (NaCl) are formed in the ionizer and mixed with DOP vapor produced in the boiler. The vapor condenses on the nuclei forming a homogeneous, uniform DOP aerosol. Particle size is controlled by varying the ratio of the mass of the condensable vapor to the number of nuclei.

Particle diameters were determined using the angular distribution of color and light polarization methods outlined in the Hand-book of Aerosols. Penetration measurements were made using a NRL linear read out forward scattering photometer.[8]

Test results are shown in Figure 12. One can observe from the family of curves that if the filter medium velocity exceeds the AACC CS-1 recommended velocity of 5 FPM, particle penetration increases significantly.[9] Exceeding the 5 FPM medium velocity decreases the effect of diffusion and reduces collection efficiencies on sub-micron particles as shown in Figure 12, and as also reported by others.[10]

V. Conclusions

As a result of this study it can be concluded that:

1. Separator type filters are stronger than the separatorless type when tested under the same conditions as outlined in this report.

2. Overall HEPA filter performance is significantly improved by maximizing the amount of filter medium with the use of smaller height separators.

3. Particle collection efficiency for glass fiber HEPA medium in the range tested drops significantly when the filter medium velocity exceeds 5 FPM.

Filter Type	Mfg's Rate Flow	*Initial DOP % Pen.	*Final DOP % Pen.	*Increase DOP % Pen.	Test Period
Type "A" Separatorless	1500	.002	100	99.998	4 min.
Type "A" Separatorless Divider	1500	.005	6.0	5.995	5 min.
Type "B" Separatorless	1500	.030	.65	.62	62 min.
Type "C" Tapered Sep.	1500	.006	.030	.024	62 min.
Type "D" Mini Separator	1500	.005	.017	.012	62 min.
Type "E" Standard HEPA	1000	.010	.020	.010	62 min.

*DOP Penetration Tests conducted using Q107 Penetrometer (136-300-175A)

Table I   Entrained water tests.

637

Filter Type	Air Flow CFM	Initial DOP % Pen.	Initial ΔP In. W.G.	DOP Pen. Prior to Visible Rupture %	Final DOP % Pen.	Max. ΔP In. W.G.
Type "A" Separatorless	1000	.001	4.0	0.30	1.5	20.0
Type "E" Standard Separator	1000	.001	4.2	0.001	6.0	31.25
Type "A" Separatorless	1500	.001	4.1	0.012	0.06	13.25
Type "D" Mini Separator	1500	.001	4.0	0.004	0.004*	30.25
					At Visible Rupture	

*No sign visible rupture.

In Situ Cold DOP Penetration Tests (2)

Table II   Excessive pressure tests.

Filter Type	Flow CFM	Initial Wt.		Final Wt. Corrected to 6.0" W.G.		Sodium Oxide Held		Media Surface Area ft²
		lb.	oz.	lb.	oz.	lb.	oz.	
Type "A" Separatorless	1500	30	14	32	6	1	8	250
Type "D" Mini Separator	1500	34	8	37	5-1/2	2	13-1/2	320
Type "C" Tapered Sep.	1500	36	6	37	3-1/2		13-1/2	246

Table III   Sodium oxide smoke loading.
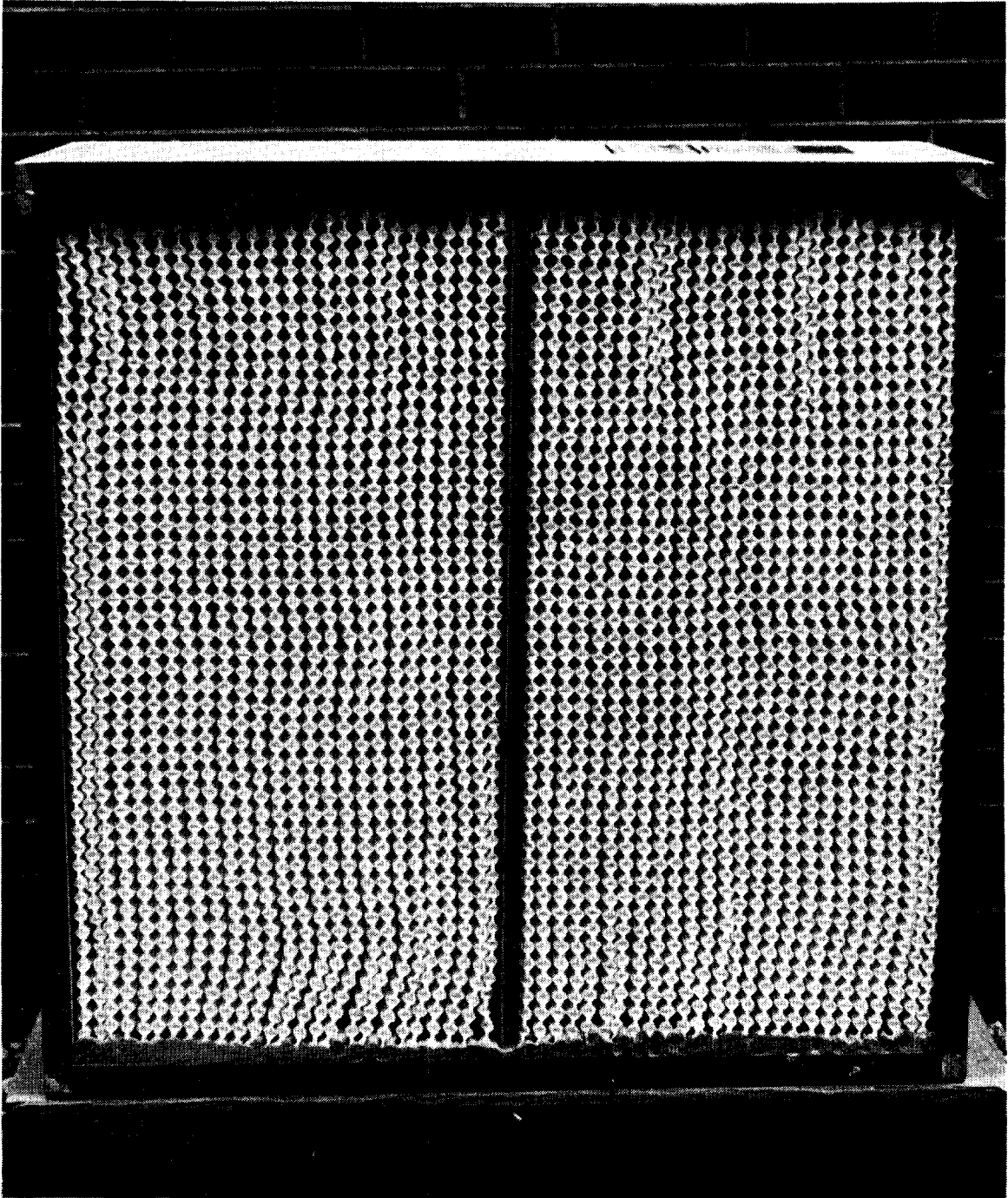
Type "A" - Separatorless Filter
"Figure 1A"
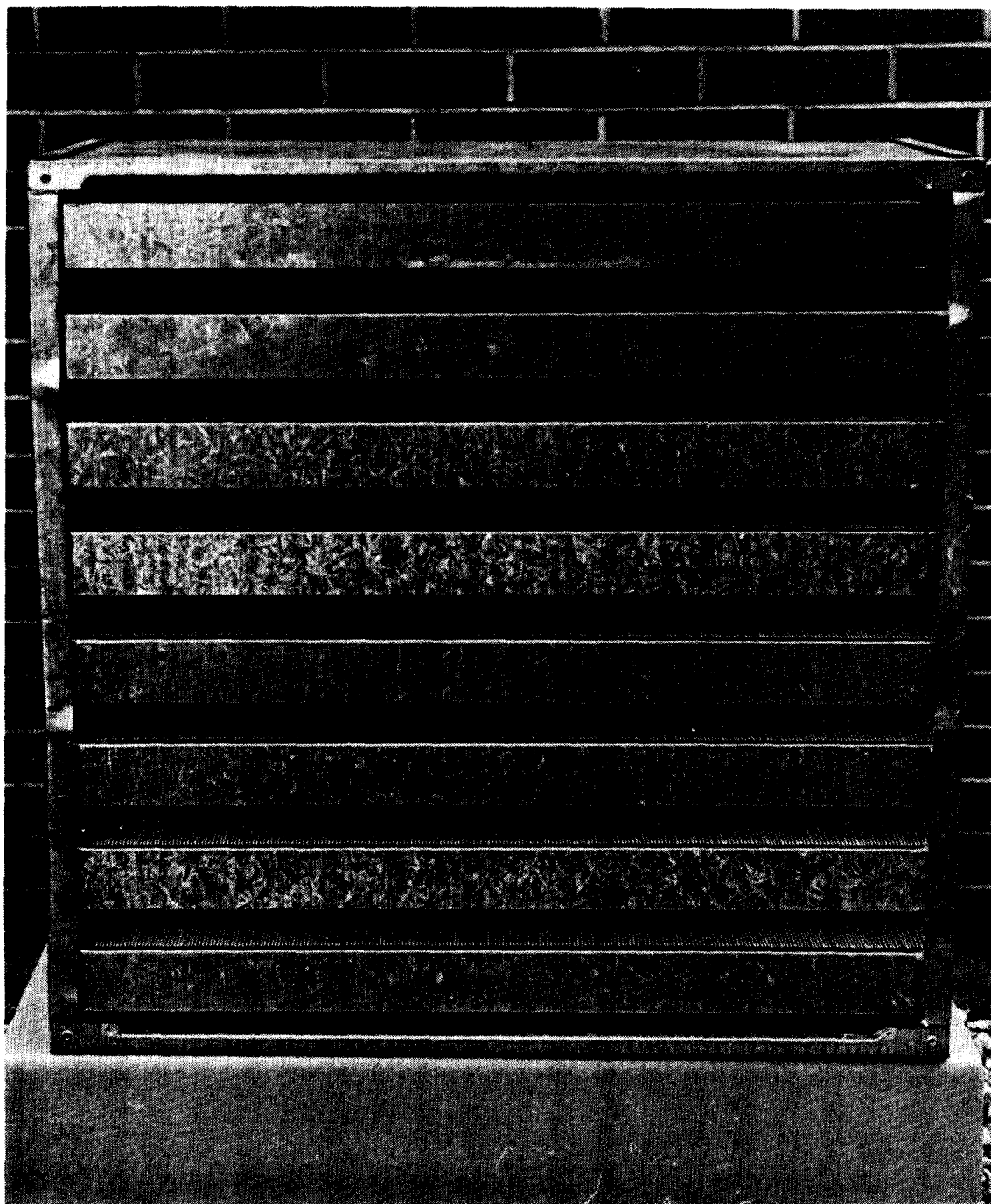
Type "B" - Separatorless Filter
"Figure 1B"
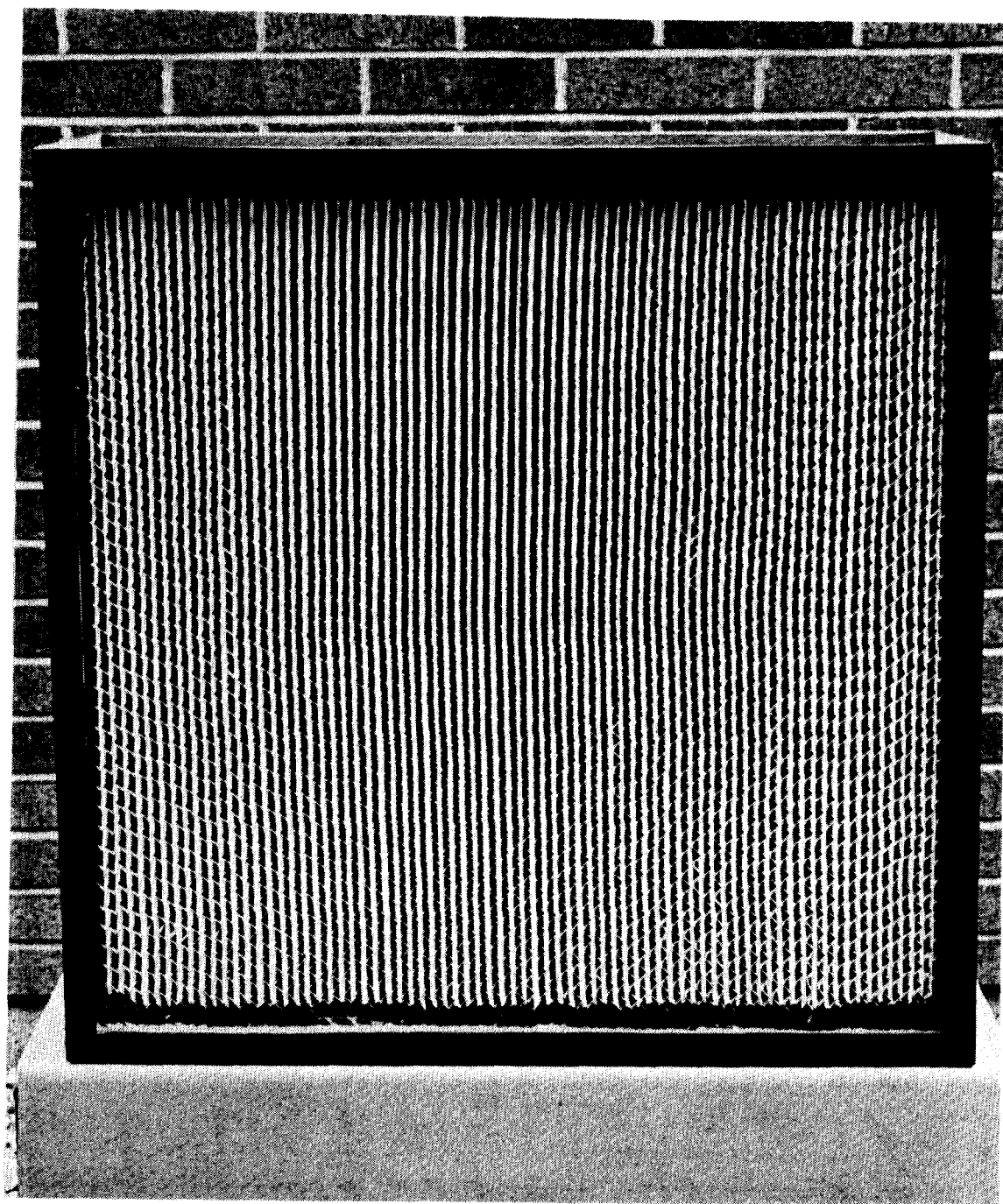
Type "C" - Tapered Separator Filter
"Figure 1C"
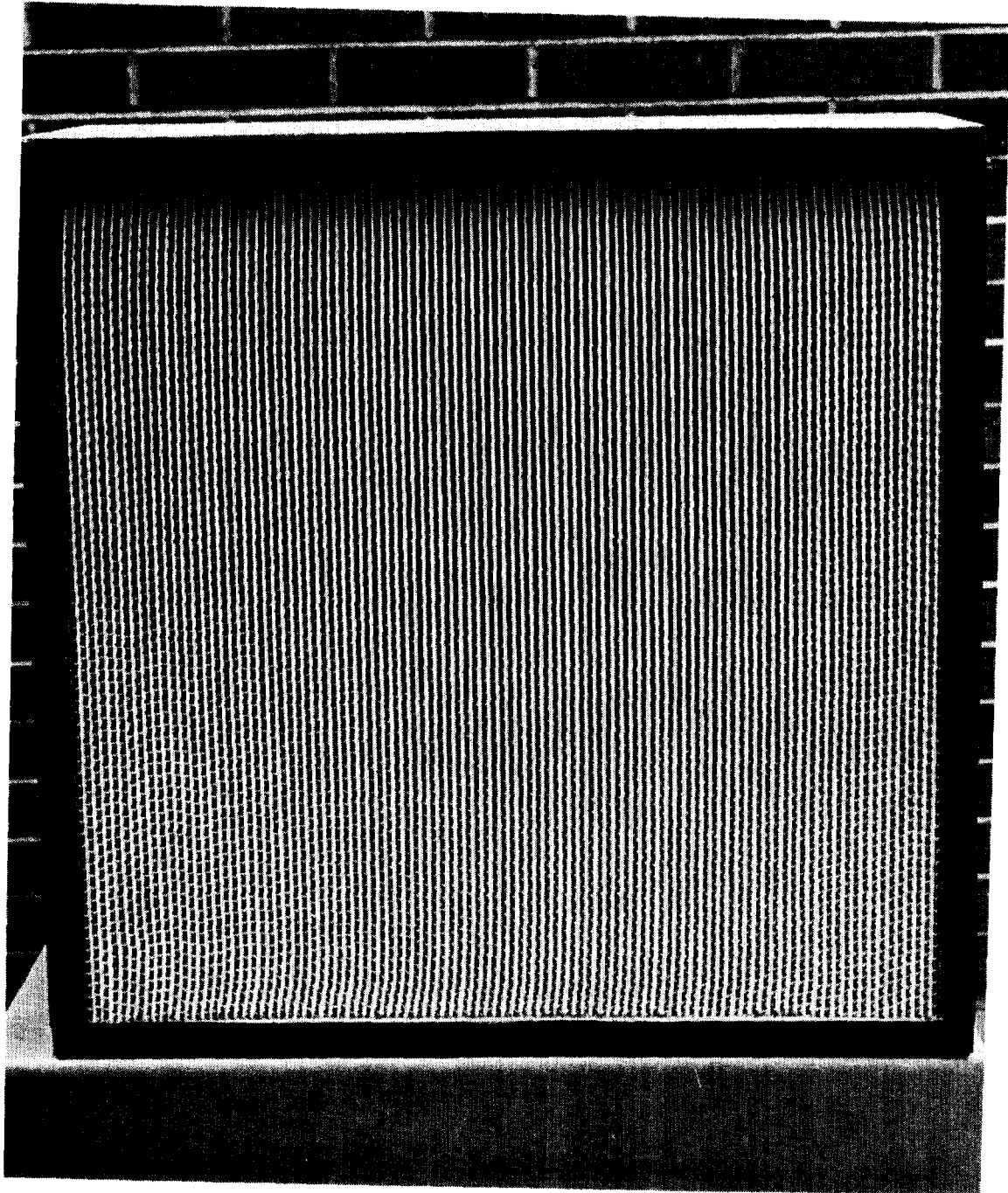
Type "D" - Mini Separator Filter
"Figure 1D"
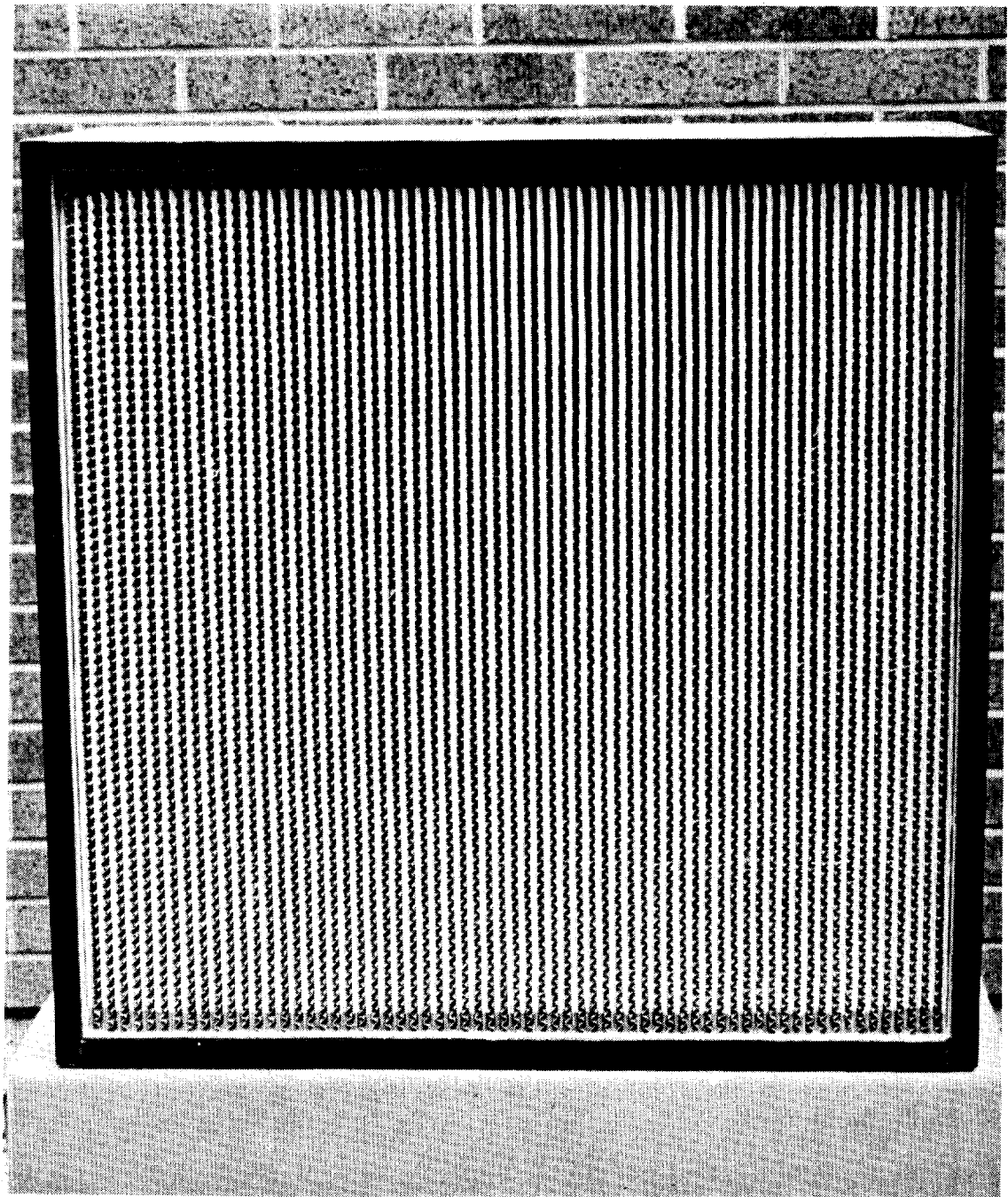
Type "E" - Standard Separator Filter
"Figure 1E"
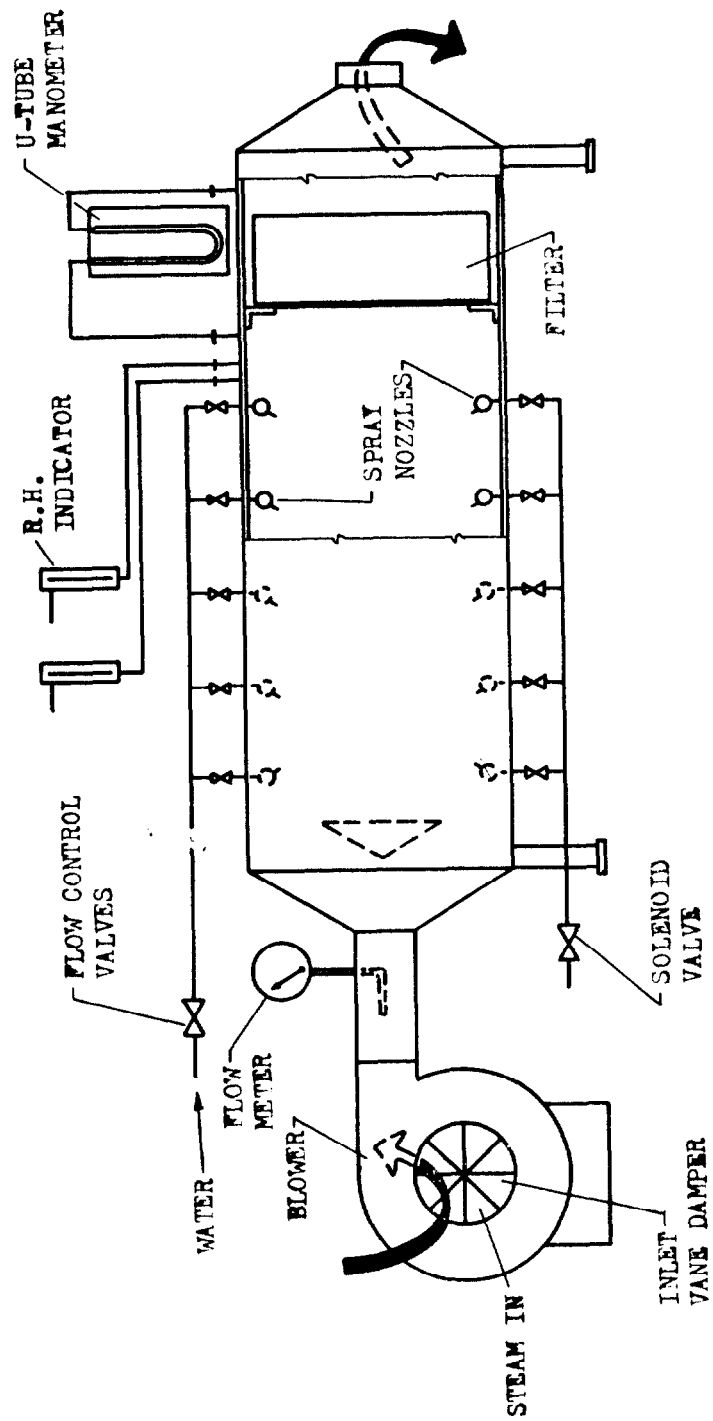
Figure 2   MSA moisture over pressure test system.
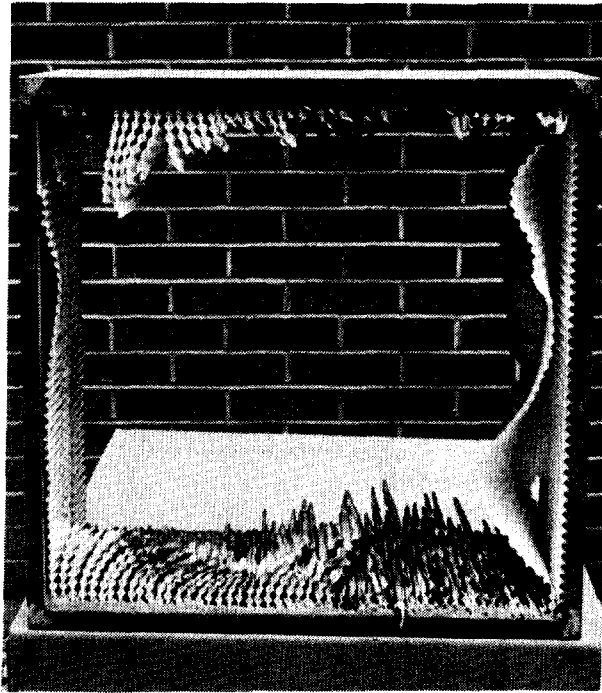
Shows complete blow-out when filter is not supported
by hardware cloth and center separator.
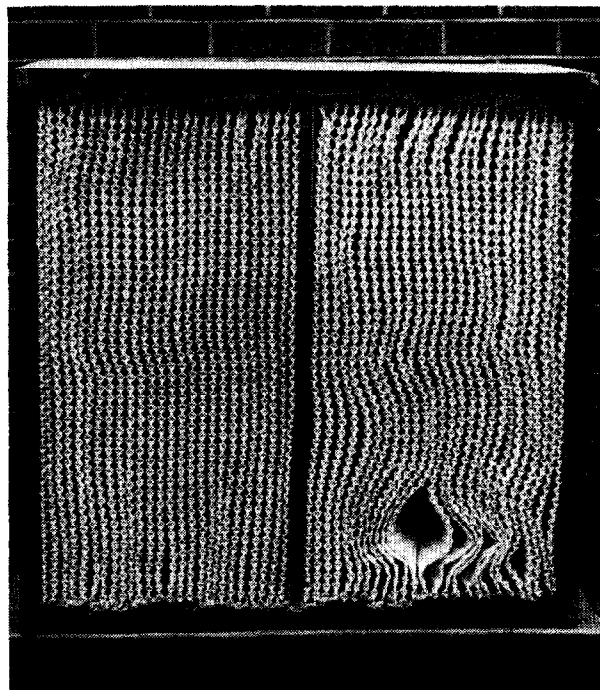
Shows heavy structural damage even when filter is
supported by hardware cloth and center divider.

Type "A" - Separatorless Filter
"Figure 3A"
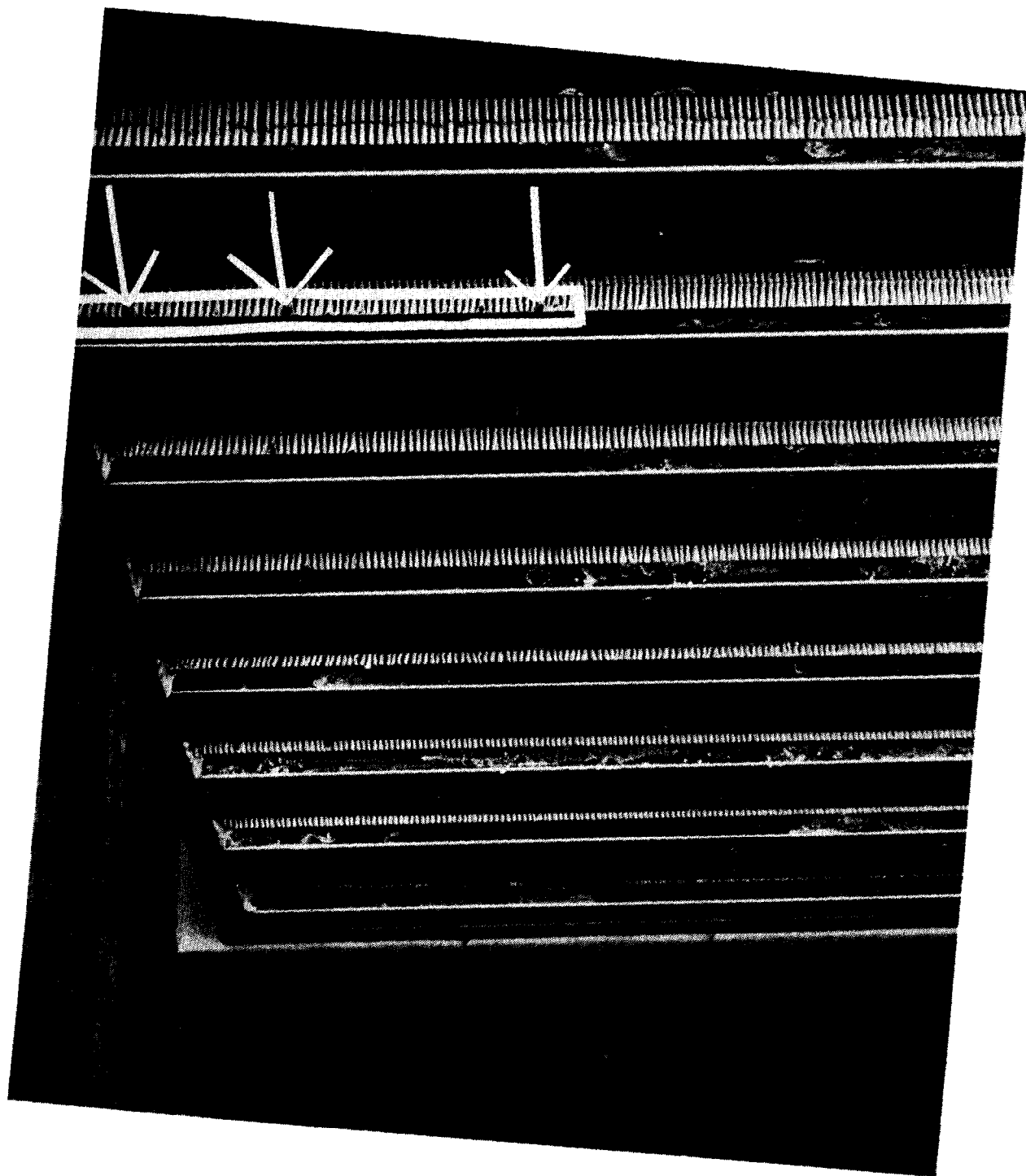
Type "B" - Separatorless Filter
"Figure 3B"
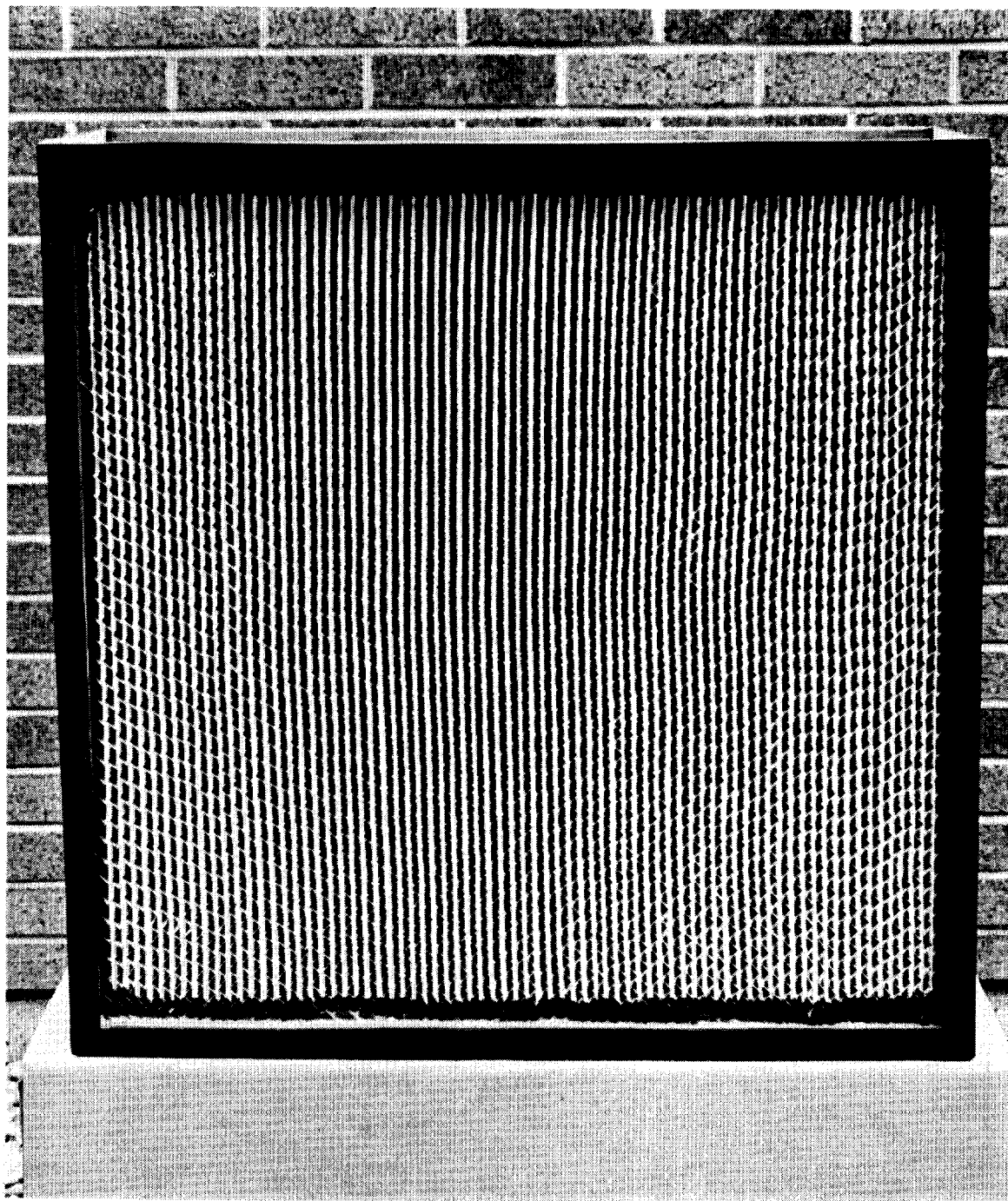
Type "C" - Tapered Separator Filter
"Figure 3C"
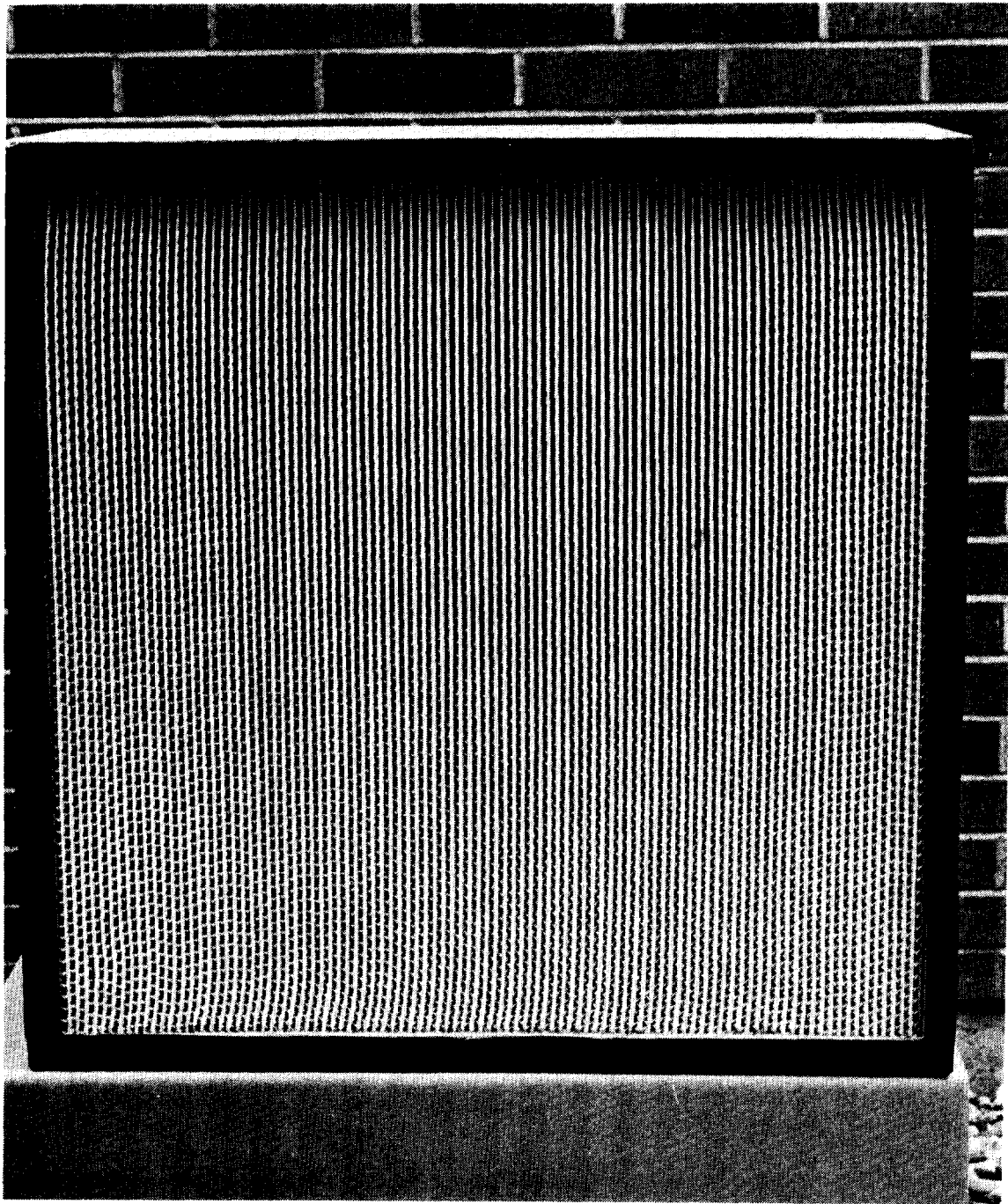
Type "D" - Mini Separator Filter
"Figure 3D"
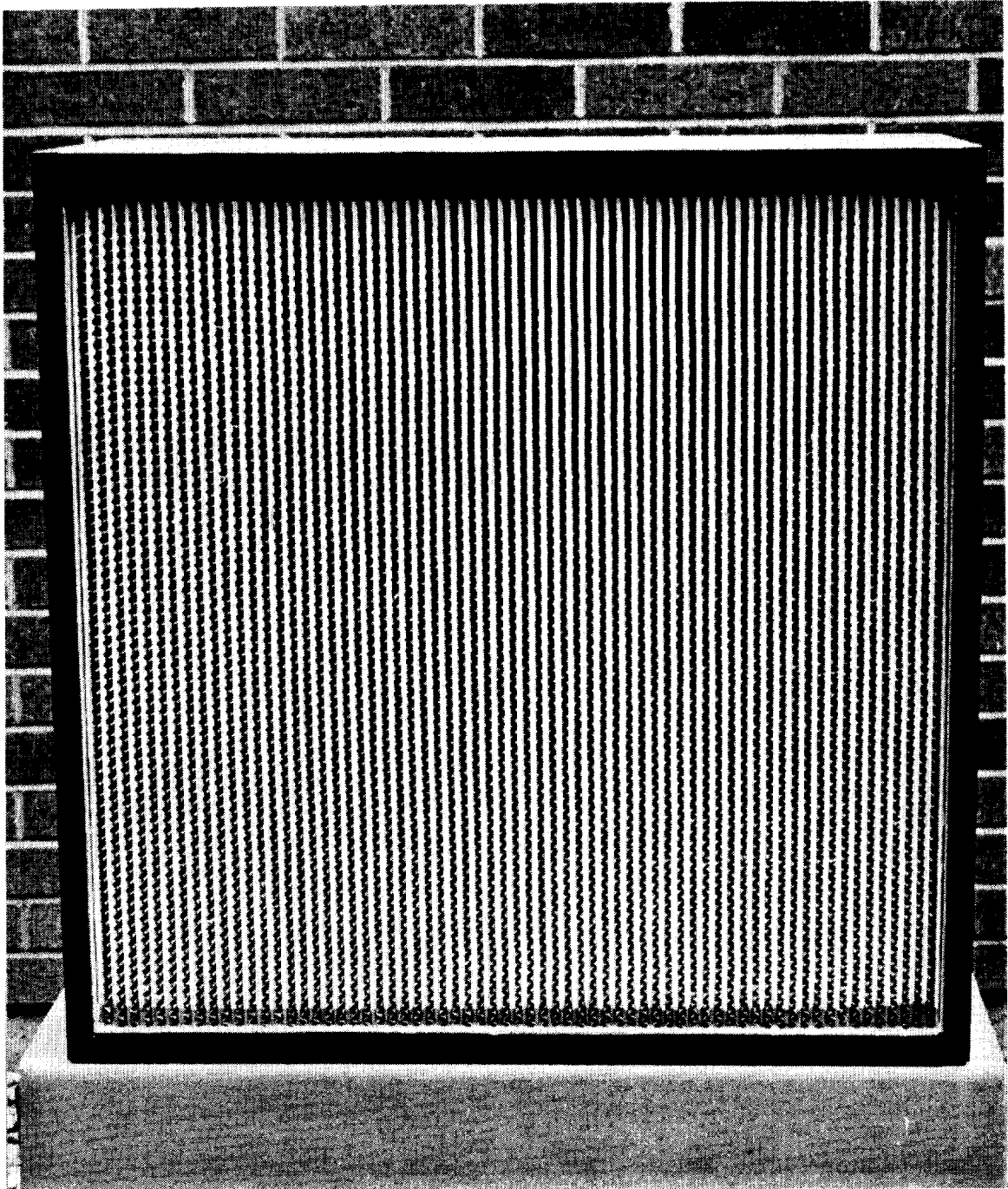
Type "E" - Standard Separator Filter
"Figure 3E"
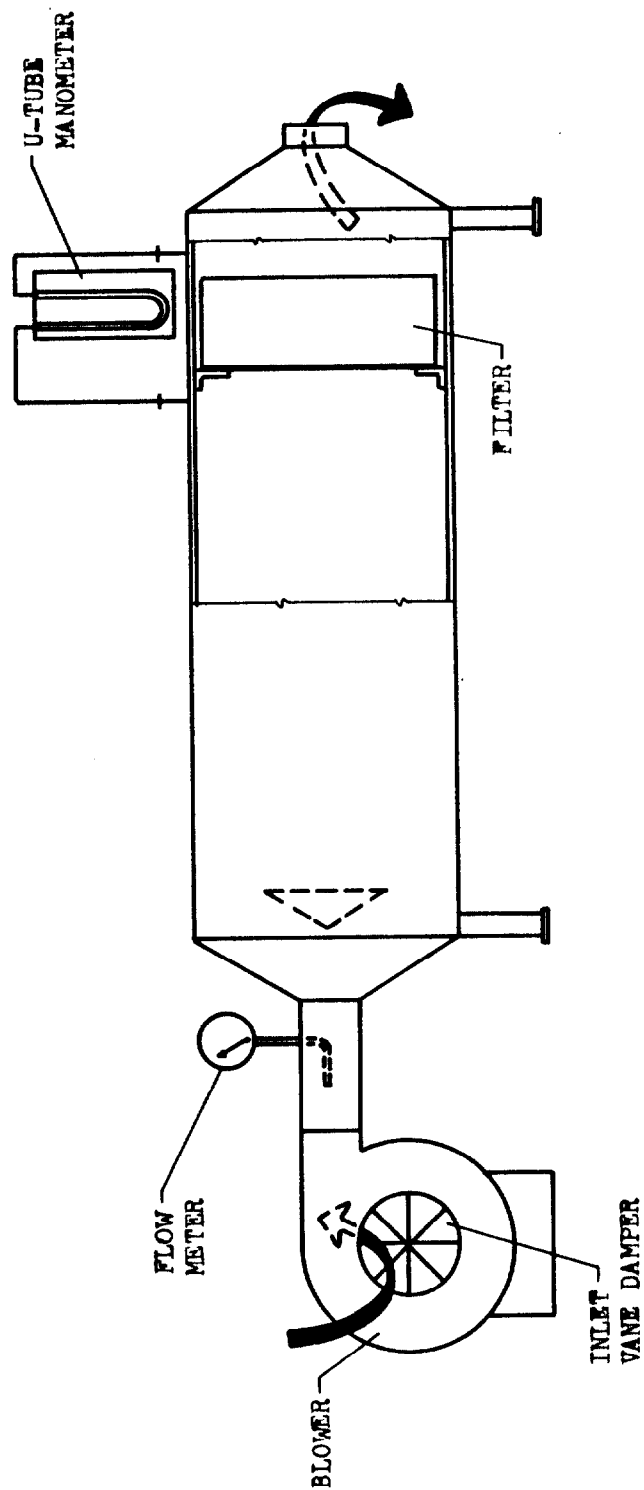
Figure 4   MSA high pressure test system.
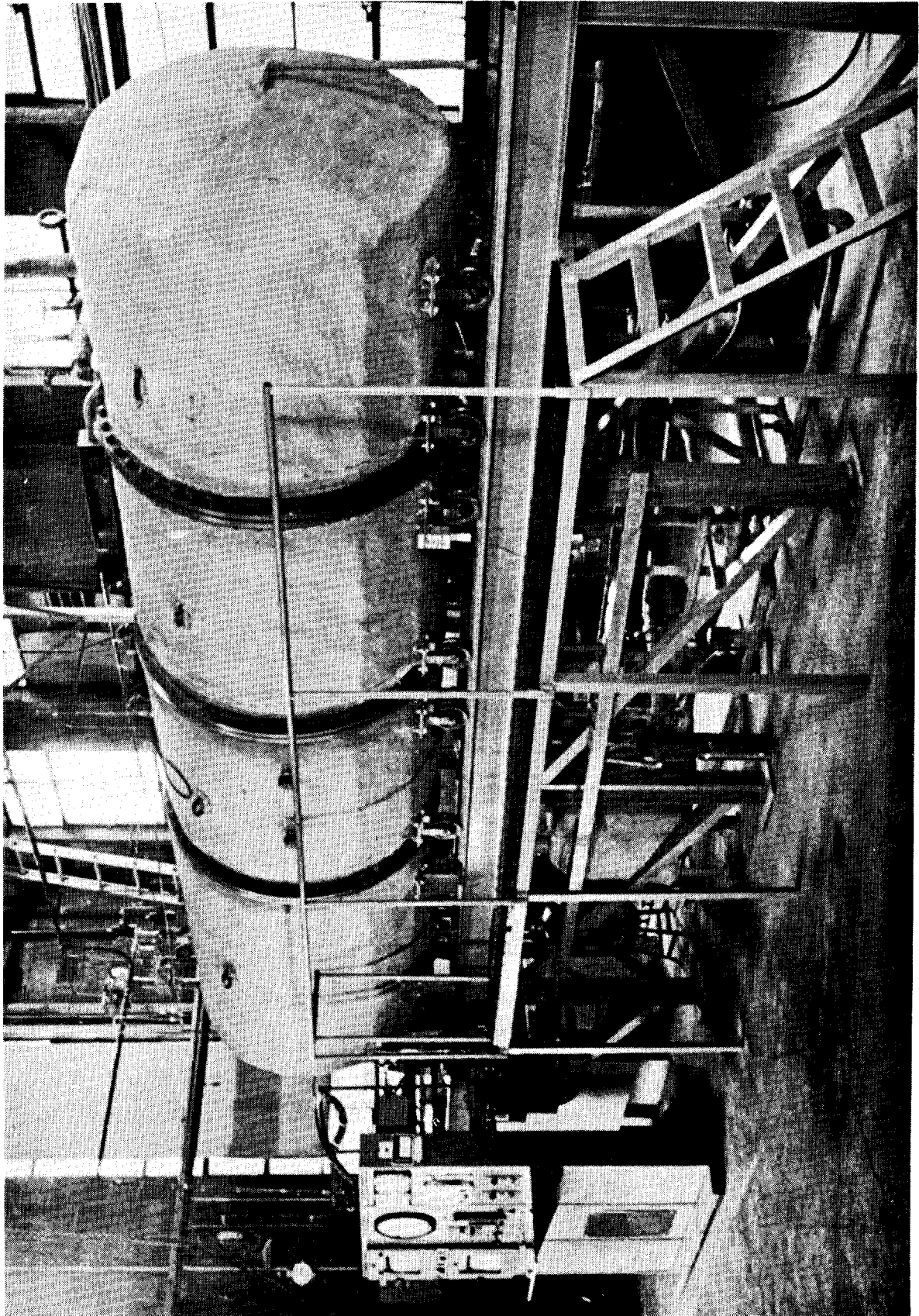
FIG. 5 - ENVIRONMENTAL TEST FACILITY (ETF), GENERAL VIEW

1. Type "A" Separatorless Filter
2. Type "E" Separator Filter
3. Type "D" Mini Separator Filter (1500 CFM Model)
4. Type "C" Tapered Separator Filter
5. Type "B" Separatorless Filter
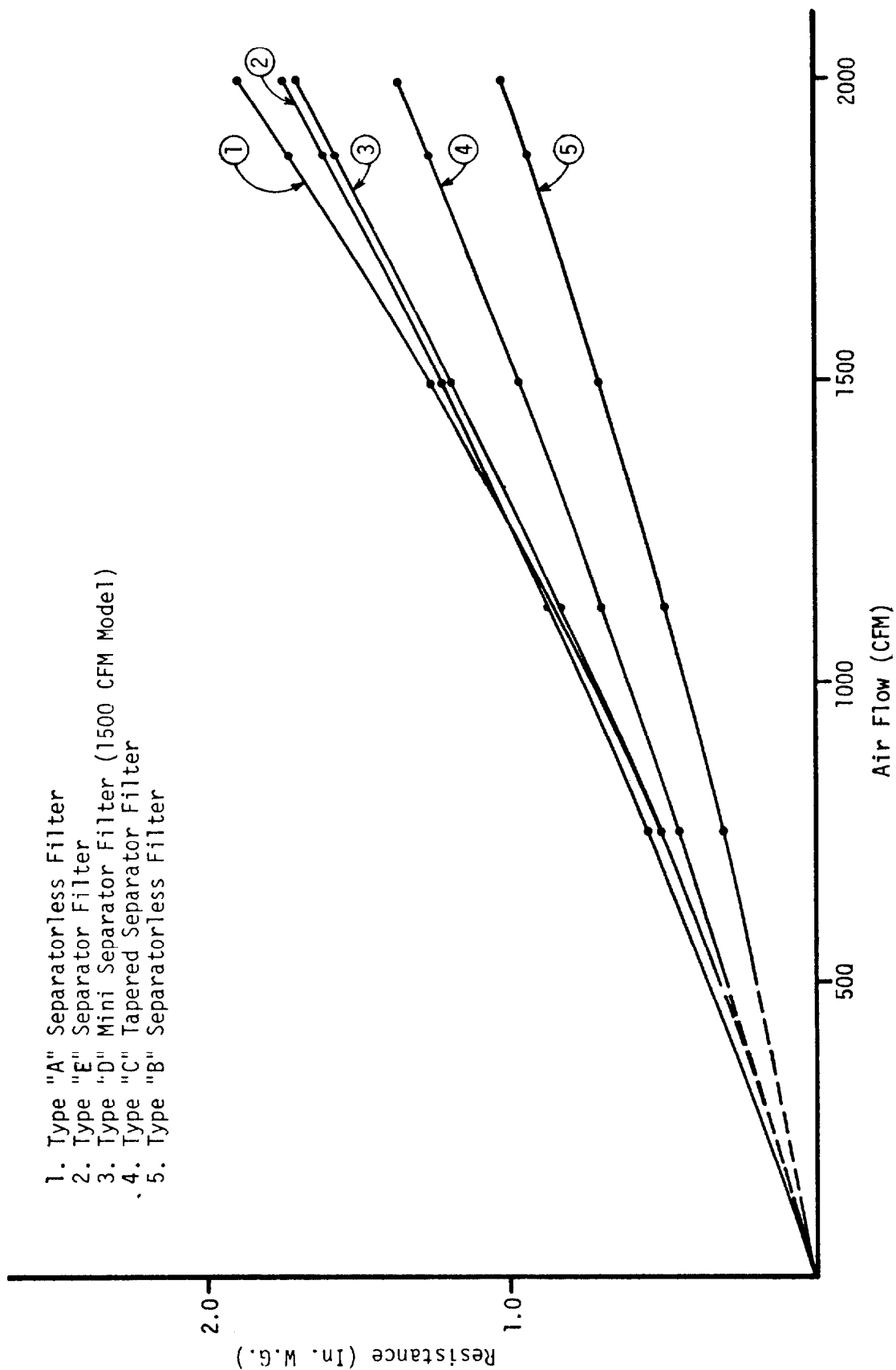
Figure 6   Clean filter air flow curves.
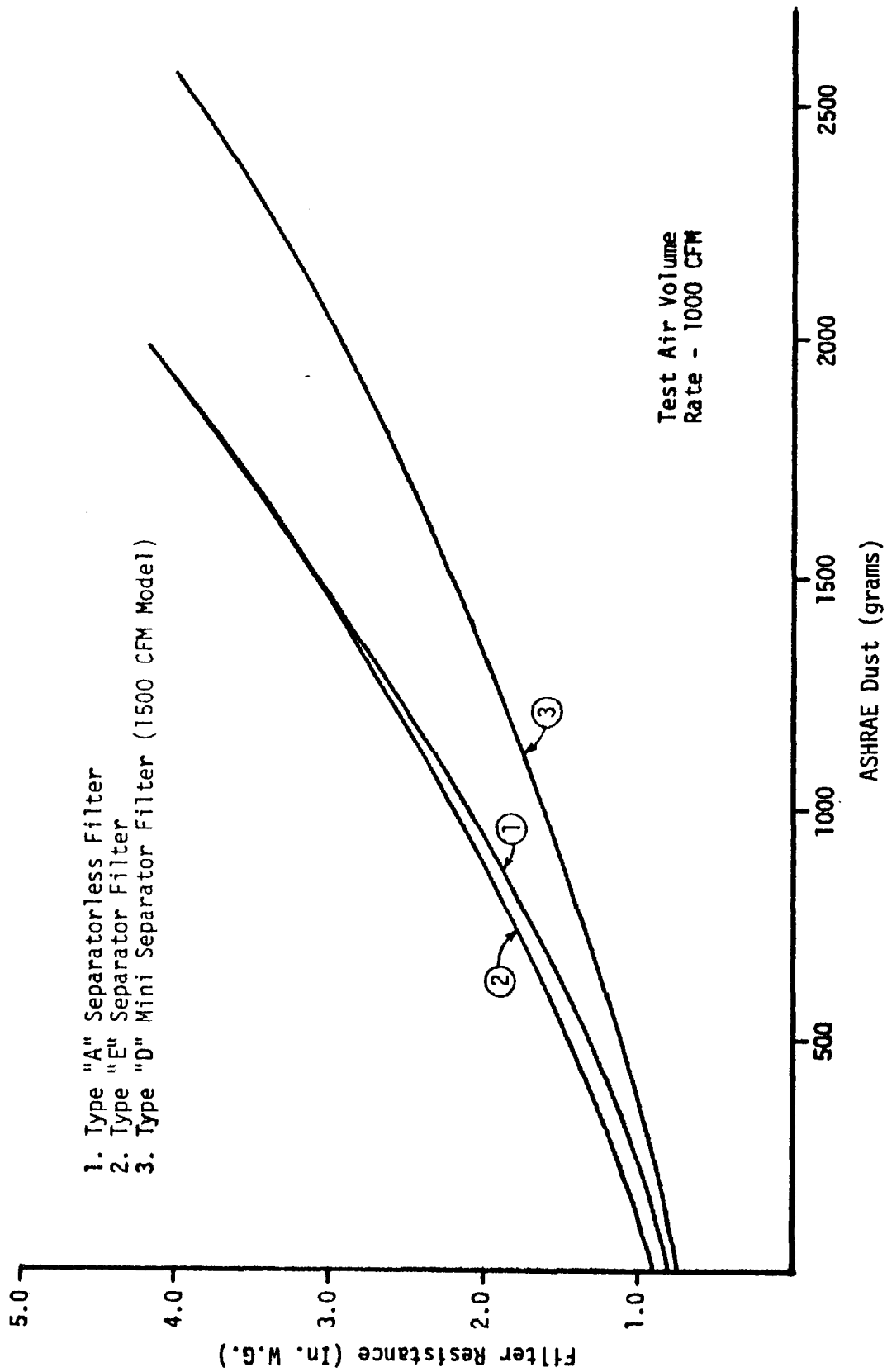
Figure 7   ASHRAE 52-68 dust loading curves.
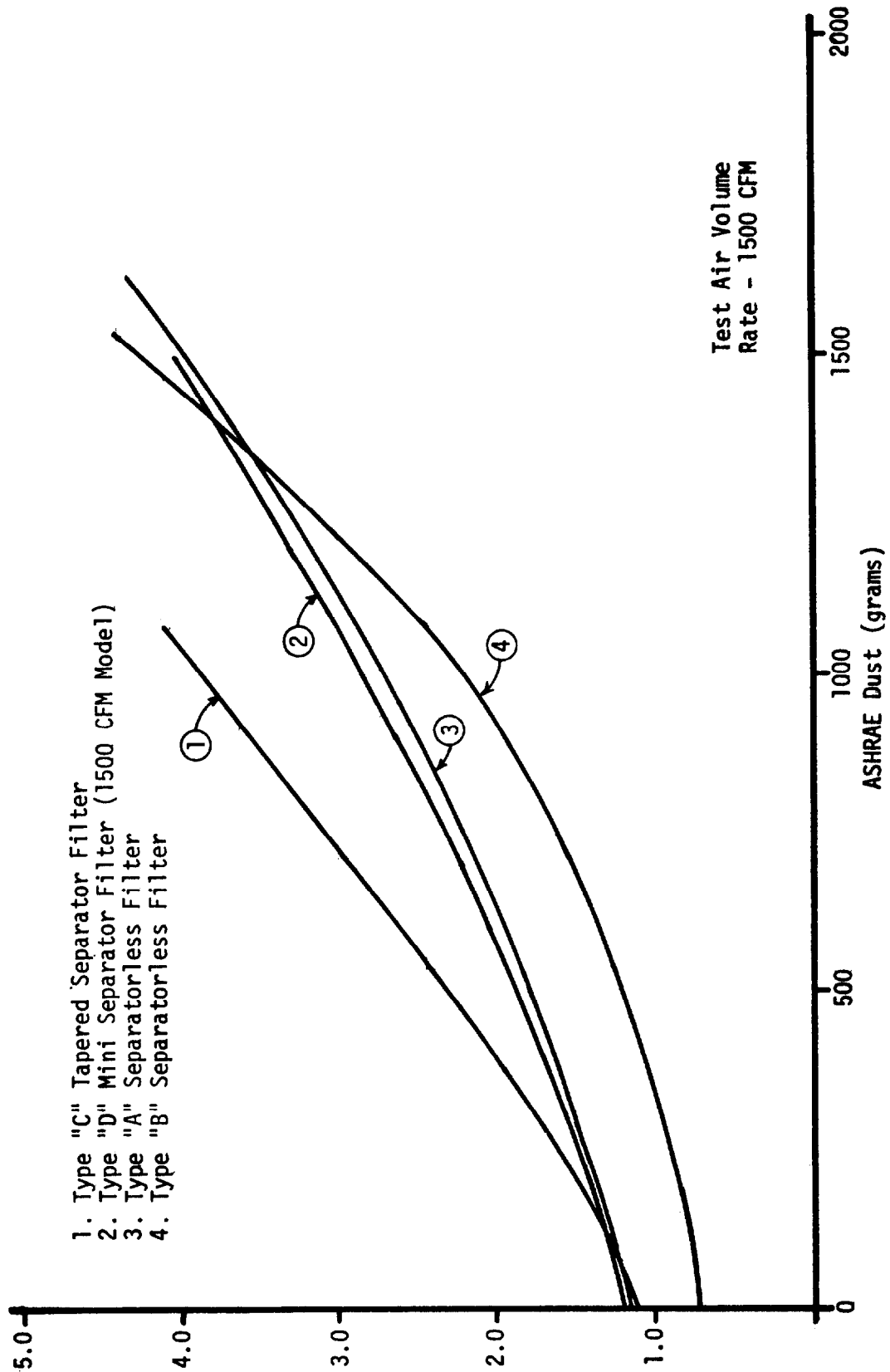
Figure 8   ASHRAE 52-68 dust loading curves.
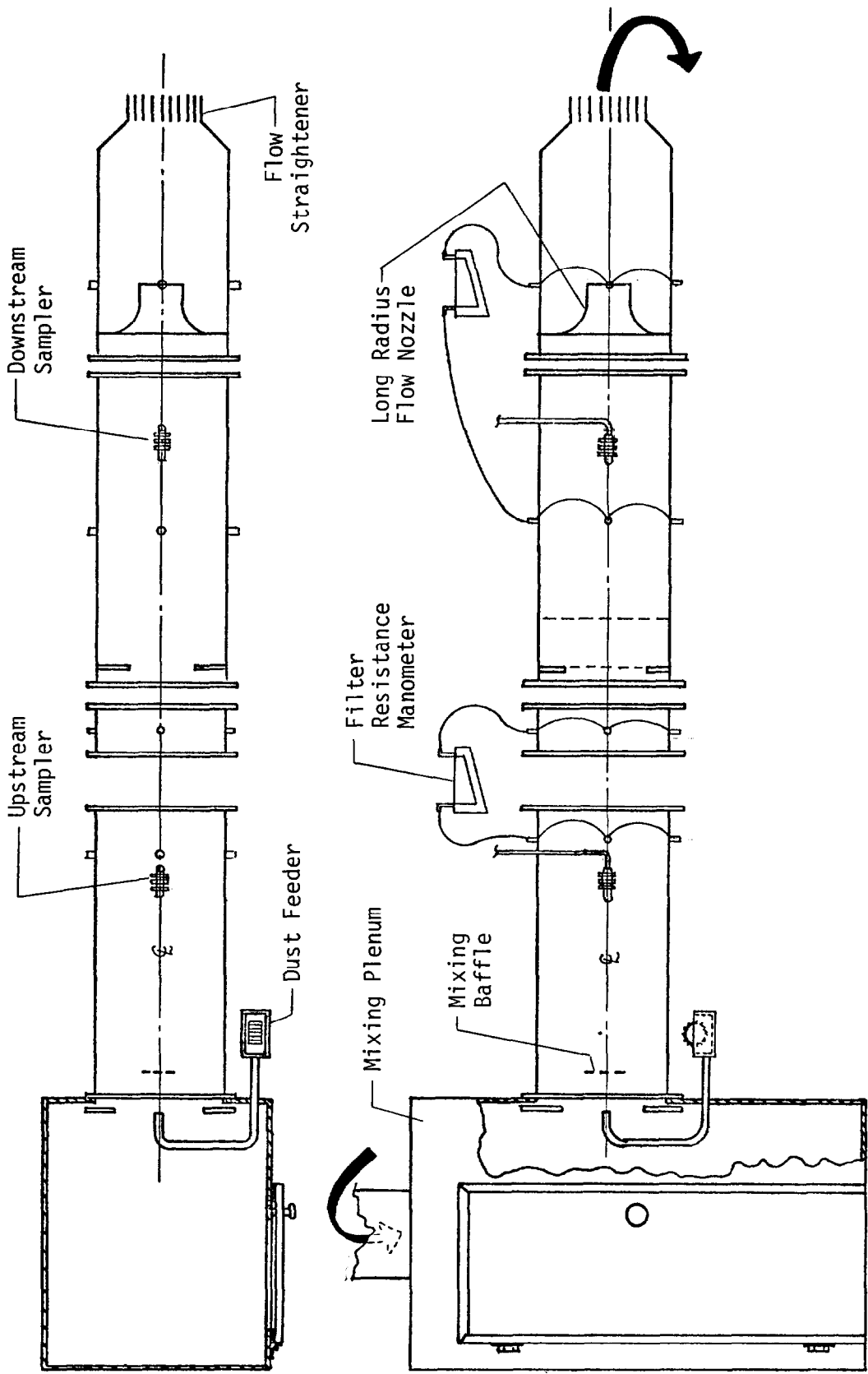
Figure 9   ASHRAE 52-68 test duct.
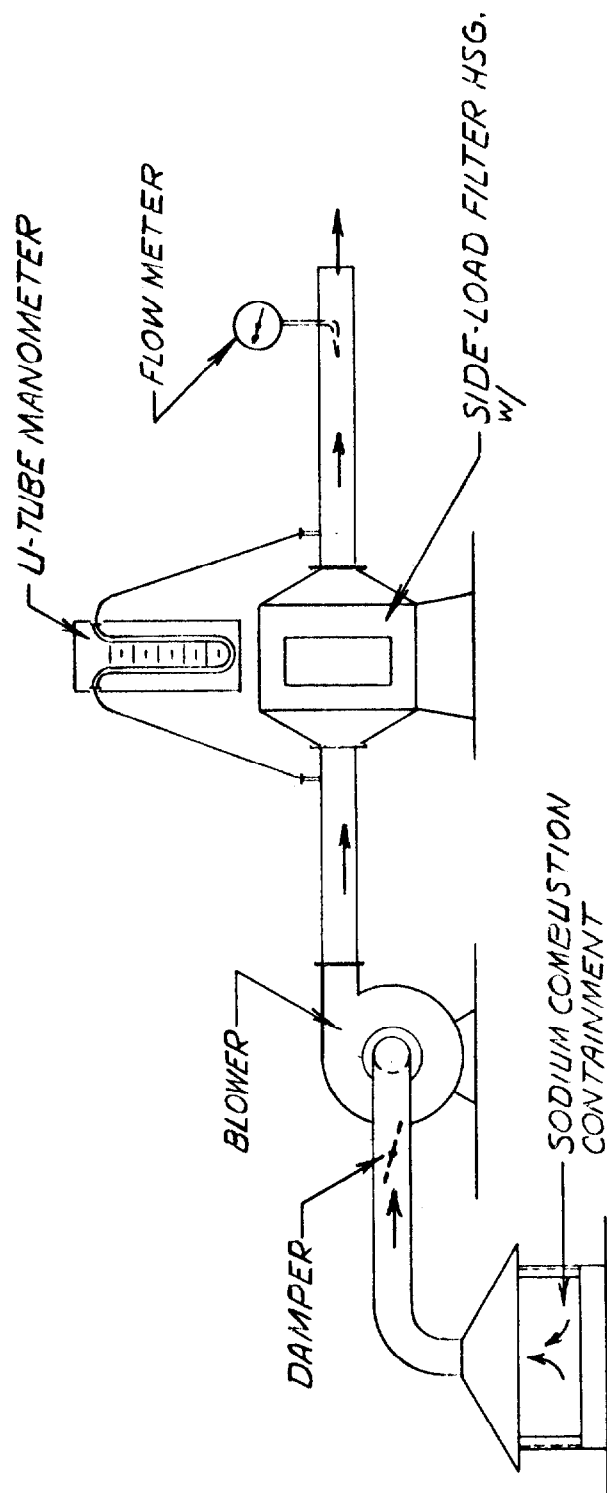
Figure 10   MSA sodium fume test duct.
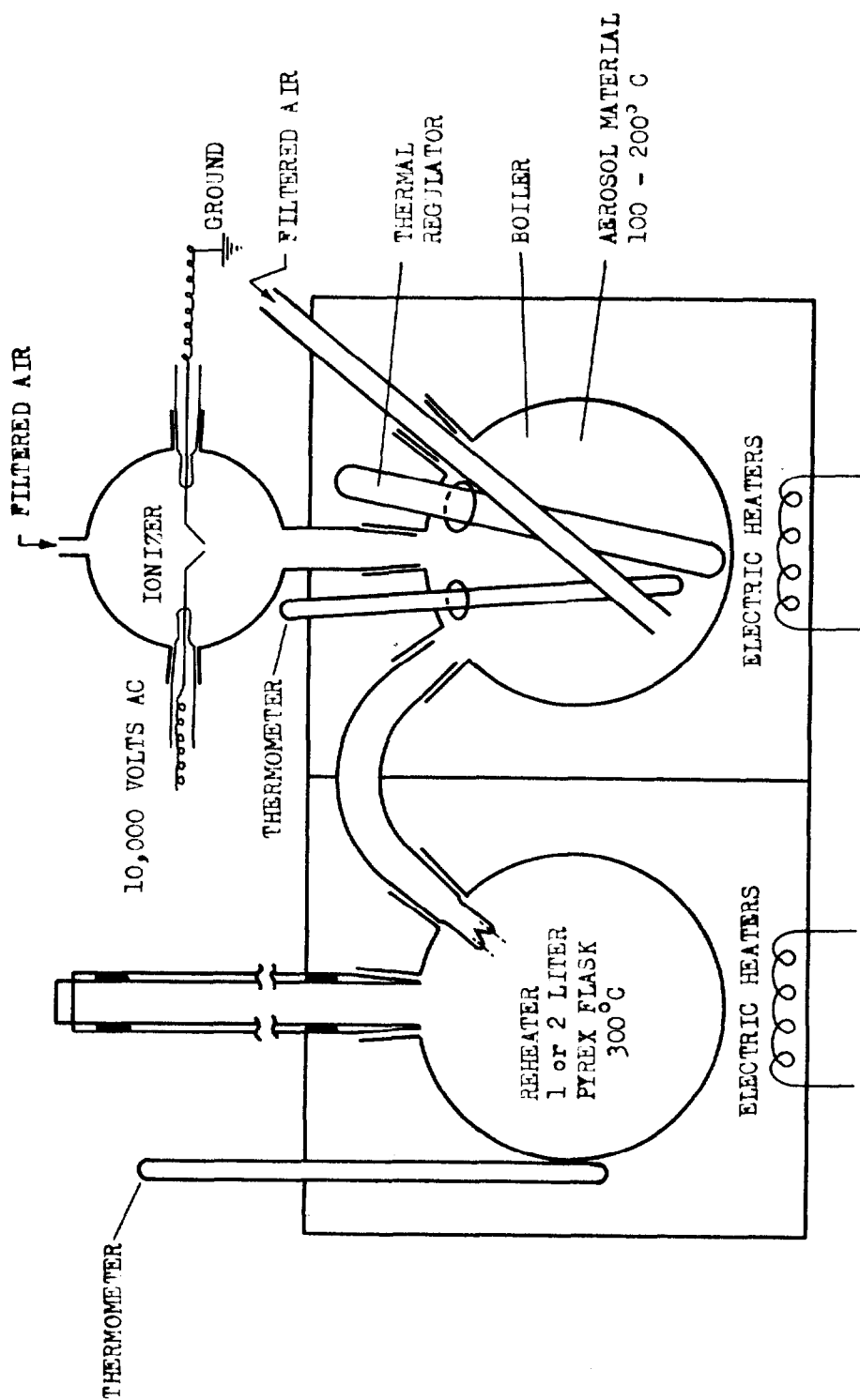
FIGURE 11 HOMOGENEOUS AEROSOL GENERATOR
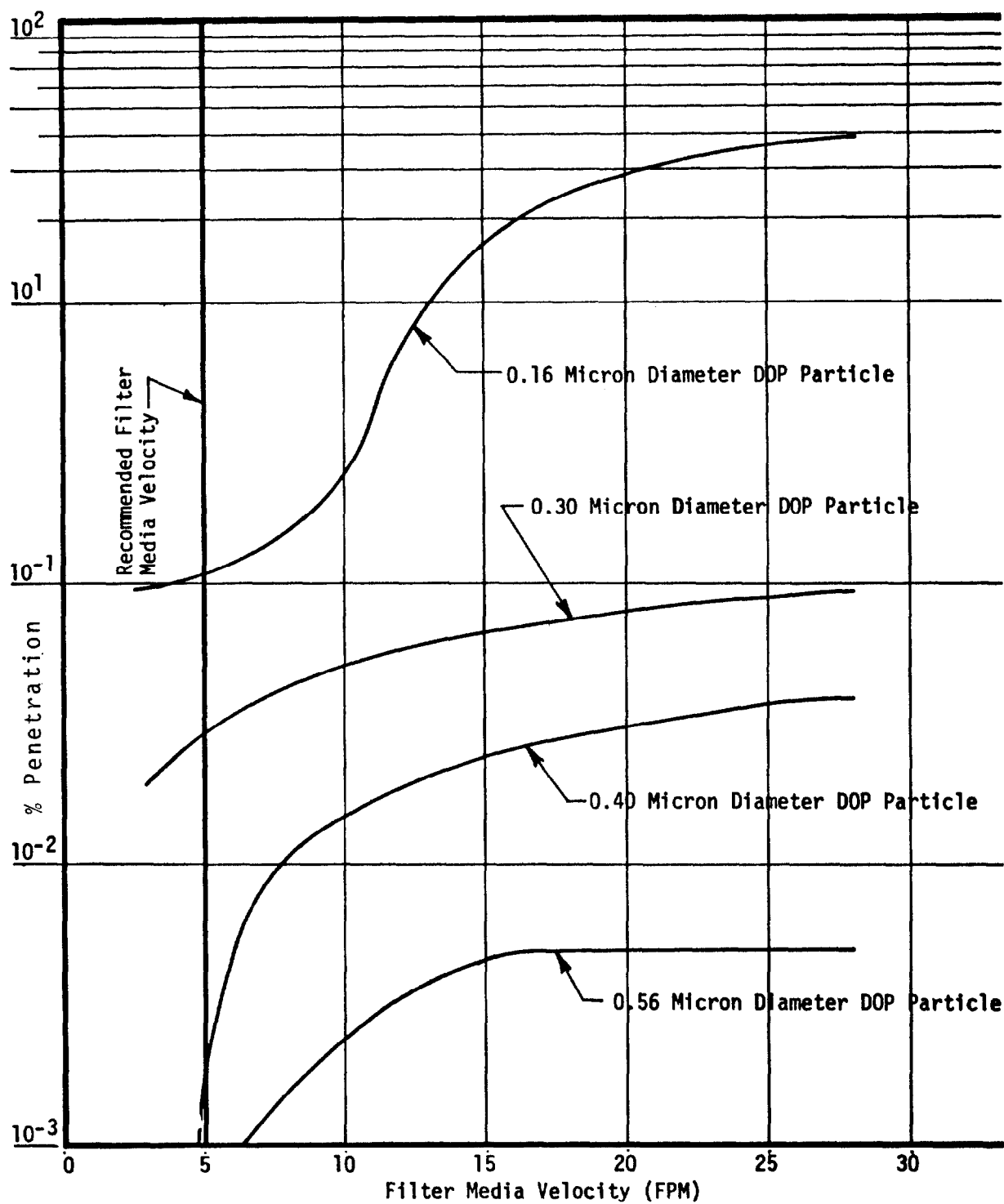
Figure 12   Particle size penetration curves.

VI. References

1. C. A. Burchsted, and A. B. Fuller, ORNL-NSIC-65, Section 3.2.2, (January, 1970).

2. E. C. Parish, and R. W. Schneider, "Tests of high efficiency filters and filter installations at ORNL", ORNL-3442, (June 3, 1963).

3. G. H. Griwatz, J. V. Friel, J. L. Bicehouse, "Entrained moisture separators for fine particle water-air-steam service", MSAR 71-45, AEC Contract AT 45-1 - 2145, (March, 1971).

4. F. J. Viles, P. Himot and M. W. First, "High capacity-high efficiency filters for sodium aerosols", NYO-841-10, (page 2), (Aug. 1967).

5. K. T. Whitby, A. B. Algren, R. C. Jordan, and J. C. Annis, "The ASHAE air borne dust survey", Heating Piping and Air Conditioning, (Nov. 1957).

6. G. Langmuir and K. B. Blodgett, "Smokes and filters", OSRD Report 3460, (1944).

7. Handbook on Aerosols - AEC - (pp 77, 78, 84, 85, 86), (1950).

8. H. W. Kundson and L. White, "Development of smoke penetration meters", NRL Report P2642, (Sept. 14, 1945).

9. C. A. Burchsted, "Minutes meeting April 27, 1976, Institute of Environmental Sciences Nuclear Energy Committee", (Paragraph 4-b, page 2), (May 18, 1976).

10. J. Truitt, "Effect of velocity on efficiency of absolute filter media for removal of stainless steel - UO_2 Aerosol", ORNL Nuclear Safety Research and Development Program Bi-Monthly Report for January-February, 1971, USAEC Report, ORNL TM3342, Oak Ridge National Laboratory, (1971).

DISCUSSION

CADWELL: Did you do any prolonged service life tests on these filters to the extent of a year or more?

GUNN: No, we didn't. We started but we didn't finish.

CADWELL: How many filter units were tested to develop the data for the Type A Separatorless filter?

GUNN: Approximately 28 filters.

CADWELL: Measurements of effective filter media area would indicate areas different from those included in your study.

EDWARDS: How do you explain that the Type A Separatorless filter passed all QPL requirements, and the mini-separator filter did not?

GUNN: We found essentially no difference in test performances between our "mini type" and "mini type" as supplied by another who passed all QPL tests. However, it is my understanding that we also passed all tests except the media radiation requirement. Meeting or not meeting this requirement would not effect the results reported in this study.

EDWARDS: Why did your test criteria exceed the requirements of the military specification?

GUNN: We did not intend to verify the Mil-Spec in this study.

EDWARDS: Your opening statement implied a cooperative venture between MSA and other   filter vendors when, in fact, Flanders Filters was not notified nor invited to submit filters for testing.

GUNN: I did not indicate anywhere in my speech and/or paper that this was a cooperative venture.

EDWARDS: How can you be sure that the products tested were intended for use in the nuclear industry?

GUNN: We can only go by what the vendors so indicated.

PENETRATION OF HEPA FILTERS BY ALPHA RECOIL AEROSOLS*

W. J. McDowell and F. G. Seeley
Oak Ridge National Laboratory
Oak Ridge, Tennessee 37830

and

M. T. Ryan
University of Lowell
Lowell, Mass. 01854

Abstract

The self-scattering of alpha-active substances has long been recognized and is attributed to expulsion of aggregates of atoms from the surface of alpha-active materials by alpha emission recoil energy, and perhaps to further propulsion of these aggregates by subsequent alpha recoils. Workers at the University of Lowell recently predicted that this phenomenon might affect the retention of alpha-active particulate matter by HEPA filters, and found support in experiments with ^{212}Pb. Tests at Oak Ridge National Laboratory have confirmed that alpha-emitting particulate matter does penetrate high-efficiency filter media, such as that used in HEPA filters, much more effectively than do non-radioactive or beta-gamma active aerosols. Filter retention efficiencies drastically lower than the 99.9% quoted for ordinary particulate matter were observed with ^{212}Pb, ^{253}Es, and ^{238}Pu sources, indicating that the phenomenon is common to all of these and probably to all alpha-emitting materials of appropriate half-life. Results with controlled air-flow through filters in series are consistent with the picture of small particles dislodged from the "massive" surface of an alpha-active material, and then repeatedly dislodged from positions on the filter fibers by subsequent alpha recoils. The process shows only a small dependence on the physical form of the source material. Oxide dust, nitrate salt, and plated metal all seem to generate the recoil particles effectively. The amount penetrating a series of filters depends on the total amount of activity in the source material, its specific activity, and the length of time of air flow. Dependence on the air flow velocity is slight. It appears that this phenomenon has not been observed in previous experiments with alpha-active aerosols because the tests did not continue for a sufficiently long time. A theoretical model of the process has been developed, amenable to computer handling, that should allow calculation of the rate constants associated with the transfer through and release of radio-active material from a filter system by this process.

I. Introduction

The phenomenon of alpha recoil or alpha "creep" has been recognized for many years. As early as 1910 Russ and Makower[1] proposed that the expulsion of aggregates of material by alpha recoil energy might account for the observed self-scattering of alpha active material.* In 1915 Lawson[2] investigated the phenomenon, confirmed that the proposed mechanism existed, and gave it the name "aggregate recoil." The work of Lawson was subsequently summarized by Rutherford[3]. Chamie[4] and Jedrezezowski[5] used photographic methods to investigate and confirm aggregate recoil processes. A variety of alpha emitting materials including radium, polonium, and thorium "emanation" were used in these experiments. In 1973 Vento[6] studied aggregate recoil particles of lead-212 and its daughter products by autoradiographic methods and determined that the particles showed a size distribution with an average of about 10^3 atoms/particle (diameter $\approx$ 0.003 μm), a size for which the expected HEPA filter efficiency should be higher than 99.97%. Alpha creep has been familiar to many persons working with polonium, plutonium, and the transplutonium isotopes.

About 1973 Ryan, Skrable, and Chabot at Lowell Technological Institute proposed that this process of expulsion of aggregates from the surface of alpha-active materials by alpha emission recoil energy, and perhaps further propulsion of these aggregates by subsequent alpha recoils, might affect the retention of alpha active materials by HEPA filters. Using ^{212}Pb plated on needles as sources** of aggregate recoil particles, they obtained experimental confirmation of this hypothesis[7]. They demonstrated, by a combination of counting and autoradiographic methods, that recoil aggregates were generated from the source and were found on downstream filters in amounts greater than would be expected if the particles were being retained with the rated filter efficiency.

This paper presents the results of subsequent work at Oak Ridge National Laboratory in which lead-212, einsteinium-253, plutonium-238, and plutonium-239 were used as sources of aggregate recoil particles for filter penetration tests.

II. Experimental Methods

All tests were on a laboratory scale. The filters used were 47-mm diameter Gelman, Type A. According to the manufacturer's literature,[8] these filters have a minimum retention of 99.98% for 0.3-micron sized particles, and have physical characteristics that are similar to those of commercial HEPA filters. For testing, the filters were held either in a Gelman in-line filter holder (product No. 1235) in which the filters were in physical contact, or in a device of our construction in which the filters were held separate. There was no significant difference in results with the filters in contact or separate. These methods of holding the filters and of mounting sources of alpha-active materials are shown in Figure 1. Two types of sources were used, (1) metallic deposits plated either electrostatically or electrolytically on stainless-steel or gold needles, or (2) metal oxides deposited in the fibers of a filter disc. The ^{212}Pb sources were prepared by electrostatic plating in the device shown in Figure 2. The needle was placed in

---

*It can easily be shown that the daughter-atom of an alpha decay event will have approximately 100 keV of energy or roughly 10^5 times that necessary to break chemical bonds.

**Daughters of ^{212}Pb (^{212}Po) provide the alpha emissions necessary to propel ^{212}Pb aggregates containing both ^{212}Pb and equilibrium amounts of these daughters products.

ORNL DWG 76-44IRI

NEEDLE

CAP

SEPTUM

BRASS CHAMBER

TEFLON FILLER

TEFLON GASKET

GLASS FIBER FILTER DISC

228Th

Figure 2   Lead–212 generator.

ORNL–DWG 76-1043

SUPPORT DISC

SUPPORTING GRID

FILTER STACK

SOURCE NEEDLE IF USED

EXIT AIRFLOW TO VACUUM

O-RING

AIRFLOW FROM PREFILTER AND FLOWMETER

TO VACUUM

SOURCE FILTER

CLEAN FILTER

O-RINGS

FILTER SUPPORT GRIDS

AIRSTREAM FROM PREFILTER + FLOWMETER

Figure 1   Experimental filter units.

proximity to a ^{228}Th source and maintained at a potential of about -9 volts. The 55-sec ^{220}Rn escaped through the filter stack and decayed to 0.16-sec ^{216}Po and then to 10.64-hr ^{212}Pb. Positive ions of both these species were collected on the needle. Sources of 0.5 to 25.0 µCi were prepared in this way. Sources of ^{253}Es on needles were prepared by conventional electroplating methods. Sources on filter discs were prepared by placing 25 to 100 microliters of a nitrate or chloride solution of the element on a filter disc, adding formic acid or ammonium hydroxide (to destroy the nitrate and/or hydrolyze the metal salt), and drying under infared lamps for approximately 30 minutes. These sources were presumed to be either metal oxides or oxy salts (MOX). Sources of 10^7 to 10^8 dpm were usually prepared in this way.

The lengths of the runs were determined by the half-life of the nuclide used and the length of time necessary to accumulate a meaningful amount of activity on the downstream filters. The half-lives of the nuclides, their specific activities, and the lengths of typical runs are listed in Table I. Initially many single-experiment runs were made; however, it became obvious that with runs of several

Table I   Nuclides examined for aggregate recoil filter penetration.

Nuclide	$T_{1/2}$	g/Ci	Lengths of Runs
^{212}Pb	10.4 hrs	7.18×10^{-7}	4-30 hrs
^{253}Es	480.0 hrs	4.0×10^{-5}	2-20 days
^{238}Pu	87.4 y	5.8×10^{-2}	20 days
^{239}Pu	24,413 y	16.3	20 days

days duration efficient use of time demanded multiple-experiment runs, and the device shown in Figure 3 was built. In all cases, individual flow meters monitored the air flow through each filter stack. Flow rates were initially varied from 10 to 34 linear feet per minute (LFM), but later experiments, including all those with ^{238}Pu and ^{239}Pu, were run at 5 LFM, consistent with the usual flow rate through HEPA filter media. No measurable dependence of transfer on flow rate was observed in the experiments where it was varied. Each type of filter assembly used was tested for retention of a di-n-octyl phthalate mist by standard methods (DOP test) and found to perform as expected.

Liquid scintillation counting was the primary analytical method used. Source needles were leached and a portion of the solution was added to the scintillator, or the needle itself was immersed in the scintillator. (Tests indicated that the addition of a needle to the sample did not affect counting results.) Filter-disc sources were dissolved in dilute HF and diluted to a known volume, and an aliquot of this solution was added to the scintillator solution. Downstream filters were counted by immersion of the entire filter in the scintillator. Tests with known amounts of various alpha emitters dried on filter discs indicated this method of counting to be 100% efficient and reliable and reproducible within counting statistics. Studies of the decay rate for ^{212}Pb and of alpha and gamma spectra for the other isotopes confirmed that the activity seen on downstream filters originated from the source.
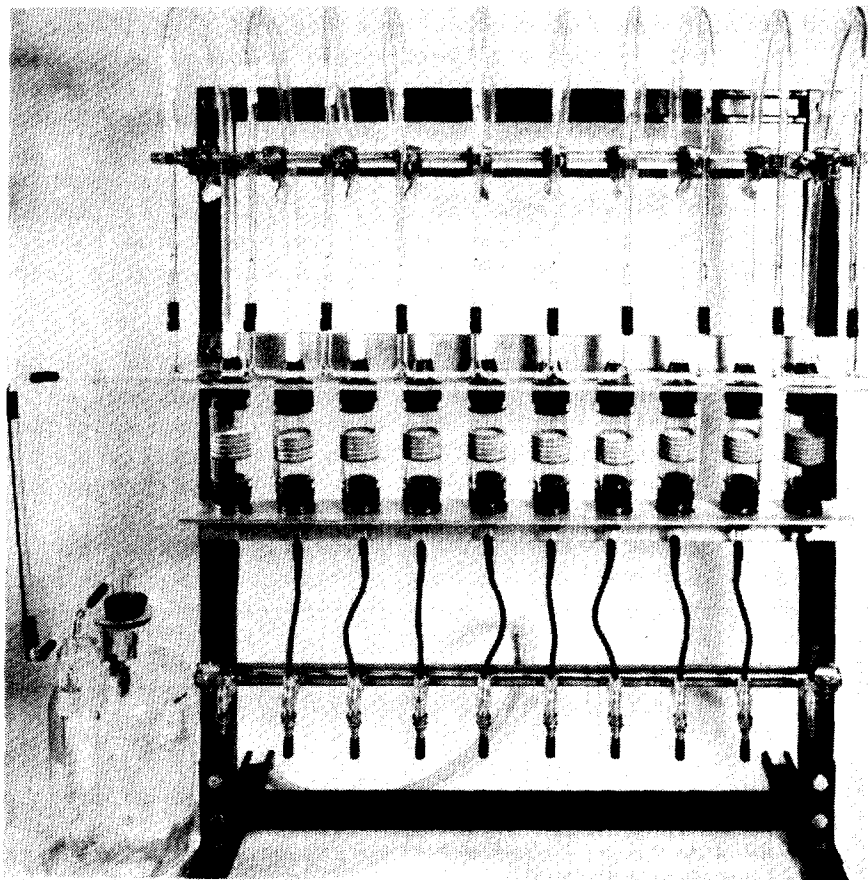
Figure 3   Ten-unit filter manifold.

III.   Results and Discussion

General Observations

It should be emphasized in the beginning that in all these tests, the source material was firmly fixed to the needle or filter support.   No normal dust or aerosol was generated to challenge the filter system.   However, in all tests using sources containing alpha emitters, positive evidence of migration of the source material through a set of 4 or 5 filters in series was observed.

The fact that all of the alpha-active preparations produced migration of the source material through the filter stack is consistent with the idea of the expulsion of aggregate recoil particles from the source material and subsequent propulsion of these particles by alpha recoil energy.   It should be noted here that in the case of ^{212}Pb, the migration of the non-alpha-active ^{212}Pb itself was observed, indicating that an aggregate of atoms is indeed expelled and propelled.

Tests in which only the beta-gamma active material ^{152,154}Eu was used showed no evidence of migration, but later tests with ^{152,154}Eu mixed with ^{238}Pu showed migration of the ^{152,154}Eu.   This again indicates the existence of aggregates.

The data obtained for aggregate recoil penetration of the filters by particles from the various sources are shown in Table II.   The amount of material on downstream filters is small in all cases and represents only a minute fraction of the

source activity. However, the fraction of activity on the second and each succeeding downstream filter is much larger than would be expected from established filter efficiency and the amount on the filter immediately preceding it and does not represent a rate of decrease of activity consistent with filter efficiency. Further, it should be remembered that what we are observing appears to be a continuous process of release and transport, dependent on the amount of activity on the filter rather than on the concentration of any challenging aerosol. High-efficiency filters are, indeed, expected to perform with their rated efficiency with normal aerosols of alpha active materials over short periods of time, as has been shown by the extensive tests of Ettinger, et al.[9] The fact that the effect of aggregate recoil was not seen in those tests is attributed to the relatively short duration of the tests. Conversely, we believe that our observations can be explained only by the operation of an aggregate recoil mechanism as proposed above continuing over a relatively long period of time.

Mathematical Model

The change, with time, in the number of active atoms, N, on an alpha-active source can be described by the equation

$$\frac{dN_s}{dt} = - (K_s + \lambda) \, N_s(t), \tag{1}$$

in which λ is the usual radioactive decay constant, and K_s is the rate constant for transfer of atoms by the aggregate recoil process. If aggregate recoil particles are resuspended in the air stream and re-collected on the next downstream filter, then the change in activity on the first downstream filter after the source filter can be described by

$$\frac{dN_1}{dt} = K_s N_s(t) - (K_1 + \lambda) \, N_1(t). \tag{2}$$

The rate of change of activity on any downstream filter, m, is thus

$$\frac{dN_m}{dt} = K_{m-1} N_{m-1}(t) - (K_m + \lambda) \, N_m(t); \; m = 2,3,\ldots,M. \tag{3}$$

If it is assumed that $K_m = K_{m-1}$, etc., and $K_m > K_s$, this family of differential equations may be solved [10] to obtain an expression for the amount of activity on any filter at any given time,* giving:

$$N_m(t) = \frac{N_s(o) K_s k^{m-1}}{(K-K_s)^m} \, e^{-(\lambda + K_s)t} \, P(m, \, (K-K_s)t), \tag{4}$$

where:

$$P(m,x) = \frac{1}{\Gamma(m)} \int_o^x e^{-u} u^{m-1} du. \tag{5}$$

A computer code for fitting the data in Table II to equation 4 by a nonlinear least-squares analysis has been written, and values of K_s and K have been obtained for each set of data. Values of the transfer rate constants are listed in Table III. The errors for these transfer rate constants may be estimated by

---

*It is possible to solve the separate differential equations for the source and each filter obtaining K_s, K_1, K_2, etc., but this requires experimental values for N_s at $t = 0$ and $t = t$ more accurate than can be reasonably obtained for successful application.

Table II   Aggregate recoil filtration data

Source	Source Activity (dpm)	Run Time	Airflow (L.F.M.)	Activity on Filter (dpm)			
				1	2	3	4
Lead-212	9.6×10^6 (a)	4 h	34	123	22	107	50
	1.16×10^6 (a)	4 h	10	6,040	105	54	40
	5.48×10^7 (a)	4 h	10	509	259	45	99
	4.10×10^7 (a)	8 h	10	632	211	221	292
	2.69×10^7 (a)	4 h	10	1,650	23	23	18
	1.31×10^7 (a)	22 h	10	156	9	18	11
	4.93×10^7 (a)	4 h	8	162	32	17	8
	4.05×10^7 (a)	4 h	16	45	5	4	2
	1.82×10^7 (a)	4 h	24	61	4	5	8
	8.60×10^6 (a)	8 h	16	28	3	6	5
	2.14×10^7 (a)	8 h	24	53	22	21	20
	1.84×10^7 (a)	8 h	8	57	52	28	12
	2.60×10^7 (a)	16 h	8	56	17	16	15
	2.67×10^7 (a)	16 h	16	74	7	3	6
	2.19×10^7 (a)	16 h	24	378	31	11	6
	2.87×10^7 (a)	30 h	8	43	2	3	6
	5.18×10^6 (a)	30 h	16	29	4	2	3
Plutonium-238	3.7×10^8 (b)	20 d	5	1,373	16	10	3
	3.5×10^8 (b)	20 d	5	1,754	21	13	20
	3.6×10^8 (b)	20 d	5	1,175	18	7	71
	3.5×10^8 (b)	20 d	5	3,680	116	22	23
	3.7×10^8 (b)	20 d	5	637	22	17	30
	3.6×10^8 (b)	20 d	5	675	29	7	8
	3.6×10^8 (b)	20 d	5	2,598	30	17	9

Table II (Contd.) Aggregate recoil filtration data

Source	Source Activity (dpm)	Run Time	Airflow (L.F.M.)	Activity on Filter (dpm)			
				1	2	3	4
Einstein-ium-253	1.52×10^8 (b)	10 d	23	3,454	36	7	5
	1.69×10^7 (b)	48 h	10	839	22	19	7
	5.0×10^7 (b)	11 d	10	5,110	29	17	99
	1.32×10^7 (a)	11 d	10	348	11	7	3
	9.0×10^6 (a)	20 d	10	5,134	205	100	46
	7.48×10^7 (b)	20 d	10	5,511	14	9	7

Table III Summary of Transfer Rate Constants

Nuclide	Source Rate Constant (K_s)	Downstream Rate Constant (K)
^{238}Pu	$2.44 \times 10^{-6} d^{-1} \pm 9.38 \times 10^{-8} d^{-1}$	$8.59 \times 10^{-3} d^{-1} \pm 3.58 \times 10^{-3} d^{-1}$
^{253}Es	$1.16 \times 10^{-6} h^{-1} \pm 4.68 \times 10^{-7} h^{-1}$	$2.44 \times 10^{-3} h^{-1} \pm 7.87 \times 10^{-4} h^{-1}$
^{212}Pb	$4.17 \times 10^{-8} h^{-1} \pm 3.37 \times 10^{-8} h^{-1}$	$2.81 \times 10^{-3} h^{-1} \pm 1.53 \times 10^{-3} h^{-1}$

propagation of the known counting errors of each filter. The standard deviations associated with these transfer rate constants are included in Table III.

Release calculations. From the model above, the release from filter m during time interval t is

$$R_m(t) = \int_0^t N_m(\tau) \, d\tau = N_s(o)\left(\frac{K_s}{K_s + \lambda}\right)\frac{K}{K + \lambda}^m \left\{ P(m, (K + \lambda)t) - e^{-(K_s + \lambda)t}\left(\frac{K + \lambda}{K-K_s}\right)^m P(m, (K-K_s)t) \right\} . \quad (6)$$

Evaluation of this equation by computer methods[10] allows calculation of amounts of activity released by aggregate recoil under various conditions. Figure 4 shows the total release in μCi as a function of time for ^{238}Pu. The conditions assumed for these calculations are: (1) a set of four filters in series and (2) at time zero the first filter collects a unit amount (1 Ci) of the alpha active material. In each case the activity released is significantly greater than that expected from normal filter penetration of particles in the aggregate particle size range. Because of the design of the experiments and the method of calculation, the curve shows release due to aggregate recoil only.

ORNL DWG 76-737RI
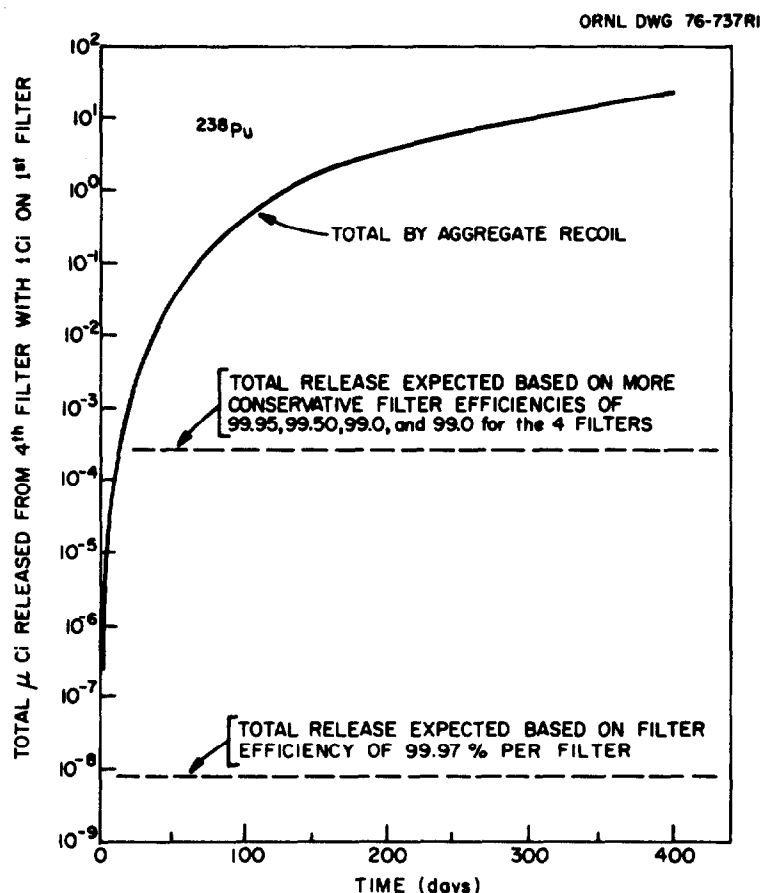
Figure 4   Calculated release of ^{238}Pu from a set of four HEPA filters, with 1 Ci initially collected on the first filter, as a function of elapsed time.

Figure 5 shows total releases calculated for three nuclides, ^{212}Pb, ^{253}Es, and ^{238}Pu, as a function of elapsed time in units of half-life. The release rates appear to increase rather sharply for 1 to 2 half-lives. Nuclides with longer half-lives eventually release a larger fraction of their source activity because the recoil-promoted migration through the filter system continues for a longer period of time.

ORNL DWG 76-745RI
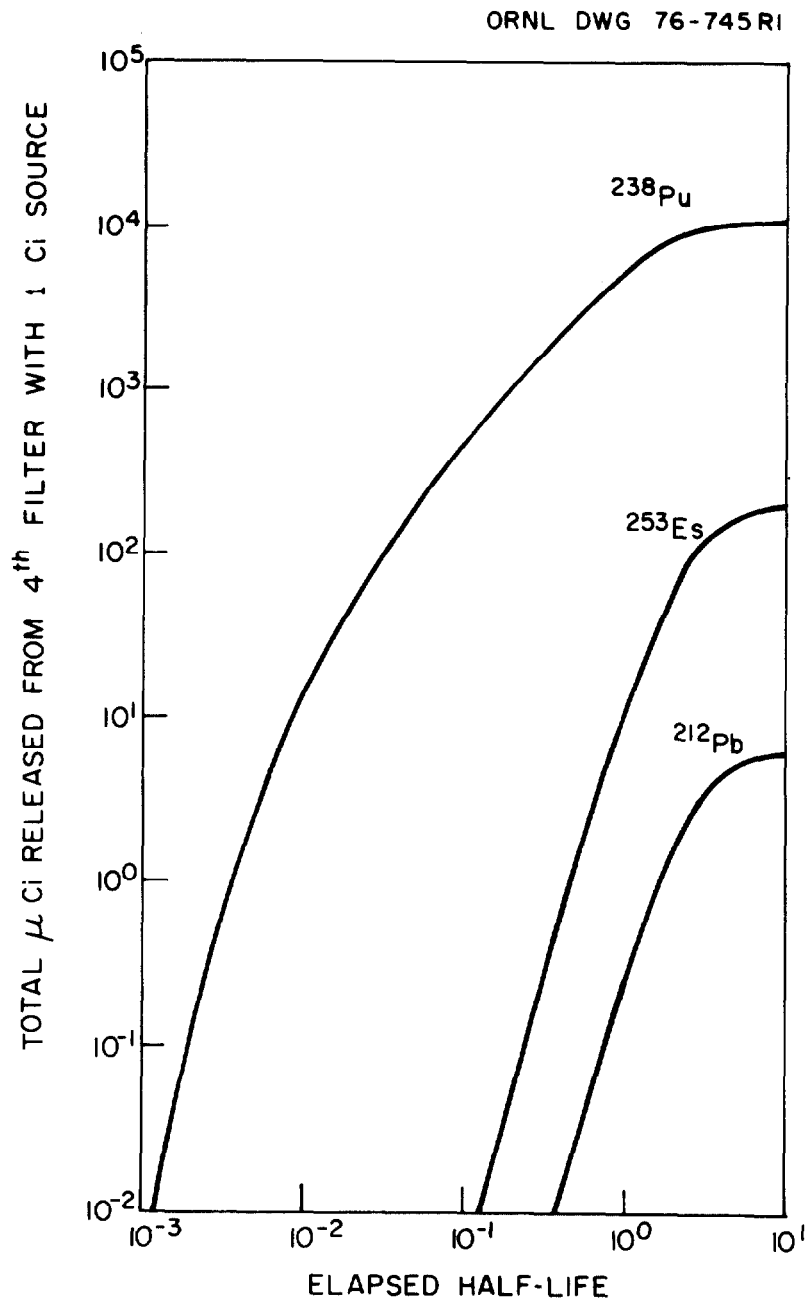
Figure 5   Calculated release of nuclides from a set of four HEPA filters, with 1 Ci initially collected on the first, as a function of elapsed half-lives.

Figure 6 allows comparison of the effectiveness of the aggregate recoil process in the penetration of a four-filter system for nuclides of different half-lives. Here we assumed all the nuclides to have approximately the same atomic weight and transfer rate constants as ^{238}Pu and calculated the total release to be expected during 300 days with initially 5 grams of the hypothetical nuclide on the first filter. Penetration by long half-life nuclides is slight because of their low specific activity (not much activity in 5 grams), and very short half-life nuclides do not penetrate effectively because much of the nuclide disappears through radioactive decay before it can migrate through the filter system. The Maximum effectiveness for the conditions selected appears to occur at about $T_{1/2}$ = 150 days. It is interesting to note in this connection that ^{210}Po ($T_{1/2}$ = 138 days) is particularly notorious for its alpha "creep" behavior.

ORNL DWG 76-740 RI
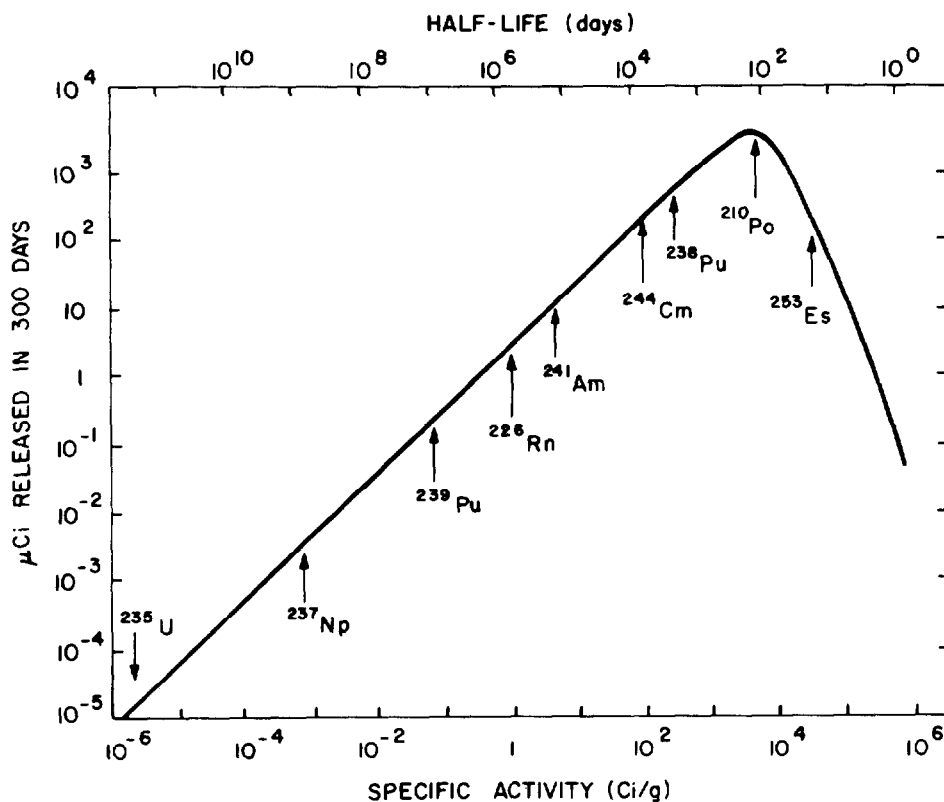
Figure 6   Calculated μCi of activity released in 300 days from 5 g each of hypothetical nuclides (physically resembling Pu), initially collected on the first of four filters, as a function of specific activity.

By appropriate application of the release equations, it is possible to calculate concentrations of airborne material released from a filtration system. Figure 7 shows a plot of the calculated air concentration of ^{238}Pu released by aggregate recoil from a series of 4 standard, 1000 CFM, HEPA filters. Two loading situations are evaluated: (1) with 0.25 Ci placed on the first filter at time zero and (2) with the load accumulated over 1 year at 0.042 Ci/month (0.25 Ci load at 6 months). Real situations would probably be included within these extremes of one-time or continuous loading. Concentrations being released at the end of one
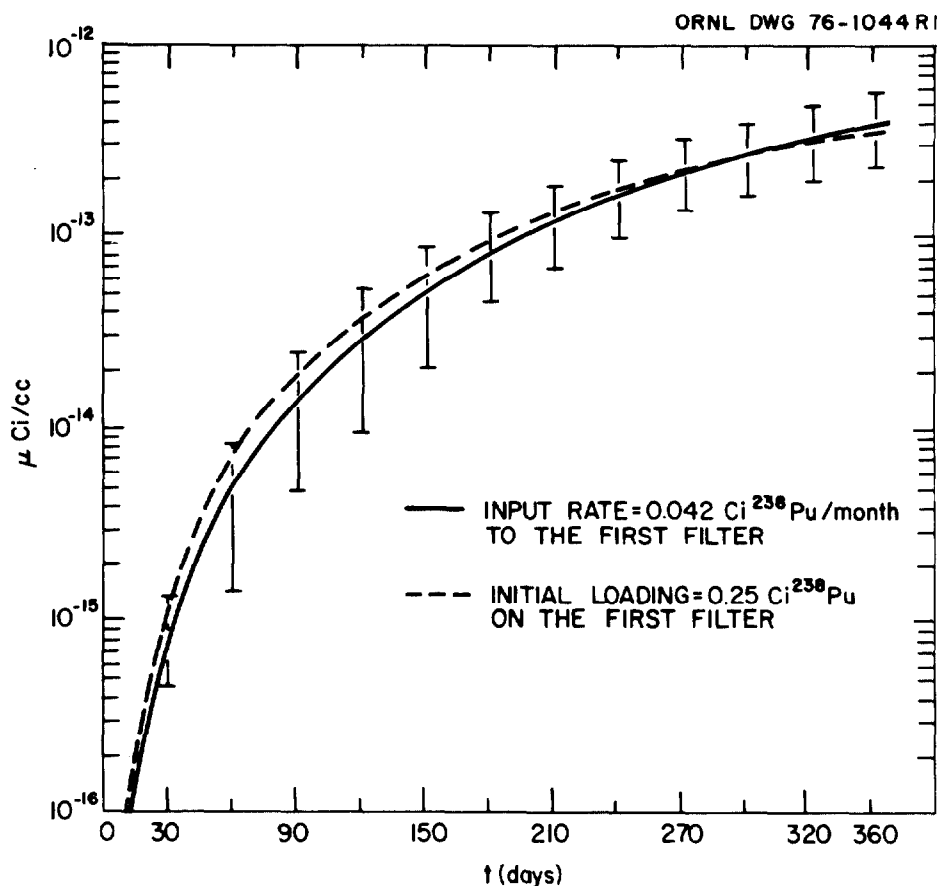
Figure 7   Calculated concentration (μCi/cc) of ^{238}Pu in air released from four 1000 CFM HEPA filters in series.

year are the same for both cases, within the accuracy of the calculations, and amount to about 3.5×10^{-13} μCi/cc. Preliminary work with ^{239}Pu indicates that, with loadings of the same amount of activity, releases would be similar. These concentrations are sufficiently large to warrant attention by those responsible for containment of alpha-emitting radioactive material.

Consequences and Prevention

The conclusion should not be drawn from this work that more alpha-active material has been released through air filters than was known. Exit air streams have been monitored and releases are, in general, well documented. However, there have been reports of unexplained slow increases in alpha activity in exit air from alpha processing facilities. These instances were usually attributed to development of leaks in the filter system, and new filters were installed. This work suggests, instead, that the observed increases in exit-air alpha activity were due to the aggregate recoil particle penetration of the filter system. It is thus appropriate to consider how this phenomenon might be prevented. Since the mechanism of aggregate recoil requires the residence of a significant amount of alpha activity on a filter for an extended time, any procedure that prevents long-term build-up of activity in the filter system will prevent the excessive migration

of alpha recoil particles. Tactics that immediately suggest themselves include frequent filter changes (perhaps of only the first filter, guided by a knowledge of the amount of activity on the filter), a washable filter, or precleaning of the air by some method that continuously removes particulates from the system. Many additional tests on both laboratory and engineering scale are needed to develop effective and economical methods of preventing aggregate recoil penetration of HEPA filters.

IV. Conclusions

Aggregate recoil particles from a source of alpha activity appear to penetrate HEPA filters much more effectively than would be expected on the basis of filter efficiency for similar sized stable aerosols. It is probable that an important portion of the alpha activity now released in air streams from alpha material processing facilities is due to the alpha aggregate recoil phenomenon. Significant total releases and significant exhaust air concentrations due to this mechanism are possible. Preventative measures are desirable and appear feasible.

V. References

1. W. Makower and S. Russ, Philosophical Mag. 19, 100-102 (1910).

2. R. W. Lawson, Wien. Ber., 217, 1 (1918).

3. E. Rutherford, J. Chadwick, and C. D. Ellis, Cambridge University Press, London, 1930, pp 557-558.

4. C. Chamie, Compt. Rend. 184, 1243-1244 (1927).

5. M. Jedrezezowski, Compt. Rend. 188, 1043-1045 (1929).

6. J. A. Vento, Thesis, Lowell Technological Institute (1975).

7. M. T. Ryan, K. W. Skrable, and G. Chabot, Health Physics 29, 798-799 (1975).

8. Gelman Instrument Co., Publication No. PB 322, p 9 (1974).

9. H. J. Ettinger, J. C. Elder, and M. Gonzales, Progress Report for Period March 1 through June 20, 1972, Report LA-5012-PR (July, 1972).

   H. J. Ettinger, J. C. Elder, and M. Gonzales, Progress Report for Period July 1 through December 31, 1972, Report LA-5170-PR(Jan., 1973).

   H. J. Ettinger, J. C. Elder, M. Gonzales, Progress Report for Period January 1 through June 30, 1973, Report LA-5349-PR (July, 1973).

   H. J. Ettinger, J. C. Elder, M. Gonzales, Progress Report for Period July 1 through December 31, 1973, Report LA-5544-PR (March, 1974).

   J. C. Elder, H. J. Ettinger, M. Gonzales, and M. Tillery, Progress Report for Period January 1 through June 30, 1974, Report LA-5784-PR (Nov., 1974).

10. C. W. Nestor, ORNL-CSD-INF-76/4, (June, 1976).

DISCUSSION

ETTINGER: The model you use does not include the function size. Very possibly, size is very important. We find from experimental work we've done at Los Alamos and from operating data at plutonium facilities (where the aerosols are realistic in terms of what comes out of these facilities) that we do not see the effect. It is very possible that alpha recoil is a real physical phenomenon but, in relation to the type of aerosols that come out of real plutonium situations, it is not a significant factor. Your test data indicate, at least in the text, that the plus or minus value on K is just a counting error and not an overall error based on a least squares fit to the data. Looking at the tabulated data in your report, I had a feeling that the plus or minus value might be fairly high because there seem to be no trends in counts when going from filter two to three to four. Sometimes, filter 4 had more activity and, in fact, I think the slide you showed,using an average of all of these tests, showed that filter 4 had, I think, two or three times as much activity as filter 3. I wonder if you've looked at that trend, or lack of trend, between filters 2, 3 and 4?

MCDOWELL: We've been concerned about this lack of trend. The explanation that we've come up with, which we believe is right, is that it is probably a matter of particle statistics. A very few particles could account for the activity that we're seeing on the filter. Therefore, counting statistics, in this situation, are probably more accurate than particle statistics. Whether you've got two particles or three particles on the filter could make the difference in the uncertainity in the count that you observe, whereas your count of what is there might be pretty accurate. I did not do the statistical evaluation of the K's. This was done by someone in our math division and they tell me that it is an estimate of the goodness of the fit to the equation derived from the uncertainties in counting and the scattering of the data.

STAFFORD: I wanted to reemphasize Harry's comment that we have not seen this type of decrease in efficiency much of the time when we've looked at our plutonium process exhaust filters. They are changed, generally, because of an increase in pressure drop. Reviewing our data, we have not seen a decrease in efficiency over the past several years. Did you look at the particle size distribution of your plutonium 238 aerosol?

MCDOWELL: No, we did not. In fact, we didn't generate an aerosol. Our aerosol generated itself. I'd like to reemphasize that, in all cases, we started out with a solid material which spontaneously produced particulate material that migrated and that we saw this with alpha active material and with alpha-beta-gamma active material. We know nothing about the particle size except to assume that it's similar to what had been previously mentioned with lead 212 which I spoke about.

BALSMEYER: I'm wondering if some of your statistical variation was related to the experimental setup. For instance, the distance between your filter media? Did you look at that at all?

MCDOWELL: No, we did not. We tried to look at relative humidity. That didn't seem to have any effect. The one thing that we were able to see some variation in that we had some control over was the way the source was prepared. This seemed reasonable to use because a source with a much finer particle size will have more surface area and the production of aggregate recoil particles from such a source ought to be more efficient. We don't have good data on it but there does seem to be a trend in that direction, i.e., that sources produced in such a way that they have a high surface area, produce more material traveling downstream.

BURCHSTED: I'd like to ask John Geer if Rocky Flats has anything to add to this since Rocky Flats operates systems with multiple filter banks that trap materials in this category.

GEER: I don't think we have seen anything that we would recognize as being due to the phenomena you're speaking of. Dick Woodard has done some work that indicates that there might be a few particles getting through, but we're not able to relate that to these phenomena. However, we have noted in the past that apparently there is some penetration, some slight penetration. We're trying to find a mechanism for it and we're interested in your comments.

KNOX: I'm addressing my question to Harry Ettinger. The phenomena that Jack reported here depend on time as well as on quantity. Did you have your multiple filters in test long enough to give time effects a chance to appear?

ETTINGER: I sent the data to Jack about a month ago. We sent data that showed no trend of penetration through HEPA filters that had been in place, I think, over a two year period. In addition, we did some laboratory work in which we put plutonium aerosol on a small HEPA filter, eight by eight by six inches, and put it away for approximately one year. At the end of one year, we tested it to see whether the plutonium on it had any effect. Although this is a somewhat different situation, we could see no effect. Again, the field data over a two year time span should show the effect that Jack has seen in his work.

MCDOWELL: I'd like to say that what we were observing is an effect produced by the alpha active material. It's not an effect of the filter. We don't think there's any degradation of the filter. So, putting a filter away with plutonium on it and testing it later by any kind of test should show no effect. As I understand it, the other data on penetration that came out of the operating data, involved a second filter in the system. There was a glovebox filter, a first bank and a second bank filter. Looking at the data I just showed and reflecting on this problem, it's true that what Harry had sent me showed no increase that could be attributed to alpha recoil. But, if we had looked at the second filter, we would not have seen any increase either. It's only apparent when you look at several filters. I think you'd have to have about three in series before you saw the effect, or at least three sampling stations. You can't see it just by looking across one filter.

EXHAUST FILTRATION ON GLOVEBOXES
USED FOR AQUEOUS PROCESSING OF PLUTONIUM

R. W. Woodard, K. J. Grossaint, and T. L. McFeeters
Rockwell International
Atomics International Division
Rocky Flats Plant
Golden, Colorado

Abstract

The report covers information obtained during the study of ventilation of glovebox systems used for wet process operations associated with plutonium recovery. Analytical data are presented on:

- concentration of chemical components in exhaust air

- concentration of radioactive material

- chemical species deposited on, or found in, HEPA filters in the exhaust systems.

I. Introduction

Air exhausted from glovebox lines, in which plutonium is processed by "wet" chemical operations, is filtered using high efficiency particulate air (HEPA) filters to reduce the plutonium activity to a level acceptable for discharge to the atmosphere. Although HEPA filters are effective in this service, they require frequent replacement, thus adding to the volume of waste which must be handled.

An opportunity exists at the Rocky Flats Plant to observe large scale filter systems associated with chemical process operations. It is the objective of one phase of a project funded by the Energy Research & Development Administration (ERDA) to utilize plant conditions to find better ways of using HEPA filters and acquire data for development of improved HEPA filters and prefilters for chemical service. Successful achievements of these objectives would reduce the quantity of waste associated with disposal of contaminated filters.

II. Description

Figure 1 depicts the flow of air through the system used in chemical process operations. Room air enters a typical glovebox line through HEPA filters at point (1), and into the glovebox where it becomes contaminated with chemical fumes and radioactive particulate. Exhaust filters, point (2) filter out most of the particulate matter from the air leaving the box. Air and gaseous components
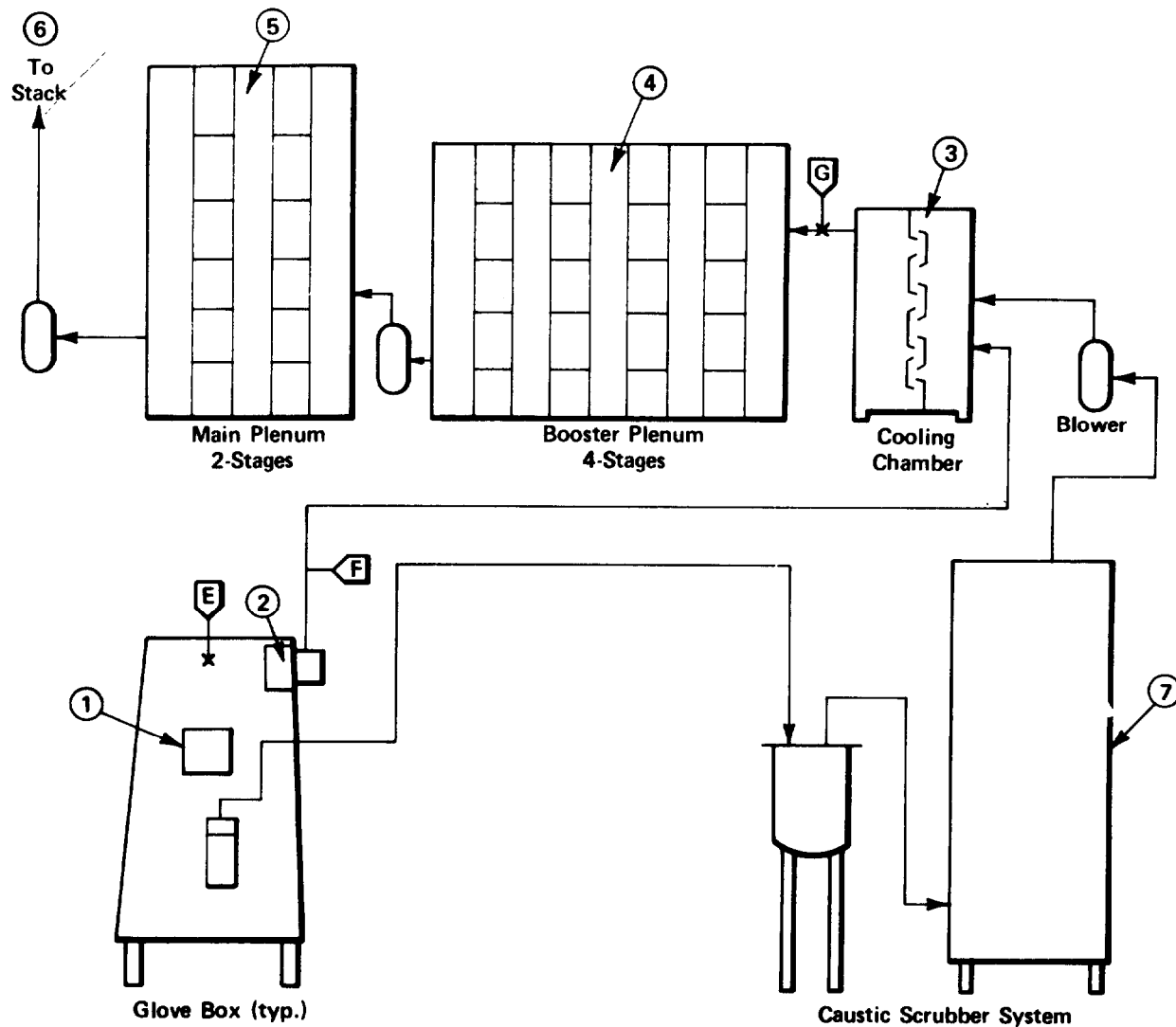
FIGURE 1
VENTILATION SYSTEM
CHEMICAL OPERATIONS

passing through the filter are collected by headers and flow through a cooling chamber (3), a multi-stage booster plenum (4), the building's main exhaust plenum (5), and then discharged through an exhaust stack (6). Some glovebox lines are provided with a supplemental exhaust system which passes the air vented from highly corrosive operations through a scrubber in which potassium hydroxide is circulated (7). The scrubbed exhaust air is then combined with the main exhaust air at the cooling chamber.

Chemical attack has been observed on all stages throughout the filter system but is most severe at the glovebox exhaust filter.

Figure 2 shows a glovebox in the chemical recycle facility. The volume of this box is 5.66 m^3 (200 ft.^{3}) and airflow is on the order of 2 m^3/min. (70 ft.^{3}/min.), thus giving about 20 air changes per hour. The process carried out in the box is leaching of solids which contain plutonium. The leach solution is 9 $\underline{M}$ nitric acid containing .1 to .2 $\underline{M}$ fluoride ion. Vapors from this mixture attack components of HEPA filters so vigorously that the filters at the box exhaust must be changed every few weeks. An example of a severely degraded glovebox exhaust filter is shown in Figure 3. Note how the media has become weak and is sluffing away from the upper edge of its frame. Collection headers, Figure 4, remove air exhausted from the glovebox lines.

A view of the caustic scrubber is shown in Figure 5. As mentioned previously, the scrubber system handles corrosive vapor drawn from processes in a limited number of boxes.

Figure 6 shows the cooling chamber. Headers which collect the exhaust from the various chemical process lines and the caustic scrubber converge at this point. The cooling chamber contains no filters but is equipped with heavy steel baffles and sprays for cooling, if required.

A 30-inch diameter line carries exhaust from the cooling chamber to a filter plenum, Figure 7, which houses four stages of HEPA filters, 30 filters per stage. Approximately 425 m^3/min. (15,000 ft.^{3}/min.) of air flow through the plenum. The 1st stage of HEPA filters is changed every two to three months. Subsequent stages in the plenum last six months to a year.

Figure 2. Glovebox Plutonium Recovery
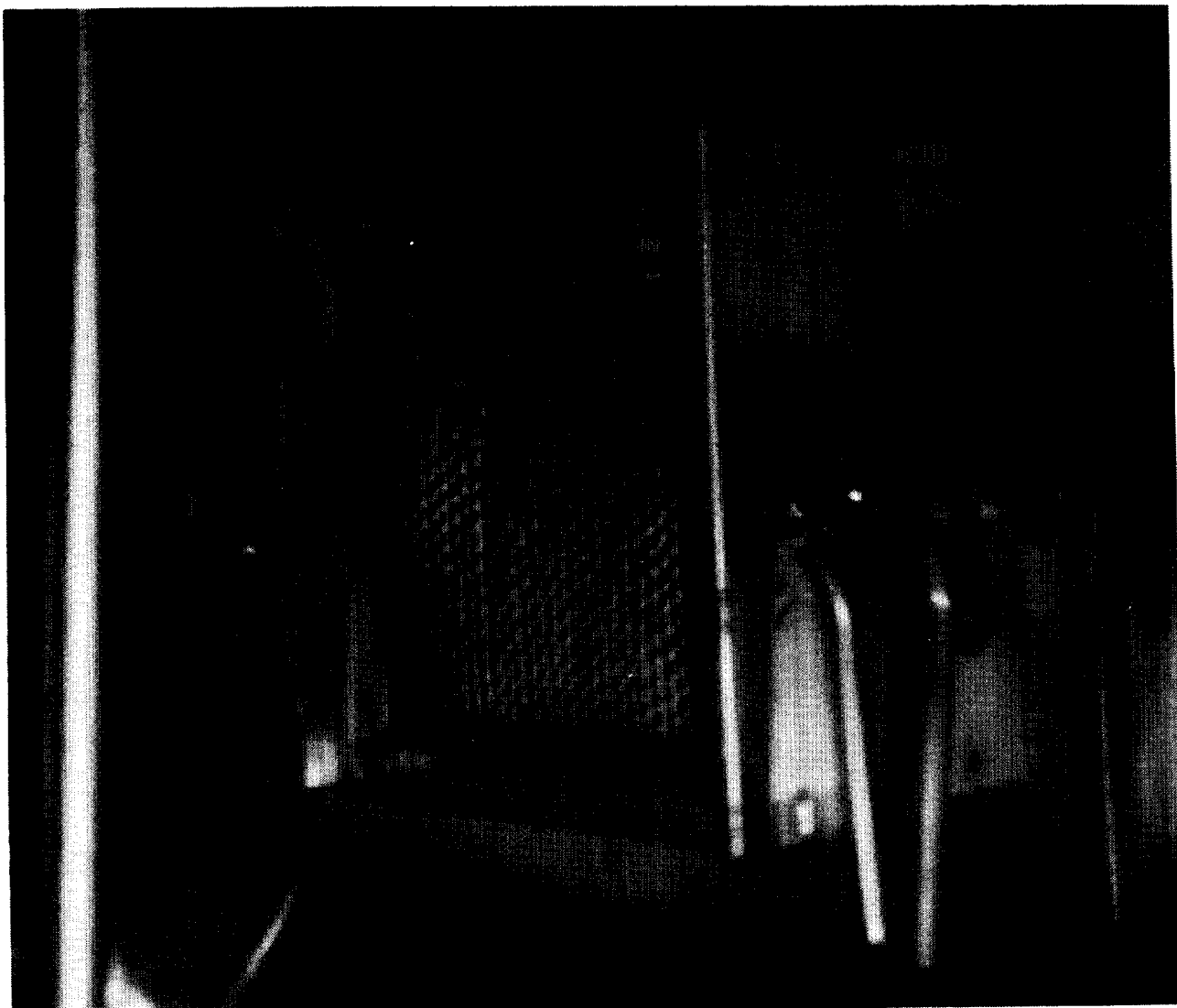
Figure 3. Glovebox Exhaust Filter
Degraded by Chemical Attack
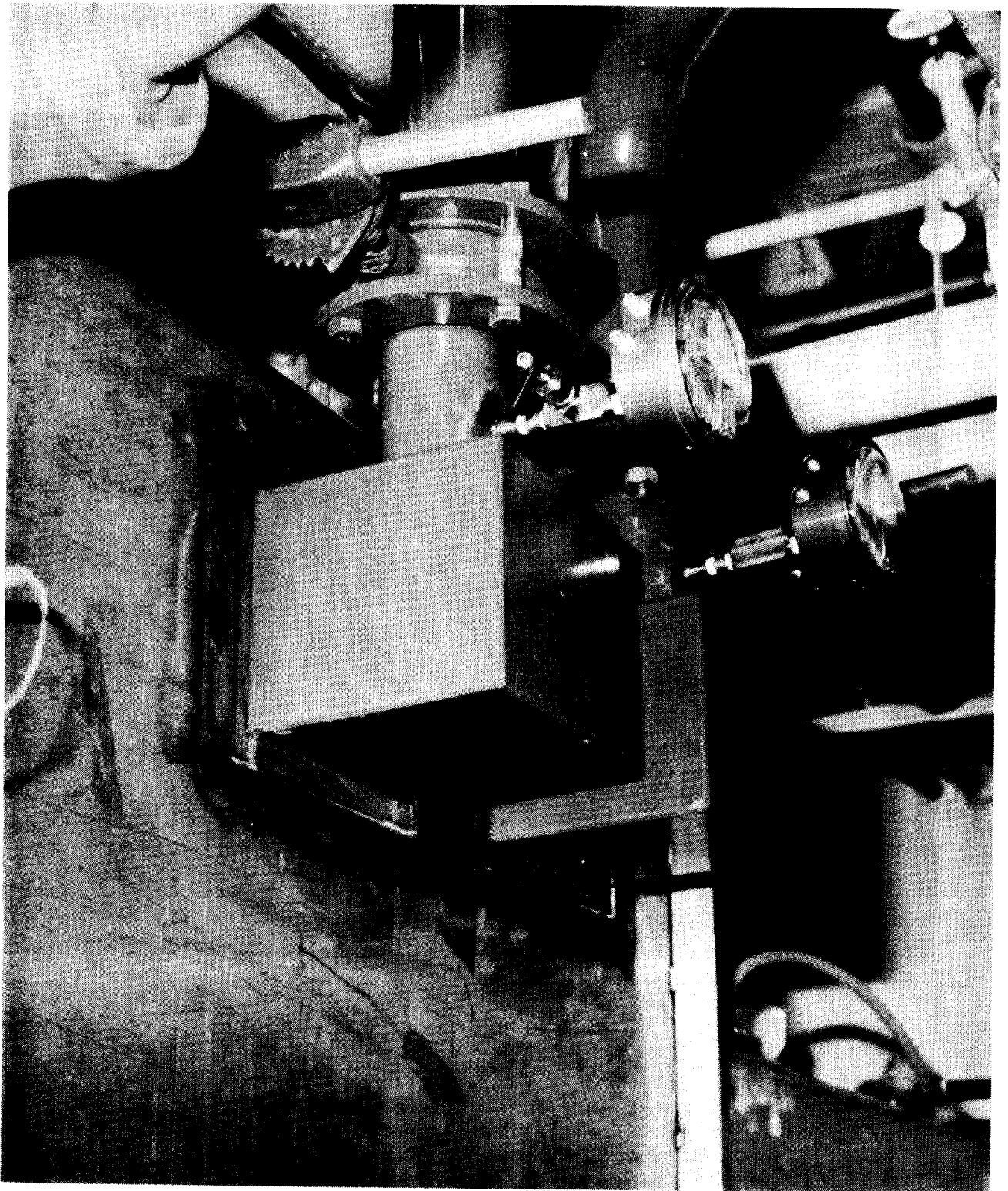
Figure 4. Collection Headers at Glovebox
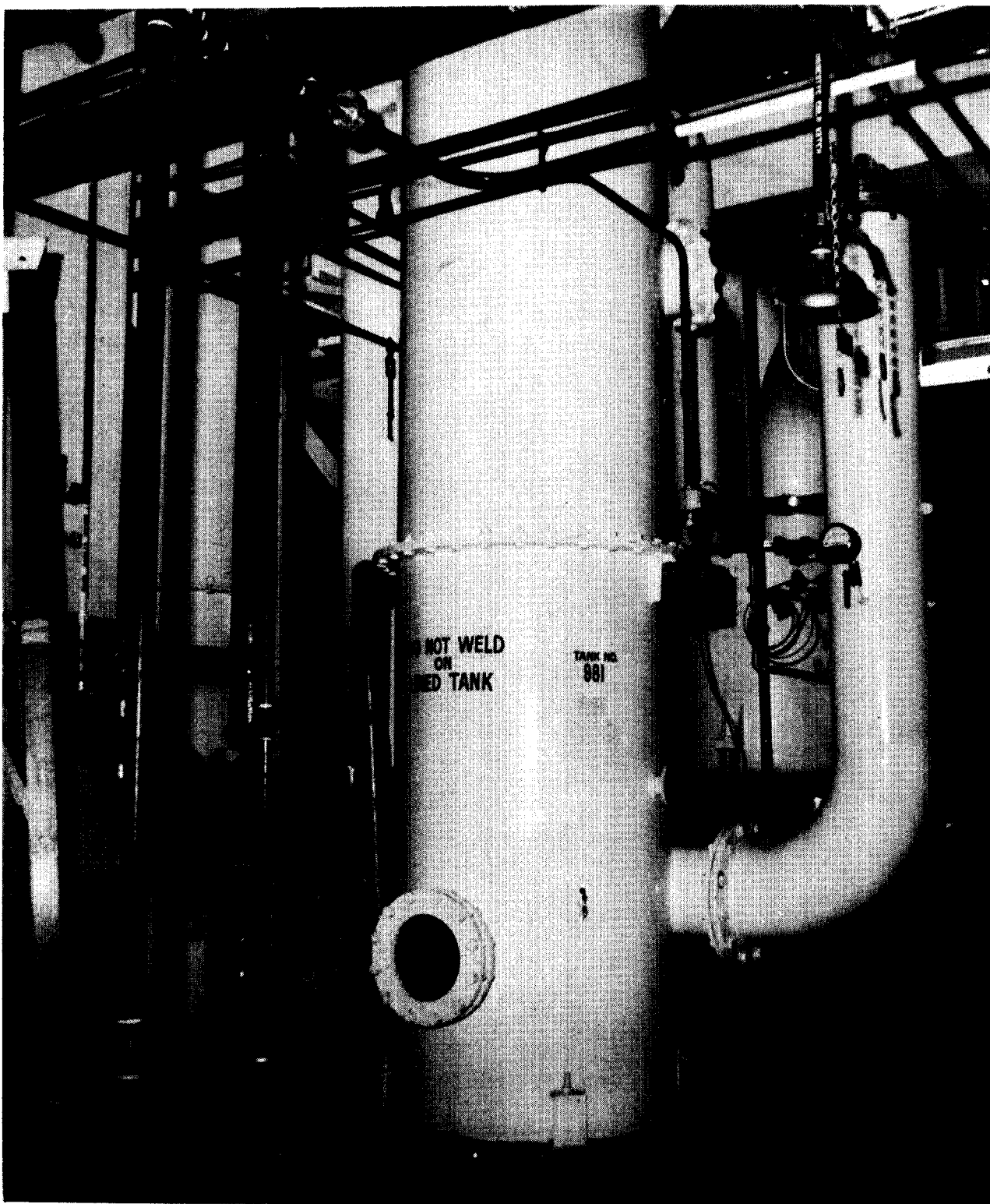
Figure 5.   Caustic Scrubber
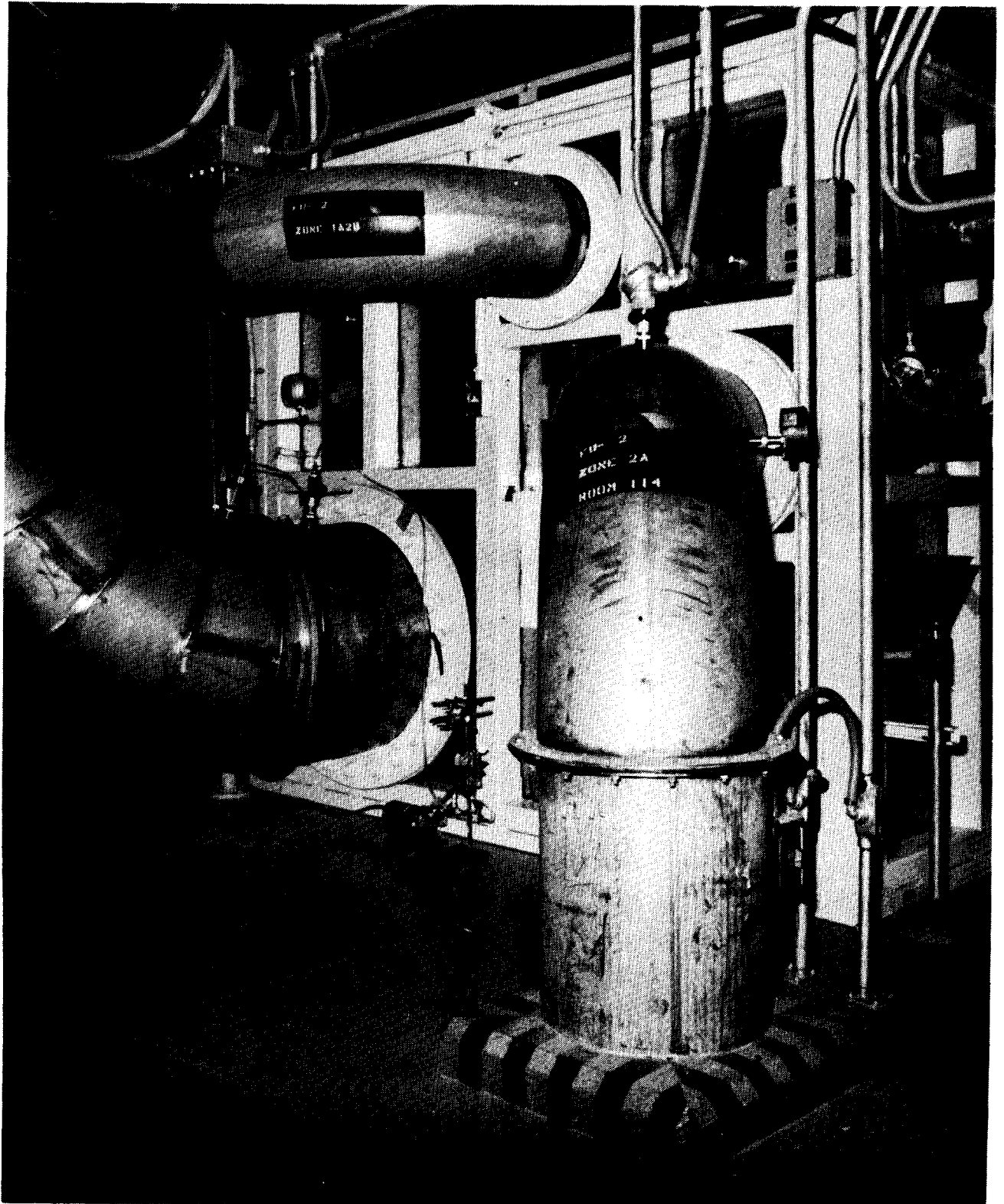
Figure 6. Cooling Chamber
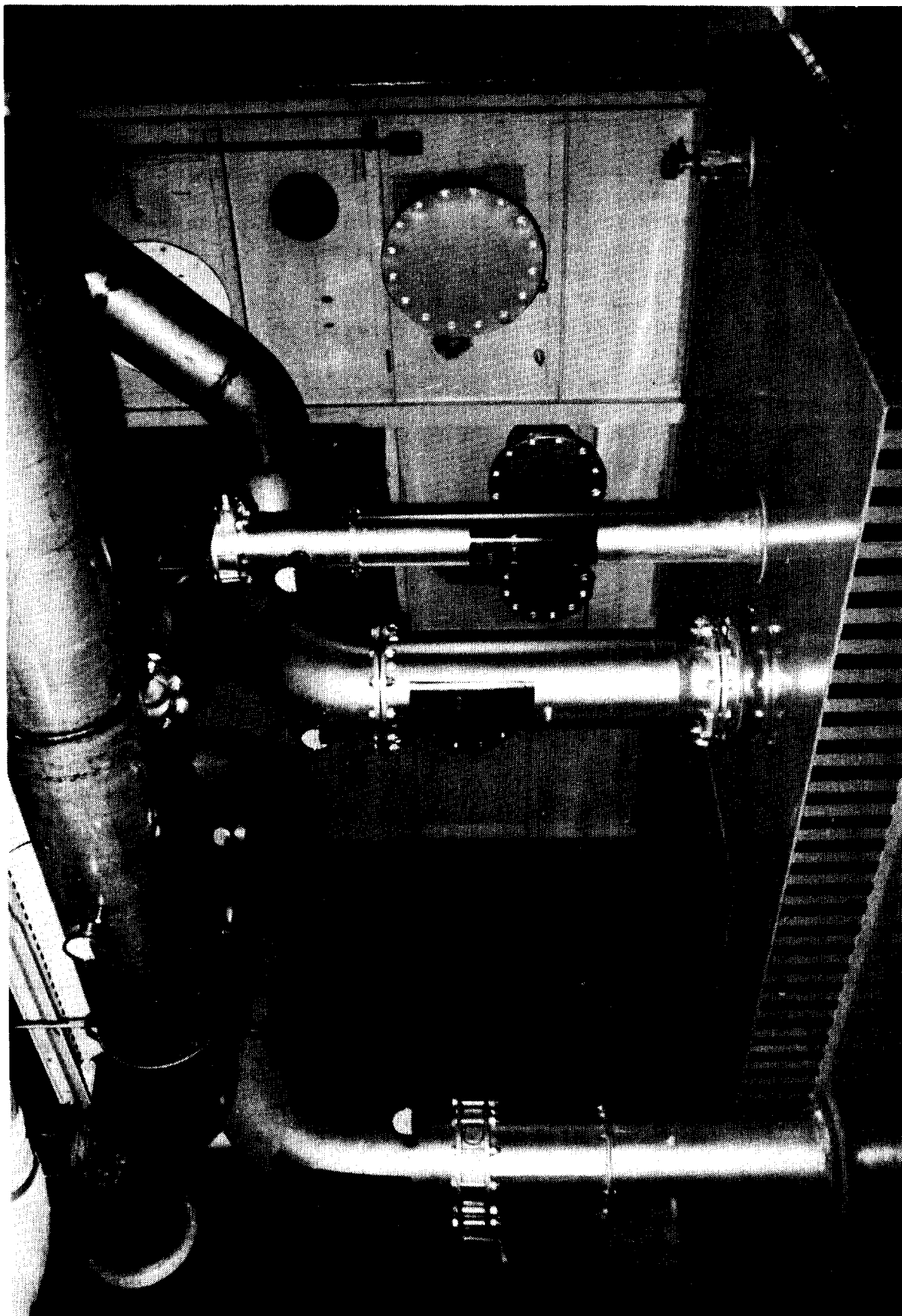
Figure 7. Collection Headers and Four-Stage Filter Plenum

Sampling of Exhaust Gases

A sampling program was begun to obtain background information on the concentration of various chemical and radioactive components of the glovebox air effluents. This program is still under way.

The sketch shown in Figure 1 also indicates the locations at which samples have been taken. Location E is a sample point in the interior of a glovebox in which plutonium is being leached from a refractory residue. Samples taken at this point would be expected to be highest in concentration of radioactive particulate and chemical components. F is a sample point located just a few feet downstream of the glovebox exhaust filter. G is located in the 30-inch diameter duct leading from the cooling chamber.

Sampling experience on radioactive particulate point E in the box, and point F downstream of a HEPA filter (Table I) shows the plutonium alpha activity observed upstream (E) and downstream (F) of the glovebox filter.

TABLE I		
Alpha Activity Upstream and Downstream		
of Glovebox Exhaust Filter		
"E" (Box) $d/m/m^3$	"F" (Header) $d/m/m^3$	Filter Eff. (%)
3.65×10^7	1.7×10^5	99.54
7.52×10^6	4.0×10^4	99.47
5.73×10^6	2.0×10^3	99.97
3.14×10^7	4.0×10^4	99.87
1.58×10^7	2.8×10^4	99.82
Average: 1.94×10^7	6.2×10^4	99.68

Membrane filters Millipore®* (.8 μ AA) were used to collect samples at points E and F.

The distribution of particle size of material taken from the membrane filters used in the glovebox atmosphere at point E was determined using a Quantimet 720 particle size analyzer which combines optical and electronic counting and sizing systems.

* Millipore® is the registered trademark of Millipore Corporation, Bedford, Mass., USA.

The distribution of particulate grouped in size intervals is shown in Table II.

TABLE II

Distribution of Pu Particulate

Sampled in Glovebox (E)

Size of Interval (μ)	% of * Total
< 0.3	10.2
0.4 - 0.7	23.2
0.8 - 1.3	36.7
1.4 - 3.4	23.1
3.5 - 6.8	5.4
6.9 - 13.6	1.3
> 13.7	.1

* Average of 8 determinations

A log probability plot, Figure 8, of the particle size distribution by count shows 50 percent of the total number of particles are 0.9 micrometers or less in size. Calculations show this would account for less than 0.5 percent of the total mass.

Chemical Components

Samples of air taken at the glovebox locations mentioned above were analyzed for chemical components (Table III). NO_x concentration observed in the box enclosure (point E, Figure 1) ranged from 0 to 171 parts per million (ppm) by volume. The wide range of NO_x concentration is attributed to the types of operation and level of activities in the glovebox. Exhaust air samples from the box (point F) ranged from 0 to 160 ppm NO_x.

Using liquid nitrogen to freeze condensible components, a sample taken of air in the box was calculated to contain 0.8 ppm by volume of fluoride in the box and ranged from 0.2 ppm to 2.5 ppm in the exhaust air from the box. The concentration of water varied but was usually in the range of 1500 to 3000 ppm. Acidity (H^+) found in the gas stream is attributable, in part, to nitric acid vapor.
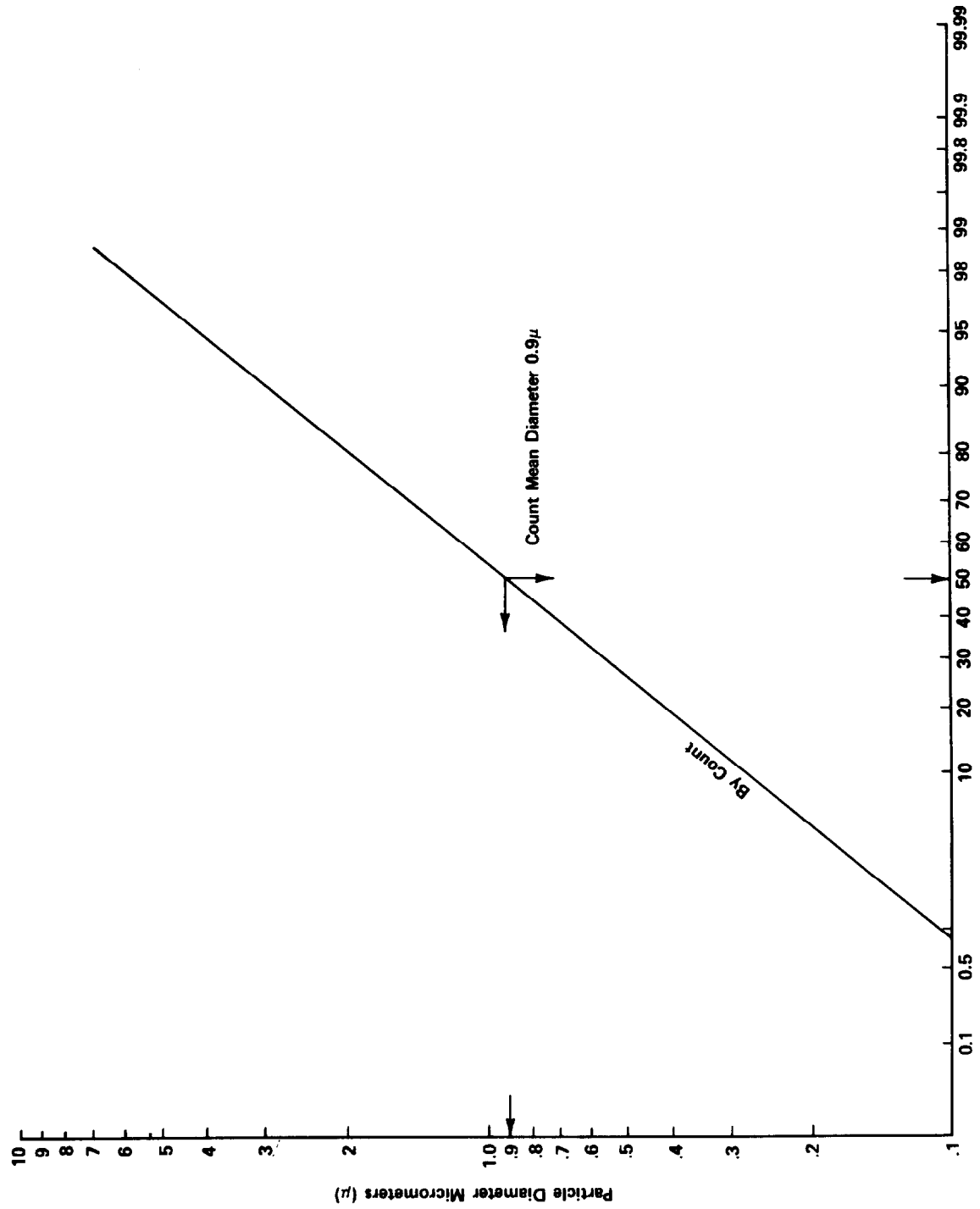
FIGURE 8. PARTICLE SIZE DISTRIBUTION

TABLE III

Concentration of NO_x, F, H_2O, H^+

Vol. ppm at Sample Location *

Component	In Glovebox (E)	Glovebox Exhaust (F)	Cooling Chamber Exhaust (G)
NO_x	0 - 171	0 - 160	.50 - 6.0
F	.8	.2 - 2.5	.14 - 0.6
H_2O		1500 - 3000	
H^+	1.9	4.2	

* Samples obtained over a four-month period under varied operating conditions.

Samples taken at the cooling chamber exhaust (point G, Figure 1) over a four-month period were found to be low in NO_x concentration and averaged about 1.0 ppm by volume, although readings as high as 6.0 ppm were observed. Fluoride at sample point G ranged from below the limit of detection, .14 ppm, to as high as .63 ppm. The analytical data indicate that the concentration of chemicals in the exhaust air, especially fluoride, is not high but their effect on HEPA filters is evident.

Samples of components of HEPA filters which have been in service in the booster plenum have been compared with unused component materials using a variety of analytical techniques.

Using thermogravimetric analysis and covering the temperature range to 1000°C, the volatile content of new media is about 4.0 percent (Table IV). After a filter is used in the 1st stage of the plenum, the volatiles increase to about 18 percent after a two and one-half month exposure. Volatiles on the 3rd stage media measured 4 percent even after an exposure of ten months. Volatiles in new asbestos base separator material are usually in the 25 percent range. After two and one-half months of use the volatile content measured in a 1st stage sample is close to 50 percent and after ten months exposure in the 3rd stage, increased to 61 percent.

TABLE IV
Volatile Content of Filter Components
Percent Weight Loss to 1000°C

Sample	New	1st Stage 2 1/2 Mo.	3rd Stage 10 Mo.
Glass Media	4	18	4
Asbestos Separator	25	50	61

The data indicate that filter media in the 1st stage adsorbed volatiles, including H_2O, HF, and HNO_3. These components would also react with particulate matter trapped in the media. Volatile content of the 3rd stage media showed minimal difference from unexposed media. In contrast, the weight of volatiles in the separator increased with length of service - even in the 3rd stage, and indicates material in the separator is reacting with gaseous component in the exhaust airstream.

Hot water leach of weighed filter samples were examined for acid and leachable ions using specific ion electrodes (Table V). New media was found to have a pH of 8.9, fluoride <.06 percent, and nitrate .09 percent. Leach solution of media exposed in the 1st stage of the filter plenum gave a pH of 3.9, fluoride 2.2 percent, and nitrate 9.8 percent. Media exposed in the 3rd stage of the filter plenum for ten months gave a pH of 3.15, fluoride .45 percent, and nitrate 1.6 percent.

Leaches performed on samples of filter separator material taken from the 1st stage filter after two and one-half months service, yielded a pH of 3.9, fluoride .22 percent, and nitrate 19.6 percent. A separator sample, after ten months exposure in the 3rd stage, yielded a pH of 3.4, fluoride .24 percent, and nitrate 36.5 percent. The soluble substance leached from the separator was identified to be predominately magnesium nitrate, along with soluble silicate(s).

TABLE V

Water Leach of Filter Components

Sample	New	1st Stage Filter After 2 1/2 Mo.	3rd Stage Filter After 10 Mo.
Media:			
pH	8.90	3.90	3.15
F	.06%*	2.20%	.45%
NO_3	.09%	9.80%	1.60%
Separator:			
pH		3.9	3.4
F		.22%	.24%
NO_3		19.60%	36.50%

* Weight percent based on weight of sample leached

The leach data correlate with the thermogravimetric analysis. It is of special interest that the separator in the 3rd stage had adsorbed more nitrate than that from a 1st stage sample, indicating continued reaction during the exposure period.

Mass Spectral outgas of media and separator samples provide another means of observing chemical effects on these materials (Table VI). With new filter media only small amounts of moisture, carbon dioxide, carbon monoxide, etc., were observed. On 1st stage filter media in service for two and one-half months, the major substances which outgased included silicon tetrafluoride, water, nitrogen oxides; minor components included hydrogen fluoride, ammonia, and carbon dioxide. Third stage filter media in service ten months outgased water as the major component and ammonia, silicon tetrafluoride, and nitrogen oxides in minor concentrations.

Outgas data taken on samples from new separators gave only water as a major component. Used separators from the 1st and 3rd stages gave major components: water, nitrogen oxides, and carbon dioxide with minor amounts of silicon tetrafluoride.

TABLE VI

Mass Spectral Outgas of Filter Components

Sample Source	Outgas Components	
Filter Media – New	Major:	None
	Trace:	H_2O, CO, CO_2, Hydro-carbons
Separator – New	Major:	CO_2, CO, H_2O
	Trace:	CH_3OH, CH_2O, Binder Decomp.
Filter Media – Used in 1st Stage	Major:	SiF_4, H_2O, NO, CO
	Minor:	HF, NH_3, CO_2
Separator – Used in 1st Stage	Major:	H_2O, NO, N_2O, CO_2
	Minor:	SiF_4
	Trace:	HF, Hydrocarbons, HCl, HNO_3
Filter Media – Used in 3rd Stage	Major:	H_2O, NH_3, SiF_4, N_2O, NO, DOP
	Minor:	NO_2, HCl, CO, CO_2, Fluorosiloxanes
Separator – Used in 3rd Stage	Major:	H_2O, NO_2, NO, N_2O, CO
	Trace:	SO_2, Hydrocarbons

III. Summary

In summary, the trends noted by the analytical work indicate that fluoride in the exhaust gas preferentially adsorbs on the glass filter media whereas the nitrate preferentially reacts with the chemicals associated with the asbestos separator. The partitioning is more pronounced in the 3rd stage filters where there is less deposition of particulate matter in the media. The concentration of fluoride in 3rd stage filter components is lower than on the 1st stage, even after longer exposure, suggesting depletion of fluoride as it passes through a number of stages of filter media.

The cumulative effect of fluoride compounds in the degradation of filters is undoubtedly quite complex. The properties of glass fibers may be greatly affected by alteration of the oxygen-bridged

polymeric silicate ions $(Si_xO_y)^n$ or formation of stable compounds such as CaF_2, SiF_4, and NaF.

The take-up of nitrate in media is relatively high only on the 1st stage filters where it combines with, or is a part of, the particulate matter being filtered. Nitrate is heavily absorbed by the asbestos separators in filters of all stages.

The sampling program will be continued as new components are developed and operational changes are made. An area that will receive special attention is at the glovebox line, the source of chemical and particulate contaminants.

It is intended to explore the use of prefilters at the glovebox exhaust of a type which are resistant to acid fumes and take out the larger particulate which should contain most of the plutonium. A <u>cleanable</u> prefilter would be attractive from both the standpoint of plutonium economy and reduction of the numbers of filters discarded.

Since asbestos base separators react with nitric acid vapor and oxides of nitrogen, attention will be given to variations of separator composition.

<u>Acknowledgement</u>

ENTRAINMENT SEPARATOR PERFORMANCE

M.W. First and D. Leith
Harvard Air Cleaning Laboratory

Abstract

Clean and dust-loaded ACS entrainment separators mounted up-stream of HEPA filters were exposed to a combination of fine water mist and steam at about 70°C from one to four hours. In every trial, the ACS entrainment separator prevented measureable deterioration of performance in the following HEPA filter. Droplet size-efficiency evaluation of the ACS entrainment separators showed that, within the accuracy of the measurements, they meet all service requirements and are fully equal to the best separator units available for service on pressurized water reactors.

I. Introduction

A loss of coolant accident in a PRW nuclear reactor imposes severe conditions on the air cleaning elements that comprise an important part of the engineered safeguards system. A major source of air cleaning system stress would be the very large amounts of condensed water in the form of mist and droplets that would be entrained with the containment vessel air, released fission products, and uncondensed steam. This condensate could flood the particulate filters and activated charcoal adsorption units in the absence of efficient liquid water separation devices. The detrimental effects of large amounts of condensed steam on particulate filters and activated charcoal adsorption units was recognized many years ago, and remedial measures have included increasing the water repellency and steam resistance of absolute filter papers [1] as well as the introduction of entrainment separators (also called moisture separators and mist eliminators) upstream of the principal elements of the air cleaning train.

Peters [2] investigated the mist separation characteristics of full-scale 2-in. thick mats of "Teflon" yarn wrapped over stainless steel reinforcing wire* when exposed for 10 days to a simulated loss of coolant atmosphere and found that these units were capable of preventing failure of downstream absolute filters while maintaining flow at or close to design values. Rivers and Trinkle [3] described a moisture separator that was developed for the Connecticut Yankee Atomic Power Plant and found to be capable of protecting downstream absolute filters for a minimum of 24-hours when subjected to design flow rates of a "saturated air-steam mixtures at pressures up to 40 psi and 261°F, the maximum predicted conditions." These moisture separators consisted of "three type M-105 phenolic-bonded glass fiber pads" mounted in a frame approximately 8-in. deep and placed downstream of a set of louvers.** MSAR 71-45 [4] described

*York Separator, Style 321. Otto H. York Co.
** American Air Filter Co., Louisville, Ky.

tests of five commercially available entrainment moisture separators and found that two of these units AAF Type T** and MSA Type G † were capable of removing greater than 99% of droplets in the 1-10 μm size range when handling a simulated PWR postaccident atmosphere at rated flow rate for a number of hours. The MSA Type G Separator is 5-in. deep and consists of multiple layers of 9 μm glass fiber and 0.006-in. diameter knitted wire pads.

The present study was undertaken to evaluate the usefulness of a new commercially available entrainment separator for service in PRW power reactor engineered safeguards systems.

II. Test Program

Ten separate trials were conducted in each of which an unused 1,000 CFM nominal capacity filter was protected by a new ACS entrainment separator of equal air flow rating located upstream of it. In each, the combination was subjected for a prolonged period to a high concentration of water droplets in the 1-10 μm diameter range suspended in a saturated steam-air mixture at about 70°C. Droplet concentration measurements were made upstream and downstream of each entrainment separator and droplet collection efficiency determinations were made for four important size ranges. Three new absolute filter and new separator pairs were tested for periods of one hour and three identical pairs were tested for periods of four hours each. Four additional pairs of new elements were tested for four hours after having been loaded with Cottrell-precipitated fly ash.

Before and after exposure to the droplet laden steam-air mixture for the prescribed length of time, the efficiency of each absolute filter was checked at an airflow rate of 600, 1000, and 1600 cfm using a dioctylphthalate (DOP) test aerosol having a mass median diameter of 0.6 μm and a geometric standard deviation of 1.65. In every case, ACS entrainment separators protected downstream absolute filters to the degree that no decrease in efficiency could be detected after prolonged exposure to the droplet-steam aerosol.

III. Test Facilities

A dimensioned schematic of the test facility designed for this program is shown in Figure 1. The steam-air mixture entered the filter and entrainment separator housing though a rectangular section where additional steam and water droplets were injected and where a thermocouple was located to record the temperature of the aerosol as it reached the entrainment separator. At the entrainment separator and absolute filter, the housing cross section enlarged from 20-in. square to 24-in. square to provide sumps for water drainage. Between separator and filter there was a 5-ft. long section equipped with Plexiglas view port.

**American Air Filter Co., Louisville, KY.
† Mine Safety Appliances Co., Pittsburgh, PA.

Downstream of the filter, there was an 8-in. diameter duct with a Venturi meter for measuring flow rate, a flow regulator, and a Buffalo Forge Co. centrifugal blower with a 48-in. diameter impeller and 25 HP motor, capable of moving 2000 cfm of air at 40-in. w.g. After the blower, the flow entered a switch that made it possible to send the flow to the waste air system or back to the test section for recirculation. The recirculation mode was used whenever elevated temperature steam-air-droplet trials were conducted but the entire stream was exhausted to the waste air system whenever filters were tested with DOP. All surfaces of the test apparatus except the duct leading from the switch to the waste air system were heat insulated with 3.5 in. of commercial fiberglas blanket covered with aluminum foil.

Each entrainment separator and absolute filter was mounted firmly in the test tunnel against 1-in.flat-ground flanges. Gasket material 1/8-in. thick, self-adhesive closed sponge rubber, was applied to the flanges to assure a good seal. The absolute filters were equipped by the manufacturer with Neoprene sponge gaskets. Each separator or filter was held firmly in position by eight clamps. In every case, before exposing separator or filter to the droplet and steam mixture, an in-place filter test was performed with DOP to demonstrate that the separator and filter were mounted satisfactorily.

Steam was injected in the system at 3 psi through a 3/4-in. pipe located upstream of the separator. A dense fog of water droplets was generated by a bank of 39 Spraying Systems Co.* 1/4 J nozzles. These are two-fluid atomizing nozzles that required compressed air as well as water. They were operated at a manifold pressure of 7.5 psi to the compressed air side and a water flow of 2.2 lpm. Air pressure was measured with a pressure gauge mounted on the inlet air manifold and water flow rate was measured with a rotameter located just upstream of the inlet liquid manifold. Figure 2 shows the bank of 39 nozzles as they were located in the injection section. During the steam-droplet tests, the aerosol was recirculated but, because injection of steam, water, and compressed air was continuous, it was necessary to bleed off a fraction of the gas stream to the laboratory waste air system to avoid overpressurizing the test facility.

Water drains were provided at four points along the housing as shown in Figure 1; one drain was upstream and one was downstream of the entrainment separator, other drains were upstream and downstream of the filter. The rate at which water drained from the sections upstream and downstream of the separator was measured using a graduated container and stopwatch. The liquid flow from the drains on either side of the absolute filter were so low that they could only be measured by noting the total amount of liquid collected over the course of a four-hour run.

* Spraying Systems Co., North Avenue at Schmale Road, Wheaton, IL.

Pressure taps were located up and downstream of the entrainment separator and absolute filter to measure pressure drop across these units and across the Venturi flowmeter to measure system flow. Pressure taps were connected to manometers to provide continuous visual observation of pressure drop at these three points in the system. In addition, the pressure taps were connected through a sequential switching system to a pressure transducer that made it possible to record pressures on a strip chart. Figure 3 is a photograph of the pressure drop and temperature monitoring instruments and strip chart recorder. The temperature in the test section was measured with an iron-constantin thermocouple pair. One side was placed in the injection section and the other was placed in an ice water bath. The thermocouple was recalibrated with boiling water prior to each separator test and the output was continuously monitored and recorded on a strip chart. All data pertaining to pressure drop, temperature, water flowrate, and compressed air were recorded in a lab book at ten minute intervals; water drain flowrates were recorded each twenty minutes.

Droplet concentration and size measurements were made with 4-stage May-Cassella cascade impactors located inside the test housing upstream and downstream of the entrainment separator. Each of the four impactor stages was fitted with a glass slide coated with freshly generated magnesium oxide (MgO) deposited by passing the slide through the fume rising from a burning magnesium ribbon. When the test atmosphere was drawn through the impactor, water droplets present in the gas deposited on successive stages according to decreasing droplet size. When a droplet hits the coated slide, a crater forms in the soft, smooth magnesium oxide that has the same diameter as the droplet. Crater diameters were measured under the optical microscope to establish droplet size parameters. During the sampling, the impactor was mounted inside the moisture eliminator-filter housing and operated to sample isokinetically. The characteristic droplet diameters collected on each stage were found to be: stage 1, 29 µm; stage 2, 12.5 µm; stage 3, 5.3 µm; stage 4, 3.1 µm.

A. ACS Entrainment Separator

The moisture separators used in these tests were manufactured by ACS Industries, Inc., Woonsocket, R.I. and designed specifically for this application. The manufacturer's description of the separators is as follows:

"They are composed of a 5-1/2" thick pad of knitted mesh enclosed in a welded frame of stainless steel sheet metal. The mesh is manufactured using a parallel knitted style composed of .006" T304 SS and multifilament fiberglass. The knitted composite mesh is crimped and the pad is constructed by building up layers of mesh, in such a way as to obtain a pre-determined density. Interspersed through the pad thickness are a number of layers of plain wire mesh to assist in the removal of entrained liquid from the interior of the mesh pad.

"The frame consists of a single length of 16 gage, T304 SS sheet formed with a 3/4" lip on both edges and finally formed into a 24" square. The pre-assembled mesh pad is inserted into the frame which

697

is closed and heliarc welded at one corner. Square cross grids made of 1/8" T304 SS rod on 5" centers are welded into place on both faces of the mesh pad. Drain holes are drilled in one side of the square frame and the unit is marked to indicate that the holes are on the bottom when it is installed. On the top two rows of horizontal grid members on both faces, 3-1 1/2" long pieces of 1/8" T304 SS rod are welded on each grid rod at an upangle (6 per side) to act as prongs to insure that the mesh pad doesn't settle or pack down and pull away from the top of the frame when installed upright.

"These units are designated as ACS Model 101-55." A drawing reflecting the above description is shown in Figure 4.

B. Absolute Filters

Catalog No. 7C83-L, size F filters were purchased from Flanders Filters, Inc. Face dimensions of these units were 24-in.square and depth, 11 1/2-in. Filters were fabricated from glass fiber paper, aluminum foil separators, plastic foam sealant, and double flanged chromatized steel frame. Rated efficiency for homogeneous 0.3 μm DOP is not less than 99.97%. Rated pressure drop is not more than 1.0 in. w.g. at 1000 cfm. Manufacturer's data, stamped on each filter, are listed in Table 1.

IV. Test Program

Ten individual tests were made with all-new moisture separator-filter pairs. Tests 1, 2, and 3 were each of one hour duration and were conducted with clean, new separators and filters. Tests 4, 5, and 6 were each of four hours duration and were conducted with clean, new separators and filters. Tests 7, 8, 9, and 10 were each conducted with new separators and filters which first had been loaded with dust. Each of these latter tests was of four hours duration. In test 7, the moisture separator-filter pair was loaded in tandem with 29 pounds of dust. For tests 8, 9, and 10, the separator-filter pairs were loaded in tandem with one pound of dust. The dust used for loading the moisture separators and filters prior to steam-water droplet testing was seived Cottrell-precipitated pulverized coal fly ash having a count median diameter of 0.6 μm and a geometric standard deviation of 3.0. This prepared coal fly ash test dust is equivalent to NBS dust without the addition of small amounts of cotton linters and carbon black that are sometimes added to shorten test time and to improve the readability of the discoloration papers. As neither addition serves any useful purpose for, or influences the results of the tests performed in this study, they were omitted.

After inserting a separator and absolute filter into the test tunnel, a DOP in-place filter test, carried out in conformity with the methods recommended in ORNL-NSIC-65 [5] was performed on the separator and on the filter at air flow rates of 600, 1000, and 1600 cfm to establish that the unit was undamaged and that there was no leakage around the mounting flanges. A TDA*, seven-nozzle hetero-

---

*Air Techniques, Inc., Baltimore, MD.

geneous (cold) DOP generator, operated at 30 psi, was used. Upstream and downstream DOP concentrations were measured with a TDA-2D* photometer. When leakage was found, the filter or separator affected was reseated the filter mounting clamps, retightened and additional DOP tests performed until it was established that no leakage occurred. Beakers were placed in the housing at distances of 1, 2, 3, and 4 feet downstream of the entrainment separator to indicate the rate at which droplets or condensation reached the floor of the dropout section at various distances downstream of the separator.

A run was started by feeding steam to the recirculation loop and water and air to the spray nozzles. The temperature inside the test section was monitored and the test period started after the unit reached a stable equilibrium temperature of about 70°C (15 to 30 minutes).

Water and airflow rates to the spray nozzles and flow rate through the entire system were carefully monitored and adjusted whenever necessary. Generally, once equilibrium conditions were established, these flows were stable. Visual observation of droplet carryover downstream of the separator was attempted during each trial but, because of the steam, the Plexiglas observation port was always fogged making meaningful observations impossible. Near the end of each trial, cascade impactor samples were taken downstream of the separator for droplet size analysis. At the conclusion of the trial, the water, air, and steam feeds were discontinued immediately and the water level in the four droplet collecting beakers on the floor of the tunnel was measured and recorded.

The efficiency of the absolute filter after exposure to the steam-droplet-air atmosphere was checked by performing once again the prescribed DOP in-place filter test at 600, 1000, and 1600 cfm. The test section was then opened, the separator and filter removed and examined visually.

The number concentration of droplets in each size range produced by the 39 nozzle spray manifold was calculated from single nozzle tests by applying a suitable multiplication factor. The results are given in Table 2. Droplet concentrations downstream of the entrainment separator and ahead of the absolute filter were measured at the conclusion of each test. After the size of droplets collected on each impactor stage had been determined, it was only necessary to count the number of droplets present on each stage to develop the downstream droplet size distribution and calculate droplet collection efficiency.

V. Test Results

Table 3 summarizes temperature and pressure drop measurements for each of the ten trials. Temperature and pressure drop were stable during all tests for both clean and dirty separators and filters.

---

*Air Techniques, Inc. Baltimore, MD.

Table 4 summarizes water drainage measurements for each of the ten trials. Close to 99.9% came from the drains before and after the entrainment separator. Table 5 shows the results of in-place filter tests performed before and after each of the trials for entrainment separators and absolute filters. No degradation in filtering ability of the filters was observed after exposure to a steam-droplet atmosphere in any of the tests. In all cases, the entrainment separator successfully protected the absolute filter from damage.

Table 6 is a summary of droplet size vs collection efficiency data for the moisture separators determined from analysis of cascade impactor data. The results are plotted in Figure 5 with the curve for the MSA entrainment separator. They show that the collection efficiency vs droplet diameter relationship for the ACS entrainment separator is identical, within experimental reliability, with that of the MSA separator.

After each trial, between 1.5 and 2 ml of water was found in each beaker placed on the floor of the rectangular test section between moisture eliminator and filter regardless of beaker location or duration of test. This demonstrates that few large droplets were blown off the downstream face of the moisture eliminator.

VI. Summary and Conclusions

Ten ACS entrainment separators have been tested for their ability to protect absolute filters from damage when exposed to a droplet laden steam atmosphere similar to that expected during an accident at a PWR. The test aerosol contained high concentrations of water droplets in the 1 to 10 μm diameter range at temperatures in the vicinity of 70°C. Pressure was atmospheric.

In all cases, the separators protected the absolute filters from damage on the basis of acceptable in-place DOP filter tests conducted at 600, 1000, and 1600 cfm. The droplet diameter vs collection efficiency characteristics of the ACS entrainment separators were found to be comparable to those of the MSA entrainment separator, as reported in Reference 4.

The demister units that were tested met "qualification requirements similar to those found in MSAR 71-45 [4] and, as a consequence, may be presumed to be acceptable to the Nuclear Regulatory Commission staff as defined in Regulatory Guide 1.52[6].

Table 1   Absolute filters used for tests.

| Test # | Serial # | Factory Measurements | |
		Airflow Resistance at 1000 cfm in. w.g.	Homogeneous DOP % Penetration
1	A445098	0.74	0.004
2	A445100	0.72	0.006
3	A445095	0.86	0.002
4	A445099	0.78	0.010
5	A445104	0.80	0.002
6	A445097	0.70	0.006
7	A445105	0.80	0.004
8	A445096	0.76	0.006
9	A445102	0.80	0.002
10	A445103	0.78	0.005

Table 2   Number concentration of droplets
from a 39-Nozzle bank of Spraying Systems 1/4-J nozzles.

Stage Droplet Diameter micrometers	Number Concentration $\#/cm^3$ of air
29.0	646
12.5	661
5.3	121
3.1	91

Table 3   Temperature and pressure drop
at test conditions.

Test	Temp.°C	Pressure Drop, in. w.g. Separator	Filter
1	55	0.80	0.90
2	66	1.02	0.92
3	56	0.87	1.05
4	75	1.05	0.95
5	66	0.91	0.96
6	74	0.94	0.96
7	69	2.60	1.40
8	72	1.13	0.93
9	73	0.92	0.92
10	73	0.87	0.87
Average *		0.95± 0.10	0.94± 0.05

+ = standard deviation

* Excluding test 7, in which 29 pounds of dust were fed to the separator and filter. All pressure drop data taken at 1000 cfm.

Table 4   Water drain rates.

	Separator		Filter	
Test	Upstream	Downstream	Upstream	Downstream
1	-- no data --		-- no data --	
2	1.77 lpm	0.335 lpm	0.0014 lpm	0
3	1.74	0.265	0.0011	0
4	1.90	0.340	0.00074	0.00015
5	1.99	0.139 ·	0.00098	0.00023
6	1.93	0.087	0.00106	0.00031
7	1.90	0.035	0.00083	0.00008
8	1.93	0.160	0.00375	0.00052
9	1.93	0.093	-- no data --	
10	1.97	0.056	0.00478	0.00042
Average:	1.90 lpm	0.17 1 pm	0.0018 lpm	0.00028 lpm
% of total drained		99.9%		0.11%

Table 5 DOP penetration for separators and absolute filters before and after steam and droplet exposure.

Test	Separator, %		Absolute Filter, %	
	Before	After	Before	After
1	80-90	100	<0.01	<0.01
2	98-100	87-100	<0.01	<0.01
3	90-100	98-100	<0.01	<0.01
4	95-96	93-97	<0.01	<0.01
5	93-97	94-98	<0.01	<0.01
6	93-95	93-95	<0.01	<0.01
7	95-97	93-95	<0.01	<0.01
8	90-93	90-95	<0.01	<0.01
9	78-87	92-97	<0.01	<0.01
10	84-90	90-100	<0.01	<0.01

Table 6 Droplet collection efficiency of entrainment separators.

Test	Droplet diameter, μm			
	29	12.5	5.3	3.1
1	---------------- no data ----------------			
2	99.87%	99.95%	99.88%	99.99%
3	99.89%	99.98%	99.93%	99.92%
4	99.99%	99.96%	99.72%	99.91%
5	99.92%	99.67%	99.20%	99.85%
6	99.78%	99.67%	98.51%	99.91%
7	99.79%	99.67%	97.58%	99.63%
8	99.75%	99.91%	99.36%	99.46%
9	99.30%	99.72%	---- no data -----	
(10 -no data-)	99.79%	99.82%	99.17%	99.81% Average
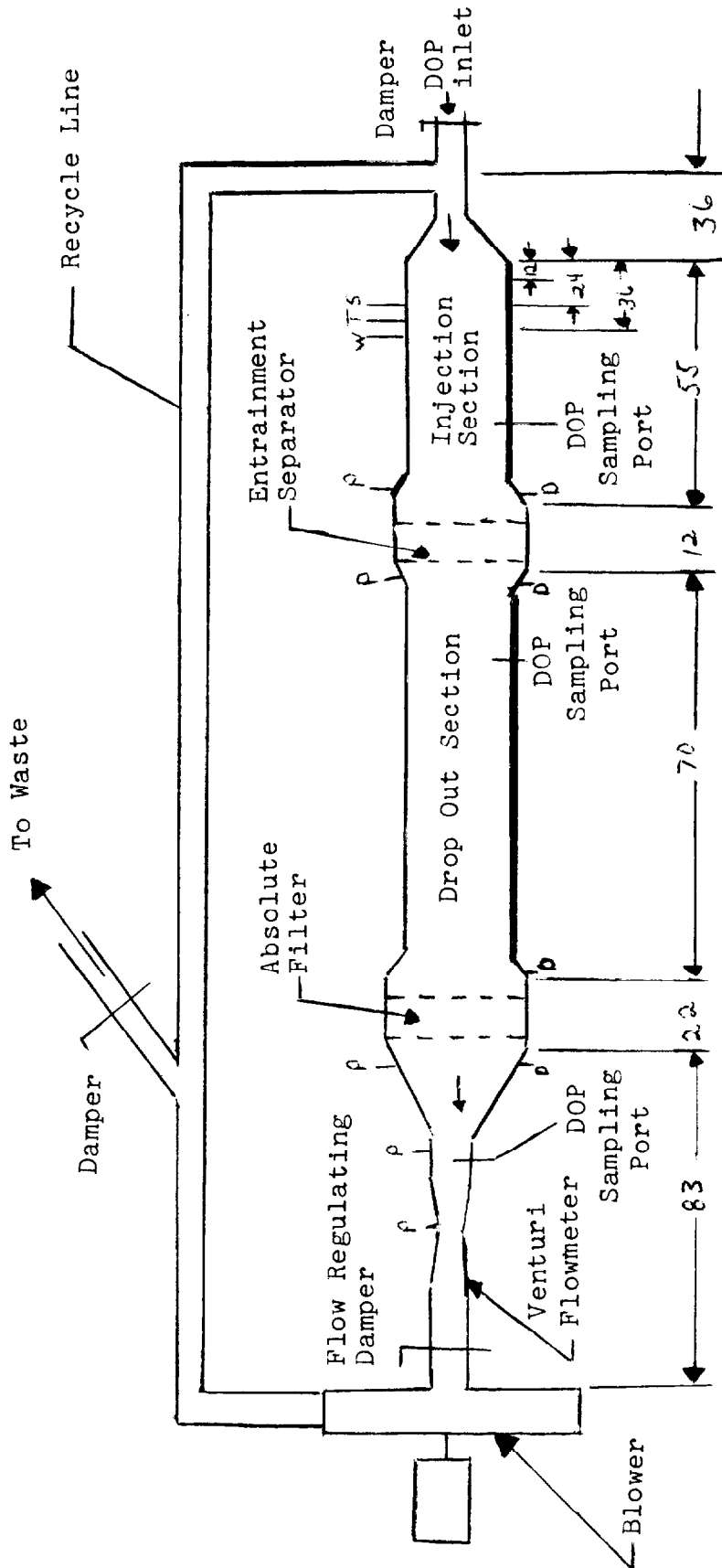
FIGURE 1   SKETCH OF APPARATUS

S – Steam Injection

T – Temperature Meas.

W – Spray Nozzles

P – Pressure Tap

D – Drain

All Dimensions in Inches
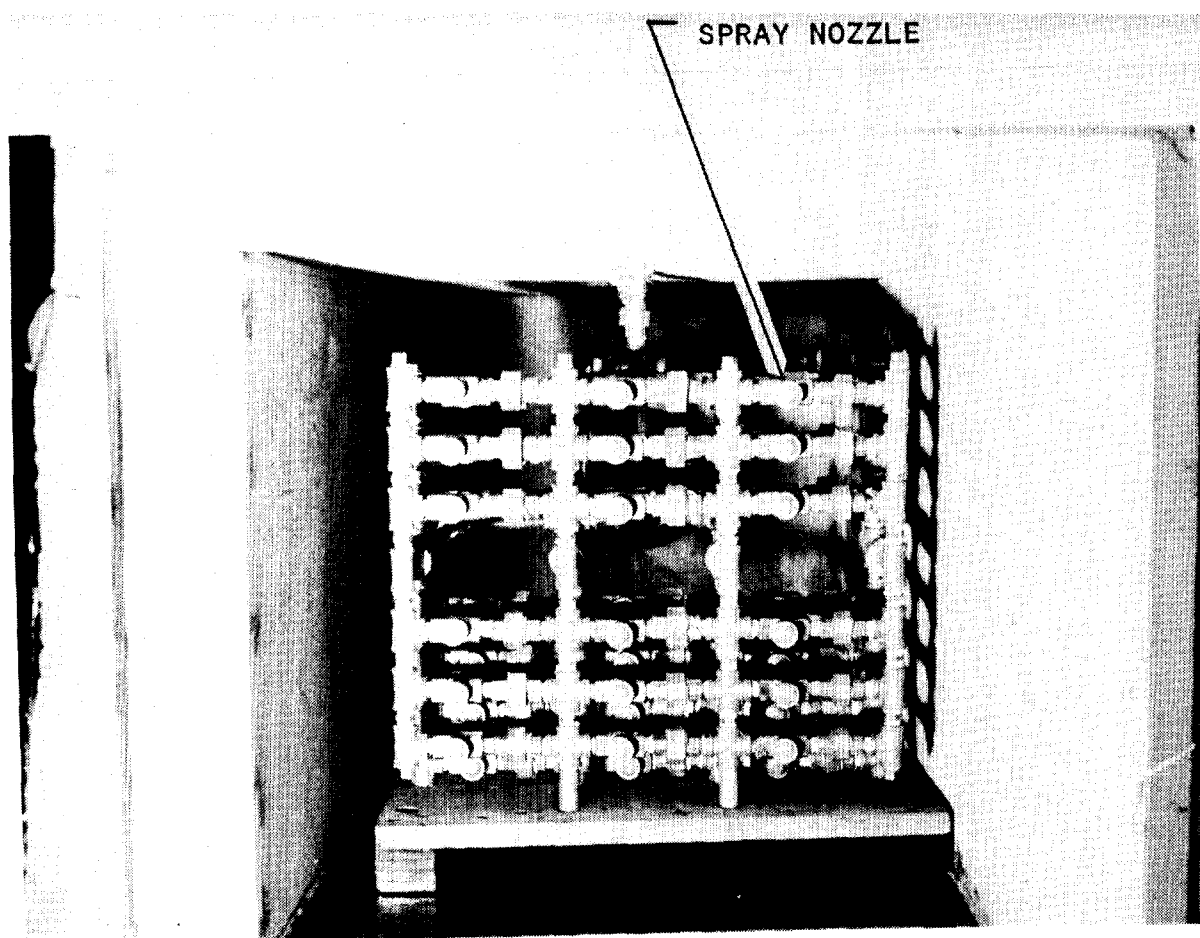
FIGURE 2

PHOTOGRAPH OF NOZZLES, INTERIOR OF INJECTION SECTION
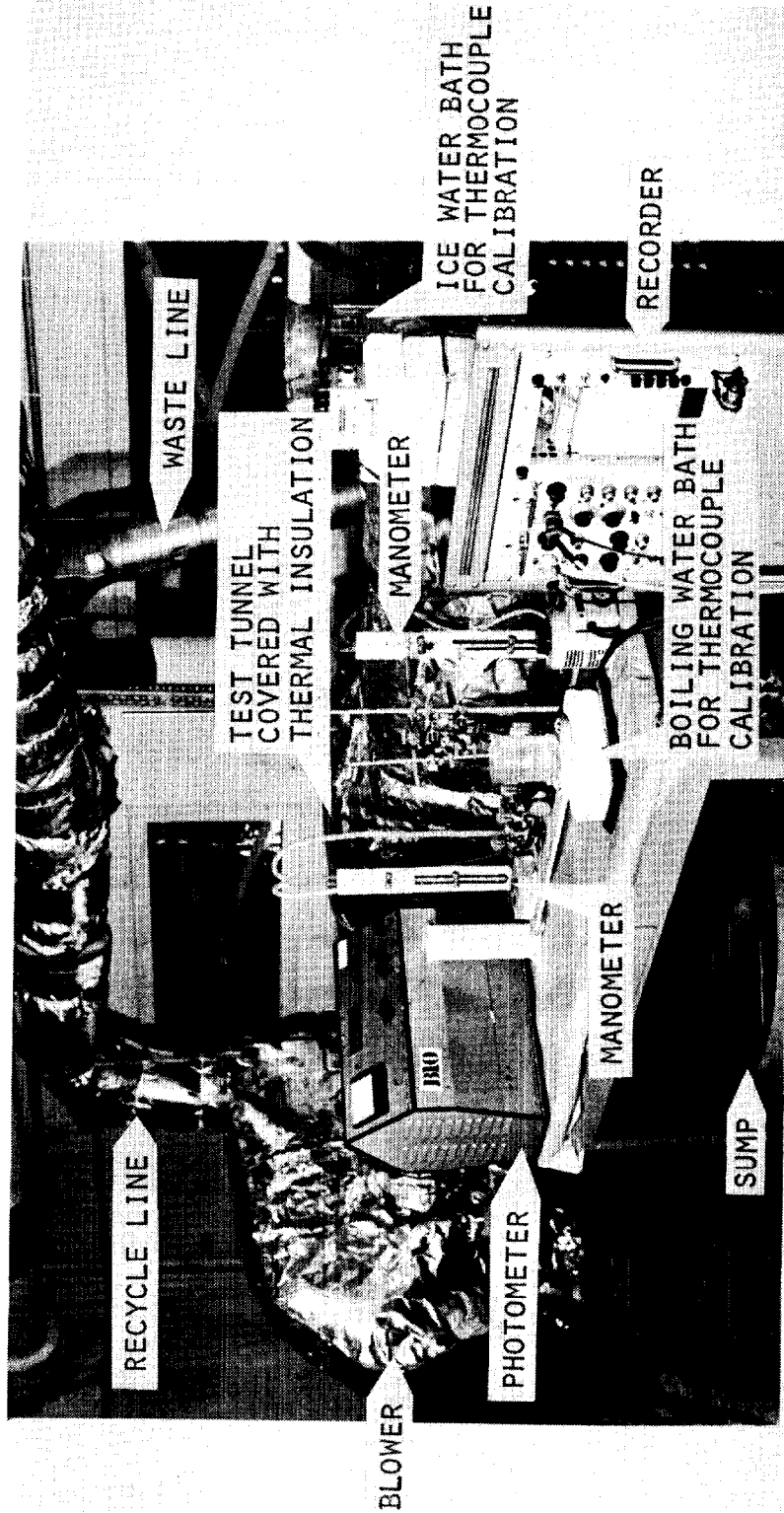
FIGURE 3

PHOTOGRAPH OF EQUIPMENT USED
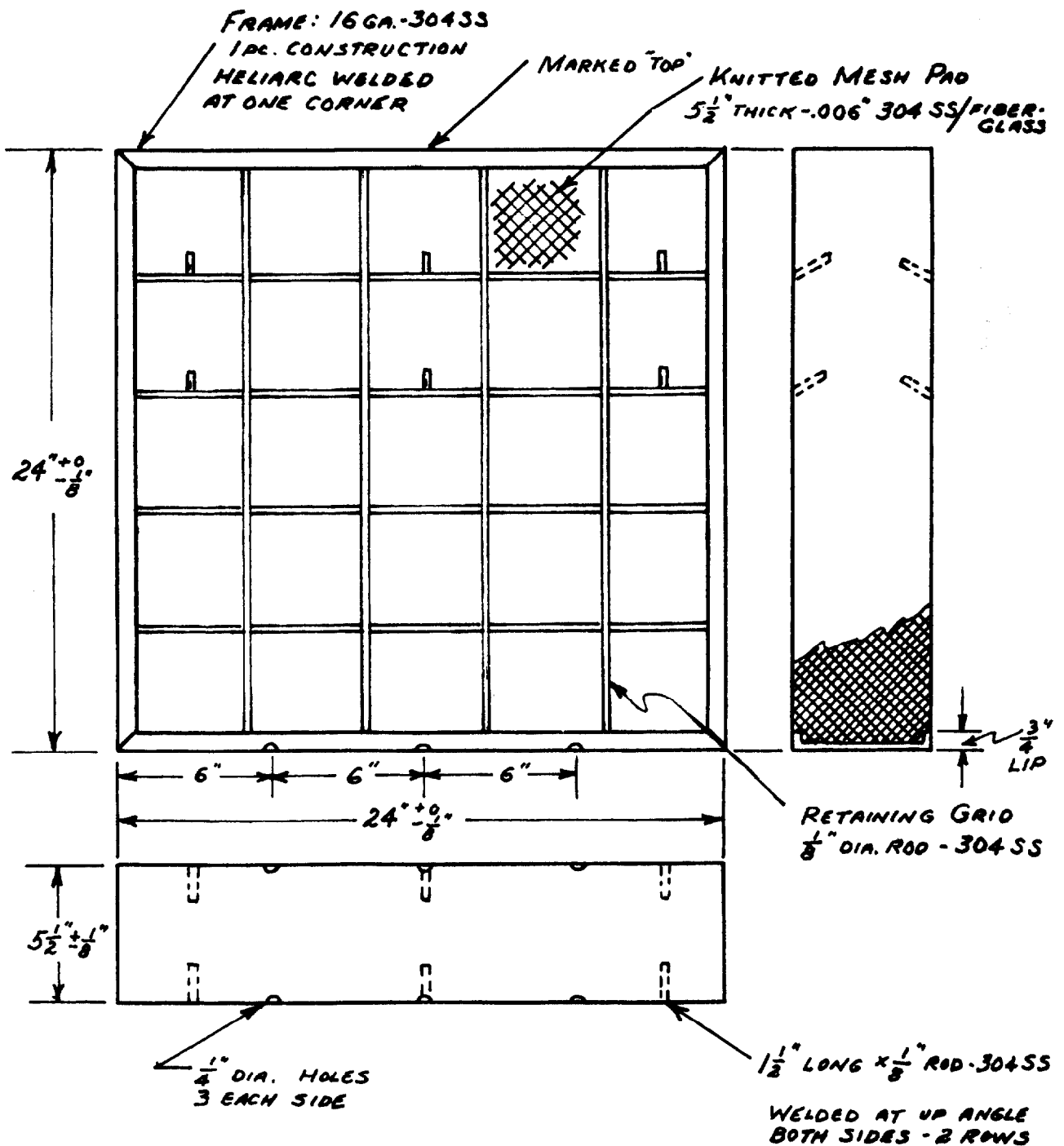
FIGURE 4   ACS ENTRAINMENT SEPARATOR

Date *Jan '75*	Customer		Cust. Part No.
Scale *1" = 1'*	Material	Part Name	Part No. *MODEL 101-55*
Dr. By *J.L.*	*As noted*	*Moisture Separator*	
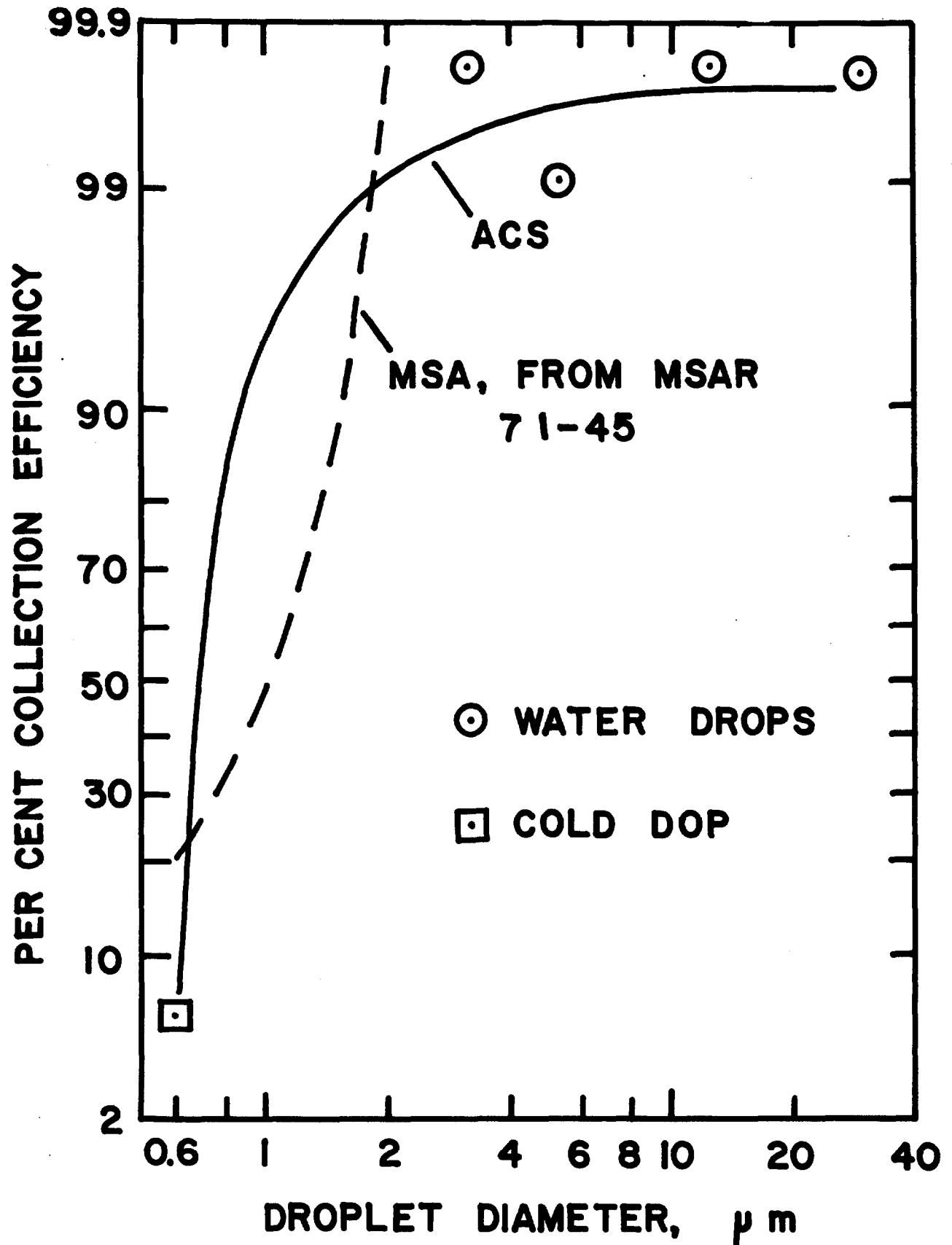
FIGURE 5   Per Cent Collection Efficiency vs Droplet   Diameter,
MSA and ACS   Entrainment Separators

References

1. MIL-F-51079 B,"Filter Medium, Fire-Resistant, High-Efficiency," Military Specification, 4 April 1974.

2. Peters, A.H., Application of Moisture Separators and Particulate Filters in Reactor Containment, DP-812, Office of Tech. Services, U.S. Dept. of Commerce, Washington D.C., Dec. 1962.

3. Rivers, R.D. and Trinkle, J.L., Moisture Separator Study, NYO-3250 -6, American Air Filter Co., Inc., Louisville, Ky., June 1966.

4. MSAR 71-45, Entrained Moisture Separators for Fine Particle Water-Air-Steam Service: Performance, Development and Status, MSA Research Corp., Evans City, PA., March 1971.

5. Burchsted, C.A., Fuller, A.B., and Kahn, J.E., Nuclear Air Cleaning Handbook, ERDA 76-21 (ORNL NSIC 65, Rev. 1), Energy Research and Development Administration, Washington, D.C., 1976.

6. Regulatory Guide 1.52, Design, Testing, and Maintenance Criteria for Engineered-Safety-Feature Atmosphere Cleanup System Air Filtration and Adsorption Units of Light-Water-Cooled Nuclear Power Plants, USNRC.

DISCUSSION

GEER: Based on the MSA report, we are going to try the MSA filter as a prefilter to the poor one you saw in Woodard's paper. We hope to have it installed soon so we will have some operating data in a couple of months.

T. T. ALLAN: What is the purpose of the 7-ft distance between the entrainment separator and the HEPA filter as shown in the apparatus diagram? If the face velocity through the entrainment separator is evenly distributed, can this distance be reduced? By how much? This is important because of the limited space requirements in many installations.

FIRST: The 7-ft distance between entrainment separator and HEPA filter was chosen because that distance was used for the qualification tests cited in Reference 4. Obviously, this is not a very informative answer. The effect of this distance is to permit very large droplets that may accumulate and become detached from the downstream side of the entrainment separator to fall to the sump by gravity before reaching the HEPA filter. I don't know by how much this distance can be reduced because it has not been tested, to the best of my knowledge. It seems reasonable to conclude that the greater the distance between entrainment separator and HEPA filters, the better.

MARBLE: How can this test qualify a separator to meet "no visible downstream plume" when report says "windows fogged so we could not observe downstream conditions?"

FIRST: The windows fogged because they were not covered with thermal insulation and the inner surfaces were below the dew point when tests were conducted with warm, saturated air on the inside. When tests were conducted at ambient temperature, no visible downstream plume was observed even when air saturation was assured by recirculating the air through the spray banks in a closed system.

MARBLE: How did you determine that saturation was obtained, or was it only close?

FIRST: Steam was added upstream of the spray nozzles to heat and saturate the air. During passage through the spray nozzle banks, the temperature of the air was lower below its dew point and condensation occurred. This assured saturation as there was a small degree of cooling in the remainder of the test tunnel.

MARBLE: Do you have pressure rise data on the HEPA filters?

FIRST: These are reported in the paper. Briefly, pressure rise was insignificant in all cases.

GOVERNMENT-INDUSTRY MEETING ON FILTERS, MEDIA, AND MEDIA TESTING

W. L. Anderson
Naval Surface Weapons Center
Dahlgren, Virginia

An informal working group has been responsible for many of the accomplishments achieved thus far in the high efficiency filtration programs of ERDA. Originally constituted at the 7th Air Cleaning Conference, the group consisted of a handful of individuals meeting in a night session at a local motel to discuss current problems in a "bull-session" format. At the 10th Conference in New York, the group was officially recognized with Mr. Gilbert as chairman. Attendance has increased from the 32 who attended the organizational meeting to a level of about 60; this level has been maintained at the last several sessions by limiting attendance to invitation only. At the 13th Conference in San Francisco, leadership of the group was transferred from Mr. Gilbert to Dr. First; this change had been requested by Mr. Gilbert following his retirement from ERDA.

The most recent session of the working group was held this past Sunday afternoon (Aug 1) and was devoted to a series of discussions on subjects of current interest. It was the first meeting under the new leadership but followed the precedent of earlier meetings in that it related to the operating requirements placed on high efficiency filter and the capacity of industry to meet them. To this end, the collected talents of the assembled body were unified toward the solution of problems of the particulate filter, its components and test methods. A prepared agenda listed six items with discussion leaders identified for each. The individual leaders were extremely well prepared and all items were discussed, evaluated, and resolved with dispatch.

At this the 14th Conference in Sun Valley, Idaho, a total of 63 persons comprised the assembled body; although the majority were from industry, representatives from government, government contractors, academic institutions, and four foreign nations were in attendance. Included were representatives of all the industrial complex; from the specifiers, the basic component suppliers, the unit manufacturers, and finally the end item users. Research organizations from R&D government laboratories and academic institutions contributed status reports on work currently underway. Users at various levels expressed their problems and actively participated in the discussions.

It is my intent to review for you, in abstract form, the items of the committee deliberations. The items will be discussed in the order of their agenda listing. In accordance with the new format, prepared papers were reviewed and the intimate discussions and deliberations were conspicious by their absence.

1. Standardization of Test Methodology. This subject was reviewed for the group by William Heyse, Dexter Corporation, Windsor Locks, Conn.

Standards and instruction manuals are lacking in specific details to assure that comparable testing can be accomplished at all sites whether they be production control, quality assurance, and/or specification conformance. This is particularly true in resistance, penetration, test flow, and physical testing of both the media and the filter unit. The previous utilization of primary standards, round-robin testing, and/or referee laboratory evaluation to assure uniformity in testing was abandoned when the Naval Research Laboratory terminated their filter development programs in 1971. Attendees agreed that test methods and procedures should be updated and that some form of program be developed for coordinating testing at the concerned laboratories.

   a. Recommendation. The Q127 Test Manual be reviewed and revised to bring it up to present day standards. Specific ASTM, ANSI, TAPPI, and other standards should be specified so that all groups are adhering to the same test conditions. The position/desirability of a referee laboratory be determined; if accepted, a laboratory should be so identified and begin to function as a point of contact and a single source of data comparison.

   b. Action. The chairman will appoint a Ad Hoc group to up grade the test procedures, examine the referee lab position, and screen potential candidates for the final selection of the referee lab.

2. Microfiber Fiber Diameter Determination. The discussion of this subject was presented by Clifford Cain, Johns-Manville (JM), Denver, Colorado.

Glass fiber diameters have previously been determined by the Williams Freeness Test that was established and calibrated by the Naval Research Laboratory in the early 1950's. The original curve was considered valid for fibers down to just less than 1 micron diameter but in later years was extrapolated to include fibers as low as 0.1 micron diameter. Information developed over the years indicated that the calibration curve might be in error over this extrapolated portion. Mr. Cain reported on his findings that this reported fiber diameter discrepancy was a fact and that corrections should be made in the previously reported size ranges 0.05 to 0.75 micron diameter; simply stated these lower fiber diameters were actually larger than stated in the suppliers literature. R&D efforts to show effects of temperature, pH, dispersion and physical test techniques on the Williams method were presented. Preliminary evidence was also obtained to show a technique for estimation of meaningful fiber size distributions. A new Williams fiber diameter calibration curve was obtained and verified by surface area (BET) techniques.

a. Recommdnation. JM shall adopt the new calibration curve and use it for determining future fiber diameters. An effort should be made by JM to correlate the new calibration techniques to production facilities in an attempt to produce more uniform and reproducible fiber lots. The experimental data presented should be documented so that it is available for other research groups.

b. Action. JM will issue new sales literature stating the correct fiber diameters for codes 100, 102, 104, and 106. The data presented will be assembled in a manuscript form and offered to a technical journal for publication.

3. Fiber Migration from HEPA Filters. Discussions on this subject were presented by C. D. Skaats, Rockwell International, Golden, Colorado.

Industrial hygiene and medical authorities have been concerned about the release of glass fibers from HEPA filter units supplying air to ventilation systems. This concern was amplified when medical evidence indicated that glass fibers deposited in human lungs were potential sites for carcinoma development. Attendees were in agreement that binder additives to the media would enhance fiber retention and under standard operating conditions, no hazard should exist in their use. In the absence of existing experimental data, Mr. Skaats and Dr. Leineweber of JM reported on the operation of a typical system and their attempts to detect fiber migration from the HEPA unit. Sampling was conducted for 6 hours using the Nucleopore collection techniques with optical and electron microscopy for fiber identification. Since no fibers could be found on their samples, they concluded that no fibers were released from the HEPA units.

a. Recommendation. Attendees should endorse the results of the experiment and distribute the information to their customers and fellow workers. The results should be documented and published, perhaps as a letter to the editor. Some quantitative definition of the word no should be determined. Sensitivity of detection stated as fiber count per sample volume should be determined.

b. Action. Mr. Skaats will review the physical parameters of the experiment and report back on the quantitative value of fiber detection.

4. Qualified Products List (QPL) for HEPA Units. Max Negler of Edgewood Arsenal, Maryland presented the findings in this area.

After two years of testing the QPL for HEPA filter units is now available. Manufacturers have submitted samples for qualification to Edgewood, tests have now been completed, and certification is now imminent. It should be pointed out that the long time delay was at least partially attributed to a discrepancy of radiation test results

between Edgewood and Savannah River. Technical problems in determining radiation exposure conditions resulted in a reworking of the test conditions and a restructuring of the ultimate results. Since a total of five manufacturers had each submitted samples in 7 different categories, a comprehensive listing of acceptance or rejection was not possible. Some suppliers had all products accepted, some had partial acceptance, and some failed all qualifications. Contact with the various unit fabricators will be necessary before one can determine which of their units are listed on the qualified products roster.

    a. Recommendation. QPL listings as presented be accepted and appropriate letters of qualification issued to the producers. It was further recommended that QPL testing be continued and those producers who failed to qualify on their first effort be encouraged to resubmit updated units.

    b. Action. Edgewood issue 1st phase QPL approval/status letters to industry. Filter Media samples and/or units be resubmitted as soon as possible for follow-on QPL testing.

5. Draft Mil. Specs. on HEPA Media and Units. Discussion leader for revision of the Mil Specs. was Mr. Max Negler of Edgewood, Md.

Mil Specs F-51068 and F-51079 are under revision to include all changes made to date. The filter specification (51068) revisions are relatively minor and include physical and marking changes as well as inclusion of QPL requirements. The media specification (51079) was revised to a greater extent. The acidity determination was eliminated and media tensile strengths were lowered in several areas. The number and size of test specimens was also changed. In addition, provision for a QPL will be included in the filter medium specification, and the SPEC will be expanded to cover two grades of media. Grade A will meet all requirements of 51079; Grade B will meet all requirements of the specification except gramma irradiation testing, and will not have a minimum thickness requirement.

    a. Recommendation. The revisions be adopted and the revised Mil. Spec. be issued as soon as possible.

    b. Action. ERDA review the proposed tensile changes and decide whether the adopted values are adequate for their requirements. ERDA should issue a revised Bulletin 306 stating the requirement changes they deem necessary.

6. DOP Toxicity During Man Testing. Sam Steinberg of ATI, Baltimore, Maryland reviewed the present status of the subject.

Inquiries into the toxicity of DOP when used for man-testing of protective facepieces have increased over the recent past; many of these have originated from commercial sources. Since no maximum allowable concentrations (MAC) have been established for this specific compound, some concern exists over its relative toxicity. A search of the literature indicates that DOP is non-toxic and attendees agreed that in their opinion no hazard exists in the proposed use. Statements from a toxicity expert (Stokinger) has resulted in a similar opinion that this class of material is not considered to be toxic and as such no special MAC is required. After considerable discussion it was decided that the assembled group was not qualified to state an official position on the subject; NIH or NIOSH would be the appropriate government agency to issue such a position statement.

a. <u>Recommendation</u>. A task group be formed to solicit and collect <u>information from</u> a variety of sources (medical, toxicologists, producers) on the toxicity levels of DOP. This information would be submitted to the government agency responsible for establishment of MAC's; a request would be made for an acceptance level that could be applied to man test conditions.

b. <u>Action</u>. The chairman will appoint necessary membership for the task group to carry out the recommendations.

In conclusion, it should be re-emphasized that this informal working group, with its diversified representation, provides a means for a comprehensive and expedient solution to the problems of the absolute filtration industry. The total effort has proven invaluable because it permits the surfacing and review of problems that might otherwise be lost in the quagmire of bureaucracy and management. The meetings are intended to be and actually are a working level distribution of data and expertise as well as a progress report of ongoing projects in the particle filtration areas. To this end, we feel that we have been successful and future sessions are contemplated.

CLOSING REMARKS OF SESSION CHAIRMAN: (C. A. Burchsted)

We had a number of papers on electrical effects and a number of papers on sand. Don Orth of Savannah River discussed the advantages and problems of selecting sand for sand filters at the Savannah River plant.

Mr. Schuster discussed the operation of electrical field air cleaners and Mr. Reid spoke about static collection on filter beds. This was followed by Gary Nelson who talked about electrostatic collection of filter beds and the electronic experiments at Livermore Laboratory.

Chuck Skaats reviewed his experiences with three filter manufacturers and discussed construction problems. I think his discussion demonstrates clearly that qualification tests of a filter are no substitute for the one-by-one, quality assurance testing that ERDA conducts for the Commission and makes available to commercial users on a cost basis.

After that, Charlie Gunn compared the performance of a number of HEPA filters of different construction under very adverse conditions. We don't see such conditions very often in real situations, but they can occur and are very important factors in the qualification of filters.

Jack McDowell gave the most controversial paper on the list. If there are questions that anyone would like to discuss with Jack on the alpha mechanism, I would suggest they do so.

Lastly, Mr. Woodard on chemical operations, Dr. First on the testing of demisters, and Anderson's summary of the filter meeting.

SESSION VII

LUNCHEON MEETING

Tuesday, August 3, 1976
CHAIRMAN: G. Wehmann

CONTINUING CHALLENGES IN NUCLEAR AIR CLEANING
D. W. Moeller

CONTINUING CHALLENGES IN NUCLEAR AIR CLEANING

Dade W. Moeller
Harvard Air Cleaning Laboratory
Harvard School of Public Health
Boston, Massachusetts

Abstract

The safe operation of nuclear facilities is heavily dependent upon the adequate performance of air cleaning systems. Although many problems have been solved, new questions and new challenges continue to arise. These are well illustrated by weaknesses in air cleaning and ventilating systems revealed by the Browns Ferry fire, and the need to develop additional data on the reliability of such systems, particularly under emergency conditions, as revealed by the Reactor Safety Study. Assessments of the degree to which engineered safety features can compensate for deficiencies in nuclear power plant sites continue to challenge those involved in risk/benefit evaluations. Additional challenges are being generated by the air cleaning requirements associated with the commercial development of the liquid metal fast breeder reactor.

I. Introduction

Air cleaning systems play a major role in the safe operation of nuclear facilities, under both routine and postulated accident conditions. Many problems have been solved, but new questions and new challenges continue to have an impact in this field. Significant events which have occurred since the 13th Air Cleaning Conference two years ago include the Browns Ferry fire, publication of the Reactor Safety Study, and a variety of changes resulting from the formation of the Nuclear Regulatory Commission (NRC). Presented in this paper is a review of the implications of these and other events as seen primarily from my activities and personal observations as a member of the Advisory Committee on Reactor Safeguards. The comments are restricted to programs and activities within the United States and are primarily directed to problem areas, as contrasted to the many successes which could be cited. Although mention is made of fuel fabrication and chemical processing plants, the major focus is on selected air cleaning systems associated with nuclear power plants. Although various ACRS reports serve as a basis for much of the paper, the comments offered do not reflect official views of the Committee and should not be interpreted as such.

II. Recent Developments

For purposes of this presentation, recent developments which have had an impact on air cleaning operations are described below under three categories - Operating Experience, Theoretical and Experimental Evaluation, and NRC Regulatory Activities.

A. Operating Experience

1. The Browns Ferry Fire

The one single event which has had the greatest recent influence on the design, installation and operation of nuclear air cleaning systems is the fire which occurred in the Browns Ferry Nuclear Station near Decatur, Alabama, on March 22, 1975. Immediately following the fire, the U.S. Nuclear Regulatory Commission appointed a Special Review Group to institute a program to identify the lessons learned from this event and to make recommendations for the future in the light of these lessons. The report of the Special Review Group was published earlier this year[1] and the NRC subsequently issued a Branch Technical Position (APCSB 9.5-1) outlining "Guidelines for Fire Protection for Nuclear Power Plants."[2] Both of these reports contained recommendations relative to ventilation and exhaust systems.

a. Recommendations of the Special Review Group

Shortly after the Browns Ferry fire began, ventilation was lost due to failure of the electrical power supply to the ventilation system and to its control subsystem. As a result, even if venting the smoke through the installed ventilation system had been planned in the design, it would not have been possible due to inoperability of the system.

On the basis of its assessment, the Special Review Group recommended that ventilation systems in all operating plants be reviewed and upgraded as appropriate to assure their continued functioning if needed in a fire. Specific suggestions included:

(1) Control and power cables for a ventilation system important to fire control should not be routed through areas the system must ventilate in the event of a fire.

(2) Ventilation designs should be provided with the capability of isolating fires by use of cutout valves and dampers.

(3) Capability for the control of ventilation systems to deal with fire and smoke should be provided, but such provisions should be made compatible with requirements for the containment of radioactive materials. It must be recognized, however, that these provisions and requirements may not be mutually compatible and in some cases may be in direct conflict with each other. For example, operating ventilating blowers to remove smoke may fan the fire; the same action may also result in a release of radioactive materials, either directly by transport of radioactive particles with the smoke or by decreasing the effectiveness of the filters provided to contain the radioactivity. It is obvious that some compromise will be necessary and that flexibility of operation may be needed, depending on the nature of any event that may occur. The Special Review Group recommended that the pros and cons be considered in the development of detailed guidance.

The Special Review Group also noted that, in the event of a serious fire in the cable spreading room, the control room might have become uninhabitable because of smoke and toxic fumes. In the situation at Browns Ferry, smoke and CO_2 entered the Control Room through openings in the floor at the point where the cables entered the Control Room.

b. Recommendations of the NRC Regulatory Staff

The Branch Technical Position included the recommendations of the Special Review Group, plus the following additional items related to the design and operation of ventilation systems.

(1) The products of combustion which need to be removed from a specific fire area should be evaluated to determine how they will be controlled. Smoke and corrosive gases should generally be automatically discharged directly outside to a safe location. Smoke and gases containing radioactive materials should be monitored in the fire area to determine if release to the environment is within permissible limits of the plant Technical Specifications.

(2) Any ventilation system designed to exhaust smoke or corrosive gases should be evaluated to assure that inadvertent operation or single failures will not violate the controlled areas of plant design. This requirement includes containment functions for protection of the public and maintaining habitability for operations personnel.

(3) Fixed automatic sprinkler systems, or alternative methods as described in Regulatory Guide 1.52[3], should be installed to protect charcoal filters.

(4) The fresh air supply intakes to areas containing safety related equipment or systems should be located remote from the exhaust air outlets and smoke vents of other fire areas. This is to minimize the possibility of contamination of the intake air with the products of combustion.

(5) Stairwells should be designed to minimize smoke infiltration during a fire.

(6) Smoke and heat vents may be useful in specific areas such as cable spreading rooms and diesel fuel oil storage areas and switchgear rooms. When used, they should be installed at a minimum ratio of 1 square foot of venting area per 200 square feet of floor area. The conversion factor for power venting is 300 cubic feet per minute equals 1 square foot of gravity venting area.

(7) Self-contained breathing apparatus, using full face positive pressure masks, should be provided for fire brigade, damage control and control room personnel. Control room personnel may be furnished breathing air by a manifold system piped from a storage reservoir if practical. Service or operating life should be a minimum of one half hour for the self-contained units. These recommendations were in direct response to the problems noted by the Special Review Group (and cited above).

(8) Where total flooding gas extinguishing systems are used, area intake and exhaust ventilation dampers should close upon initiation of gas flow to maintain necessary gas concentration.

2. Hydrogen Explosions (Selected Examples)

Although not comparable to the Browns Ferry fire in terms of the seriousness of their impact, hydrogen explosions have continued to be a problem in nuclear power plant facilities. A review of Licensee Events Reports, for example, shows that at least half a dozen such explosions, primarily within off-gas systems, have occurred in the last 18 months. The two events below were considered of special interest since both resulted from the impact of cold weather on an air cleaning system.

a. Cooper Nuclear Station

In January, 1976, a buildup of ice in the upper portion of an exhaust stack at the Cooper Nuclear Station resulted in back-pressure and the accumulation of hydrogen in the off-gas building. Later there was an explosion which completely demolished the off-gas building. Fortunately, there were no personnel injuries. Corrective action included heat tracing and insulation of the upper ten feet of the elevated release point pipe.[4]

b. Brunswick Steam Electric Plant, Unit No. 2

In January, 1976, there was an explosion in the stack filter house at the Brunswick Steam Electric Plant, Unit No. 2. The cause was later determined to be the improper positioning of a demister which permitted moisture to collect and freeze on a HEPA filter, causing an increase in resistance to flow. Pressure buildup resulted in blowing a number of off-gas loop seals which permitted both airborne radioactive materials and hydrogen gas to enter the stack filter house. Corrective action included proper positioning of the demister, plus a number of other measures.[5]

B. Experimental and Theoretical Evaluations

1. Routine and Accidental Releases

One of the primary needs in terms of defining performance requirements for air cleaning systems is an improved set of models for describing source terms for accidental releases of radioactive materials from nuclear power plants. Studies are also needed for improved definition of the fission product inventory within containment as a function of time. Guides currently used[6][7] require assumption of an instantaneous release. Hsia and Chester[8] have recently developed mathematical models for estimating the release rate for specific radionuclides into containment for light water reactors, assuming a LOCA coupled with a failure of the Emergency Core Cooling System. Their study shows that even for volatile radionuclides such as ^{133}Xe, ^{131}I, and ^{90}Sr several hours are required for a significant fraction of the curie inventory to gain access to the environment. (It is assumed that there is containment failure and that the core has not yet melted through the pressure vessel.)

For example, a typical large PWR with a hole in the containment building approximately the size of one of the equipment doors and an inoperative recirculating filter-adsorber is modeled. In this case upwards of 6 hours are required for a release to the environment of 10% of the core inventory of ^{131}I. Their models also show that in a case similar to the above, but with an operating filter-adsorber, the release to the environment can be reduced an order of magnitude. If the containment and filter-adsorber integrity are maintained, the release to environment can be reduced more than five orders of magnitude.

Other efforts with respect to the development of models for assessing accident situations include those for predicting the effectiveness of containment spray systems over a wide range of temperatures, pressures, and chemical compositions.[9] Similar models are needed for calculating the effectiveness of charcoal adsorption systems over a range of temperature and moisture conditions, for determining removal efficiencies for various potential leak paths through containment, for estimating the effectiveness of pool scrubbing (for Boiling Water Reactors) as a removal mechanism, and for predicting the role of plateout as a radionuclide removal process within containment.

In the case of the analysis of routine releases, the development of models appears to have progressed much further. The NRC Staff has recently published two reports[10][11] which, together with Regulatory Guide 1.112[12], provide methodologies for calculating source terms for nuclear power plants under normal operating conditions. The Commission has also published a detailed review of the wide range of models available for estimating fission gas release from reactor fuels under both routine and accident conditions.[13] Specific efforts by reactor vendors to provide better definition of radionuclide source terms under normal operations include models developed to take into account observed increases in the amount of radioactive material (particularly radioiodine) in reactor coolant systems following a power or system pressure transient.[14]

Models, such as these, can provide a very useful tool to air cleaning specialists. Thorough evaluation and application of modeling techniques, for example, can lead to better understanding of the basic mechanisms involved in specific removal processes and this, in turn, can lead to significant feedback in the form of refinements in the theory and design of improved air cleaning systems. This type of approach, combined with experience gained through operating systems, can also help to clarify the degree of removal effectiveness required for each of the variety of sources to be considered.

2. Failure Probabilities for Air Cleaning Systems

In October, 1975, the U.S. Nuclear Regulatory Commission published the final version of its Reactor Safety Study.[15] One of the innovative contributions of this report was that it contained a series of analyses related to generic types of failure mechanisms which could conceivably lead to failure of air cleaning systems.

The results of two such analyses are cited below. The first relates to an analysis of a Containment Spray Injection System for a Pressurized Water Reactor and is based on data for the Surry Power Station, Unit 1, in Virginia. The second relates to an analysis of a Secondary Containment System for a Boiling Water Reactor and is based on data for the Peach Bottom Atomic Power Station, Unit II, in Pennsylvania. Essentially all of the information presented is quoted directly from Appendix II of the published report.

a. Containment Spray Injection System

The Containment Spray Injection System (CSIS) is part of the engineered safety features installed to compensate for the effects of a loss of coolant accident (LOCA) within a Pressurized Water Reactor. The CSIS delivers cold water containing boron through spray heads to the containment volume from the refueling water storage tank during the first half hour after the postulated large LOCA incident. The principal function of the system is to reduce the pressure within containment and to provide the preferred path for delivery of additives such as NaOH to the containment atmosphere for initial airborne fission product removal.

The point estimates reported for various types of failures which would lead to the unavailability of the CSIS in the event of a large LOCA were:

Type of Failure	Probability of Occurrence
Single	3.2×10^{-4}
Double	4.4×10^{-7}
Test & Maintenance	1.5×10^{-4}
Common Mode	1.9×10^{-3}

The median estimate of CSIS unavailability for the postulated large LOCA was:

Median Failure Probability $= 2.4 \times 10^{-3}$

It may be noted that the greatest or highest probability of failure resulted from common mode failure. According to the analysis, the largest contributors to this situation would arise from two faults, both of which result from human errors. The first is common mode failure of the Consequence Limiting Control System due to miscalibrations of several sensors which prevent the proper signal reaching the CSIS in the event of a large LOCA. The second was the possibility that both CSIS pump flow recirculation valves were left open after the monthly pump test due to operator error. As has been pointed out in the past, this stresses the extreme importance for air cleaning specialists to design systems which are less subject to human error.

b. Secondary Containment System

In the event of a LOCA in a Boiling Water Reactor, there is a probability that radioactive materials may be released beyond the confines of the primary containment. A Secondary Containment System is provided to protect against such an event. This System consists of the reactor building, portions of the reactor building heating and ventilation system, and the Standby Gas Treatment System (SBGTS). In addition to these system elements, appropriate instrumentation is provided for monitoring radiation exposures and depicting system status. The purpose of the Secondary Containment System is to limit the ground level release of radioactive materials and to provide a means for controlled elevated release of the reactor building atmosphere.

In the course of the Reactor Safety Study[15], the probability of the unavailability of the Secondary Containment was assessed for two undesirable events. For an unfiltered ground level release, the overall probability of unavailability was estimated as:

Probability
(unfiltered ground level release) = 3.5×10^{-5}

For an unfiltered elevated release, the probability of unavailability was estimated as:

Probability
(unfiltered elevated release) = 5.6×10^{-5}.

For the unfiltered ground level release, the chief contributors to the assessed unavailability were four sets of hardware double faults involving the blockage of redundant sets of filters and intake ducting of the SBGT system. For the unfiltered elevated release, the single faults were the major contributors and consisted primarily of the unavailability of A.C. power for the heaters in the SBGT system. Loss of function of the heaters was assumed to result in loss of function of the filter bank due to excessive moisture reaching the filter. The amount of release was assumed to be dependent upon the amount of reduction in charcoal filter efficiency caused by excessive moisture and upon the volume of air which could pass through the wet filter elements. Double failures such as heater failure and a circuit breaker failing open could result in the same effect.

For unfiltered releases both at ground and elevated levels, test and maintenance were not considered to contribute to unavailability of the system in an emergency since no in-service testing or maintenance which would result in system unavailability is permitted. Another assumption made in the estimation of system unavailability was that activation of the fire protection deluge system would result in loss of the affected filter bank but would not cause a release of contaminants to the atmosphere.

As with the evaluation of the Containment Spray Injection System, these analyses were instrumental in highlighting potential weaknesses in the Secondary Containment System and in describing interplay among subsystems which could be improved. Such anal-

yses could also be used to determine the cost effectiveness of proposed improvements, as well as to demonstrate instances in which current practice may not be warranted. It would also appear that application of similar techniques to reliability estimates for routine nuclear air cleaning systems might be a very worthy field of investigation. Such application could very well lead to the design and installation of systems and subsystems of increased reliability and performance.

C. NRC Activities

From the standpoint of the U.S. Nuclear Regulatory Commission, there are two types of activities which provide some indication as to which aspects of air cleaning are considered of primary importance by its staff at the present time. One is the nature or degree to which improved air cleaning systems are being backfitted into existing plants; the other is the degree to which air cleaning problems are listed in its status reports on safety problems. Summarized below are lists of topics currently occupying the interests of the NRC staff in both of these areas.

1. Air Cleaning Backfitting Requirements

A review of NRC actions over the past 3 years shows the following air cleaning system modifications being required within operating nuclear power plants.[16] Although not every item has been required for every plant, these items were selected as representing generic types of requirements for nuclear facilities.

a. Improved surveillance and performance requirements for filter systems;

b. Development of technical specifications for limiting conditions for operation and surveillance for filter systems including adsorbers and high efficiency particulate air filters;

c. Installation of augmented or modified off-gas systems to assure radioactive emissions as low as reasonably achievable;

d. Modification of off-gas recombiner systems to improve system reliability, performance, and safety;

e. Grounded off-gas system high efficiency filters to increase system safety by reducing the probability of an explosion;

f. Modification of penetration room ventilation systems to increase reliability in the event of an accident;

g. Required evaluation of facilities in conformance to Appendix J, 10 CFR 50, regarding Containment Leak Testing;

h. Increase in capacity of the auxiliary building special ventilation system to assure negative pressure within the Category I ventilation zone;

i. Increased requirements on systems used for preventing a hydrogen explosion in containment following a LOCA.

2. Current Air Cleaning Studies and/or Investigations

Through its Technical Safety Activities Reports[17], the NRC Division of Systems Safety provides an ongoing account of the status of various studies underway to resolve problems related to reactor safety. The most recent report lists the following air cleaning items which are receiving attention.

a. Review of current data to update models for estimating fission product releases during accident conditions;

b. Development of safety guides for the design, evaluation and testing of containment spray systems for fission product removal;

c. Development of a mathematical model for methyl iodide removal by containment sprays;

d. Determination of the hazardous effects of airborne gases which may be accidentally released on or in the vicinity of a nuclear reactor site; development of a diffusion model for calculating concentrations at short distances in order to determine the hazards from toxic chemicals or radioactive gases that could potentially reach control room intake locations;

e. Measurement of air infiltration into control rooms to determine the effectiveness of isolation for protection of control room operators against external airborne contamination; development of a staff position with respect to isolation requirements for control room ventilation systems;

f. Evaluation of dose consequence problems of PWR and BWR (Mark III) containments with continuous purging;

g. Development of a Regulatory Guide specifying acceptable methods for design, testing, and maintenance of HEPA filters and iodine removal systems used in plant ventilation systems under normal operating conditions;

III. Air Cleaning as an Engineered Safety Feature

For many years, it has been the policy of the U.S. Atomic Energy Commission, and now the U.S. Nuclear Regulatory Commission, to recognize the use of engineered safety features as an effective means for limiting radiation doses to the population residing near a nuclear power plant. This policy is of special importance to air cleaning specialists since air cleaning systems are considered one of the primary forms of such safety features. The basis for this policy is exemplified by the wording in 10 CFR Part 100[18] which states:

"Where unfavorable physical characteristics of the site exist, the proposed site may nevertheless be found to be acceptable if the design of the facility includes appropriate and adequate compensating engineering safeguards."

A. Reports of the ACRS on Engineered Safety Features

In a report issued in 1964[19], the ACRS affirmed its concurrence with the principle stated above and made the following additional statements relative to this matter. Although these statements were made over a decade ago, they are well worth repeating today:

"It is important to recognize that engineered safeguards are designed to allow the siting of reactors at locations where, without such safeguards, protection of the public would not be adequate. The advantages of a remote site cannot be exactly balanced by engineered safeguards. On the other hand, the advantages of a remote site may be temporary, if appreciable increases in population density occur near the reactor. Few sites presently in use are such that some engineered safeguards are not desirable. Thus, the protection of the public ultimately depends on a combination of engineered safeguards and adequate distances. Engineered safeguards which can justify decrease of the distances must be extraordinarily reliable and consistent with the best engineering practices as used for applications where failures can be catastrophic. To be worthy of consideration, engineered safeguards must be carefully designed, constructed and installed, equipped with adequate auxiliary power, and continuously maintained. Certain designs are based on sound engineering principles supported by materials acceptance tests; others require developmental and proof testing. In any case, provisions for regular and careful testing are required where deterioration may be expected. The acceptance of engineered safeguards to mitigate unfavorable aspects of reactor sites should continue to be based on positive evidence that these design objectives can be attained. In addition, there will probably be a continuing need to develop new devices and design concepts as reactors are proposed for less and less remote sites."

"In each case, the engineered safeguard must be considered with respect to the specific nuclear plant for which it is intended. It is equally important to assess the degree of confidence that the safeguard will function properly in an emergency. An engineered safeguard that must remain operable for the life of the plant but cannot be tested without ruinous effects would not usually be accorded the same importance as one that can be tested periodically."

In subsequent deliberations over the past decade, the ACRS through its Siting Evaluation Subcommittee has given further consideration to engineered safety features. In drafts of reports never formally issued, but subsequently made public[20], the Committee made the following additional recommendations pertaining to such safeguards:

1. Because of the small likelihood that proof of the efficacy of engineered safety systems under accident conditions will be obtained as a consequence of actual accident experience, extra margin

should be provided in the design of these systems wherever such provision is practical and will clearly improve safety.[21]

2. Improved testing provisions for and reliability of engineered safeguards should be endorsed for all reactors.[22]

The reason that this matter was assigned to the ACRS Siting Evaluation Subcommittee was due to the fact that applicants were proposing to locate power reactors at sites in areas of increased population density. The series of meetings of the Subcommittee contributed to the development of an ACRS position that large power reactors might be acceptable at sites having population densities somewhat greater than had been previously approved, but only if certain kinds of improvements were made in their design and construction and if additional safeguards were provided. The history of these deliberations was most recently summarized in an ACRS report in 1974.[20] This history has shown that, whenever a choice is available, regulatory authorities would generally prefer the use of distance to engineered safety features as a protective approach.

The history of these and other deliberations also shows that there is a limit to which engineered safety features can compensate for population densities. In other words, there are sites, particularly near major metropolitan areas, where the population density is considered too large for a nuclear power plant to be located, regardless of the extent to which it would be equipped with engineered safeguards. Notable examples are the cases of the proposed site for the Burlington Nuclear Generating Station in New Jersey and the proposed site for the Newbold Island Reactor near Trenton, New Jersey. In the former case, the ACRS unanimously stated that it did "not see how the site could be approved"[23] and the application was subsequently withdrawn. In the latter case, the Atomic Energy Commission staff persuaded the applicant to shift the plant to a more acceptable, less populated, site.

The challenges of decisions in this problem area continue to exist today and are exemplified by a report issued by the ACRS in December, 1975[24], wherein the Committee suggested that:

"Studies be conducted on the degree to which engineered safety features or alterations in plant design should be used to compensate for specific site deficiencies. In particular, it would be useful to determine whether there are characteristics for which compensating engineering changes should not be applied."

B. Reports of the ACRS on Specific Safety Features

1. Reactor Containment Systems

In its 1964 report[19] the ACRS also stressed the importance of containment as a specific engineered safety feature and cited double containment as appearing to have particular promise as a means for minimizing the release of airborne fission products following a postulated accident in a nuclear power plant.

Later, in its review of the proposed Newbold Island Reactor[25], previously mentioned, the Committee commented favorably on the double containment approach proposed for this facility. At the same time, however, because of the high population density of the site proposed for this plant, the Committee was careful to reserve judgment as to the adequacy of even this type of containment, which included air recirculation and filtration, for this plant at this site.

Continual prodding by the Committee and the AEC and NRC staffs down through the years has led to the design and construction of improved reactor containments and the specification of reduced maximum leakage rates for such facilities. Today, double containment systems consisting of an inner steel shell and an outer concrete vessel, with an intermediate annulus, are becoming increasingly common for both Pressurized and Boiling Water Reactors.

Some of the problems and considerations involved in such containments are illustrated by the recent NRC Staff and ACRS review of the GESSAR-238 standardized plant design which had been submitted for preliminary design approval by the General Electric Company. In its report on this design, the ACRS enumerated questions on two air cleaning items.[26]

One pertained to the proposal that the plant be operated with continuous venting of the containment. A second pertained to the seismic capability of the off-gas system and conformance with the dose limitations of Regulatory Guide 1.29.[27] Final resolution of the first item was that the containment could be continuously purged so long as the exhaust was passed through a cleanup system and discharge lines were limited in size. Following this practice, the containment would be sealed on a high radiation alarm, and any later purging for hydrogen control would be through the Standby Gas Treatment System. This approach makes the effective operation of containment heavily dependent on rapid acting valves to seal the purge lines. Resolution of the second item involved designing the off-gas system to withstand an Operating Basis Earthquake. The fact that it was not required to withstand a Safe Shutdown Earthquake was based on theoretical and experimental evaluations which showed that, even if the charcoal adsorption beds were fractured, the evolution of the adsorbed radioactive gases would be relatively slow.

2. Containment Spray Systems

Another engineered safety feature of interest to air cleaning specialists which has received attention from the ACRS over the years is the matter of containment spray systems.[28] The basic purpose of such sprays is to provide a mechanism for reducing the pressure within containment following a LOCA. In most plants, the system also has the capability for removing a portion of the airborne fission products from the containment atmosphere. Such systems are now common-place as a part of engineered safety features since they have proven to be a very effective economic trade-off as compared to the costs which would be involved in purchasing additional land to achieve greater isolation of a nuclear power plant.

In early plants, sodium hydroxide (NaOH) was used as an additive to the spray since it was a very effective radioiodine removal agent. In addition, the NaOH served as a pH adjustor. Since the spray also contained boric acid, adjustment of the pH to the alkaline range (pH 9-12) was necessary to keep certain metallic parts of the reactor vessel, and other safety related systems, from being damaged by stress corrosion.

Later, to increase the radioiodine removal efficiency, another material, sodium thiosulfate, was added to containment sprays. This enhanced their removal capability for organic iodine, but again, to keep the sodium thiosulfate stable, the pH of the boric acid solution had to be maintained in the alkaline range (using NaOH).

As contrasted to the above, there is another class of containment sprays which do not contain iodine removal additives at all. Their sole purpose is containment depressurization. When this type operates, initially only borated water is sprayed within containment. As the water collects in the containment sumps, it washes through baskets of trisodium phosphate (TSP) which raise its pH to a neutral range (pH = 7). Again, this adjustment in pH is necessary for protection against stress corrosion. Plants using sprays of this type depend upon the use of charcoal filters for radioiodine removal.

Another additive proposed for years for use in containment sprays, but only recently considered for actual use, is hydrazine. Tests have shown that addition of this chemical to boric acid sprays in trace quantities will provide effective radioiodine removal. As in the case of systems using boric acid alone, hydrazine systems would employ TSP powder baskets for pH adjustment.

As may be noted from the above, containment spray systems have been the subject of a number of evaluations in the past years and a range of systems are in use today. Concurrent with these developments, the ACRS has raised a variety of questions and has made a number of recommendations regarding such systems. These were most recently outlined in its report on the "Status of Generic Items Relating to Light-Water Reactors: Report No. 4,"[29] and included the following:

a. A review and evaluation should be made of the variety of experiments which have been conducted on the effectiveness of various containment sprays, specifically with respect to the removal and retention of airborne radioactive materials of the types anticipated to be present within containment following a LOCA. This review should include consideration of the adequacy of definition of the physical and chemical forms of the anticipated airborne radionuclides, and the applicability of the evaluative tests for estimating removal efficiencies of the various proposed sprays under the conditions of temperature, pressure, and radiation doses expected to exist under post-LOCA conditions.

b. The Committee also recommends that, if compounds, such as hydrazine, have distinct advantages, action be taken to encourage their use. At the same time, the Committee suggests that studies be conducted to determine if there are better additives which might be considered.

730

IV. Other Challenges in Air Cleaning

Nuclear safety is a dynamic field and present positions are constantly undergoing review and evaluations. Many examples of emerging problems and challenges have been cited by other speakers at this Conference. Several other new developments and/or problems which could have an impact on air cleaning systems are mentioned below. The list is by no means comprehensive. It is simply a sampling of a few of the emerging challenges.

A. Development of Liquid Metal Fast Breeder Reactors

Within the next few years, a decision will be made as to the extent to which the Liquid Metal Fast Breeder Reactor (LMFBR) will be used in meeting our future energy needs. If large scale development of the LMFBR is undertaken and plutonium recycling is approved, this will involve the construction and operation of commercial fuel fabrication facilities to prepare plutonium fuels for fast breeders, as well as mixed oxide fuels for light water reactors. Such facilities will require air cleaning systems of high efficiency and reliability, since release limits for plutonium to the environment will undoubtedly be extremely restrictive.[30] Also implied in plutonium recycling is the operation of a number of large scale fuel reprocessing plants. Such operation will involve air cleaning challenges for the commonly known radionuclides such as ^{85}Kr and ^{3}H as well as the "newer" problem nuclides such as ^{129}I and ^{14}C.

In connection with the operation of LMFBRs, it might be noted that the NRC staff has stated[31] that the Clinch River Breeder Reactor will be required to have engineered safety systems adequate to cope with identified design basis accidents to ensure that off-site doses are less than 10 CFR 100 guidelines. For design purposes at the construction permit review, the operative guideline of the NRC staff has been to limit off-site doses for emergency releases to 20 rems whole body and 150 rems thyroid, as contrasted to the values of 25 and 300 rems, respectively, specified in 10 CFR Part 100.[18] Since postulated airborne releases from an LMFBR under accident conditions could include plutonium as well as perhaps activated sodium, the NRC staff has specified additional design guideline dose limits of 7.5 rems for the lung and 15 rems for the bone. Again the challenges to air cleaning specialists to design systems to meet these requirements will be extremely demanding.

B. Role of Ventilation in Assuring the Performance of Electronic Equipment Under Emergency Conditions

As noted earlier, the NRC review of the Browns Ferry fire pointed out a number of problem areas with respect to the performance of ventilation and/or air cleaning systems under emergency conditions. One additional potential problem is the functioning of ventilation systems in order to assure the continued satisfactory performance of electronic equipment under such conditions.

Most of the electronic equipment in nuclear facilities is now solid state. If normal power to ventilation systems is lost in an

emergency situation, the D.C. input to electrical panels will cause rapid temperature increases. Since solid state equipment in logic panels can yield unpredictable operation at temperatures as low as 125°F, maintenance of adequate ventilation becomes an extremely important matter. In the case of control rooms, continuous ventilation is also necessary to maintain temperatures low enough for human habitation.

Although "service" systems of this type are generally designed to be redundant, it is reasonable to assume that sooner or later one of the two systems (usually the "active" system) is going to fail. When it does, the failure constitutes an emergency and nuclear facility operators must then call upon the single remaining alternative service system. As a consequence, the emergency, as postulated, leads to a situation in which redundancy in the backup system is no longer available.

This is an area to which air cleaning and ventilation specialists need to direct more attention. The expensive approach would be to provide "post-emergency" redundancy through the installation of three ventilation trains, the third one being a simple and less efficient, but nonetheless adequate, system. Another approach might be to provide only two trains with the second one being a passive system, or to provide a two train system supported by a guaranteed limited time for repair of any defects and restoration of service. This last approach, however, is not a very sure course of action.

C. Increasing Emphasis on Waste Management

During the past several years, there has been an increasing emphasis on the development of techniques for the long term management of radioactive wastes. This has included attention not only to the problems of high level liquid wastes but also to the problems of the large volumes of low level solid wastes being generated in all facets of the nuclear industry. Major consideration is being given in the latter case to the use of incineration as a method for reducing the volumes involved. This will require extensive air cleaning for the particulates and gases generated in the combustion process, particularly in the case of wastes containing the transuranics. Also needing greater attention is the development of air cleaning filters and adsorbers which can, themselves, be readily reduced in size and volume for final disposal.[32] Studies show that air cleaning operations are a significant source of solid wastes. For example, the annual volume of waste filters from a typical 1,000 MWe nuclear power station totals some ten cubic meters.[33] For a mixed oxide fuel fabrication plant, it is estimated that, of the total radioactive material content being sent to waste disposal, 18% will be that contained in the HEPA filters.[33] As would be expected, most of this activity will consist of alpha emitters.

D. Feedback of Information from Operating Reactors

The recent establishment within NRC of a new Division of Operating Reactors offers a chance for increased benefits to air cleaning system design, maintenance, and operation via the feedback of information from operating nuclear power stations. Although much

useful information results from the feedback of "Licensee Event
Reports" and "Abnormal Occurrence Reports," there remain defects in
these systems from the standpoint of the provision of information
in a form most useful to air cleaning specialists. For example, such
events are not always categorized in a way so as to be readily recog-
nized as being important in air cleaning, nor are they always re-
corded in the computer storage bank under terminology commonly used
within the air cleaning industry. This is an area which needs atten-
tion. Consideration might be given to the formation of a small
committee of air cleaning specialists to advise the NRC on this
matter.

Acknowledgment

The author wishes to express his appreciation to his colleagues
on the Advisory Committee for Reactor Safeguards and to officials
of the Nuclear Regulatory Commission for their helpful advice and
suggestions in the preparation of this paper.

References

1. Hanauer, Stephen H., Chairman, Special Review Group, "Recommen-
   dations Related to the Browns Ferry Fire," Report NUREG-0050,
   U.S. Nuclear Regulatory Commission, Washington, D.C. (February,
   1976).

2. Branch Technical Position APCSB 9.5-1, "Guidelines for Fire Pro-
   tection for Nuclear Power Plants," U.S. Nuclear Regulatory Com-
   mission, Washington, D.C. (1976).

3. "Design, Testing, and Maintenance Criteria for Atmosphere Clean-
   up System Air Filtration and Adsorption Units of Light-Water-
   Cooled Nuclear Power Plants," Regulatory Guide 1.52, U.S. Nuclear
   Regulatory Commission, Washington, D.C. (June, 1973).

4. Lessor, L.C., Station Superintendent, Cooper Nuclear Station,
   Letter to Mr. E. Morris Howard, Director, Office of Inspection
   and Enforcement, Region IV, U.S. Nuclear Regulatory Commission,
   Arlington, Texas (January 21, 1976).

5. Utley, E.E., Vice President, Bulk Power Supply, Brunswick Steam
   Electric Plant, Unit No. 2, Letter to Mr. Norman C. Moseley,
   Director, Region II, U.S. Nuclear Regulatory Commission, Atlanta,
   Georgia (February 2, 1976).

6. "Assumptions Used for Evaluating the Potential Radiological Con-
   sequences of a Loss of Coolant Accident for Boiling Water Reac-
   tors," Regulatory Guide 1.3, Revision 2, U.S. Nuclear Regulatory
   Commission, Washington, D.C. (June, 1974).

7. "Assumptions Used for Evaluating the Potential Radiological Con-
   sequences of a Loss of Coolant Accident for Pressurized Water
   Reactors," Regulatory Guide 1.4, Revision 2, U.S. Nuclear Regu-
   latory Commission, Washington, D.C. (June, 1974).

8. Hsia, D.Y. and Chester, R.O., "A Study of the Fission Product Release from a Badly Damaged Water-Cooled Reactor," Report ORNL-TM-4702, Oak Ridge National Laboratory, Oak Ridge, Tenn. (June, 1974).

9. Postma, A.K. and Pasedag, W.F., "A Review of Mathematical Models for Predicting Spray Removal of Fission Products in Reactor Containment Vessels," Report WASH-1329, U.S. Atomic Energy Commission, Washington, D.C. (June 15, 1974).

10. "Calculation of Releases of Radioactive Materials in Gaseous and Liquid Effluents from Boiling Water Reactors (BWR-GALE Code)," Report NUREG-0016, U.S. Nuclear Regulatory Commission, Washington, D.C. (April, 1976).

11. "Calculation of Releases of Radioactive Materials in Gaseous and Liquid Effluents from Pressurized Water Reactors (PWR-GALE Code)," Report NUREG-0017, U.S. Nuclear Regulatory Commission, Washington, D.C. (April, 1976).

12. "Calculation of Releases of Radioactive Materials in Gaseous and Liquid Effluents from Light-Water-Cooled Power Reactors," Regulatory Guide 1.112, U.S. Nuclear Regulatory Commission, Washington, D.C. (May, 1976).

13. "The Role of Fission Gas Release in Reactor Licensing," Report NUREG-75/077, U.S. Nuclear Regulatory Commission, Washington, D.C. (November, 1975).

14. Lutz, R.J., Jr., "Iodine Behavior Under Transient Conditions in the Pressurized Water Reactor," Report WCAP-8637, Westinghouse Electric Corporation, Pittsburgh, Penn. (November, 1975).

15. "Reactor Safety Study: An Assessment of Accident Risks in U.S. Commercial Nuclear Power Plants," Appendix II, Report WASH-1400 (NUREG-75/014), U.S. Nuclear Regulatory Commission, Washington, D.C. (October, 1975).

16. Rusche, B.C., "Status of ACRS Recommendations," Letter to R.F. Fraley, Executive Director, Advisory Committee on Reactor Safeguards, Washington, D.C. (March 22, 1976).

17. Heineman, Robert E., "Technical Safety Activities Report," Division of Systems Safety, U.S. Nuclear Regulatory Commission, Washington, D.C. (December, 1975).

18. "Reactor Site Criteria," Title 10, Part 100, Code of Federal Regulations, U.S. Nuclear Regulatory Commission, Washington, D.C.

19. "Report on Engineered Safeguards," Advisory Committee on Reactor Safeguards, Washington, D.C. (November 18, 1964).

20. Report on "ACRS Documents Relating to Siting Evaluation," Advisory Committee on Reactor Safeguards, Washington, D.C. (August 13, 1974).

21. Draft Report on "Location of Power Reactors at Sites of Population Density Greater than Indian Point - Zion," Advisory Committee on Reactor Safeguards, Washington, D.C. (July 14, 1969).

22. Minutes of Meeting of the Reactor Siting Subcommittee, Advisory Committee on Reactor Safeguards, Washington, D.C. (March 20, 1965).

23. "Minutes of the 88th Meeting Held on August 10-12, 1967," Advisory Committee on Reactor Safeguards, Washington, D.C. (Issued on July 11, 1968).

24. Report on "Review of Siting Policies for Licensing Nuclear Facilities," Advisory Committee on Reactor Safeguards, Washington, D.C. (December 10, 1975).

25. Report on "Public Service Electric and Gas Company - Newbold Island Site," Advisory Committee on Reactor Safeguards, Washington, D.C. (September 10, 1969).

26. "General Electric Standard Safety Analysis Report (GESSAR-238)," Advisory Committee on Reactor Safeguards, Washington, D.C. (March 14, 1975).

27. "Seismic Design Classification," Regulatory Guide 1.29, Revision 2, U.S. Nuclear Regulatory Commission, Washington, D.C. (February, 1976).

28. Major, Richard K., "Report on Containment Spray Technology," Advisory Committee on Reactor Safeguards, U.S. Nuclear Regulatory Commission, Washington, D.C. (December 1, 1975).

29. "Status of Generic Items Relating to Light-Water Reactors: Report No. 4," Advisory Committee on Reactor Safeguards, Washington, D.C. (April 16, 1976).

30. Seefeldt, W.B., Mecham, W.J., and Steindler, M.J., "Characterization of Particulate Plutonium Released in Fuel Cycle Operations," Report ANL-75-78, Argonne National Laboratory, Argonne, Illinois (May, 1976).

31. Denice, Richard, Assistant Director for Special Projects, U.S. Nuclear Regulatory Commission, Letter to Lochlin W. Caffey, Director, Clinch River Breeder Reactor Project Office, Washington, D.C. (May 6, 1976).

32. Burchsted, C.A., "Removal of Particulates from Nuclear Offgas," paper presented at the International Symposium on the Management of Wastes from the LWR Fuel Cycle, Denver, Colorado (July 14, 1976).

33. Steindler, M.J. and Trevorrow, L.E., "Description of the Fuel Cycle and Nature of the Wastes," paper presented at the International Symposium on the Management of Wastes from the LWR Fuel Cycle, Denver, Colorado (July 13, 1976).

SESSION VIII

SYSTEM DESIGN FOR NUCLEAR FACILITIES

Tuesday, August 3, 1976
CHAIRMAN: J. Murrow

THE REMOVAL OF RADIOACTIVE AEROSOLS FROM THE POST ACCIDENT ATMOSPHERE
OF AN LWR-CONTAINMENT
G. Haury, W. Schoeck

GAS CLEAN-UP SYSTEM FOR VENTED CONTAINMENT
J. L. Kovach

STANDARDIZATION OF AIR CLEANUP SYSTEMS FOR NUCLEAR POWER PLANTS
E. Nicolaysen, K. E. Carey,
J. J. Wolak

CONTROL ROOM VENTILATION INTAKE SELECTION FOR THE FLOATING NUCLEAR
POWER PLANT
D. H. Walker, R. N. Nassano,
M. A. Capo

EVALUATION OF CONTROL ROOM RADIATION EXPOSURE
T. Y. Byoun, J. N. Conway

OPENING REMARKS OF SESSION CHAIRMAN:

In a day and a half we have heard about particulate and gaseous
collection, monitoring, fire, disposal of collected materials, effects
of natural and manmade disasters, and now we are going to learn how
systems can be, and should be, designed to further the safeguards
that Dr. Moeller spoke to us about during lunch.

THE REMOVAL OF RADIOACTIVE AEROSOLS
FROM THE POST ACCIDENT ATMOSPHERE
OF AN LWR-CONTAINMENT

G. Haury and W. Schoeck
Laboratorium fuer Aerosolphysik und Filtertechnik
Projekt Nukleare Sicherheit
Kernforschungszentrum Karlsruhe, Germany

Abstract

The computer code NAUA has been developed to model the removal of the airborne radioactive particles in the post accident atmosphere of an LWR-containment. It calculates the aerosol processes coagulation, diffusion, sedimentation and thermophoresis, the steam condensation on the particles, and significant thermodynamic effects such as heat removal by the containment spray system.

With the first version NAUA-Mod1 calculations have been done which show the dominant role of the condensation process. The number concentration and the size of the so formed droplets affect very strongly the rate of subsequent coagulation between droplets and the remaining dry particles. This effect is further enhanced by temperature decrease due to spraying.

The paper dicusses the structure and potential of the NAUA code, and presents the results of a parametric study on the important removal effects. Some problems of the physical behavior of the aerodispersed system in the post accident LWR-atmosphere are discussed which cannot be solved by the modelling alone. Therefore, the investigation of the condensation process and of the proprties of the three phase particle droplet steam system will be part of the supporting experimental program.

I Introduction

The events in the course of a hypothetical accident in a light water reactor could be divided into three main groups which are physically quite different, the release of radioactive material from the melting core into the containment, the removal of radioactivity from the atmosphere inside the containment, and the transport phenomena and radiological impact to the environment. As the amount of released radioactive material can be very high in melt down accidents following blow down, the removal processes inside the containment are of great importance as a means of mitigating the radiological consequences.

The physical and chemical properties of the radioactive material immediately suggests a classification into the groups of chemically nonreactive noble gases, volatile fission products mainly iodine compounds, and solid particulate material. The latter includes most of

the long lived isotopes as e.g. Co, Sr, Ce, and Pu.

Mathematical modelling of the time dependent behavior of the gaseous radioactive elements and compounds is not very difficult as soon as the physical and chemical processes of removal are known. In the case of the aerosolic matter, however, even if the removal processes were understood, the modelling would still remain complicated by interactions between the particles themselves and, particularly in the LWR case, by the presence of large amounts of condensable water vapor released during blow down. This water will condense on part of the aerosol, and thus introduce a third, liquid phase to the system.

The subject of this paper will be to discuss a mathematical model and results of preliminary calculations of the time dependent aerosol behavior in the post accident atmosphere of an LWR containment.

II Theoretical basis of the model

Many descriptions of aerosol removal in closed containments start from the suggestion that the decay rate of any kind of mean airborne concentration C be proportional to C itself

$$dC/dt = -\alpha.C \tag{1}$$

which immediately leads to an exponential decay. General experience contradicts this exponential law, and the model is adjusted by introducing time dependent factors α, which are obtained empirically from experimental work. This numerically simple approach enables the model to handle multicomponent systems with moderate computation times.

The opposite approach, the one we use, is to model as closely as necessary the physical processes in the aerosol system. This leads to more complicated mathematical structures and consequently to necessary reductions in the geometrical complexity of the model containment in order to keep computation times adequately low.

We consider our approach to be more reliable for two reasons: First, in the large volumes of a reactor containment, the aerosol removal is governed by the physical aerosol processes rather than by the geometry of far off containment walls, and second, decay factors in eq.(1) are valid only for the experimental conditions from which they were deduced, and cannot be transferred to other situations with greatly different parameters. The use of experimental data should be limited to cases where the microscopic processes are well understood both in the experiment and in the calculated situation.

Starting from these considerations we constructed the NAUA code (NAUA = NAch-Unfall-Atmosphaere = post accident atmosphere) using the microscopic aerosol removal processes coagulation, sedimentation, thermophoresis, and diffusion, and the interaction process with the condensing water vapor, which is a molecular high speed process. These processes are considered to be the most important, in future versions

of the code other mechanisms, as e. g. gravitational coagulation, may be added if necessary.

The model further includes homogeneous steam and particle sources of arbitrary time dependence.

III Numerical concept of the code

In calculations of time dependences, the most important parameter of aerosols is the size of the individual particle or the size distribution of the aerosol. Sizes of irregularly shaped particles can be defined in numerous ways, we choose the mass equivalent radius as a measure, because the particle mass is proportimal to the radioactivity. The effect of the irregular shape is accounted for by means of form factors whenever necessary. In discussing the structure of the model, we will concentrate on particle radius and particle properties. Detailed descriptions of the underlying physical mechanisms are given in earlier reports [1].

The code is separated into two main subunits because of numerical reasons. The first is called NAUCON, and calculates the condensation of steam on the particles and the thermodynamic properties of the gas phase. The equation given by Mason [2] is used to calculate the change of particle radii

$$r \, dr/dt \; = \; A \, (S(t) - \exp(B/r)) \tag{2}$$

where S is the degree of saturation, which is close to one in the LWR post accident atmosphere, and A and B are thermodynamic functions of the gas-steam system.

The second subunit of the code, NAUPAR calculates the aerosol removal processes. The change of the population of a size class n(r) is given by

$$dn(r,t)/dt = Q(r,t) - (\alpha_s(r) + \alpha_D(r) + \alpha_T(r)) \; n(r,t)$$

$$- \int K(r,r_1) \; n(r,t) \; n(r_1,t) \; dr_1 \tag{3}$$

$$+ \iint K(r_2,r_3) \; n(r_2,t) \; n(r_3,t) \; dr_2 \; dr_3$$

Here Q is the particle source term and the alfas are coefficients for deposition by sedimentation, diffusion and thermophoresis respectively. The two integrals describe the action of coagulation. The first integral is the coagulation rate f r o m the size class under consideration to all others, the second describes coagulation i n t o this size class, where obviously $r^3 = r_2^3 + r_3^3$.

Eq.(3) is the PARDISEKO equation which was used to calculate aerosol removal in LMFBR containments [3]. In the LWR case this equation

739

cannot be used, because n(r) is no more a continuous function and the coagulation integrals cannot be solved with the necessary precision. Thus the coagulation integrals have been replaced by a much simpler particle counting and classifying routine that, by definition, conserves the mass during coagulation. Because the new method cannot be represented by an equation of the type of eq.(3), its description will be omitted here. A detailed discussion is given elsewhere [4]. Another advantage is the higher computation speed of the new technique.

The already mentioned form factors are used in the NAUA model to account for the differences between the reality and the idealized mathematical model which e.g. always uses spherical particles. Presently three form factors are used. The first one f_m is needed in eq.(2), which is valid for condensation on water droplets only, and not on irregularly shaped solid particles. The rate of steam condensation is dependent on the degree of wetting of the particle, too, f_m thus depends on the actual radius of every individual particle. The second form factor, the aerodynamic form factor f_b describes the change in mobility due to the fluffy structure of the fuel particles. The coagulation form factor f_S, finally, accounts for the fact that the target particles are considerably larger than is represented by the mass equivalent radius.

All three factors are size dependent and unknown for fuel aerosols. Their values will be measured in the experimental part of the program. At the moment, values from pevious work on LMFBR aerosol behavior are used for f_b and f_S, f_m is set to one.

In order to test the performance of the code under varying conditions, and to identify the most relevant parameters that need experimental investigation a sensitivity study has been executed. Because the response of the aerosol system to changes in steam density is always instantaneous, it is reasonable to discuss the condensation processes and the long term removal separately, as will be done in the following sections.

IV Short term calculations of steam condensation

Steam condensation on fuel-like particles is the elementary process of the NAUA model for which the least experience exists. It has been studied intensively with variations of all possible parameters, the most important results will be discussed now.

As a result of the condensation, which acts only on the bigger particles of the initial size distribution, bimodal particle-droplet distributions are generated within a few seconds. Fig.1 shows as an example the resulting bimodal distributions that are created from an initial dry particle size distribution of log-normal shape with a mean geometric radius of 0.1 μm and a standard deviation of $\ln\sigma = 0.4$. It is apparent that the temperature of the system has little influence. This is valid for all other effects, too, which are not very sensitive to temperature, with the exception of steam density of the containment
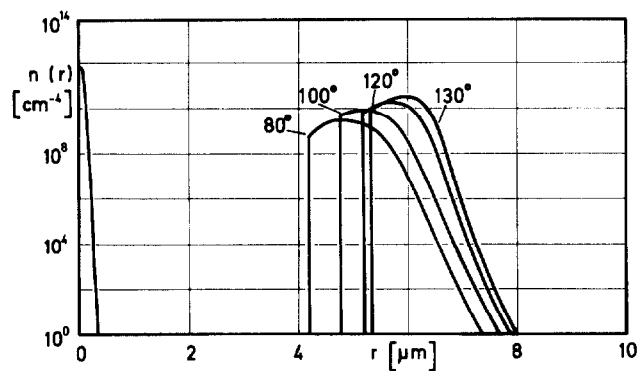
Figure 1   Bimodal size distribution developed
at different temperatures.
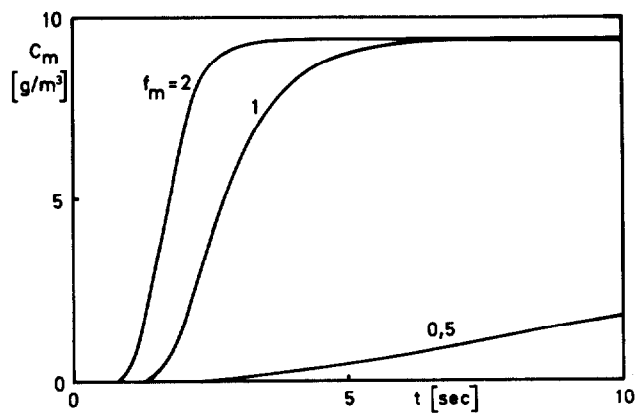
Figure 2   Time dependence of droplet mass
concentration with different
condensation form factors f_m.

atmosphere. Thus temperature dependences will not be discussed in this paper, the influence of steam density, however, is shown in the next section.

A large bandwidth of particle size distribution parameters has been used in calculations of steam condensation together with various time dependent steam source terms. The differences in the resulting bimodal size distributions are great, but is was not possible to evaluate any quantitative simple law to connect input and output of the condensing steam-aerosol system. The complete model has to be employed in order to obtain reliable results.

Further calculations have been done to assess the influence of the non-sphericity of the particles on the condensation process. Since no experimental work has been published on this problem we varied the form factor f_m. Starting values for the initially dry particles are $f_m = .5$, 1, and 2. Fig.2 shows the time dependent mass concentration of the growing droplets, the total condensable steam concentration being 10 g/m^3 in all three cases. For $f_m = 0.5$ it takes more than two minutes until all the steam has condensed on the particles, in the other cases a few seconds are sufficient for the droplet formation. The great difference that is also exhibited in the number and size of the droplets emphasizes the need for exact experimental data. The steam condensation on fuel particles will be investigated closely in the first phase of the experimental program.

V Long term calculations of aerosol removal

Using an $f_m = 1$, long term calculations have been done to study the influence of the aerosol parameters and of containment spraying on the removal process. To do this it was necessary to input into the model some properties of the containment and some assumptions on the accident sequence. The containment properties are mainly geometric and thermodynamic data, and were taken from the Reactor Safety Study [5]. The temperature function T used in our calculations is shown in Fig.3. When necessary it was extended to longer times. It will be shown, however, that a further temperature decrease beyond the first 30 minutes will contribute little more to the removal of particles. Thus in most cases the temperature was held constant after the rapid decrease in the first half hour. As already mentioned, the main effect of temperature is to change the amount of condensable water vapor in the system. The density of condensable steam is shown by function C_w in Fig.3.

Among the other data the particle source term has the greatest influence on the behavior of the aerosol-steam system. On the other hand very little is known of these data, particularly when the particle size distributions and the single particle properties are required. As a rough estimate for particle sizes, we used experimental results of generation of fuel aerosols by exploding wire technique which were done in our laboratory previously [6], and by a direct arching method which was developed by one of us recently. The most reasonable values for a particle size distribution of fuel aerosol in
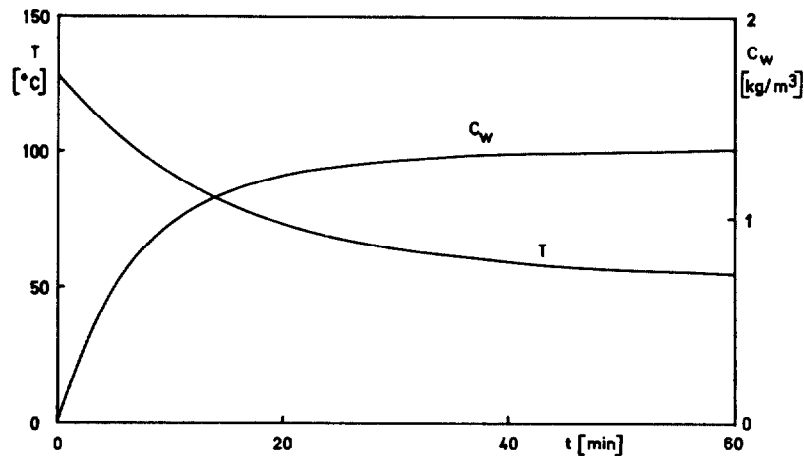
Figure 3   Time dependence of containment temperature T
            and steam density C_W used in the long term
            calculations.

the melt down and evaporation phases are a mean geometric radius of
0.1 μm and a standard deviation of 0.4, assuming a log-normal size
distribution. We have used these values in our long term calculations.
The total released mass is 1000 kg as given in [5]. In the
calculations reported here, we assumed a source with constant rate but
with variable duration. Another removal mechanism of great importance
is the action of a spray system. Its effect on particles is not yet
investigated very well, we consider the most relevant effect to be the
rapid decrease of temperature which frees large amounts of condensable
steam (Fig.3). Whereas temperature decrease through cold containment
walls mainly leads to water condensation on the walls, the result of
the spray action as a volume effect is that the steam condenses on the
particles, because the surface of the particles is greater by orders
of magnitude than the surface of the containment walls or of the spray
droplets. Thus in our model we assumed the action of spraying to be
that all condensable steam condenses on the particles. The real
fraction and its dependence on the various parameters will be subject
to investigations in the experimental program.

Table I shows the scheme of parameter variations in the long term
calculations. Case D1 is the reference case with which all others are
compared. The values f_b = 3.5 and f_s = 8.2 are taken from previous
LMFBR safety experiments [6].

Fig.4 shows the time dependence of particle number and mass
concentrations C_n and C_m for the reference case D1. The most
interesting result is that, at the end of the particle source action,

743

case #	particle source	f_b	f_s	spray
D1	30 min	3.5	8.2	off
D2	120 min	3.5	8.2	off
D3	30 min	1.0	8.2	off
D4	30 min	3.5	2.0	off
W1	30 min	3.5	8.2	on
W2	120 min	3.5	8.2	on

Table I   Scheme of parameter variations
for long term calculations.

the total released mass of 1000 kg (40 g/m^3) is airborne. It takes some hours for the coagulation process to form big enough particles, before the sedimentation becomes effective. In our case the temporal separation of the dominance of coagulation and sedimentation phases is so large that it exceeds the duration of the particle source. This can be seen clearly in Fig.5 where the cases D1 and D2 with different source term duration are compared. Only an insignificant delay of mass removal is visible, because the coagulation phase is much longer than either source term interval.

It should be emphasized, that this result was calculated with an aerosol behavior model that depends strongly on aerosol properties which are not exactly known. Fig.6 represents the results of calculations with variations of the particle properties, namely form factors f_b and f_s.

f_s acts on the coagulation rate only. Therefore, in case D4 the coagulation rate was lower than in case D1. After a prolonged coagulation phase, the aerosol removal rate finally approximates the same value as in case D1.

In case D3 the particle mobility was increased by putting $f_b = 1$. The factor f_b acts on all removal processes simultaneously. So an immediate beginning of the removal without a distinct coagulation phase and a much faster decay of the mass concentration is observed. Thus with an $f_b = 1$ also a dependence on source term duration could be expected that is more pronounced than in Fig.5.
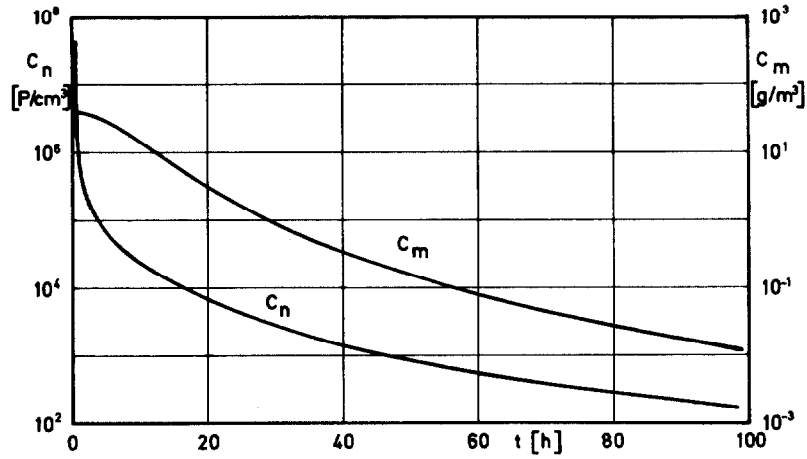
Figure 4   Time dependence of airborne particle
            mass and number concentrations C_m
            and C_n in the reference case D1.
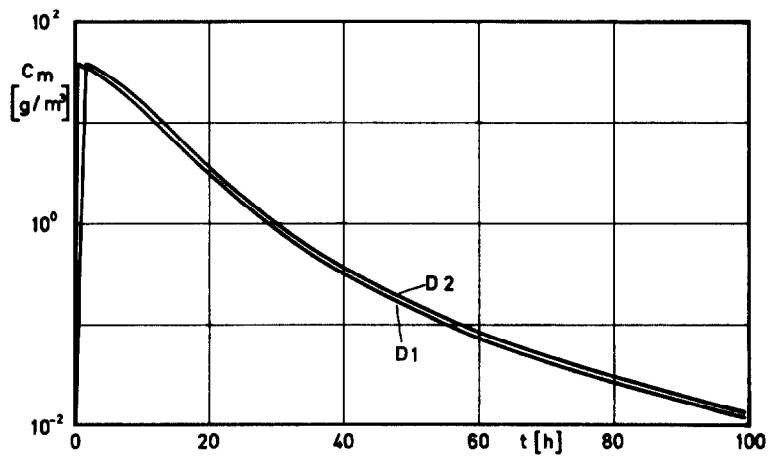
Figure 5   Airborne particle mass concentration
            with different source term duration.
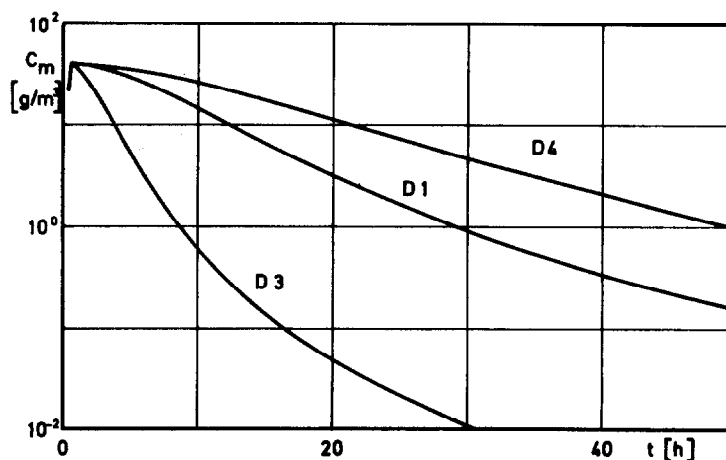
Figure 6   Airborne particle mass concentration
            with different particle form factors.

The fact that both the influence of the source term and the long term
behavior   are   very   sensitive to the particle form factors emphasizes
the importance of their direct experimental measurement, which will be
part of our experimental program.

So far we did not consider the effect of condensation of large amounts
of water vapor that will take place during the action of containment
spray systems. In Fig.7 the airborne mass concentration for cases W1
and W2 are shown. The time dependence is quite different from that of
the 'dry' D cases. First of all nearly the total mass consists of
condensed water droplets, as only 40 g/m^3 maximum of solid material
were released. The mass concentration closely follows the curve C_W of
condensable steam that is set free due to the temperature decrease.
After   20   minutes,   the   droplets   have   grown so big that the
sedimentation becomes noticeable. All the time the coagulation acts
only between the source particles and the already existing droplets,
and is enhanced by their great size difference. A short time after the
end of the particle source action, all particles will have vanished
due to coagulation into the droplets, and the long term decay of
airborne solid mass is determined almost only by the sedimentation of
the droplets.

This is illustrated in Fig.8 where the airborne mass of solid material
(without the condensed water fraction) for cases W1 and W2 is compared
with case D1. The difference between cases W1 and W2, that was
obscured by the great water content in Fig.7, is now clearly visible.
The decay of solid mass or of radioactivity is faster in both cases
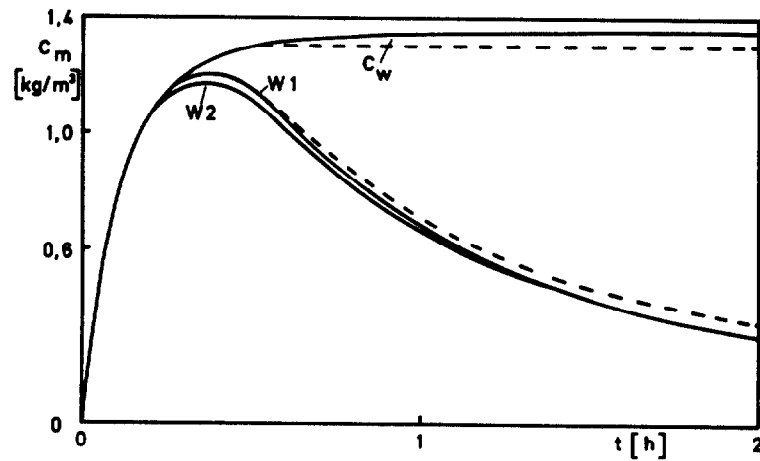
Figure 7   Airborne mass concentrations in the
            calculations with spray W1 and W2
            and condensable steam density C_W.
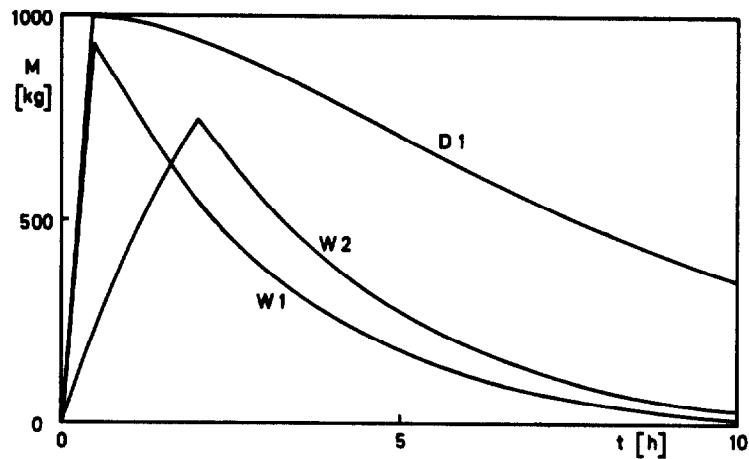
Figure 8   Total airborne mass of solid material in
            the containment for the spray cases W1 and
            W2 compared to the case D1 without spray.

than in case D1 without spray. However, the fractional content of solid matter, that is shown in Fig.8, is only a rough estimate. The measurement of the distribution of solid particulate material inside the droplets as a function of the system parameters is one of the great problems that have to be solved experimentally.

It should be noticed finally that the effect of spraying is most significant in the beginning when the temperature is still high. A shut off of the spray system after 30 minutes will cause only a short delay of the removal of airborne mass, as is shown by the dashed lines in Fig.7.

VI Experimental Program

As has been shown, some of the unknown physical parameters of the aerodispersed system have great influence on the time dependence of the airborne particle mass concentration. If the NAUA code calculations are intended to be more valuable than conservative assessments, the measurement of these parameters becomes unavoidable.

The construction of the experimental facility has been started, with whith investigations of the microscopic effects such as form factors, condensation phenomena or particle distribution in the droplets can be done as well as integral experiments on spray system efficiency, wall effects and code verification. It is planned that the construction and testing of the facility will be completed in the first half of 1977. The assembling of the instrumentation and development of new measurement techniques, especially for the droplet mesurement, will be finished early enough to be used in the testing period.

References

[1] G.Haury et al, 'PNS Halbjahresberichte', No.II/1974, KFK report 2130, (1975) and No.I/1976, to be published

[2] B. I. Mason, The Physics of Clouds, Oxford, 1971

[3] H. Jordan and C. Sack, 'PARDISEKO 3, a computer code for determining the behavior of contained nuclear aerosols', KFK report 2151, (1975)

[4] G. Haury and W. Schoeck, 'Parameterrechnungen mit dem NAUA-Modell', PNS Arbeitsbericht No. 78/76 (1976)

[5] USNRC, 'Reactor Safety Study', WASH 1400, NUREG 75/014, (1975)

[6] H. Jordan, W. Schikarski, H, Wild, 'Nukleare Aerosole im geschlossenen Containment', KFK report 1989, (1974)

GAS CLEAN-UP SYSTEM FOR VENTED CONTAINMENT

J. L. Kovach
Nuclear Consulting Services Inc.
Columbus, Ohio

Abstract

Component selection and sizing analysis was performed for both operational and post accident vented containment for light water reactors.

The criteria used was the decrease of pressure and retention of significant health hazard isotopes which would be present in the containment after a loss of coolant accident.

Time-pressure curves were developed for different vent volumes together with fission product capacity for the various components of the system.

The analysis indicates that the design of post accident venting systems is feasible and the protection afforded can justify the cost of the system.

Two types of operation were analyzed; treatment external to the containment and vent to the atmosphere, and treatment external to the containment with recirculation to the containment.

I Introduction

The ventillation systems for nuclear power stations are still primarily in the realm of sheet metal work. Although the gaseous waste treatment systems may involve chemical process technology, the expertise of the chemical solvent vapor handling techniques have not permeated the nuclear industry. The use of deep bed adsorption systems to recover solvent vapors has been practiced for over 70 years, and aspects of this process can be well suited for any major release clean-up or post accident venting of the containment. In the following,design and operation criteria for such systems is evaluated.

II Clean-up Volumes

Figure 1 is a reproduction from WASH 1400 (1) for a typical PWR where the containment free volume is 1.8×10^6 ft^3. The volumes to be cleaned-up and vented are at the following rates:

Daily Vent % Containment Volume	CFM
100	1,250
200	2,500
300	3,750
500	6,250

Therefore even at a 2,500 cfm rate the failure pressure range will not be reached and at approximately 200 minutes after LOCA the pressure inside the containment would be decreasing even with no containment safeguards operating.

Similar values can be generated for BWRs also, however both the size and cost is less therefore, the sizing evaluation here is based on PWR only.

III   Design Concept

The air (gas) motive force exists in the containment itself. The pressure differential is sufficient to result in the required flow because total pressure drop through the system is, at most, several psi. Therefore the basic clean-up process does not require blowers.

The first analysis is based on an iodine and particulate fission product removal at the 3,000 CFM flow rate corresponding to venting 3 containment volumes per day. The temperature exiting from the containment is assumed at 130°C.

The following components are considered for this application.

a) Heat Exchanger using water to lower gas temperature to ~50°C.

b) Sand Bed filters for particulate removal (99.97% Efficiency).

c) Iodine removal bed based on decay (99.99 + % Efficiency).

The cost estimates for such components in 304 stainless steel are

a) $180,000.00
b) $105,000.00
c) $285,000.00
Total: $570,000.00 redundant, code construction.

The iodine adsorption bed sizing is based on long term operating life, where the iodine may be transported through the bed; however it is decayed in a similar manner to the noble gas delay beds. The design of such bed is discussed in detail in Part VI of this paper.

For elemental iodine decay in the adsorbent bed approximately 10,000 lbs of carbon is required assuming an inlet concentration of 1.0 mg iodine FP/m^3.

The sizing data for sand beds is based on operational experience at the Savannah River Plant of USERDA (2) (3).

This mode of operation would result in venting to an outside location and the noble gases would not be delayed to an appreciable extent in the system.

If a recirculation mode is used, i.e., the particulate and iodine FP decontaminated noble gas-containing-air is reinjected into the containment, the rate of return would be approximately one third of the total gas removed because a large part of the steam is condensed. The rate of returnable gas is approximately 1000 CFM.
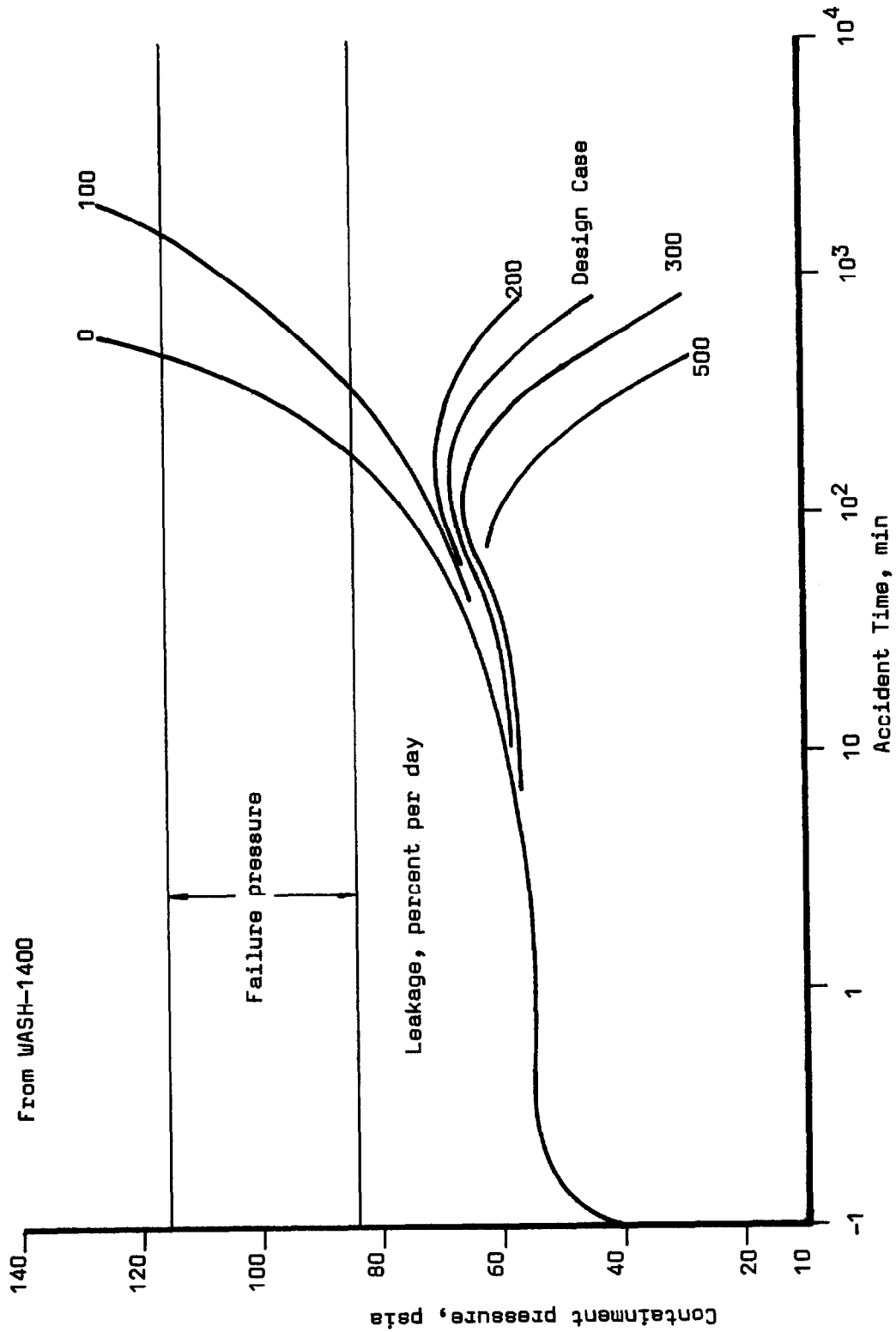
Figure 1. PWR containment pressure as a function of leak rate for an assumed LOCA with no containment safeguards.

If reinjection is used, an airmoving device capable of boosting the residual gas to approximately 60 psia is required; the cost of such a compressor is estimated at $40,000.00 each.

IV Clean Up Components

Sand Bed Filter

Vertical bed using base grating with graduated particle size packing. Approximate gas velocity through bed at < 20 FPM, bed depth 80-100 inches. The efficiency for such beds was measured for particulate fission products and uranium or plutonium aerosol of above 99.99% (4) (5) (6).

Iodine Removal Bed

Grated bed is most beneficial where the roughing adsorber contains non-combustible 80-90% minimum efficiency packing followed by or in a separate bed with impregnated carbon or other high efficiency adsorbent. Velocity at > 40 FPM; bed volume to be sized for long-term decay type removal process, where self-regeneration takes place. Efficiency for iodine fission products 99.99%. Detail of such sizing is discussed in Part VI of this paper.

V Estimation of Installed Cost

Direct Costs

Equipment	$650,000
Installation (75%)	487,500
Structures and Buildings	125,000
Subtotal.	$1,262,500

Indirect Costs

Engineering Design (18%)	$227,250
Field Erection (50%)	631,250
Owner's Cost (5%)	63,125
Contingency (25%)	315,625
Interest During Construction (30%)	378,750
Subtotal.	$1,616,000
TOTAL	$2,878,500

VI Sizing of Iodine Decay Beds

Elemental iodine is removed from contaminated atmosphere in activated carbon beds by adsorption. In flowing air stream a concentration band is formed in the inlet side of the adsorber from 0 iodine concentration to the inlet concentration. Once this concentration band is formed it moves along the depth of the adsorbent bed at a constant rate.

A similar concentration gradient is formed when methyl iodide is decon-taminated by isotope exchange. Both processes are controlled by bulk diffusion, i.e. intergrain diffusion in laminar flow systems, while the rate controlling

step becomes a much faster pore diffusion in turbulent flow systems. The reason for this phenomenon is that in turbulent flow, the movement of an iodine or methyl iodide molecule to the surface of the carbon grain becomes much faster.

When adsorption of a radioactive molecule takes place the above described manner of achieving equilibrium is not applicable, because as a result of the radioactive decay the movement of the concentration gradient will not stay constant but will decrease in rate as it moves along the adsorbent bed and finally will become stationary. (7)

As a result of radioactive decay the mean life of a radioactive isotope is

$$\mathcal{T} = 1/\lambda \tag{1}$$

Denoting the radioactive atom of an adsorbing molecule as X* the following will take place on the surface.

When the molecule is adsorbed, upon decay of X* a recoil nuclei will be ejected into the gas phase or into the body of the solid adsorbent. The adsorption site (active site) will be freed and may be used for the adsorption of a molecule containing the undecayed X* isotope, if the fragments of the original molecule and the daughter isotope do not interfere. (Although the possibility of new active site generation,i.e. extended surface or porosity by the radiation and the recoil atoms is indicated, its effects are not discussed here.)

The process is somewhat simplified when the decay product is only weakly adsorbed. Such is the case during the adsorption of halogen isotopes either in the form of Hal⁻ or (Hal)$_2$ or more specifically I⁻ or I$_2$. The decay products Kr, Xe and other noble gases are not chemisorbed at all and are only weakly adsorbed by Van der Waals forces. Therefore it can be assumed that one adsorption site is freed-up on each iodine isotope decay.

In theory, if only radioactive isotopes are present,the possibility of the "perpetual" operation of the adsorbent bed exists with complete adsorption of the continuously introduced iodine upon sites continuously freed up by radioactive decay of the adsorbed iodine and subsequent release of the daughter product into the gas phase.

At zero time the surface of the adsorbent is completely free from radioactive iodine. At time t=0, beginning from the inlet section $x_0 = 0$,the iodine containing gas stream is passed through at a concentration of C_0 and a gas velocity of v. The superficial gas velocity is always much greater than the rate of movement of the concentration band (or adsorption wave front), therefore the iodine concentration will sharply (exponentially) decrease along the length of the adsorbent bed. Thus, initially, the radioactive iodine content of the first portions of the emerging gas stream will be negligibly low even for relatively short adsorbent depths. This initial condition is shown on Figure No. 2.

If the introduction of the iodine containing gas stream is maintained,the inlet section of the adsorbent bed is gradually filled with iodine resulting in the formation of the adsorption wave front; behind this front the adsorbent is at equilibrium with the inlet iodine concentration and in front of it there is a sharp fall to zero concentration. As the front moves forward, because of

partial freeing of the adsorbent surface as a result of decay into a weakly adsorbed molecule, the rate of movement of the front (in contrast to its movement in case of non-radioactive molecules) will continuously be slower until it stops completely at some depth of the adsorbent bed designated L.

The value for L depends on λ, the geometry of the adsorbent bed, the gas flow rate v, the capacity of the adsorbent for iodine, the temperature of the system, the relative humidity of the system, the inlet concentration C_0, and the form of the iodine species present. When the wave front has reached this section L along the adsorber a steady state system is achieved.

In the following only initial and limiting case equations are shown as a rough guide for the practical application of this design method.

By setting $C(x,t)$ to denote the concentration of the radioactive gas per unit volume of the adsorber charge at a given time t and at a given distance x from the inlet of the adsorber. The corresponding concentration of the radioactive gas adsorbed per unit volume of the adsorbent is denoted by $A(x,t)$. The maximum amount of the radioactive gas component adsorbed (at equilibrium) per unit volume of the adsorbent is denoted by N_0. The balance equation in the gas phase will be:

$$\frac{\partial C}{\partial t} = u \frac{\partial C}{\partial x} - Kf(C)(N_0 - A) \tag{2}$$

and in the adsorbed phase:

$$\frac{\partial A}{\partial t} = Kf(C)(N_0 - A) - \lambda A \tag{3}$$

where $Kf(C)(N_0 - A)$ characterizes the adsorption rate, i.e. the quantity of radioactive gas adsorbed per unit time per unit volume of adsorbent on the available free sites $N_0 - A$.

The value of λA denotes the rate of decay of the adsorbed iodine per unit time per unit volume of adsorbent.

At low concentration the concentration dependence $f(C)$ can be described by the Langmuir equation:

$$f(C) = \frac{C}{C + b_0} \tag{4}$$

In general b_0 is very much smaller than the inlet concentration C_0. Such function corresponds to a low dependence of the adsorption rate on the space concentration almost up to complete adsorption of the starting radioactive gas.

The value K characterizes the adsorption rate and is the reciprocal of the time required for the adsorption of the iodine by the adsorbent. Both experimental data and theoretical evaluations show that K increases in turbulent flow for the earlier described reasons.

At the initial moment t=0

$$C(x,0) \text{ and } A(x,0) = 0 \tag{5}$$

and in the inlet section at x=0

$$c(0,t) = const. = C_0 \tag{6}$$

The initial stage of the adsorption up to the formation of the stable adsorption wave is characterized by the concentration distribution illustrated in Figure No. 2. The distance l over which the concentration falls by a factor of two is given approximately by

$$l = \frac{u}{K} \tag{7}$$

While the ratio of the outlet concentration C_f to the initial concentration C_0 is

$$\frac{C_f}{C_0} = \exp(-\frac{x}{l}) \simeq \exp(-\frac{Kx}{u}) \tag{8}$$

where x is the full length of the adsorber bed.

This ratio is established after a short time:

$$\mathcal{T}_1 = \frac{x}{u} \tag{9}$$

which is required for the passage of a portion of the gas through the apparatus and then will increase slowly.

As a result of the high rate of adsorption, particularly in turbulent flow, the length of the adsorption wave front will be very much less than the depth of the adsorber, therefore C_f will be orders of magnitude lower than C_0.

In the next stage of the adsorption process as the adsorption wave front is established, the concentration distribution of the radioactive iodine in the gas phase and on the adsorbent is shown on Figure No. 3.

Balance equations can best be used to determine the wave front velocity u.

The amount of the radioactive iodine entering in time dt per unit section of the adsorber equals $uC_0 dt$. The front of the adsorption wave moves by udt in the same length of time; the amount of iodine adsorbed per unit section of the adsorber equals approximately $vN_0 dt$ because the maximum adsorption capacity A_m is close to N_0.

However in the same length of time, of the adsorbed radioactive iodine $\approx$ $N_0 x$ (per unit section of the adsorber) a λdt fraction will decay. The total amount of radioactive iodine decaying equals $N_0 x \lambda dt$.

Because of the law of conservation of matter:

$$uC_0 = vN_0 + N_0 x\lambda \tag{10}$$

Considering that

$$v = \frac{dx}{dt} \qquad (11)$$

and integrating Eq (10):

$$v = v_0 \exp(-\lambda t) \qquad (12)$$

where the initial velocity of the front u_0 at $x = 0$ is

$$v_0 = u \frac{C}{N_0} \ll u \qquad (13)$$

From equation (12) it follows that the motion of the front will practically cease after a time:

$$\tau \approx \frac{3}{\lambda} \qquad (14)$$

which is approximately three times the half life of the radioactive iodine.

The length of the adsorption wave front can also be calculated by

$$L_a \approx \frac{v_0}{\lambda} \approx \frac{uC_0}{\lambda N_0} \qquad (15)$$

from equation (10) when v=0.

When the movement of the adsorption wave front ceases some final concentration distribution is established in the adsorbent bed as illustrated on Figure No. 4.

In the part from the inlet section to $x=L_a$, the adsorbent is at equilibrium while the concentration in the gas phase drops to a value of:

$$C_1 \approx b_0 \qquad (16)$$

Beyond this layer there is a sharp exponential fall in the concentration C and A according to equation (8). Thus the final outlet concentration is approximated by

$$\frac{C_f}{C_0} = \exp\left[-\frac{(x-L_a)}{1}\right] \qquad (17)$$

Therefore near complete decay of the radioactive iodine can be achieved in approximately twice the length of the adsorption wave front:

$$x = 2L_a \qquad (18)$$

Expressed on a volumetric basis, $V_a = SL_a$ is used to denote the value of the adsorbent containing the adsorption wave front and $V = Sx$ will be the adsorbent volume. From equation (15):

$$V_a = \frac{uC_o}{\lambda N_o} \tag{19}$$

and from equation (18):

$$V = 2V_a \tag{20}$$

Therefore the quantity of required adsorbent can be calculated to permit decay of the iodine without breakthrough.

In case of isotope exchange the number of active sites (when excess iodine is deposited on the surface, which is the case above 2% I_2 present) is approximately the same as the sites available for adsorption.

All estimates should account for poisoning of the bed by adsorption of non-iodine species on the adsorbent surface. Experimental data indicates that poisoning takes place only in a narrow inlet section of the adsorber; thus the correction should be additive and not factored into the sizing calculation.

Symbols

A = quantity of radioactive gas adsorbed at concentration C.
b = constant in Langmuir equation.
C = concentration of radioactive gas.
l = length of bed in which the concentration falls by a factor of two.
L = length of the adsorption wave.
N = quantity of radioactive gas adsorbed by unit volume of adsorbent.
S = cross section of the adsorber.
t = time.
u = velocity of the adsorption wave front.
v = superficial gas velocity.
V = volume of the adsorbent.
x = length along the adsorbent.
X* = denotes decaying isotope.
λ = decay constant.
τ = mean lifetime of decaying isotope.

Subscripts

a = properties of adsorption wave front.
f = final.
m = maximum.
o = initial.

Figure 2

Figure 3

Figure 4
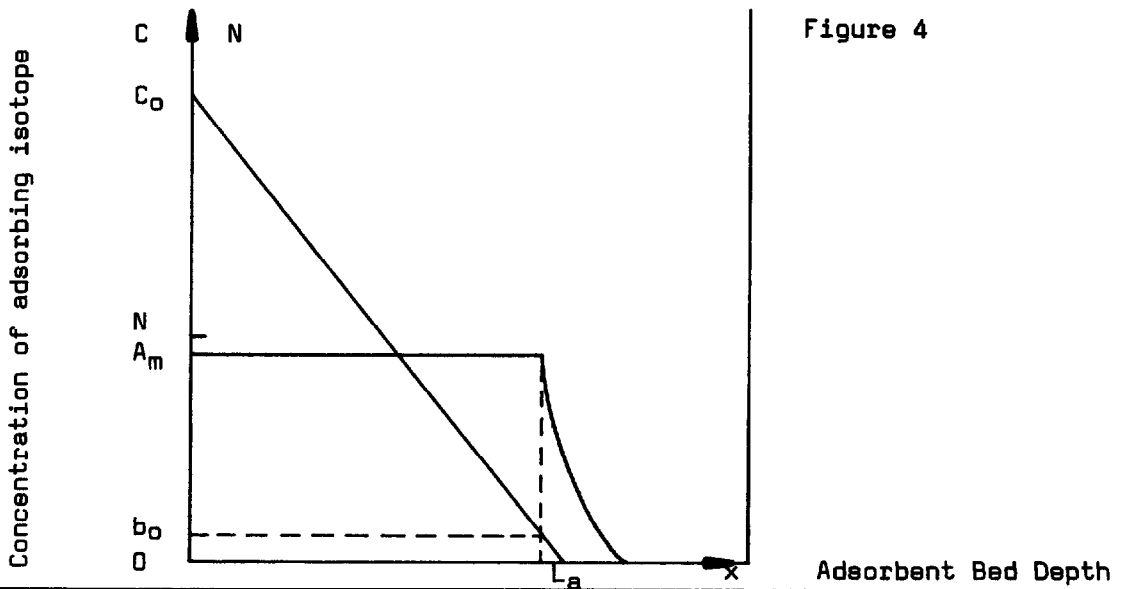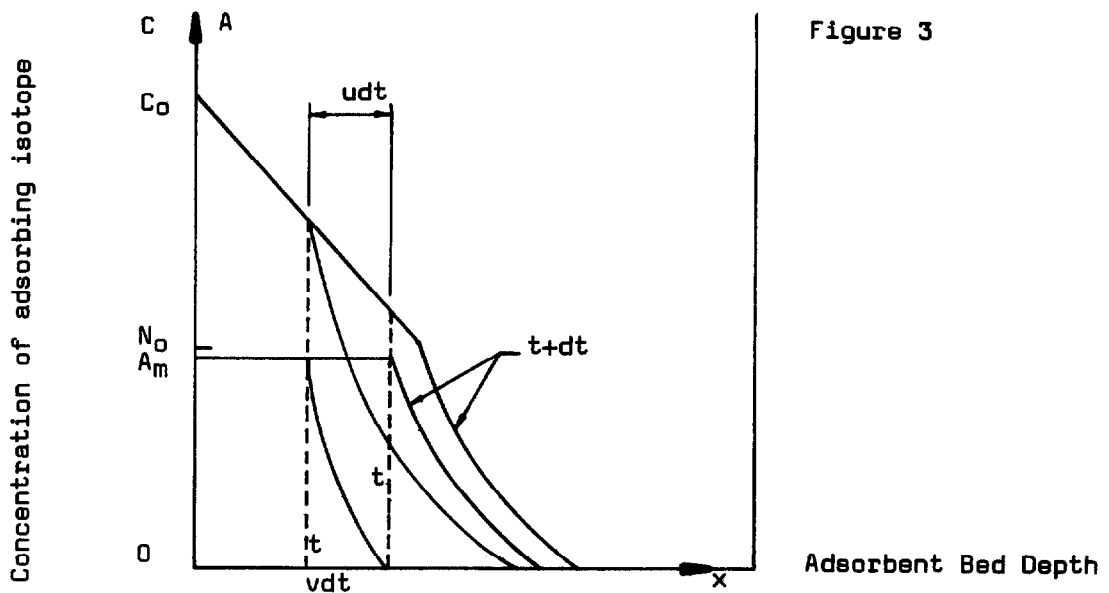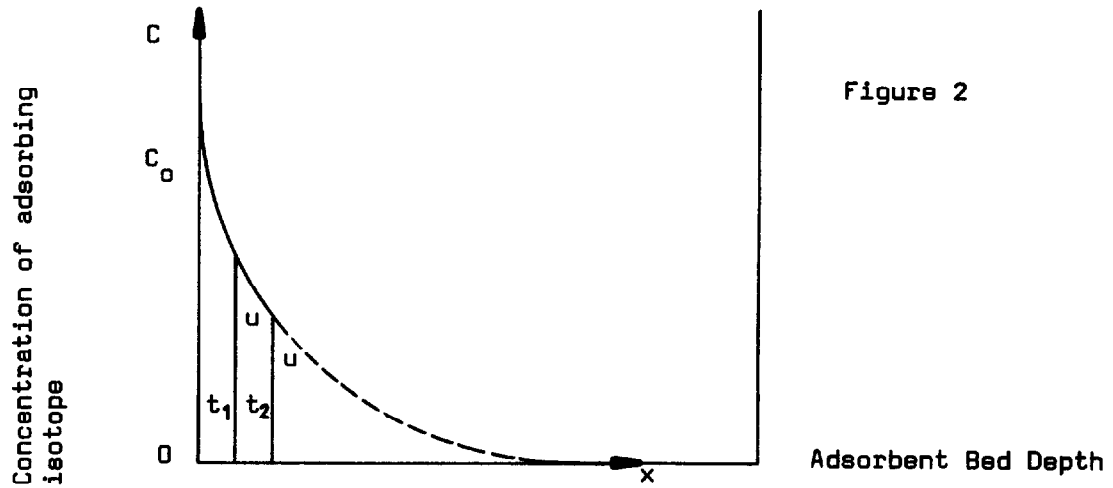
References

1. "Reactor safety study", Appendix VIII, <u>USAEC Report</u> WASH-1400 (1974)

2. Sykes, G. H. and Harper, J. A. "Design and operation of a large sand bed for air filtration." <u>Treatment of Airborne Radioactive Wastes.</u> IAEA Vienna (1968)

3. Zippler, D. B. "Evaluation of multistage filtration to reduce sand filter exhaust activity." <u>USAEC Report,</u> CONF 740807 (1974)

4. Thomas, J. W. and Yoder, R. E. "Aerosol size for maximum penetration through fiberglas and sand filters." <u>A.M.A. Arch. Ind. Health</u> Vol. 13, No. 545 (1956)

5. Kovach, J. L. and Newton, R. G. "Deep bed activated carbon for liquid, solid, aerosol and gaseous filters." <u>USAEC Report</u> CONF 700816 (1970)

6. Cheever, L. in <u>ZPPR FSAR</u> (1968)

7. Roginskii, S. Z. and Todes, O. M. "Physicochemical characterization of the dynamics of sorption of radioactive substances." <u>Radiokhimiya</u>, 4, No. 1, 39-44 (1962)

DISCUSSION

COLLARD: Did you evaluate the dimensions of a delay bed for iodine when the charcoal used is an unimpregnated one?

KOVACH: We have postulated a case where the quantity of adsorbent in the system is increased to the point where it would completely delay even xenons, if not the kryptons, in the system. Cost can determine whether it is better to use a very large external system or to pump back about a third of the total flow into the containment. On a cost basis, it looks much more economical to pump it back and allow the noble gases to decay, at least for a certain length of time, in the containment before venting to the outside.

FORSBERG: Is it correct to assume that this system could be designed so no electric power would be required for operation?

KOVACH: Electric power would be required only if you are returning the gas. If not, you don't need air motive power because the containment is pressurized. Total pressure drop for the system can be calcualted. It is about 3 psi.

LORENZ: Mention was made of very deep and, I presume, large charcoal beds. For those of you who aren't familiar with the possibilities of combustion of charcoal, a word of caution. As the size of charcoal beds increases the chance of spontaneous combustion also increases. The probability of spontaneous combustion depends upon the reactivity of the charcoal, the air supply rate, and the temperature of the bed (whether elevated by decay heat or some other means). I

refer you to a brief discussion in the 13th AEC Air Cleaning Conference paper entitled "Behavior of Highly Radioactive Iodine on Charcoal" by Lorenz, Martin, and Nagao.

KOVACH: You are correct. In the paper, we were discussing the use of inorganic non-carbon adsorbents to pick up most of the iodines and the use of mixed media for an adsorption system.

MILLER: Is the purpose of this system to more quickly accelerate the depressurization of the containment or to allow a higher containment leakage rate?

KOVACH: Either/or. This process permits you to vent under control and to depressurize the containment more than you otherwise could.

MILLER: Is it your intention to modify or replace the existing iodine safety systems in primary containment such as the spray systems?

KOVACH: We have not looked at eliminating sprays and using this type of an approach as a tradeoff.

MILLER: Is it logical to assume that you could not release the vented gases directly to the environment because of the noble gas dose?

KOVACH: Not necessarily. A dose evaluation is required for this type of safety approach. The main thing we wanted to be sure of was that all particulates and iodine, plus everything else that's volatile, except noble gases, is removed as close to 100 per cent efficiency when the contaminant is depressurized. After initial recirculation for a period, the system can be operated in the vent mode.

DIETZ: What are some approximate dimensions and quantity requirements of adsorbent for the proposed system?

KOVACH: Approximately 10,000 lbs (on carbon basis) for the postulated design case.

STANDARDIZATION OF AIR CLEANUP SYSTEMS
FOR NUCLEAR POWERPLANTS

E. Nicolaysen - Supervising Mechanical Engineer - Nuclear
K. E. Carey   - Associate Mechanical Engineer   - Nuclear
J. J. Wolak   - Associate Mechanical Engineer   - Nuclear

Gibbs & Hill, Inc.
Engineers, Designers, Constructors
New York, New York

Abstract

The Gibbs & Hill, Inc. (G&HI) approach to standardization of the air cleanup systems serving the controlled access areas in pressurized water reactor (PWR) powerplants was developed in the course of designing a succession of powerplants including Fort Calhoun Unit 1, Angra Unit 1, C.N. Almaraz Units 1 and 2, Comanche Peak Units 1 and 2, Fort Calhoun Station Unit 2 and the G&H standard plant.

The G&HI designs emphasized operability, maintainability, quality, testability, redundancy, constructability, and operation convenience at minimum cost. The later designs have been strongly influenced by Nuclear Regulatory Commission (NRC) Regulatory Guide 1.52, (1). All designs have, to some extent, been influenced by conditions related to the geographical locations of the stations.

The relationship and interplay of these factors is illustrated by discussions of the Comanche Peak Units 1 and 2, Fort Calhoun Station Unit 2, and the G&HI standard plant designs.

The features covered by this discussion are:

1. Physical and general arrangements (GA)
2. Modular design
3. Effects on total system design
4. Interrelationship with engineered safety features (ESF)
5. Compliance with NRC Regulatory Guide 1.52
6. Methods of energy conservation
7. Maintainability of the filter trains
8. Testability
9. Reliability of filter train systems
10. Economics of the design
11. Manufacturing and shipping processes

The standard plant, has to some extent, complicated the system design by requiring a design that can be built on a variety of sites. The design innovations to standardize the air-filtration system necessitated by this requirement are discussed in this paper.

Introduction

Historically, the ventilation system was a stepchild in the design of nuclear powerplants, mainly because the average design engineer did not have a full appreciation of the physical size of the air cleanup components and thus allocated insufficient floor space for this equipment. This led to designing air cleanup trains customized to fit into available spaces which resulted in adequate but less than desirable ventilation system designs. GHI was no exception in this matter as shown in Wash-1234 (2). Visits by the authors to powerplants under construction, air cleanup system vendor facilities, as well as the publication of Wash-1234 and NRC Regulatory Guide 1.52 convinced G&HI that a better approach to an air cleanup system design was needed. Four steps were taken to achieve a better design:

1. The Heating, Ventilating, and Air Conditioning (HVAC) engineer made certain that sufficient space for all the ventilation equipment had been allocated during the initial phases of the GA layout.

2. Centralization of the air cleanup units and other ventilation equipment, while maintaining separation criteria, was pursued.

3. An economic study was performed to determine if capital and operating cost of refrigeration equipment would be offset by savings in filter costs, smaller ducts, and smaller equipment sizes for sites where the available cooling water temperature was above 70 F.

4. After discussions with vendors, an economic study was performed to determine if several smaller identical air cleanup units, completely shop-manufactured and shipped intact to the jobsite, would be less expensive than larger custom built units, which were shop-assembled, then dismantled, and finally field-reassembled.

From the results of the studies and a judicious allocation of equipment space and location, G&HI arrived at a standard design, based upon use of modular air cleanup units, which we believe is unique to the power industry. The design can be applied to any size nuclear powerplants by either adding or subtracting modules.

This paper presents the standardization of the air cleanup system and gives a brief discussion of the application of the design to the system design on the Comanche Peak, Fort Calhoun Station Unit 2 and the G&HI standard nuclear powerplant. Topics include the system designs, mode of operations, maintenance and testing, economics, and the impact on the design by the NRC regulatory guides and standards, and similiar regulations.

General System Description

Air cleanup units are necessary to minimize the radioactive gaseous and particulate effluents released to the environs during normal operation (3), to remove fission products in a postaccident environment, and to protect plant operators from the accidental

release of radioactive gases (4). The ventilation systems requiring the use of air cleanup units include the controlled access area ventilation (CAAV), control room HVAC, hydrogen purge, and containment preaccess filtration.

The CAAV system encompasses the ventilation of the controlled access sections of the auxiliary building, safeguards areas, and the fuel-handling building, all known as the nuclear island. The system also provides for containment purging and ventilation during reactor shutdown.

The CAAV system uses a modular design arrangement for both the supply and exhaust. The supply is comprised of several 30,000-scfm air-filtration cooling and heating modules and the exhaust is comprised of several 15,000-scfm air cleanup modules. The supply modules, six for a single 1130-MW reactor plant such as Fort Calhoun Station Unit 2, (see Figure 1) eight for a two unit plant such as Comanche Peak (see Figure 2), are connected in parallel to a common air intake plenum. Outside air is drawn in through a missile- and tornado-protected seismic Category I intake by the supply units and discharged into a common distribution plenum. A main supply header is attached to this plenum for the auxiliary building (controlled access portions), the safeguards building, the fuel-handling building, and for containment purging. The quantity of modules is a function of plant physical size, not of plant geographical location, since the entering air is cooled to a predetermined temperature.

The exhaust modules, 12 in the case of Fort Calhoun Station Unit 2, (see Figure 1), 16 for Comanche Peak (see Figure 2), are connected in parallel to the plant vent stack plenum. Each exhaust module is also connected to a common suction plenum which contains branches for the auxiliary building, safeguards building, fuel-handling building, containment, and the condenser vacuum pump discharge. Two of the exhaust modules are classified as ESF and are maintained on a standby mode. Dampers in the common suction plenum of the exhaust allow the fuel-hanlding building exhaust to be routed through the ESF modules during refueling periods. The exhaust modules are separated into two equipment rooms which are located on different elevations, thus enabling separation of redundant modules. (see Figures 3 and 4).

The control room HVAC system is designed to insure that the habitability of the control room is maintained during all operational transients and following design basis accidents (DBA). The air cleanup equipment of the system consist of the emergency filtration and the emergency pressurization modules.

The system is provided with ductwork which supplies approximately five percent fresh makeup air from a missile-protected air intake and 95 percent of recirculation air from the conditioned space (see Figure 5). The system is provided with dampers which also allow the system to operate on 100 percent recirculation air (see Figure 6). The emergency filtration module, which is sized at 4000-scfm for a single-unit control room and at 8000-scfm for a double-unit control

room, consists of a fan and air cleanup unit; it draws a portion of the recirculation air from the return air ductwork and discharges this air to the suction side of the air-conditioning units. The capacity of the emergency filtration module is sufficient to filter the control room volume once every hour.

The emergency pressurization module, which consists of a fan and an air cleanup unit with a capacity of 1000 scfm, draws outside air in through the missile-protected intake and discharges it to the suction of the emergency filtration module. The quantity of air handled by the emergency pressurization module is sufficient to maintain the control room at a slight overpressure (.25 inches wg).

The emergency filtration and the emergency pressurization modules are provided with 100-percent standby capacity. The redundant components are physically separated, assigned to two separate and independent trains with only common supply and return ductwork.

The hydrogen purge system is designed to maintain the concentration of hydrogen within the containment below three-percent by volume following a LOCA. The purge system is provided with supply and exhaust modules. The supply module, consisting of a prefilter and supply blower, draws 1000 scfm of outside air in through a missile-protected seismic Category I intake and discharges into a supply header. The supply header routes the purge air into the containment distribution ductwork through a single penetration.

The exhaust module, also consisting of a fan and an air cleanup unit with a capacity of 1000 scfm, draws the containment atmosphere through a single penetration through a suction header. The containment atmosphere is routed to the plant vent stack through the exhaust module discharge header.

The hydrogen purge supply and exhaust modules are provided with full redundancy. The redundant modules are physically separated from each other by being located on different elevations of the auxiliary building, each having connections to the common purge supply and exhaust headers.

Additional connections on the hydrogen purge supply header and hydrogen purge exhaust header are provided in the case of the Comanche Peak Station. This enables the system to purge either one of the containments, fulfilling the protection requirements for both units with a single system.

The containment preaccess filtration system is designed to reduce the concentrations of radioactive particulate and gaseous iodine to permit limited personnel access to the containment during a hot standby or shutdown without containment purging.

The preaccess filtration modules, consisting of a fan and air cleanup units draws air from the lower levels of the containment and the discharge is routed through ductwork to the operating level. Two 50-percent modules are used, each sized for 15,000 scfm and located on the intermediate levels of the containment.

The design is based on the use of two supply module sizes, i.e., 1000 scfm and 30,000 scfm, and three air cleanup module sizes of 1000 scfm, 4000 or 8000 scfm, and 15,000 scfm.

Module Description

The air cleanup units design incorporated the guidelines of NRC Regulatory Guide 1.52 and the recommendations of ORNL-NSIC 65 (5). Specific problems in previously designed air cleanup units as shown in Wash-1234 were also considered. Particular attention was paid to adequate lighting and service space (both inside and outside of the unit) to facilitate maintenance and testing (see Figure 7). Prime consideration was given to the shortening of maintenance time thus reducing cost and exposure to the personnel.

The normal exhaust air cleanup units and fans are designed for normal operation only. These units are used in the containment pre-access filtration and CAAV systems. The components comprising the air cleanup units are as follows in sequential order: prefilter, HEPA filter, adsorber, and HEPA filters. Moisture separators and electric heaters are not used since the relative humidity does not exceed 70 percent, as shown on Figure 8. The fans are direct-drive single-inlet centrifugals. Centrifugal fans are required since the systems resistance approaches 15 inches wg with dirty filters. The direct-drive limits the amount of maintenance required for each fan. Adjustable inlet vanes are provided for each fan to maintain the design flow requirements over the range of system resistance.

ESF air cleanup units are used in the hydrogen purge exhaust, control room pressurization, control room recirculation and the controlled access emergency exhaust. The components comprising the ESF air cleanup units are in sequential order as follows: moisture separators, electric heater, prefilter, HEPA filter, adsorber, and HEPA filters. The controlled access emergency exhaust units are the only exception to this in that prefilters are not used.

Moisture separators, although inefficient when compared to prefilters used within the air cleanup modules, are used in lieu of prefilters in the CAAV ESF air cleanup modules.

The reduction in the life of the HEPA filter resulting in the use of the moisture separator is considered justified for two reasons. First, the function of the filtration units, using the moisture separator section is to act as a redundant standby to those air cleanup modules which operate normally and to operate only during refueling and in the event of an accident condition. Secondly, to maintain the same standard size of the other modular filtration units, the prefilter has been replaced by the moisture separators. It was felt that the disadvantage in shortening the HEPA life was far outweighed by the savings realized in maintaining the same basic housing size.

The same direct-drive single-inlet centrifugal fans are used as in the normal modules. Adjustable inlet vanes are provided for each fan to maintain the design flow required.

Component Description

Moisture separators are provided in the air cleanup units and function in an adverse environment of moisture-laden air. The moisture separators are designed to remove an entrained water and steam mixture from the air entering the air cleanup modules. The removal of the water and steam mixture protects the prefilters, HEPA filters, and adsorbers from water damage and plugging. The moisture separator section of the air cleanup module is built up from a number of cartridges each capable of handling approximately 1500 scfm, and each consisting of stainless steel baffles and a stainless steel fiberglass mesh. The addition of the fiberglass enables the moisture separator to act as a medium efficiency filter. To reduce the potential of fire, the moisture separators are rated UL Class I (6).

Electric heaters are provided downstream of the moisture separator section. These heaters are designed to heat the passing airstream and reduce the relative humidity to below 70 percent, thus allowing the filters and adsorber to maintain their design efficiency. The electric heater casings are of stainless steel construction. The elements are the extended-fin type with chromized steel enclosing the resistance heating wire.

The prefilters are the first set of particulate filters located in the normal air cleanup unit. Prefilters remove the larger particulates thus extending the life of the more efficient and expensive HEPA filters located downstream by preventing premature loading. The prefilter section consists of a number of filter cartridges each capable of handling approximately 1200 scfm at one-inch wg. Prefilters are constructed of fiberglass media with a chromized steel casing. In order to reduce the potential of fire, the filters are rated UL Class I.

The second set of particulate filters located in the air cleanup modules are HEPA filters. The HEPA filters are designed to remove fine particulate from the exhaust air which may be radioactive. The third set of particulate filters are also HEPA filters. This HEPA filter section is located downstream of the charcoal adsorber and is provided for removal of potentially radioactive carbon particules released from the adsorber bed. Each HEPA filter section is comprised of a number of filter cartridges each capable of handling approximately 1500 scfm of air. The HEPA filters are of the separatorless design, constructed of a fiberglass media with a stainless steel casing. In order to reduce the potential of fire, the HEPA filters are designed to satisfy the requirements of UL-586 (7).

The adsorber section is located downstream of the first HEPA filter section. The adsorbent removes radioactive gaseous iodine (either elemental iodine or organic iodines) from the exhaust air. The adsorbent material is activated, impregnated charcoal. This material is contained in vertically oriented bed modules fabricated from stainless steel. The face of each module is either a perforated stainless steel sheet or mesh. The adsorber section is capable of handling 1000, 4000 or 8000, and 15,000 scfm, with a resulting face

velocity enabling a 0.25-second (per 2-inches of adsorbent material) residence time of the exhaust air within the adsorbent. The design of the adsorbent section allows for gravity feeding of the adsorbent through the top of the adsorber section and withdrawing of the adsorbent through drain piping located at the bottom of each bed.

Mode of Operation

The air cleanup modules, modes of operation are tabulated in Table 2. During normal plant operation for Comanche Peak, Fort Calhoun Station Unit 2 and the G&HI standard plants four of the CAAV air cleanup modules, the hydrogen purge air cleanup modules, and the control room emergency air cleanup modules do not operate.

As indicated in Table 1, during startup and normal operation, four supply and eight exhaust modules operate continuously, while the remaining CAAV modules are on standby. Following plant shutdown, one additional supply and two additional normal exhaust modules are required to function for containment purging. During the refueling mode, the operation of two exhaust modules are terminated and left on standby since the fuel-handling building exhaust filtration is accomplished by using the two emergency exhaust modules.

During startup, normal operation, and shutdown, the CAAV emergency exhaust and standby modules do not normally operate. However, periodic testing and inspection may be performed. The tests and inspections will include sequencing of dampers, unit flow tests, heater capacity tests, filter and adsorber penetration tests, adsorber efficiency tests, filter resistance tests, and visual inspection of the module.

The emergency exhaust modules are operated during refueling mode, serving as the fuel-handling building ventilation exhaust. In the event of a fuel-handling accident at least one exhaust module is capable of maintaining the fuel-handling building at a slight negative pressure thereby limiting the potential offsite release of radioactive iodine and other radioactive particulates, to the environs in accordance with 10 CFR part 50, Appendix I. The normal ventilation system is not required to operate in the event of a LOCA. In the event of a LOCA, at least one emergency exhaust unit is manually operated to maintain the controlled access areas at slight negative pressure with respect to the uncontrolled access areas and the outside.

During the winter months, both energy and filter usage are conserved by terminating the operation of several modules, thus reducing the flow through the CAAV system. Sufficient number of two-position volume dampers and flow indicating meters are located in the system to allow two system balance points, summer and winter, and still allow sufficient ventilation airflow within areas of potential radioactive leakage.

The parallel operation of 8 to 12 exhaust modules requires constant surveillance of the flow to ascertain that the modules are paralleling. This is accomplished by using flow straighteners and multi pitot-tube monitors in the inlet of each module with either

direct or remote readout so that an operator can adjust the fan inlet vanes to maintain the flow constant as the filter resistance increases because of dust loadings.

The hydrogen purge system air cleanup modules and the control room air cleanup modules are only used following a DBA. These modules all have 100-percent redundancy. The hydrogen purge system is only operated in case the containment hydrogen recombiners fail.

Maintainability, Testing, and Reliability

It should now be evident that we are dealing basically with only three different size air cleanup modules, all designed in the same manner, which is, from a maintenance point of view, a desirable arrangement. All modules in the nuclear island are identical to the containment modules which means the same maintenance procedure can be used for all. The hydrogen purge modules are identical to the emergency pressurization modules which are essentially smaller versions of the other air cleanup modules using the same components.

The air cleanup modules use cartridge-type prefilter sections with rated efficiencies of 85 percent according to the NBS dust spot method of testing. A high-efficiency prefilter is used to extend the life of the HEPA filters which decreases the frequency of filter replacement. Prefilters specified for the air cleanup system have an initial air resistance of 0.35 inches wg and are replaced when the final air resistance reaches 1 inch wg. High-efficiency prefilters of the automatic-roll type are also used in conjunction with the supply air handling units to maintain relatively clean areas throughout the power station.

Separatorless high-efficiency (99.9 percent at 0.3 micrometer as in reference (1)) particulate air HEPA filters have been used to extend the filter replacement frequency, thus reducing maintenance cost and radiation exposure to personnel. The apparent lower initial air resistance and larger dust-holding capacity of separatorless-type HEPA filters coupled with operating these filters to a final air resistance of 3.5 to 4.0 inches wg, extends the life of the filters and reduces the frequency of the maintenance cycle.

In specifying the charcoal adsorber section of the filtration unit, maintainability was an important consideration. The gasketless adsorber section using vertically oriented charcoal beds and horizontal airflow with a remote means of filling and emptying the charcoal bed was chosen. This method eliminated the need for maintenance personnel to come in direct contact with the contaminated carbon, reduced personnel exposures during adsorber replacement, and eliminated servicing gaskets to ascertain zero bypass leakage.

Air cleanup filter housings have been designed and specified in order to conform to be accessibility guidelines described in NRC Regulatory Guide 1.52 and ORNL-NSIC-65. This facilitates replacement of filters and minimizes the radiation exposure to maintenance personnel in accordance with Regulatory Guide 8.8. The units have been provided with adequately sized access doors, sufficient lighting, 5 feet of separation between filter frames and a maximum filter bank

height of six feet (three 24 inch by 24 inch filters high).

The air cleanup modules are furnished with test ports located in accessible locations on the side of each filter housing, together with portable injection and sampling grids for DOP and Freon, in order to facilitate test procedures when performing in-place testing of the HEPA filters and charcoal adsorbers. Sample adsorber canisters and local pressure gauges which monitor filter resistance are provided to maintain surveillance on each of the air cleanup modules. Permanently installed flow meters are also provided to maintain surveillance and avoid time-consuming pitot tube traversing. The test procedures and the testability requirements are in accordance with ANSI N101.1, ANSI N509, ANSI N510, and the guidelines included in NRC Regulatory Guide 1.52 and ORNL-NSIC-65.

All air cleanup modules which are designated ESF remain on standby during the normal plant mode of operation. The ESF units will operate only 10 hours a month in accordance with NRC Regulatory Guide 1.52. Therefore, it is anticipated that the proposed requirement of testing ESF atmospheric cleanup systems after 720 hours of operation will not be attained during a year of reactor operation. However, an annual test of the air cleanup modules is conducted for both the ESF and normal modules.

The feature of using only three sizes of modules allows for interchangeability of parts, enabling efficient and fast replacement of any part while a standby module is operating thus allowing overall system reliability of the highest order.

Economics

As shown earlier, there is a definite requirement to determine what the minimum temperature increase in the plant must be in order to maintain the relative humidity below 70 percent. With a maximum temperature of 104 F imposed by electrical equipment, this increase is minimum 11 F if saturated air is assumed to be entering the plant. A study determined that the use of refrigeration equipment to increase the temperature difference would be economically favorable since increased ΔT resulted in lower flow rates and hence smaller filter trains, ducts, fans and so on. The lower limit in reducing the airflow is the quantity of air required to maintain the airborne radioactivity levels below 10 CFR Part 20 maximum permissible concentrations (MPC). The Comanche Peak Station, the Fort Calhoun Station Unit 2 and the G&HI standard plant have been designed with a specific inlet air temperature. Comanche Peak and Fort Calhoun Unit 2 use chillers while the standard plant may use chillers or evaporative coolers depending upon the particular site requirements, the cooling water temperatures, and the availability of makeup water.

The modular system allows for energy conservation. By designing the system with two or more system air balancing points, i.e., for seasonal operation, the plant airflow can be reduced to cool operating equipment during the winter months by shutting down several air cleanup and supply modules and by balancing the system so that the 10 CFR Part 20 MPC requirements are met.

The modular design allows for much lower capital cost of the air cleanup trains since the engineering cost is minimal. Jigs can be used in the manufacturing process resulting in an assembly-line type arrangement.

G&HI has estimated, based on manufacturing techniques, shipping and field erection costs, that this design results in capital cost savings of approximately 20 percent over the customized design.

The Comanche Peak station uses four different air cleanup module sizes. The original design called for only three sizes but redesign of the layout in the containment deprived us of sufficient space to maintain the size desired, therefore, the containment preaccess filtration system had to be redesigned to fit into the available space. This particular problem was corrected in the Fort Calhoun and the standard plant stations.

The size of 15,000-scfm nominal was selected as the module size for the nuclear island in all three plants primarily because this size is readily shipped by truck without specific permission and routing. A 15,000-scfm air cleanup train that can be completely assembled and tested in the manufacturing plant and then shipped intact to the josite, eliminating costly field assembly, lends itself to a minimum cost system of highest reliability and maintainability.

Cost analysis showed that in the long run the gasketless air cleanup systems were less expensive and easier to maintain than the tray type. This may not be the case for the smaller systems. However, the G&HI position is that mixing of the two types of systems defeats the purpose of standardization; therefore, the tray types are not considered for the applications discussed.

In addition, the cost analysis performed to justify the use of refrigeration equipment proved that approximately $1,000,000 could be saved in filter replacement cost over 40 years for the Comanche Peak Station, due to the lesser air quantities required.

Summary

In summary, the G&HI air cleanup design can be applied to any size nuclear powerplant by either adding or subtracting modules. This fulfills the intended air cleanup function and also is the most economical approach from both the capital investment and the operating and maintenance cost points of view.

TABLE 1

AIR CLEANUP MODULE (ACM) MODE OPERATION

		Number of Modules Operative						
CAAV	Number Units Installed	Initial Startup	Startup Following Shutdown	Normal	Plant Shut-down (1)	Re-fueling	Loss of Offsite Power	LOCA
Normal Ventilation								
Supply module	6 [8]	4 [5]**	4 [6]	4 [6]	5 [6]	5 [6]	-	-
Exhaust ACM	10 [14]	8 [10]	8 [12]	8 [12]	10 [12]	8 [12]	-	-
Emergency Ventilation								
ESF exhaust module	2	-	-	-	-	2	1	1
Hydrogen Purge								
Supply module	2	-	-	-	-	-	1	1
Exhaust ACM	2	-	-	-	-	-	1	1
Control Room								
Emergency recirculation ACM	2	-	-	-	-	-	1	1
Emergency pressurization ACM	2	-	-	-	-	-	1	1

(1) Includes containment purging

*Numbers in brackets [ ] are for Comanche Peak Units 1 and 2. Numbers without brackets are Fort Calhoun Unit 2 and the G&HI standard plant.

**Unit 1 operating only

References:

(1)   U.S. Nuclear Regulatory Commission
       Regulatory Guides (RG)

       a)   RG 1.52, Design Testing, and Maintenance
             Criteria for Atmosphere Cleanup System Air
             Filtration and Adsorption Units of Light-
             Water-Cooled Nuclear Powerplants, 1973

       b)   RG -8.8, Information Relevant ·to Maintaining
             Occupational Radiation Exposure As Low As is
             Reasonably Achievable, 1975

(2)   U.S. Nuclear Regulatory Commission
       Wash-1234, Engineered Safety Features
       Air Cleaning Systems for Commercial
       Ligh-Water-Cooled Nuclear Powerplants, 1974

(3)   Code of Federal Regulations, 10CFR20, Appendix B,
       Concentration in Air and Water Above Natural
       Background

(4)   Code of Federal Regulations, 10CFR50,

       a)   Appendix A, General Design Criteria
             for Nuclear Powerplants

       b)   Appendix I, Numerical Guides for
             Design Objectives and Limiting Conditions
             for Operation to Meet the Criterion "As
             Low As Practicable" for Radioactive
             Material in Light-Water-Cooled Nuclear
             Power Reactor Effluents

(5)   Energy Research and Development Administration
       ORNL-NSIC-65, Design, Construction and Testing
       of High-Efficiency Air Filtration Systems for
       Nuclear Application, 1970

(6)   Underwriters' Laboratories, Inc. (UL)-900
       Safety Standard for Air Filter Units, 1971

(7)   Underwriters' Laboratories, Inc. (UL)-586
       Safety Standard for High-Efficiency Air Filter
       Units, 1971

(8)   American National Standards

a)   N101.1, Efficiency Testing of Air
     Cleaning Systems Containing Devices
     for Removal of Particles, 1972

b)   N509, Draft Standard for Nuclear
     Powerplant Air Cleaning Units and
     Components, 1975

c)   N510, Standard for Testing of Nuclear
     Air Cleaning Systems, 1975
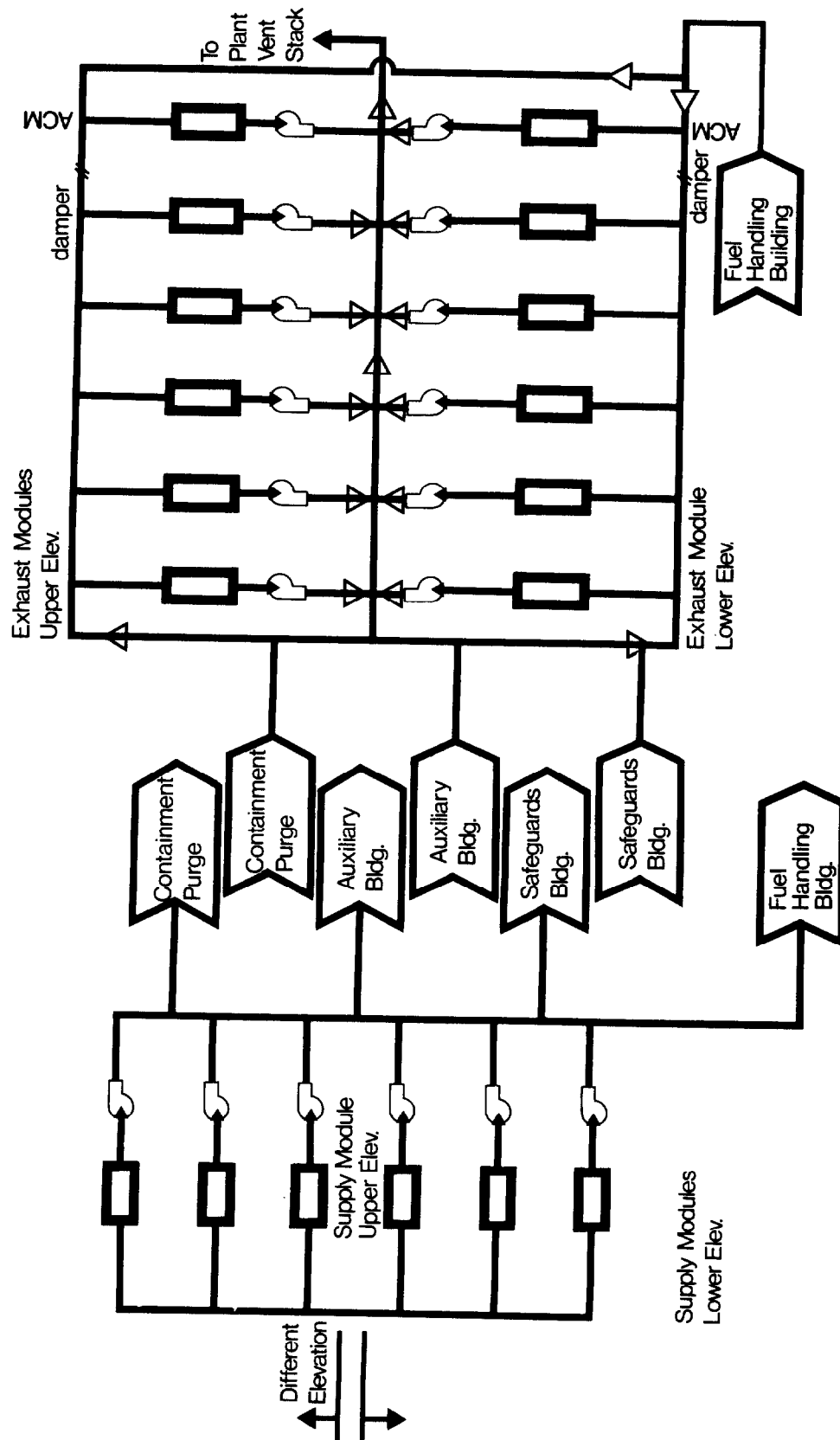
Figure 1 Controlled Access Area
Ventilation Single Unit
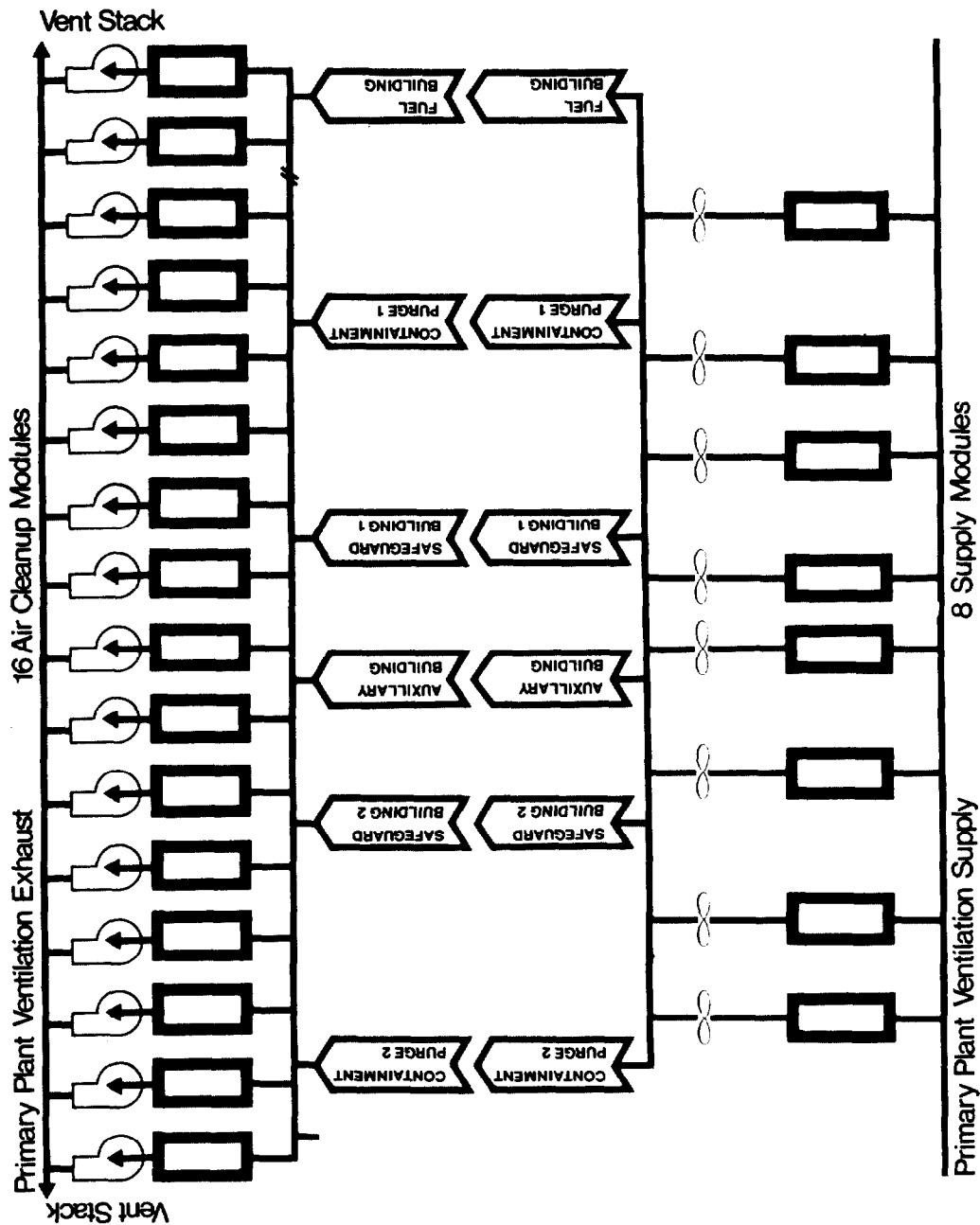
Figure 2 Controlled Access Area
Ventilation Two Unit
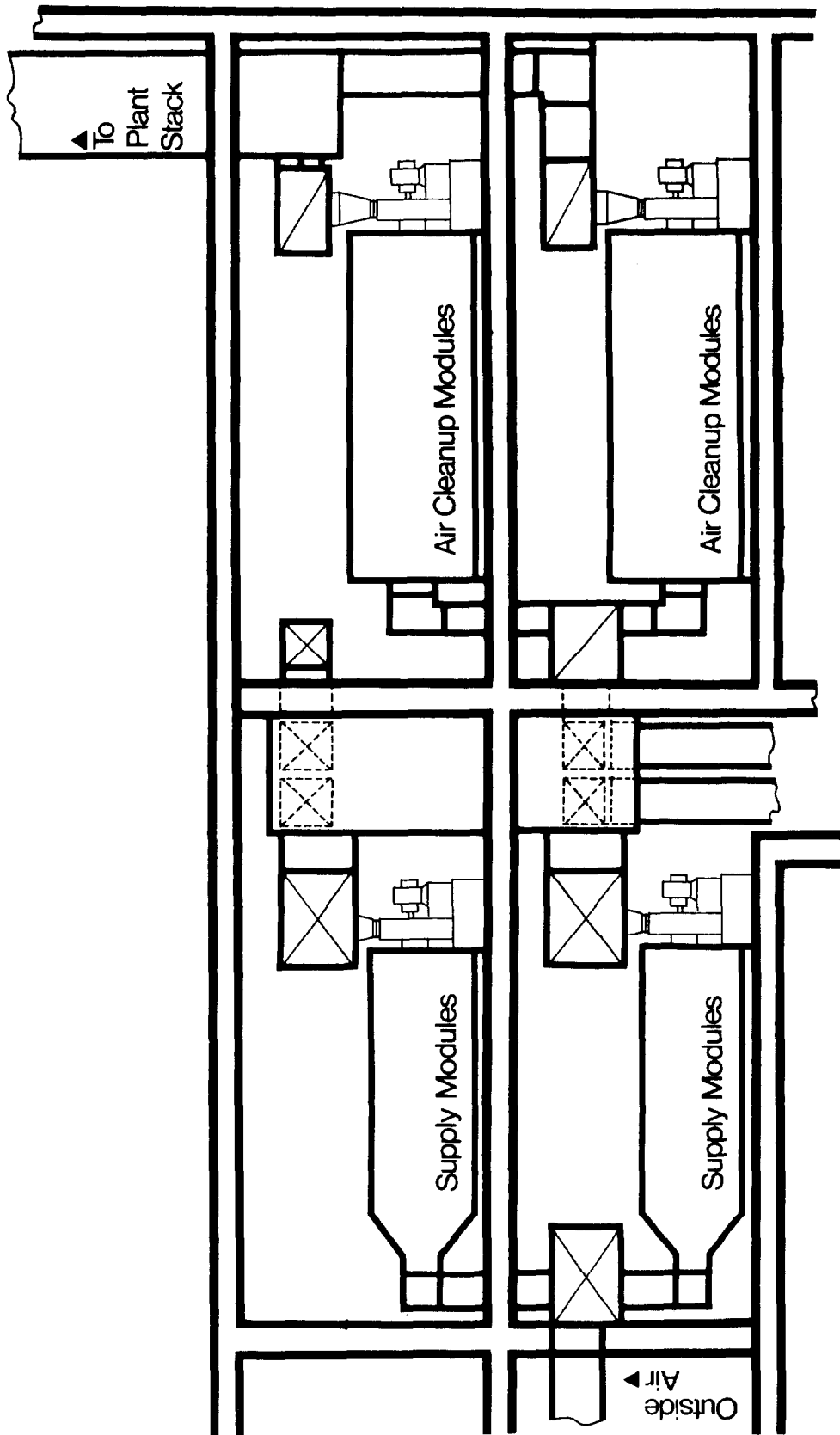
Figure 3 Physical Arrangement
Fort Calhoun Station Unit 2
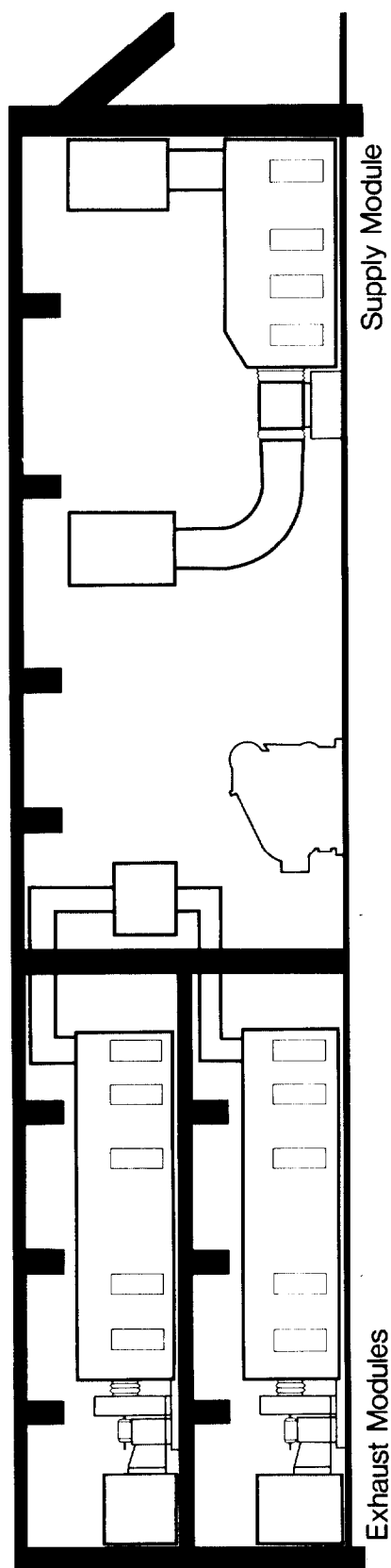
Figure 4 Physical Arrangement
Comanche Peak Units 1 & 2
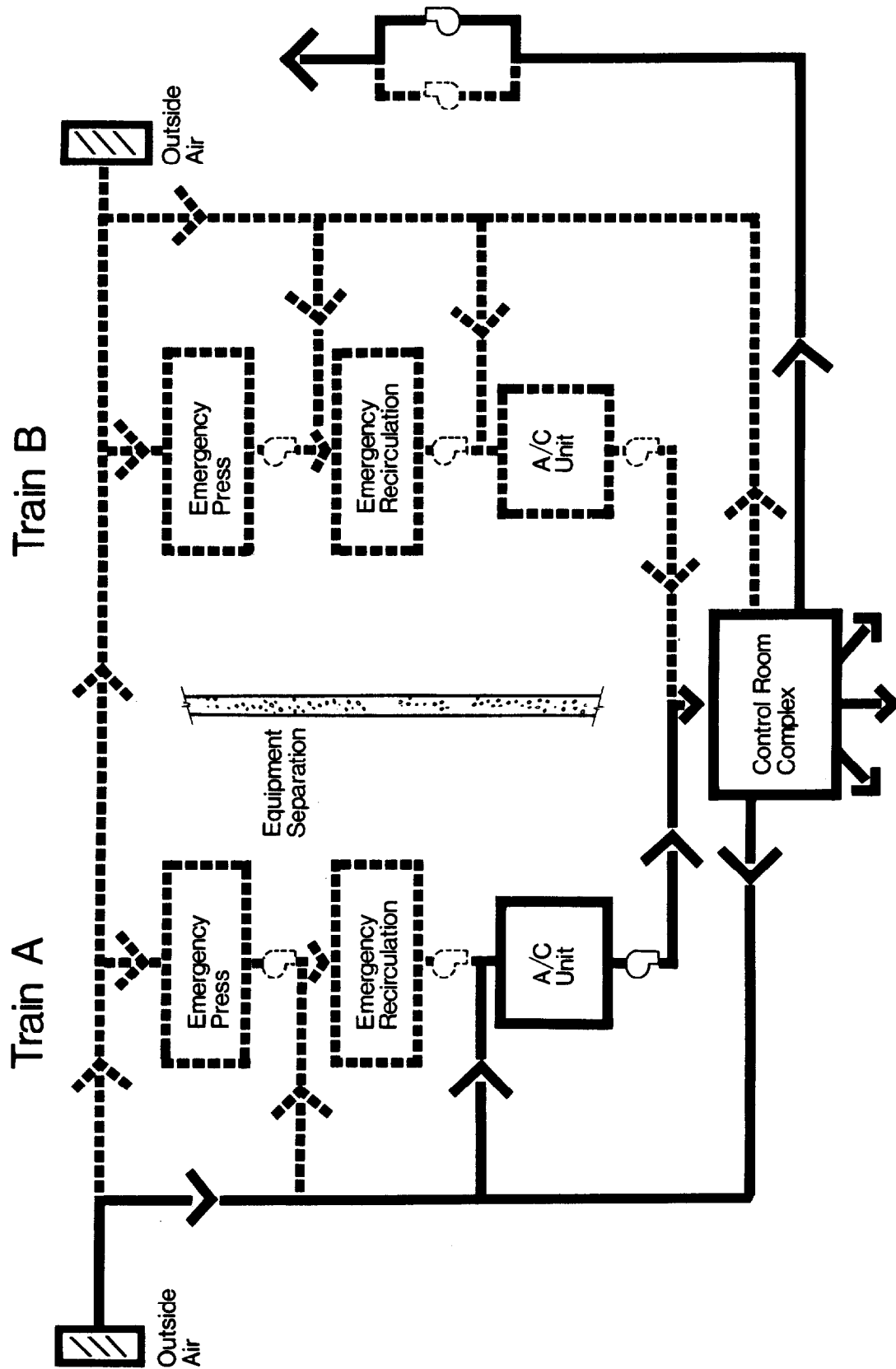
Figure 5 Control Room HVAC Normal Mode of Operation
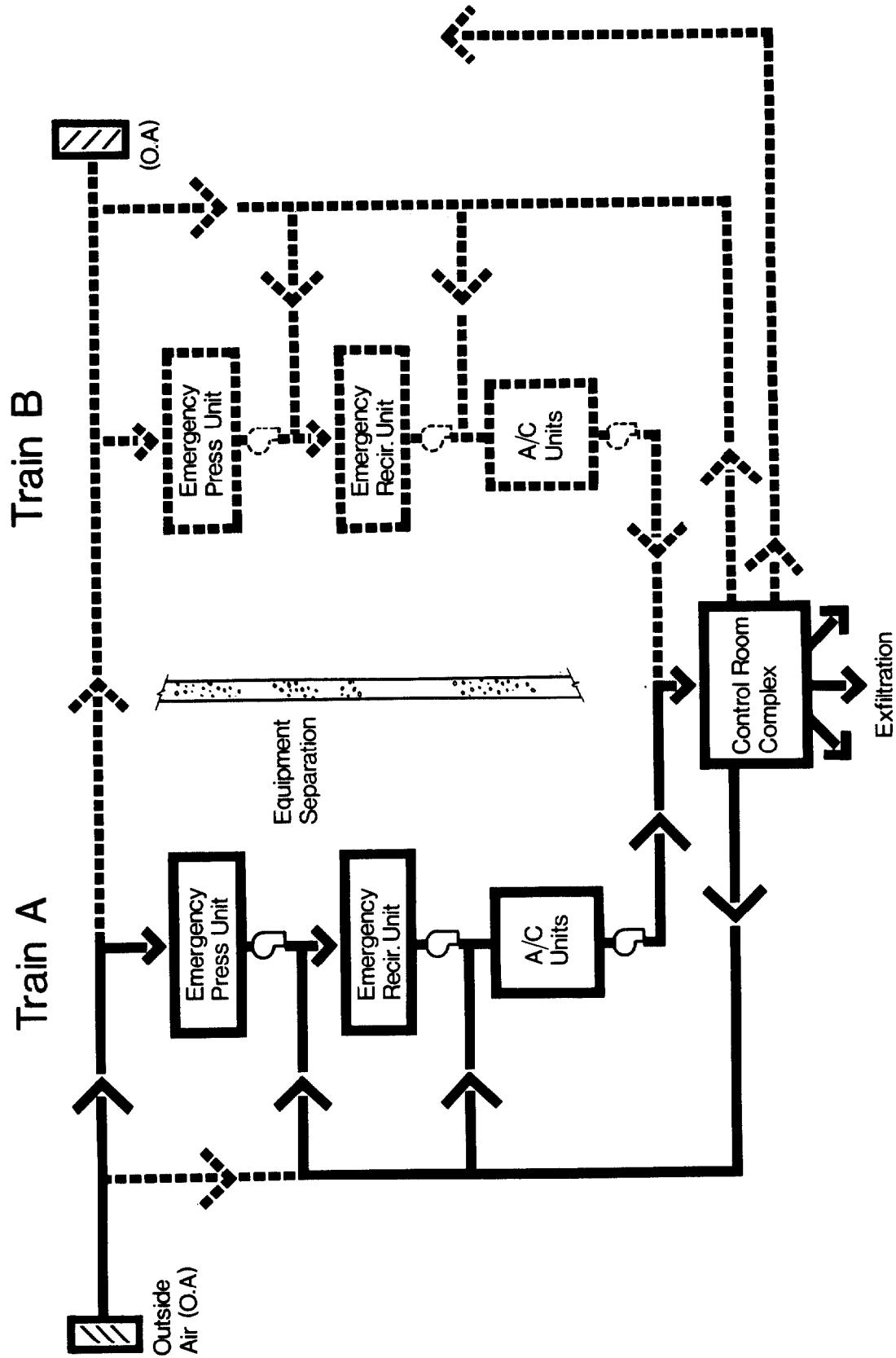
Figure 6   Control Room HVAC Emergency Recirculation
Mode of Operation
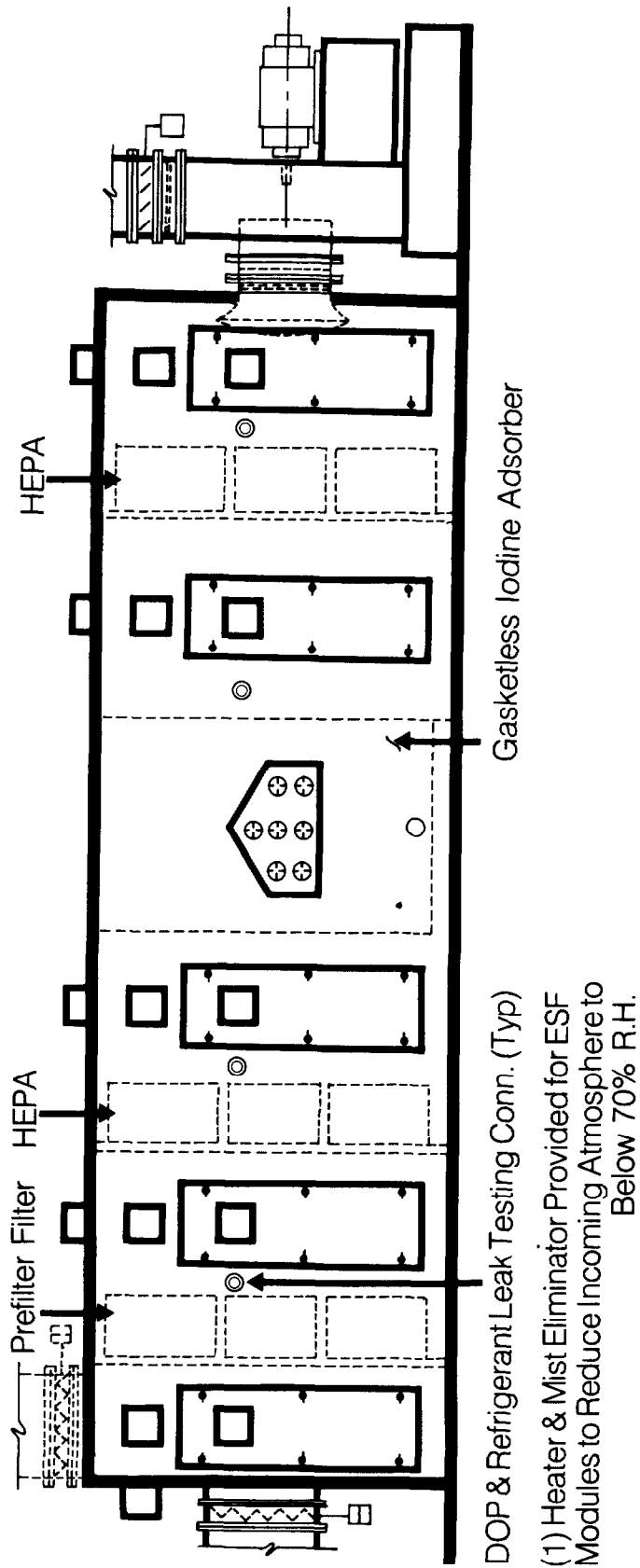
Figure 7 Air Cleanup Unit

Prefilter Filter HEPA

HEPA

HEPA

Gasketless Iodine Adsorber

DOP & Refrigerant Leak Testing Conn. (Typ)

(1) Heater & Mist Eliminator Provided for ESF Modules to Reduce Incoming Atmosphere to Below 70% R.H.
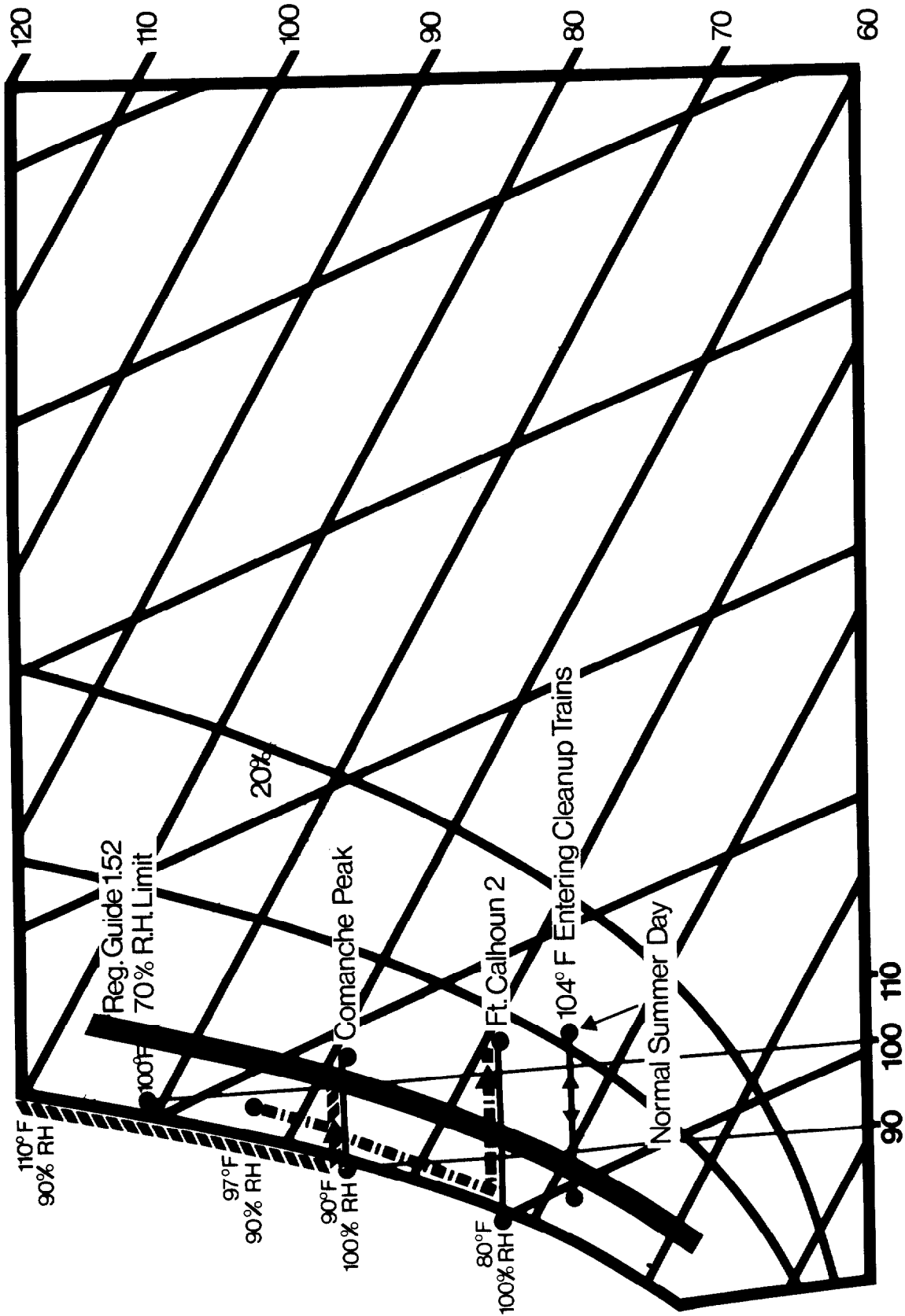
Figure 8 Design Basis for "Saturated Air Entering Plant"

DISCUSSION

ZEIDMAN: Is it right that you were standardizing the first packages at 15,000 CFM?

NICOLAYSEN: We are using three packages of 15,000, 4,000, and 1,000 CFM. In the Comanche Peak Station we are using 8,000 CFM units for the control room since it is a twin unit station.

ZEIDMAN: That would be relatively small for us. Doesn't this lead to space problems because the modules restrict flexibility in the sense that space and equipment become "prearranged" into fixed design modules?

NICOLAYSEN: By ascertaining that sufficient space is allocated as soon as the general arrangement drawings are being prepared, we have no restrictions as to space. For the Comanche Peak Station, our two main equipment rooms were on the top elevation and could be expanded or contracted to fit the need.

ZEIDMAN: Do you recommend using the standard units even if you are up to a million CFM?

NICOLAYSEN: I would recommend cooling to reduce the airflow and the use of this design. I did a study on cost benefits on cooling. A station saved a million bucks in filter costs alone by putting in chillers.

KAHN: I was wondering why you tied the fan to a 15,000 CFM unit in your modular approach. It seems to me it would generate quite a bit of interaction between the fans of a 12-unit system.

NICOLAYSEN: We looked at the pro's and con's of using fans in parallel separate from the filter banks. It requires additional space to do it that way. Furthermore, it is much easier to compensate for the filters becoming dirty in this manner since each module contains an airflow monitoring device and variable inlet vanes for the fans. Another advantage with the fans being the 15,000 CFM size is that during the winter, when we do not require as much equipment cooling, we can shut off units and reduce the airflow. However, we must maintain sufficient airflow to stay within the M.P.C. requirements of 10 CFR 20. We conserve energy in this manner.

KAHN: In your engineering safety feature systems, do you have 100% duplication?

NICOLAYSEN: One hundred % redundancy. In the control room slide, you saw the separation. On one side of the separation wall there was the operational unit; on the other, a standby.

KAHN: The loss of a single component, such as the fan, loses the total unit?

NICOLAYSEN: Yes. It loses the unit. But using only three different sizes of fans, you can have spares on hand and in a couple of hours you have a new fan on the line.

BELLAMY: My first question pertains to how you can justify a seismic category one, safety class three, filter housing for the normal ventilation system modules.

NICOLAYSEN: The modules in the controlled access ventilation system are all alike but for the replacement of the prefilter with a moisture separator - electrical heater combination in the modules designated ESF. Since the design is to standardize, it is just as easy to qualify twelve as Category I as to qualify two. Furthermore, we originally designed all the modules such that any one could be used to exhaust the fuel building during refueling, having the moisture separator and heater located within this building separate from the modules. Then you came up with the 720 hr ESF testing requirement, that's why the two dampers went in. In addition, the system is designed already and I do not seen any reason to redesign it.

BELLAMY: My second question concerns the philosophy behind operating the engineering safety feature modules during all modes of refueling. Why not have them on a radiation monitoring signal to turn them on when there is sufficient radiation in the area?

NICOLAYSEN: We could. This is part of the technical operating procedures.

BELLAMY: That is a flexible unit.

NICOLAYSEN: According to Regulatory Guide 1.52, it is not possible to bypass. That is why we guard against it by saying, "All right, use the ESF system during the refueling cycle."

MUNSON: I would like to inquire about the capability of standard fans to handle the various system pressures that will occur with different duct requirements in a custom designed station.

NICOLAYSEN: We designed the ducts to have approximately the same pressure drop all the way through by balancing the pressure drops in the system. The flow is also balanced by using air monitors and balancing dampers in all major trunk lines. This is part of good ventilation design. You have to have this, otherwise you can't balance air flow.

CONTROL ROOM VENTILATION INTAKE SELECTION
FOR THE
FLOATING NUCLEAR POWER PLANT

D. H. Walker, R. N. Nassano, M. A. Capo

Offshore Power Systems
Jacksonville, Florida

Abstract

In the event of accidents on or near a nuclear plant, it is necessary to provide sufficient protection to the plant operators in the control room to permit them to safely shut down the plant and to maintain the plant in a safe shutdown condition. One consideration in providing this protection is the adequacy of the air supply to the control room. Hazards or conditions usually considered in design of the control room air supply are release of radioactivity from the plant as a result of an internal plant accident and release of a toxic gas near the plant as a result of a nearby accident.

To assist in the design of the control room air supply for a floating nuclear plant, a comprehensive wind tunnel measurements program, employing scale models of two floating nuclear power plants located within a scale model of a typical breakwater, was performed at the Colorado State University under the direction of Offshore Power Systems. The purpose of the program was to provide data for:
1) selecting locations on the standard plant for the two alternate control room ventilation intakes, and, 2) determining applicable dispersion factors between the release locations and the selected intakes required for hazard analyses. This paper describes the measurements program and the methods employed by Offshore Power Systems in analyzing the experimental data that lead to the selection of the intake locations and the values of X/Q for control room hazard analyses.

I. Introduction

One consideration in the overall design of the control room for a nuclear power plant is to assure that the plant can be shut down and maintained in a safe shutdown condition (following certain postulated accidents). Accidents involving release of radioactivity (from the plant) or release of toxic gases (external to the plant) are usually considered in the plant design. The criteria to be met in the event of such accidents are specified by the Nuclear Regulatory Commission. [1,2,3]

Floating nuclear power plants may be sited off-shore[4] and as a result the operating crew may be required to remain on the plant for a few days following a postulated accident. It is therefore important that the air intakes be located such that an adequate air supply will be available following such an accident. The ventilation system design for the control room on the floating nuclear plant is to have dual intakes which are physically separated. The purpose of the dual intakes is to allow for drawing of outside air from a region where the concentration of radioactivity or toxic gas, if any, is relatively low. If there were to be gaseous release under very stable atmospheric conditions with low wind speed, a relatively concentrated plume of small lateral dimension could be carried toward and past one of the intakes. This condition appears to be the most severe from the standpoint of ventilation system design.

A wind tunnel measurements program, employing scale models of two floating nuclear power plants located within a scale model of a typical breakwater, was performed at the Colorado State University[5] under the direction of Offshore Power Systems to determine:

1. The locations on the plant for the two alternate control room ventilation intakes and

2. The dispersion factors between the release locations and the intakes for hazards analysis.

The applicability of scaled wind tunnel tests to determine the extent of mixing (at full scale) when both the release point and the intakes are located on or near complex structures is discussed by Merony[5], Halitsky[6], and in the Peach Bottom PSAR[7].

II. Description of Experiment

The model, located in the wind tunnel, included the two model power plants and the model breakwater, constructed to a linear scale of 1:450. The model is shown in Figure 1.

Ten sample ports, representing potential control room ventilation·intakes, were placed on each of the side-by-side plant models during the test. Figure 2 illustrates the location of several sample ports on two isometric views of a plant. The sample ports are labeled 6 (16) through 15 (25), where the numbers in parentheses refer to the corresponding locations on an adjacent plant.

The location of simulated release points on the plant are also shown in Figure 2. These include the plant vent stack, steam relief valve vents, containment vessel surface, and the house boiler exhaust. Metered quantities of gas were vented from the release point of interest to simulate the exit velocity and to account for the bouyancy effects due to the temperature difference between the released gas and the ambient atmosphere (if any). For this purpose, helium and compressed air were mixed in metered amounts.

The floating nuclear plant design[4] has a shield building surrounding and separated from the containment. The space between the shield building and the containment is maintained at negative pressure by a ventilation system both during normal operation and during postulated accidents, such as a loss-of-coolant accident (LOCA). Radioactivity which may leak from the containment in the event of a LOCA would then be a controlled release from the plant vent stack. Some radioactivity release could also occur from the surface of the shield building as a result of bypass leakage. As shown in Table 1, each of these potential release modes was considered in the experimental program. Releases from the plant vent stack at relatively low velocity following an accident is typical of the floating nuclear plant design[8]. Some tests at higher exit velocities were performed to determine what effect increasing the stack velocity might have on dilution between the vent and potential intake locations.

III. Experimental Information

Table 1, taken from Reference 5, gives an overview of the tests performed during the experimental program. Table 1 shows that the following variables were considered: source release point on either Plant A(α) or Plant B(β), plant vent stack height, atmospheric stability (neutral, N, or stable, S), wind velocity(V_a),

stack velocity (V_c), and wind angle. The alphanumerics (eg, B3 listed in the table reference specific tests as described in the CSU data report[5].

A schematic plan view of two adjacent plants located inside a breakwater is shown in Figure 3. (While this arrangement is for the Atlantic Generating Station' Units 1 and 2, it may also be used at other sites). Figure 3 illustrates the wind angles used throughout the experimental program. Also shown are the standard intakes on each plant, as well as typical sample locations and release points.

Although experimental data were obtained for all of the experimental release points shown in Table 1, this paper deals only with the plant vent stack and containment releases and their application to potential control room hazards analysis. Data concerning potential release of toxic gas outside the plant and breakwater were also obtained during the test program. These data and these analyses are not discussed in this paper but are included in Reference 4.

Qualitative Test Results

Tests with visible plumes were performed so that overall effects could be observed qualitatively. For these visual tests, gas was bubbled through a container of titanium tetrachloride before venting. The plume was illuminated with arc-lamp beams. Figure 4 is a still photograph showing a well defined plume exiting the stack from one plant model and passing over the top of the adjacent plant model. In addition to the still photographs, a series of color motion pictures of the visual test releases was obtained.

On the basis of visual observations, the following qualitative conclusions were reached:

1. Releases from the plant vent stack at low velocity may potentially envelope the upper part of the plant structure,

2. Releases from the plant vent stack with higher exit velocities did not appear to entrain between the various building cavities.

3. Releases from the containment surface may envelope the entire structure, but are quite well mixed providing significant dilution.

4. Although wind orientation and atmospheric stratification influence the character of flow over the plants, there is no strong evidence of a "worst" situation with respect to concentration at air intakes.

Quantitative Test Results

For quantitative measurement of the extent of mixing between the release point and the sample intake location, a mixture of Krypton-85 and air was vented. Samples were collected at each of the intake locations. Subsequently the samples were analyzed by counting of radioactivity. The counts for each sample point were then transformed into concentration values. The experimental data were reported in terms of $V_a(x/Q)$, where V_a is the wind velocity and x/Q is the atmospheric dispersion factor.

The experimental concentrations are presented in Reference 5 for each test at each sample location on the plants. In addition, the test data were provided to Offshore Power Systems as computer printouts and as card data decks. The

latter data were employed in the analysis of the experimental results, described in Section IV.

IV. Analysis of Experimental Data

The experimental data were analyzed in two phases. The first phase was to select the most favorable location for an alternate air intake, considering both plants. The standard intake is located on the south side of the plant as shown in Figure 2, where the standard intake is labeled #6 for Plant A and #16 (in parenthesis) for Plant B. The second phase of the analysis dealt with derivatior of the dispersion factors between the release and intake location for use in control room dose calculations.

Selection of Alternate Intake Locations

The test data were segmented into series for analysis, with a series being comprised of the data for all wind directions for release from a single release point, with other variables (stack height, wind velocity, and stack velocity) held constant. Next, the "worst" wind direction within each series was determined on the basis of the largest value (least mixing) of $(V_a \chi/Q)$ measured at the standard intake location. These data are presented in Tables 2 through 5. Each line or bracketed set in the tables represent a set of data. The worst wind direction and the $(V_a \chi/Q)$ value for the standard intake are listed in columns 5 and 6. $(V_a \chi/Q)$ values for other potential alternate intakes are listed in the subsequent columns. Tables 2 and 3 apply to intakes on Plant A for neutral and stable stratification, respectively. Tables 4 and 5 apply to intakes on Plant B for neutral and stable stratification, respectively.

For several test series, all concentrations were less than detectable limits at standard intake location 6 (Plant A) or standard location 16 (Plant B). For those cases (shown by ** on Tables 2 through 5), three wind directions were chosen which geometrically represent the potentially worst wind directions relative to the standard intake. Note that the source of release is given in the first column of each table. Generally, the tabulated data indicate concentration of potential second intakes for the worst condition at the standard intake (6 or 16). One would want to switch to a second intake when the conditions at the standard intake become unfavorable.

The data from Tables 2 through 5 were next reduced to the form shown in Table 6. Table 6 illustrates the most favorable second intake location for each test series analyzed. An x indicates the intakes which had the observed lowest value of $V_a (\chi/Q)$ for a particular test series. For some test series there is more than one preferred intake, since several sample locations had concentrations below detectable levels for a particular test series. Generally, these data show that intake #12 is the preferred second location on Plant A and intake #18 is the preferred second location on Plant B.

Floating nuclear power plants are to be of standard design, and hence the alternate air intake must be at the same location on each plant. Table 7 combines the data on preferred intake locations on Plant A and Plant B to indicate the alternate intake which is the best overall alternate location as indicated by the test program. The values in the right hand column of Table 7 were obtained by adding the appropriate totals from the bottom of Table 6 for a set of matching intakes on the two plants. From Table 7 it can be observed that the preferred combination is intake #8 on Plant A and intake #18 on Plant B. Thus, these locations on the southeast side of each plant were selected as the alternate intake

locations for design.

The next step in this analysis was to determine which of the intakes on each plant would be employed for the various wind directions. The measured values of V_a (χ/Q) for the selected dual intakes for all wind directions on both Plants A and B were tabulated. These tabulations are given in Tables 8 and 9 for Plants A and B, respectively.

Only data for release from the plant stack of standard height (195 feet), and from the containment for the lower wind velocity of V_a = 5 feet/second (1.5 m/sec) (typical minimum mixing) were considered. Data for both the neutral and stable atmospheric stratification conditions were considered as shown in Tables 8 and 9. The data for the dual intakes are grouped in these two tables according to release points (stack or containment) and the plant from which release occurs. For each experimental wind angle a maximum observed value of V_a (χ/Q) is listed at the bottom of the table for each of the four intakes on the two plants (intakes 6 and 16 and intakes 8 and 18) for both plant vent stack and containment releases. These maxima were plotted versus wind direction (angle) for both the plant stack and containment release points for both Plants A and B as shown graphically in Figures 5 through 8. (It should be noted that the value of V_a applicable to these data is 5 ft/sec or 1.5 m/sec.). Specifically, Figures 5 and 6 apply to intakes on Plant A, for release from the plant vent and containment, respectively; whereas Figures 7 and 8 apply to intakes on Plant B, for release from the plant vent and containment, respectively.

In the unlikely event of an accident such as a loss-of-coolant, most of the radioactivity which could affect operation in the control room is released from the plant vent stack. Therefore, data on release from the plant vent stack were the primary data used to determine which intake would be employed as a function of wind direction, Figures 5 and 7. The selection technique will be discussed using Figure 5 as the example. The maximum values of V_a (χ/Q) for intake #6 are shown on Figure 5 as a dashed curve·and for intake #8 as a dotted curve. The solid curve is an envelope curve based on the lower value of the two curves for all wind angles, i.e., it represents the intake providing the more favorable dilution. From Figure 5 it can be observed that on Plant A intake #8 is pre-ferred over the ranges 330° to 360° and 0° to 180° while intake #6 is preferred over the range 180° to 330°. (Referring to Figure 6, it is observed that the preferred intake as a function of direction is generally the same for the con-tainment release).

A similar technique was employed to select the preferred on-line intake for Plant B. From Figure 7, the envelope curve shows that intake #16 is preferred over the ranges 310° to 360° and 0° to 140° while intake #18 is preferred from 140° to 310°.

Figure 9 shows a plan view of Plants A and B and indicates the preferred intakes as a function of wind direction for both plants.

A wind direction indicator on each plant will be used to select automati-cally which intake should be utilized in the event of an accident. The operator can override the automatic feature if necessary.

Selection of Dispersion Factors

To calculate potential doses in the control room from airborne radioactivity

release following a hypothetical accident, dispersion factors between the release point and the intakes are needed. For the dose analysis for the floating nuclear plant, the applicable χ/Q's were developed from the experimental data.

From Figures 5 through 8, maximum values of V_a (χ/Q) were selected for the on-line intake (solid curves) for each plant and each release mode. These maximum values are summarized in Table 10. The two least favorable values for plant vent stack release and for containment release, required for dose evaluation, are 1.8×10^{-5} and 6.0×10^{-4} respectively.

V. Summary

Offshore Power Systems has employed a series of scale model wind tunnel tests for selecting the location of dual and alternate ventilation intakes for the control room on standard design Floating Nuclear Power Plants and for determining dispersion factors between the point of release and the intakes for accident analyses. The location of the alternate intakes and the accident analyses employing these dispersion factors has been approved by the Nuclear Regulatory Staff in their Safety Evaluation Report for the plant[9].

Furthermore, the dispersion values for control room dose analyses[9] for the plant vent are about a factor of 20 lower than dilution from the plant vent that would be calculated from reference 6. The atmospheric dispersion factor derived from the test data for releases from the containment was essentially in agreement with that derived via reference 6. These data demonstrate the general applicability of the methods in reference 6 for calculating dilution when releases are from the containment surface (within the building complex). The data also show the significant additional dilution attained from a release elevated slightly above the containment.

VI. References

1. Code of Federal Regulations, 10CFR Part 50, Appendix A, General Design Criteria 19, Control Room.

2. U.S. Nuclear Regulatory Commission, Standard Review Plan, Section 6.4, Habitability Systems, June, 1975.

3. Murphy, K. G. and Campe, K. M., (1975), Nuclear Power Plant Control Room Ventilation System Design for Meeting General Criterion 19, 13th AEC Air Cleaning Conference, 401-428.

4. Docket No. STN 50-437, Plant Design Report, Offshore Power Systems, May, 1973 (plus amendments).

5. SA-1000-14A45A, (1974), Wind Engineering Study of Atmospheric Dispersion of Airborne Materials Released from a Floating Nuclear Power Plant, Merony, R. N., Cermak, J. E., Connell, J. R., and Garrison, J. A., Colorado State University.

6. Slade, P. H., Meteorology and Atomic Energy, July, 1968, p. 221-255.

7. Docket Nos. STN 50-277 and 50-278, Unit 2 Vent Plume Behavior, Peach Bottom Atomic Power Station, Philadelphia Electric Company, March, 1974.

8. Docket Nos. STN 50-477 and 50-478, Preliminary Safety Analysis Reports, Atlantic Generating Station Units 1 and 2, Public Service Electric and Gas Company, March, 1974.

9. NUREG 75/100, (September, 1975), Safety Evaluation Report Related to Offshore Power Systems Floating Nuclear Plants (1-8), Office of Nuclear Reactor Regulation, U.S. Nuclear Regulatory Commission.
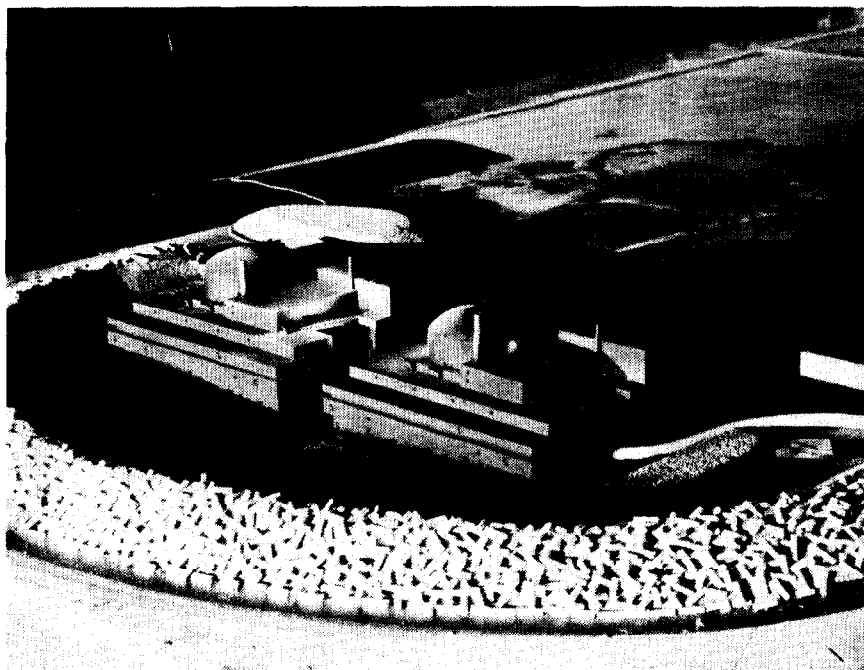
FIGURE 1

Photograph of Plant Scale Models

Enclosed Within Scale Model of

Breakwater at The Colorado State

University Wind Tunnel

VIEW FROM NOMINAL SE

VIEW FROM NOMINAL SW
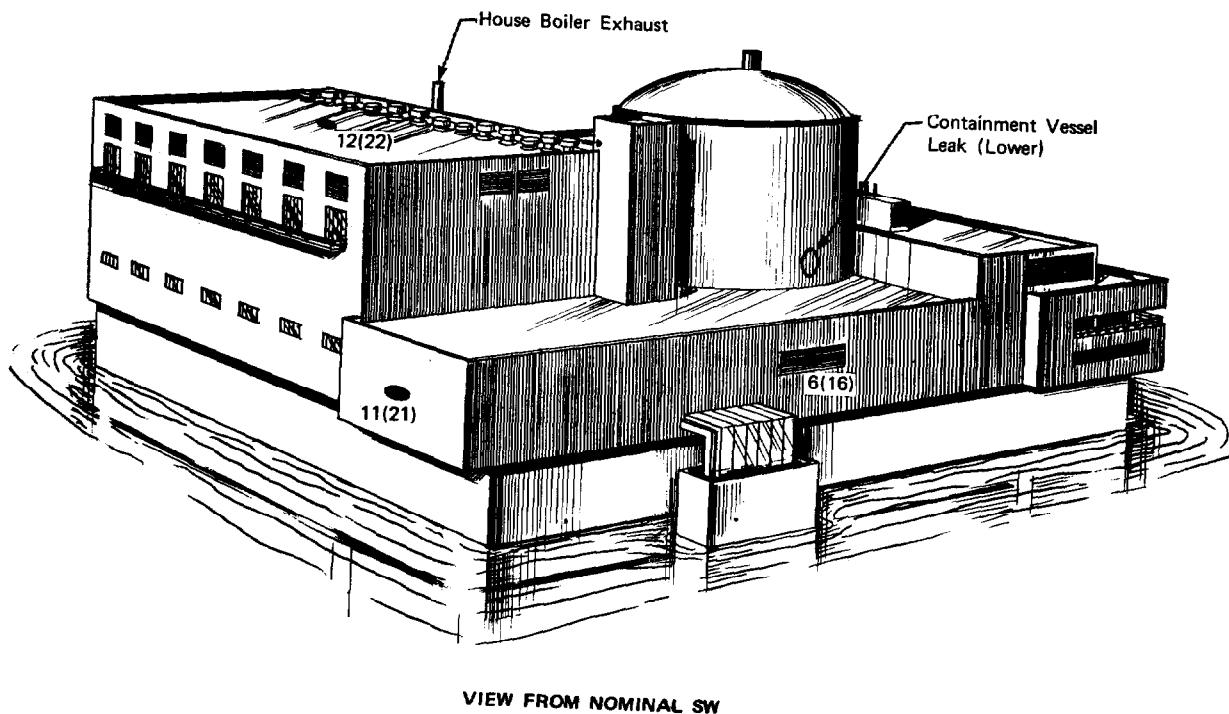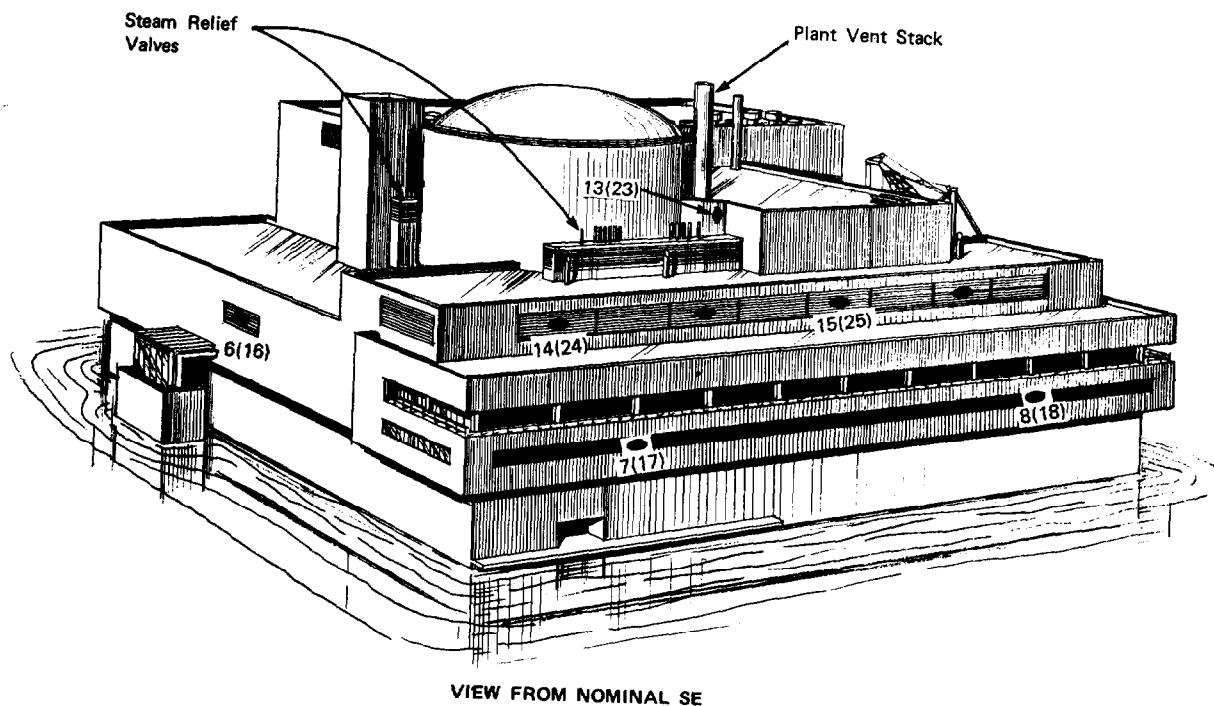
FIGURE 2

FLOATING NUCLEAR PLANT — ISOMETRIC VIEWS ILLUSTRATING
RELEASE LOCATIONS AND SAMPLING LOCATIONS

TABLE 1

SUMMARY OF TEST CONDITIONS

Source	Height (ft)	Stability	V_a (ft/sec)	V_s (ft/sec)	Angle / Bldg	0° (α)	45° (α)	90° (α)	(β)	135° (β)	180° (β)	225° (β)	270° (β)	(α)	315° (α)
*Plant Vent Stack	195	N	5	.05		B1	B2	B3	B4	B5	B6	B7	B8	B9	B10
				10		B11	B12	B13	B14	B15	B16	B17	B18	B19	B20
			25	.05		B21	B22	B23	B24	B25	B26	B27	B28	B29	B30
				15		B31	B32	B33	B34	B35	B36	B37	B38	B39	B40
		S	5	.05		B41	B42	B43	B44	B45	B46	B47	B48	B49	B50
				15		B51	B52	B53	B54	B55	B56	B57	B58	B59	B60
	245	N	5	.05		B61	B62	B63	B64	B65	B66	B67	B68	B69	B70
			25	.05		B71	B72	B73	B74	B75	B76	B77	B78	B79	B80
		S	5	.05		B81	B82	B83	B84	B85	B86	B87	B88	B89	B90
				15			B180				B181				B182
*Containment Vessel	---	N	5	Lo		B91	B92	B93	B94	B95	B96	B97	B98	B99	B100
			25	Lo		B101	B102	B103	B104	B105	B106	B107	B108	B109	B110
		S	5	Lo		B111	B112	B113	B114	B115	B116	B117	B118	B119	B120
**Diesel Generator Exhaust	113	N	5	125								B121	B122		B123
			25	125								B124	B125		B126
	125		5	125								B127	B128		B129
			25	125								B130	B131		B132
**House Boiler	---	N	5	50								B133	B134		B135
			25	50								B136	B137		B138
**Steam Relief Valves	---	N	5	Hi								B139	B140		B141
			25	Hi								B142	B143		B144

NOTE: V_a = Wind Velocity   N = Neutral

   V_s = Vent Stack Flow Velocity   S = Stable

* 25 Sample Locations each test

** 4 Sample Locations each test
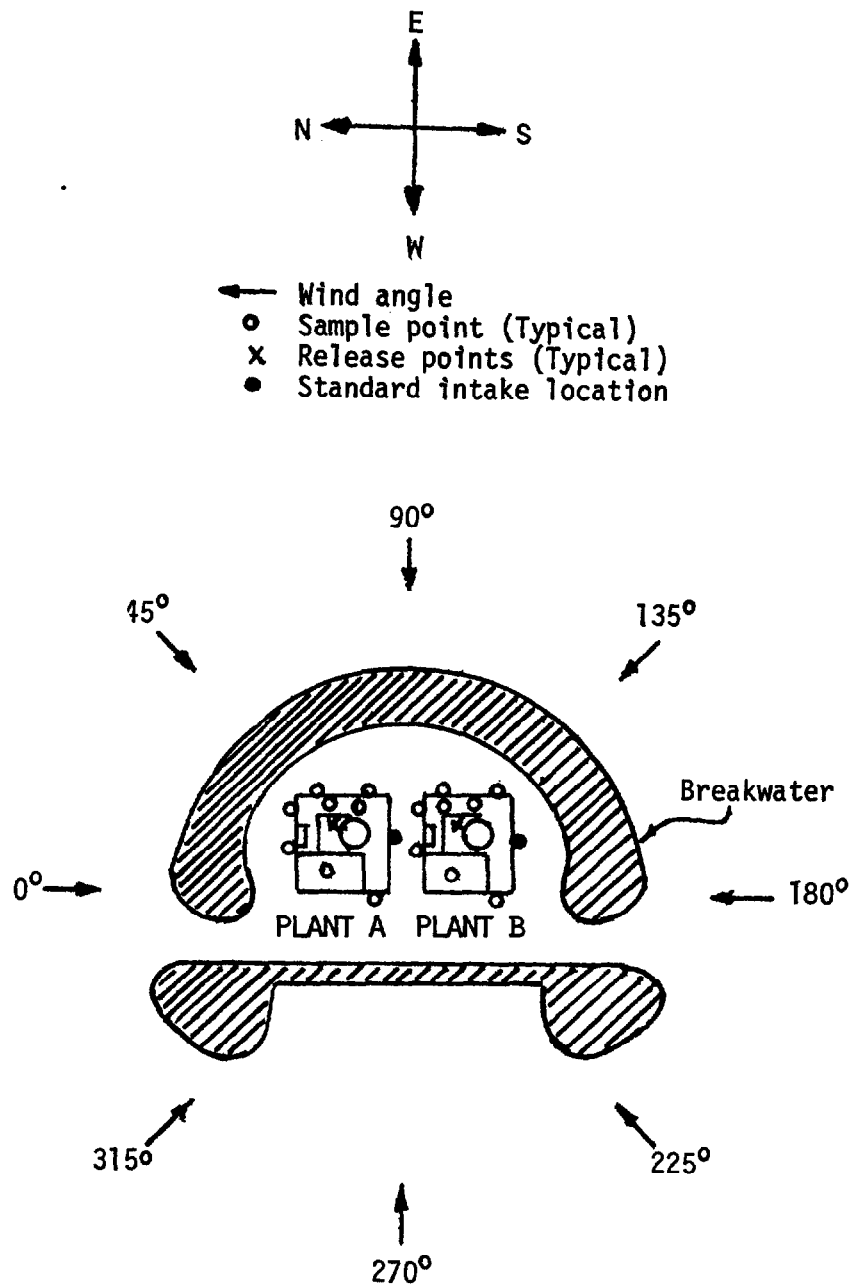
FIGURE 3

Schematic Plan View of Adjacent Plants

Inside Breakwater Illustrating Wind

Angles Employed During Test Program

(Atlantic Generating Station)
Units 1 and 2
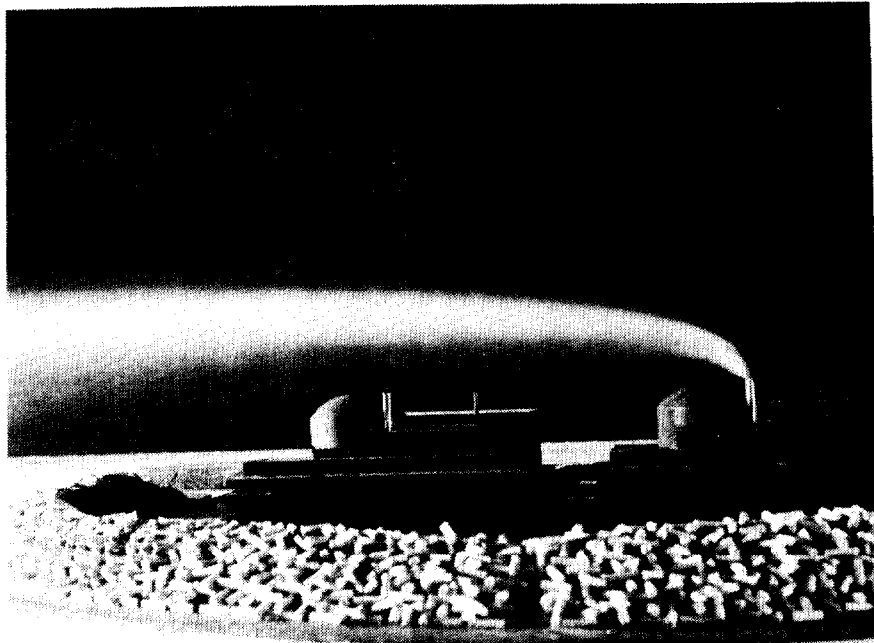
FIGURE 4

Photograph of model

During Test Illustrating

Well Defined Plume

TABLE 2

$(V_a \chi/Q)$'s AT INTAKES ON PLANT "A" FOR WIND DIRECTIONS WHICH PRODUCE HIGHEST VALUE OF PARAMETER AT INTAKE #6

NEUTRAL STRATIFICATION

Source	Stack Ht.	V_a ft/sec	V_s ft/sec	Wind Dir.*	: $(V_a\chi/Q)$ (M^{-2}) AT INTAKES									
					6	7	8	9	10	11	12	13	14	15
Stack-A	195'	5	.05	0°	--	--	--	--	4.2(-5)	1.3(-5)	--	--	--	--
"	"	=	=	45° }**	--	7.5(-4)	2.5(-5)	--	--	5.3(-5)	--	7.3(-4)	1.0(-3)	2.7(-4)
"	"	=	=	315°	2.7(-5)	7.6(-7)	1.7(-6)	--	--	4.3(-6)	--	2.9(-6)	8.9(-7)	1.8(-6)
"	"	=	10	90°	--	--	--	2.4(-6)	4.1(-6)	--	5.1(-6)	--	--	3.3(-5)
"	"	25	=	0°	--	--	--	--	--	1.7(-4)	--	--	--	--
"	"	=	=	45° }**	--	8.3(-4)	--	2.3(-4)	--	--	--	--	1.7(-3)	2.3(-4)
"	"	=	=	315°	--	3.5(-6)	1.7(-6)	2.6(-6)	1.5(-6)	4.1(-6)	3.0(-6)	2.3(-6)	2.6(-6)	2.4(-6)
"	245'	5	15	0°	2.2(-5)	--	--	--	--	--	--	--	--	--
"	"	25	.05	0°	4.2(-5)	--	--	--	--	--	--	--	--	--
"	"	=	=	270°	8.2(-6)	--	--	--	8.2(-6)	--	--	1.6(-5)	--	--
Stack-B	195'	5	.05	180°	1.6(-4)	1.4(-4)	--	3.1(-4)	1.5(-4)	1.0(-4)	--	5.7(-4)	1.9(-4)	4.3(-4)
"	"	=	10	180°	1.3(-5)	2.1(-5)	1.4(-5)	1.3(-4)	7.8(-5)	2.0(-6)	8.6(-6)	4.5(-4)	1.6(-4)	1.7(-4)
"	"	25	=	90°	8.3(-5)	--	--	--	--	--	--	--	--	--
"	"	=	15	180°	5.3(-5)	1.9(-4)	1.1(-4)	3.5(-4)	5.4(-4)	6.7(-6)	3.5(-5)	1.7(-3)	5.7(-4)	6.0(-4)
"	245'	5	=	225°	4.2(-5)	--	3.3(-5)	--	--	--	--	--	--	--
"	"	25	.05	135°	2.1(-5)	6.6(-6)	--	--	8.2(-6)	--	--	--	--	6.7(-5)
Cont.-A	N/A	5	1.5	0°	2.9(-4)	4.9(-6)	3.4(-6)	1.2(-6)	--	1.3(-6)	7.1(-6)	2.3(-4)	1.5(-5)	4.6(-6)
"	"	25	2.5	0°	1.0(-3)	1.1(-5)	1.3(-5)	4.4(-6)	4.3(-7)	1.7(-6)	--	1.1(-4)	2.4(-5)	1.2(-5)
Cont.-B	N/A	5	1.5	180°	5.3(-5)	2.0(-4)	1.8(-4)	2.8(-4)	7.9(-4)	4.9(-6)	4.8(-5)	8.1(-4)	8.6(-4)	7.1(-4)
"	"	25	2.5	270°	3.2(-4)	4.5(-4)	3.9(-5)	8.9(-6)	9.4(-6)	1.7(-6)	--	1.2(-4)	3.6(-4)	1.0(-4)

* These directions were chosen from all the available data (ie. 8 different wind directions). They represent the direction which gave the largest $V_a\chi/Q$ at intake #6.

** For these tests the data at intake #6 was too low to be detectable for any wind direction. Since intake #6 was south of the release point for both cases, the 0°, 45°, and 315° angles were chosen to be the worst directions.

TABLE 3

(V_aX/Q)'s AT INTAKES ON PLANT "A" FOR WIND DIRECTIONS WHICH PRODUCE HIGHEST VALUE OF PARAMETER AT INTAKE #6
STABLE STRATIFICATION

Source	Stack Ht.	V_a ft/sec	V_s ft/sec	Wind Dir.*	(V_aX/Q) (M^{-2}) AT INTAKES									
					6	7	8	9	10	11	12	13	14	15
Stack-A	195'	5	.05	45°	3.4(-5)	2.4(-5)	1.4(-5)	5.0(-6)	2.5(-5)	1.9(-4)	3.2(-5)	1.5(-5)	2.0(-5)	1.4(-5)
"	"	"	15	270°	1.3(-5)	9.5(-7)	1.4(-6)	8.2(-7)	8.1(-7)	8.8(-7)	7.2(-7)	9.2(-7)	5.5(-7)	7.8(-7)
"	245'	"	.05	0° **	--	--	--	--	--	--	--	--	--	--
"	"	"	"	45° **	--	--	--	--	--	--	--	3.2(-6)	--	--
"	"	"	"	315°	--	--	--	--	3.9(-5)	--	--	3.2(-6)	2.4(-5)	--
"	"	"	15	315°	2.9(-6)	1.5(-6)	2.9(-7)	1.4(-6)	7.2(-7)	1.4(-6)	1.3(-6)	1.7(-6)	1.3(-6)	1.8(-6)
Stack-B	195'	5	.05	180°	1.0(-4)	5.7(-5)	5.1(-5)	6.5(-5)	8.7(-5)	5.9(-5)	6.6(-5)	--	2.4(-4)	--
"	"	"	15	135°	3.3(-6)	3.7(-6)	2.4(-6)	3.3(-6)	3.8(-6)	5.8(-6)	2.9(-6)	3.2(-6)	2.6(-6)	3.2(-6)
"	245'	"	.05	135° **	--	1.3(-5)	--	1.9(-5)	7.1(-5)	3.3(-4)	--	--	--	6.3(-6)
"	"	"	"	180° **	--	--	--	--	1.2(-4)	--	--	2.0(-4)	--	1.1(-4)
"	"	"	"	225°	--	--	--	--	--	--	--	6.3(-6)	--	1.3(-5)
"	"	"	15	225°	1.2(-6)	2.1(-6)	2.1(-6)	1.3(-6)	1.3(-6)	1.1(-6)	2.6(-7)	8.5(-7)	8.5(-7)	1.3(-6)
Cont.-A	N/A	5	.5	0°	3.1(-4)	9.9(-6)	8.3(-6)	1.6(-6)	4.1(-6)	4.9(-6)	2.9(-6)	5.1(-6)	3.2(-6)	3.6(-6)
Cont.-B	N/A	5	.5	180°	6.3(-6)	1.5(-5)	2.9(-5)	1.7(-4)	1.4(-4)	1.5(-4)	1.8(-4)	8.1(-4)	6.3(-4)	5.9(-4)

* These directions were chosen from all the available data (ie, 8 different wind directions). They represent the direction which gave the largest V_aX/Q at intake #6.

** For these tests the data at intake #6 was too low to be detectable for any wind direction. For these cases three directions were chosen (0°, 45°, and 315° if the intake #6 is south at the release point) or (135°, 180°, and 225°) if intake #6 is north of the release point).

TABLE 4

(V$_a$χ/Q)'s AT INTAKES ON PLANT "B" FOR WIND DIRECTIONS WHICH PRODUCE HIGHEST VALUE OF PARAMETER AT INTAKE #16

NEUTRAL STRATIFICATION

Source	Stack Ht.	V$_a$ ft/sec	V$_s$ ft/sec	Wind Dir.*	16	17	18	19	20	21	22	23	24	25
					— (V$_a$χ/Q) (M^{-2}) AT INTAKES									
Stack-A	195'	5	.05	0°	1.1(-4)	--	--	--	--	--	--	6.7(-6)	6.7(-5)	7.3(-5)
"	"	"	10	0°	4.7(-5)	9.7(-7)	2.9(-6)	3.5(-6)	2.4(-6)	2.0(-6)	4.7(-6)	1.0(-4)	6.4(-6)	5.6(-6)
"	"	25	.05	0°	4.2(-5)	--	1.9(-4)	1.3(-4)	--	--	--	3.0(-4)	--	--
"	"	"	15	0°	3.6(-4)	7.4(-6)	1.6(-5)	1.8(-5)	4.3(-5)	4.5(-5)	2.4(-5)	1.1(-3)	9.2(-5)	5.6(-5)
"	245'	5	.05	0°	6.7(-5)	--	--	--	--	--	--	1.1(-3)	--	--
"	"	25	.05	0°	2.1(-4)	6.6(-6)	--	5.2(-5)	--	--	1.6(-5)	5.8(-4)	3.3(-5)	2.0(-5)
Stack-B	195'	5	.05	180°	4.2(-5)	5.3(-5)	--	5.8(-4)	3.4(-4)	--	8.3(-5)	3.1(-4)	--	8.0(-5)
"	"	"	10	0°	2.4(-5)	1.2(-6)	4.5(-7)	1.6(-6)	3.8(-7)	4.6(-7)	5.7(-7)	8.6(-7)	1.5(-6)	--
"	"	25	.05	0°	--	--	--	--	--	--	--	--	--	--
"	"	"	"	45°}**	--	--	--	--	--	1.7(-4)	--	--	--	3.3(-5)
"	"	"	15	315°	2.2(-5)	8.3(-4)	--	2.3(-4)	--	--	--	--	1.7(-3)	2.3(-4)
"	245'	5	.05	0°	4.2(-5)	3.5(-6)	1.7(-6)	2.6(-6)	1.5(-6)	4.1(-6)	3.0(-6)	2.3(-6)	2.6(-6)	2.4(-6)
"	"	25	.05	90°	8.2(-6)	5.2(-5)	--	3.0(-5)	--	9.5(-5)	2.9(-5)	--	--	--
Cont.-A	N/A	5	1.5	315°	1.5(-4)	2.2(-4)	2.2(-4)	2.5(-4)	3.4(-4)	3.2(-5)	3.5(-4)	1.5(-4)	2.1(-4)	2.6(-4)
"	"	25	2.5	0°	2.4(-4)	1.6(-5)	4.2(-5)	1.1(-4)	1.1(-3)	1.3(-4)	1.1(-3)	4.7(-4)	1.6(-4)	1.9(-4)
Cont.-B	N/A	5	1.5	0°	2.9(-4)	4.9(-6)	3.4(-6)	1.2(-6)	--	1.3(-6)	7.1(-6)	2.3(-4)	1.5(-5)	4.6(-6)
"	"	25	2.5	0°	1.0(-3)	1.1(-5)	1.3(-5)	4.4(-6)	4.3(-7)	1.7(-6)	--	1.1(-4)	2.4(-5)	1.2(-5)

* These directions were chosen from all the available data (ie, 8 different wind directions). They represent the direction which gave the largest V$_a$χ/Q at intake #16.

** For this test the data at intake #16 was too low to be detectable for any wind direction. Since intake #16 was south of the release point, the 0°, 45°, and 315° angles were chosen to be the worst directions.

TABLE 5

$(V_a\chi/Q)$'s AT INTAKES ON PLANT "B" FOR WIND DIRECTIONS WHICH PRODUCE HIGHEST VALUE OF PARAMETER AT INTAKE #16

STABLE STRATIFICATION

Source	Stack Ht.	V_a ft/sec	V_s ft/sec	Wind Dir.*	$(V_a\chi/Q)$ (M^{-2}) AT INTAKES									
					16	17	18	19	20	21	22	23	24	25
Stack-A	195'	5	.05	0°	8.5(-5)	2.3(-5)	2.7(-5)	2.3(-5)	9.9(-6)	1.1(-5)	2.9(-5)	5.0(-4)	6.9(-5)	3.0(-6)
"	=	=	15	315°	3.4(-6)	2.9(-6)	2.1(-6)	3.1(-6)	3.3(-6)	2.7(-6)	2.9(-6)	2.0(-6)	2.9(-6)	2.7(-6)
"	245'	=	.05	0°	3.9(-5)	--	--	--	--	--	--	1.7(-4)	--	--
"	=	=	15	45°	1.6(-6)	--	--	1.5(-6)	1.3(-6)	1.4(-6)	7.7(-7)	1.4(-6)	1.5(-6)	8.5(-7)
Stack-B	195'	5	.05	135°	5.0(-5)	4.9(-5)	3.1(-5)	1.1(-5)	3.7(-5)	3.0(-6)	3.5(-5)	9.7(-5)	4.1(-5)	2.5(-5)
"	=	=	15	315°	3.4(-6)	3.4(-6)	2.3(-6)	3.9(-6)	3.3(-6)	3.6(-6)	3.2(-6)	3.3(-6)	3.4(-6)	3.5(-6)
"	245'	=	.05	0°	--	--	--	--	--	--	--	3.2(-5)	--	--
"	=	=	"	45°}**	--	--	--	--	--	--	--	2.2(-5)	--	--
"	=	=	"	315°	--	--	--	--	--	--	--	1.7(-6)	--	--
"	=	=	15	315°	2.9(-6)	1.5(-6)	2.9(-7)	1.4(-6)	7.2(-7)	1.4(-6)	1.3(-6)	1.7(-6)	1.3(-6)	1.8(-6)
Cont.-A	N/A	5	.5	0°	1.1(-4)	1.5(-4)	2.7(-4)	4.4(-4)	6.9(-4)	4.5(-5)	5.5(-4)	1.8(-4)	2.1(-4)	2.4(-4)
Cont.-B	N/A	5	.5	0°	3.1(-4)	9.9(-6)	8.3(-6)	1.6(-6)	4.1(-6)	4.9(-6)	2.9(-6)	5.1(-6)	3.2(-6)	3.6(-6)

* These directions were chosen from all the available data (ie, 8 different wind directions). They represent the direction which gave the largest $V_a\chi/Q$ at intake #16.

** For this test the data at intake #16 was too low to be detectable for any wind direction. Since intake #16 was south of the release point, the 0°, 45°, and 315° angles were chosen to be the worst directions

TABLE 6

PREFERRED ALTERNATE INTAKES FOR VARIOUS EXPERIMENTAL CONDITIONS

SOURCE	Stability Class	Stack Height (ft.)	V_a	V_s	PLANT A — PREFERRED ALTERNATE INTAKES									PLANT B — PREFERRED ALTERNATE INTAKES								
					7	8	9	10	11	12	13	14	15	17	18	19	20	21	22	23	24	25
Plant A Stack Release	N	195	5	.05		X				X				X	X	X	X	X	X			
	"	"	"	10	X									X								
	"	"	25	.05		X		X		X	X			X				X	X	X	X	X
	"	"	"	15					X					X								
	"	245	5	.05	X	X	X	X	X	X	X	X	X	X	X	X	X	X	X		X	X
	"	"	25	.05	X	X	X			X	X		X		X		X	X		X		
Plant A Stack Release	S	195	5	.05		X																X
	"	"	"	15							X										X	
	"	245	"	.05	X	X	X			X	X		X	X	X	X	X	X	X		X	X
	"	"	"	15		X								X	X							
Plant B Stack Release	N	195	5	.05		X				X					X			X			X	
	"	"	"	10						X												X
	"	"	25	.05	X	X	X	X	X	X	X	X	X		X		X		X	X		
	"	"	"	15						X					X							
	"	245	5	.05	X		X	X	X	X	X	X		X	X	X	X	X	X	X	X	X
	"	"	25	.05		X	X		X	X	X	X	X		X		X					
Plant B Stack Release	S	195	5	.05							X		X			X						
	"	"	"	15		X									X							
	"	245	"	.05		X				X		X		X	X	X		X	X			X
	"	"	"	15				X							X							
Cont. A Release	N	N/A	5	1.5				X										X				
	"	"	25	2.5						X				X								
	S	"	5	.5			X											X				
Cont. B Release	N	N/A	5	1.5					X									X				
	"	"	25	2.5						X										X		
	S	"	5	.5	X										X							
TOTALS					7	10	9	7	8	13	6	7	6	10	13	7	9	10	8	3	5	7

TABLE 7

POTENTIAL ALTERNATE INTAKE PREFERENCE CONSIDERING TWO PLANTS

INTAKE COMBINATION PLANT A – PLANT B		NUMBER OF PREFERENCES FROM EXPERIMENTAL DATA
7	17	17
8	18	23
9	19	16
10	20	16
11	21	18
12	22	21
13	23	9
14	24	12
15	25	13

SELECTED ALTERNATE INTAKE: 8(Plant A); 18(Plant B)

TABLE 8

V_a (X/Q) FOR SELECTED INTAKES ON PLANT A VS. WIND DIRECTION ANGLE

Standard Intake #6
V_a (X/Q) (M-2)

SOURCE	Va	Vs	STABILITY	0°	45°	90°	135°	180°	225°	270°	315°
VENT-A	5	10	N	2.4(-5)	5.7(-6)	2.7(-5)	1.2(-6)	2.7(-6)	1.9(-7)	5.9(-6)	1.3(-5)
VENT-A	5	15	S	1.2(-6)	2.5(-6)	6.4(-7)	3.2(-6)	2.2(-6)	9.4(-7)	1.3(-5)	3.4(-6)
VENT-B	5	10	N	-	-	6.4(-8)	5.2(-6)	1.3(-5)	8.3(-7)	1.7(-6)	-
VENT-B	5	15	S	-	-	3.0(-6)	3.3(-6)	3.1(-6)	1.6(-6)	5.1(-7)	-
MAXIMUM				2.4(-5)	5.7(-6)	2.7(-5)	5.2(-6)	1.3(-5)	1.6(-6)	1.3(-5)	1.3(-5)
CONT-A	5	LOW	N	2.9(-4)	-	-	3.6(-7)	2.8(-5)	3.4(-6)	3.3(-6)	1.9(-4)
CONT-A	5	LOW	S	3.1(-4)	6.5(-6)	6.2(-6)	1.3(-6)	3.3(-6)	2.1(-6)	2.2(-6)	8.8(-5)
CONT-B	5	LOW	N	-	-	5.7(-7)	1.2(-5)	5.3(-5)	6.2(-6)	5.3(-5)	-
CONT-B	5	LOW	S	-	-	-	1.2(-5)	6.3(-4)	2.6(-7)	1.3(-6)	-
MAXIMUM				2.9(-4)	6.5(-6)	6.2(-6)	1.2(-5)	6.3(-4)	6.2(-6)	5.3(-5)	1.9(-4)

Alternate Intake #8
V_a (X/Q) (M-2)

SOURCE	Va	Vs	STABILITY	0°	45°	90°	135°	180°	225°	270°	315°
VENT-A	5	10	N	4.5(-7)	1.8(-6)	1.7(-6)	1.5(-6)	3.4(-6)	1.1(-4)	1.2(-5)	3.1(-5)
VENT-A	5	15	S	1.5(-6)	1.5(-6)	4.3(-7)	3.4(-6)	1.4(-6)	2.9(-6)	1.4(-6)	2.3(-6)
VENT-B	5	10	N	-	-	-	2.5(-7)	1.4(-5)	2.5(-5)	6.9(-6)	-
VENT-B	5	15	S	-	-	2.1(-6)	2.4(-6)	2.8(-6)	1.2(-6)	1.2(-6)	-
MAXIMUM				1.5(-6)	1.8(-6)	2.1(-6)	3.4(-6)	1.4(-5)	1.1(-4)	1.2(-5)	3.1(-5)
CONT-A	5	LOW	N	3.4(-6)	2.4(-6)	-	7.2(-7)	1.5(-4)	3.5(-5)	1.4(-4)	1.3(-4)
CONT-A	5	LOW	S	8.3(-6)	2.6(-6)	6.3(-6)	3.8(-7)	9.1(-6)	3.9(-4)	3.1(-5)	9.6(-5)
CONT-B	5	LOW	N	-	-	-	6.9(-5)	1.8(-4)	4.2(-5)	7.4(-5)	-
CONT-b	5	LOW	S	-	-	-	2.1(-6)	2.9(-5)	2.4(-4)	1.4(-5)	-
MAXIMUM				8.3(-6)	2.6(-6)	6.3(-6)	6.9(-5)	1.8(-4)	3.9(-4)	1.4(-4)	1.3(-4)

TABLE 9

V_a (X/Q) FOR SELECTED INTAKES ON PLANT B VS. WIND DIRECTION ANGLE

Standard Intake #16
V_a (X/Q) (M^{-2})

SOURCE	Va	Vs	STABILITY	0°	45°	90°	135°	180°	225°	270°	315°
VENT-A	5	10	N	4.7(-5)	4.2(-5)	5.7(-7)	-	-	-	2.4(-6)	1.7(-5)
VENT-A	5	15	S	3.2(-6)	2.7(-6)	1.8(-6)	-	-	-	1.6(-6)	3.4(-6)
VENT-B	5	10	N	2.4(-5)	5.7(-6)	-	1.1(-6)	2.7(-6)	1.9(-7)	6.4(-6)	1.3(-5)
VENT-B	5	15	S	1.2(-6)	2.5(-6)	2.6(-6)	3.2(-6)	2.2(-6)	9.4(-7)	8.1(-7)	3.4(-6)
MAXIMUM				4.7(-5)	4.2(-5)	2.6(-6)	3.2(-6)	2.7(-6)	9.4(-7)	6.4(-6)	1.7(-5)
CONT-A	5	LOW	N	1.4(-4)	7.4(-5)	3.6(-7)	-	-	-	1.6(-5)	1.5(-4)
CONT-A	5	LOW	S	1.1(-4)	3.3(-6)	4.1(-6)	-	-	-	1.1(-5)	2.7(-5)
CONT-B	5	LOW	N	2.9(-4)	-	1.5(-6)	3.6(-7)	2.8(-5)	3.4(-6)	5.9(-6)	1.9(-4)
CONT-B	5	LOW	S	3.1(-4)	6.5(-6)	2.9(-6)	1.3(-6)	3.3(-6)	2.1(-6)	7.7(-7)	8.8(-5)
MAXIMUM				3.1(-4)	7.4(-5)	4.1(-6)	1.3(-6)	2.8(-5)	3.4(-6)	1.6(-5)	1.9(-4)

Alternate Intake #18
V_a (X/Q) (M^{-2})

SOURCE	Va	Vs	STABILITY	0°	45°	90°	135°	180°	225°	270°	315°
VENT-A	5	10	N	2.9(-6)	2.5(-6)	8.3(-7)	-	-	-	7.1(-6)	1.1(-5)
VENT-A	5	15	S	2.4(-6)	1.5(-6)	3.8(-7)	-	-	-	1.1(-6)	2.1(-6)
VENT-B	5	10	N	4.5(-7)	1.8(-6)	4.5(-7)	1.5(-6)	3.4(-6)	1.1(-4)	5.6(-4)	3.1(-5)
VENT-B	5	15	S	1.5(-6)	1.5(-6)	2.7(-6)	3.4(-6)	1.4(-6)	2.9(-6)	1.4(-6)	2.3(-6)
MAXIMUM				2.9(-6)	2.5(-6)	2.7(-6)	3.4(-6)	3.4(-6)	1.1(-4)	5.6(-4)	3.1(-5)
CONT-A	5	LOW	N	1.4(-4)	-	-	-	-	-	4.0(-4)	2.2(-4)
CONT-A	5	LOW	S	2.7(-4)	3.6(-6)	6.3(-6)	-	-	-	2.9(-5)	3.5(-4)
CONT-B	5	LOW	N	3.5(-6)	2.4(-6)	-	7.2(-7)	1.5(-4)	3.5(-5)	2.1(-4)	1.3(-4)
CONT-B	5	LOW	S	8.3(-6)	2.6(-6)	1.3(-7)	3.8(-7)	9.1(-6)	3.9(-4)	2.8(-4)	9.6(-5)
MAXIMUM				2.7(-4)	3.6(-6)	6.3(-6)	7.2(-7)	1.5(-4)	3.9(-4)	4.0(-4)	3.5(-4)

FIGURE 5   MAXIMUM Va (x/Q) ON PLANT "A" VS.
WIND DIRECTION FOR RELEASE FROM
PLANT VENT

Legend
------ Intake #6
•••••••• Intake #8
——— Intake on Line

FIGURE 6   MAXIMUM V_a (X/Q)'s ON PLANT "A" VS. WIND DIRECTION FOR DIRECT CONTAINMENT RELEASE

FIGURE 7   MAXIMUM V_a (X/Q) ON PLANT "B"
VS. WIND DIRECTION FOR
RELEASE FROM PLANT VENT

Legend
— — — Intake #16
. . . . Intake #18
——— Intake on Line

FIGURE 8   MAXIMUM V_a (χ/Q) ON PLANT "B" VS. WIND DIRECTION FOR DIRECT CONTAINMENT RELEASE

FIGURE 9   PLAN VIEW OF NUCLEAR PLANTS SHOWING STANDARD AND ALTERNATE VENTILATION INTAKES AND PREFERRED INTAKE VS WIND DIRECTION

TABLE 10

MAXIMUM V_a (χ/Q) FOR ON-LINE INTAKES

PLANT	STACK VENT RELEASE	CONTAINMENT RELEASE
A	1.8×10^{-5} (from Figure 5)	6.0×10^{-4} (from Figure 6)
B	1.6×10^{-5} (from Figure 7)	3.3×10^{-4} (from Figure 8)

Note: Units of M^{-2}, where V_a = 1.5 m/sec

DISCUSSION

SCHUERMAN: How did the Reynolds numbers compare between model and prototype?

NASSANO: The Reynolds number for the model was equal to the Reynolds number for the prototype.

EVALUATION OF CONTROL ROOM
RADIATION EXPOSURE

T. Y. Byoun and J. N. Conway
Breeder Reactor Division
Burns and Roe, Inc.
700 Kinderkamack Road
Oradell, New Jersey 07649

Abstract

This paper discusses the development, and practical
test applications of a computer program "AID" (Accident
Inhalation Dose). The "AID" computer code calculates the
external cloud doses (gamma, whole body and beta skin) and
the resultant inhalation doses after a radiological release
based upon site meteorological data and a wide range of
possible ventilation and filtration designs.

I. Introduction

At the 13th AEC Air Cleaning Conference, a paper was
presented by K.G. Murphy and K.M. Campe of the Directorate
of Licensing entitled, "Nuclear Power Plant Control Room
Ventilation System Design for Meeting General Criteria 19."[1]
After evaluating this paper, it was apparent that it could
provide the basis for a computer code to analyze a variety
of possible ventilation and filtration options which might
be selected to meet General Design Criteria 19 of 10 CFR 50,
Appendix A. In the course of developing this code, it was
decided that it should function as a practical design tool
by permitting easy parametric changes of:

1. Filter efficiency

2. Filtered recirculation rate in the Control Room

3. Filtered intake rate entering the Control Room

4. Filtered recirculation rate in the Reactor Containment Building

5. Filtered exhaust rate from the Reactor Containment Building

6. Source-receptor configurations

This computer code allows the user to either analyze a previously selected ventilation/filtration system or to selectively vary any of the above variables until an acceptable system is created. Since this computer code is very inexpensive to run (less than $3.00 per run), it has been our practice to fix those variables which are already frozen in the design and then to allow the computer code to optimize each of the remaining variables on successive runs. This approach allows us to see the effect on the ventilation design as each of the remaining variables is iterated until an acceptable design evolves.

II. Method of Analysis

Under a reactor accident condition, the radioactive isotopes of the core inventory may become airborne inside the containment. The continuous activity release from the containment would contaminate the air in the vicinity of the control room (CR) air intake(s) depending upon the on-site meteorological conditions. The exposure or inhalation of the airborne activity which is introduced into the CR via ventilation systems will contribute to the operating personnel radiation dose during the post-accident period.

The mathematical models incorporated into the "AID" program based on the above scenario consist of the containment model, meteorological data treatment, the ventilation system simulation for both the containment and the CR, and the time-integrated dose model. The diagrams of the system which can be handled by the "AID" are shown in Figures 1 and 2.

The time-integrated radiation exposure based on the above models can be expressed as follows:

$$D_i = F_{ij} \cdot \int_{T_1}^{T_2} A(t) \cdot \frac{X}{Q} \cdot R(t) \, dt, \tag{1}$$

where:

D_i = the time-integrated radiation exposure (Rem) due to i^{th} radioisotope

F_{ij} = effective dose conversation factors for the jth organ, that is, whole body, beta-skin, lung, bone, and thyroid

$A(t)$ = activity release rate (ci/sec) from the containment at time, t, after an accident

X/Q = effective atmospheric dilution factors (sec/m^3) based on the site meteorological data

$R(t)$ = activity dilution factor inside the CR depending upon the ventilation condition.

1. Containment Model

The term, $A(t)$, in equation (1) is the function of the containment leakage rate, ℓ, and containment cleanup system design (See Fig. 1):

$$A(t) = q_{oi} \cdot EXP\left[-(\lambda_i + \ell + \mathcal{E}_2' \, \mathcal{V}_2'/\mathcal{V}_c)t\right] \cdot \ell \cdot (1 - \mathcal{E}_3') \qquad (2)$$

where:

q_{oi} = source strength (C_i) of ith isotope at time zero after an accident

λ_i = decay constant (1/sec) of ith isotope

$\mathcal{E}_2' \text{ and } \mathcal{E}_3'$ = filter efficiency of the containment recirculation and exhaust filter, respectively

$\mathcal{V}_2'$ = in-containment recirculation rate (CFM)

$\mathcal{V}_c$ = free volume of the containment.

2. Control Room Filtration Systems

The activity dilution factor in the CR, $R(t)$, in equation (1) is a function of the CR filtration system design (See Fig. 1) and is shown as:

$$R(t) = \frac{\mathcal{V}_1(1-\mathcal{E}_1) + \mathcal{V}_3}{\mathcal{V}_1 + \mathcal{V}_2\mathcal{E}_2 + \mathcal{V}_3} \cdot \left\{ 1 - EXP\left[-(\mathcal{V}_1 + \mathcal{V}_2\mathcal{E}_2 + \mathcal{V}_3)t/\mathcal{V}_R\right]\right\} \qquad (3)$$

where:

$\mathcal{V}_1, \mathcal{V}_2, \text{ and } \mathcal{V}_3$ = air-intake rate through filter ($\mathcal{V}_1$), filtered recirculation rate ($\mathcal{V}_2$), and unfiltered air infiltration rate ($\mathcal{V}_3$) in the unit of CFM

$\mathcal{E}_1 \text{ and } \mathcal{E}_2$ = efficiency of the filter trains for intake and recirculation, respectively

$\mathcal{V}_R$ = control room free volume (ft^3).

3. Meteorological Data Treatment

The effective dilution factor (χ/Q-value) is treated as a function of site meteorological data as well as the source-receptor configuration. Adjustment factors to account for the long term meteorological averaging consist of: (1) occupancy factor, (2) wind speed factor, and (3) wind direction factor. (1)

The possible source-receptor configuration are expected to be: (a) diffuse vs. point release-point receptor, (b) ground vs. elevated release, and (c) single vs. multiple air-intake arrangements. Three different formula for the χ/Q evaluation are incorporated into the "AID" program depending upon the above source-receptor configurations.

(3.A) Evaluation of Diffusion Coefficients

Standard deviations for both horizontal crosswind (σ_y) and vertical crosswind direction (σ_z) are based on the Pasquill's diffusion curves. (2) For the desired Pasquill's stability condition (from Type A to Type G), the program "AID" estimates the coefficients by using the interpolation formula given below: (2)

$$\sigma_y(x) = \alpha \cdot x^\beta , \tag{4}$$

$$\alpha = \ln\left\{ \sigma_y(x_2)/\sigma_y(x_1) \right\} / \ln\left(x_2/x_1 \right) \tag{4a}$$

$$\beta = \sigma_y(x_1) \cdot x_1^{-\alpha} \tag{4b}$$

where:

$\sigma_y(x)$ = standard deviation of the gas concentration in the horizontal crosswind at distance, X , from the release point

$\sigma_y(x_1)$ and $\sigma_y(x_2)$ = standard deviations σ_y , at reference distances X_1 and X_2 which are permanently stored into the program as a function of the stability condition.

The coefficient for vertical crosswind direction, σ_z , is evaluated by using the same equations given above.

(3.B) χ/Q -Values as a Function of Source-Receptor Configuration

(B.1) Volume Source Formula [2]

$$\chi/Q = \frac{1}{\pi u_o \Sigma_y \Sigma_z} \cdot EXP\left(-\frac{h^2}{2\Sigma_z^2}\right) \qquad (5)$$

where:

u_o = five percentile wind speed in meter/sec

h = effective height of source (meters)

$$\Sigma_y = \left(\sigma_y^2 + a/2\pi\right)^{1/2} \qquad (5a)$$

$$\Sigma_z = \left(\sigma_z^2 + a/2\pi\right)^{1/2} \qquad (5b)$$

a = the cross-sectional area of the containment (m^2)

The above equations are for general cases, such as volumetric release, elevated releases, or point-ground level releases.

(B.2) Diffuse Release and Point Receptor [2]

$$\chi/Q = u_o^{-1} \cdot \left\{\pi \sigma_y \sigma_z + a/(K+2)\right\}^{-1} \qquad (6)$$

where:

$K = 3/(s/d)^{1.4}$ for single air-inlet arrangement (6a)

$K = 0$ for dual inlets (6b)

s = distance between the containment surface and receptor (meters)

d = containment diameter in meters.

Equation (6) could be applied for the following cases: [1]

(1) Diffuse release-point receptor, or vice versa

(2) Point release-point receptor with source-receptor elevation difference greater than 30% of containment height

(3) Dual air-inlets located on the major plant structures contiguous to the CR (see eq. 6b)

(B.3) Remotely-Placed Dual Inlets[1]

$$\frac{X}{Q} = \frac{0.16}{L u_o X} \qquad (7)$$

where:

X = distance from source to the closest inlet (meters)

L = vertical mixing layer in meters taken as the containment height divided by 2 for the consideration of building wake factor.

Equation (7) could be applied when the dual inlets are placed about 180 degrees apart from the release point and each inlet is located well away from the major structure.[1]

(3.C) Long Term Meteorological Data Averaging

The five percentile $\frac{X}{Q}$ calculated from equations (5) to (6) is reduced on the basis of long term averaging considerations. These consist of: (1) wind speed factors, w_s , (2) wind direction factors, w_d , and (3) occupancy factors, w_o .

The first step to calculate the wind speed and wind direction factors is to determine the number of 22.5° wind sectors that result in receptor exposure.[1]

$$
\begin{array}{lllll}
n & = & 10 & \text{if} & 0.0 \le s/d \le 0.38 \\
n & = & 8 & \text{if} & 0.38 < s/d \le 0.50 \\
n & = & 7 & \text{if} & 0.50 < s/d \le 0.63 \\
n & = & 6 & \text{if} & 0.63 < s/d \le 0.82 \\
n & = & 5 & \text{if} & 0.82 < s/d \le 1.24 \\
n & = & 4 & \text{if} & 1.24 < s/d \le 2.47 \\
n & = & 3 & \text{if} & \quad\quad\;\; s/d > 2.47.
\end{array} \qquad (8)
$$

Notations used in eq. (8) are described previously in eq. (6a).

The wind speed factor for the "p"-percentile wind speed, w_s, is given by using the annual joint frequency data of wind direction and speed shown in Table 1, and the following equations:

$$w_s = \frac{u_o}{u_p} \qquad (9)$$

$$p = \sum_{i=N_1, j=1}^{i=N_2, j=\ell} f_{ij} \bigg/ \sum_{i=N_1, j=1}^{i=N_2, j=8} f_{ij} \qquad (10)$$

$$u_p = \left(u_\ell - u_1\right)/2 \tag{11}$$

where:

u_o and u_p = wind speeds of five percentile and "p"-percentiles, respectively

f_{ij} = annual joint frequency data for i^{th} wind sector and j^{th} wind speed as shown in Table 1

ℓ = ℓ^{th} wind speed column in Table 1 which would give "p"-percentile speed

N_1 and N_2 = N_1^{th} and N_2^{th} 22.5° wind sectors which are calculated by using eq. (8). (Winds blowing from $N_1 \sim N_2$ sectors will result in the receptor exposure.)

p = the wind speed percentile to be used for different time intervals.

The wind speed percentiles, p, applicable during subsequent time intervals after an accident are: (1) 5% during 0-8 hr. period, (2) 10% during 0-24 hr. period, (3) 20% for 1-4 days, and (4) 40% during 4-30 days period.[1]

The wind direction factor, W_d, is given by evaluating the fraction of time frequency of the receptor exposure (See Table 3),[1]:

$$F_d = \sum_{i=16, j=8}^{i=N_2, j=8} \sum_{i=N_1, j=1} f_{ij} \tag{12a}$$

$$\sum_{i=1, j=1} f_{ij} = 1 \tag{12b}$$

Based on the above fraction of time of wind blowing from source to receptor, the wind direction factors, W_d, during subsequent time intervals after an accident are used:[1]

$$W_d = 1 \text{ for 0-8 hrs. period} \tag{13a}$$

$$W_d = 0.75 + 0.25 \cdot F_d \text{ for 0-25 hrs. period} \tag{13b}$$

$$W_d = 0.5 + 0.5 \cdot F_d \text{ for 1-4 days period} \tag{13c}$$

$$W_d = F_d \tag{13d}$$

4. Dose Models

The "AID" program calculates the external cloud doses (gamma, whole body and beta-skin) and inhalation doses (thyroid, lung, and bone dose). Effective dose conversion factors, F_{ij}, in equation (1) are illustrated below:

(4.A) External Whole Body (WB) Dose[2]

$$F_{ij} = 0.25 \, E_{\gamma i} \tag{14a}$$

for the WB dose based on the semi-infinite cloud model

$$F_{ij} = 0.25 \cdot E_{\gamma i} \cdot V_R^{0.338} / 1173 \tag{14b}$$

for the external WB dose due to the activities dispersed inside the control room (CR).

where:

$E_{\gamma i}$ = total gamma ray disintegration energy (MeV/sec) of ith isotope[4]

$V_R^{0.338} / 1173$ = Geometry factor for the immersed cloud in the CR based on 0.733 MeV of average gamma energy.[1]

(4.B) Beta-Skin Dose[2]

The beta-skin dose calculation in the "AID" code has two options; with and without taking a credit of dead skin depth:

$$F_{ij} = 0.23 \, \bar{E}_\beta \; ; \text{ for surface dose} \tag{15}$$

$$F_{ij} = 0.23 \, \bar{E}_\beta \cdot \alpha \cdot \left\{ c^2 \left[3 - \exp(1 - Vd/c) \right] - \frac{Vd}{c} \left(2 + \ln \frac{c}{Vd} \right) + \exp(1 - Vd) \right\} \tag{16}$$

for the depth beta dose[2]

where:

$\bar{E}_\beta$ = average beta energy per disintegration (MeV/dis)

$$\bar{E}_\beta = 0.33 \cdot E_\beta^{max} \cdot \left(1 - z^{1/2}/50 \right) \cdot \left\{ 1 + \left(E_\beta^{max} \right)^{1/2} / 4 \right\} \tag{16a}$$

z = number of electrons per atom

E_β^{max} = maximum beta disintegration energy (MeV/dis)

d = dead skin depth in gr/cm^2

c = 2 for 0.17 MeV $\leq E_\beta^{max} <$ 0.5 MeV

c = 1.5 for 0.5 MeV $\leq E_\beta^{max} <$ 1.5 MeV

c = 1 for 1.5 MeV $\leq E_\beta^{max} <$ 3 MeV

$$\alpha = \left[3c^2 - (c^2 - 1)e \right]^{-1} \tag{16b}$$

$$\nu = 37.2/\left(E_\rho^{max} - 0.036\right)^{1.37} \tag{16c}$$

$$\left[3 - exp\left(1 - \frac{\nu d}{c}\right) - \frac{\nu d}{c} \cdot \left(2 + \ln \frac{c}{\nu d}\right)\right] = 0 \quad \text{if } d \geq c/\nu \tag{16d}$$

(4.C) Inhalation Dose

Inhalation doses which can be estimated by "AID" program are thyroid, bone, lung, and whole body doses.

$$F_{ij} = \langle BR \rangle \cdot \overline{W}_{ij} \tag{17}$$

where:

$\langle BR \rangle$ = standard man's breathing rate (m^3/sec)

$\overline{W}_{ij}$ = j^{th} organ inhalation dose conversion factors $(Rem/c_i \cdot \text{-inhaled})$ due to i^{th} isotope [3]

5. "AID" -- Flow Diagram

The simplified flow diagram of the "AID" program is shown in Fig. 3.

The main input data required for "AID" program consist of:

(1) Containment leakage and geometry data (containment diameter, height, free volume),

(2) site meteorological data -- annual joint frequency data as a function of wind direction and speeds (See Table 1),

(3) initial activity data as a function of isotope,

(4) source-receptor configuration,

(5) filtration system conditions for both containment and control room based on the desired model shown in Fig. 2,

(6) option control card.

III. Discussions

A series of parametric studies on the control room(CR) accident dose analysis is usually required to develop acceptable alternate CR filtration system design which meet the regulatory requirements. The CR habitability system design features which are impacted by the above dose analysis are mainly:

(1) CR filter efficiency requirements,

(2) filtered recirculation rate(CFM) requirements foi
the control room or for the reactor containment,

(3) single air-inlet vs. multiple inlet arrangements
including the location of the inlets,

(4) leak tightness of the control building to prevent
the unfiltered infiltration of the radioactivities
and to minimize the air-intake rate required for the
pressurization of the CR.

The "AID" program is a practical tool for these parametric
studies since it enables the designer to make a timely decision on
the above design in the preliminary design stage. The special
features of the "AID" code are as follows:

(1) Built-in routine for the versatile treatment of
the meteorological data, including wind sector
averages, and the long term X/Q -value adjustment
factors, with minimum input requirements.

(2) Various options for different source-receptor
configurations.

(3) Options for the site boundary analysis and activity
concentration analysis in a certain cell due to
the activity release from an adjacent cell.

(4) Several options in choosing the filtration system
models for the containment and the control room
are available (See Fig. 2).

(5) Time-dependent containment leakage rate can be
handled.

(6) A library of 295 isotopic data including the organ
dose conversion factors.[3,4]

(7) Automatic updating routines for different control
room/containment recirculation rates, source-receptor
distances, and time intervals.

IV. Conclusion

The "AID" program has proven itself to be an extremely
valuable tool which we have used for both the scoping and de-
tailed analyses that must be performed for a nuclear power plant
to determine the control room vertilation design. This program
is presently be used for this purpose for the Clinch River Breeder
Reactor Plant. Results of a typical sample problem are included.

The authors wish to express their appreciation to Mr. F. Patti, Burns and Roe, Inc., for his continous guidance and advice and Messrs. A.E. Klickman, P.J. Babel and E.P. Stergakas for their thorough checking and criticisms in the development of the "AID" program.

References

(1) K.G. Murphy and K.M. Campe, "Nuclear Power Platn Control Room Ventilation System Design for Meeting General Criterion 19": Proceedings of the 13th AEC Air Cleaning Conference, Vol. 1, CONF-740807, pp. 401-430, August, 1974.

(2) D.H. Slade, Editor, "Meteorology and Atomic Energy", TID-24190, pp. 102-113, 331-332, and pp. 406, July, 1968.

(3) E. Specht, et. al., "Description of the COMRADEX-II Code". TI-001-130-048, pp. 41-70, Atomics International, February, 1975.

(4) Nuclear Data Group ORNL, D.H. Horen, et. al., Editor, "Nuclear Level Schemes A=45 through A=257", Academic Press, Inc., 111 Fifth Ave., N.Y., N.Y. 10003, 1973.
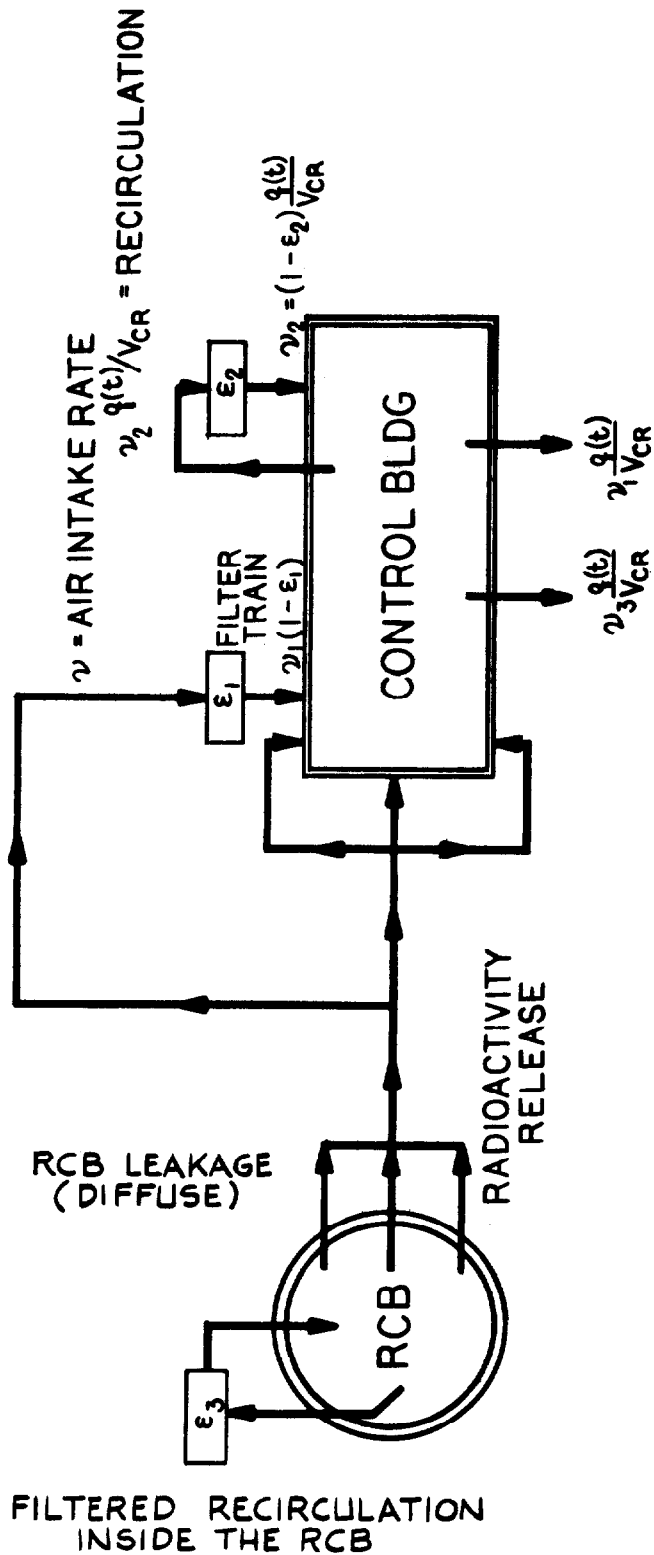
NOTE:

V_{CR} = TOTAL FREE VOLUME OF THE CONTROL ROOM

$q(t)$ = AMOUNT OF CONTAMINATED AIR INTRODUCED TO THE CONTROL ROOM AS A FUNCTION OF TIME AFTER ACCIDENT

$\varepsilon_1, \varepsilon_2$ = FILTER EFFICIENCIES

FIG. I CONTROL BLDG EMERGENCY VENTILATION SYSTEM MODEL
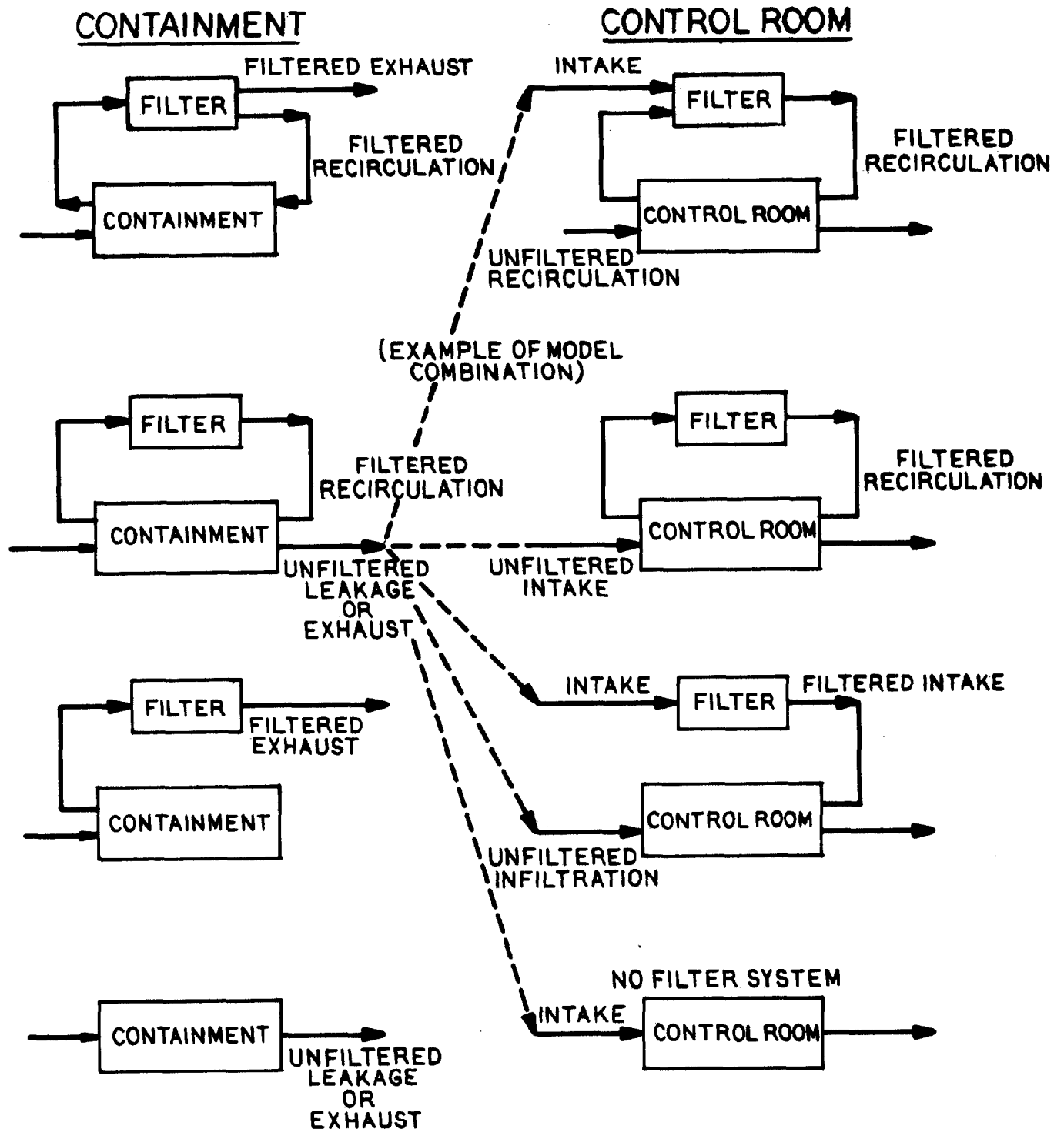
FIG. 2 "AID" OPTIONS OF FILTER MODELS FOR CONTAINMENT AND CONTROL ROOM

FIGURE 3 - SIMPLIFIED FLOW DIAGRAM OF THE
COMPUTER CODE "AID"
(ACCIDENT INHALATION DOSE)
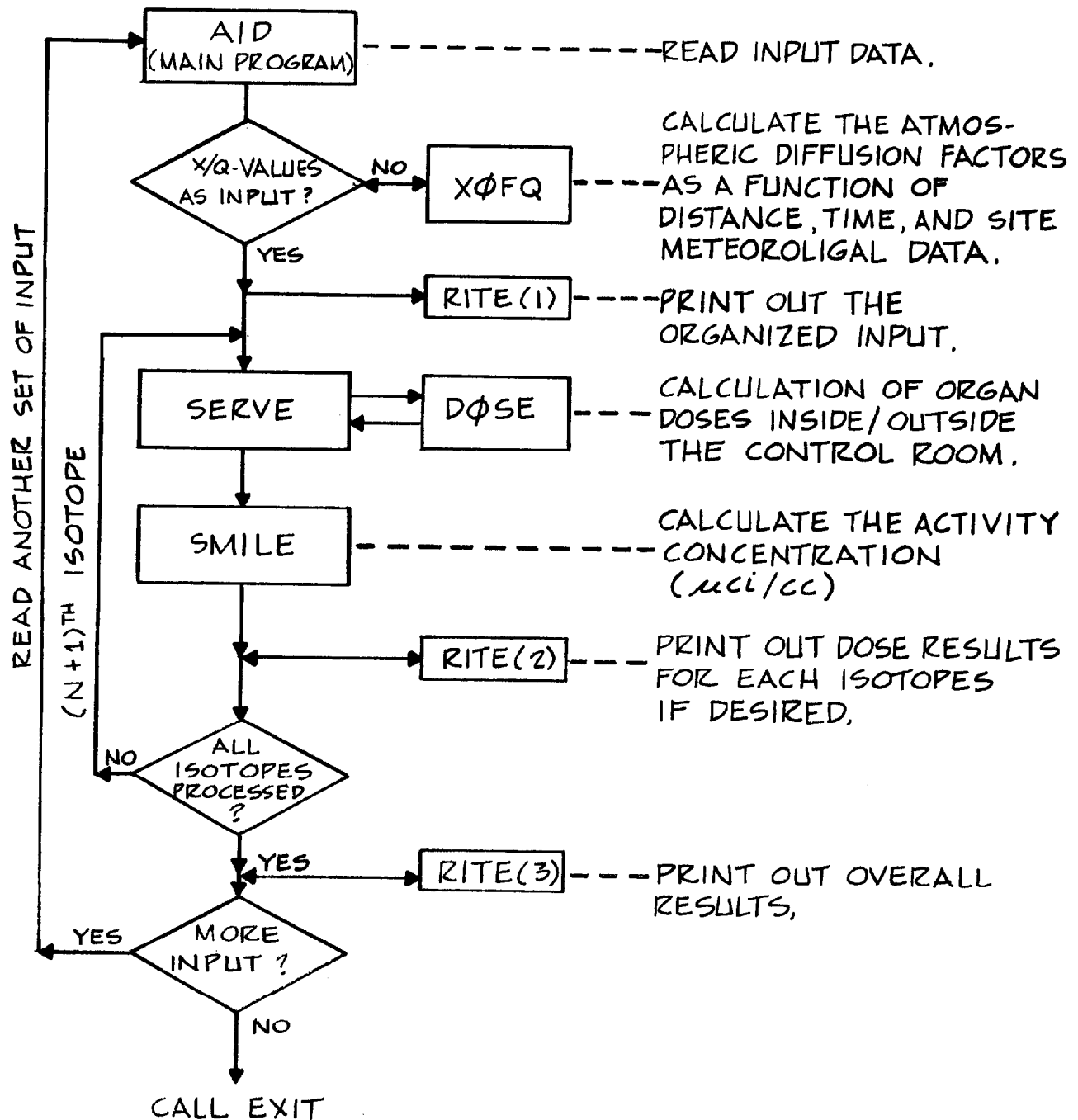
TABLE 1 - <u>ANNUAL JOINT FREQUENCY OF WIND DIRECTION</u>
<u>AND WIND SPEED (MEASURED DATA)</u>

WIND SPEED (U_j) / WIND DIRECTION (i)	ANNUAL JOINT FREQUENCY DATA (F_{ij}) AS FUNCTIONS OF WIND DIRECTION (*) AND WIND SPEED (**)						
	U_1	U_2	.	.	.	U_7	U_8
N (i = 1) (*)	$f_{1,1}$	$f_{1,2}$	.	.	.	$f_{1,7}$	$f_{1,8}$
NNE (i = 2)	$f_{2,1}$	$f_{2,2}$	.	.	.	$f_{2,7}$	$f_{2,8}$
NE (i = 3)	.	.	.	.	.	.	.
.	.	.	.	.	.	.	.
.	.	.	.	.	.	.	.
.	.	.	.	.	.	.	.
NW (i = 15)	.	.	.	.	.	$f_{15,7}$	$f_{15,8}$
NNW (i = 16)	$f_{16,1}$	$f_{16,2}$	.	.	.	$f_{16,7}$	$f_{16,8}$

(*) N (i = 1): WIND DIRECTION BLOWING FROM 22.5 DEGREE SECTOR OF THE NORTH DIRECTION (i = 1,2, ... 16)

(**) U_j : j^{TH} WIND SPEED (KNOTS OR METER/SEC)

SAMPLE PROBLEM

Based upon a radiological release from the Reactor Containment, "AID" runs were made for Case I - Single Control Room Intake and for Case II - Dual Control Room Intakes. The only variable used was the Control Room filter recirculation rate. The initial "AID" run defined the threshold recirculation rate necessary to meet the Guideline Dose for each organ.

FOR CASE I - A&B (SINGLE CONTROL ROOM INTAKE)

ORGAN NAME	THRESHOLD RECIRC. RATE (CFM) TO MEET GUIDELINE DOSE FOR EACH ORGAN	DOSE RESULTS (REM) CORRESPONDING TO THE THRESHOLD RECIRCULATION RATE FOR EACH ORGAN				
		WHOLE BODY	BETA-SKIN	THYROID	LUNG	BONE
WHOLE BODY	2,000	4.0	4.1	11.3	17.0	140.
BETA-SKIN	2,000	4.0	4.1	11.3	17.0	140.
THYROID	1,000	6.9	4.1	18.7	30.6	252.
LUNG	4,000	2.3	4.1	6.3	9.1	74.
BONE	12,000	1.0	4.1	2.3	3.2	26.

Based upon the above information two options were selected for further evaluation. Specific runs were made for each option with the results as shown below.

CASE A. SINGLE INTAKE AND SINGLE FILTER TRAIN:
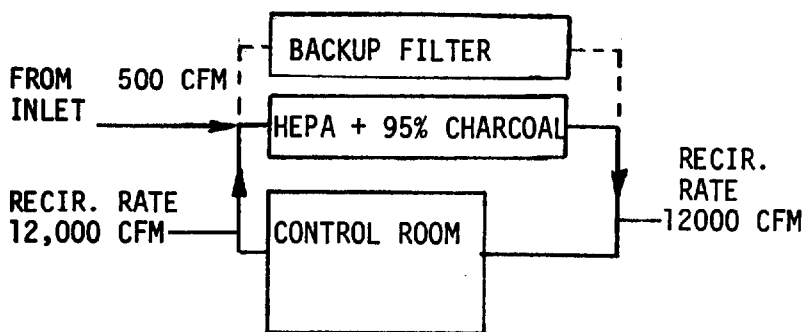
ORGANS	DOSES (REM)
WHOLE BODY	1.0
BETA-SKIN	4.1
THYROID	2.3
LUNG	3.2
BONE	26.0

CASE B. SINGLE INLET AND COMBINED FILTER TRAINS:
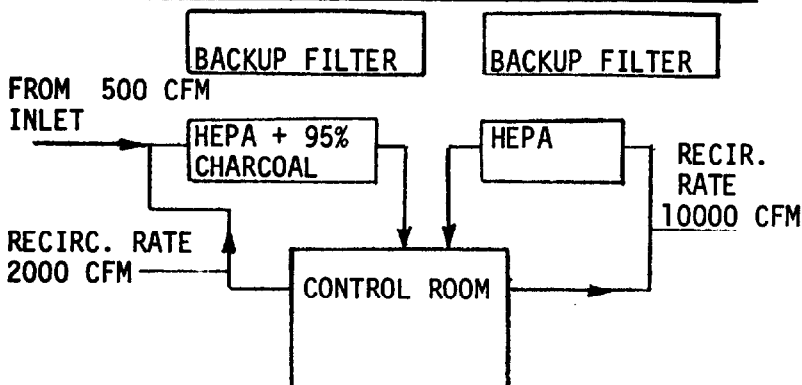
ORGANS	DOSES (REM)
WHOLE BODY	1.0
BETA-SKIN	4.1
THYROID	11.3
LUNG	3.2
BONE	26.0

FOR CASES II - A&B (DUAL CONTROL ROOM INTAKES)

ORGAN NAME	THRESHOLD RECIRC. RATE (CFM) TO MEET GUIDELINE DOSE FOR EACH ORGAN	DOSE RESULTS (REM) CORRESPONDING TO THE THRESHOLD RECIRCULATION RATE FOR EACH ORGAN				
		WHOLE BODY	BETA-SKIN	THYROID	LUNG	BONE
WHOLE BODY	1,000	4.5	1.2	7.4	20.2	170.
BETA-SKIN	1,000	4.5	1.2	7.4	20.2	170.
THYROID	1,000	4.5	1.2	7.4	20.2	170.
LUNG	2,000	2.4	1.2	4.2	10.6	89.
BONE	8,000	0.7	1.2	1.2	2.8	23.2

Based upon the above information two options were selected for further evaluation. Specific runs were made for each option with the results as shown below.

CASE A. DUAL INLETS AND SINGLE FILTER TRAIN:
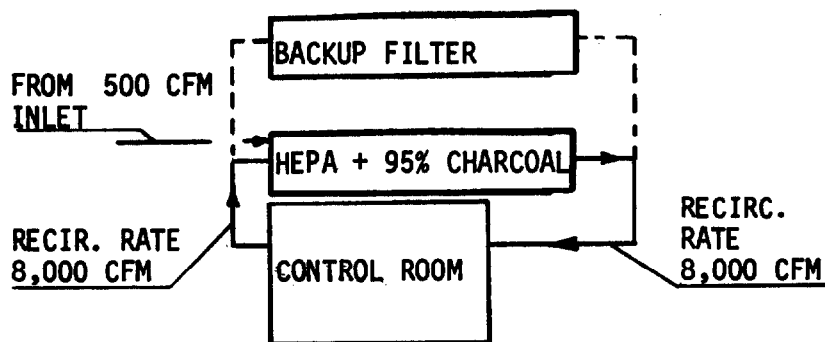
ORGANS	DOSES (REM)
WHOLE BODY	0.7
BETA-SKIN	1.2
THYROID	1.2
LUNG	2.8
BONE	23.2

CASE B. DUAL INLETS AND COMBINED FILTER TRAINS:
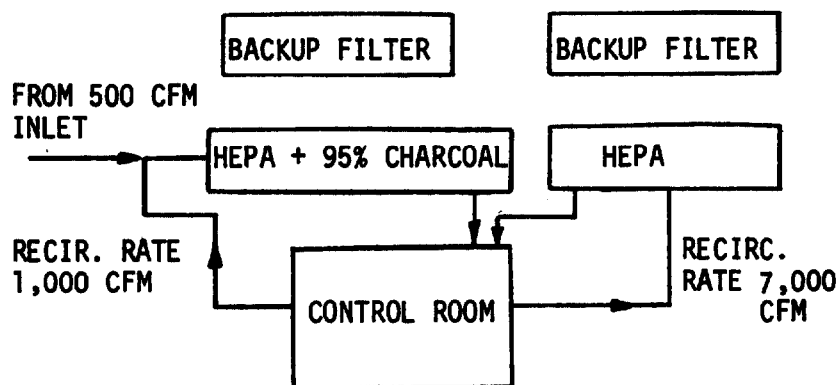
ORGANS	DOSES (REM)
WHOLE BODY	0.7
BETA-SKIN	1.2
THYROID	7.4
LUNG	2.8
BONE	23.2

DISCUSSION

MUNSON: I would like to inquire about the recirculated HEPA filter. What is it doing?

CONWAY: In our case, it is reducing the average concentration in the control room. We needed it because of plutonium. It was a specific requirement there.

MUNSON: Is this requirement directly related to the outdoor intake air cleanup by-pass that must be assumed in the dose calculation? I am sort of surprised to see particulate in the control room.

CONWAY: It was our initial intent not to have recirculation, but we found that we couldn't handle it by any other mechanism. We had run outside air quantities down to 500 CFM. We decided it was an absurdity and below the amount we needed to pressurize the load. At that point, there was no other avenue open to us.

MUNSON: Is that the assumed amount that you have to consider?

CONWAY: Yes, and it really hurt us. In this calculation, we went to the minimum number that is allowed by NRC. I believe it was in the order of 3 CFM. That alone was significant.

SESSION IX

OPEN END

Tuesday, August 3, 1976
CHAIRMAN: M. W. First

COORDINATION OF FIRE TERMINOLOGY IN ASTM
J. R. Gaskill

ULTRAHIGH EFFICIENCY SPARKPROOF ELECTROSTATIC PRECIPITATION
J. K. Thompson, R. C. Clark,
G. H. Fielding

EFFECT OF EXPOSURE TIME IN THE PREHUMIDIFICATION OF CHARCOALS FOR
METHYL IODIDE TRAPPING
V. R. Deitz, C. H. Blachly

IODINE EMISSION DURING A PROGRAMMED HEATING OF IMPREGNATED CHARCOALS
IN CARRIER AIR
V. R. Deitz, J. B. Romans

AN EXPERIMENTAL INVESTIGATION OF THE RELATIONSHIP BETWEEN BED PACKING
AND FLOW DISTRIBUTION
H. C. Parish, R. C. Muhlenhaup,
W. W. Vogelhuber

A CONTAINMENT AND RECOVERY SYSTEM FOR FUEL-REPROCESSING PLANTS
T. R. Galloway

REDUCING AIR CLEANUP SYSTEM COSTS
H. R. Reedquist, Jr.

ABSOLUTE FILTERS: EFFECTIVE FILTERING MEDIA
G. H. Cadwell, Jr.

OPENING REMARKS OF SESSION CHAIRMAN:

Session 9 is called "Open End" for a specific purpose. The intention is to open the session to short topics, to things that are in progress in the research labs but have not yet developed to the point where they are suitable for formal papers. It is to permit people to ask questions, to make comments, and to ask other people questions which will elicit useful answers. This is not intended to be a session for leftover papers or last minute formal papers, but, rather, a chance to discuss with colleagues many points which, perhaps, did not come up adequately or at all in the structured sessions. For that reason, the time allotted to each of the speakers will be brief.

COORDINATION OF FIRE TERMINOLOGY IN ASTM*

James R. Gaskill
University of California, Lawrence Livermore Laboratory
Livermore, California 94550

During the past few years, legal and technical questions have arisen concerning certain terms used in the field of fire technology. Such expressions as "non-combustible," "self-extinguishing," "slow-burning," have been challenged by government agencies and by fire protection engineers.

The American Society for Testing and Materials (ASTM) has in its various standards and testing committees subcommittees whose function is the development of appropriate terminology associated with the standards and test methods. When it became evident two or three years ago that the several different committees were each defining the same term in somewhat different ways, it was decided within the Society to set up coordinating groups each associated with a particular technology. At the present time two such working groups exist: WG-1 — concerned with terminology in the field of fire technology; and WG-2 — concerned with a similar function in regard to building materials.

Although in the interest of efficiency working groups are restricted as to numbers, committees having an interest in the particular technology are invited to provide representation and expertise. Thus, on Working Group I, we have representation from the Fire Tests Standards Committee, the Fire Hazards Standards Committee, committees on plastics, wood, rubber, textiles, and electrical insulating materials. Some members cover more than one area of interest, e.g., the National Bureau of Standards, ISO (TC-92 — International Fire Tests Standards), the Consumer Products Safety Commission, and the National Fire Protection Association.

WG-1 has accumulated a list of several hundred terms from within ASTM and from outside organizations. It has established priority lists for terms to be considered, and then proceeds to ballot on and discuss results of these ballots following the usual ASTM procedures. When coordinated terms have been finally agreed upon, they are sent to committees having an interest in these terms for comment and possibly further refinement.

It is proposed to publish terms in a particular field of technology in the form of a glossary which may eventually become a technical dictionary.

The two tabulations included herewith represent lists of terms which have been coordinated by WG-1 and are currently under various stages of review as indicated. We have found it necessary to go back to fundamental terms because in many cases the standard dictionary definitions are not deemed adequate. I present them here today for

your general consideration with the idea that perhaps a similar coordinating effort should be made in the field of air-cleaning technology.

TERMINOLOGY IN FIRE TECHNOLOGY

I. Coordinated Terms Currently Under ASTM General Review

ablation   (n) - a self-regulating heat and mass transfer process in which incident thermal energy is expended by loss of material from exposed surfaces.

afterglow (n) - emission of light, usually subsiding, from a material undergoing combustion, but occurring after flaming has ceased.

char (v) - to form carbonaceous material during pyrolysis or during incomplete combustion.

char (n) - carbonaceous material formed by pyrolysis or incomplete combustion.

combustion (n) - a chemical process of oxidation that occurs at a rate fast enough to produce both heat and light either as glow or flames. Note: Some oxidation, such as that of hydrogen, emits radiation outside the visible spectrum.

fire exposure (n) - the heat flux of fire, with or without direct flame impingement, to which a material, product, building element or assembly is exposed.

flame (n) - a hot luminous zone of gas or matter or both in gaseous suspension that is undergoing combustion.

flame spread (n) - the propagation of flame along or across a surface.

flash point (n) - the lowest temperature, corrected to 101.3 kPa (1013 millibars) of pressure, of a sample at which application of an ignition source causes the vapor of the sample to ignite under specified conditions of test.

glow (n) - (1) visible light given off by a substance because of its high temperature; (2) visible light, other than from flaming, emitted from a solid undergoing combustion.

ignition (n) - the initiation of combustion. Note: The combustion may be evidenced by glow, flame, detonation or explosion. The combustion may be sustained or transient.

pyrolysis (n) - irreversible chemical decomposition caused by an increase in temperature without oxidation.

self-ignition temperature - (misleading term - not recommended).

smoldering (n) - combustion of a solid material without flame, often evidenced by smoke. Note: Smoldering can be initiated by small or low-temperature sources of ignition, especially in loose materials, and may persist for an extended period of time after which a flame might be produced.

standard temperature/time curve - in fire testing, a curve used to define the prescribed furnace temperature with progressing time; that given in Method E-119, unless otherwise specified.

temperature (n) - the thermal state of matter as measured on a defined scale.

II. Coordinated Terms under Review by Interested Committees

fire severity (n) - the potential of a fire to inflict damage. Note: An evaluation of fire severity includes the properties - temperature, effective heat flux, rate of heat release, and duration - of the fire. Estimating fire severity also requires consideration of the thermal characteristics of a product, or component of a fire enclosure.

fire severity test exposure (n) - the measure of fire severity resulting from a standard fire test exposure. Note: As applied to ASTM methods E-119, E-152, and E-163 - the ratio of the area of the temperature/time curve of the average test furnace temperature to that under the standard temperature/time curve. In each case time is measured from the start of the test to the end of the test or time-of-failure; temperature is measured above a base point of 20°C (68°F).

flame spread rate (n) - the surface distance or area covered by a propagating flame per unit of time.

flame spread index (n) - a number or classification indicating a comparative measure of flame spread or flame spread rate as determined by a specific test method. Note: As applied to a particular test method, a flame spread index should be defined as to what it measures, e.g., distance, area, distance/time, or area/time, and should include the appropriate dimensions.

fire retardant (n) - a substance added to or incorporated into a material which by such incorporation or addition hinders the ease of ignition, flammability or combustibility of the resulting product.

smoke (n) - the visible and invisible airborne products - solids, liquids, and gases - evolved when a material undergoes pyrolysis or combustion.

DISCUSSION

FIRST: I'll exercise the chairman's privilege and make a comment. I'm one of the people that Mr. Gaskill has argued with about the term "smoke." I believe that optical density is an important characteristic of smoke and I asked him why he wished to redefine a word in common usage when it's not necessary. Perhaps, Mr. Gaskill will tell us why he prefers to call "the visible and invisible airborne products of a material that undergoes pyrolysis or combustion", "smoke" instead of "decomposition products."

GASKILL: "Smoke" is to be used to designate decomposition products by a particular process called pyrolysis. It is a special phenomenon in the field of fire. Although one can break up a product chemically and get a number of products out of it, I think we use "smoke" when discussing the phenomena associated with heat, flame, and radiation in fires. It is peculiar to that subject. Apparently, a number of my colleagues in ASTM agree with me.

ULTRAHIGH EFFICIENCY SPARKPROOF ELECTROSTATIC PRECIPITATION

J. K. Thompson, R. C. Clark and G. H. Fielding
Chemical Dynamics Branch
U. S. Naval Research Laboratory
Washington, D. C. 20375

Abstract

Low-conductivity nonmetallic plates for two-stage electrostatic precipitators allow design improvements and simplifications such that efficiencies of 99.99+ percent appear attainable at an air speed of 250 fpm and a pressure loss of 0.1 inch of water.

Text

In production designs, the two-stage electrostatic precipitator has been limited to filtration efficiencies of 85-95 percent. This performance has been satisfactory in many recirculating air systems, where little would be gained by higher efficiency operation. In many other situations however, including some in the nuclear industries, only those filtration efficiencies in the 99.9+ percent range are acceptable.

Over 25 years ago, an NRL team began to study possible improvements in two-stage electrostatic precipitator design, using the Westinghouse Model PH-12 Home Precipitator as a model. Our first effort was to place two of these units in series. The result was puzzling: the efficiency of two units in series was the same as that of either unit alone. This suggested localized areas of low filtration efficiency which were in the same locations in both units. We now began probing the downstream face of one of the units with a suction tube connected to an NRL Smoke Penetrometer. In a matter of minutes a definite pattern of low-efficiency areas was evident. It was clear that a significant fraction of the airflow through the precipitator (and this was shown to be true of other two-stage ESP's) was bypassing the collection fields through gaps between the high-voltage plates and the grounded aluminum housing. Closing these gaps with phenolic plastic strips and plates raised filtration efficiencies more than tenfold; to 99.5 percent or better. We now believe that at least part of the residual inefficiency was due to design factors which would be corrected automatically in the new design principle discussed below.

We were reaching for still higher efficiencies. Three of the modified precipitators were placed in series in a single housing. Efficiencies rose to levels beyond the sensitivity of the NRL light-scattering meter. However, a microbiological technique indicated efficiencies in excess of 99.999% for the triple unit. This was at an air speed of 250 fpm, and a resistance of about 0.1" of water. The finished device was large, heavy, and the modifications in the commercial design were all made and fitted by hand. It should be possible, however, to produce an ultra-high performance two-stage

electrostatic precipitator following the principles of our no-bypass design.

One problem remained in the no-bypass design, and we are only now in the process of solving it. Filling the bypass gap between high-voltage elements and ground with plastic members is not entirely practical. Carbon tracking may occur, and with it permanent electrical leaks or dead shorts.

A new invention, the low conductivity collector plate, appears to make fully feasible the no-bypass concept in commercial designs. The new plates are nonmetallic, and have a low but appreciable electrical conductivity. The plates offer no significant resistance to the electrical current caused by the desposition of charge aerosol particles, but do not permit the concentrated and relatively high currents required to produce tracking of plastic insulation or inter-plate sparking. Other advantages are: (1) collector plates can now be supported solely at their edges, thus eliminating complex and heavy insulated support systems; (2) this change in turn allows more uniform airflow and the option of higher airflow, shorter collecting plates, or higher efficiency; (3) plate-to-ground sparking becomes impossible or improbable to any degree desired, and this in turn opens the way to; (4) the advantages of higher-voltage operation; and (5) the safe collection of highly flammable or pyrophoric dusts such as aerosols of uranium or plutonium.

DISCUSSION

FIRST: Could you tell me how these new devices behave in the presence of high humidity? Have you had a chance to check that?

FIELDING: No, we haven't. We're just getting underway. We've run a few tests.

THE EFFECT OF EXPOSURE TIMES IN THE PREHUMIDIFICATION OF IMPREGNATED CHARCOALS *

Victor R. Deitz and Charles H. Blachly
Naval Research Laboratory
Washington, D. C. 20375

INTRODUCTION

An integral step in the test procedure for determining the trapping efficiency of methyliodide at 25°C is the prehumidification of the impregnated charcoal. The specifications (1) direct that the prehumidification with air at 95 $\pm$ 2% RH be continued until the temperatures recorded at the entrance and exit of the charcoal bed are equal. Since this operation may require about five hours, it is convenient to allow the prehumidification to extend overnight (sixteen hours). This Note is concerned with the unexpected adverse influence on methyliodide trapping by exposures of charcoals to prehumidification at long contact times.

RESULTS

The penetration of methyliodide as a function of time of pre-humidification is illustrated (Figures 1, 2 and 3) for a number of impregnated charcoals. After the designated prehumidification with air at 95 $\pm$ 2% RH the addition of the methyliodide (two hours) and the desorption step (two hours) were made in air flows of 25 liters/min also at 95 $\pm$ 2% RH. The increased penetration with increase times of prehumidification is quite unexpected and it does not appear to have been reported hitherto. In the cases of no prehumidification, several minutes were allowed for the flow of air to reach a steady state before starting the dose; both the dose and the desorption steps used carrier air also at 95 $\pm$ 2% RH. The least penetration was observed with no prehumidification of the charcoal.

The weight-gains of the various samples were determined upon continuous exposure to air humidified at 95-96% RH. As shown in Figure 4, the gain in weight of these charcoals leveled off in about 20 to 40 hours, but the penetration of methyliodide continued to increase after longer periods of prehumidification. After about 100 hours of prehumidification, the MBV-base charcoals leveled off at about 2.4% penetration, an unsatisfactory value (Figure 2). The penetration through KI_x impregnated charcoals also appeared to level off, but this occurred at a most unsatisfactory value (Figure 3). The leveling-off of the weight-gain after a relatively short time suggests that the quantity of adsorbed water is not the controlling parameter in the enhanced penetration of methyliodide. It does not appear to be a question of filling the porous structure of charcoal with adsorbed water and thus blocking access to adsorption sites.

DISCUSSION

The specification that the prehumidification be continued until equal temperatures are recorded at the entrance and exit of the charcoal bed assures only that the heat of adsorption of water vapor has been reduced to a non-measurable quantity. One explanation may be that multilayers of adsorbed water are formed and the mass transfer of methyliodide vapor across the interface is significantly reduced. The formation of multimolecular layers is similar to the formation of multimolecular clusters in imperfect gases (2) and there is no reason to expect that surface multilayers simply grow in depth over the entire surface and thus approach bulk water. Instead, the barrier layer of water may have finite openings between the clusters through which the methyliodide may eventually diffuse given sufficient residence time. This model has suggested additional experimentation that is now in progress.

A reaction mechanism was suggested (3) for methyliodide trapping in which the hyperiodite ion may be the reactive species, viz.

$$MeI(131) + K^+OI^- \rightarrow MeOI + K^+I^- (131)$$

$$MeOI + K^+OH^- \rightarrow MeOH + K^+OI^-$$
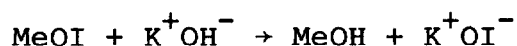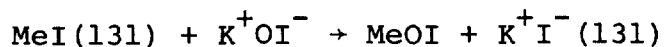
It may be possible that large surface coverage with adsorbed water interferes with the above mechanism. Since the reactivity of the prehumidified charcoal is recovered after drying, it may be a valid explanation.

An important aspect of the above findings is the relevancy to plant practice. The incoming air drawn into the charcoal filter may at times reach a high relative humidity. A. Gary Evans of the Savannah River Laboratory has noted (4) that while the humidity in experimental units may average about 70% RH, the daily high values after sundown may attain near saturation. Thus, a charcoal filter in operation may be subjected to a significant flow of saturated air. The extent to which such exposures influence the efficiency of a charcoal filter is as yet unknown.

REFERENCES

1.   RDT M 16-17 Revised June, 1976, ERDA Division of Reactor Research and Development.

2.   Mayer, J. E. and Mayer, M. G., "Statistical Mechanics", p. 312, New York (1940).

3.   Deitz, Victor R. and Blachly, Charles H., 14th ERDA Air Cleaning Conference (1976).

4.   Evans, A. Gary, Savannah River Laboratory, private communication of unpublished data.
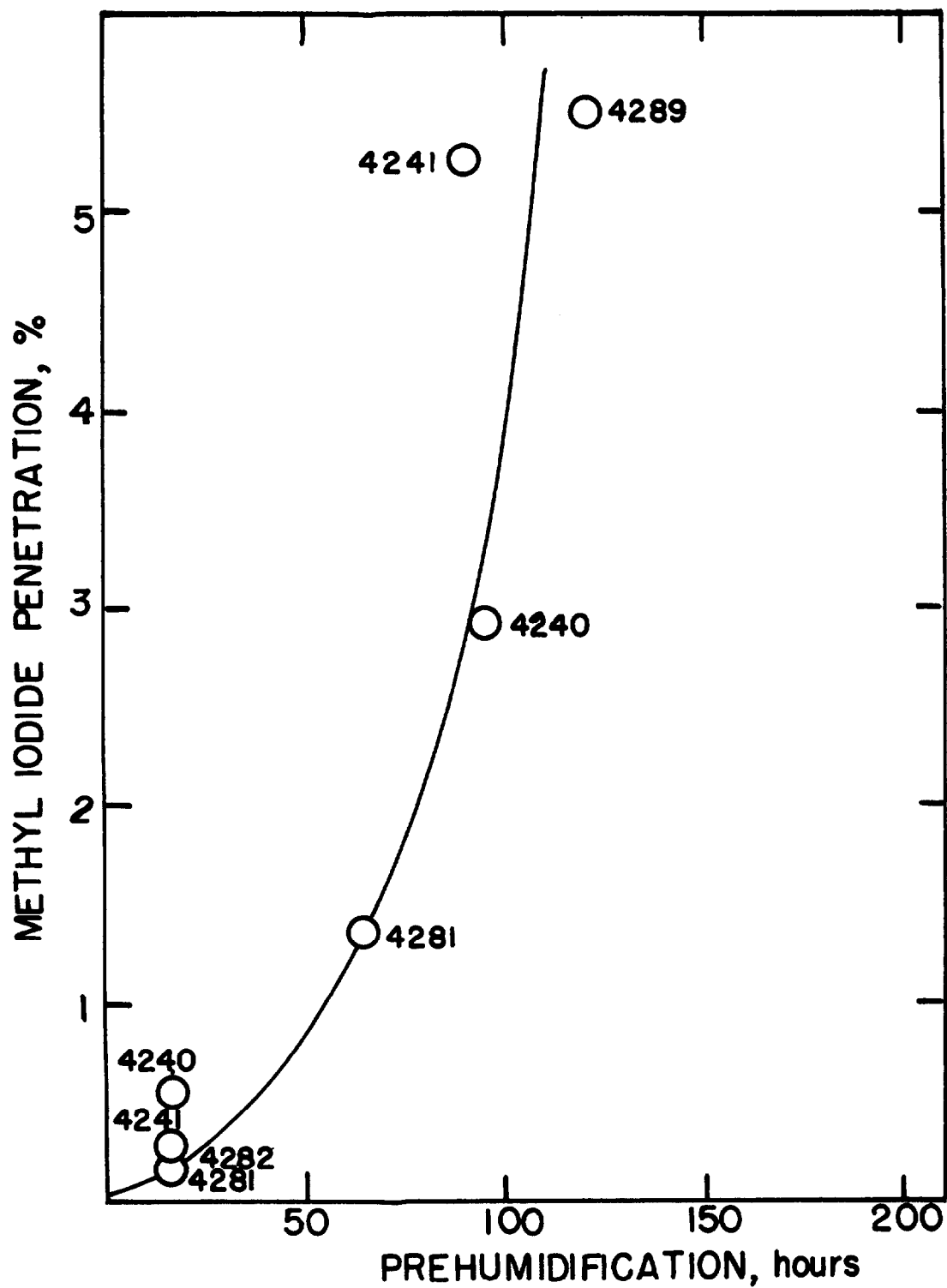
Figure 1: Penetration of methyliodide as a function of the prehumidification time using iodate-iodide impregnations on Gx 202 (a wood charcoal).
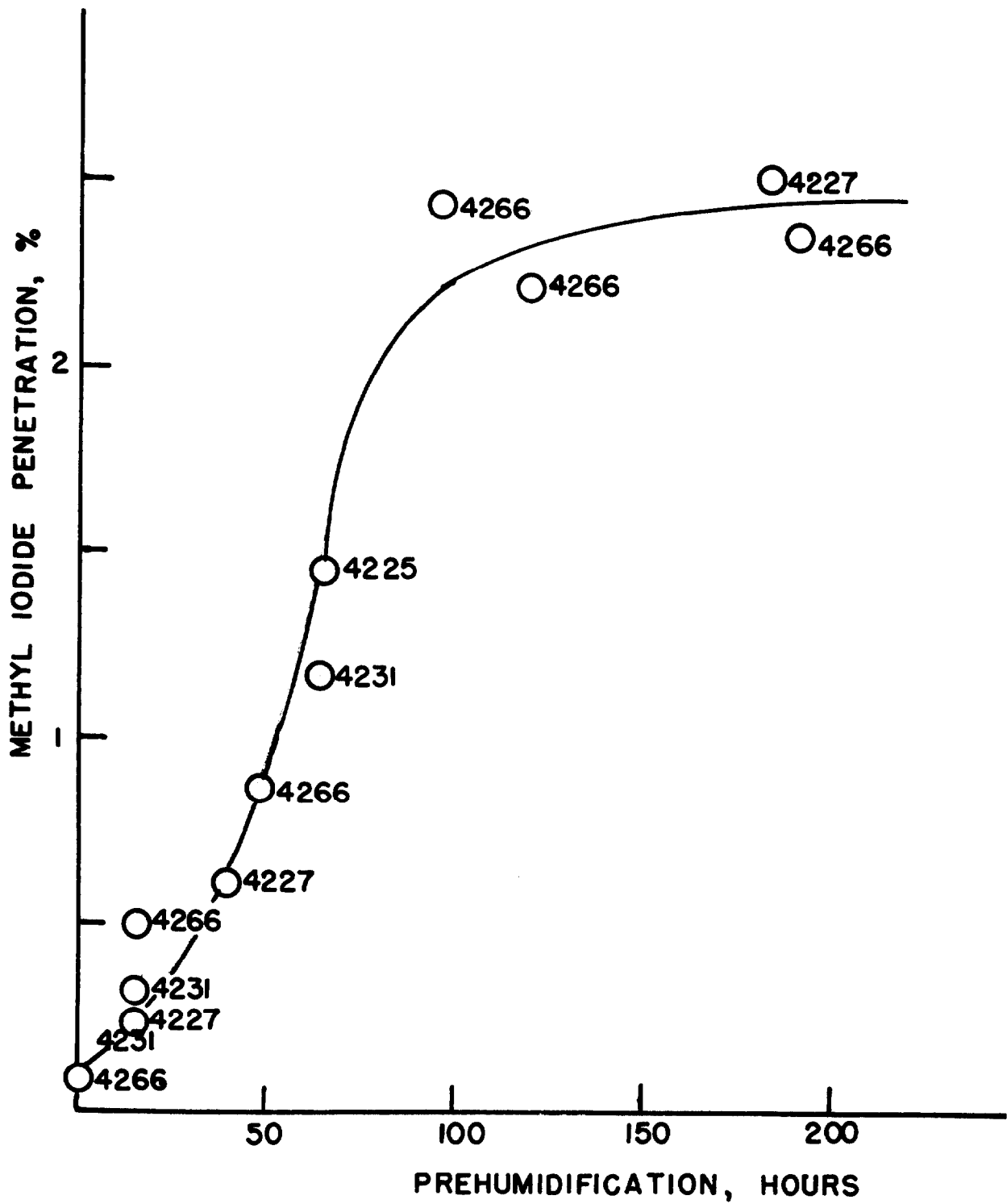
Figure 2:   Penetration of methyliodide as a function of
            prehumidification time using iodate-iodide
            impregnations on MBV (coal-base charcoal).
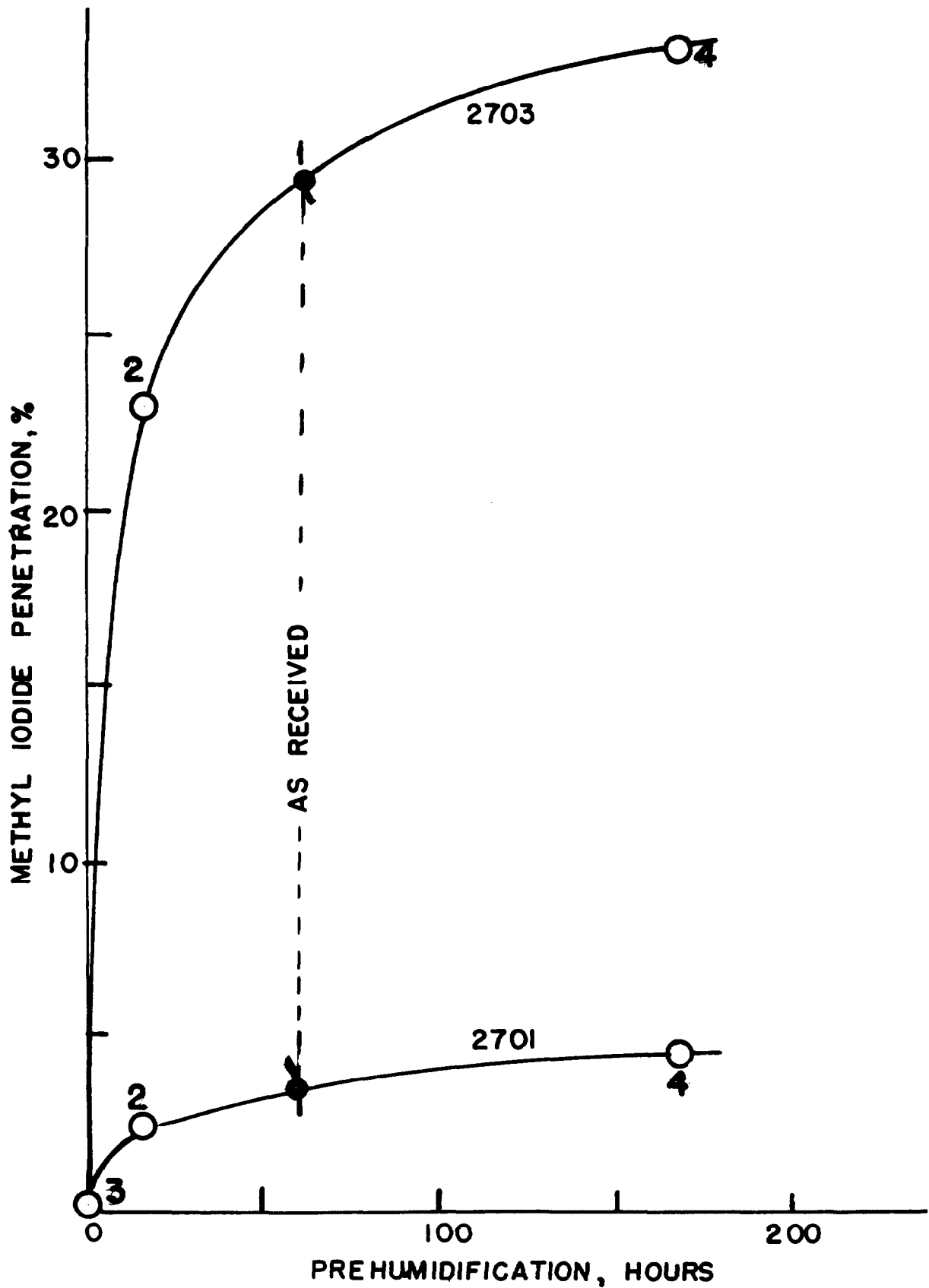
Figure 3:   Penetration of methyliodide as a function of prehumidification time for two KI_x impregnated charcoals.
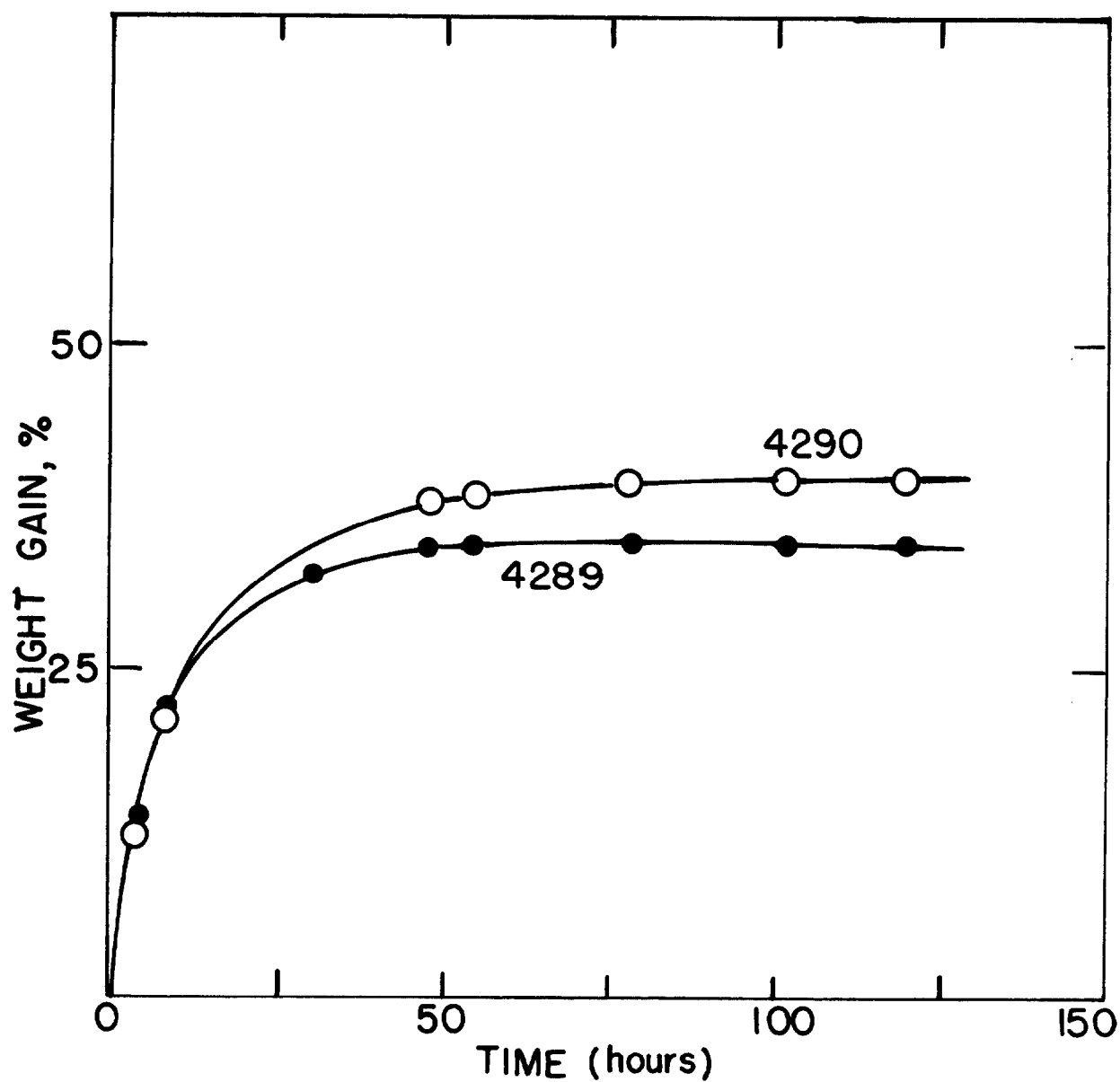
Figure 4: Weight-gain of two impregnated charcoals exposed
continuously to humidified air (95-96% RH).

DISCUSSION

FIRST: The MAST instrument is not specific for ozone. Would it not have been better to have used a chemiluminescence instrument that is specific for ozone? Also, I was wondering whether you should precondition the charcoal by heating it to 200°C for a period. Then you wouldn't have this phenomenon as the charcoal heated. In other words, is this a unique phenomenon for some volatile species that may be remaining in this charcoal and once you drive them off at a higher temperature, are permanently gone?

DEITZ: It is a fact that the MAST microcolombmeter responds to many oxidants. However, no signal was detected in the effluent gases from a thermal analysis of the charcoal up to ignition temperatures. Also, no iodine was emitted from crystals of potassium iodate and as previously mentioned, no emission from pre-heated crystals of potassium iodide.

A successful combination is KIO_4 plus KI; an impregnation containing this mixture does not require any preliminary treatment. The formation of KI is a desirable sink for radioiodine and it is very promising that these impregnations yield successful trapping of methyl iodide.

The iodine emission behavior ties very closely with Evans' desorption test at 180°C. We are also determining the emission at constant temperatures (160-250°C) and are finding linear curves for the emission of total iodine as a function of time at constant temperature.

KOVACH: Dr. Deitz, none of these charcoals is a real commercial charcoal. At least I've never run into any of the 2701 or any woodbase charcoal that is being used. So we don't really know if our good commercial carbons like the BC747 or the NSC585 fiber or the various carbons would behave the same way. These are all experimental charcoals.

DEITZ: We have used many commercial charcoals as impregnant carriers in the investigations now in progress.

KOVACH: They are commercial charcoals, but they are not being used in nuclear power stations, at least currently. The question I have is particularly related to the purity of the potassium iodine. I don't see the advantage of going to very high potassium iodide on charcoal that has up to 5% water soluble non-iodine. All sorts of junk, really, on the charcoal.

DEITZ: It is true that charcoals contain non-carbon constituents, but we are interested in particular in the emission of iodine after impregnation and whatever else is present does not appear to contribute significantly to the formation of gaseous iodine compounds.

KOVACH: At how high a temperature are you drying your experimental charcoals when you prepare them?

DEITZ: About 125°C.

<u>RIVERS</u>:   I assume the carbon labelled "2701" in your report was a sample of AAF 2701 which we sent you. That is not an experimental carbon; it is commercially available. 2703 is experimental. Could you elaborate on the notation "as received" on the slide?

<u>DEITZ</u>:   The notation "as received" in Figure 3 corresponds to the methyl iodide penetration observed for the two samples (2701 and 2703) as received; the laboratory prehumidification was 16 hours. Both samples were then dried in a convection oven overnight at 105°C and immediately tested with no laboratory prehumidification; the penetration was very small (0.088 and 0.14%, resp.). Dried samples were then prehumidified for 16 hours and the penetration was 2.49 and 23.1%, respectively. Finally, the dried samples were prehumidified for 1 week (168 hours) and the penetration was 4.42 and 33.2%, respectively. We concluded that the samples as received had been exposed to water vapor for a period equivalent to about 60 hours of laboratory prehumidification.

<u>RIVERS</u>:   I wonder what will be the effect on the overall penetration after going through the entire cycle under this exposure, e.g., after you heat it up to 230°C? Is this emission a significant mass or is it just a very tiny portion in spite of the fact that you can detect it so strikingly?

<u>DEITZ</u>:   At present, we are using thermal analysis of impregnated charcoals as a measure of thermal stability. The charcoals are dosed with methyl iodide and immediately subjected to an analysis of the thermal desorption products. The order of magnitude of the products coming off at 180°C is about the same magnitude as Gary Evans finds in his desorption tests. The orders of magnitude of the iodine that we determine may be ascribed to the stability of the iodine complexes in the impregnated charcoals.

<u>RIVERS</u>:   I was interested in the earlier one, coconut carbon 2701. Does it have a siginficant penetration when it's put through the cycle?

<u>DEITZ</u>:   The results for methyl iodide penetration on 2701 and 2703 will be given in the next paper.

IODINE EMISSION DURING A PROGRAMMED HEATING OF IMPREGNATED CHARCOALS IN CARRIER AIR

Victor R. Deitz and James B. Romans
Naval Research Laboratory
Washington, D. C. 20375

INTRODUCTION

Unpublished results from this Laboratory have shown that there is considerable emission of carbon monoxide from impregnated charcoals heated (5°/min) in air flows at temperatures significantly below spontaneous ignition. This behavior raised questions as to the stability of the various iodide impregnations on charcoals when subjected to programmed heating in like manner; also, how would they compare to the stability of trapped iodine and/or methyl iodide on such charcoals? This Note is concerned with a thermal analysis of impregnated charcoals, reporting determinations of elementary iodine and organic iodides in air flows of 5 L/min.

PROCEDURE AND RESULTS

The effluent gases from the test procedure for the determination of the spontaneous ignition temperature (SIT) of an activated charcoal were sampled (126 ml/min) and the flow directed into a microcoulometric detector (MAST Instrument) (1,2). The charcoal was heated at 15°/min to 120°C and then at 5°/min until the SIT was attained. The MAST Instrument responds to elementary iodine and the output (mv) can be continuously recorded. A calibration was made against known vapor pressures of iodine crystals held at suitably low temperatures.

The emissions of molecular iodine are reported for three impregnated charcoals. The results for a KI_x-impregnated wood-base charcoal, 2701 (Figure 1), and for two (KIO_3+KI+KOH)-impregnated charcoals, 4289 and 4290 (3) (Figures 2 and 3), make an interesting comparison (see points in circles). The latter impregnations appeared to be more stable at a given temperature than the KI_x impregnation, a most desirable behavior with respect to DBA considerations. The small increase in I_2 emission (Figures 2 and 3) was followed by a marked decrease. This behavior raises interesting possibilities as to its significance in the nuclear application. Is the iodine changed to some thermally stable salt or is it converted to volatile organic compounds that are not counted by the microcoulometer?

To answer these questions, the effluent sample from the SIT test was passed first through a quartz tube (2 mm i.d.) heated to approximately 600-650°C and then directed into the microcoulometric detector (4). It is known that the alkyl iodides, such as methyl iodide, are pyrolyzed into elementary iodine and hydrocarbons (5). Hence, if volatile organic iodides are present in the effluent gases, the total iodine measured would be enhanced. The results (points in squares in Figures 2 and 3) demonstrate that this is indeed the case. Heating of impregnated charcoals must yield organic iodides. The KI_x impregnations are least stable, but these do not appear to form a significant amount of organic iodides. The new impregnations with oxyiodine

salts (3) evolve less and, in addition, the emission after peaking at 250-260° decreases significantly until the actual SIT is approached.

CONCLUDING REMARKS

In the thermal analysis of some impregnated charcoals there are present chemical reactions that form volatile organic iodides at temperatures lower than ignition, thus raising the possibility of iodine release. The magnitudes of the SIT of nuclear grade charcoals appear to be of secondary importance.

The impregnations on charcoals of the oxyiodide-HMTA formulation are of greater stability than the present KI_x impregnations.

The total iodine emission integrated to a specified temperature (e.g. 180°C) is a small fraction ($\sim 10^{-6}$) of the total iodine in the impregnation; the emission varies somewhat with both charcoal and impregnation formulation for a specified temperature.

The experimental procedure is now being applied to follow the iodine emission at constant temperatures for time periods up to 24 hours. These results will complement the desorption tests at 180°C already reported by A. G. Evans (DP 1280, Savannah River Laboratory).

REFERENCES

1.   Thomson, W. G. and Grossman, R. E., Proc. 9th AEC Air Cleaning Conf. 1966, 1134-1149.

2.   Grossman, R. E. and Thomson, W. G., TID-20426, "NS Savannah Ventilation System Filter Testing", November 1963. AEC Division Technical Information.

3.   Deitz. V. R. and Blachly, D. H., 1976 Proc. ERDA Air Cleaning Conference.

4.   McFee, D. R. and Bechtold, R. R., Jr. Am. Indus. Hygiene Assoc. 32, 766-770 (1971).

5.   Cottrell, T. L., "The Strength of Chemical Bonds", Butterworths Scientific Publications, 310 pp. (1954).

ACKNOWLEDGEMENT

Figure 1: Emission of I_2 (points in circles) and of total iodine (points in squares) from KI_x impregnated charcoal
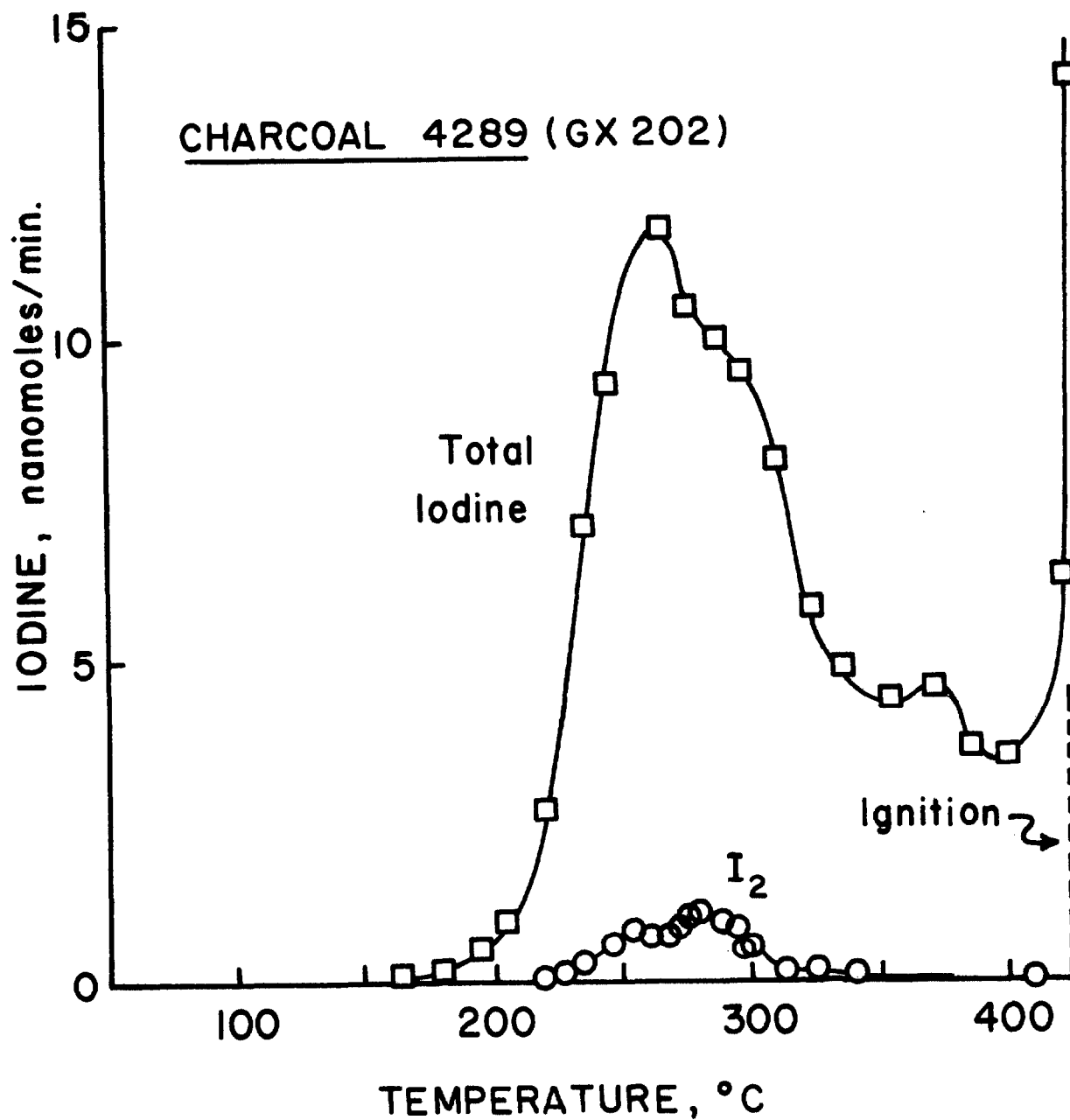
Figure 2: Emission of I_2 (points in circles) and of total iodine (points in squares) from a wood charcoal impregnated with $KI+KIO_3+KOH+HMTA$ (3).
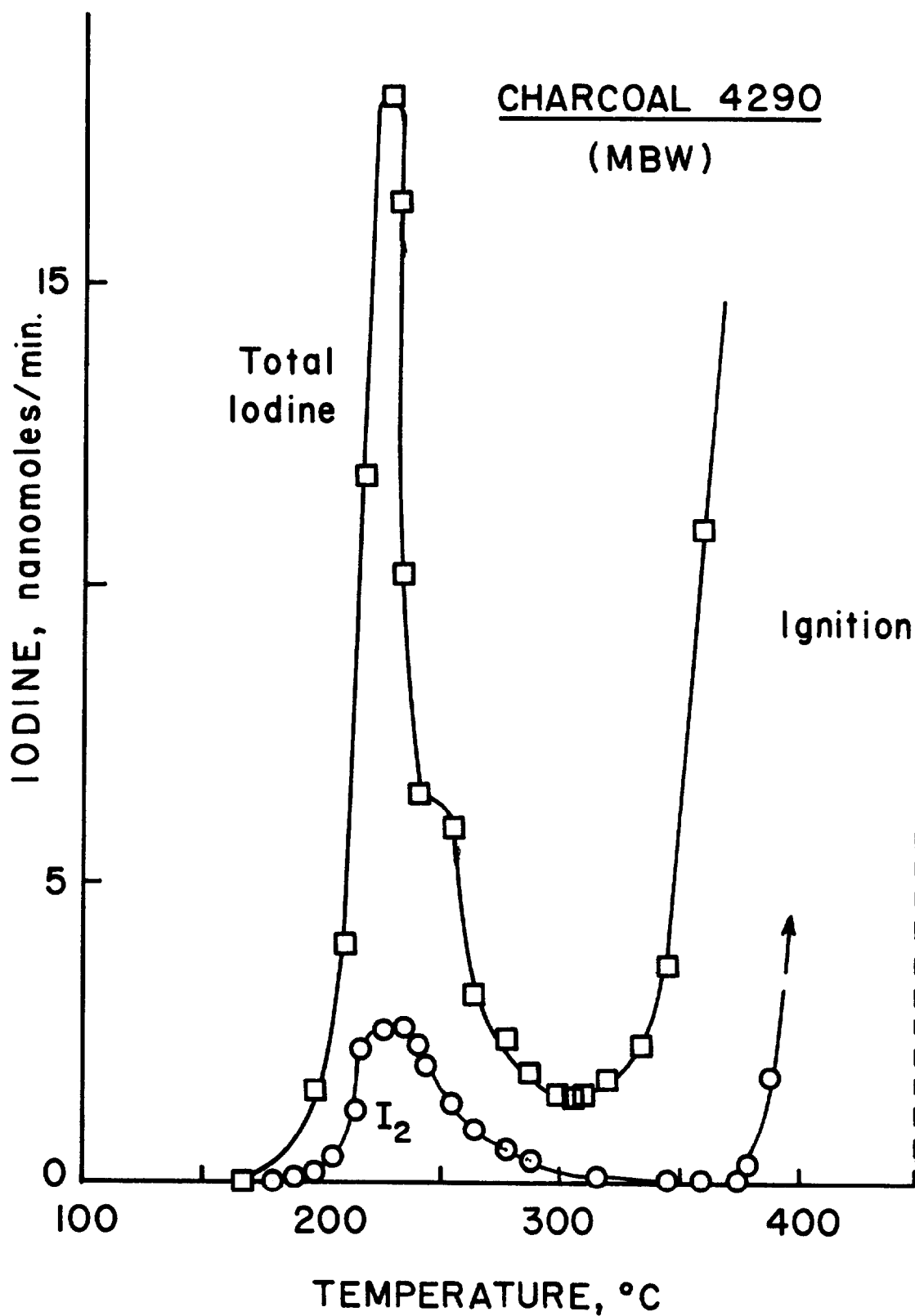
Figure 3: Emission of I_2 (points in circles) and total iodine (points in squares) for a coal base charcoal impregnated with $KI+KIO_3+KOH+HMTA$ (3).

DISCUSSION

RIVERS: The heating-elution curves shown are quite detailed, the result of some very sensitive measuring equipment. I hope everybody recognizes that the quantity of elution shown represents less than 0.01% penetration in the course of a test, even though the carbons were heated all the way to their ignition point. We reported some similar data at the 13th AEC Air Cleaning Conference. There is some evidence that a carbon with good physical adsorption properties (like coconut) will capture radioiodine well at lower temperatures, but release some of it on heating. A system with a lower initial adsorption, but strong chemical bonding of the iodine compounds, may have less overall penetration under conditions where the bed is subjected to decay heating. I was struck by the data in Staples paper in Session 4 which showed about 39% loss of adsorbed I_2 from the silver zeolite when it is heated to 150°C for substantial periods. Maybe we need a very careful look at the probable heating condition for these beds. Incidentally, would you expect the elution curve for 2701 to come back to the baseline before ignition, in the same manner as 4289 and 4290 samples did in Figures 2 and 3?

DEITZ: The iodine emission from 2701 (and 2703) does not return to the baseline before ignition. In fact, when viewed through a depth of about 10 cm, a purple cloud of iodine vapor is visible. The thermal stability of a KI_x impregnation on charcoal appears to be inferior to the samples 4289 and 4290 (Figures 2 and 3), the impregnations of which were basic solutions of KIO_3 + KI + hexamethyltetraamine.

FIRST: If you were to put dry air through your charcoal for 200 hours, would you return to your base reading?

DEITZ: Yes, but if you want to do it in less time, the charcoal can be placed in an oven. When the humidified charcoal is dehydrated, the initial low penetration is recovered. However, if the prehumidification is done at 95 and an attempt made to dry at 80 or so, the effort is analogous to trying to dry wet clothes on a wet day. Very little water would be removed from the charcoal. We are presently measuring the adsorption and desorption isotherms of water on impregnated charcoals in order to establish the extent of the hysteresis involved.

BELLAMY: I would like to make sure I understand this. All of the results you have just talked about are for new, unused carbons, so the effect cannot be compared to what Mr. Hunt talked about yesterday. Is that true?

DEITZ: Yes. As you know, our samples are now being aged by exposure to air flows drawn from the environment on the roof of the NRL Chemistry building.

BALLAMY: Can a committee just pick a standard prehumidification time and everybody run a test for the same number of hours?

DEITZ: We cannot solve this problem by committee work. It

calls for some more experimental work. When the water layer builds on the surface of charcoal, a barrier is formed to the mass transfer of methly iodide into the structure. More work must be done to understand the clustering of water molecules on the surface at high relative humidity and perhaps there are ways to minimize the effect.

KOVACH: What is the total air velocity that you are using in prehumidification? Is it the same as you use in the test?

DEITZ: The normal flow is twenty-five liters per minute but at times it is cut in half.

KOVACH: Have you looked at how clean the air is that you are using? Do you have any hydrocarbons? If it is compressed air, do you make sure you have absolutely no water vapor left from your compressors or any organic impurities?

DEITZ: The air supply of 25 liters per minute is passed through a bed of charcoal in a two inch diameter tube and then through a high efficiency particulate filter.

KOVACH: So you know for sure that you have no organic con- taminant in the air stream. I am just trying to make sure. Is it water that causes the problem or are we facing other contaminants?

DEITZ: I believe that it is adsorbed water. When the char- coal is dried and the test started again, the same methyl iodide penetration is obtained after 16 hours. The behavior is quite repro- ducible.

MUNSON: I would just like to inquire if keeping the charcoal dry prevents this behavior, and I think you seem to say that. If the charcoal is continuously heated above the dew point, will the charcoal maintain its efficiency?

DEITZ: I don't know what is being done in industry. We would greatly appreciate some commercial information. Obviously, the cheapest procedure is to pull in outside air. When this is done, the increase in relative humidity at nightfall is an important factor.

WILHELM: Did you every try to get an x-ray picture of your charcoal? The charcoal is impregnated with potassium iodide and this forms a very small crystallite. If you run this charcoal in a wet atmosphere for a long time, the crystalite starts to grow. The sur- face area of the crystalites grow, and with this growth, the reaction on the surface becomes slower and slower because it has less surface. That could be a reason for what you have seen.

DEITZ: In reply to your first question, we have obtained quite a few electron transmission micrographs of charcoal, with and without impregnations. It is very interesting to see from the strong contrasting silhouettes where the impregnation is located. We will send you some photographs is you desire. The charcoal is amorphous material and the impregnations form minute crystals at random locations. These crystalites can best be studied with electron diffraction tech- niques. The electron diffraction results show the presence of single crystal patterns. These are present in the inner porosity of the char- coal.

JONAS: Do you think one might distinguish between the amount of H_2O on the charcoal and the time of prehumidification, relative to its methyl radioiodide penetration, by prehumidifying the charcoal for 16, 25, 50 and 100 hours at a lower RH, e.g., 60 or 80% RH?

DEITZ: We are now prehumidifying samples at various relative humidities. Early researchers at NRL showed that dry charcoal and wet charcoal take up oxygen over periods of many days at a constant temperature in direct proportion to the moisture content. There is a very slow and continuous reaction of moist air with charcoal.

AN EXPERIMENTAL INVESTIGATION OF THE RELATIONSHIP BETWEEN BED PACKING AND FLOW DISTRIBUTION

H. C. Parish, R. C. Muhlenhaupt
and W. W. Vogelhuber
CVI Corporation
A Subsidiary of Pennwalt Corporation
Columbus, Ohio

Abstract

A testing program was conducted to evaluate different methods for filling carbon beds in terms of the resultant air flow distribution through the beds. Three filling methods were included:

1) Deposit carbon in the bed in an uncontrolled and random manner (with respect to fill rate and/or distribution) with no packing effort.
2) Uncontrolled deposition as in 1) above but followed by an attempt to pack by vibration.
3) Filled and packed simultaneously, using a gravity pack method.

The test results indicate that the filling method is a very significant factor in determining the quality of the resultant air flow distribution. A gravity packing method provided the best results while the uncontrolled fill with no effort to pack gave very poor results. The combination of an uncontrolled fill with subsequent packing by vibration also provided poor flow distribution.

I. Introduction

For all ESF (Engineered Safety Feature) Systems, Regulatory Guide 1.52 (Reference 1) requires that the flow distribution within carbon adsorber beds must not vary by more than ± 20% from the average. For Non-ESF Systems, the NRC (Nuclear Regulatory Commission) has recently published ESTB No. 11-2 (Reference 2), which also requires a maximum flow deviation of ± 20% from the average.

In addition, it is instructive to estimate the effect of velocity on performance. Some calculations have been performed using a method developed in CVI Technical Note No. 26 (Reference 3) to evaluate relative performance at various velocities. Penetration of CH_3I was estimated to increase by 70% to 90% for a 20% increase in velocity. A 50% increase in velocity could increase penetration by 200% to 300%, depending on the quality of the carbon. These increases were estimated assuming inter-particle diffusion to be the rate limiting step. Therefore, poor flow distribution can have a very significant effect on adsorber performance, due to increased penetration in the high velocity areas.

Another consideration is the weathering effect. The rate of weathering is related directly to velocity. Therefore, if the velocity is 50% higher through some area of the bed, then the adsorbent would be expected to weather 50% faster in that area, an important economic consideration.

Thus, uniform flow distribution is important because of regulations, performance and economic factors. Good design practice, therefore, demands that steps be taken to assure a uniform flow through the adsorber.

One of the most important design considerations, although frequently not given adequate consideration, is to insure that the flow resistance of the adsorbent be uniform throughout.

It is also sound engineering practice to make the flow resistance through the adsorber large relative to the inlet/outlet resistances. When this condition is met, any tendency to promote a non-uniform flow pattern by the inlet/outlet sections is overpowered by the larger flow resistance in the adsorber and the flow is thus smoothed out.

With these design principles in mind, it is significant to note that carbon will exhibit a 300% variation in flow resistance if the packing density is allowed to vary from minimum to maximum as indicated in Reference 4.

From previous testing reported in Reference 5, the packing density can be substantially affected by the packing method. It was found that a gravity pack method provides the maximum packing density while an uncontrolled fill generally produces the minimum packing density and an uncontrolled fill followed by mechanical shock (vibration) provides an intermediate packing density.

The effect of various packing methods on flow distribution was evaluated by measuring the flow distribution through a section of a full scale adsorber with the adsorber being filled and packed by various methods. This paper describes the test program and discusses the results.

II. Experimental Procedure

The test was conducted on a specially constructed element out of a full scale adsorber. Figure 1 is a sketch representing a typical all welded adsorber in the plan view. Figure 2 is a cross-section of the test apparatus in a side view. The test apparatus can be described as representing an element or slice taken from one full scale bed along with its associated one half inlet and one half outlet air plenum (see Figure 1). The test section was 6" in width (direction normal to the 2 dimensional flow plane) but all other dimensions are representative of the full scale system. The test unit was oriented vertically to facilitate filling of the carbon.

The test apparatus was considered to be a very realistic model of production assemblies because:

1) The depth of carbon in the test apparatus represented, for practical purposes, the minimum depth of carbon in full scale systems. The test section had a bed depth of 2-1/8 inches, the full scale systems vary from a minimum of 2-1/8 to 2-3/16 inches for nominal 2 inch beds.
2) Since the standard inlet and outlet plenums handle air from two carbon sections while the inlet and outlet plenums for the test assembly handled air to only one carbon section, the test assembly inlet/outlet plenums were one-half the width of their full scale system counterparts. Therefore, the air velocities were the same for the inlet and outlet plenums in the test assembly as in the full scale system.
3) The test assembly used a bed length of 7 feet, representing the longest bed that had been manu-factured to that time by CVI. Thus, in all the significant dimensions, (i.e., in the plane of flow) the test assembly corresponded to a full scale system.

The test apparatus featured holes in the inlet and outlet air plenums at locations A2 thru A7 and B1 thru B6, as shown in Figure 2, through which a pitot tube or hot wire anemometer could be inserted to determine the air velocities in the inlet and outlet plenums. The faces of the unit (the outer sides of the inlet and outlet plenums - see Figure 2) were made of plexiglass so that the correct positioning of the pitot tube and hot wire anemometer could be visually confirmed. The holes were taped over except when in use and then the probes were "packed" around the hole to preclude air leakage.

Air flow was provided by a Spencer Turbine unit with a manually operated throttling valve and orifice flow meter to provide flow control. A schematic drawing of the test setup is illustrated in Figure 3.

It was intended that the flow be adjusted to provide an average superficial bed velocity of approximately 40 fpm for the first tests. However it was subsequently determined that the actual velocity was 35.4 fpm; thus, for consistency, the remaining tests were conducted at nominally the same flow rate of 35.4 fpm.

Test Procedure

Air velocities on the order of 40 fpm (standard face velocity in I_2/CH_3I removal systems) are very difficult to measure reliably with conventional equipment. This is even more true in the presence of a much higher velocity normal to the face velocity. Therefore, rather than attempting to measure the face velocity directly, the volumetric flow rate through various carbon sections was determined directly by changes in flow in the inlet and outlet plenums. The face velocity was then calculated directly from the volumetric flow rate and the face area for the various sections.

Therefore, the primary measurements taken in the tests were velocities in the air inlet and outlet plenums at measuring stations A2, A3. . . A7 and B1, B2. . . B6, as shown in Figure 2, measuring the velocities in the direction of the plenum axis.

Referring to Figure 2, the air enters the test unit at the bottom of the inlet plenum. As the inlet plenum is traversed from bottom to top, some of the air stream is continuously withdrawn from the inlet plenum and passes through the carbon bed to the outlet plenum.

Since the pressure gradient through the bed is much larger than the pressure gradient in the direction along the length of the inlet/outlet plenums, it follows that the air flow through the carbon is essentially normal to the flow in the plenum.

Each section of the test assembly must satisfy the continuity equation. The section in Figure 2 illustrates a typical flow balance based on the Section 2-3. Applying the continuity equation to the section illustrated in Figure 2 (changes in pressure are negligible in terms of density change so continuity is expressed in terms of volumetric flow rate).

$$\dot{V}_{B2} - \dot{V}_{B3} = \dot{V}_{A3} - \dot{V}_{A2} \, . \tag{1}$$

where the symbol $\dot{V}$ is used to indicate the volumetric flow rate.

Applying the continuity equation to the inlet plenum for the section shown in Figure 2:

$$\dot{V}_{2.3} = \dot{V}_{B2} - \dot{V}_{B3} \; . \tag{2}$$

Summarizing, the approach used in the test program was to measure the plenum velocities, in the direction of the plenum axis, from which the volumetric flow rates ($\dot{V}_{B1}$, $\dot{V}_{B2}$, . . . $\dot{V}_{B6}$ and $\dot{V}_{A2}$, $\dot{V}_{A3}$, . . . $\dot{V}_{A7}$) were determined.

A velocity traverse was performed for several representative sections prior to the test from which a centerline coefficient was determined. Throughout the test, the centerline velocity was measured and the centerline coefficient was used to calculate the volumetric flow rate at that section.

III. Data Analysis

Having determined the flow rates in the air plenums at various stations, the change in flow rate between any two adjacent stations in the air plenum can be equated to the flow rate through the carbon between those two points (see Equation 2). Having determined the flow rate, the average superficial face velocity can be calculated for the area between the stations, using data from both the inlet and outlet plenums.

The plenum velocities at points A2 thru A7 and B1 thru B6 are entered as data into a computer which calculates the corresponding volumetric air flow rate at each of the measuring stations. The computer also sums the flow rate at each elevation, for example, $\dot{V}_2 = \dot{V}_{A2} + \dot{V}_{B2}$. Assuming the air flow through the carbon is perpendicular to the screen for the reasons given previously, the total plenum flow rate at any elevation will be constant and equal to the total flow rate into the unit. Thus, it would be expected that $\dot{V}_1 = \dot{V}_2 = \dot{V}_3 = \dot{V}_4 = \dot{V}_5 = \dot{V}_6 = \dot{V}_7$, although the measured values are certain to vary somewhat from station to station because of measurement error.

Since the calculation of the face velocities ($V_{1,2}$, $V_{2,3}$ thru $V_{6,7}$ in Figure 2) are determined from the flow differences $\dot{V}_{B2} - \dot{V}_{B1}$, $\dot{V}_{B3} - \dot{V}_{B2}$, etc., the calculated face velocities are very sensitive to small deviations in flow rate. In effect, the procedure used involves numerically evaluating the derivative of the flow ($d\dot{V}/dx$) in the inlet or outlet plenum, this derivative being proportional to the corresponding face velocity through the carbon. It is well known that the derivative of a "non-smooth" function can be very erratic which underscores the need for smooth flow rate data in the inlet and outlet plenums.

Therefore, the measured flow rate data in the plenums were smoothed, subject to the condition that the total plenum air flow rate at any elevation was a constant to satisfy the principle of continuity. These steps were accomplished by first normalizing the data from the outlet plenum to that of the inlet plenum as follows. Prior to smoothing the data, the computer averages the indicated flows from the inlet and outlet plenums for each elevation to obtain the indicated total air flow rate at each station. These were then averaged to obtain the average total air flow rate.

The average total flow rate was then used as the flow rate at the inlet and outlet, i.e., at points A1 and B7. The average flow from all stations was used rather than the measured flow at A1 and B7 because the measured flows at these points were considered suspect due to inlet/outlet effects. The velocity traverses performed at both of these measuring stations confirmed this. These velocity traverses across the plenums generally indicated a flat velocity profile, typical for fully developed turbulent flow except at the sections A1 and B7. There was a steep velocity gradient from front to back at B7. Therefore, if the velocity probes were not placed exactly right, the measured velocity would be significantly off. Section A1 appeared to have a vena contracta effect to complicate measurement at that station.

The measured flow rate for the outlet plenum at each interior station is then subtracted from the average total air flow rate to obtain the corresponding flow rate for the inlet plenum. Thus, for each elevation (except A1 and B7), there are two data points representing the flow rate in the inlet plenum, one datum point being measured directly, the other calculated from the average total air flow rate and the measured flow rate at that elevation in the outlet plenum. These data were then subjected to a least squares curve fitting procedure to obtain a "best fit" curve which was then used in subsequent calculations to represent the best estimate for flow rate in the inlet plenum at any elevation.

Figure 4 is a reproduction of a typical work sheet to illustrate the above procedure (in this example the carbon was filled by pouring, i.e., loosely packed). The pitot tube data is handwritten at the top of Figure 4. The seven inlet and seven outlet plenum velocities are then entered into the computer which calculates and prints out the inlet and outlet plenum flow rates, the total flow rate for each station and the average total air flow rate. The flow rates in the outlet plenum were then subtracted from the average total air flow rate by hand and are shown handwritten next to the outlet flow rate column.

The inlet plenum flow rate data used in the curve fitting procedure is plotted in Figure 5 for the example case with the measured flow rate data represented by the circle symbol and the flow rate data calculated from (the average total air flow rate less the outlet plenum flow rate) represented by the square symbol. The end points, corresponding to positions at 0 and 80 inches from the inlet are based on the average total air flow rate at the inlet and zero flow at the outlet, respectively, to satisfy the principle of continuity.

It can be seen from Figure 5 that the data measured in the inlet plenum and the data measured in the outlet plenum agree quite well.

The data, as tabulated in Figure 4 and plotted in Figure 5, were used to determine a best fit curve for a 2nd order equation, using the method of least squares. The end points at 0 and 80 inches from the inlet were weighted to force the curve to go through those points. The resultant best fit curve is shown in Figure 5. From an examination of Figure 5, the data points look reasonably consistent and are fitted well by the 2nd order equation. It should be noted that mathematically, by assuming a 2nd order equation, the face velocity is forced to vary linearly from one end to the other. This can be seen in the data of Figure 6 thru Figure 15. The reason for this is that the face velocity is determined, in effect, by differentiating the flow rate along the length of the plenum as:

$$V = \text{Constant} \cdot \left(\frac{\Delta \dot{V}}{\Delta x}\right) = \text{Constant} \cdot \left(\frac{d\dot{V}}{dx}\right) \tag{3}$$

where

V = average face velocity for carbon over increment Δx

$\Delta \dot{V}$ = incremental change in volumetric flow rate between stations

Δx = incremental distance between stations

Since the flow rate data is fit by a second order equation:

$$\dot{V} = Ax^2 + Bx + C \tag{4}$$

and

$$V = \text{Constant} \cdot \left(\frac{d\dot{V}}{dx}\right)$$

then

$$V = \text{Constant} \cdot (2A x + B) \tag{5}$$

Therefore, V is forced to be a linear function of x (distance). If a 2nd order equation did not fit the data so well (for example, see Figure 5), then a higher order equation should be used. However, the curve fits were all sufficiently good that it was decided that a higher order curve fit would not be justified and would not be statistically meaningful based on the number of data points. It might also be noted that if the flow data of Figure 5 formed a straight line, the constant "A" in Equation 5 would be zero and the velocity would be constant across the bed. The data in Figure 5 obviously could not be considered to fit a straight line and therefore, by inspection, it could be concluded that the face velocity is non-uniform.

The "best fit" curve from Figure 5 is then taken to represent the true flow distribution for the inlet plenum and the quantity (average total air flow minus inlet plenum flow) the flow distribution for the outlet plenum. The flow distribution for the inlet plenum can then be used to calculate the face velocity profile using Equation 5.

The face velocity profile based on the data from Figure 5 is plotted in Figure 6 pictorially as velocity arrows at various elevations.

For this test, featuring a loosely packed bed, it can be seen that the face velocity is far from constant, varying from a minimum of 19.5 fpm to a maximum of 57.1 fpm.

Results

The results of the tests are presented in Figures 6 thru 15. The test apparatus is represented schematically along the ordinate in each of the figures with the measuring stations shown by number. The numbering system is consistent with that used in Figure 2 with Station No. 1 at the inlet, Station No. 7 at the outlet and with Stations No. 2 thru No. 6 approximately evenly spaced between. The average velocity between measuring stations is shown as an arrow at the midpoint between stations. The magnitude of the velocity is read from the abscissa.

Each of the figures includes pertinent test information including the Test Number, a description of the fill technique, percent maximum packing density and measured flow resistance.

The maximum packing density is based on the highest measured density from all in-house tests on a given carbon. The static pressure differential was measured at each of the five interior stations (2 thru 6) to determine the average flow resistance for each fill of the test bed except for Test No. 26.

Data taken on carbon filled by pouring, without control over distribution or rate of fill, is plotted in Figures 6 thru 8. The result was a series of loosely packed beds, as evidenced by the measured percent of maximum packing density and the measured flow resistance. It is apparent that the resultant face velocities are very non-uniform.

Test No. 26 (Figure 9) used the same uncontrolled pouring method. However, after pouring, an electric vibrator was attached to the side of the test assembly and energized. Operation of the vibrator continued until the carbon quit settling (surface of carbon dropped about 3" during vibration). Additional carbon was added to bring the level up to normal height. The apparent density increased from 28.0 to 29.7 lbm/ft³ with vibration or from 85.4% to 90.5% of maximum-packing density. It is apparent from Figure 9 that the velocity is still very non-uniform, varying from 17.8 fpm to 51.5 fpm. Given a cursory consideration, it might be expected that vibration should improve the flow distribution somewhat over the data from Figures 6 thru 8 since there was some increase in packing density. However, the carbon used in Test No. 26 had an abnormally large mesh size which would have the effect of decreasing the flow resistance. Also, variation in packing density within a bed is another mechanism which can create flow channeling. The characteristic response of any non-rigid mechanical system to vibrational excitation is the formation of several nodes and antinodes (i.e., minimal and maximum displacements). It would be expected that the packing density would vary accordingly from one location to another, being maximum at the antinodes and minimum at the nodes. Thus, it is considered likely that vibration could very well make any existing flow channeling worse, even though the average packing density and flow resistance are increased. For comparison, the same large mesh carbon was used with a gravity pack technique. The corresponding data are plotted in Figure 14 and 15 and will be described later.

Data on gravity packed carbon beds are plotted in Figures 10 thru 15. The data in Figures 10, 11, 12, and 13 show high average flow resistances with a ∆P/L of 0.420 to 0.458 in. w.g./in. of bed depth compared to 0.171 to 0.192 in. w.g./in. for the uncontrolled, poured beds of Figures 6 thru 8. Also, the measured packing density was 100% of maximum compared to the 86.5% for the loosely packed beds. Most significant, the corresponding flow distribution was much improved, particularly the data in Figures 11, 12, and 13.

A closer examination of the data represented in Figure 10 indicates that these data are not as reliable as data taken in the other runs. The data from Run No. 6 and Run No. 7A (Figure 10 and 11) were taken on the same packed bed (i.e., same fill) under the same conditions and at the same flow rate so that the velocity distribution should be the same. Yet the flow from Run No. 7A (Figure 11) is much more uniform. In examining the plenum flow data of Run No. 6, the data are more scattered than for any of the other runs. The plenum flow data from Run No. 6 and Run No. 7A are shown for comparison in Figure No. 16 and Figure No. 17, respectively. By inspection, the plenum flow data of both Figures 16 and 17, could be well represented by a straight line, which would mean a uniform face velocity. For contrast, refer to Figure 5 where the plenum flow is decidedly non-linear (i.e., the face velocity is non-uniform).

An index of the scatter is the error of fit (i.e., the square root of the sum of the differences squared) which is computed and printed along with the other curve fitting data. The error of fit for the data in Figures 10 thru 13 is summarized in Table 1.

Table 1

Figure No.	Error of Fit
10	6.98
11	4.77
12	4.80
13	4.36

Therefore, it is reasonable to assume that the actual flow distribution from that particular fill is more nearly represented by the data of Figure 11 than by the data of Figure 10.

The data represented in Figures 14 and 15 were taken on gravity packed beds but with an abnormally large mesh size carbon. This is the same carbon for which data were plotted in Figure 9 (Test No. 26). In

comparing the data for gravity packed beds with the data on a bed packed by vibration, it can be seen that the gravity packed bed provided a much better flow distribution.

V. Summary

Proper packing of carbon beds is an important factor in providing good flow distribution which, in turn, is a prerequisite to the following:

1) Conformance to Standards and Regulations
2) Minimizing weathering effects and premature carbon replacement with attendant economic impact.
3) Good adsorber performance

Proper packing requires both a uniform packing density throughout the system and a near maximum packing density for the given material.

The primary purpose of the effort described in this paper was to evaluate the effect of different methods for filling carbon beds on the resultant air flow distribution through the beds. The results of this testing program indicate that the gravity packing method provides a more uniform flow distribution than either no packing or packing by vibration.

This result is not surprising considering that, properly done, a gravity packing technique produces the maximum packing density and provides an inherently uniform packing density. On the other hand, it is considered improbable that a system of any size could be vibrated uniformly throughout, suggesting very strongly that the packing density would also be non-uniform.

References

1. USAEC Regulatory Guide 1.52, June 1973
2. Branch Technical Position — ETSB No. 11-2 "Design, Testing and Maintenance Criteria for Normal Ventilation Exhaust System Air Filtration and Adsorption Units of Light-Water-Cooled Nuclear Power Reactor Plants" Attached to Standard Review Plan Section 11.3 of NUREG 075/087, Standard Review Plan for the Review of Safety Analysis Reports for Nuclear Power Plants, USNRC, September 1975.
3. Parish, H., "CVI Technical Note No. 26", November 9, 1972
4. Pittsburgh Activated Carbon Specification Sheet 23-108, Type PCB Granular Carbon
5. Parish, H., "CVI Technical Note No. 30", November 6, 1975

STATION	P_{IN} (IN.W.G.)	V_{IN} (FPS)	P_{OUT} (IN.W.G.)	V_{OUT} (FPS)
1	0.310	36.66	0	0
2	0.186	28.82	.003	3.66
3	0.160	26.81	.009	6.34
4	0.120	23.15	.035	12.50
5	0.046	14.33	.073	18.05
6	0.007	5.59	.155	26.31
7	0	0	.260	34.07

```
ENTER SEVEN INLET VELOCITIES
? 36.66,28.82,26.81,23.15,14.33,5.59,0
ENTER SEVEN OUTLET VELOCITIES
? 0,3.66,6.34,12.5,18.05,26.31,34.07
```

STATION	INLET FLOW RATE (CFM)	OUTLET FLOW RATE (CFM)	TOTAL FLOW RATE (CFM)
1	137.5	0.0 — 126.6	137.5
2	108.1	13.7 — 112.9	121.8
3	100.5	23.8 — 102.8	124.3
4	86.8	46.9 — 74.7	133.7
5	53.7	67.7 — 55.9	121.4
6	21.0	98.7 — 27.9	119.6
7	0.0	127.8 — 0.0	127.8

```
AVERAGE FLOW RATE (BASED ON FLOW RATE) =  126.6 CFM

PRINT BED FLOW RATES AND VELOCITIES ?   (1 - YES, 2 - NO)
? 2
? 2  CONTINUE ?   (1 - YES, 2 - NO)
? 2
```

Figure 4. Sample work sheet indicating inlet, outlet, and total plenum flow rates.

TEST SECTION

BLOWER

ΔP

ORIFICE FLOW METER
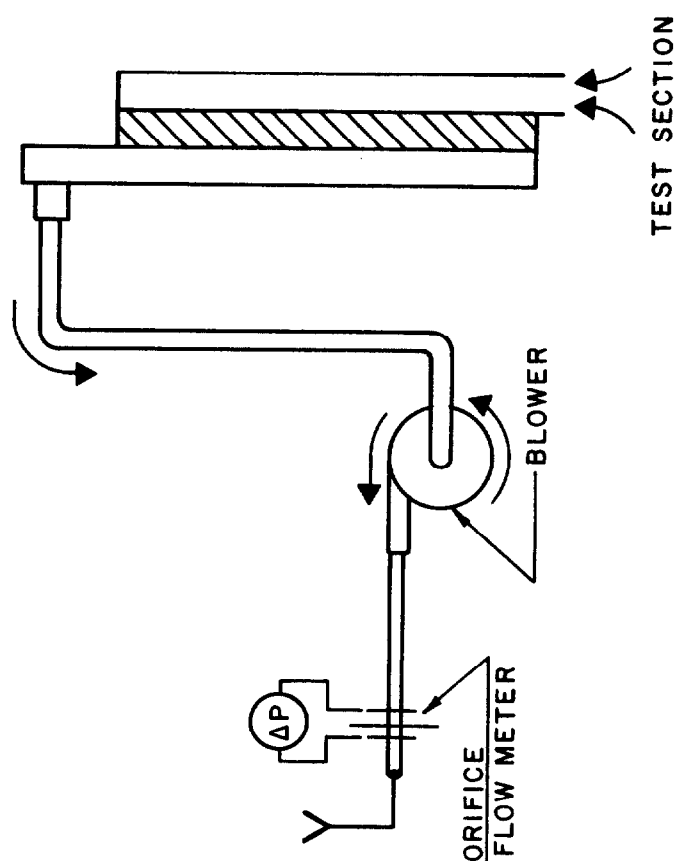
Figure 3. Flow schematic for test setup.

Figure 2. Cross section of apparatus in side view.

Figure 1. Cross section of typical all-welded adsorber in plan view.

☐ = INLET PLENUM FLOW RATE
CALCULATED FROM OUTLET PLENUM
AND TOTAL FLOW RATES

⊙ = INLET PLENUM FLOW RATE
MEASURED DIRECTLY
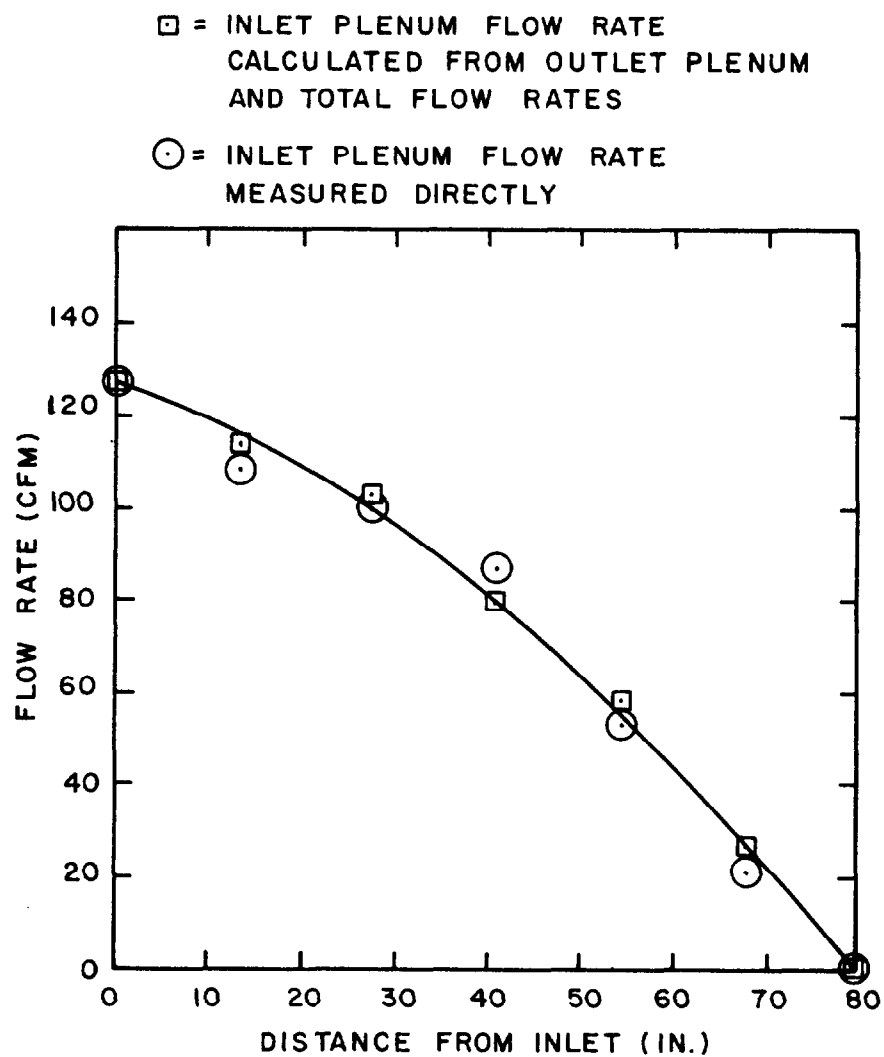
Figure 5. Sample indicated plenum flow rate and
best fit curve for Test No. 3A.

TEST DATA

1) TEST NO. – 9
2) FILL TECHNIQUE – POURED (LOOSE)
3) % OF MAXIMUM PACKING DENSITY – 86.5 %
4) AVERAGE FLOW RESISTANCE
   (ΔP/L AT 35.4 FPM) = 0.171 IN·W·G/IN
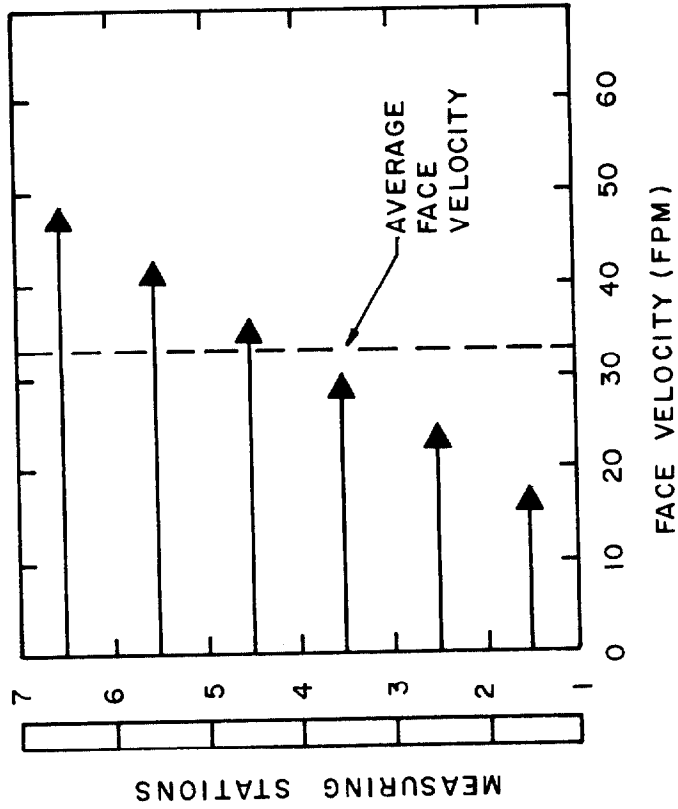
Figure 7. Face velocity distribution – Test No. 9.

TEST DATA

1) TEST NO. – 3A
2) FILL TECHNIQUE – POURED (LOOSE)
3) % OF MAXIMUM PACKING DENSITY – NOT MEASURED
4) AVERAGE FLOW RESISTANCE
   (ΔP/L AT 35.4 FPM) = 0.192 IN·W·G/IN
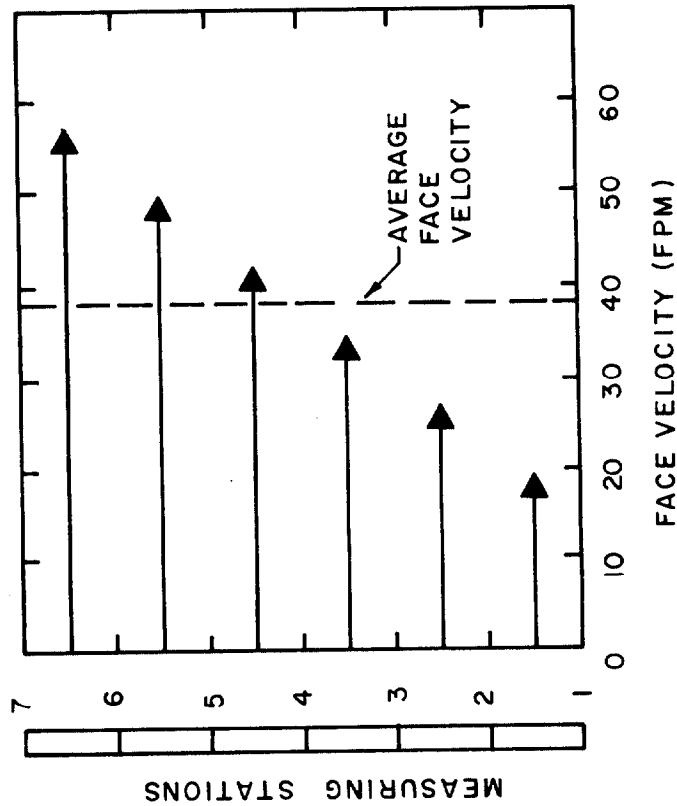
Figure 6. Face velocity distribution – Test No. 3A.

TEST DATA

1) TEST NO. –26
2) FILL TECHNIQUE – POURED & VIBRATED
3) % OF MAXIMUM PACKING DENSITY – 90.5 %
4) AVERAGE FLOW RESISTANCE (ΔP/L AT 35.4 FPM) = NOT MEASURED

NOTE: THIS DATA TAKEN ON BC-727 WITH AN ABNORMALLY LARGE MESH SIZE
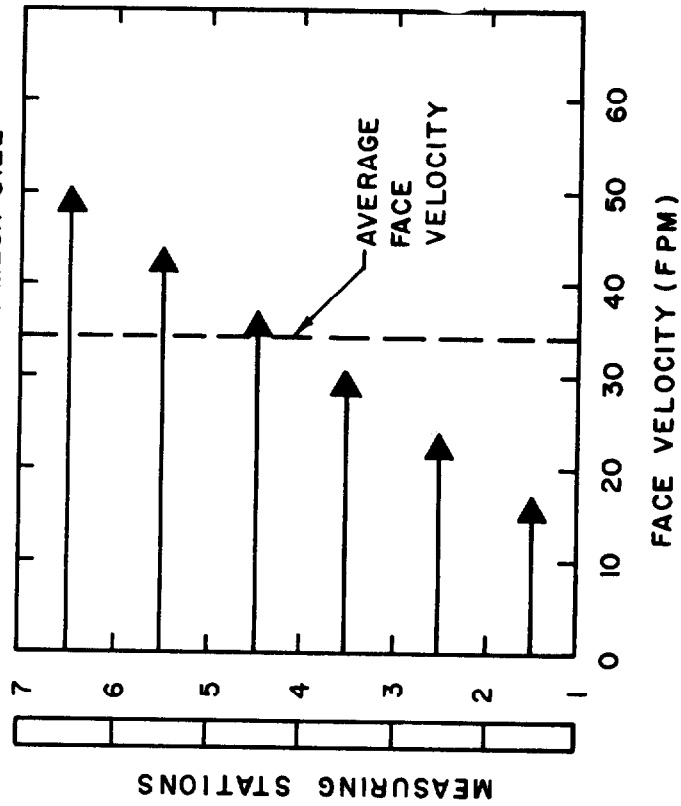
Figure 9. Face velocity distribution — Test No. 26.

TEST DATA

1) TEST NO. –11
2) FILL TECHNIQUE – POURED (LOOSE)
3) % OF MAXIMUM PACKING DENSITY – 86.5 %
4) AVERAGE FLOW RESISTANCE (ΔP/L AT 35.4 FPM) = 0.171 IN-W-G/IN
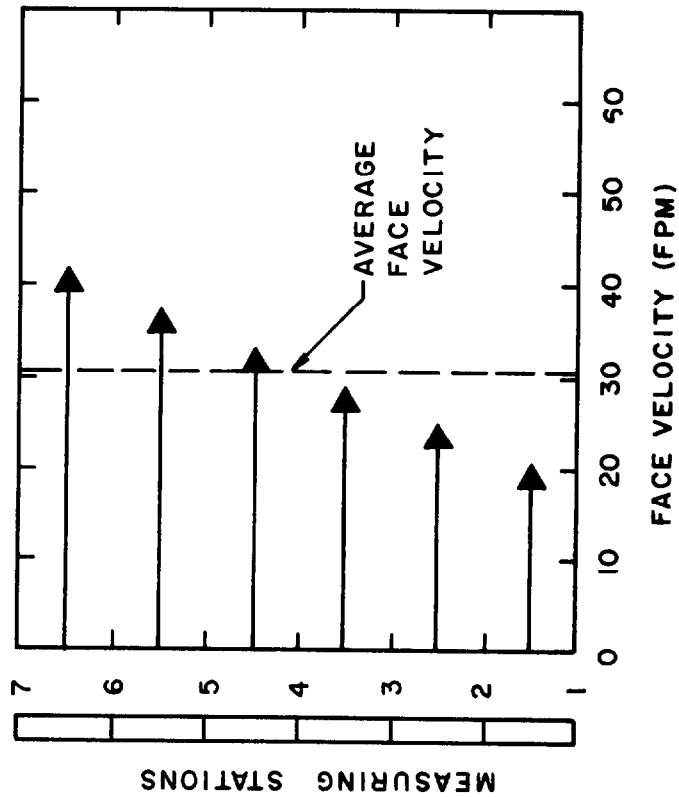
Figure 8. Face velocity distribution — Test No. 11.

TEST DATA

1) TEST NO. – 7A

2) FILL TECHNIQUE - GRAVITY PACKED (DENSE)

3) % OF MAXIMUM PACKING DENSITY – NOT MEASURED

4) AVERAGE FLOW RESISTANCE (ΔP/L AT 35.4 FPM) = 0.420 IN·W·G/IN
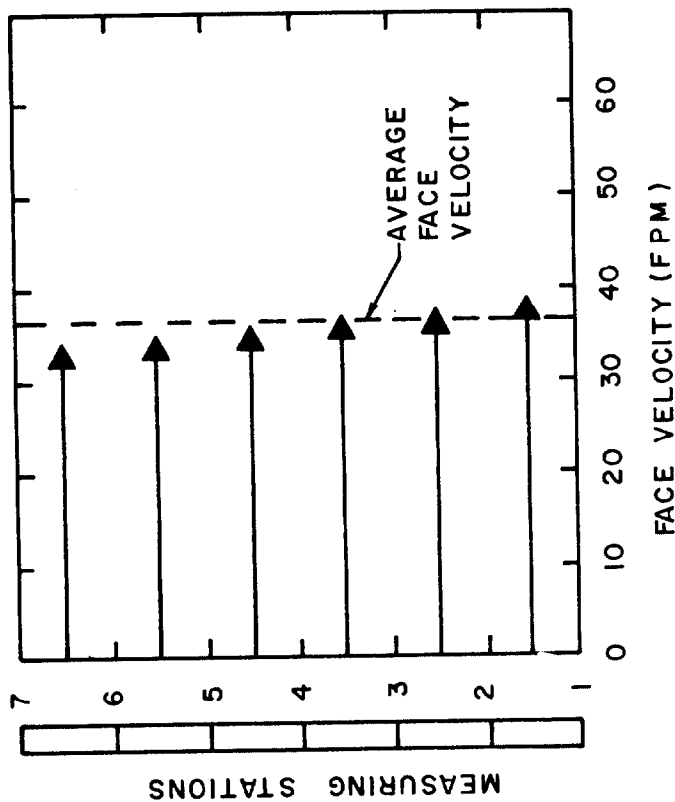
Figure 11. Face velocity distribution – Test No. 7A.

TEST DATA

1) TEST NO. – 6

2) FILL TECHNIQUE - GRAVITY PACKED (DENSE)

3) % OF MAXIMUM PACKING DENSITY – NOT MEASURED

4) AVERAGE FLOW RESISTANCE (ΔP/L AT 35.4 FPM) = 0.420 IN·W·G/IN
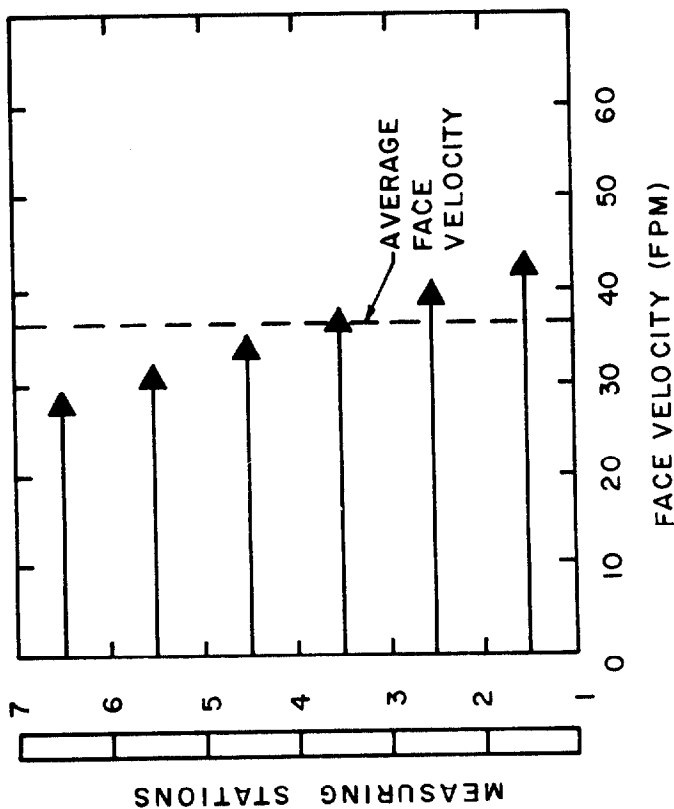
Figure 10. Face velocity distribution – Test No. 6.

TEST DATA

1) TEST NO. – 15
2) FILL TECHNIQUE – GRAVITY PACKED (DENSE)
3) % OF MAXIMUM PACKING DENSITY – 100 %
4) AVERAGE FLOW RESISTANCE (ΔP/L AT 35.4 FPM)=0.458 IN·W·G/IN
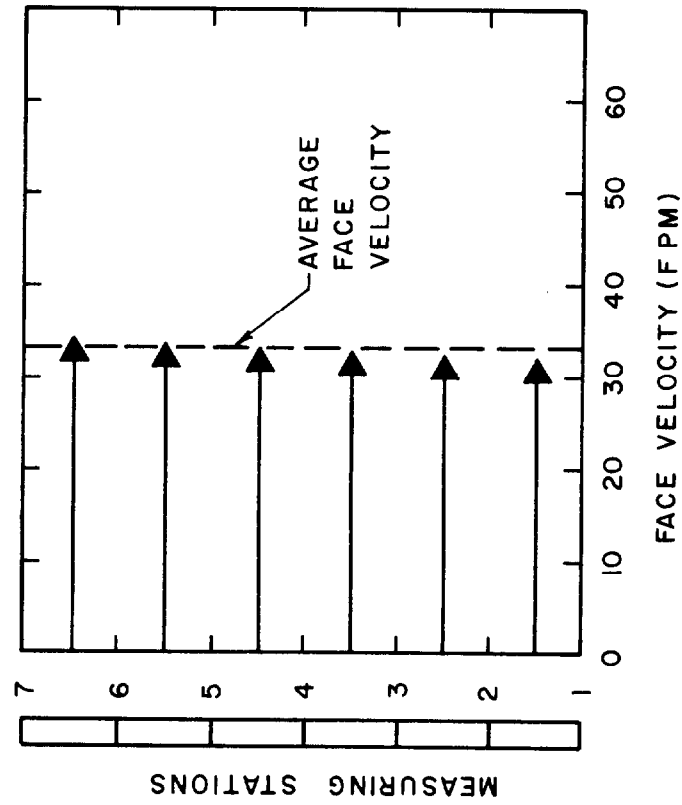
Figure 13. Face velocity distribution — Test No. 15.

TEST DATA

1) TEST NO. – 14
2) FILL TECHNIQUE – GRAVITY PACKED (DENSE)
3) % OF MAXIMUM PACKING DENSITY – 100 %
4) AVERAGE FLOW RESISTANCE (ΔP/L AT 35.4 FPM)=0.458 IN·W·G/IN

Figure 12. Face velocity distribution — Test No. 14.

TEST DATA

1) TEST NO. - 24

2) FILL TECHNIQUE - GRAVITY PACKED (DENSE)

3) % OF MAXIMUM PACKING DENSITY - 100%

4) AVERAGE FLOW RESISTANCE (ΔP/L AT 35.4 FPM) = 0.298 IN·W·G/IN

NOTE: THIS DATA TAKEN ON NEW BC-727 WITH AN ABNORMALLY LARGE MESH SIZE

Figure 15. Face velocity distribution — Test No. 24.

TEST DATA

1) TEST NO. - 23

2) FILL TECHNIQUE - GRAVITY PACKED (DENSE)

3) % OF MAXIMUM PACKING DENSITY - 100%

4) AVERAGE FLOW RESISTANCE (ΔP/L AT 35.4 FPM) = 0.298 IN·W·G/IN

NOTE: THIS DATA TAKEN ON NEW BC-727 WITH AN ABNORMALLY LARGE MESH SIZE
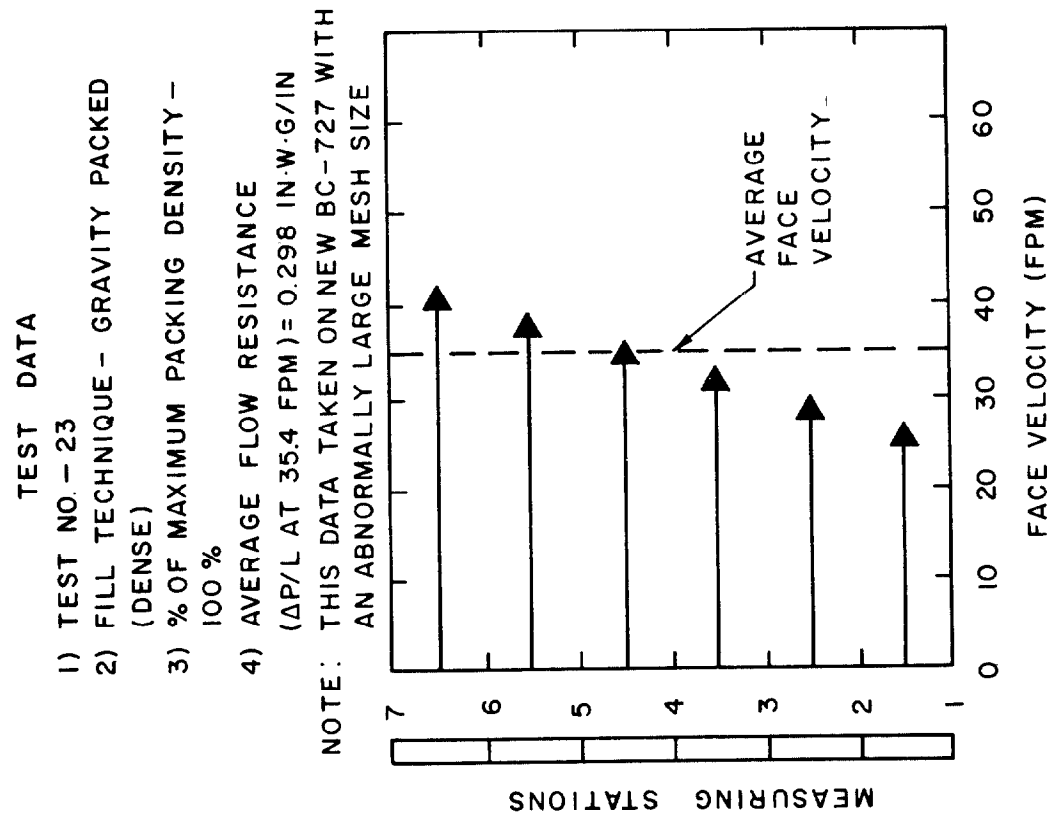
Figure 14. Face velocity distribution — Test No. 23.

865

Figure 17. Indicated inlet plenum flow rate and best fit curve for Test No. 7A.

Figure 16. Indicated inlet plenum flow rate and best fit curve for Test No. 6.

DISCUSSION

FIRST: Would you tell me how you measure 30 feet per minute with a pitot tube?

PARISH: Because of the time limitations, I didn't have time to discuss this in sufficient detail, I am afraid, but what I tried to indicate was that we did not try to measure the face velocity in and out of the carbon. What we measured was the velocity down the plenum, which has a much higher velocity than 30 to 40 feet per minute.

FIRST: How does this relate to the differential velocity over your face?

PARISH: If you would like to take the time, we could go back to the first slide which shows the test unit. The flow down the plenum is on the order of 1,500 feet per minute which you can measure quite well. If you know the difference in flow from one station to the next, you can then calculate the flow through the carbon from the continuity equation. From the volumetric flow rate through the carbon over the area between stations and from the area you can calculate the velocity.

FIRST: Your calculation may be correct, but it dosen't prove your point.

PARISH: I would like to say one other thing in that respect. I have some slides available which will appear in the paper that I could also show you. Using this technique, we measured the flow in the inlet plenum and outlet plenum individually and then compared the difference between the total flow and the flow in the outlet plenum. We got a very high degree of consistency, which should relieve your mind as to the validity of that approach.

BURCHSTED: Did you make any measurements directly downstream of the bed itself?

PARISH: You are talking about face velocity?

BURCHSTED: Outlet velocity.

PARISH: At the face of the bed?

BURCHSTED: Yes.

PARISH: Not in this effort. We had tried that previously, and I think this is the point that Dr. First was getting at. It is a very difficult thing to do. We tried it before. We have gotten some numbers, but we decided that it was basically an unsatisfactory approach, and that is why we went to this scheme for testing.

BURCHSTED: I suspect you get a lot of deviation, according to where you make the measurement across the bed. If you have directional effects, there will be no uniformity to the flow velocity.

STRAUSS: The first qeustion I would raise was asked by you, Mr. Chairman, and I noted the answer. The second is a remark, but first I want to know what bed thickness you have.

PARISH: This is a two inch bed. It actually measured about two and an eighth. It was intended in every way to be consistent with the standard conventional filter bed.

STRAUSS: I agree with you fully that the flow distribution is very important to get uniform removal of impurities. Because the bed described in our paper that you referred to is 10 times deeper, there are some differences in filling and in flow distribution. The velocity decrease we mentioned is due to the geometric form and is nearly uniform over the total crosssection of such a deep bed.

MARBLE: We tested a 4" flat bed 1" from the back face at 40 FPM. We found no real uniformity of flow. Some readings were as high as 500 FPM. How could you get such uniform readings in your system and how did you take the side vectors into account?

PARISH: I can understand. You would have difficulty trying to measure 40 feet per minute. That's correct.

MARBLE: I think that is what Dr. First was getting at.

PARISH: I would agree with him, too. I agree that you and everybody else would have difficulty measuring 40 feet per minute with a pitot tube. The thing I am trying to get across is that we did not attempt, in this effort, to measure 40 feet per minute. If there is time, I would like to go back to that first slide.

MARBLE: How did you take care of the fact that you had vectors in the plenum?

PARISH: Let me try to explain it this way: We measured the flow, not the velocity, to certain discreet sections of the bed. From the flow, we can calculate the velocity. The velocity normal to the bed, the 40 feet per minute nominal velocity, is insignificant compared to the velocity we are measuring, which, as I pointed out earlier, was on the order of 1,500 per minute.

STIEHL: There are 2 effects you are demonstrating: the change of pressure drop of a bed by varying the packing density and the change of velocity distribution in the experimental duct system by varying the pressure drop. Did you measure the influence of packing density to the linear velocity distribution in a rectilinear flow direction?

PARISH: That would be possible, and we could use that to demonstrate, say, the effect of a non-uniform packing density. However, one of the things that we are illustrating here would be obviated with that approach. In other words, if you are flowing straight in and straight out, then you would not have a variation in ΔP across the bed, which is what led to the non-uniformity in the first few slides. Yes, you could measure the flow uniformity if you flowed directly in and out, but that is not directly representative of typical filter systems.

STIEHL: I think you mix two principles. One is the change of density of the packed bed and the other is the distribution of the velocity in between the two beds in the channel in the duct where you approach the layer itself.

PARISH: We did, to an extent, mix them. We treated the first one by itself. In the first several slides that I showed you, we were measuring the effect of the velocity between two beds. In the third from the last slide, we introduced the effect of variations in packing density within the bed itself, illustrating that it overwhelmed the plenum velocity effect. Therefore, it was only a qualitative illustration of the effect of variations in packing density within the bed. By varying the packing density, or distribution, if you will, we completely reversed the picture. Instead of having the flow tending to be highest on the outlet end, now the flow was highest on the inlet end; even though the plenum velocity effect was still there. So I agree, it was not real clean, but we did show, I think, the significance of the effect.

A CONTAINMENT AND RECOVERY SYSTEM
FOR FUEL-REPROCESSING PLANTS*

T. R. Galloway
Lawrence Livermore Laboratory, University of California
Livermore, California 94550

Abstract

We identify tritium containment and removal problems in a fuel-reprocessing plant and explore conceptual process designs for reducing emissions to the environment to below 1 Ci/day. The conceptual design recommended would allow an air atmosphere in the reprocessing-plant hall, and would use a continuous-catalytic-oxidizer/molecular-sieve-adsorber cleanup system to maintain a $40-\mu Ci/m^3$ tritium level ($5~\mu Ci/m^3$ HTO) against 180 Ci/day leakage from components and process piping.

Containment Goals

Environmental Impact

Most fuel reprocessing plants routinely emit about 1500 Ci/day. The lowest practicable level for most tritium-handling facilities is around 3 Ci/day or 10^{-6} times the daily inventory handled, whichever is least. The goal in the fusion-reactor-engineering community is to reduce the total tritium loss to the environment to below 1 Ci/day. This level will be used as a standard in this study.

Losses from a fuel-reprocessing-plant containment hall with an approximate volume of 350 000 m^3 could be kept at this low level only if the tritium concentration within the gas cover (inside the hall) were kept low (i.e., around 40 $\mu Ci/m^3$). In addition, the entire wall surface would have to be either hermetically sealed or covered with a rare-metal getter (scavenger). The getter approach can be rejected on the grounds of cost and scarcity of materials; it would take 10 t of cerium, titanium, or some other rare metal to cover the walls of a 350 000-m^3 containment hall with a 1-mm-thick foil. At ambient temperatures, a stainless steel shell (alloys 304, 316, or 321) 2 mm (1/16 in.) thick would provide the needed permeation barrier[1]. The necessary welding and construction technology already exists. Such a shell, erected within a concrete building, would make it possible to meet our permeation standard (below 1 Ci/day) even in the case of an incredible accident in which 2.3 kg of T_2 (the assumed total inventory of a fusion facility) were ignited and dumped, releasing HTO or T_2O or both into the containment hall and quickly increasing the concentration up to 24.5 ppm (65 Ci/m^3).

The hermetic shell would be assembled on standoffs or studs cast into the concrete shell of the building. This would create a space between the building and the stainless steel liner. Tritium levels in the space would have to be kept below 5 $\mu Ci/m$. If we arbitrarily

state that the facility must be capable of containing T_2, HTO, or T_2O at the high accident-level concentrations described above ($65\ Ci/m^3$), and of reducing the concentrations to $40\ \mu Ci/m^3$ in 3 days of containment-hall air processing, then we can compute the length of the standoff required. If a 24.5-ppm spill leaks into this space for 3 days at 0.03 Ci/day (the permeation through 2 mm [1/16 in] of stainless steel) and if the level within the space must remain below $5\ \mu Ci/m^3$, the standoff distance for a 350 000-m^3 hall must be 79 cm. This release, under the worst possible meteorological dispersion conditions ($\chi/Q < 6.7 \times 10^{-4}$), would result in a minimal 0.002 mrem exposure to the general public. The design concept is economical and very safe; it would also qualify as providing for secondary containment of the hall.

Occupational Safety

The routine safety of the worker must be the prime consideration in setting normal ambient operating levels within the hall. We have selected $40\ \mu Ci/m^3$ of gaseous tritium as the ambient containment hall level [8 times the maximum permissible concentration (MPC)] for very particular health and safety as well as state-of-the-art hardware reasons. A worker can be exposed at $5\ \mu Ci/m^3$ (100% MPC) for 40 hours per week without any clothing protection if the HTO fraction remains below 12% by volume. Such environments (with once-through air) are not atypical of production facility work environments in the U.S. Mound[2] is demonstrating $40\ \mu Ci/m^3$ in a recirculating highly-processed system, and Los Alamos[3], on a smaller scale is demonstrating $0.5\ \mu Ci/m^3$ for 10^6 isolation between a processed glove box (at $1\ Ci/m^3$) and a room. For design purposes, the level chosen for normal operating conditions should be well below 100% MPC. ERDA recommends[4] that levels of 20% MPC should be used for design purposes. Such a standard would limit work assignments to 8 hours per week in a containment hall with a $40\ \mu Ci/m^3$ tritium concentration and would further require analytical evidence for HTO fractions below 2%. As an alternative, the worker could be protected by light-weight suits that would not interfere with his needs for agility and dexterity. Such light-weight suits (overalls with plastic over- and undergarment) with an independent air supply typically[5] can provide protection factors of 100 or more if changed hourly, and ventilated suits can provide factors up to 1400. Thus, it can be seen that the nominal level of $40\ \mu Ci/m^3$ offers many operational options, while still remaining close to the economic and safety optimum.

As mentioned above, there must be some assurance that our operational design could maintain HTO levels below 2%, and this question is critical to its practicality. The HTO can be produced from pure T_2 or HT by isotopic exchange with H_2O in the water-laden air within the hall, by autoradiolysis of T_2 in air (oxygen), by catalytic conversion of T_2 or HT on active metal surfaces exposed, and by radiolysis of T_2 or HT in air caused by radiation fields. If care is taken to eliminate hot, precious-metal (catalytic) surfaces, excess water vapor, and a buildup of T_2, then the formation of HTO can be kept at manageable levels. Estimates of the conversion rates have been made by fitting available data[6,7] to a rate equation. The results are as follows:

$$HTO = T_2(0)[1 - \exp(-kT_2(0)\theta)] , \qquad (1)$$

where θ is time for conversion in hours, $T_2(0)$ is the initial T_2 concentration in $\mu Ci/m^3$, k is the rate constant (k = 29 × 10^{-10} $m^3/\mu Ci \cdot h$ at 100% humidity; k = 6.24 × 10^{-10} $m^3/\mu Ci$-HR for dry air), and HTO is the calculated concentration of HTO in $\mu Ci/m^3$. At $T_2(0)$ levels of 40 $\mu Ci/m^3$, the rate of formation of HTO would always be less than 1.0 × 10^{-6} $\mu Ci/m^3 \cdot h^{-1}$. The conversion rate does not get significant until levels of 65 Ci/m^3 (over 10^6 times larger than those planned for in design) are approached. For the incredible accident case, 11 Ci/m^3 of HTO would be found in the first hour. From this analysis, we see that it is extremely important to keep T_2 at low concentrations.

The above predictions of HTO formation have been made assuming T_2 conversion by isotopic exchange and autoradiolysis in humid air. The effects of the availability of substantial areas of active metal surfaces on this conversion rate have been examined elsewhere[7]. A comparison of oxidation rates under various conditions is made in Table I. It can be seen that, overall, the enhancement effect results in concentrations some 500 times over those in dry air. However, it is clear from the HTO conversion rates that when the concentrations are kept low (i.e., 40 $\mu Ci/m^3$) and when the air within the containment hall is continuously processed and not allowed to sit stagnant for very long periods of time, the percentage of HTO present will remain well below the 2% figure desired for the design case (20% MPC HTO).

Process System Leakage

Containment Hall Processing

Now that it has been established that a tritium gas (2% HTO) level of 40 $\mu Ci/m^3$ is a safe working environment within the hall, we can proceed to examine the constraints that this level places on the process units within the containment hall. Experience in our facility at LLL and at other tritium research and development facilities in the U.S. suggests that whether a continuous air recirculation or a once-through air exhaust system is used, the ambient room levels will

Table I   HTO levels (in $\mu Ci/m^3$) produced under various containment hall conditions by oxidation of T_2 (initial T_2 concentration = 40 $\mu Ci/m^3$).

Time (h)	Dry air	Humid air	Catalyzed by steel*	Rad. field on steel**
1	9.96 × 10^{-7}	4.01 × 10^{-6}	9.75 × 10^{-5}	0.6 × 10^{-3}
2.5	2.49 × 10^{-6}	1.00 × 10^{-5}	2.44 × 10^{-4}	1.58 × 10^{-3}
50	4.98 × 10^{-5}	2.01 × 10^{-4}	4.88 × 10^{-3}	$\sim$3.1 × 10^{-2}
2 000	1.99 × 10^{-4}	8.00 × 10^{-3}	1.92 × 10^{-1}	$\sim$5.0
10 000	9.98 × 10^{-3}	4.00 × 10^{-2}	0.96	$\sim$25.0

* In humid air.
** Radiation field taken to be 40 000 R/h, on steel-catalyzed surfaces in humid air.

ultimately be dependent upon the cleanliness of the work, i.e., on how much outgassing of tritium occurs from leakage and deadsorption. The ambient level for a given room volume depends on the air replacement rate within this volume and the tritium outgassing rate. Our operating experience with once-through air exhaust systems suggests that 20 changes of air per hour are needed to keep room levels at about 15 μCi/m^3. Of course, when laboratory operations are not clean, the level will increase correspondingly.

In Table II, we give the results of a mass-balance analysis relating the maximum tritium outgassing rate that can be tolerated (based on the 40-μCi/m^3 level) to given air-flow rates in the 350 000-m^3 hall.

A processing system that could maintain the 40-μCi/m^3 level is shown in Fig. 1. This system would catalytically oxidize the T_2 and HT to HTO and capture the HTO on a molecular sieve. Operation at high temperature (350°C) would permit oxidation of tritiated hydrocarbons. The higher-boiling refractory organics could be trapped by an activated carbon column. Waste air would be recycled for the most part into the hall itself, with a small bleed stream exhausted to the stack, hopefully below 40 μCi/m^3. The processed air would enter the hall near floor level, where most of the workers would be located. The bulk flow of the reprocessed air would be 58.8 m3/s (100 000 cfm) or better. The air velocity near the worker might be in excess of 3.3 m/min (10 fpm); however, the net velocity upward through the interior of the containment hall would be only 0.33 m/min (1 fpm) or so. Thus, the fact that air is blowing past the worker (< 120 fpm) does not constitute a safety enhancement.

Spill Accident

The waste-gas processing system, the consequences of an accidental spill of the entire inventory (2.3 kg T_2), and estimated worker re-entry times after such a spill must now be considered. This problem is a difficult one because of the transient behavior of T_2O and T_2 adsorbed layers on all exposed surfaces, but neglecting the adsorption-controlled outgassing problems, we can make an estimate of the processing time required to reduce the 65-Ci/m concentration from the incredible accident, to the 40-μCi/m^3 operating level. Using the Mound Laboratory studies[8] for the determination of the catalytic oxidation kinetic rate data, a plug-flow reactor can be designed.

Table II   Maximum tolerable outgassing within containment hall to maintain 40-μCi/m^3 level.

Air flow		Volume changes per hour	Outgassing tolerated (Ci/day)
(m^3/s)	(cfm)		
0.36	607	1/24	1.0
5.88	10 000	0.05	18.0
58.8	100 000	0.5	180.0
2352	4 000 000	20.5	7200.0
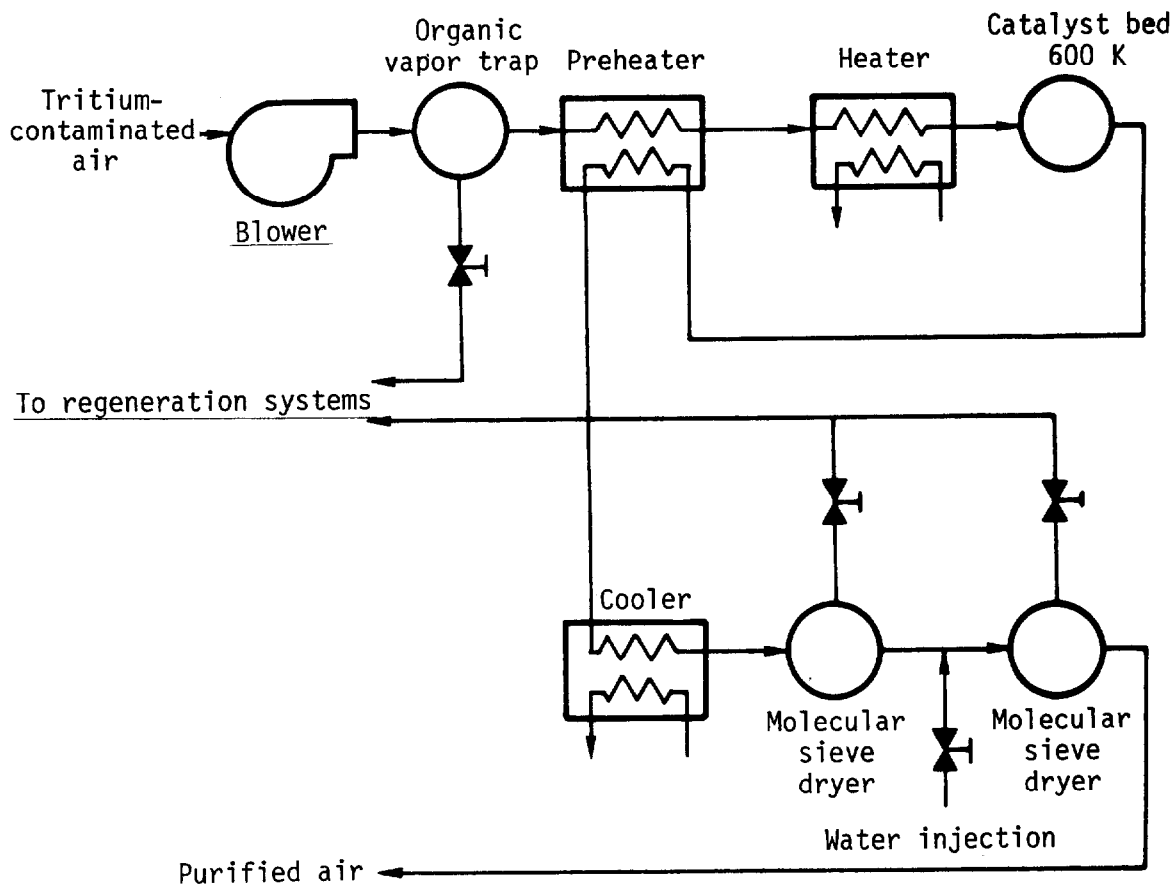
Figure 1   Catalytic oxidation and molecular-sieve adsorption of tritium.

A schematic for such a recirculating tritium-removal system is shown in Fig. 2. The tritium (T_2) concentration (in g/m^3 of total gas) is given as T and subscripted according to location. It is assumed that the containment-hall atmosphere is well mixed and that the volumetric removal of gas (mostly T_2O) is negligible compared to the recirculating flow Q_2.

A mass balance on the containment hall can be made by expressing the difference between inlet and outlet concentrations and the decrease in the prevailing level:

$$T_2 (\Theta) - T_1 (\Theta) = -\frac{V}{Q_2} \frac{dT_2(\Theta)}{d\Theta} , \qquad (2)$$

where Θ is the process time and V the containment hall volume. A similar balance can be made around the removal process unit:

$$Q_2[T_2 - T_1] = Q_3 T_3 \qquad (3)$$
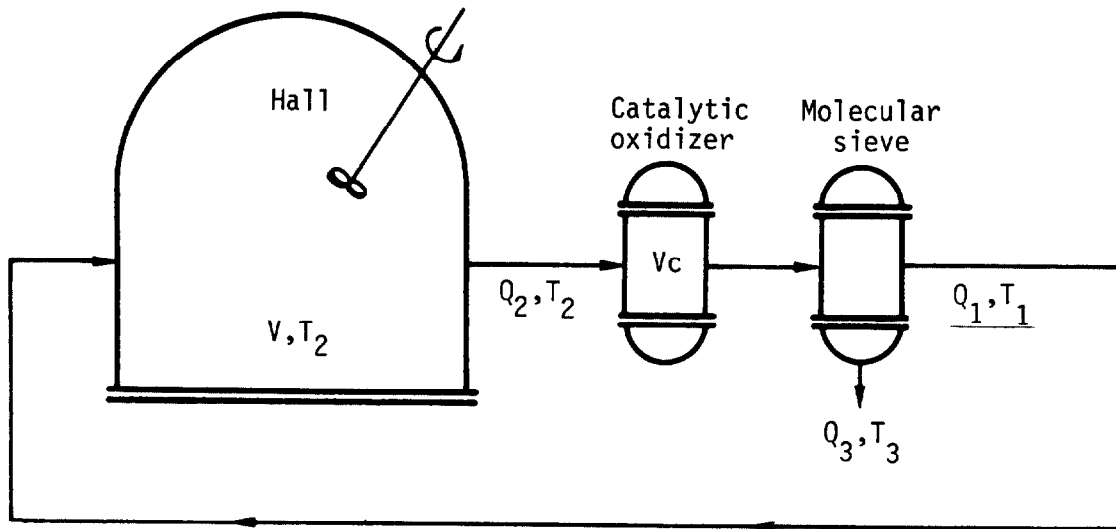
Figure 2   Model for prediction of tritium spill cleanup
dynamics.

or

$$\frac{T_1}{T_2} = 1 - \frac{Q_3 T_3}{Q_2 T_2} \, . \tag{4}$$

The plug-flow-reactor design equation can be written[9] as:

$$\frac{T_1(\theta)}{T_2(\theta)} = \exp\left[-k\frac{Vc}{Q_2}\right] , \tag{5}$$

where Vc is the catalyst volume and k is the first-order kinetic rate
constant,

$$k = 2.27 \times 10^5 \, \exp[-7100/RT] , \tag{6}$$

as determined at Mound[8]. Although this plug-flow approach is sim-
plistic in that it neglects pore diffusion and dispersion effects,
for low-temperature (300 K) operation, these effects are insignifi-
cant.

Eliminating $T_1(\theta)$ between Eqs. (2) and (5) results in:

$$T_2(\theta) \left[1 - \exp\left(-k\frac{Vc}{Q_2}\right)\right] = -\frac{V}{Q_2} \frac{dT_2(\theta)}{d\theta} \, . \tag{7}$$

Integrating,

$$\int_{T_2(0)}^{T_2(\theta)} \frac{dT_2}{T_2} = -\left[1 - \exp\left(-k\frac{Vc}{Q_2}\right)\right] \frac{Q_2}{V} \int_0^\Theta d\theta \, ,$$

results in

$$\frac{T_2(\Theta)}{T_2(0)} = \exp\left\{-\left[1 - \exp\left(-k\frac{Vc}{Q_2}\right)\right]\frac{Q_2}{V}\Theta\right\}. \tag{8}$$

In Table III, the results of the model calculations relating safe "re-entry times" as a function of required catalyst volumes are shown. Catalyst beds larger than 200 m3 are not practical because of the cost; thus, re-entry times range from around 1 day to 6 months for reasonable bed designs. Re-entry times of several days to a week or so would be acceptable; catalyst volumes from 10 m3 to around 100 m3 are therefore needed. There are many areas where costs can be cut if an optimization of the design is made to suit the particular specialized requirements for the containment hall processing.

We have looked briefly at one way of containing tritium in a fuel-reprocessing plant so as to limit the release to the environment to 1 Ci/d. The use of a gas cleanup system to provide a safe working environment and to make re-entry of personnel possible within a reasonable time after a large spill has been discussed.

Table III Tritium reduction after the incredible accident
[Q = 58.8 m³/s (100 000 cfm); $T_2(0)$ = 65 ci/m³;
V = 350 000 m³; Temp. = 300 K].

Elapsed time (h)	Tritium level (μCi/m³) for various catalyst volumes			
	0.17 m³	1.7 m³	16.7 m³	167 m³
30 (1 day)	6.05×10^7	3.21×10^7	1.71×10^5	0
600 (1 month)	1.54×10^7	48.03	0	0
3 000 (4 months)	6.56×10^4	0	0	0
10 000 (1 year)	2.12×10^{-3}	0	0	0
4 years	0	0	0	0
Approximate plant cost (millions of dollars)*	0.1	1.0	10.0	100.0

*Basis: honeycomb catalyst at 60 000 dollars/m³, constituting 10% of plant cost.

References

1. T. S. Ellemen and K. Verghese, "Surface effects on tritium diffusion in niobium, zirconium, and stainless steel," *J. Nucl. Mater.* 53, 229-306 (1974).

2. C. J. Kerschner and J. C. Bixel, "Tritium effluent control laboratory," *Proc. 13th AEC Air Cleaning Conference*, San Francisco, August 12-15, 1974. U.S.AEC Conf. 740807, Vol. II, pp. 948-971.

3. J. L. Anderson, F. A. Damiano, and J. E. Nasise, "Tritium handling facilities at the Los Alamos scientific laboratory," *Proc. 23rd Conference on Remote Systems Technology*, San Francisco, November 1975, pp. 77-88.

4. "Standards for Radiation Protection," *U.S. Energy Research and Development Administration (ERDA) Manual*, Chapter 0524, pp. 1-25, Jan. 1, 1975.

5. R. V. Osborne, "Absorption of tritiated water vapor by people," *Health Phys.* 12, 1527-1537 (1966).

6. G. J. Casaletto, L. H. Gevantman, and J. B. Nash, *The Self-Radiation Oxidation of Tritium in Oxygen and Air*, U.S. Naval Radiological Defense Laboratory, San Francisco, US NRDL-TR-565, May 8, 1962.

7. A. Alan Moghissi and Melvin W. Carter, *Tritium*, Messenger Graphics, Phoenix, Arizona, 1973.

8. J. C. Bixel and C. J. Kerschner, "A study of catalytic oxidation and oxide absorption for the removal of tritium from air," *Proc. 2nd AEC Environmental Protection Conference*, Albuquerque, New Mexico, April 16-19, 1974, pp. 261-284.

9. O. Levenspiel, *Chemical Reaction Engineering*, Second Edition, John Wiley, N.Y., 1972.

REDUCING AIR CLEANUP SYSTEM COSTS

Howard R. Reedquist Jr.
CTI-NUCLEAR, inc.
Denver, Colorado

I. Introduction

The majority of Air Cleanup System specifications issued this last year, for Air Cleanup System manufacturers to bid to, have contained numerous errors. These errors range from omissions and conflicting requirements to more stringent requirements than are required by government specifications and are obtainable by the industry. This increases the engineers time and manufacturers time and costs in resolving and correcting these errors, thus frequently delaying the schedule and increasing the Air Cleanup Systems cost.

II. Causes and Solutions

During the past years we have reviewed many such technical specifications in support of our Sales Department in preparing bid proposals for Air Cleanup Systems. As an engineer, my interest is in establishing the technical requirements of the equipment and proposing a cleanup system design that meets the users requirements, as he states them in his specification.

But what the engineer wants or needs in his Air Cleanup System is not always what he indicates in his technical specifications to bidders. A few reasons are apparent.

First: He is often an H.V.A.C. or Mechanical Engineer, newly hired by the expanding Architect Engineer or utility, who has not worked with specifications of Nuclear Air Cleanup Systems before, and is scheduled to issue his Air Cleanup System Technical Specification in a couple months.

Second: He has quickly read a number of the government regulations and specifications, and has become lost in the paper mill of confusing and sometimes conflicting requirements.

Third: He has reviewed a number of product catalogs, some of which are obsolete, and has become confused by the alternatives.

Fourth: He looks for a quick way out of his dilemma to issue his technical specification on schedule -- and he apparently has two or three alternatives.

The first alternative, one that has been used many times, is to obtain a copy of a previously issued Air Cleanup System specification from another division of his company, that is working on another nuclear plant. Using this as a guide, he uses the same text, changing the CFM and instrumentation to fit his particular requirements. But his new technical specification now has inherited any errors that the original specification had, and perhaps some more stringent requirements than his air filter units may really need.

Examples to illustrate this include:

1. Eight independent omissions in one specification, listed as controlled by the specification, for heating coil fin configuration and materials, prefilter test requirements, HEPA filter type for MIL-F-51068, HEPA filter test requirements, and fan drive arrangement and other construction features.

2. Incorrect HEPA filter section flow rates $2\frac{1}{2}$ times the capacity of other parts of the Air Cleanup System.

3. Air flow measurements in the middle of an Air Cleanup System housing, accurate to within 5% of the system's rated flow, with instrument terminals for remote readout and recording. The air flow velocity pressure the engineer was going to measure was 0.006 in. w.g., while the air flow velocity pressure at the inlet and outlet were 0.1 in. w.g.; a still difficult but measurable figure.

4. A charcoal adsorber section with a 12-inch head of charcoal above the filter beds with viewing ports and lights above the charcoal to verify that it would not settle after properly filling the 4-inch beds. This required unnecessary stainless steel, welding and inspection, windows, lighting and wiring, and charcoal.

A second alternative, used less frequently, is for the engineer to lift the most stringent requirements from several specifications and the highest performance levels from the various product catalogs he is able to obtain in his limited time. But this leads to some conflicting or unrelated performance requirements in his specifications, when the highest performance is used from various products, and more stringent requirements than his Air Cleanup Systems may really need.

Examples to illustrate this include:

1. Charcoal adsorbent impregnated with 5% TEDA, but with the charcoal ignition temperature above the requirements of the RDT M16-IT at a value obtainable only with a 2% TEDA or 3% KI_3 Impregnation.

2.   Moisture and over pressure dust loading tests for one HEPA filter from each roll of filter media used on filters meeting the requirements of MIL-F-51079 with QAS testing. The price of this destructive testing was twice the price of the total quantity of HEPA filters to be built per the MIL Specs and individually tested at a QAS station.

3.   Prefilters of 85% ASHRAE Dust Spot Test efficiency to be individually tested with 0.3 micron DOP smoke per military Standard 282.

4.   Air Cleanup Systems used in normal recirculating control room air and auxiliary buildings, for air that men are working in, which have the following component requirements:

A.   Withstand temperatures up to 300 degrees Farenheit.
B.   Withstand a radiation dose of 1×10^6 Rads.
C.   Include a water deluge system for fire extinguishment in the charcoal adsorber due to decay heat from adsorbed radioactive iodine.

In preparing a proposal, we assume that the engineer really wants what his technical specification states, and therefore attempt to propose and price a design which meets his specification. Some Air Cleanup System manufacturers question unusual requirements with the engineer, some include it in their design and pricing, and some omit it, taking an exception to the specification. Now the Engineer must wade through proposals which include and omit various items in their price, and to the Purchasing Department, it is like pricing apples and oranges.

An option which we believe results in a better technical specification, is for the engineer to review and design his Air Cleanup Systems using ORNL-NSIC-65, or its replacement when available, ERDA 76-21, as a guide and handbook. In addition, his specification should require that the design, construction, and testing of the systems and their components are to meet the requirements of ANSI N-509 and 510, as applicable. These standards call out the remaining government and industry standards, which therefore do not need listing again in your technical specification. Add to this, consultation with one or more of the manufacturers who have built Air Cleanup Systems to a number of government and engineers' specifications, and are familiar with what is required and what performances in components are available, and you will have a better, more precise, technical specification for your Air Cleanup Systems.

Conclusion

By working with your engineers, the Air Cleanup System manufacturers, or a knowledgeable independent consultant, can supply them with information they are unaware of and can obtain information that they are having difficulty obtaining. We can help them design their system and work out their technical problems so that they may arrive at a satisfactory design to meet the Air Cleanup System performance requirements and prepare a technical specification that correctly and precisely identifies these requirements.

An accurate specification identifying what is really required, reduces the Air Cleanup System manufacturer's time and cost in preparing bid proposals, thus reducing his operating costs, and eliminates unnecessary repetitive phone calls to the engineer from each Air Cleanup System manufacturer. Thus, the engineer reduces his initial specification preparation time, reduces the number of calls he receives to clarify his specification, reduces his time required to evaluate the proposals submitted in response to his specification, and reduces the price manufacturers ask to meet his specification. In addition, he becomes more knowledgeable about the requirements and performance his Air Cleanup Systems will meet.

ABSOLUTE FILTERS: EFFECTIVE FILTERING MEDIA

George Cadwell
Flanders Filters, Inc.
Washington, North Carolina

The amount of effective filtering media in an absolute filter, i.e. that media which is available to remove particulates, is a function of the method used to construct the filter. The effective filtering media is not necessarily equal to the total amount of filtering media in the filter.

This may seem like a profound statement of oversimplification, but I believe it is relevant now for two reasons:

1. On August 1, 1976, we learned that, for the first time a separatorless filter passed all of the testing performed by Edgewood for QPL listing.

2. Certain data have been presented here which are in disagreement with data gathered from experience in evaluating the performance of separatorless filters over extended periods of service life.

Experience indicates that separatorless or molded type filter applications have approximately 3 times the service life of filters of conventional construction with flat roll media and corrugated separators. This experience is derived from applications where filters have been in service for periods ranging from six months to three years.

The phenomenon of effective filtering media vs total filtering media was detected during tests to determine the reasons for the proven extended life of the molded filter element.

As a part of these tests, filters constructed with both molded filter packs and separator type filter packs were subjected to surface dust loading by ASHRAE test dust without linters. After the filters had been surfaced loaded, they were cut apart and samples of the filtering media were removed. It was noted that the media from filters made with separators showed alternating bands of black and white throughout the depth of the filter. The black bands indicated those areas of the filtering media that had been exposed to the test dust. The white bands indicated those areas where the crowns of the separators had pressed against the filtering media to block the effective use of the media.

The percentage of effective filtering media in a separator type filter was calculated by measuring the band width between the crowns of the separators and the widths of the white bands indicating blockage of the media by the crowns of the separators. From these measurements, the total effective area of filtering media for various types of size 24" x 24" x 11-1/2" filters were calculated as follows:

TYPE FILTER PACK

	Mini-Pleat	Standard	Molded
Width of Separator Shielding Band-In	.06	.08	.05
Width of Media-Crown to Crown-In	.30	.43	.70
Effective Media-Crown to Crown-In	.24	.45	.65
Percent Effective Filtering Media	80.0	81.4	92.9
Total Filtering Media – Sq. Ft.	292.3	263.1	289.4
Effective Filtering Media – Sq. Ft.	233.8	214.2	268.8

It is concluded that the greater proven service life of the molded filter element is the result of greater area of effective filtering media and the lower initial pressure drop of the molded element.

The affects of the filter media thickness have not been evaluated at this time. Standard roll filtering media is used in thicknesses of 15 to 19 mils. Molded filter elements are made from media of 22 to 25 mil thicknesses.

DISCUSSION

FIRST: Do I understand from the slide you showed that those pleats are floating in air and don't touch each other? You showed 100 per cent of the filter medium available.

CADWELL: That was an error, it should have been 92.9%. That's why I made the point of extended service life for the separatorless filter. We find that when you have this per cent of filter media in the filter, airflow resistance is equal to a single layer of paper at equal filtration velocity.

DEMPSEY: I am very glad to see this trend toward increasing the capacity of filters. It is a very important matter down the road for waste management. Lately, we have heard a great deal about at least two manufacturers in Europe who place twice as much paper in the same area. I would be very interested to know if anyone has tested them for performance.

CADWELL: I think Chuck Skaats may be testing some now.

SESSION X

LMFBR AIR CLEANING SYSTEMS

Wednesday, August 4, 1976
CHAIRMAN: C. Newton

THE AEROSOL BEHAVIOR IN LMFBR ACCIDENTS: RESULTS OF TUNA EXPERIMENTAL
    PROGRAM AND COMPARISON WITH PARDISEKO CODE
                                    W. O. Schikarski

AN EVALUATION OF ALTERNATIVE AIR CLEANING SYSTEMS FOR EMERGENCY USE
            IN LMFBR PLANTS
                                    J. D. McCormack, R. K. Hilliard
                                    A. K. Postma, L. D. Muhlestein

EVAULATION OF IN-VESSEL AIR CLEANING SYSTEMS FOR AN LMFBR
                                    W. C. Hinds, E. F. Mallove,
                                    M. W. First

OPENING REMARKS OF SESSION CHAIRMAN:

As you know, air cleaning systems have long been an important
safety feature in nuclear installations and are often provided for
lightwater reactors as a means of reducing radiological consequences
of postulated accidents.

You may be wondering why we have a separate session on LMFBR air
cleaning. The reason, quite simply, is that postulated accidents for
LMFBR's and the environments that they lead to are significantly dif-
ferent than those postulated for lightwater reactors.

The main difference, of course, is the sodium coolant which does
lead to a potential for large releases of sodium oxide and sodium
hydroxide aerosols. Such aerosols do provide quite a challenge for
an air cleaning system. Early research indicated that HEPA filters
rapidly plugged when challenged with sodium oxide and sodium hydroxide
aerosols. Therefore, if one is to use some sort of a filtration sys-
tem, a prefilter would be necessary.

The work to data on prefilters is very encouraging and a number
of options appear to be viable. Spray systems, which are sometimes
used in light water reactors, are also a candidate for LMFBR air
cleaning systems. We cannot, of course, use water because of its in-
compatibility with sodium, but other materials are under investiga-
tion and show promise.

A point I would like to leave with you is that ERDA is agres-
sively pursuing the development of air cleaning systems as an en-
gineered safety feature for LMFBR's.

THE AEROSOL BEHAVIOR IN LMFBR ACCIDENTS:
RESULTS OF TUNA EXPERIMENTAL PROGRAM AND
COMPARISON WITH PARDISEKO CODE

W.O. Schikarski
Laboratorium für Aerosolphysik und Filtertechnik
Kernforschungszentrum Karlsruhe, Germany

Abstract

Aerosol behavior in contained vessels is of high significance for LMFBR safety analysis. In the TUNA program UO_2-particle concentrations have been measured in a 2.2 m^3 and a 0.022 m^3 vessel as function of time. A corresponding computer code PARDISEKO III was developped which is capable to describe the concentration time function for different geometries and gas temperatures. The aerosol processes most important for aerosol behavior have been identified. The significant experimental results are reported and compared with theory. Open problems in the complete description of aerosol behavior in LMFBR containments are discussed.

I. Introduction

The activity release and transport into the environment in the case of a severe accident in a nuclear power plant is of high significance in any reactor safety analysis. For the LMFBR the special problems of formation, transport, behavior and (eventually) release to the environment of aerosols originated from core disassembly and other sources are of particular interest.

In the Nuclear Research Center Karlsruhe a research program has been carried out which dealt with the behavior of nuclear aerosols in contained systems. The program has been completed in 1974 with his first phase and covered the investigation of the time functions of UO_2 aerosol concentration in dry and N_2 filled atmosphere, the determination of the aerosol processes involved and the modelling of the airborne aerosol system by computer code.

This paper describes the more important experiments, their results, the general findings on aerosol processes, the computer code developped and the still existing problems.

II. Experiments on Nuclear Aerosols

Goals

The goals of the program were the following:

- Determination of the particle size and related parameters of nuclear aerosols (i.e. aerosols formed in typical accidents in LMFBR's with core disassembly) as function of accident conditions

- Determination of the particle number concentration and aerosol mass concentration as function of time in the containment system considered

- Determination of physical and chemical properties of nuclear aerosols, their

interaction processes and the influence of these processes on the aerosol behavior

- Development of suitable models capable to extrapolate of the experimental results to real containment geometries.

The ultimate goal of the program is the reliable description of the activity release in severe accidents of a LMFBR.

Experimental Results

The experiments have been carried out in the experimental facility TUNA (Teststand für die Untersuchung nuklearer Aerosole) which has been described elsewhere[1] in detail. In this facility a number of aerosol measurement techniques are concentrated around a stainless steel vessel of 2,2 m^3 free volume simulating a nuclear reactor containment. The main characteristics of TUNA are given in table 1, a schematic graph is given in figure 1.

The UO_2-aerosols investigated in this part of the experimental program were produced in all cases by the exploding wire technique. A sintered UO_2 cylinder of 40 mm length and 4 mm diameter is preheated by an irradiation furnace until it becomes electrically conductive. Then a puls current from a bank of capacitors is lead through the cylinder, heating it up and vaporizing parts of the material. A rather fine aerosol is produced by this way as has been reported in [2]. The typical conditions under which the UO_2-aerosol have been formed in all experiments are given in table 2.

Typical aerosol measurement methods were used, namely for the particle number concentration the condensation nuclei counter, for aerosol mass concentration the activation analysis, for particle size analysis the usual electron or light microscope techniques.

Because of the necessity of modelling the aerosol behavior for extrapolation to real containment conditions the exact description of the particle number concentration as function of time is the most important part of the program. Determining the particle number concentration the following test runs have been carried out (the most important ones are mentioned only):

- Vaporization of UO_2 in N_2 in the main vessel of TUNA and subsequent measurement of particle number concentration as function of time at room temperature

- Vaporization of UO_2 in N_2 in the small adjacent vessel (aerosol chamber) and subsequent measurement of particle number concentration as function of time at room temperature

- Vaporization of UO_2 in N_2 in the main vessel and subsequent measurement of particle number concentration at function of time for different gas temperatures.

The results of these tests are summarized in figure 2,3 and 4. The range between the solid lines (fig. 2) represents the error range. All experimental measuring points (11 tests) were within that range of error.

main vessel	material	stainless steel
	volume (cylindrical)	2.22 m^3
	surface	8.8 m^2
	hight	2.9 m
	diameter	1.0 m
	distance from probe to bottom	3.1 m
aerosol chamber	(on top of the vessel) material	stainless steel
	volume (cylindrical)	0.02 m^3
	surface	0.5 m^2
	hight	0.34 m
	diameter	0.30 m
	distance from probe to bottom	0.17 m

<u>Table 1</u>   Data of TUNA

probe (cylindrical) dimensions	UO_2 sintered
length	40 mm
diameter	4 mm
electrical energy inserted	ca. 500 Wsec/g
energy insertion time*)	ca. 3 msec (0.1 msec)
vessel conditions	
pressure	1 at
temperature	20 °C
relative humidity	10 %
atmosphere	N_2 filtered
purity of the UO_2 aerosol	
impurities (total)	< 0.1 %
impurities elements	Ta.W.Ni.Mn.

*) Experiments No. 147 and 166 have been carried out with
time constants of 0.1 msec, experiments No. 152 and 163
with time constants of 3 msec. An influence of time
constants on the primary particle behavior has not
been observed.

<u>Table 2</u>   Conditions of aerosol formation in TUNA

An important characteristic of aerosol behavior in closed systems is the initial
particle size distribution. Extensive measurements of these parameters revealed
the following result:

- The initial particle size distribution is logarithmic normal but does not
  necessarily remain exact log-normal during the whole course of the life of the
  aerosol system

- The initial mean geometric diameter (projected area) depends on the energy

inserted into the UO_2 probe. For 500 Ws/g the MGD was 0.08 μm with σ=1.85. Higher inserted specific energy resulted in smaller particle size.

Discussion of Experimental Results and Comparison with Theory

Early presumptions upon the most important aerosol processes acting in an airborne, dry and contained aerosol system resulted on the basis of general considerations of aerosol physics in the statement, that at least the agglomeration process (coagulation) and the settling process (sedimentation) are effective[3]. As can be seen from fig. 4 the effect of temperature on the aerosol concentration decay curve is significant also. Therefore, thermophoresis (aerosol transport in a temperature gradient) contributes also and has to be incorporated in the modelling. Furthermore, the diffusion process which takes into account the fact that along the containment wall will always exist a concentration gradient has to be taken into account.

More or less (depending on containment geometry , particle concentration, gas temperature and other parameters) all four processes are effective. The computer code PARDISEKO III, developped on the basis of the TUNA experimental program results, includes all these aerosol processes in an adequate form[4]. The essential mathematical equations of PARDISEKO III are listed in the appendix of this paper.

In the comparison of experimental and theoretical (PARDISEKO III) results it was found that an aerosol model comprising the above mentioned aerosol processes can describe the aerosol behavior satisfactory if essentially the following aerosol related parameters are known (see appendix):

$$c_p(0) = \text{initial particle number concentration}$$
$$r_g = \text{initial mean geometrical particle radius}$$
$$\sigma^g = \text{standard deviation of radius distribution}$$
$$\delta_D = \text{mean diffusion boundary layer thickness}$$
$$\delta_T = \text{mean thermal boundary layer thickness}$$
$$f = \text{collision form factor}$$
$$\kappa = \text{dynamic form factor}$$
$$\rho = \text{density of particle material}$$

Along with these aerosol parameters, of course, a number of non-aerosol parameters (gas viscosity, gas and wall temperatures, containment geometry, thermal conductivity of carrier gas and others) must be known. However, these parameters are easy to determine or to measure. From the aerosol parameters the first three $(c_p(0)$, r_g, $\sigma)$ were measured in the experimental program. δ_D and δ_T were estimated from literature data (see[1]), where f and κ were used as fitting parameters.

These two form factors describing the deviation from behavior of a spherical particle in comparison to the real irregularly shaped particle related to the aerosol process considered (f = collision form factor relates to coagulation, κ = dynamic form factor relates to diffusion, sedimentation and thermophoresis) appeared to be the focal point in the aerosol modelling theory.

κ has been measured by other authors for a variety of particles of different material except UO_2, whereas f can only be determined indirectly. Using κ = 3.5 according to literature data for other particles (here κ lies between 2 and 6) and assuming f = 8.2 a time function for $c_p(t)$ was calculated with PARDISEKO showing good agreement between experiment and theory (fig. 2, curve I). For comparison κ and f were varied (see fig. 2). Curve II is based on f = 1.0 and κ = 1.0 which means spherical particles only. Curve III is based on f = 1.0 and κ = 3.5 and curve IV

on $f = 8.2$ and $\kappa = 1.0$.

A further prove of the assumed values for f and κ can be taken from fig. 4. Here PARDISEKO was applied to an aerosol system at elevated temperatures. Again, with the same form factors as used in curve I of fig. 2 the best agreement between experiment and theory was achieved. Moreover, for the case of the small chamber experiments (fig. 3) again the applied κ and f values as in curve I of fig. 2 gave the best agreement.

It should be mentioned, however, that in all PARDISEKO calculations the theoretical density of the particle material was assumed. This is not in agreement with the experimental findings, since all UO_2 particles investigated showed a more porous structure than a compact structure. There exists, however, certainly a close correlation between particle form factors and particle density. Therefore, a combination of $\overset{\circ}{\rho}$ with κ and f will probably be a better approach from the standpoint of aerosol physics. Nevertheless the form factors discussed are of great importance in aerosol modelling and cannot be neglected if the behavior of irregularly shaped particles is described.

III. On the State of the Art of Aerosol Modelling

In the foregoing chapters the TUNA program results in comparison with PARDISEKO theory was discussed. Concerning the behavior of nuclear aerosols in a LMFBR post-accident atmosphere the present state of knowledge can be described as follows:

a) The time function of an instantaneously formed aerosol concentration in a contained system can be satisfactorily described by the PARDISEKO III code, if some assumptions (form factors) are made which from the standpoint of aerosol physics are reasonable.

b) In the accident analysis not only UO_2 (or PuO_2) aerosols are important. For the SNR-300 four aerosol sources are considered (see table 3). Only two of them are instantaneously formed. Although PARDISEKO III is capable of calculating several timely overlapping sources the confirmation by experiments is still lacking.

c) Since the aerosol system in a core disassembly accident is formed of several sources the problem of mixed aerosols (consisting of UO_2, Na, fission products etc.) should be investigated. The properties (physical, chemical) of these aerosol sources should be investigated.

d) In all so far known experiments on aerosol behavior in contained systems only small volumes have been used (up to 10 m^3). In that volumina the influence of thermal convections is small and negligible. The effect of thermal convections in real containments on aerosol concentration time functions remains to be investigated.

e) In the post-accident containment atmosphere of LMFBR's a considerable amount of vaporized sodium will exist. Since depending on temperature and pressure conditions some of the sodium will condense the influence of condensation on particle behavior should be investigated.

IV. Summary

The TUNA program on the behavior of nuclear aerosols in contained systems has

SOURCE ORIGIN	COMPOSITION	TIME OF FORMATION	INITIAL PARTICLE DIAMETER	REMARKS
CORE DISASSEMBLY	UO_2-PuO_2, FISSION PRODUCTS STEEL, SODIUM	INSTANTANEOUS	< 0.08 μm (INCREASING)	HIGH INITIAL CONCENTRATION
NA-RESIDUAL O_2 REACTION	Na_2O	INSTANTANEOUS	0.1 μm (INCREASING TO CA. 0.4 μm)	
NA-EVAPORATION FROM CORE CATCHER	NA	LONG TERM (DAYS)	0.1 μm (INCREASING TO CA. 0.3 μm)	RECONDENSATION AEROSOL WITH TRACE FISSION PRODUCTS AND FUEL
H_2O-EVAPORATION FROM CONCRETE	NAOH	LONG TERM (DAYS)	?	
GFK/LAF I	AEROSOL SOURCES IN ACCIDENT OF LMFBR			33346

table 3

been carried out in his first phase by using inert UO_2 aerosols in an inert N_2 atmosphere. These experiments which did not yet simulate real containment conditions served to explore what aerosol processes are involved in aerosol behavior. The results show that the most important aerosol processes are

- coagulation
- sedimentation
- thermophoresis and
- diffusion

In modelling aerosol behavior it has been clarified that certain aerosol parameters (form factors) play an important role and cannot be neglected. The computer code PARDISEKO III describes satisfactorily the experimental results and is a tool in the calculation of activity release in heavy accidents. Further research is necessary concerning the influence of thermal convection and condensation as well as of the properties of mixed aerosols.

Acknowledgement

In the course of the TUNA program a number of colleagues in the Laboratory of Aerosol-Physics and Filter-Technology in the Nuclear Research Center Karlsruhe have contributed to the experimental and theoretical results. In particular the work of H. Wild and H. Jordan is greatly appreciated.

Appendix

Model equations of PARDISEKO III according to[4]

$$\frac{\partial n(r_e,t)}{\partial t} = S(r_e,t) - (\alpha_D(r_e) + \alpha_S(r_e) + \alpha_T(r_e) + \alpha_L(r_e)) \, n(r_e,t)$$

$$+ \int_0^{r_e/\sqrt[3]{2}} K(\sqrt[3]{r_e^3 - r_e'^3}, r_e') \, n(\sqrt[3]{r_e^3 - r_e'^3}, t) \, n(r_e', t) \frac{r_e^2 \, dr_e'}{(r_e^3 - r_e'^3)^{2/3}}$$

$$- n(r_e,t) \int_0^{\infty} K(r_e, r_e') \, n(r_e', t) \, dr_e'$$

n = Particle size distribution
r_e = Mass equivalent radius
S = Source function

$\alpha_D = \dfrac{kTB(r_e)}{\delta_D} \cdot \dfrac{A_D}{V}$ = Deposition rate coefficient due to diffusion

$\alpha_S = \dfrac{4\pi}{3} \, r_e^3 \rho g B(r_e) \dfrac{A_S}{V}$ = Deposition rate coefficient due to sedimentation

$\alpha_T = \dfrac{9\eta^2 r_e}{\rho g} \left(\dfrac{1}{1+3Kn}\right) \left(\dfrac{k_g/k_s + 2.48Kn}{1+2k_g/k_s + 4.96Kn}\right) \dfrac{T-T_W}{T} \dfrac{B(r_e)}{\delta_T} \dfrac{A_T}{V}$

= Deposition rate coefficient due to thermophoresis

α_L = Leak rate coefficient

$K = 4\pi kTf(B(r_e) + B(r_e'))(r_e+r_e') + \varepsilon(r_e,r_e')\dfrac{4\pi}{3}\rho g f^2 \cdot \left| r_e^3(B(r_e) - r_e'^3 B(r_e')) \right| \cdot (r_e+r_e')^2$

= Coagulation function

$B = \dfrac{1}{6\pi\eta r_e} (1+AKn+QKnC^{-b/Kn})$ = Mobility

$$C_T(t) = \int_0^\infty n(r_e,t)dt = \text{Particle number concentration}$$

$$C_M(t) = \int_0^\infty \frac{4\pi}{3} \rho r_e^3 \, n(r_e,t)dr_e = \text{Aerosol mass concentration}$$

References

(1)   H. Jordan, W. Schikarski, H. Wild
      "Nukleare Aerosole im geschlossenen System"
      KFK-1989 (1974)

(2)   W. Schikarski
      "The Karlsruhe Research Program on Nuclear Aerosol and its Relation to
      the Hazard of Fast Sodium Reactors"
      Int. Symp. Oper. and Develop. Experience in the Treatment of Airborne
      Rad. Wastes, IAEA New York (1968)

(3)   W. Schikarski, H. Wild
      "Experiments on the Behavior of UO_2-Aerosols in Fast Breeder Reactor
      Containments"
      Congrès International sur la Diffusion des Produits de Fission, Saclay,
      France (1969)

(4)   H. Jordan, C. Sack
      "PARDISEKO III, a Computer Code for Determining the Behavior of Contained
      Nuclear Aerosols"
      KFK-2151 (1975)

1 aerosol chamber	8 manometer
2 coaxial cable	9 pressure transducer
3 preheater electrical penetration	10 power supply and condenser bank
4 TUNA main vessel	
5 aerosol measuring ports	11 off-gas filter
6 gas heater (internal, external)	12 pump
7 thermocouple rig	13 inlet filter
	14 gas supply
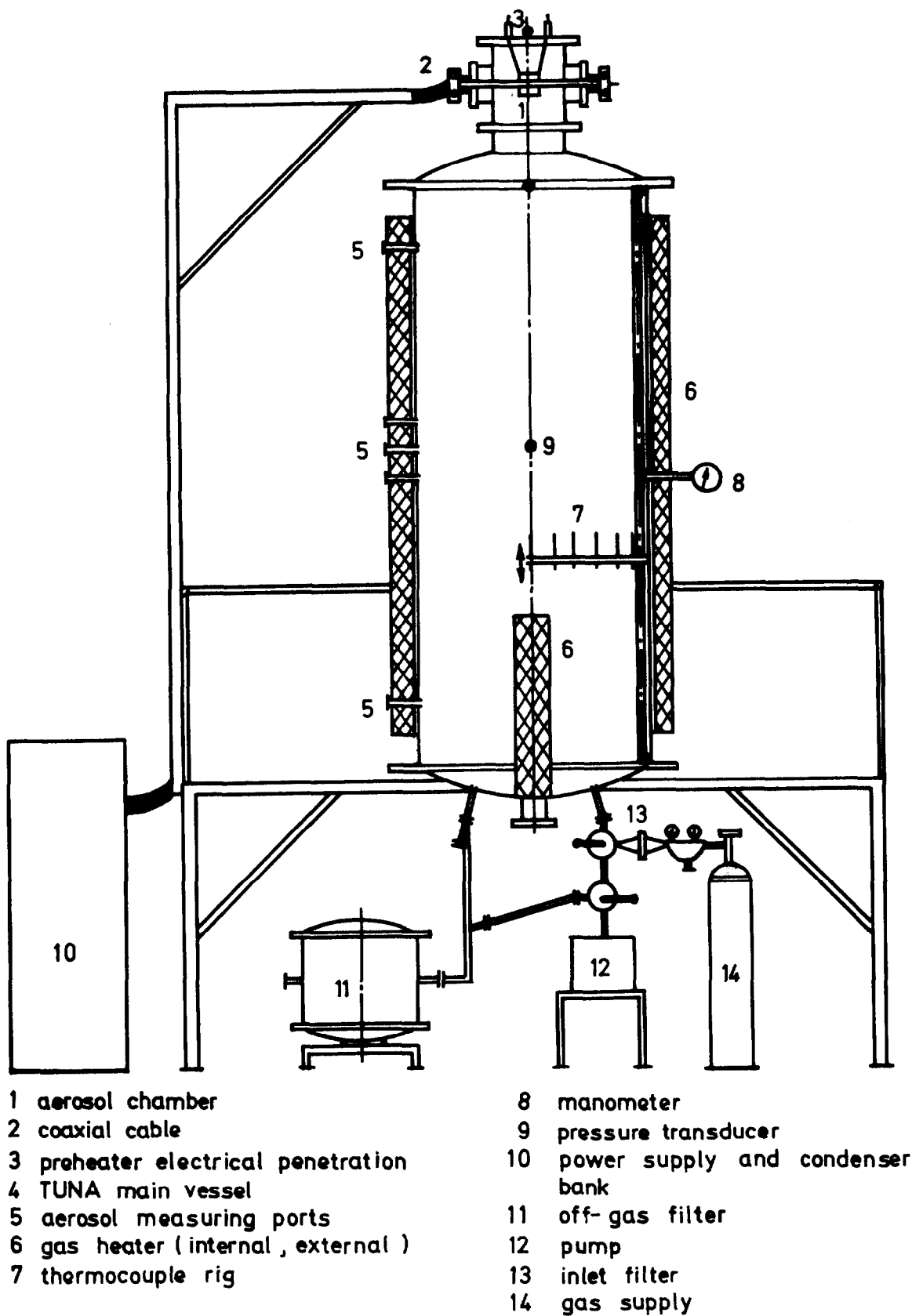
Figure 1   TUNA , schematic
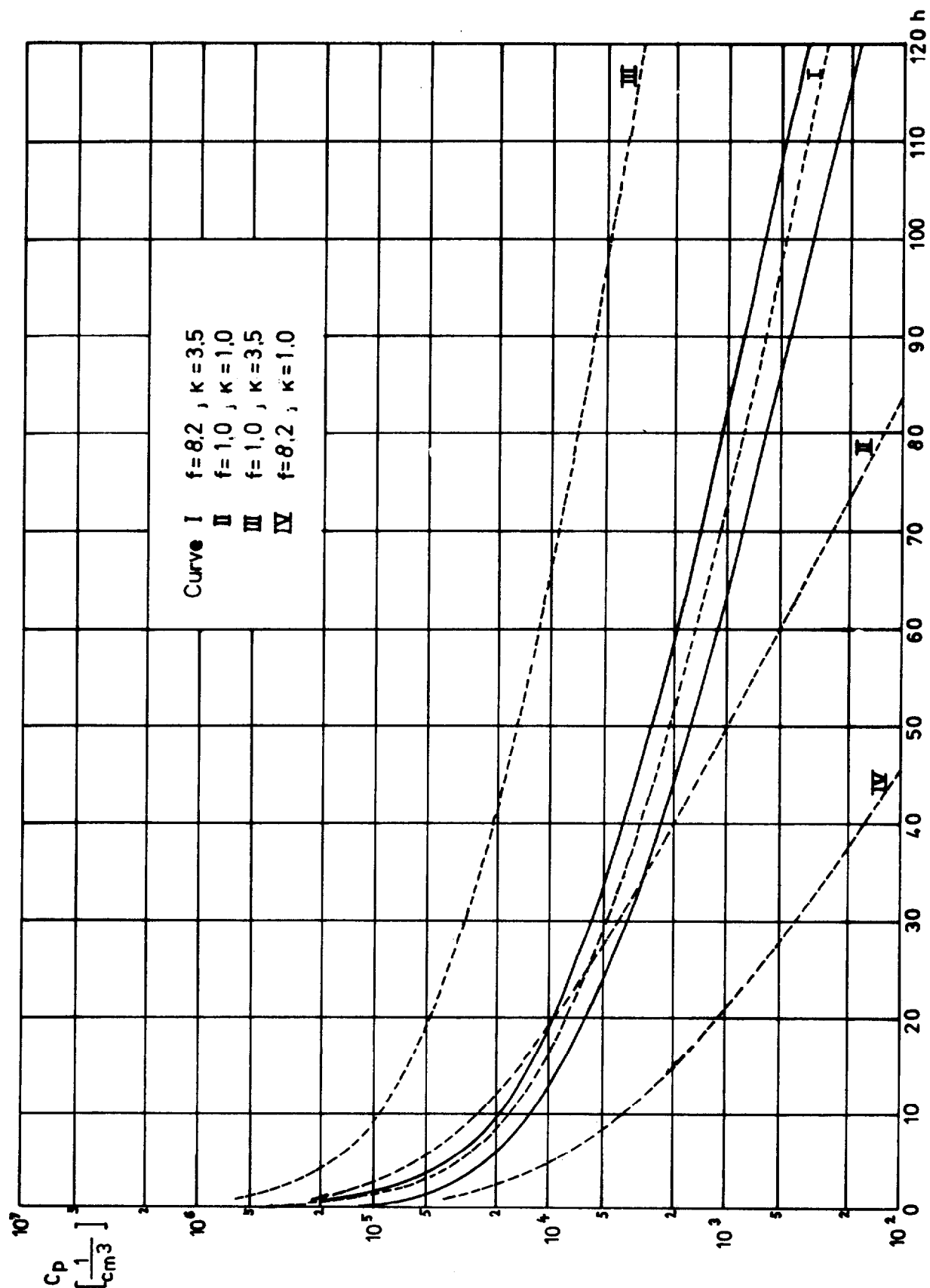
Figure 2   Comparison Experiment - Theory (TUNA vessel) UO_2 particle number concentration as function of time at room temperature
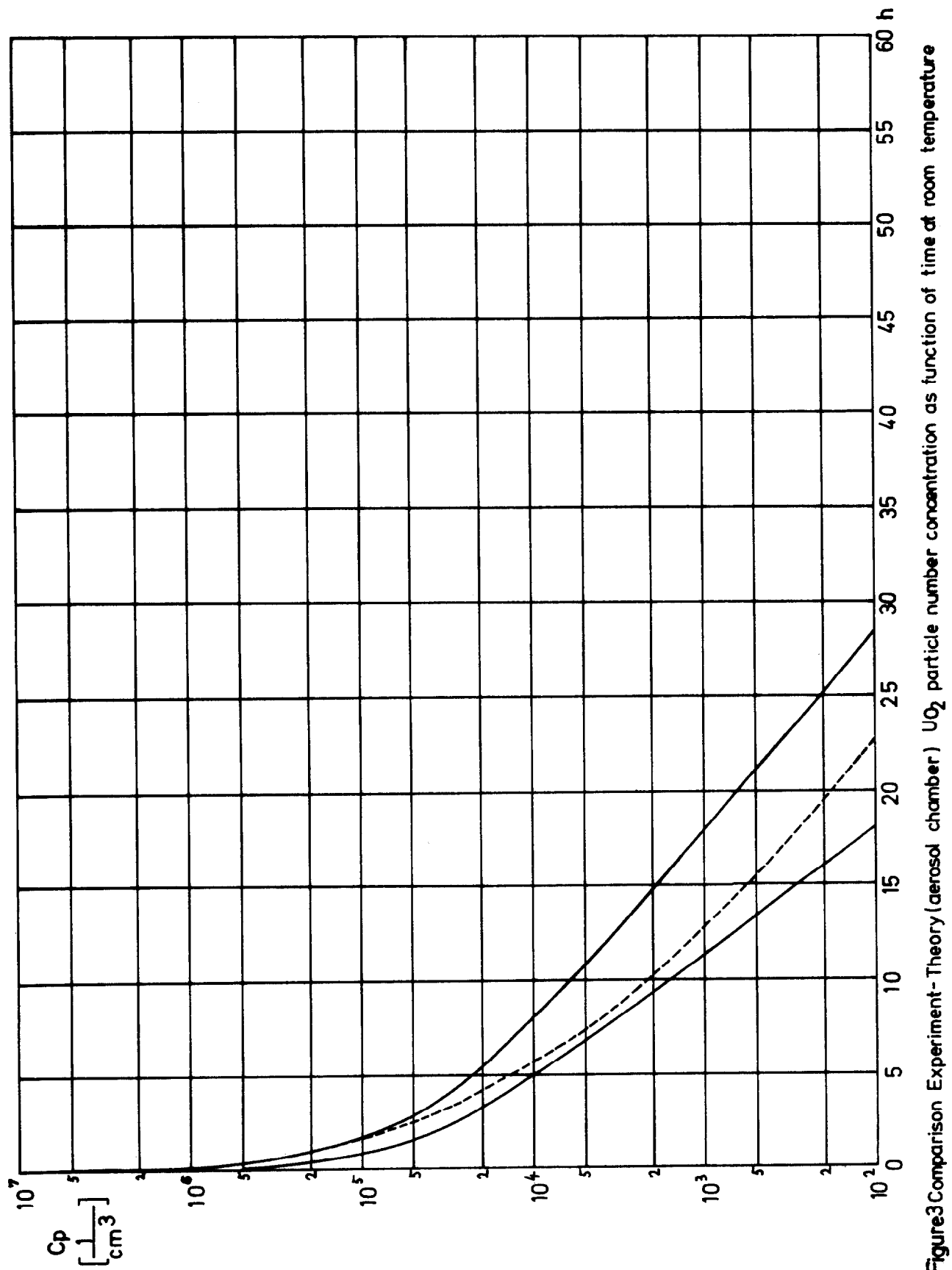
Figure3 Comparison Experiment-Theory (aerosol chamber) UO_2 particle number concentration as function of time at room temperature

Figure 4   Comparison Experiment –Theory (TUNA vessel) UO_2 particle number concentration as function of time at different gas temperatures
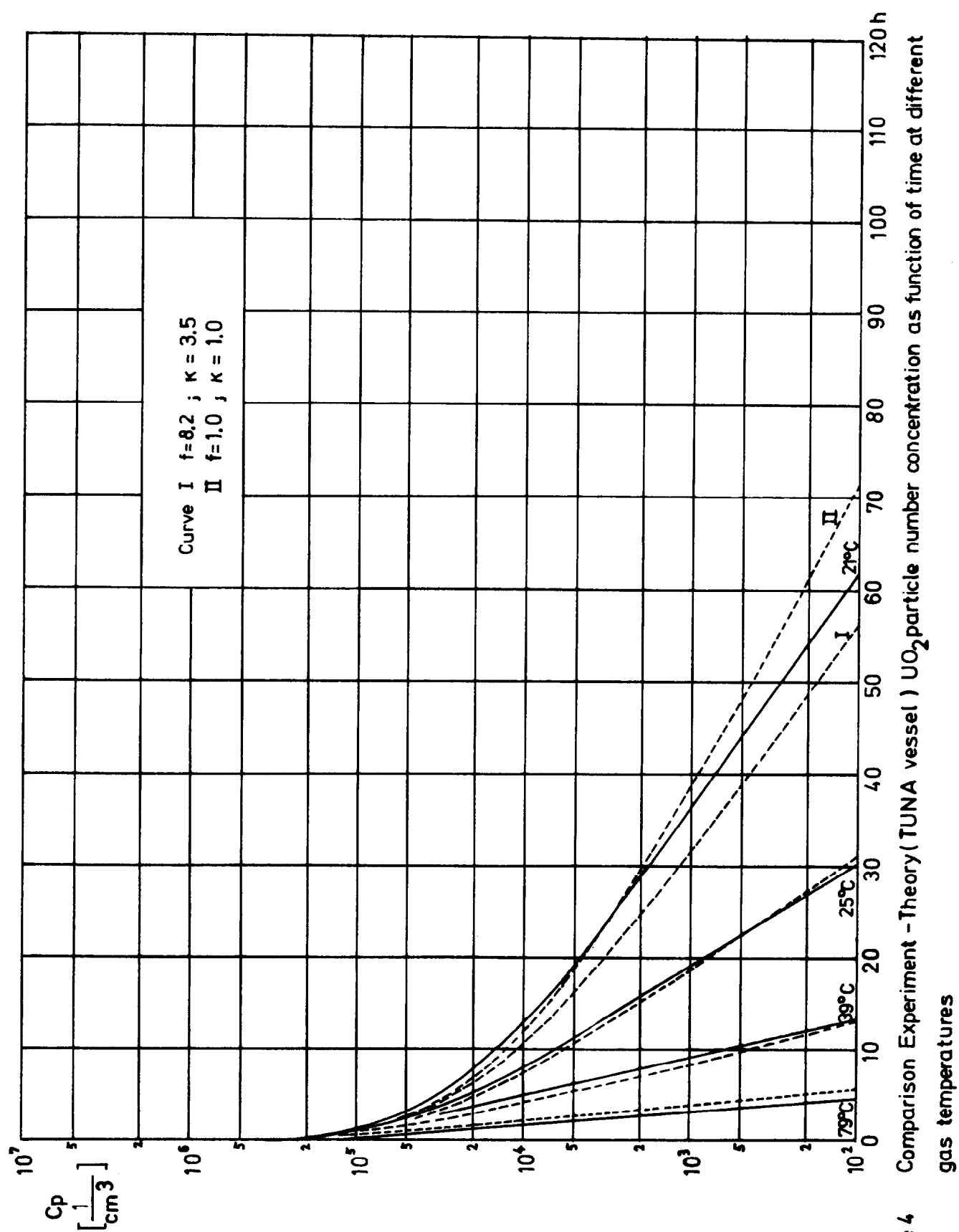
DISCUSSION

NEWTON: I personally consider this paper on aerosol behavior very important for a number of reasons. For one thing, it is a natural attenuation mechanism which, if we understand if sufficiently well, gives us a great deal of attenuation credit. Also, it permits an assessment of the real benefits of air cleaning systems to be evaluated. That is, one can compare what the radiological doses will be with and without an air cleaning system. Finally, of course, by understanding the aerosols generated from these accidents better, we're able to characterize the aerosol that challenges the air cleaning system that we're trying to design.

AN EVALUATION OF ALTERNATIVE AIR CLEANING SYSTEMS

FOR EMERGENCY USE IN LMFBR PLANTS

(USERDA Contract AT(4501)-2170)

J. D. McCormack, R. K. Hilliard, A. K. Postma, and L. D. Muhlestein
Hanford Engineering Development Laboratory
Richland, Washington

Abstract

Twenty-four air cleaning systems, with widely differing air cleaning techniques, are evaluated for feasibility as engineered safety features in LMFBR plants. System designs are considered for both containment and containment/confinement type plants. A source term for release from the reactor vessel is postulated. The systems are designed to provide a 2-hr dose reduction factor of 10 or an overall decontamination factor of 100 for containment and containment/ confinement uses, respectively. Each air cleaning system is evaluated against criteria developed for this purpose, the merits and weaknesses are discussed, and development needs are outlined. For single containment systems, a recirculating-prefilter/HEPA-filter system is shown to be useful with minimal development needed to substantiate the design assumptions. In-vessel acoustic aerosol agglomeration offers attractive potential but requires considerably more development. For containment/confinement use, a sand bed filter with HEPA and charcoal backup can accommodate a sodium fire in the confinement building, as well as the postulated radiological source term. The need for development of a high-capacity, low-efficiency sand bed filter is suggested.

I. Introduction

Air cleaning systems are used extensively in existing nuclear facilities for controlling normal plant effluents and for mitigating the radiological consequences of postulated major accidents. The systems can be divided into three categories: containment atmosphere cleanup systems, ventilation exhaust systems, and process off-gas systems. Systems with similar functions for use in Liquid Metal Fast Breeder Reactors (LMFBRs) are in a developing stage and for application to postulated major accidents will require significant modification and development before their practicability can be demonstrated.

The feature of an LMFBR which has the largest impact on air cleaning for accident mitigation purposes is the use of sodium as the coolant. Although each reactor must be evaluated on an individual basis, radiological analyses of site boundary doses for postulated severe accidents in LMFBRs show that inhalation of aerosol particles containing plutonium may be a concern rather than thyroid dose from radioiodine, as is the case in light water reactors (LWRs).[1] Thus, aerosol attenuation is the highest priority for LMFBR emergency air cleaning systems (EACSs). A second feature of an LMFBR which strongly affects the design requirements for an EACS is the release of sodium during the postulated accident, with its attendant high aerosol mass concentration and chemical reactivity considerations.

898

The purpose of the work reported in this conference was to evaluate all air cleaning concepts which appeared to have merit for use as accident consequence mitigating systems in LMFBR plants and to recommend the systems which have the greatest potential for development into practical engineered safety systems. Realization of this end goal would provide the designers of future commercial LMFBRs with a valuable option in designing containment systems to meet regulatory guidelines. The Nuclear Regulatory Commission (NRC) has expressed confidence in the reliability of air cleaning systems to perform their intended function in LWR plants.[2] Although the dose reduction factor (DRF) attainable by an EACS is smaller than some of the attenuation processes which can be postulated,[1] the probability of attaining the design DRF is essentially unity. This provides added incentive to develop a suitable EACS for future LMFBR plants.

The work reported here included the definition of reference plant (1000 MW$_e$) features important to the EACS design, selection of an EACS design basis source term, definition of criteria for rating the various EACS candidates, making rudimentary conceptual designs of twenty-four candidate EACSs, evaluating the candidates against the criteria and ranking them against each other, and finally, selection of the systems which appear most promising for development.

II. Definition of Reference Containment Designs

Discussion

The ambient conditions and operational requirements for an emergency air cleaning system depend strongly on the type of containment system provided for the reactor plant. Thus, the selection and description of the plant containment features is a prerequisite step before an evaluation of air cleaning systems can be made. A review of existing LMFBR plant containment designs revealed that no one type of containment system can be designated as being standard for future large LMFBR plants.[3-6] For the purpose of this study, several reference designs were selected to provide a basis for establishing EACS design and operating conditions and requirements.

The three containment types summarized in Table 1 were selected for the present EACS study. Each of these three designs imposes significantly different requirements on an EACS, and each appears to offer an economically viable option to future reactor designers. The reactor is the same for each of the three reference plants: 1000 MW$_e$, 2430 MW$_{th}$, 15,300-kg heavy metal oxide (13,500 kg as heavy metal), and fuel material is 25 percent PuO$_2$, 75 percent UO$_2$.

Single Containment Design

The single containment design is physically similar to the FFTF with the open head compartment option. It is also similar to the containment system provided for the British DRF.

At the present time, the type and size of future EACSs is unknown. For purposes of this study, an air cleaning system working on air in the containment vessel, with an effective removal rate (λ) of 5 hr^{-1}, was assumed. The system could be located either entirely

TABLE 1

SUMMARY OF REFERENCE CONTAINMENT DESIGN PARAMETERS

Parameter	Case I	Case II	Case III
Type of Containment	Single Containment	Double Containment	Containment-Confinement
Brief description	Single, low-leakage, cylindrical steel shell surrounding all primary sodium systems.	Sealed, inerted, high-pressure inner containment surrounding reactor vessel and head compartments. An outer low-leakage cylindrical steel shell surrounds the inner compartment.	Sealed, inerted, high-pressure inner containment surrounding reactor vessel and head compartments. A ventilated rectangular building surrounds the inner containments.
Inner containment			
Atmosphere	N/A	99% N_2/1% O_2	99% N_2/1% O_2
Size	N/A	40' D x 50' H, hemispherical top	40' D x 50' H (12.2 m x 15.2 m) hemispherical top
Volume, $ft^3(m^3)$	N/A	29,300 (830)	29,300 (830)
Leak rate, %/day	N/A	100	100
Outer containment			
Atmosphere	Air	Air	Air
Size above operating floor	160' D x 60' straight cylinder with hemispherical top	160' D x 60' (48.8m x 18.3m) straight cylinder with hemispherical top	105' x 204' x 105' (32.0 m x 62.2 m x 32.0 m)
Volume, $ft^3(m^3)$	2.25 x 10^6 (63700)	2.25 x 10^6 (63700)	2.25 x 10^6 (63700)
Leak rate, %/day	0.1	0.1	15,000 CFM (ventilation) (7.1 m3/s)

internal to the containment vessel or in an external loop. This system could be either a recirculation type (e.g., filters) or a direct application system (e.g., sprays). The design DRF for two hours resulting from operation of this system is ten. For longer periods of time, the DRF would be greater than ten.

Double Containment Design

The principal physical difference between single and double containment schemes is the addition of a sealed dome over the reactor head compartment. The outer containment vessel was taken to be identical with that provided for the single containment case.

The physical size of the inner containment dome was selected as a hemisphere large enough to cover the reactor head compartment. This dome would be removed during refueling operations.

The double containment design is similar in concept to the CRBR design, based on the inerted closed head option, and to FERMI. It is similar to SEFOR which used 10 psi inerted primary vaults as well as an outer steel containment vessel. This design is also conceptually similar to the design proposed for 1000 MW$_e$ by AI.[5] Of these previous designs, only the AI conceptual design included an emergency air cleaning system.

The assumed air cleaning system is one which cleans the air in the outer containment atmosphere with an effective λ of 2 hr^{-1}. This system gives a smaller dose reduction factor than the EACS used for the single containment case, and will treat much less concentrated aerosols because the primary volume allows appreciably more settling and plating than would occur in a single containment. An alternate air cleaning approach would be to clean the gas enclosed in the primary volume.

Containment/Confinement Design

The containment/confinement design is, in effect, a double containment scheme in which the outer barrier is a ventilated building rather than a low-leakage containment shell. The outer building is maintained at a slightly negative pressure by an exhaust system which discharges air through suitable cleanup devices to a stack so that radioactive materials leaked from the primary containment are removed by filters or scrubbers. The containment/confinement concept trades a high leakage rate of processed air (filtered, elevated release) for a low leakage rate of unprocessed air.

The physical size and features of the primary containment volume were assumed to be identical to the double containment plant. The outer confinement building size and the capacity of the EACS were taken from the General Electric 1000 MW$_e$ follow-on study.[6] The design is similar in appearance to several existing designs. The British PFR uses an inner containment scheme with an outer steel structural building. An important difference is that PFR uses a recirculating air cleaning system rather than a single pass system.

Although the specific kind of air cleaner (filter, scrubber, etc.) need not be specified, the total flow rate is specified as 15,000 CFM (7.1 m³/s). The efficiency required for this system must be high compared to the systems chosen for containment plants. Based on preliminary analyses, it appears that the EACS system will have to achieve a decontamination factor of about 100 or more to give bone doses equivalent to that of a double containment plant.

III. EACS Design Basis Source Term

Basis for Selection of Design Basis Source Term

Definition of the design basis source term (DBST) for the air cleaning study provides a means for evaluating the conditions imposed upon, and performance of, containment systems incorporating an EACS. In selecting the DBST for this study, emphasis was placed on the quantities and type of radioactive materials and sodium which could become airborne, and therefore represent an air cleaning requirement.

A hypothetical core disruptive accident (HCDA) appears to be the most severe type of accident which can be postulated for evaluating containment system performance. ERDA is currently supporting a major analytical and experimental program to develop a source term model describing the release of fuel and fission products from the core to the cover gas and then from the reactor vessel to the head compartment.[7] At the present time, such a model is not completely available and releases postulated in this report are based on parametric studies, judgment, and precedent.

Additional interactions associated with postulated post-HCDA melt-through of the reactor vessel were not assumed to add to the initial short-term releases.

Aerosol Source Terms

The phrase "source term," as used in this paper, refers to the release of materials from the primary reactor vessel to the next level of containment. For the single containment plant, the release is directly into the outer, air-filled containment building via the open head compartment. For both the double containment and containment/confinement plants, the release is into an inerted inner containment volume.

The mass releases of radioactive materials and sodium from the reactor vessel are summarized in Table 2. The aerosol properties were developed by using HAA-3b code[8] calculations.

Comparison of Containment Concepts

An evaluation of various containment concepts is beyond the scope of the present study. However, the analyses performed here provide some bases for a general comparison. It must be strongly emphasized, however, that variations in each of the reference plant designs could greatly alter the conclusions.

Table 3 is a compilation of data selected from the previous sections of this report for total mass and plutonium leaked to the

902

TABLE 2

ASSUMED INSTANTANEOUS AEROSOL SOURCE

Parameter	Release Directly to Containment Building	Release to Sealed Primary Containment
Composition, µg		
Fuel (as oxide)	1.53×10^{11}	1.53×10^{11}
Volatile solids	4.50×10^{10}	4.50×10^{10}
Halogens	2.80×10^{9}	2.80×10^{9}
Na_2O	6.38×10^{11}	2.99×10^{10}
Total	8.39×10^{11}	2.31×10^{11}
Gas volume, cm^3	6.4×10^{10}	8.2×10^{8}
Initial aerosol mass concentration, µg/cm^3	13.1	280
Initial concentration, particles/cm^3	7.95×10^{7}	7.70×10^{8}
Particle Density, g/cm^3	2.74	6.0
Particle density modification factor, α	0.25	0.25
Initial particle mass median diameter (MMD), µm	1.0	1.0
Geometric standard deviation, σg	2.0	2.0
Mass fraction as Pu	0.0402	0.146

TABLE 3

COMPARISON OF CONTAINMENT CONCEPTS

(for Source Term and Reference Plant Designs
Defined in this Paper)

| | Single Containment | | | Double Containment | | Containment/ Confinement | |
	No Cleanup	Natural Fallout, α=0.25	With EACS, λ=5 hr⁻¹	Natural Fallout, α=0.25	With EACS, λ=2 hr⁻¹	EACS CF=100	EACS DF=1000
TOTAL MASS LEAKED, g							
2 hours	110	43.	11.	0.05	0.014	3.5	0.35
t = 30 days	4.3x10⁴	48.	11.	0.5	0.015	5.6	0.56
PLUTONIUM LEAKED, g							
2 hours	2.8	1.2	0.27	0.0073	0.002	0.51	0.051
t = 30 days	1100	1.4	0.27	0.073	0.0022	0.81	0.081
BONE DOSE @ 1 MILE, rem							
2-hour exposure	650	270.	62.	1.8	0.5	6.3	0.63
30-day exposure	2.4x10⁵	320.	62.	18.	0.54	10.	1.
BONE DOSE @ 6.2 MILE, rem							
30-day exposure	1.8x10⁴	23.	4.5	1.3	0.04	4.5	0.45

environment. Using standard meteorological data,[9] an arbitrary site exclusion radius of 1 mile (1609 m) and a population center distance of 6.2 miles (10,000 m), the bone doses are calculated for the three reference containment designs. The information is presented for plants with and without an EACS operating, and for two EACS efficiency levels for the containment/confinement plant. The ranking, in order of ascending dose, is the same at each distance and is as follows:

Rank	System
1	Double Containment with EACS
2	Containment/Confinement, DF=1000
3	Double Containment without EACS
4	Containment/Confinement, DF=100
5	Single Containment with EACS
6	Single Containment without EACS

The comparison of containment systems made in Table 3 indicates that, if a double containment system is provided, an EACS may not be required. This conclusion cannot be substantiated until additional information becomes available on accidents not considered in this report, e.g., a reactor melt-through, and until federal regulations are established for accident guideline dose limits on plutonium inhalation. However, for the accident conditions described here and for the presently suggested guideline bone dose of 150 rem, it appears that for a double containment plan an EACS would not be required to meet most siting requirements, although it would certainly add to the margin of safety. Therefore, for the purpose of evaluating EACSs for development, only the single containment and containment/confinement type systems will be considered at this time. Table 4 presents the most probable ranges of values for the important accident conditions which impact EACS design for the remaining two containment systems. Because a sodium fire in the confinement building would impose a severe loading on the EACS, Table 4 also includes a list of environmental conditions for the case of a postulated large sodium fire in the confinement building. For the purposes of this report, it is assumed that the DBST and the sodium fire would not occur simultaneously.

IV. Criteria and Procedure for Evaluating EACS Concepts

The conservative EACS operating conditions have been summarized in Table 4 for the two containment systems. Because of the obvious differences in EACS requirements for these two systems, separate evaluation criteria have been defined for both types of containment. For each case, the criteria are classed into six main groups, each with several individual criteria. Table 5 lists the criteria for single containment.

Somewhat different criteria have been developed for the containment/confinement system. For this containment concept, the EACS is an integral part of the plant confinement design and, as a result, a minimum decontamination factor of 100 is specified and the weighting factors have been changed somewhat, with additional weight being placed on the reliability and compatibility sections. The criteria for evaluating an EACS in containment/confinement systems are given in Table 6. The total of the weighting factors remains at 100, as in

TABLE 4
PARAMETERS CHARACTERIZING ACCIDENT ENVIRONMENT
FOR TWO CONTAINMENTS WITH EACS

Parameter	Probable Value for Single Containment[a]	Probable Values[c] for Confinement Bldg.	
		DBST[d]	Sodium Fire
1. Aerosol source	Puff release followed by sodium pool fire. Upper bound 1% of fuel, 25% halogens, 25% volatile solids, 100% noble gases, 5000 lbs sodium	Leakage from primary containment after HCDA	40 lb/min sodium released into confinement bldg
2. Maximum containment gas temperature	300°F	-10 to 110°F	-10 to 300°F
3. Maximum containment pressure	10 psig	0 psig	0 psig
4. Containment pressure transient	0.2 psi/sec for 15 sec	0	0
5. Containment atmosphere humidity	0 to saturated	10 - 100% RH	0 - 100% RH
6. Maximum aerosol mass concentration	20 $\mu g/cm^3$	0.02 $\mu g/cm^3$	25 $\mu g/cm^3$
7. Mass collected by EACS (maximum)	2000 kg	1 kg	1000 kg[e]
8. Water/sodium weight ratio for aerosol particle	0 - 10	1 - 100	1 - 10
9. Aerosol size distribution	1.7 μm MMD, $\sigma = 2$	4.0 μm MMD, $\sigma = 2$	2 μm MMD, $\sigma = 2$
10. Particle material density	2.7 g/cm^3	6 g/cm^3	2.3 g/cm^3
11. Particle density modification factor	0.25	0.25	0.25
12. Effective density of particles	0.7	0.25	0.25
13. Aerodynamic equivalent diameter[b]	1.4 μm AED	1.5 g/cm^3	0.6 g/cm^3
14. FP decay heat in EACS collected mass 10^6 Btu/hr			0
t = 1 hr	10	.01	
t = 2 hr	10	.01	
t = 7 hr	5	.01	
t = 24 hr	3	.007	

(a) EACS $\lambda = 5$ hr^{-1}
(b) equivalent particle with density of 1.0 g/cm^3
(c) for 15,000 CFM ventilation rate
(d) not considering a sodium fire in confinement building
(e) as NaOH

TABLE 5

CRITERIA FOR EVALUATING LMFBR EMERGENCY AIR CLEANING
SYSTEMS IN SINGLE CONTAINMENT PLANTS

Criteria Description	Weight Factor
1. SYSTEM EFFECTIVENESS	<u>27</u>
The EACS shall be effective in reducing the release of radioactive substances to the environment under DBST conditions.	
a. A dose reduction factor (2-hr) of ten can be achieved for aerosol particles	9*
b. Decay heat can be dissipated adequately	7*
c. Either dry or sticky particles can be treated effectively	7*
d. System effectiveness is not degraded by the radiation dose caused by the accident over the required operating period	4*
2. SYSTEM RELIABILITY	<u>23</u>
The EACS shall have a high degree of reliability in startup and continuance of operation during the entire accident period.	
a. The EACS shall have a high probability of startup after initiation of the DBST release	6*
b. The system shall be capable of withstanding the pressure pulse associated with the DBST	5*
c. The system does not degrade during periods of unuse	4*
d. The system shall be capable of dependable operation over the required period of time under accident conditions of temperature, pressure, humidity and aerosol loading	6*
e. The system requires simple components and conservative design stress	2
3. CONTAINMENT COMPATIBILITY	<u>18</u>
The presence and operation of the EACS shall not degrade the normal effectiveness of the containment building.	
a. Inadvertent operation of the EACS shall not harm plant equipment or constitute a hazard to personnel	5
b. Operation of the EACS shall not significantly increase the pressure within the containment building by gas injection, energy release or other means	5*

* denotes mandatory criterion.

TABLE 5 (continued)

Criteria Description	Weight Factor

c. The size of the EACS shall be compatible with   4*
    installation within or adjacent to the contain-
    ment building (less than 10% of the volume of
    the RCB)

d. The EACS shall maintain the collected aerosol   4*
    mass in a subcritical configuration

4. TECHNOLOGICAL CREDIBILITY   14

The effectiveness of the EACS shall be clearly
demonstrable by experience, mathematical models and
testing.

a. The air cleaning concept is based on highly   3
    developed technology

b. The EACS can be tested in-place for operability   5
    and efficiency

c. The EACS performance can be predicted by verified   4
    mathematical models

d. The EACS equipment scaleup from currently avail-   2
    able sizes to LMFBR plant application is small

5. SYSTEM CHARACTERISTICS AND FLEXIBILITY   11

The EACS performance shall not be critically dependent
on the accident environment conditions and shall
accommodate possible future design changes.

a. The EACS is effective for the entire particle   3
    size spectrum expected during the accident

b. The system performance is not highly sensitive   4
    to the atmosphere temperature, pressure and
    relative humidity

c. The system energy consumption is low   1

d. The system can be modified to add halogen removal   2
    components, hydrogen recombiners, containment coolers

e. The post-accident recovery is facilitated by the EACS   1

6. FABRICATION EFFORT   7

The system shall be readily designed, fabricated and
installed at reasonable cost and in a time frame
consistent with plant construction.

a. The system cost is low. Capital cost is less than   5
    $10 million; operating costs are low

b. Materials and techniques used in construction are   1
    readily available and easily fabricated

c. Components and equipment are readily available   1

                                                     ‾‾‾‾
                                                    100

TABLE 6

CRITERIA FOR EVALUATING LMFBR EMERGENCY AIR CLEANING
IN A CONTAINMENT/CONFINEMENT PLANT

Criteria Description	Weight Factor
1. SYSTEM EFFECTIVENESS	24
The EACS shall be effective in reducing the release of radioactive substances to the environment under DBST conditions.	
a. A decontamination factor of 100 can be achieved for aerosol particles	12*
b. Either dry or sticky particles can be treated effectively	7*
c. System effectiveness is not degraded by the radiation dose caused by the accident over the required operating period	5*
2. SYSTEM RELIABILITY	29
The EACS shall have a high degree of reliability in startup and continuance of operation during the entire accident period.	
a. The EACS shall have a high probability of startup after initiation of the DBST release	10*
b. The system does not degrade during periods of unuse	6*
c. The system shall be capable of dependable operation over the required period of time (30 days for DBST, 1 day for Na fire) under the accident conditions of temperature, pressure, humidity, and aerosol loading	10*
d. The system requires simple components and conservative design stresses	3
3. CONTAINMENT COMPATIBILITY	7
The presence and operation of the EACS shall not degrade the normal effectiveness of the confinement building.	
a. Inadvertent operation of the EACS shall not harm plant equipment or constitute a hazard to personnel	4
b. The size of the EACS shall be compatible with installation within or adjacent to the confinement building (<12,000 ft^2)	3*
4. TECHNOLOGICAL CREDIBILITY	21
The effectiveness of the EACS shall be clearly demonstrable by experience, mathematical models and testing.	
a. The air cleaning concept is based on highly developed technology	5

* denotes mandatory criterion.

909

TABLE 6 (continued)

Criteria Description	Weight Factor

b. The EACS can be tested in-place for operability and efficiency — 8*

c. The EACS performance can be predicted by verified mathematical models — 5

d. The EACS equipment scaleup from currently available sizes to LMFBR plant application is small — 3

5. SYSTEM CHARACTERISTICS AND FLEXIBILITY — <u>12</u>

The EACS performance shall not be critically dependent on the accident environment conditions and shall accommodate possible future design changes.

a. The EACS is effective for the entire particle size spectrum expected during the accident — 3

b. The system performance is not highly sensitive to the atmosphere temperature, pressure and relative humidity — 4

c. The system energy consumption is low — 2

d. The system can be modified to add halogen removal components and other air cleaning devices if needed — 2

e. The post-accident recovery is facilitated by the EACS — 1

6. FABRICATION EFFORT — <u>7</u>

The system shall be readily designed, fabricated and installed at reasonable cost and in a time frame consistent with plant construction.

a. The system cost is low. Capital cost is less than $10 million; operating costs are low — 5

b. Materials and techniques used in construction are readily available and easily fabricated — 1

c. Components and equipment are readily available — 1

___

100

the previous case.

Certain criteria are thought to be of such importance to the system that they are considered mandatory requirements and a minimum rating score of 2.0 is required. These mandatory criteria are noted in Tables 5 and 6 by an asterisk.

Using the requirements established previously in Table 4 for the EACS design base, a conceptual design of the candidate air cleaning system was completed. On the basis of this preliminary design, the system was rated with a score of 0 to 4 (to the nearest 0.1), based on the extent that it met each criterion.

A system score is determined by summing the individual criterion scores which are the product of the criterion weight and the rating factor. The maximum system score possible is 400. Systems with criteria with low scores were examined for possible design changes which could lead to improved ratings.

Scope Design of Systems

As noted above, ratings were obtained for systems based on the preliminary design. These systems were examined for possible areas of improvement and several promising systems were designed in more detail. Whenever possible, performance information for removal of alkali metal fumes was used.[10-13] For many systems, however, such information was not available and the designs were based on conservative interpretation of standard air cleaning texts and reports.

V. Description of Air Cleaning Systems Evaluated

System Classification

The chief radiological hazards resulting from the DBST defined in Section III are the plutonium and solid fission products released to the containment building as respirable-size aerosol particles. Radioactive materials released in other forms, e.g., halogen vapor and noble gases, are of concern and their hazard should be investigated. However it is believed that most of the halogens would be associated with aerosol particles[14,15] and that the chief air cleaning objective is the removal of the aerosol particles. Consequently, the systems selected for evaluation in this report are aimed at removal of particulates. Iodine removal may become the objective of future studies.

Many types of air cleaning equipment are available for controlling particulate air pollutants. They can be classified into three general groups according to their mode of operation in LMFBR service: (1) gas recirculation, (2) direct in-vessel application, and (3) gas purge. In the gas recirculation mode, the EACS removes the contaminants from a flowing gas stream in a recirculating loop which can be located either entirely internal or external to the containment building. Direct in-vessel application systems operate directly on the containment building atmosphere without incorporating a duct air flow system. An example of this class is the containment building spray system used in many LWR plants. In the gas purge mode (also known as single-pass mode), the EACS is located in a ventilation system which discharges directly to the environs usually through a stack.

Air Cleaning Systems to be Evaluated

Particle removal from the containment atmosphere may be accomplished by air cleaning components used singly or several types may be arranged into systems. The types of components and systems considered in this study are listed in Table 7.

TABLE 7
TYPES OF CANDIDATE AIR CLEANING COMPONENTS AND SYSTEMS

For Recirculating or Purge Modes

Filters
Prefilters (various types, including demisters)
Bag Filters (various types)
Deep Bed Graded Media Filters
Sand Filters
High-Efficiency Particulate Air (HEPA) Filters
Cyclone Separators
Mechanical Separators
Electrostatic Precipitators
Dry
Wet
Wet Scrubbers
Spray Chamber
Centrifugal Scrubber
Venturi Scrubber
Packed Bed
Fluidized Bed
Acoustic Agglomerator
Settling Chamber
Charcoal Bed

For Direct In-Vessel Application Modes

Containment Building Liquid Spray
Containment Building Powder Discharge
Foam Dispersal
Acoustic Agglomerator
Electrostatic Precipitator

These components are arranged into the systems shown in Figure 1 for study in the single containment case. Figure 2 shows the systems for the containment/confinement case.

VI. Evaluation Results

Numerical Ratings for EACSs

The numerical ratings and weighted group scores for both single containment and containment/confinement plant systems are tabulated in Table 8. The ratings represent the best judgment of the authors and were arrived at after both independent and joint assessments of how well each criterion was satisfied on a system-by-system basis. Quantitative evaluations were possible for some of the criteria (e.g., cost, size, DRF, energy requirement), but many of the criteria ratings were assigned on a subjective basis.
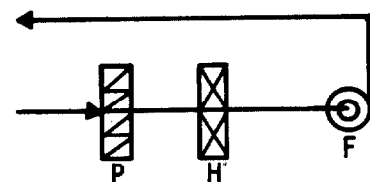
SR-1 RECIRCULATING-
PREFILTER, HEPA
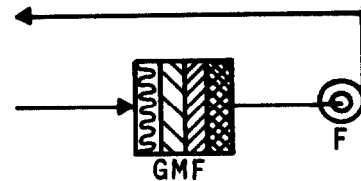
SR-2 RECIRCULATING-
GRADED MEDIA FILTER
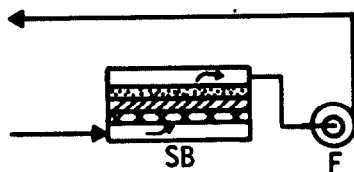
SR-3 RECIRCULATING-
SAND BED FILTER
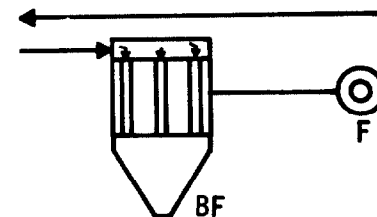
SR-4 RECIRCULATING-
BAG FILTER
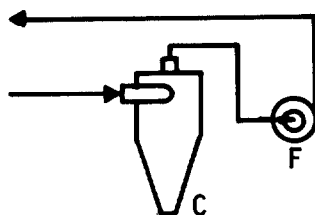
SR-5 RECIRCULATING-
CYCLONE SEPARATOR
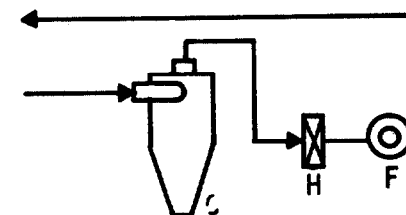
SR-6 RECIRCULATING-
CYCLONE, HEPA
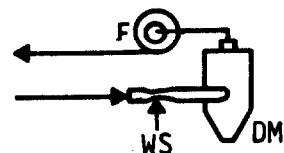
SR-7 RECIRCULATING-
WET SCRUBBER,
DEMISTER
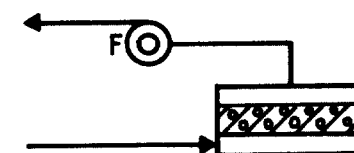
SR-8 RECIRCULATING-
FLUIDIZED BED

FIGURE 1a.   Schematic Flow Diagrams for Single Containment
EACS Candidate Systems.
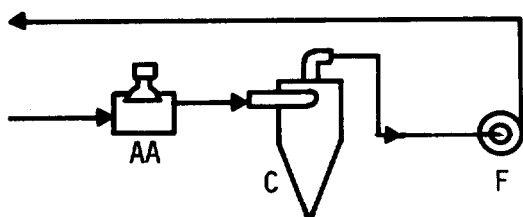
SR-9   RECIRCULATING - ACOUSTIC
       AGGLOMERATOR, CYCLONE
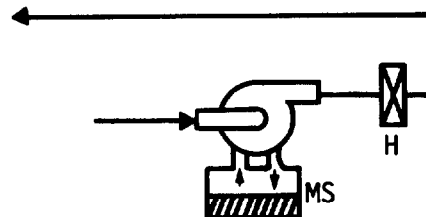
SR-10   RECIRCULATING - MECHANICAL
        SEPARATOR, FILTER
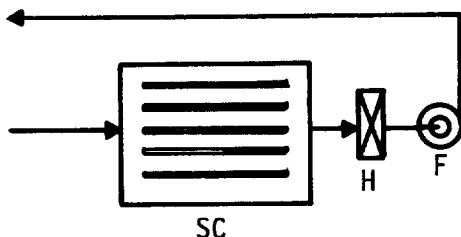
SR-11   RECIRCULATING - SETTLING
        CHAMBER, FILTER
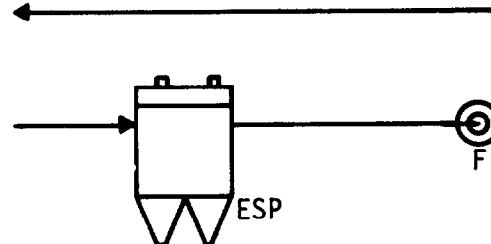
SR-12   RECIRCULATING - ELECTRO-
        STATIC PRECIPITATOR
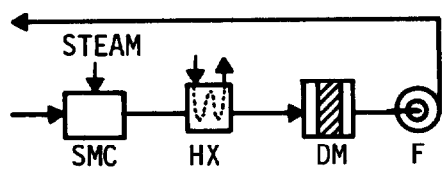
SR-13   RECIRCULATING - STEAM
        CONDITIONER, DEMISTER
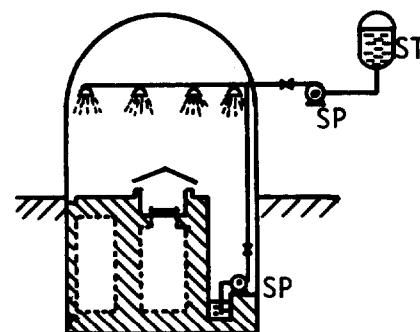
SD-14   DIRECT LIQUID SPRAY

FIGURE 1b.   Schematic Flow Diagrams for Single Containment
             EACS Candidate Systems.

914
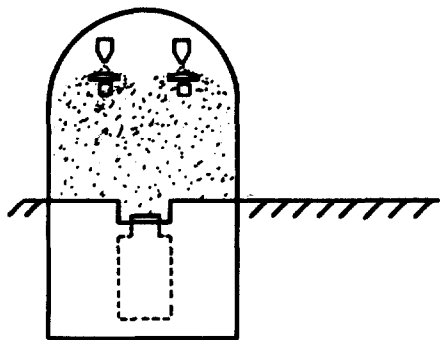
SD-15   DIRECT POWDER DISCHARGE
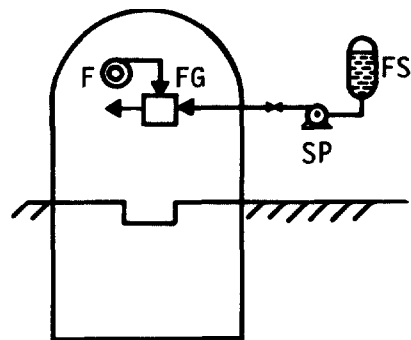
SD-16   DIRECT FOAM DISPERSAL
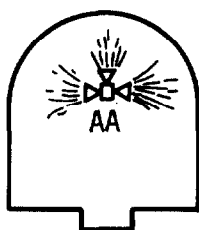
SD-17   DIRECT ACOUSTIC
        AGGLOMERATOR
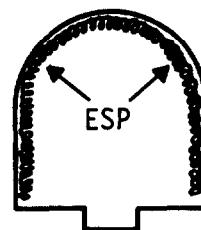
SD-18   ELECTROSTATIC PRECIPITATOR
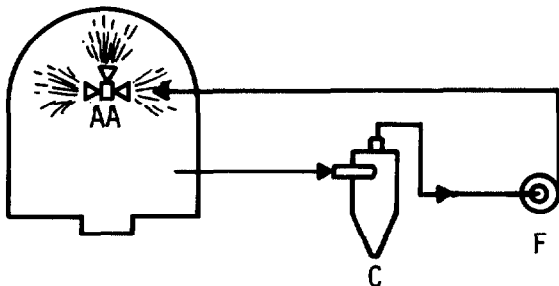
SC-19   COMBINATION - ACOUSTIC
        AGGLOMERATOR PLUS RECIRCULATING
        CYCLONE
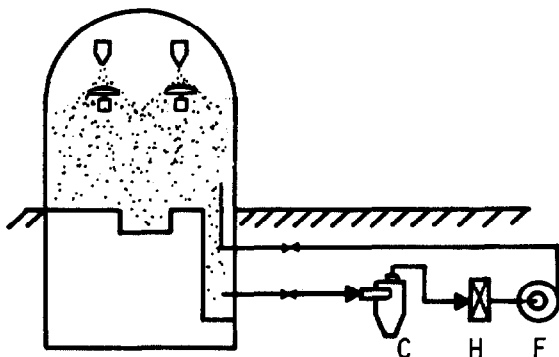
SC-20   COMBINATION - POWDER
        DISCHARGE PLUS RECIRCULATING
        CYCLONE, FILTER

FIGURE 1c.   Schematic Flow Diagrams for Single Containment
             EACS Candidate Systems.
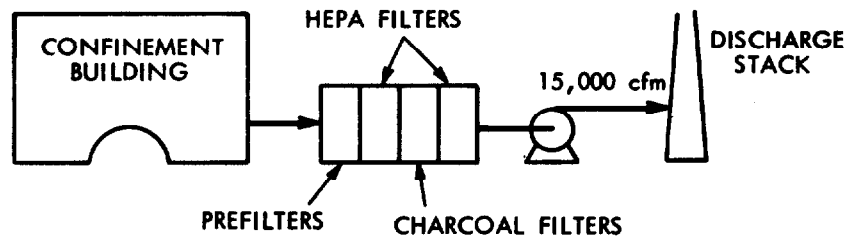
SYSTEM CF-21. PREFILTER, HEPA, CHARCOAL, HEPA
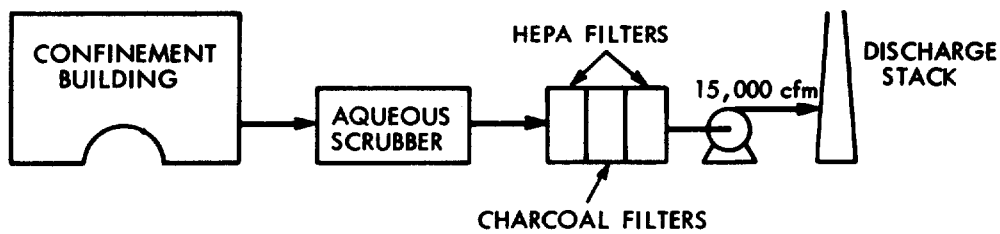
SYSTEM CF-22. SCRUBBER, HEPA, CHARCOAL, HEPA
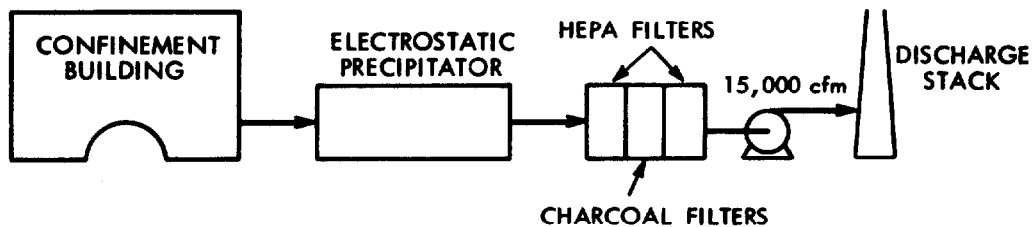
SYSTEM CF-23. ELECTROSTATIC PRECIPITATOR, HEPA, CHARCOAL, HEPA
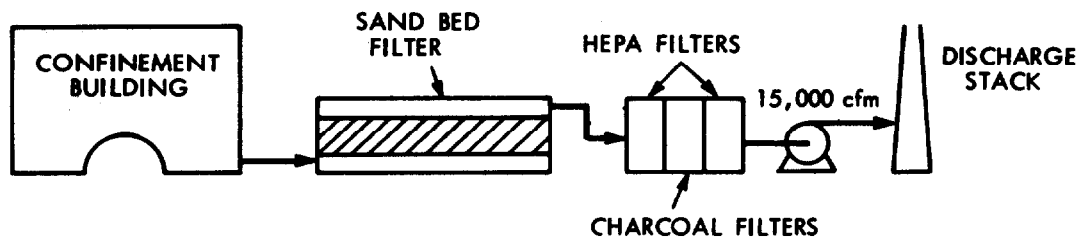
SYSTEM CF-24. SAND FILTER, HEPA, CHARCOAL, HEPA

FIGURE 2. Schematic Diagrams for Containment/Confinement
Air Cleaning Systems Evaluated.

916

TABLE 8

RANKING OF EACS CANDIDATES BY TOTAL SCORE AND BY CRITERIA GROUPS

Overall Rank	System		Total Score	Ranking by Criteria Group [a]					
				Group 1 Effectiveness	Group 2 Reliability	Group 3 Compatibility	Group 4 Credibility	Group 5 Flexibility	Group 6 Fabrication
Single Containment Systems									
1	SR-1	PF + HEPA	338.8	16	5	2	1	5	11
2(b)	SR-3	Sand bed	338.4	8	1	10(b)	2	4	18
3	SR-6	Cyclone + HEPA	327.5	11	4	8	7	9	8
4	SR-12	Electrostatic	325.7	13	12	4	4	2	13
5	SR-5	Cyclone	324.2	10	2	9	8	19	5
6	SR-2	Graded media	322.1	14	3	6	10	6	16
7	SR-4	Bag filter	313.1	18	14	5	3	7	7
8(b)	SR-7	Wet scrubber	310.7	7	11	17(b)	6	10	12
9	SD-17	In-containment acoustic	309.5	1	7	15	16	16	4
10	SR-9	Recirc acoustic + cyclone	306.5	9	9	12	14	8	15
11	SC-19	In-cont acoustic + recirc cyc	304.6	3	8	16	15	11	9
12(b)	SR-11	Settl Bed + HEPA	304.5	15	16	13(b)	5	12	20
13(b)	SD-14	Liquid spray	296.8	4	10	19(b)	11	13	1
14	SD-15	In-containment powder	296.4	2	16	11	18	14	6
15(b)	SR-10	Mech Sep + HEPA	293.0	19(b)	13(b)	3	9	17	10
16	SC-20	Powder + recirc HEPA	288.7	5	18	14	17	3	14
17(b)	SR-13	Steam + demister	276.7	6	19	18(b)	13	1	17
18(b)	SR-8	Fluidized bed	272.6	12	20(b)	1	12	15	19
19(b)	SD-18	Direct ESP	254.9	20(b)	15	7	20	18	2
20(b)	SD-16	Foam	237.9	17(b)	17(b)	20(b)	19	20	3
Containment/Confinement Systems									
1	CF-24	Sand bed	356.0	2	1	4	1	1	4
2	CF-21A	PF, HEPA	341.0	4	2	2	2	2	2
3	CF-23	ESP	336.0	3	3	1	3	3	1
4	CF-22	Wet scrubber	328.0	1	4	3	4	4	3

(a) See Tables 5 and 6 for complete definition of criteria

(b) Denotes failure of one or more mandatory criteria

As noted in Table 8, nine of the single containment systems rated unacceptably low in the mandatory criteria identified in Table 5. Two of the systems failed because of their large size (SR-3, sand bed; and SR-11, settling bed plus HEPA). Although the size criterion is somewhat arbitrary, it is felt that the added containment volumes required for the sand bed (22 percent of the RCB volume) and the settling bed (45 percent) are clearly excessive. Four systems failed because they used water which creates a potential hydrogen problem (SR-7, wet scrubber; SR-13, steam conditioner; SD-14, liquid spray; and SD-16, foam). If a suitable alternate liquid could be found to replace water in these systems, they would rate much higher and the SD-14 liquid spray system would probably be the best overall system. Two systems failed because of unacceptably low reliability for operating throughout the required period of time (SR-8, fluidized bed; and SR-10, mechanical separator plus HEPA filters). Both of these are sensitive to handling sticky particles. One system failed because it was ineffective in providing a reasonable dose reduction factor (SD-18, in-containment electrostatic precipitator).

Of the eleven single containment EACSs remaining after elimination of the failed systems, the system with the highest overall rating is the recirculating-prefilter/HEPA system, SR-1. System CF-24, the sand bed filter, had the best rating for the containment/confinement plant.

The scores of the surviving containment plant systems were reviewed to determine the development potential.

<u>Discussion of Ratings</u>

Table 8 shows that the recirculating systems rank higher in total score than those which act directly in containment. Closer examination of Table 8 reveals that this is due to the generally low ratings given the in-containment concepts for reliability, compatibility, credibility, and flexibility. The in-containment concepts (acoustic agglomeration and powder dispersal, either singly or in combination with recirculating systems) rate very high in effectiveness and fabrication. This suggests that if development effort can improve the credibility, reliability and compatibility of the two in-containment concepts they would probably become the best EACS candidates. It seems probable that the credibility group ratings, at least, could be improved considerably by proper development effort.

Figure 3 illustrates that the two in-containment concepts (SD-15, powder dispersal; and SD-17, acoustic agglomeration) or combination systems using these two concepts (SR-9, SC-19, SC-20) are generally low in credibility but high in effectiveness. The diagonal line in Figure 3 arbitrarily separates the systems into those which offer high and low incentive for improvement by development effort. The systems furthermost to the left of the line offer the most potential. Similarly, Figure 4 plots the reliability versus the credibility ratings.

Another criterion which can be used to select the most promising EACS for development is cost. In Figure 5, the numerical ratings are plotted versus the estimated installed cost for all twenty systems evaluated. The nine systems which failed the mandatory criteria are
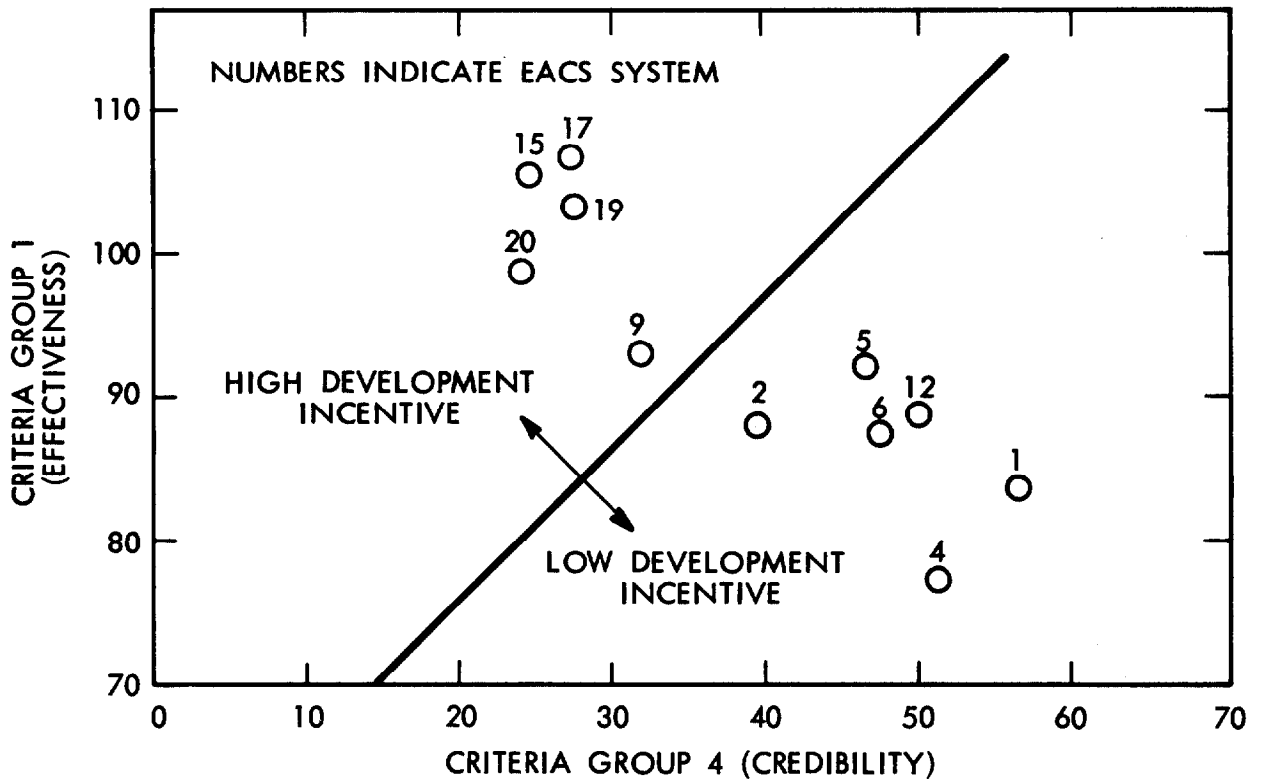
FIGURE 3.   EACS Effectiveness Versus Credibility Ratings.
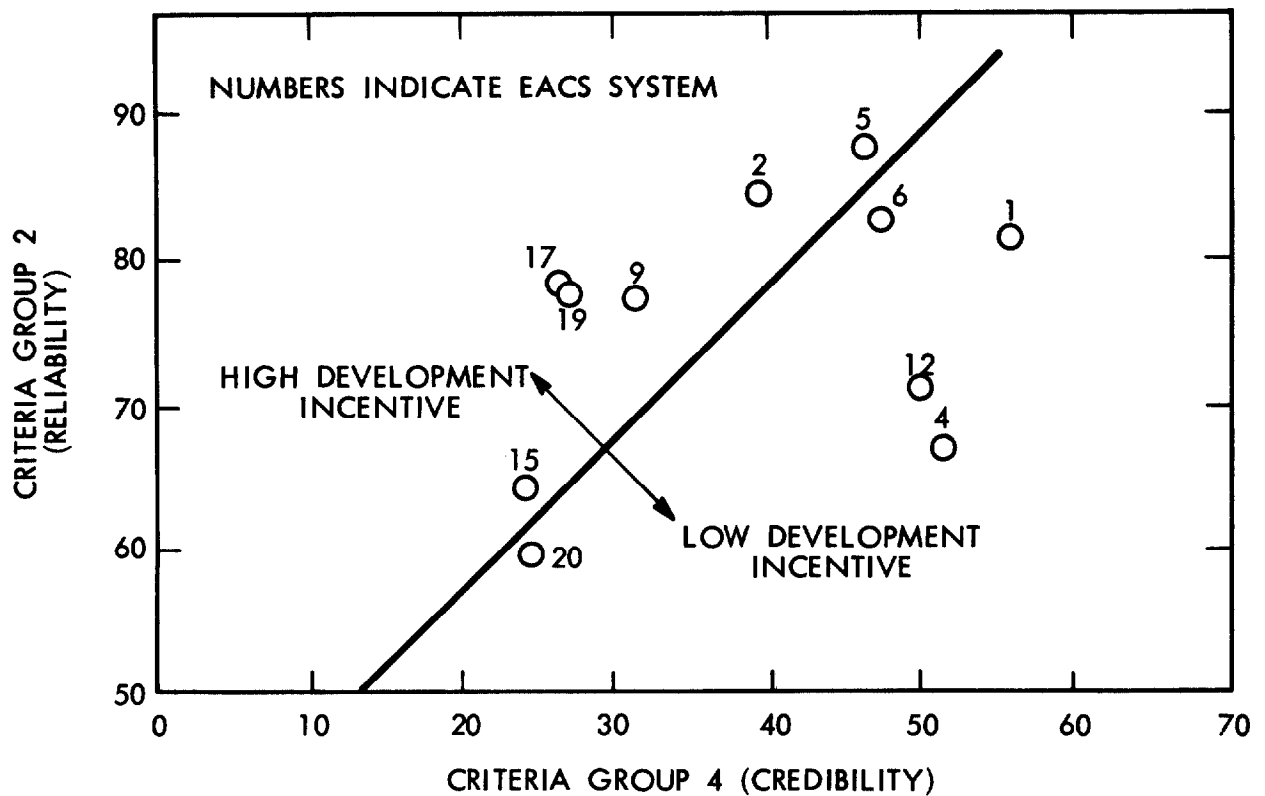
FIGURE 4.   EACS Reliability Versus Credibility Ratings.
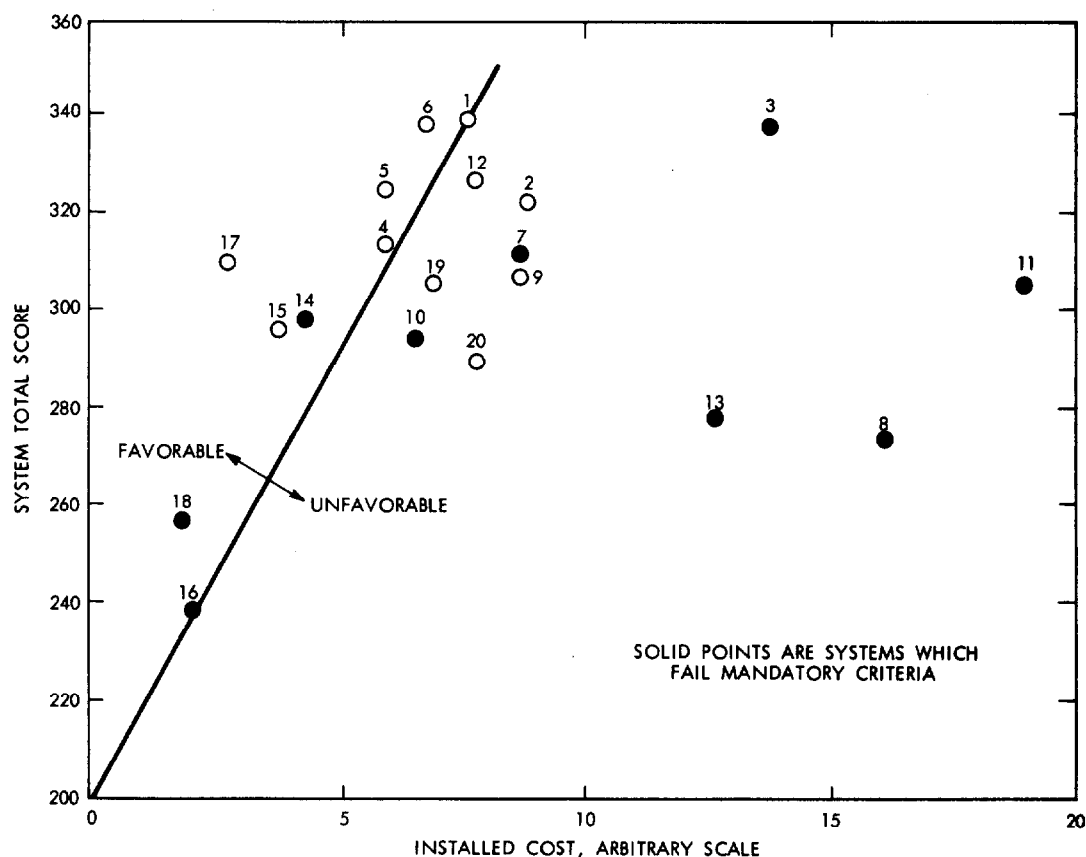
FIGURE 5.   EACS Numerical Ratings Versus System Cost.

designated by solid symbols, while the remaining eleven systems are plotted with open symbols. Since low cost and high numerical ratings are desirable, systems lying to the left of the diagonal line are the more favorable candidates. On a cost basis, system SD-17 (in-containment acoustic agglomeration) is the best system, having a reasonably high rating with the lowest cost of any of the eleven feasible systems. The powder dispersal system (SD-15) and the two cyclone systems (SR-5 and SR-6) are also cost-favorable.

Table 9 summarizes the system components which are regarded as being favorable for development, based on their use in systems which show the highest development potential. The specific development recommendations for these concepts are given in Table 10.

The analysis of the numerical ratings for containment/confinement EACS concepts is more direct, as no systems failed the mandatory criteria and fewer systems were involved. Table 8 shows that system CF-24 (sand bed - HEPA - charcoal - HEPA) has the highest total score. Second highest is system CF-21A (prefilter - HEPA - charcoal - HEPA); third is CF-23 (electrostatic precipitator - HEPA - charcoal - HEPA); and fourth is CF-22 (wet scrubber - HEPA - charcoal - HEPA).

It is not reasonable to compare system CF-21B (conventional pre-filter - HEPA - charcoal - HEPA) with the other four systems because it is not designed to handle the sodium fire accident. However, it was

TABLE 9

AIR CLEANING CONCEPTS FAVORED FOR DEVELOPMENT
FOR LMFBR SINGLE CONTAINMENT PLANTS

Air Cleaning Concept or Device	Number of Times Favored*
High-Efficiency Cyclone Separator	9
Acoustic Agglomeration	7
Powder Dispersal	4
HEPA Filters	3
Deep Bed Graded Media Filter	2
Prefilter	1
Electrostatic Precipitator	1
Bag Filter	1

*From Figures 3, 4, and 5

rated on an absolute basis against the DBST conditions and was assign-
ed a total score of 382. Although it was not given a perfect score of
400, this system clearly met or exceeded every criterion for the DBST
case.

It is concluded that on the basis of present knowledge the sand
bed filter system, CF-24 (backed up by a HEPA - charcoal - HEPA), is the
best system for cleaning the confinement building exhaust if the EACS
must handle both the DBST and a sodium fire in the confinement build-
ing. A conventional prefilter-HEPA-charcoal-HEPA system (CF-21B) is
best if a sodium fire is excluded. If two parallel, independent sys-
tems can be shown to be feasible, then the best combination is the
CF-21B filter-adsorber system for handling the radiologically
significant DBST and a separate system using only a wet scrubber
(without backup filters) for handling the sodium fire accident efflu-
ent.

Development needs for the containment/confinement systems are also
presented in Table 10. The development activities described here
represent a compilation of the necessary data and confirmatory inform-
ation found lacking during the conceptual design and evaluation of the
EACS. Completion of the development would lead to improved design and
increased confidence in the air cleaning systems.

VII. Conclusions

The work reported here substantiates the conclusion that reliable
and effective EACSs are feasible for use as engineered safety systems
for LMFBR plants, but that some development effort is needed for all
the air cleaning concepts evaluated. The work supports the following
specific conclusions:

1. Air cleaning is a promising engineered safety system for
    LMFBRs. It is virtually certain that a 2-hr DRF of 10 can
    be achieved with systems designed for single containment
    and that decontamination factors of 100 to 1000 can be
    obtained by systems designed for containment/confinement
    plants.

TABLE 10

DEVELOPMENT NEEDS FOR RECOMMENDED EACS CONCEPTS

Single Containment

Priority	Concept or Device	Development Needed
1.	Prefilter and HEPA	a) Loading capacity as a function of aerosol composition, particle size, air humidity. b) Long-term performance--chemical attack, change in flow resistance, resuspension. c) Large-scale demonstration under simulated DBA conditions.
2.	Acoustic Agglomeration	a) Measurement of agglomerated particle size and density as a function of sound intensity, frequency, wave shape; and particle concentration, size, density. Small-scale and large-scale tests. b) Theoretical treatment of acoustic agglomeration process relating particle size to acoustic conditions. c) Develop high-intensity sound generator, minimizing gas requirement.
3.	Cyclone Separator (High-Efficiency Type)	a) Large-scale demonstration tests in simulated DBA conditions: 1) Alone 2) Pretreatment for filter 3) Backup for in-line acoustic agglomerator.
4.	Powder Discharge	a) Develop suitable powder (storage, flow-ability, dispersibility, reaction with Na fire). b) Demonstrate aerosol removal in a large vessel, verifying mathematical model predictions of effects of powder size, flow rate and fall height. c) Demonstrate full-scale equipment for storing and dispersing powder.

Containment/Confinement

Priority	Concept or Device	Development Needed
1.	Sand Bed	a) Optimize sand and gravel layers to give maximum Na_2O/NaOH loading capacity. b) Characterize sand bed (1.a. above) performance. Efficiency, flow-resistance as function of aerosol particle size, concentration and gas relative humidity. c) Proof test large-scale section of prototype sand bed under simulated DBA conditions.
2.	HEPA	Same as No. 1 for single containment.
3.	Wet Scrubber	Measure efficiency for Na_2O/NaOH particle removal as function of particle size, using three types of scrubbers (wetted fiber bed, Venturi, centrifugal wet fan) at large scale (5 to 10,000 CFM).

2. The technological base for air cleaning of LMFBR plants is not sufficient to support an immediate application. For the most developed system currently available, development efforts appear to be modest. Lesser developed but potentially more attractive systems are available, and development applied to these would have a potentially high payoff in terms of reduced system cost and possibly higher DRFs.

3. For single containment plants, the best system, judged from current technology, is a recirculating system with low efficiency prefilters followed by high-efficiency particulate air (HEPA) filters. Direct in-containment acoustic agglomeration of aerosols is a highly attractive candidate system because it is small in size and low in cost. Considerably more development effort would be required to allow firm design of the acoustic agglomerator system than for the recirculating prefilter-HEPA system. A third system which appears promising is direct in-containment powder discharge, which is small and intermediate in cost. Cyclone separators were found to have usefulness individually and in combination with other components because of their high mass loading capacity and simplicity. Several other systems were judged to be feasible but less desirable because of higher cost, size, or lower reliability.

4. All systems which use liquids were judged to be unfeasible for use in single containment plants because no suitable liquid could be identified. The vapor pressure and hydrogen formation potential of aqueous liquids prevented their use. Several of these systems would be very attractive if a suitable liquid could be identified.

5. For a containment/confinement plant with a design basis source term encompassing both a radiological release and a sodium fire, the best system, judged from current technology, is a sand and gravel bed filter backed up by a HEPA-charcoal adsorber system. A significant reduction in the relatively high cost is believed possible by development of a sand bed with a high mass loading capacity. If the containment/confinement plant source term excludes a sodium fire, the best system is a conventional filter-adsorber system consisting of prefilters, HEPA filters, and charcoal adsorbers.

6. If two parallel, independent systems can be shown to be feasible, then the best combination for a containment/confinement plant is the filter-adsorber system for handling the radiologically significant source term and a separate wet scrubber system (without back-up filters) for handling the sodium fire accident effluents.

7. An aerosol property which is poorly understood but which can have an impact on the performance of some types of EACSs is the stickiness and change of particle shape caused by adsorption of water vapor. Normal reactor containment building (RCB) atmospheres contain sufficient moisture and carbon

dioxide to convert all of the released sodium oxide aerosol to sodium hydroxide and sodium carbonate. Additional water release from concrete surfaces exposed to the RCB atmosphere must be considered.

8. The 2-hr DRF provided by all the systems evaluated here was 10 because this was a design objective. Larger or smaller systems can be designed, yielding proportionate values of cost and DRF.

References

1. Carl Newton, "Program Planning for Development of Radiological Source Terms for Postulated LMFBR Accidents," Paper 1-1 in Status of Safety Technology for Radiological Consequence Assessment of Postulated Accidents in LMFBRs, ERDA-56, July, 1975.

2. R. R. Bellamy and R. W. Zavadoski, "The AEC Regulatory View of the Reliability of Air Cleaning Systems in Nuclear Facilities," Proceedings of the Thirteenth AEC Air Cleaning Conference, CONF-740807, p. 41, August 1974.

3. E. R. Appleby, "Compilation of Data and Descriptions for United States and Foreign Liquid Metal Fast Breeder Reactors," HEDL-TME 75-12, August 1975.

4. W. B. Cottrell and A. W. Savolainen, eds., "U. S. Reactor Containment Technology," ORNL-NSIC-5, Oak Ridge National Laboratory, Oak Ridge, Tennessee, August 1965.

5. R. E. Aronstein, et al., "1000-MW$_e$ Liquid Metal Fast Breeder Reactor Follow-On Study Conceptual Design Report," AI-12792 (Vol. IV), Atomics International, Canoga Park, California (no date).

6. W. R. Gee, Jr., et al., "Conceptual Plant Design, System Descriptions, and Costs for a 1000 MW$_e$ Sodium Cooled Fast Reactor," GEAP-5678, General Electric Co., Sunnyvale, California, December 1968.

7. "Status of Safety Technology for Radiological Consequence Assessment of Postulated Accidents in Liquid Metal Fast Breeder Reactors," ERDA-56, July 1975.

8. R. S. Hubner, E. V. Vaughn, and L. Baurmash, HAA-3 User Report, AI-AEC-13038, Atomics International, Canoga Park, CA, March 30, 1973.

9. Regulatory Guide 1.4, Revision 2, "Assumptions Used for Evaluating the Potential Radiological Consequences of a Loss of Coolant Accident for Pressurized Water Reactors," USAEC Directorate of Regulatory Standards, June 1974.

10. R. Dennis, et al., "Fibrous Filters for NaK Fume Removal," NYO-4811, Harvard Air Cleaning Laboratory, May 1, 1960.

11. F. J. Viles, et al., "High Capacity-High Efficiency Filters for Sodium Aerosols," NYO-841-10, Harvard Air Cleaning Laboratory, August 1967.

12. L. Bohm, et al., "The Off-Gas Filter System of the SNR-300," CONF-740807, Proceedings of the Thirteenth AEC Air Cleaning Conference, p. 620, August 12-15, 1974.

13. M. W. First and T. Baldwin, "Sodium Aerosol Filtration Studies," Proceedings of the Eleventh AEC Air Cleaning Conference, CONF-700816, p. 445, December 1970.

14. A. S. Goldin, et al., "Behavior of Iodine in Sodium Systems," CONF-700816, Proceedings of the Eleventh AEC Air Cleaning Conference, p. 356, December 1970.

15. L. Baurmash, et al., "Behavior of Iodine in the Presence of Sodium Oxide Aerosols," CONF-700816, Proceedings of the Eleventh AEC Air Cleaning Conference, p. 373, December 1970.

DISCUSSION

MOELLER: How did you determine the reliability of each of the various systems you considered?

MCCORMACK: We did not go into any detailed failure analysis. It was, in this case, fairly subjective with the authors and it was a relative ranking rather than any absolute system.

KAHN: In the first ranking of the containment systems, you had an asterisk next to the sand filter, indicating failure to meet a mandatory criterion. Was cost the mandatory criterion involved?

MCCORMACK: No, cost really isn't a mandatory criterion, but size is, and it was primarily size that gave us trouble with the sand filter. We felt that the filter housing would have to be built with the same code requirements as the containment vessel. With a system the size of a sand filter, we felt that this was a very serious obstacle.

SCHIKARSKI: Have you looked into the German sand filter design, which is a very small, compact kind?

MCCORMACK: Yes. We used some of your loading information in attempting our scope design. It is interesting that we think this is an application where, perhaps, the sand filter could be optimized to reduce size even further and to increase mass loading even if the cost was a somewhat reduced efficiency.

SCHIKARSKI: In my opinion, your ranking for the cyclones is too high to be realistic. There is much evidence that many designs of cyclones can be plugged easily by sodium oxide aerosols during long-

term operation.   Did you take this into account?

MCCORMACK: We were very concerned about the sticking of the sodium oxide or sodium hydroxide particles. This was a concern with us in the scope design of the systems. We didn't have any definite information on that feature.

BENDIXSEN: I noticed in both of your figures that the relative rankings that you have for the various air cleaning systems were very close, and, in fact, the full range varied between only eight and ten % for some dozen items. Would you comment on the relative closeness in the "test scores" and whether the differences are significant or not?

MCCORMACK: That is a feature we noticed, too, and I think probably it could be, in part, a reflection of the rating system we used. I think, in retrospect, we need to use a ranking system with a bigger range of weighting factors to spread the ratings of the systems. We have some confidence in the ranking though, because of the individual assessments that each of the authors gave the system. I think it is a reflection on the ranking system, however. It should also be noted that each system was designed to work and to meet, to the extent possible, the same objectives. Hence the system differences will tend, in many criteria, to be small.

R. J. WILLIAMS: How does consideration of natural processes of attenuation relate to selection of a system? How were estimates of natural processes made?

MCCORMACK: Natural processes do help to reduce the aerosol concentration. Natural processes were assumed to be operating concurrently with the EACS. They do not influence the system selection. Removal by natural processes was estimated by using the HAA-3 computer code which accounts for both gravitational settling and wall deposition.

EVALUATION OF IN-VESSEL EMERGENCY AIR CLEANING
SYSTEMS FOR AN LMFBR

W.C. Hinds, E.F. Mallove, and M.W. First
Harvard Air Cleaning Laboratory
Boston, Massachusetts

Abstract

The goal of direct application in-vessel air cleaning systems is to reduce the two hour integrated dose leaking from a containment vessel after a design basis accident by rapidly reducing airborne sodium aerosol concentration within the vessel. This reduction in concentration is achieved by direct action on the entire containment volume rather than by a more conventional recirculating clean-up loop. Strategies that have been evaluated include: increased sedimentation by enhanced agglomeration using powder dispersal, acoustic energy, or turbulence, and powder scavenging. Experiments were conducted by burning metallic sodium in a 90 m^3 chamber to achieve aerosol concentrations up to 10 gm/m^3. The time decay of the airborne mass was measured by sequential filter sampling and the effectiveness of each enhancement method was evaluated by comparison with decay profiles of untreated aerosols.

Experiments with induced turbulent agglomeration show 2-hour dose reduction factors (DRF's) up to 43. Under the same scale turbulence conditions it is likely that a similar DRF would be achieved in a 30 m high containment vessel. Powder dispersal scavenging tests in the same chamber showed 2-hour DRF's up to 7.2--a performance level which would also be duplicated in a 30 m high containment vessel.

I. Introduction

One of the safety features that might be incorporated into an LMFBR is an emergency air cleaning system (EACS) that can operate in the event of a sodium fire to reduce the concentration of airborne sodium fume and accompanying radioactive fission products in the reactor containment vessel. Rapid removal of aerosol particles will reduce the amount of radioactive material leaking from the containment vessel to the external environment at the design leakage rate of 0.1% of the total volume per 24 hours.

Three modes of operation of an EACS have received attention: gas recirculation through a gas cleaning device, excess gas pressure purged to the outside through a gas cleaning device, and direct in-vessel reduction of airborne concentrations by a system which acts on the entire containment vessel atmosphere at once. A primary figure of merit for an EACS is the "dose reduction factor" (DRF) achieved in a two hour period following start of the clean-up system:

$$DRF(t_*) = \frac{C_o t_*}{\int_0^{t_*} C(t)dt} \tag{1}$$

where C_o is the initial mass concentration of aerosol particles, $C(t)$ is the mass concentration-time history of the aerosol under treatment, and t_* is a time period, taken to be 2 hours. A minimum design goal is a system with a DRF (2 hour) capability of 10 in a 30m high containment vessel. Although a DRF (2 hour) of 10 might be attainable with gas recirculation or gas purging it would require such an extremely large filtration and air flow system capacity (200,000 cfm even at 100% cleaning efficiency) that it would (1) represent a significant capital investment (2) require large amounts of power that would be difficult to obtain during an emergency following a major reactor accident and (3) occupy a large fraction of the containment volume. The third mode of operation, direct in-vessel precipitation of airborne particles, has excellent potential for rapidly reducing aerosol concentration with devices that require only a low to moderate energy input. Specific emergency air cleaning systems for LMFBR's, of both the direct and recirculating type, have been suggested and theoretically analyzed in Reference 1.

A number of possible direct in-vessel systems have been eliminated from consideration for use with sodium. In particular, liquid sprays for scavenging sodium aerosols have to be abandoned in the absence of a liquid that is safe to use with sodium metal. Foam encapsulation has similar problems of chemical incompatibility with molten sodium metal. The increased sedimentation that results from enhanced agglomeration after dispersal of inert powder into sodium aerosol can be shown on theoretical grounds to require excessive amounts of powder to achieve a DRF (2 hour) of 10, however, this approach might be used to enhance the performance of other direct systems. For similar reasons, clean up systems that require deployment of large collection surfaces are unattractive, i.e., the amount of area-intensive material required is prohibitively bulky and difficult to release rapidly.

The remaining candidate direct systems are turbulence-induced agglomeration and acoustic agglomeration to enhance sedimentation, powder dispersal scavenging, and direct electrostatic deposition. The current experimental program has focused on the first three of these systems. Each of these shows considerable promise of being adaptable to practical systems. Electrostatic precipitation in a direct cleaning mode system has not yet been evaluated by us.

II. Summary of Baseline Tests

In order to evaluate the effectiveness of the direct cleaning methods being investigated, it was necessary to establish as a baseline the aerosol evolution characteristics of an unperturbed sodium pool fire. The baseline test in our air-filled 4m high 90m^3 rectangular chamber calls for melting and burning one pound of sodium inside an electrically heated, insulated steel pot. The relative humidity of the air-filled chamber at the start of the sodium fire was approximately 20% for all baseline fires. Sodium combustion in a normal atmosphere results in a very dense, white aerosol which in minutes fills the chamber. The mass concentration decay with time, the baseline property of most importance, was obtained with open-face absolute filter samples taken near the mid-chamber height.

Generally samples were taken over a 3 minute interval at 18.4 liters/minute.

The baseline sodium aerosol decay rate, shown in Figure 1, was derived from data averages of eight sodium fires. Natural decay by gravitational settling gave a dose reduction factor in 2 hours of 1.45 when measured from the peak concentration point which occurs at approximately 25 minutes after the initiation of burning. This average DRF (2-hr.) value corresponds closely to the decay characteristics of stirred settling of a spherical 4 μm monodisperse aerosol particle with a true density of 1.0 gm/cm^3. Scaling up the settling of this aerosol for a 30 m high chamber, the equivalent DRF (2-hr.) would be 1.05.

The mass median diameter (MMD) and geometric standard deviation (GSD) of the baseline aerosol cloud were determined by Andersen impactor tests and found to be nearly constant with time during the settling period as shown in Figures 2 and 3. The average MMD of 4 μm, 60 minutes after the start of the fire declined to an average MMD of 3.5 μm at 350 minutes. This behavior suggests that there may be processes present that are analogous to those involved in the "self-preserving" aerosol size distribution postulated by Lai, et al.[2] For the baseline fire the GSD stayed close to 1.8 over a period of 350 minutes, as shown in Figure 3. These size measurements are fairly consistent with results from sodium pool fires conducted by Atomics International[3] (their Figures A.1.10 and A.1.11). Their GSD over the period covered by our measurements is in the range of 1.4 to 1.6 and their MMD is slightly over 3 μm for several hundred minutes. The larger MMD and GSD found by us can be accounted for by the higher effective cut-off diameters which were assigned to each Andersen stage in our sampling, following the updated and improved values published by Rao.[4] The measured ratio of chamber floor to chamber wall deposits (mass per unit area) was in the range of 10 to 80. The spread was caused, in part, by uncertainty in the measurement of the very low wall deposits collected on filter papers.

The baseline sodium aerosol was also sampled with an aerosol centrifuge[5] which fractionates particles according to aerodynamic diameter. Centrifuge data from a number of runs gave an average MMD close to 2.0 μm and an average GSD close to 1.65. The lower MMD determined by centrifuge versus that obtained from the Andersen impactor might be due to size selective losses at the aerosol inlet. Aerodynamic size calibration of the centrifuge was performed with polystyrene latex spheres of known size and density. These give reliable calibration values over the size range of interest.

III. Chemical Composition of the Aerosol

Chemical and physical tests were performed to determine the composition of some of the filter samples. Sodium deposit measurements by atomic absorption spectrophotometry indicated high ratios of total sample mass to sodium mass. These ratios were often much larger than would be associated with a nonhydrated sodium compound. The conclusion was that most of the sodium compounds on the filter sample (see Table 1) are hydrated. The data suggest the presence of

mixtures of the following compounds: Na_2CO_3, $Na_2CO_3 \cdot 7\ H_2O$, and $Na_2CO_3 \cdot 10\ H_2O$. Tests for sodium peroxide (Na_2O_2) indicated the presence of less than 0.5% of that compound. In tests where 1 lb. of sodium was burned and peak total concentrations of 2 gm/m^3 were obtained, almost all the non-water fraction of each filter deposit consisted of Na_2CO_3 with a negligible amount as NaOH. The air filled chamber employed for these tests contains about 55 gm CO_2. This is sufficient to produce the level of Na_2CO_3 deposits seen on our filters for total aerosol concentration of 2 gm/m^3. The reaction of carbonate formation from the initial sodium oxide and sodium superoxide combustion product is:

$$Na_2O_2 + H_2O \rightarrow 2\ NaOH + 1/2\ O_2$$

and $2NaO_2 + H_2O \rightarrow 2\ NaOH + 3/2\ O_2$

followed by,

$$2NaOH + CO_2 \rightarrow Na_2CO_3 + H_2O$$
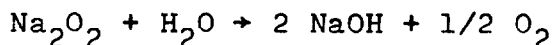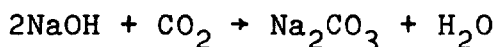
Theoretical analyses performed by other investigators[6] show reaction rates of only seconds for forming Na_2CO_3 from the hydroxide primary compound--a fact which makes these observations credible. Table 2 shows that with sufficient H_2O present in the air sodium hydroxide begins to form in significant quantities only when total aerosol mass concentrations exceed 2 gm/m^3, i.e. when greater than 1 lb. of sodium is burned in the 90 m^3 chamber. For 20% RH, there is ample excess water vapor contained in the chamber to produce sodium hydroxide levels significantly greater than those observed for larger than 1 lb. sodium fires but insufficient CO_2 to yield greater than ~1.5 gm/m^3 of carbonate.

IV. Turbulent Agglomeration Tests

The first full chamber tests of a direct precipitation method involved the use of turbulence to enhance agglomeration and speed sedimentation. A large (3000 cfm) centrifugal recirculating blower placed in the center of the chamber produced increases in the DRF (2-hr.) value from 4.2 to 8.2 when it was started shortly after the peak aerosol concentration was reached. The time decay history of the first five tests is presented in Figure 4. In an effort to separate the relative effects of centrifugal air cleaning in the blower shroud from the effect of turbulence enhanced agglomeration and sedimentation, the blower was run with and without the fan shroud in place. Operation with the shroud off takes away a major surface for centrifugal deposition, though some cleaning credit must still be taken because of particle impaction on the fan blades. Removing the shroud did not greatly change the DRF (2-hr.) from shroud-on performance, as can be seen in Figure 4.

Substantially higher DRF's were obtained with turbulent agglomeration when the peak mass concentration was raised by a factor of 2 from the baseline peak value (~2gm/m^3). Higher concentrations were generated by larger quantities of sodium and by faster burning rates induced by blowing an air jet against the sodium pool surface. Figure

5 shows the mass concentration profiles of two of these tests which
resulted in a DRF (2-hr.) of 28 and 43, respectively. Test R-21 was
conducted with air-augmented burning of 1 lb. sodium whereas test
R-22 involved air augmented burning of 3 lbs. of sodium. For both of
these tests, blower turbulence began when mass concentrations in the
chamber were above the baseline level. This confirms that higher
initial particle number concentrations accelerated agglomeration in
the expected fashion. Figure 5 shows another run with DRF (2-hr.)
greater than 8 in which turbulence was initiated after the mass con-
centration had peaked and then dropped back to 2 gm/m^3. The high
DRF (2-hr.) as shown by curve R-20 of Figure 5 is a result of longer
agglomeration time which produced a larger MMD aerosol by the time
the blower was started.

Blower induced turbulence caused agglomeration to proceed
rapidly. Large visible particles, of the order of 100 μm or more,
were seen uniformly deposited on horizontal surfaces near chamber
view ports. It is difficult to determine whether most of the agglom-
eration occurs in the strong velocity gradients near the fan wheel or
whether induced turbulence in other parts of the chamber causes most
of the agglomeration. The particle size distribution, as measured
by an Andersen impactor, shows a definite decrease in MMD with time
when the aerosol is vigorously stirred and the large agglomerates
settle in the chamber as shown by the sloping curves in Figure 2,
however there was no clear trend in GSD. That the MMD should de-
crease with time is not surprising, because turbulent agglomeration
and sedimentation can deplete the largest particles rapidly.

These turbulence tests demonstrate that DRF (2-hr.) values in
excess of 10 are readily achievable for vessels 4 meters in height.
Scale-up to containment vessel dimensions might well yield DRF's of
the same magnitude as the present tests, provided the same level of
turbulence can be induced throughout the larger volume. This assumes
that the turbulent agglomeration process would produce substantial
numbers of particles in excess of 100 μm in a matter of minutes, a
process which we believe has been observed in our tests. It is
likely that these large particles produce a further benefit by
scavenging smaller particles as they fall through the aerosol cloud.
The lower limit DRF (2-hr.) for scale-up to a 30 m chamber can be
found by imagining filling the 30 m vessel with a monodisperse aero-
sol of diameter sufficient to produce the measured DRF (2-hr.) in the
4 m high chamber. For example a DRF (2-hr.) of 43 in the small cham-
ber would scale to a DRF (2-hr.) of 5 in the 30 m vessel.

V. Powder Scavenging Tests

In an effort to test the scavenging capacity of various powders
on the sodium aerosol, we constructed a centrally mounted overhead
dust spreader in the 90 m^3 test chamber. The dust dispersal device
consists of a horizontal 16" diameter plastic disc rotated at 2000
rpm by an electric motor mounted below it. Powder is dropped through
a hole in the chamber ceiling onto the center of the disc and is
then spread by rotational action about the chamber.

Our initial tests have employed crushed limestone (intended

originally for agricultural use) which has a very low sodium content
(<1 ppm). The low sodium level in this powder permits analysis of
the sodium aerosol particles on the filter samples by atomic absorp-
tion spectrophotometry without chemical interference from the scaven-
ger dust. We recognize that carbonates are widely used for suppres-
sion of sodium fires. During powder dispersal in a sodium aerosol
cloud, the total mass on sampling filters rises considerably above
the expected baseline level but the total sodium in the samples stead-
ily declines as long as powder is injected.

Tests R-25 and R-26, shown in Figures 6 and 7 demonstrate the
cleaning effect of limestone powders when applied to the sodium aero-
sol in the manner described. The crushed limestone used in both
tests had an MMD of 200 μm and a GSD of 1.5. The measured total mass
concentration, limestone plus sodium aerosol, is seen to rise above
the normal baseline concentration during spreading. Not all the
limestone particles are represented in the total mass concentration
because of very inefficient capture of these large scavenging lime-
stone particles by the sampling system. The concentrations for sod-
ium aerosols alone, shown in Figures 6 and 7, were obtained by scaling
spectrophotometrically measured sodium mass collected on each filter
by the same constant of proportionality required to raise the initial
pre-limestone injection sodium mass samples up to the measured total
mass concentration.

In test, R-25, powder was dispersed at the maximum feed rate of
1.5 kg/minute for 21.5 minutes. The slope of the sodium concentra-
tion decay curve during this interval indicates a DRF (2-hr.) of 6.0.
In test R-26, powder was dispersed at the rate of 0.13 kg/min. for
36 minutes and was then boosted to 1.5 kg/min. for the next 60 minutes.
The DRF (2-hr.) associated with the slopes of the different dispersal
rate segments were 4.1 and 7.2 respectively. These data show that
under similar dispersal conditions in a 30 m high containment vessel,
identical, if not better, DRF's would be achieved. This is because
200 μm particles can fall 30 meters in a matter of seconds. After
they have fallen below the initial 4 m for which we have data, they
still retain their initial unit scavenging efficiency, perhaps
enhanced by the accumulated sodium aerosol coating.

VI. Acoustic Agglomeration Tests Planned

Reviews of the literature of acoustic agglomeration[7,8] hold out
great promise for this mechanism to be applied as a direct in-vessel
air cleaning system. The bulk of sonic agglomeration research and
literature has dealt with setting up finite amplitude standing waves
in precisely tuned chambers. This approach to sonic air cleaning
would not be applicable as a direct cleaning method within the very
large and irregularly shaped containment vessel. Recently, Scott[8]
has stated that progressive saw-tooth waveforms, generated, for
example, by a pulse-jet engine, would agglomerate a wider size
spectrum of aerosol particles than would a tuned, standing wave
system. The progressive wave idea would eliminate the problem of
setting up a tuned standing wave pattern within a large vessel. An
acoustic agglomeration system may also be useful as an aerosol pre-
conditioner for other direct cleaning methods such as the scavenging

system described above, even if it were found to be ineffective as a direct air cleaning method.

We have obtained and tested a (4.5 lb. thrust) Dyna-Jet pulse jet engine which burns a gasoline-air mixture and operates at roughly 250 Hz. The device is normally used to propel model aircraft. Preliminary indications are that this engine can produce sound intensities exceeding 150 dB in a localized area, a level capable of initiating sonic agglomeration phenomena. We plan to run the engine in a duct separated from the test cell atmosphere by an acoustically transparent foil membrane. The sound will be directed at the burning sodium pool to discover to what extent the anticipated rapid agglomeration of the aerosol can reduce mass concentrations through enhanced sedimentation.

VII. Conclusions

It has been demonstrated that at least two direct air cleaning systems, turbulence-induced agglomeration and powder dispersal scavenging, have an immediate prospect of satisfying a requirement for a DRF (2-hr.) equal to or in excess of 10. Acoustic agglomeration in an untuned system has good experimental and theoretical potential to serve as an aerosol preconditioning mechanism for either of these cleaning systems. Combinations of any two or more systems appear to be attractive options which should be tested by continuing research.

VII. Acknowledgement

References

1. R.K. Hilliard, J.D. McCormack, and A.K. Postma, "Evaluation of Air Cleaning System Concepts for Emergency Use in LMFBR Plants," Hanford Engineering Development Laboratory Report TC-536, (December 22, 1975).

2. F.S. Lai, S.K. Friedlander, J. Pich, and G.M. Hidy, "The Self-Preserving Particle Size Distribution for Brownian Coagulation in the Free-Molecule Region," J. Coll. and Interface Sci. 39 (2):395 (May 1972).

3. James A. Gieseke, Robert C. Behn, Allan S. Chace, and Larry D. Reed, "Analytic Studies of Aerosol Behaviour Predictions for Fast Reactor Safety," Topical Report, Task 56, Battelle Columbus Laboratories, (1975).

4. A. Rao, "An Experimental Study of Inertial Impactors," Ph.D. thesis at University of Minnesota, (June 1975).

5. M.I. Tillery, "A Concentric Aerosol Spectrometer," Am. Ind. Hyg. Assn. J., 34:62, (1974).

6. W.S. Clough and J.A. Garland, "The Behaviour in the Atmosphere of the Aerosol from a Sodium Fire," United Kingdom Atomic Energy Research Establishment Report AERE - R 6460, (1970).

7. E.P. Mednikov, Acoustic Coagulation and Precipitation of Aerosols. Translated from the Russian by C.V. Larrick, Consultants Bureau, New York, (1965).

8. D.S. Scott, "A New Approach to the Acoustic Conditioning of Ind ustrial Aerosol Emissions," J. of Sound and Vibration, 43 (4): 607-619, (1975)

Table 1   Average Ratio of Total Filter Deposit Mass to Sodium Mass During Several 1 lb. Baseline Tests.

Run	M_{tot}/M_{Na}	% of Deposit Mass Assumed to be H_2O if Primary Compound is Na_2CO_3
R-12	4.6	48
R-13	3.7	32
Theoretical Values for Pure Compounds		
Na_2CO_3	2.30	0
$Na_2CO_3 \cdot 7H_2O$	5.04	54
$Na_2CO_3 \cdot 10H_2O$	6.22	63

Table 2   Composition of the Non-Water Fraction of Filter Samples for a 4 lb. Sodium Fire in a 90 m^3 Chamber Filled with Air at 20% R.H.

Time Interval for Averaging Samples (minutes)	Total Mass Concentration Range During Sampling Period (gm/m^3)	NaOH (%)	Na_2O_2 (%)	Na_2CO_3 (%)
11 - 24	1.05 - 2.45	6	2	92
80 - 113	4.31 - 3.69	53	3	44
130 - 140	2.17 - 2.01	46	1	53

FIGURE 1

BASELINE CONCENTRATION DECAY PROFILE FOR 1.0 LB. SODIUM FIRES IN 90 M^3 AIR-FILLED CHAMBER

RUN	R.H. (%)
△ R-1	21
⊡ R-8	19
⊙ R-9	22
♦ R-10	19
⊘ R-11	18
◇ R-12	14
⊘ R-13	19
⊙ R-17	20

TIME AFTER INITIATION OF FIRE (MINUTES)

TOTAL AEROSOL MASS CONCENTRATION (GM/M^3)
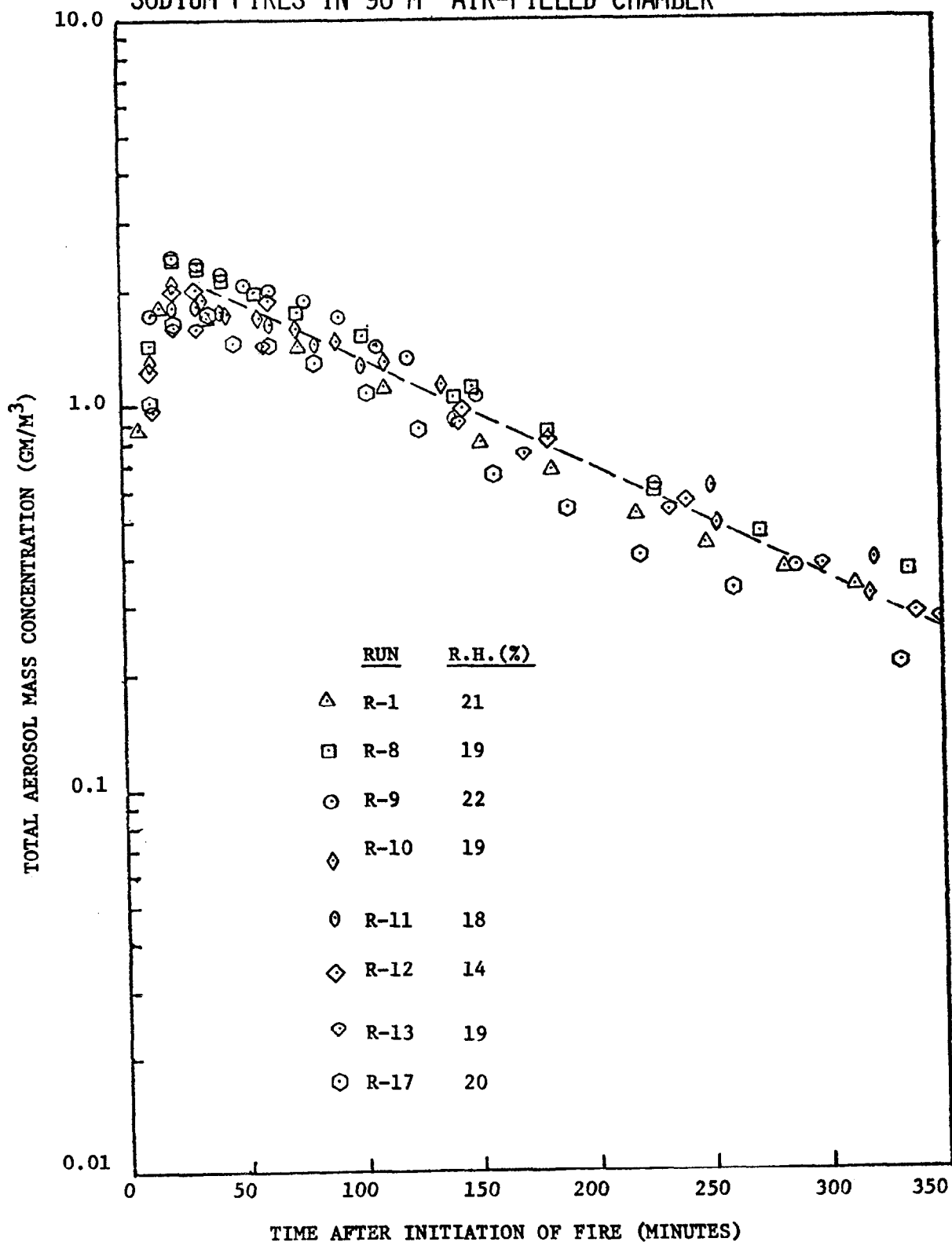
FIGURE 2.

ANDERSEN IMPACTOR MASS MEDIAN DIAMETER FOR 1.0 LB. BASELINE SODIUM FIRES
AND SEVERAL INDUCED TURBULENCE TESTS
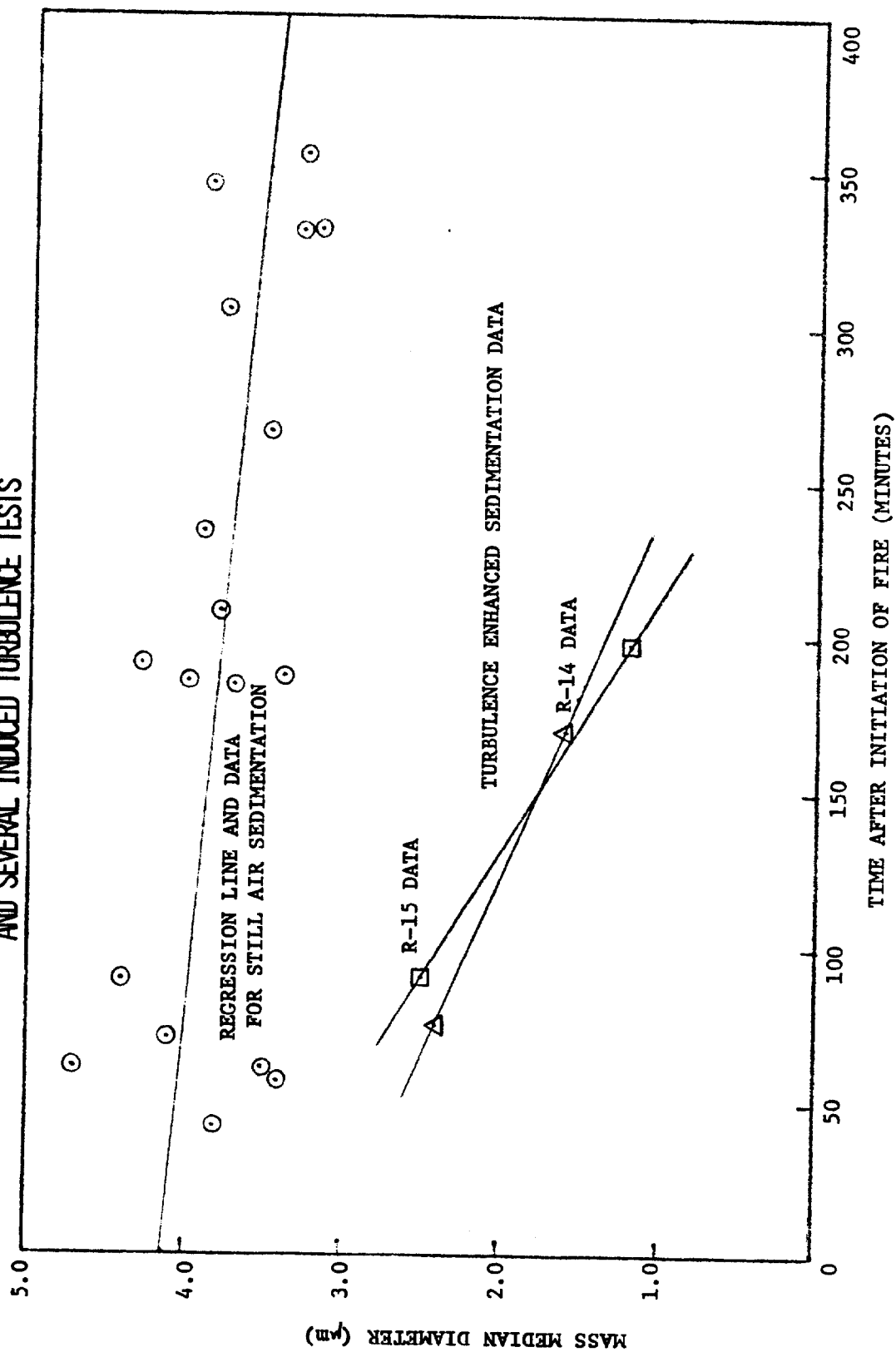
FIGURE 3.

ANDERSEN IMPACTOR GEOMETRIC STANDARD DEVIATION FOR 1.0 LB. BASELINE SODIUM FIRES
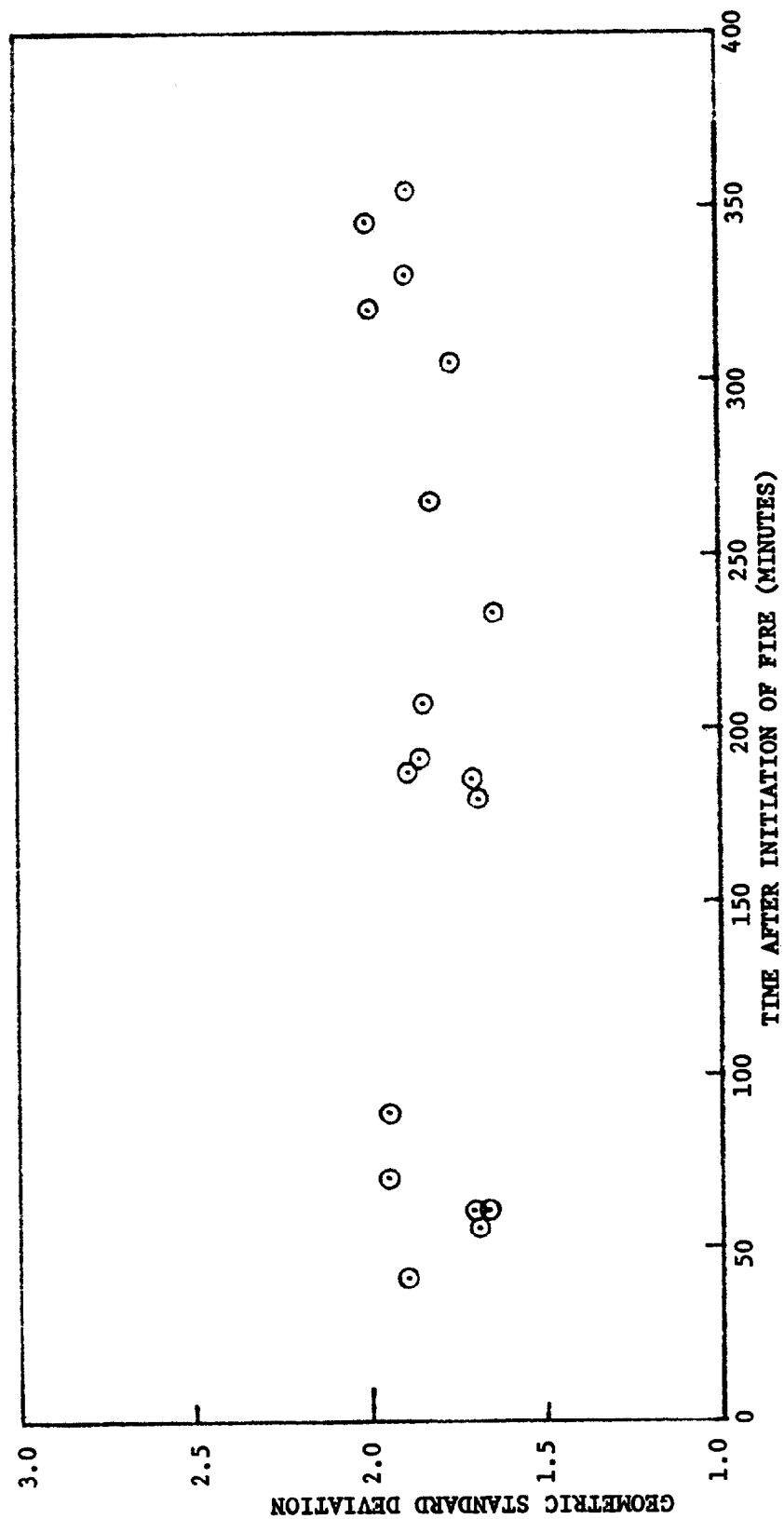
FIGURE 4.

TURBULENT AGGLOMERATION AEROSOL CLEARANCE TESTS (LOW CONC.)
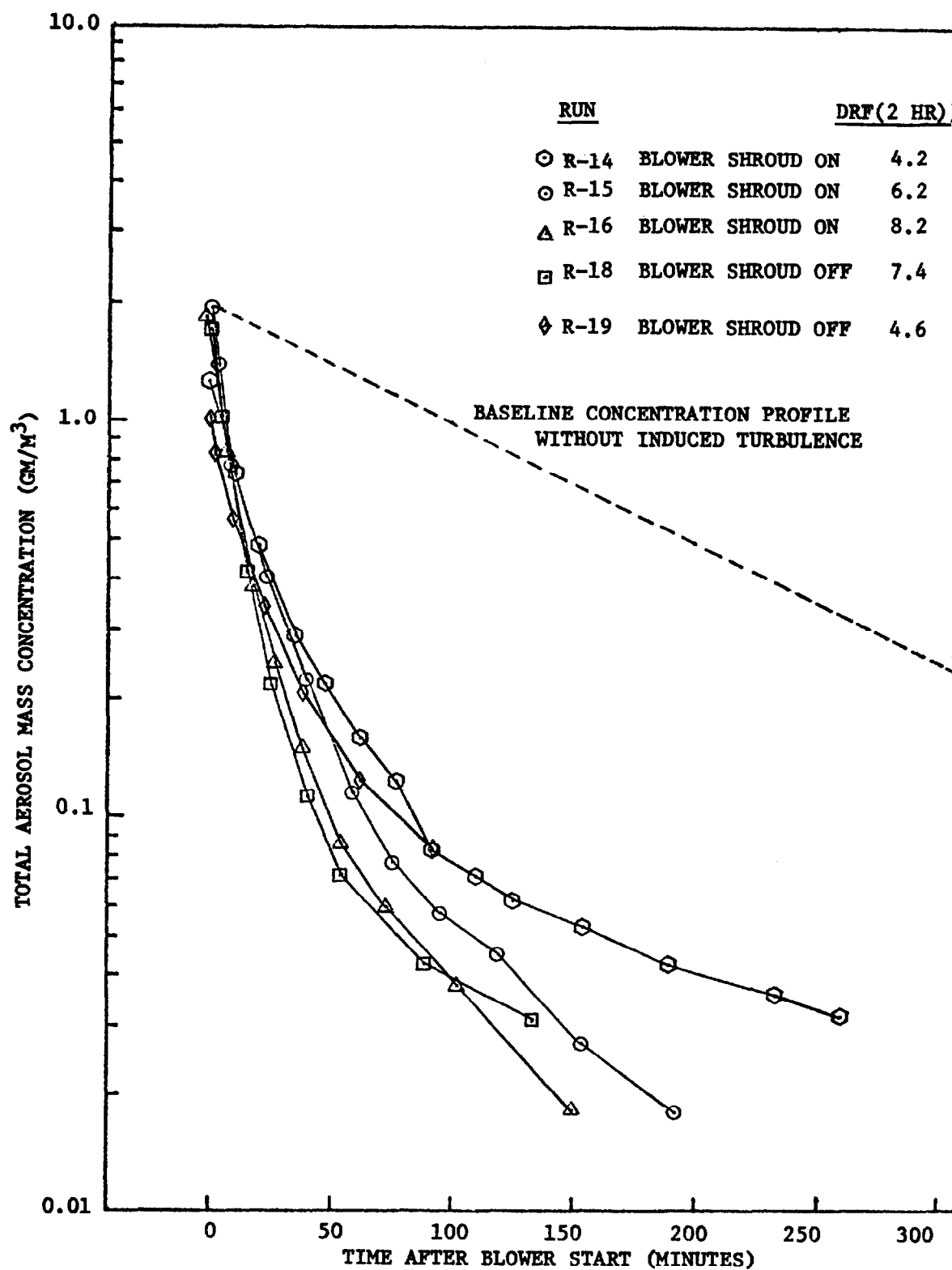
FIGURE 5.

TURBULENT AGGLOMERATION TESTS AT HIGH AEROSOL CONCENTRATION

START OF TURBULENCE
INDICATED FOR EACH RUN
BY ARROW

RUN	DRF(2 HR.)
⊙ R-20	28
⊡ R-21	25
△ R-22	43

TIME AFTER INITIATION OF FIRE (MINUTES)

TOTAL AEROSOL MASS CONCENTRATION (GM/CM³)
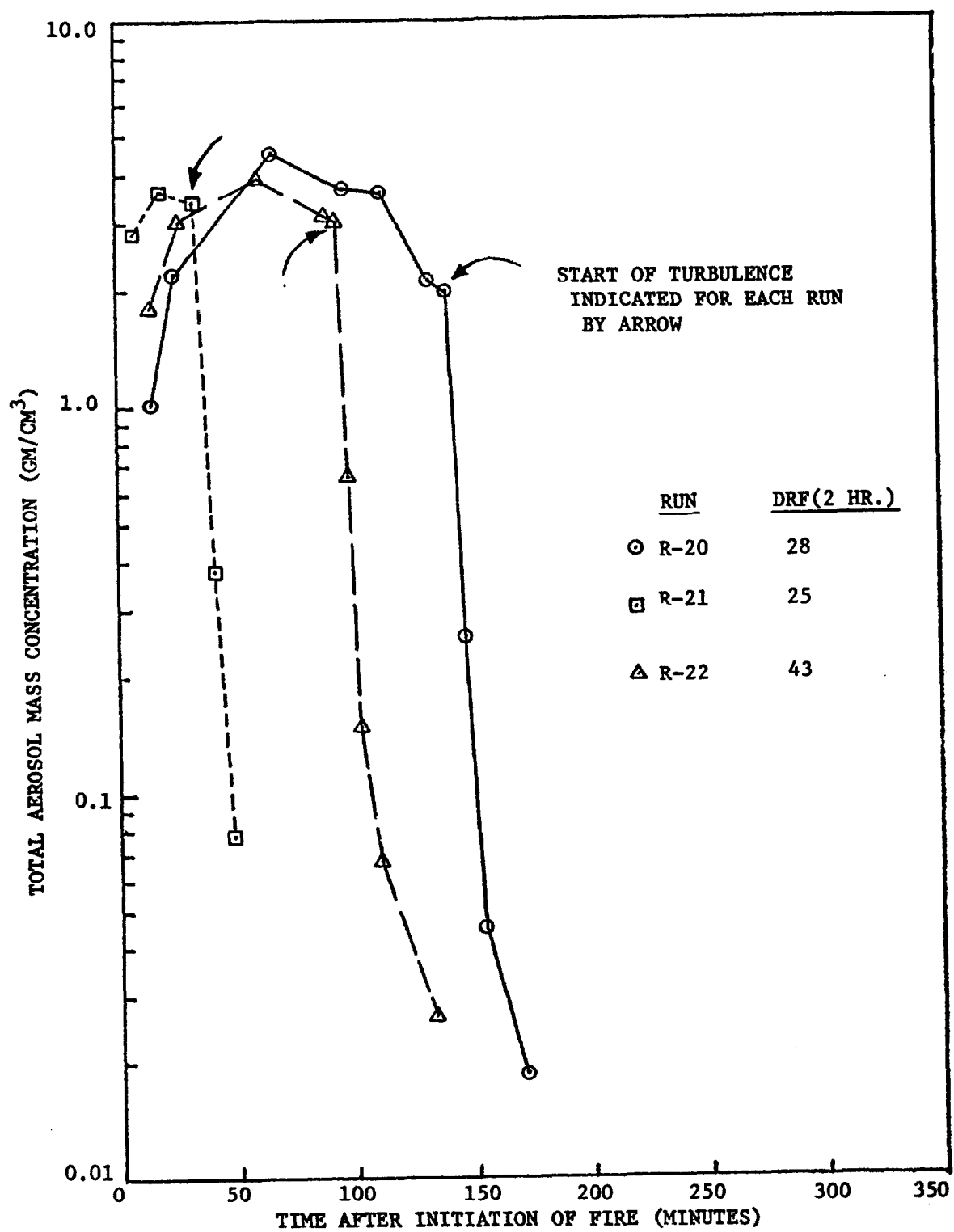
FIGURE 6.

CRUSHED LIMESTONE POWDER DISPERSAL TEST NUMBER R-25

CRUSHED LIMESTONE POWDER DISPERSAL TEST NUMBER R-25

POWDER DISPERSAL STOPS

BASELINE CONCENTRATION PROFILE
WITHOUT POWDER DISPERSAL

POWDER DISPERSAL STARTS

◻ MEASURED TOTAL AEROSOL MASS CONCENTRATION

◊ SODIUM AEROSOL PART OF TOTAL AEROSOL MASS
    CONCENTRATION

MASS CONCENTRATION OF TOTAL AEROSOL MASS AND SODIUM AEROSOL FRACTION (GM/CM³)

TIME AFTER INITIATION OF FIRE (MINUTES)
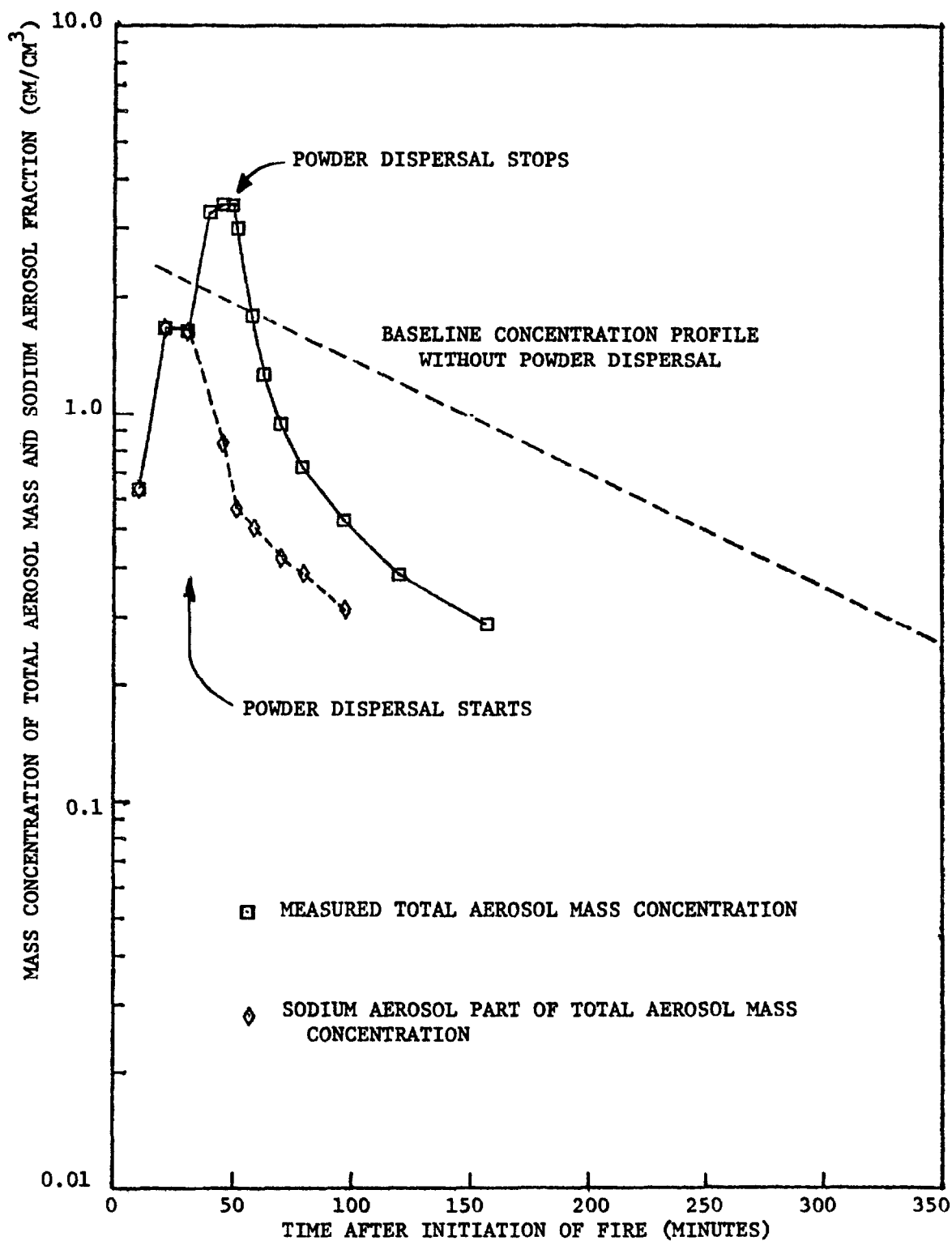
FIGURE 7.

CRUSHED LIMESTONE POWDER DISPERSAL TEST NUMBER R-26
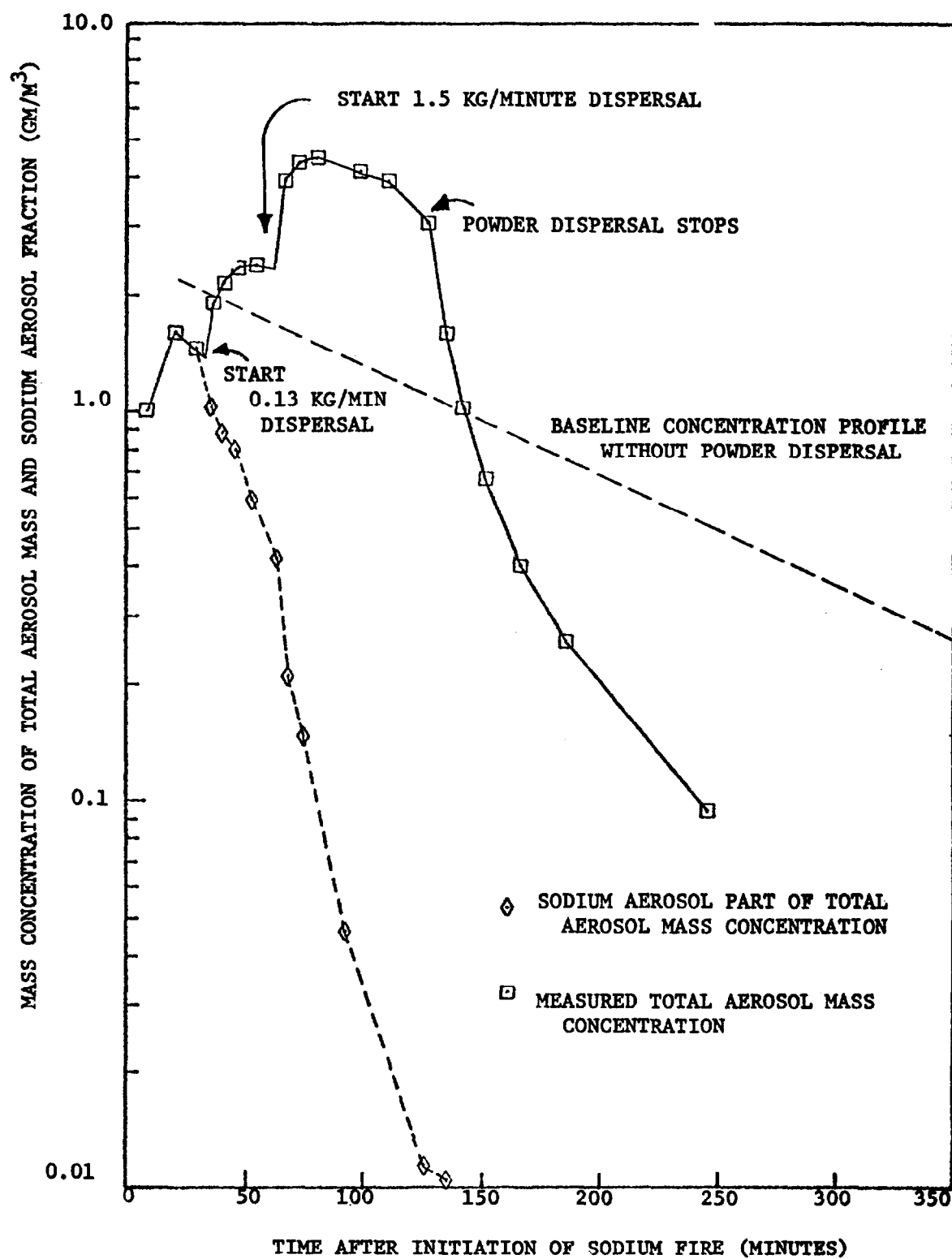
DISCUSSION

SCHIKARSKI: I'd like to congratulate you on these fine experiments. I see the problem of extrapolation to real containment size for both the concentration decay curve and the turbulence producing equipment. Do you subtract the natural convection effect, which of course, is large already? What is the remaining effect of artificial turbulence?

HINDS: This is a preliminary feasibility evaluation to see whether the concept is valid. I'm not giving any consideration to implementation. There are many ways of inducing turbulence. If we can show that it seems reasonable, we can then consider the engineering problems of how to scale up the equipment to extrapolate our information in the case of powder scavenging, the time to fall to the vessel floor is just a few seconds. We'd expect that this effect would be comparable in a containment vessel with only small differences from our chamber. Similarly, for coagulation by turbulence, we generated micrometer particles that were coagulated by turbulence and these would, also, fall very rapidly.

SCHIKARSKI: Is it your favorite method?

HINDS: It appears to have some advantages in that it gets better and better the higher the concentration.

SCHIKARSKI: Did you revise the estimates to account for natural aerosol attenuation?

HINDS: No, we did not. We considered each method of cleanup all by itself. We did not subtract natural attenuation. However, the "DRF - 2 hour" value is the ratio of the induced attenuation to natural attenuation in every case.

LORENZ: With your turbulent agglomeration, how much improvement was a result of increased plateout on the walls of the vessel?

HINDS: When we had the outlet of the blower housing directed at the ceiling, we did not see a buildup of the material on either the exhaust housing or the ceiling. We made some rough measurements of wall deposition. Wall deposition from induced turbulence was not greatly increased over natural settling.

C. T. NELSON: What is your reason for selecting a relative humidity of 20 per cent for the baseline tests? Would not a relative humidity of 40 to 50 per cent be more representative? If tests were conducted at higher humidities, would not the chemical composition of the aerosol be different than as presented in your paper?

HINDS: We selected 20% relative humidity because it is relatively dry. We intent to conduct tests at higher humidity in the future. Regarding the second question on chemical composition, I think you are correct. The chemical composition will be sodium hydroxide for high humidities. When we ran other kinds of tests at high humidity, we believe we had a liquid droplet aerosol, whereas

we had solid sodium carbonate particles at the lower relative humidity. If we do not exceed a specific aerosol concentration in the chamber, carbon dioxide will not be completely consumed and will convert the sodium aerosol particles to sodium carbonate. For many conditions, we will have a mixture of carbonate and hydroxide.

PALMER: In your paper, you state that a minimum design goal is a system with a DRF of 10. This seems extremely low for the major type of accident considered. In fact, if a DRF of only 10 is required, one would question whether any emergency air cleaning systems need to be considered.

HINDS: These tests were pilot tests to screen different direct air cleaning methods. A 2 hour DRF of 10 was arbitrarily selected to identify those methods that had potential, with further research, for high DRF values. Bear in mind, that it is the containment vessel, with a leakage rate of 0.008% of total volume in two hours, that is the primary mechanism for reducing exposure to the public. The emergency air cleaning system is intended to reduce the amount of material leaking from the containment vessel still further.

CLOSING RAMARKS OF SESSION CHAIRMAN:

In the first paper, Dr. Schikarski presented results of some aerosol behavior experiments and compared these to predictions made using the PARDISEKO code. I conclude that the agreement is very good providing that input parameters to the code are properly selected. I would note that the aerosol concentrations were low in the experiments and that no sodium or sodium compound aerosols were used.

In the second paper, Mr. McCormack presented results of a conceptual evaluation of a number of widely differing air cleaning concepts. Several of the concepts look promising. In future ERDA-sponsored research, we intend to test selected concepts; first on a laboratory scale and finally on an engineering scale.

In the third and last paper, Dr. Hinds summarized results of experiments in which the effects of turbulent-induced agglomeration and powder dispersal were determined. These results, while preliminary, look extremely encouraging. If confirmed by future experiments, such systems may result in substantial attenuation of radioactive aerosols in a containment.

In conclusion, I would say that we do not yet have a proven system for LMFBR emergency containment air cleaning. We have identified a number of concepts that look very promising, and we are proceeding to verify their performance.

SESSION XI

REMOVAL OF NOBLE GASES, TRITIUM, AND ^{14} CARBON

Wednesday, August 4, 1976
CHAIRMAN: J. A. Buckham

THE DELAY OF XENON ON CHARCOAL BEDS
G. Collard, M. Put, J. Broothaerts,
W. R. A. Goossens

THE RELEASE OF ADSORBED KRYPTON AND XENON FROM SPILLED CHARCOAL
D. W. Underhill

DEVELOPMENT OF THE CRYOGENIC SELECTIVE ADSORPTION-DESORPTION PROCESS
ON REMOVAL OF RADIOACTIVE NOBLE GASES
T. Kanazawa, M. Soya, H. Tanabe,
B. An, Y. Yuasa, M. Ohta,
A. Watanabe, H. Nagao, A. Tani,
H. Miharada

SEPARATION OF THE FISSION PRODUCT NOBLE GASES KRYPTON AND XENON FROM
DISSOLVER OFF-GAS IN REPROCESSING HTGR-FUEL
J. Bohnenstingl, S. H. Djoa,
M. Laser, St. Mastera, E. Merz,
P. Morschl

DEVELOPMENT OF THE FASTER PROCESS FOR REMOVING KRYPTON-85, CARBON-14,
AND OTHER CONTAMINANTS FROM THE OFF-GAS OF FUEL REPROCESSING
PLANTS
M. J. Stephenson, R. S. Eby

HTGR-REPROCESSING OFF-GAS CLEANING BY THE AKUT-PROCESS
H. Barnert-Wiemer, H. Beaujean,
M. Laser, E. Merz, H. Vygen

EXPERIMENTAL STUDIES ON THE KRYPTON ABSORPTION IN LIQUID CO_2 (FALC)
PROCESS
R. W. Glass, H. W. R. Beaujean,
V. L. Fowler, T. M. Gilliam,
D. J. Inman, D. M. Levins

EXPERIMENTAL DETERMINATION OF REACTION RATES OF WATER-HYDROGEN EX-
CHANGE OF TRITIUM WITH HYDROPHOBIC CATALYSTS
J. C. Bixel, B. W. Hartzell,
W. K. Park

SEPARATION OF KRYPTON FROM CARBON DIOXIDE AND OXYGEN WITH MOLECULAR
SIEVES
C. W. Forsberg

OPENING REMARKS OF SESSION CHAIRMAN:

This session deals with the removal of gaseous isotopes which could be responsible for relatively low radiation exposures to the public. Because of the low resulting radiation exposures from release, no consensus has yet been reached on whether to remove these isotopes and, if so, when to start and to what degree to do it. It is fitting that there is such an international representation at this conference and, notably, in this session, because this really is an international problem. The low-level doses caused by these effluents would, in large measure, be coming from a uniform distribution of the isotopes in the world's atmosphere. Thus, the consensus I referred to should almost surely be an international consensus. It is significant that eight of the nine papers in this session deal with noble gas removal, which is a direct indication of the state of technological development in this general area. It is also significant that the papers deal largely with removal and cover lightly, if at all, what to do with the removed isotopes. I believe this fact brings up another significant general point in this whole area that cannot be overemphasized: that is, to assure that we have an adequate storage or disposal method before undertaking isotope removal. We must keep in mind that in removing these isotopes, we are converting a low-dose, high-probability risk to a high-dose, low probability risk--we hope. Since this conference is being held in Idaho, it is fitting to draw an analogy with a hydroelectric system where this conversion was improperly made, namely, the recent failure of the Teton Dam. One of the major justifications for construction of the Teton Dam was flood control--namely, the prevention of periodic, relatively small spring floods. This low-exposure problem was prevented this May, but in June, when the defective dam broke, the result, as you know, was a devastating loss of hundreds of millions of dollars and, miraculously, only eleven lives. Therefore, as we listen to these papers on removal, we should also keep in mind the necessity of developing disposal and containment methods for the removed isotopes so that the net result of our efforts is not another Teton Dam disaster.

THE DELAY OF XENON ON CHARCOAL BEDS

G. Collard, M. Put, J. Broothaerts, W.R.A. Goossens

S.C.K./C.E.N.

Mol (Belgium)

Abstract

The dynamical adsorption of Xenon on a fixed bed of charcoal type RBL-3 has been investigated in a 15 cm diameter column applying a ^{133}Xe pulse. The experimental break-through curves were fitted by the Gaussian relationships proposed by Underhill. All data are summarized by a Van Deemter's equation the parameter values of which have determined by non-linear regression analysis of the results.

I. Introduction

The radioactive level of the gaseous effluents from a nuclear power station depends on the performance of the gas cleaning techniques in use. Up to now, it is common practice to use buffer tanks – called delay tanks – as a mean to reduce the radioactive content of the gaseous effluents of a nuclear reactor. This technique relies on the knowledge that roughly 98 % of the instant radioactivity of the noble off-gases is caused by short-lived Xenon and Krypton isotopes.

The delay of a few weeks, generally obtained now in buffer tanks, does however not satisfy anymore the "as low as practicable" principle that has to be fulfilled in the future. Therefore, fixed beds of charcoal have been proposed. A Xenon delay time of about fifty days with a corresponding noble gas de-activation factor of about 700 is now accepted for design purposes (1).

In this context SCK/CEN at Mol has performed the following three studies :

- comparison of the Xenon adsorption capacity of European charcoals;
- study of the dynamical adsorption on a selected charcoal ;
- study of the behaviour of this latter in a pilot reactor.

This paper treats the dynamical adsorption of Xenon on a fixed bed of charcoal in order to obtain the necessary design equations. A European charcoal type RBL-3 has been chosen since this material showed a high adsorption capacity in the preliminary

comparative study (2).

II. Experimental procedure

The experimental apparatus consists of three parts :
- the gas inlet where mainly stable Xe is traced with ^{133}Xe ;
- the proper adsorption column ;
- the outlet characterization section to measure the tracer concentration at any moment.

Figure 1 shows the different parts of the experimental apparatus, a view of which is given on figure 2.

(0) Magnetic valve
(1x) Manual valve
(2) Stable Xe + N₂ P = 150 atm.
(3) Mass flowmeters
(4) NaI chrystal
(5) Tracer preparation
I : Volume calibration
II : 133 Xe source
III : MC LEOD gauge

FIG. 1
FLOW SHEET OF THE EXPERIMENTAL
APPARATUS
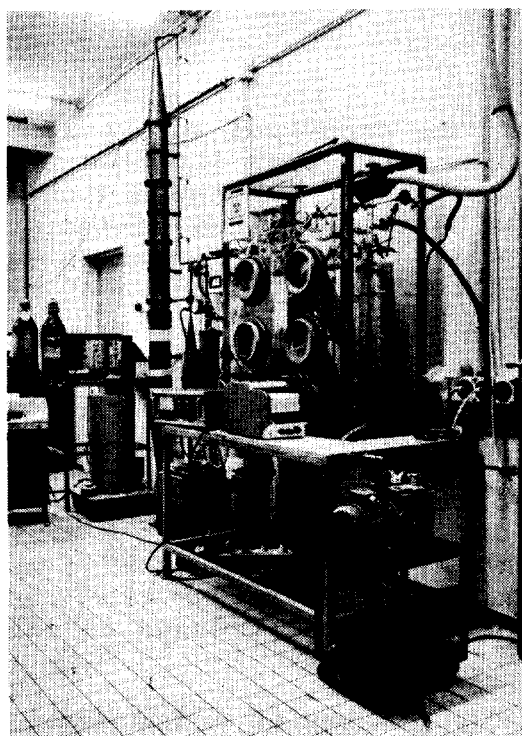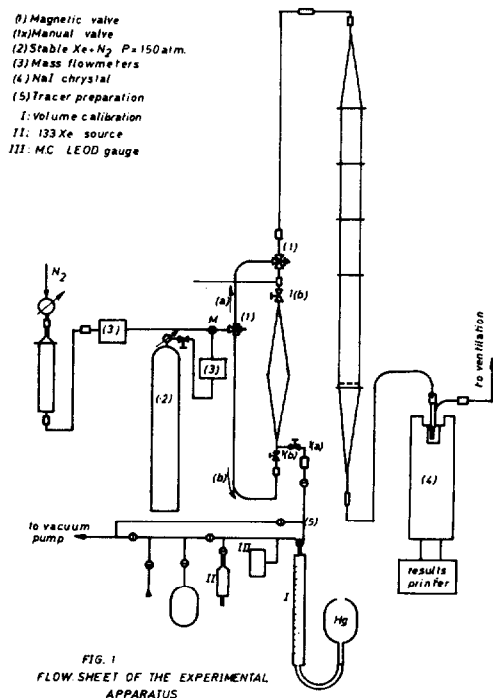
Fig. 2 Vew of the plant

In the gas inlet system a main feed stream, generally dry nitrogen, has been mixed with a side stream containing 8,000 ppm by volume of ^{131}Xe in order to obtain a Xenon inlet concentration between 50 and 600 ppm by volume. In a few runs, humid air at a relative humidity between 50 and 65 % was used as carrier gas.

The adsorption column consisted of 15 cm diameter tube, 2 m long mounted in a vertical position. This column was loaded with activated charcoal cylinders 3 by 3 mm to a height of 0.8 m. The total gas flow rate varied between 14 and 84 $10^{-6} m^3 s^{-1}$. In some final runs with dry air, the charcoal height was increased to 2 m and the gas flow rate was varied between 4.4 and 695 $10^{-6} m^3 s^{-1}$.

The gas mixture passed the column until saturation. At that moment, a pulse of radioactive ^{133}Xe was introduced by directing the main streaum for a while along a chamber previously filled with a mixture of nitrogen and ^{133}Xe at the initial Xenon inlet concentration. In this way, the radioactive pulse did neither change the over-all Xenon inlet concentration nor the steady state of the column. Moreover, entrance effects were minimized by using inlet and outlet cones with an angle of 10°C.

The break-through of the radioactive pulse was measured on line by gamma counting during 100 s with the help of a sensitive well-type NaI crystal. The dead time between consecutive countings varied from 260 to 1700 s depending on the gas flow rate used. The counting apparatus was connected to a teletype for printing and for punching on a tape which could be analysed straigth on a digital computer.

III. Mathematical analysis of the experimental data

In the computer analysis, the mean and the variance of each experimental curve were calculated. Further, each set of data points was fitted by a Gaussian function (3) and also by the Thomas's function (4). In both cases, the parameter values of these functions were calculated by minimizing the sum of the squares of the vertical distance between each experimental point and the corresponding function value. Both fittings showed no distinguishable difference, their resulting variances always differing less than 1 % from the variance of the experimental data. Therefore the Gaussian approximation was retained and Underhill's model (3) was applied.

Finally the linearity of the adsorption isotherm was verified and the dependence of the Gaussian parameters on the gas flow rate was determined.

IV. Results

The experimental conditions and data obtained are summarized in table 1.

IV.1. Capacity of the coal (fig. 3)

The capacity of the coal under these dynamical working conditions was derived by applying

$$q = \frac{G.C.t_{0.5}}{M} \tag{1}$$

where :

q = adsorption capacity of the charcoal : $Nm^3 Xe.kg^{-1}$ coal

G = carrior gas flow-rate : $Nm^3 s.^{-1}$

C = Xenon concentration : $Nm^3 Xe.NM^{-3}$ carrier-gas

$t_{0.5}$ = mean stay time of Xe in the bed : s

M = mass of the bed : kg

Table I.; Experimental results : Carrier gas : dry nitrogen

Run	Column height (m) I	Gas flow-rate $m^3 s^{-1}$ II	Xe concentration ppm volume III	Mean stay time of Xenon (t.o.s) $10^3 s$ IV	Mean stay time of carrior gas of empty column s. V	Delay Factor IV/V VI	Variance of Gaussian approxim. $10^3 s$ VII	Number theoretical plates VIII	Height of a theoretical plate $10^{-2} m$ IX	Coal capacity $10^{-3} Nm^3 kg^{-1}$ X
1	0.8	$2.1\ 10^{-5}$	200	202	673	300	22.7	79.2	1.01	0.14
2		$1.4\ 10^{-5}$	200	307	1009	304	37.6	66.8	1.20	0.14
3		$8.3\ 10^{-5}$	200	49	170	291	5.5	79.6	1.01	0.13
4		$8.3\ 10^{-5}$	200	48	170	282	5.5	75.3	1.06	0.13
5		$8.3\ 10^{-5}$	150	48	170	282	5.6	75.6	1.06	0.10
6		$8.3\ 10^{-5}$	100	47	170	276	5.3	82.6	0.97	0.07
7		$8.3\ 10^{-5}$	50	50	170	294	5.6	79.8	1.00	0.03
8		$2.1\ 10^{-5}$	200	187	673	278	20.9	80.1	1.00	0.13
9		$2.1\ 10^{-5}$	150	209	673	310	23.8	78.4	1.02	0.11
10	2.0	$1.4\ 10^{-5}$	300	695	2523	275	51.4	182.9	1.09	0.19
11		$20.8\ 10^{-5}$	300	51	170	300	4.0	164.9	1.21	0.20
12		$8.3\ 10^{-5}$	300	126	495	296	8.3	231.5	0.87	0.20
13		$11.1\ 10^{-5}$	300	98	318	308	6.1	254.5	0.79	0.21
14		$5.5\ 10^{-5}$	75	220	638	346	13.1	284.0	0.70	0.06
15		$30.5\ 10^{-5}$	75	37	115	322	3.2	131.6	1.52	0.05
16		$25.0\ 10^{-5}$	75	42	140	300	3.7	129.7	1.54	0.05
17		$0.4\ 10^{-5}$	600	2377	8835	270	255.9	86.3	2.32	0.41
18		$55.5\ 10^{-5}$	75	21.2	64	331	2.2	89.4	2.28	0.06
19		$69.4\ 10^{-5}$	75	16.8	51	330	2.0	72.2	2.77	0.06

This adsorption capacity depends on the partial of Xenon. Expressed in usual units, the following dependence was found :

$$q = 0.91 \ 10^{-3} \ p \tag{2}$$

where the partial pressure of Xenon p, is expressed in mm Hg

$$1 \text{ mm Hg} = \frac{1}{133} \text{ Pa}$$

This expression differs slightly from the equation

$$q = 1.13 \ 10^{-3} p^{1.07} \tag{3}$$

obtained under conditions in the preliminary comparative study (2) by regression analysis of the experimental results.

Both expressions (2) and (3) indicate that the partial pressure of Xenon is the only important parameter influencing the adsorption isotherm ; the composition of the carrier gas being either dry air or nitrogen showed no effect at room temperature.

The linearity of the adsorption isotherm makes the delay factor of the charcoal bed independent as well of the Xenon concentration as of the gas flow rate. This delay factor generally is put equal to the ratio of Xenon mean residence time to the mean residence time of the carrier gas in the empty column. It depends on the characteristics of the coal used and on the main gas component absorbed while other gaseous compounds (for example, humidity) might disturb the phenomena. The delay factor of Xenon has a value of the order of 300 for the coal studied.

COAL CAPACITY
10^3 (m^3 STP/ kg)

CARRIER GAS N₂
TOTAL PRESSURE 10 atm.

○ Experimental
—— Equation (3)
———Equation (3) (2)

Xe, CONCENTRATION (ppm vol)
PARTIAL PRESSURE (mmHg)
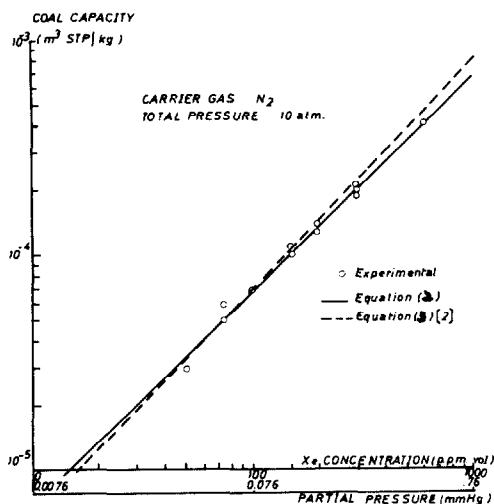
FIG. 3 ISOTHERM OF XENON ADSORPTION AT 25°C

2. Effect of gas flow rate on the variance of the break-through curve (3)

In Underhill's model, the number of theoretical plates, N, is expressed by

$$N = \frac{t_{0.5}^2}{\sigma^2} \tag{4}$$

with σ = variance of the break-through curve (s)

Moreover, the length of a theoretical plate H is given by

$$H = \frac{L}{N} \tag{5}$$

with : L = bed length (m)

According to Van Deemter the length of a theoretical plate for a given process is the result of three phenomena so that the following relationship exists :

$$H = \frac{A}{V_i} + B + C\, Vi \tag{6}$$

where V_i is the superficial velocity.

Equation (6) can be generalized and written in non-dimensional nummbers (3)

$$h = \frac{a}{v_i} + b + c\, v_i \tag{7}$$

where h = reduced height of a theoretical plate

v_i = reduced interparticle velocity.

The values of the coefficients in the latter two equations were determined for the conditions of this study by non-linear regression analysis between the experimental N value and the operating value of the superficial velocity.

This analysis gives the following expression

$$H = \frac{4.62\ 10^{-6}}{V_i} + 5.1\ 10^{-3} + 0.45\, V_i \tag{8}$$

or

$$h = \frac{0.82}{v_i} + 1.7 + 0.35\, v_i \tag{9}$$

Figure 4 shows that the curve related to equation (8) fits quite well the experimental values of the height of a theoretical plate.

Figure 5 illustrates for typical working conditions how good the experimental points are fitted by the Gaussian function the parameters values of which were calculated by applying equations (1), (2) and (8).

FIG. 4 HEIGHT OF A THEORETICAL PLATE v.s. superficial velocity

$H = 0.96 \sqrt{V}$

$H = \dfrac{4.62 \cdot 10^{-6}}{V}$

$H = 5.1 \cdot 10^{-3} m$

HEIGHT OF THEORETICAL PLATE (m)

■ experimental points
— equation (8)

SUPERFICIAL VELOCITY V (m.s⁻¹)

NORMED BREAKTROUGH VALUES (N.B.V.)

gaussion curve is computed by mean of eq (1)(2) and (8)

L bed = 0,8 m
HETP = 2,97 cm
t 0,5 = 5,1·10⁴ s

experimental points ○ run 7 □ run 6
—— gaussion curve

t (s)

FIG 5 : ILLUSTRATION OF THE UNDERHILL'S MODEL
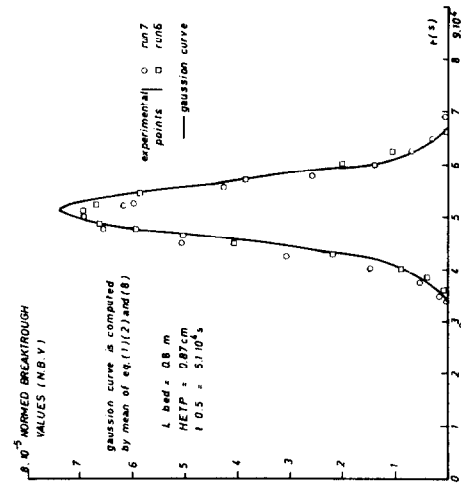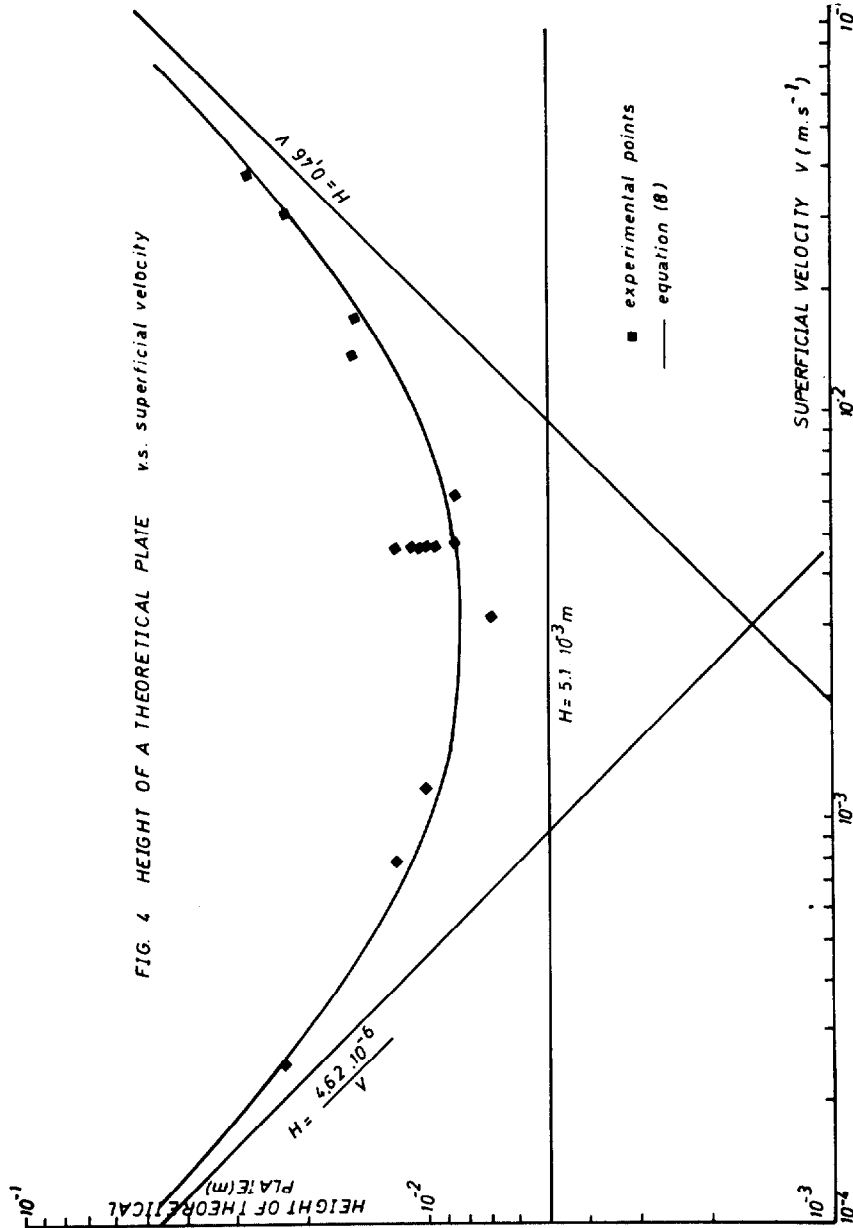
V. Additional experimental results

In order to evaluate the influence of humidity on the performance of the charcoal, five additional runs were done on the 0.80 m long bed. The conditions and results of these tests are summarized in table 2.

Table 2 : Experimental results; carrier gas : humid air

Run	Gas flow rate m^3 s^{-1}	Xe conc. ppm	Relative humidity at 25°C %	Mean stay time of the 10^3 s	Delay factor	Variance σ 10^3 s	Number of theoretical plates	Height of a theoretical plate 10^{-2} m
20	$5.5\ 10^{-5}$	600	60	33	96	3.6	87.1	0.92
21	$5.5\ 10^{-5}$	600	53	43	125	4.5	94.0	0.85
22	$8.3\ 10^{-5}$	200	64	20	118	2.3	73.1	1.09
23	$8.3\ 10^{-5}$	600	64	18	106	2.1	69.3	1.15
24	$8.3\ 10^{-5}$	50	66	18	106	2.2	70.0	1.14

By comparing the values of tables 1 and 2, it can be seen that the delay factor is reduced by a factor 3 at 60-65 % relative humidity. Nevertheless, the height of a theoretical plate is only slightly influenced.

VI. Further work

Based on the results obtained so far ((2) and present work) a pilot delay bed has been constructed on the off-gas systems of the pilot nuclear power station BR3 (10 MWe). This delay system consists of two columns 0.5 m in diameter and 5 m in height connectable in parallel or in serie. The reception runs will start as soon as BR3 will be put on power.

VII. Conclusion

In order to reduce radwaste of L.W.R. gaseous effluents, a complete study has been undertaken at SCK/CEN. The first two parts of this study have been completed, the results of which can be used to compare different European coals and to design delay beds for Xenon in dry or humid air or nitrogen. The effect of coal ageing, radioactivity and other reactor parameters will be studied in the near future and will allow to design delay beds for the retention of Xenon from reactor effluents on mathematical bases.

REFERENCES

(1)   BARTON, C.J., Separation and containment of noble gases, Nucl. Safety 15, 3, (1974) 302.

(2)   ANANTHAKRISHNAN, M., COLLARD, G., Krypton and xenon adsorption on activated charcoal, to be published.

(3)   UNDERHILL, D.W., Dynamic adsorption of fission product noble gases on activated charcoal, USAEC Report NYO-841-8 (1967).

(4)   VERMEULEN, T., <<Separation by adsorption methods>>, Advances in Chemical Engineering, Vol. II (DREW, T.B., HOOPES, J.W.Jr., editors) Academic Press Inc. - Publishers, New York (1958).

DISCUSSION

UNDERHILL: Your equation nine has coefficients which are very similar to those found in experiments which I carried out earlier using krypton at the temperature of dry ice. I believe that the values of the first two coefficients in this equation are not strongly dependent upon the temperature of fission gas that is used in the adsorbent experiments. I think the closeness of agreement between your results and the ones I have under quite different conditions may indicate that these values can be used as general values for experiments of this type. The first two coefficients should be determined by the packing of the bed and the third should be dtermined by diffusion of the fission gas in the adsorbent particles.

COLLARD: I agree completely with you and I think most people acknowledge it. Moreover, the exchange zone is so small that it will never influence very much the performance of the column. Therefore, these studies must be performed to know the range of usable gas velocities, but not to fix them in a narrow range.

UNDERHILL: One final point. I took the data that I had in these earlier experiments and examined them by using moment analysis. It did not make much difference in the values of the coefficients, but the moment analysis technique is mathematically exact. It's an exact solution to the mathematical equations for the transfer through adsorption beds. Having a mathematically exact solution allows you to take data from columns of all sizes and compare them without having to use full scale data. You do not merely rely on the Gaussian approximations.

The point is that it includes all kinds of factors and is far more general than, say, using something of the Thomas equation and, yet, is quite a simple technique.

COLLARD: Yes, I think most people acknowledge it, but there are a number of complex factors such as the exchange zone being so small that it will never influence turbulence.

RIVERS: As you stated in your presentation, the correlations on page 6 do not provide reasonable descriptions of the device. Without going deeply into filtration theory, more reasonable correlation forms might be:

For downstream concentration,

$$C_0 = C_i \, e^{-K \, L^m \, D_p^{\,n}} \qquad (1)$$

where C_i is inlet concentration. Taking logs,

$$\ln(C_0/C_i) = -K \, L^m \, D_p^{\,n}$$

and $\ln(C_i/C_0) = \ln K + m \ln L + n \ln D_p \qquad (2)$

The values of K, m and n are easily evaluated. Could you provide your data for such an evaluation? For pressure drop, we could use:

$$\Delta P = K \, G^p \, D_p^{\,q}$$

and proceed as before.

GOSSENS: We can not agree with your first sentence as you stated it. The correlations on page 6 are regression equations for the data obtained using the technique of parameter planning. These equations reflect an exact description of the data points but do not describe the performance of the device, as such, so that interpolations and extrapolations give only reasonable estimates. If correlation (1) of your question is applied on our factorial design data [this implies two "ln" in the left side of equation (2) and not one "ln" as indicated in your letter], the following constant values are obtained:

K = 3.11
m = 0.31
n =-0.33

The following table indicates that, in this way, a description of the data points can be obtained with the same degree of accuracy as that given by the first regression equation on page 6 of our paper.

values for $\ln \dfrac{C_i}{C_0}$

data point values	calculated values
4.868	4.908
4.193	4.146
6.376	6.320
5.277	5.345

We did not measure the pressure drop, but rather, the pressure increase per hour.

THE RELEASE OF ADSORBED KRYPTON AND XENON FROM SPILLED CHARCOAL

D. W. Underhill
Harvard Air Cleaning Laboratory
Boston, Massachusetts

Abstract

The rate of release of the fission gases, krypton, and xenon, depends on the depth of the spilled charcoal, the decay constant of the fission gas, and the initial distribution of fission gas within the spilled charcoal. A mathematical analysis of the rate of release is presented here which takes into account the initial distributions which may be encountered in practice. It is found that: (1) fission gases more than 15 cm from the surface generally decay within the charcoal before diffusing to the surface; (2) xenon isotopes diffuse relatively slowly and that the release of xenon can be protracted over several days and (3) the initial distribution has a strong effect on both the rate of release and the fraction of fission gas released. These equations can be applied to the release of fission gases from a charcoal adsorption bed following rupture (as for example by an earthquake). It is suggested that in order to minimize the possible release of fission gases during such an incident that during normal operation a charcoal adsorption bed be operated at a flow rate above a certain minimum for this would prevent the adsorbed fission gases from being contained within a shallow area from which their release could be relatively rapid.

I. Introduction

The use of charcoal in fission gas holdup systems has several advantages. The first and most important is that the use of a charcoal adsorbent considerably reduces the volume of the holdup system. Another advantage is that if there were a rupture in a holdup tank, the fission gases would be retained in the charcoal far longer than they would be in the ruptured tank. This paper addresses the problem of calculating the retention of krypton and xenon in charcoal spilled from a holdup bed. If these calculations prove useful in the design of nuclear containment systems, particularly if they are helpful in reducing redundant conservatism, they will have served their purpose.

II. Diffusion of Krypton and Xenon in Bulk Charcoal

The first step in calculating the loss of fission gases from spilled charcoal is to determine the diffusion coefficient for the fission gases within the bulk charcoal. The formula used for this purpose is:

$$D = \gamma_g f_g D_g + \gamma_c f_c D_c \qquad (1)$$

where D = diffusion coefficient for fission gas in bulk charcoal, cm^2/sec

γ_g = tortuosity factor for diffusion in the interparticle void volume, dimensionless

f_g = fraction of the fission gas, at equilibrium, in the interparticle void volume, dimensionless

D_g = diffusion coefficient for fission gas in the carrier gas at ambient temperature and pressure, cm^2/sec

γ_c = tortuosity factor for diffusion through the matrix of the charcoal, dimensionless

f_c = fraction of the fission gas, at equilibrium, within the adsorbent particles, dimensionless

D_c = diffusion coefficient for fission gas within an adsorbent particle, cm^2/sec

The above equation can be criticized for neglecting the coupling of diffusion between the inter- and intraparticle volumes. This simplification is valid because D_c is generally very small. In practice the term D_c can usually be neglected and D calculated as:

$$D = \gamma_g \, f_g \, D_g \qquad (2)$$

The next step is to determine reasonable values for γ_g, f_g, and D_g. The value for γ_g, as determined from many experiments in gas chromatography and chemical engineering, has a range of 0.5 to 0.9. In the results given in Table 1 a value of 0.6 was assigned to γ_g. The factor f_g can be determined from:

$$f_g = \frac{\varepsilon}{\rho K} \qquad (3)$$

where ε = fractional interparticle void volume, dimensionless

ρ = bulk density of the charcoal, gm/cm^3

K = bulk adsorption coefficient for the fission gas, cm^3/gm.

The diffusion coefficient, D_g, may be estimated using the equation of Kirschfelder, Bird, and Spotz[1].

By means of the above formulas, estimates were made of the bulk diffusion coefficients for krypton and xenon in a commercial charcoal (Barneby Cheney type 483/AK). Experimental measurements are also available giving the measured coefficients for bulk diffusion[2]. The results are shown in Table 1. As the predicted diffusion coefficients relied on estimated values for K, ε, and γ_g, the agreement between theory and experiment is as good as could be expected.

III. Integration of the Basic Differential Equation

The next step is to calculate the change in concentration across a large mass of spilled charcoal. If diffusion and radiodecay are the controlling factors, mass transfer is described by the following partial differential equation:

$$\frac{\partial C}{\partial t} = D \frac{\partial^2 C}{\partial x^2} - \lambda C \qquad (4)$$

where D = diffusion coefficient for fission gas within bulk charcoal, cm^2/sec

C = concentration of fission gas within the bulk charcoal $curies/cm^3$

λ = decay constant for fission gas, sec^{-1}

t = time, seconds

x = vertical distance, cm

Three boundary conditions are required for the solution of the above equation. The first comes from the assumption that fission gas at the bottom of the spill is not expected to diffuse appreciably into the floor. Then:

$$\frac{\partial}{\partial x} (C (x=0, t>0)) = 0 \qquad (5)$$

The second assumption, that the charcoal is spilt to a height, L, and that at the surface of the charcoal, equilibrium exists between the charcoal and a large volume of fresh air, leads to the equation:

$$C(x=L, t>0) = 0 \qquad (6)$$

The most difficult boundary condition to establish is the initial distribution of fission gas within the spilt charcoal. It is known that in the intact holdup beds before spillage occurred, the concentration of each isotope will be an exponential function of distance. We should consider the most dangerous type of spill to be one in which the most contaminated charcoal is nearest the surface of the spill. This is an extremely conservative assumption - perhaps to the point of being unrealistic - for it is far more likely that a spill would lead to mixing of the charcoal and that as a result there would be no significant concentration gradient in the charcoal. Nevertheless both cases can be examined if the concentration of fission gas is assumed to have the following initial distribution with respect to the height above the floor.

$$C(t=0) = C_o e^{-\alpha(L-x)} \qquad (7)$$

where C_o = the concentration of fission gas initially at the surface of the spill, $curies/cm^3$

α = exponential coefficient describing the initial distribution of fission gas within the charcoal, cm^{-1}. The factor, α, will equal zero is the charcoal is thoroughly mixed in spilling.

The integration of Equation 4 by means of a Fourier series leads to the following equation for the total fraction of the curies originally contained within the charcoal that would be released by time t.

$$f = \sum_{N=1}^{\infty} \left(\frac{8 + \frac{(-1)^N 16 \alpha L e^{-\alpha L}}{(2N-1)\pi}}{(2\alpha L)^2 + (2N-1)^2 \pi^2} \right) \left(\frac{\alpha L \left(1-e^{-(\frac{D\pi^2(2N-1)^2 + \lambda}{4L^2})t} \right)}{\left(1 + \frac{4\lambda L^2}{D\pi^2 N}\right)(1-e^{-\alpha L})} \right) \quad (8)$$

As $t \to \infty$ the above equation converges to:

$$f = \frac{D\alpha^2 \left(sech \left(\sqrt{\frac{\lambda}{D}} L\right) e^{-\alpha L} - 1 \right) + \alpha \sqrt{\lambda D} \tanh \sqrt{\frac{\lambda}{D}} L}{(\lambda - D\alpha^2)(1-e^{-\alpha L})} \quad (9)$$

If it is assumed that good mixing of the fission gases has taken place within the charcoal at the time of the spill, then $\alpha = 0$ and:

$$f = \sum_{N=1}^{\infty} \left(\frac{8}{(2N-1)^2 \pi^2} \right) \left(\frac{1 - e^{-(D\pi^2 (2N-1)^2 + \lambda)t/L^2}}{1 + \frac{\lambda L^2}{D\pi^2 N}} \right) \quad (10)$$

And under these conditions as $t \to \infty$:

$$f = \frac{\tanh \left(\sqrt{\frac{\lambda}{D}} L\right)}{\sqrt{\frac{\lambda}{D}} L} \quad (11)$$

Only one factor remains unresolved before calculations can be made, and that is the maximum value for α. But this factor can be determined from the fact that the concentration difference across the spilt charcoal should be no greater than that existed in the charcoal in the intact holding bed. The difference in concentration, or more precisely the ratio between the highest concentration and the lowest concentration in the intact bed should be given by:

$$\frac{C}{C_o} = e^{-\frac{km\lambda}{V}} \quad (12)$$

where k = adsorption coefficient for fission gas, cm^3/gm

m = grams of adsorbent

λ = decay coefficient for fission gas, sec^{-1}

v = flow of air through bed during normal operation, $cm/^3sec$

The ratio of the highest to lowest concentration in the spilled charcoal is given by:

$$\frac{C}{C_o} = e^{-\alpha L},\tag{13}$$

therefore, the maximum value for α is:

$$\alpha = \frac{km\lambda}{vL}.\tag{14}$$

IV. Estimated Releases from Spilled Charcoal

The results obtained using the equations developed in the previous section are shown here in a series of graphs. Figures 1-4 illustrate the loss of krypton and xenon from charcoal spills in which there was an initially homogeneous distribution of krypton and xenon in the spilled charcoal. By comparison of the results shown in these figures it is immediately apparent that (1) the release of krypton is more rapid than for xenon, (2) that the fraction that is released from a spill increases with increasing half life, and (3) that the deeper the spill the smaller the fraction of the fission gas that is released.

The effect of spill depth is clearly shown in Figures 5 and 6, which give the total fraction that can be released as a function of the depth of the spilled charcoal. Note that for beds several times deeper than $\sqrt{D/\lambda}$, the fractional release is equal to $\sqrt{D/\lambda}/L$.

The final two graphs show the effect of both bed depth and the initial distribution of fission gas on the total fraction of fission gas that will be released. For values of $\alpha L >> 1$, the fractional release can be appreciable. The real danger brought to light by this analysis is that if the fission gases are concentrated into a small volume of charcoal, then spillage of this highly active charcoal could result in a significant release of fission gas. It is suggested that in order to minimize the possible release of fission gases during such an incident that during normal operation a charcoal adsorption bed be operated at a flow rate above a certain minimum for this would prevent the adsorbed fission gases from being contained within a shallow area from which their release could be relatively rapid.

V. Summary

The results presented here give estimates of the loss of krypton and xenon by diffusion from spilled charcoal. In making these estimates the following steps were taken.

1. A theory developed for diffusion in bulk charcoal.

2. Measurement of diffusion rates and finding results which agreed with theoretical analysis.

3. Development of a theory to predict the loss of radioactive fission gases from spilled charcoal.

It has been the purpose of this paper to show what degree of the activity contained within a spill can be expected to be released and thereby give design engineers the ability to make reasonable estimates of accident conditions.

Table I   Predicted and measured bulk diffusion coefficients.

		Bulk Diffusion Coefficient, cm^2/sec	
		Predicted	Measured
Fission } Gas }	Krypton	2.1×10^{-3}	1.6×10^{-3}
	Xenon	9×10^{-5}	7×10^{-5}

References

1. R.H. Perry, ed., Chemical Engineers' Handbook, 4th edition, McGraw Hill, New York, 1963 (Equations 14-57).

2. D.W. Underhill, "Release of Krypton and Xenon from Spilled Charcoal." Accepted for publication in Nuclear Science and Engineering.

DISCUSSION

PALMER: It would seem to me that these calculations are of academic interest only. In other words, if an accident occurred of such magnitude to spill the charcoal, there would be enough other serious hazards that the release of the adsorbed krypton and xenon would be a minor concern.

UNDERHILL: That is not always true. This analysis was developed to learn what would happen if there were a severe earthquake in a nuclear reactor complex. The working assumption in the analysis is that the reactor itself would be designed to withstand an earthquake of any magnitude considered possible, but that the fission gas holdup beds were not so designed.

WATT: At the loading that you suggested, I am wondering whether decay heat would not produce sufficient temperature differences in various portions of the beds to produce convective flow rather than pure diffusion.

UNDERHILL: That is a good question. There is a minimum loading of fission gas required for heating effects to become important. I calculate that, at a loading of 100 Ci of Xe-133/kg of charcoal that the initial temperature rise would be $0.1°C$/day, and in the absence of connection and thermal diffusion, the charcoal would reach a maximum of $0.7°C$ above its surroundings. At this loading, thermal effects are not important.
                          Krypton isotopes at the same initial loading would give a similar initial temperature increase, but as a result of the shorter half life of the krypton isotopes, the final temperature rise would be considerably less.
                          Finally, it would appear that even if the interior of a mass of spilled charcoal were to heat up,   cooling of the surface areas of the charcoal by thermal diffusion would create a retentive layer which would effectively adsorb the fission gases released from the interior. This phenomenon deserves further study.

MEARDON: Has there been or is there to be consideration given to an accident condition involving the combustion of the charcoal bed? This would seem to be a maximum credible accident for this type system.

UNDERHILL: That is not always true - this analysis was developed to learn what would happen if there were a severe earthquake in a nuclear reactor complex. The working assumption in this analysis is that the reactor itself would be designed to withstand an earthquake of any magnitude considered possible, but that the fission gas holding beds were not so designed.

DEVELOPMENT OF

THE CRYOGENIC SELECTIVE ADSORPTION-DESORPTION PROCESS

ON REMOVAL OF RADIOACTIVE NOBLE GASES

T. Kanazawa, M. Soya, H. Tanabe, B. An
Kobe Steel, Ltd., Kobe, Japan.

Y. Yuasa, M. Ohta, A. Watanabe, H. Nagao, A. Tani,
Nippon Atomic Industry Group Co., Ltd., Kawasaki, Japan.

H. Miharada,
Tokyo Shibaura Electric Co., Ltd., Tokyo, Japan.

Abstract

Cryogenic selective adsorption-desorption process was developed as an effective means of removing the radioactive noble gases. A series of experiments and evaluation studies have been performed to develop a new type off gas clean up system which adopted the above process to remove the noble gases from the off gas streams of nuclear facilities.

The fundamental processes of our proposed clean up system are as follows; 1) Noble gas enrichment process to remove and enrich the radioactive noble gases from off gas, 2) Oxygen removal process to remove oxygen and oxide impurities from enriched gas and 3) Storage process to store enriched gas into cylinder. For the first process, the "selective adsorption-desorption" method was adopted. The laboratory scale experiments were performed to investigate the breakthrough and enrichment. And the engineering scale experiments are being carried out to contirm them. For the second process, "metal getter absorption" method has been developed. The static experiments were performed with heated zirconium metal getter. And the dynamic experimental apparatus is constructed and will be operated. For the third process, "adsorbent packed cylinder" method has been developed. From the laboratory experiment, it has been proved to have several advantages.

This investigation showed that the proposed methods could be applied to the off gas clean up system of the nuclear facilities.

Contents

1.   Introduction

A majority of the present BWR power plants equip with charcoal delay beds operated at ambient or reduced temperature for their off gas clean up systems.   These charcoal beds will delay noble fission gases long enough to allow the shorter lived nuclides to decay to a small fraction of their original activity, and total activity release to the environment is controlled enough below 'as low as reasonably achievable' criteria. However, as they have no decay effect to the longer lived nuclides such as Kr-85, the obtainable decontamination factor (DF) of this delay bed type system will not be able to exceed about 10^4. The DF of some conventional delay bed systems with several ten tons of charcoal is estimated as about 10^2, and almost two hundred tons of charcoal will be required for the DF of 10^4.

Consequently, for the future power plants near populous area or to build several of them in one site, it will be significant to develop a new type of off gas clean up system which should be constructed at reasonable cost compared with the delay bed type system and is able to remove even long life noble gas nuclides such as Kr-85.

From this point of view, we have started to study a total system which could effectively remove radioactive noble gas nuclides from off gas streams of nuclear facilities and store them safely for a long time period. For the noble gas enrichment process, the most important process of the total off gas clean up system, the "selective adsorption-desorption" method[1] has been developed and been proved to be promising for our purpose by the laboratory scale experiments. For the storage process, "adsorbent-packed cylinder" method has been developed. From the laboratory scale test, this storage method has been proved to have several advantageous points compared with conventional cylinder method. In case the oxygen gas in off gas stream is not removed prior to the enrichment process, oxygen and some gaseous oxide impurities in enriched gas should be removed prior to its long term storage. For this oxygen removal process, "metal getter absorption" method has been developed. Based on the experimental results of these methods, a feasibility study for the applicability of these methods to BWR off gas clean up system has been performed. Also, engineering test plant scale test facility for the enrichment process has been constructed, and its performance are now being studied.

In this article, the details of our new off gas clean up system will be shown. Also, the results of the laboratory experiments for individual processes in the total off gas clean up system and some of the results from performance test of the engineering test plant for the noble gas enrichment process will be discussed.

2.   Proposed Off Gas Clean Up System

A total off gas clean up system could consist of several subsystems. Prior to determining the construction of these subsystems or their individual processes for our total system, evaluation studies concerning safety, economy, performance and others of the many existing processes have been performed. As a result, several criteria to develop our off gas clean up system have been settled. Although the details of the discussions for this studies will not be shown here, some of the representative criteria are as follows ;

1.   apply the "selective adsorption-desorption" method to the noble gas enrichment process,

2.   operate as many subsystems under subatmospheric pressure as possible,

3.   remove oxygen and gaseous oxide impurities after noble gas enrichment process,

4.   adopt synthetic zeolite beds rather than reversing heat exchanger to remove moisture and carbon dioxide before cooling the off gas flow,

5.   circulate the enriched gas on the adsorption bed batchwise between the bed and off gas inlet flow until the required enrichment are obtained,

6.   adopt two adsorption beds system rather than three beds system for the noble gas enrichment, and

7.   adopt cryogenic "adsorbent-packed cylinder" method to eliminate any compressors for the transportation of the enriched gas to a storage container.

Based on these considerations, a total process as shown in Fig. 1 has been proposed for our off gas clean up system.

Description of the Proposed Total Process

BWR off gas is extracted from the main condenser via the steam jet air ejector (SJAE) and transferred to the plant off gas system. Its constituents are air introduced into the condenser by leakage, hydrogen and oxygen produced by radiolytic decomposition of the coolant water, small amounts of short-lived gaseous activation products, fission gases and a large volume of steam. As shown in Fig. 1, most of steam, hydrogen, oxygen and activation products are removed at an off gas pre-treatment section, recombiner and cooler, which is the same section as in conventional off gas line, resulting the principal off gas constituents are air containing moisture, carbon dioxide and noble gases.

The effluent stream of the pre-treatment section enters the moisture/carbon dioxide remover, the main portion of which consists of two adsorption beds filled with synthetic zeolite, where moisture and carbon dioxide are removed and their effluent concentration are made of the order of ppm. Since synthetic zeolite can adsorb more or less noble gases, it should be noticed that radioactivity could come out at regenerating step of the bed. At the regenerating step of the moisture/carbon dioxide remover bed, noble gas, CO_2 and moisture are desorbed in this order with increasing temperature. In our process utilizing this desorption characteristic, decrease of overall decontamination factor of the system which possibly arises from this step is eliminated by returning the initially desorbed gas, which contains most of all noble gases having been adsorbed on the bed, to the SJAE.

The effluent of the moisture/carbon dioxide remover then flows through the heat exchanger, where it is cooled to -170°C. Most of cooling source is provided with effluent stream from cryogenic adsorption bed and shortage of the cooling is supplemented with liquid nitrogen.

Subsequently, cooled off gas enters the cryogenic adsorption bed, where noble gases are removed from off gas stream, returns to the heat exchanger and is utilized as cooling source as mentioned above, and finally is released from the plant stack to the atmosphere.

Noble gas concentrator consists of two adsorption beds. Off gas or effluent of the heat exchanger, first enters one of these beds. At the time when the exit krypton concentration reaches a certain level, the flow pass is changed to the second bed (adsorption step). Then the first bed is regenerated and recooled. The present method has the special characteristics in this regeneration step. That is, the desorbed gas is recycled to SJAE (recycle step) for a certain times after a conventional regeneration step, and then the bed undergoes the following two different types of succeeding processes, regeneration at low temperature and pressure (selective desorption step) and regeneration step with increasing temperature. The selective desorption process is also conducted with increasing bed temperature but still at relatively low temperature, for instance from -170°C to -100°C. At this range of temperature increase, most of all nitrogen and oxygen adsorbed on the bed are desorbed, but yet noble gases are almost completely kept adsorbed on the bed. The desorbed gases at this step are returned to the inlet of SJAE. Thus the noble gases are doubly concentrated at the adsorption step first and then at this selective desorption step. So, the authors have named this concentration process as selective adsorption-desorption method. Concentrated noble gases are finally desorbed from the bed by raising the bed temperature up to 50°C ~ 100°C, and are sent to the noble gas storage system.

In regard to conventional noble gas enrichment methods, both thermal swing and pressure swing methods can get relatively low enrichment factor
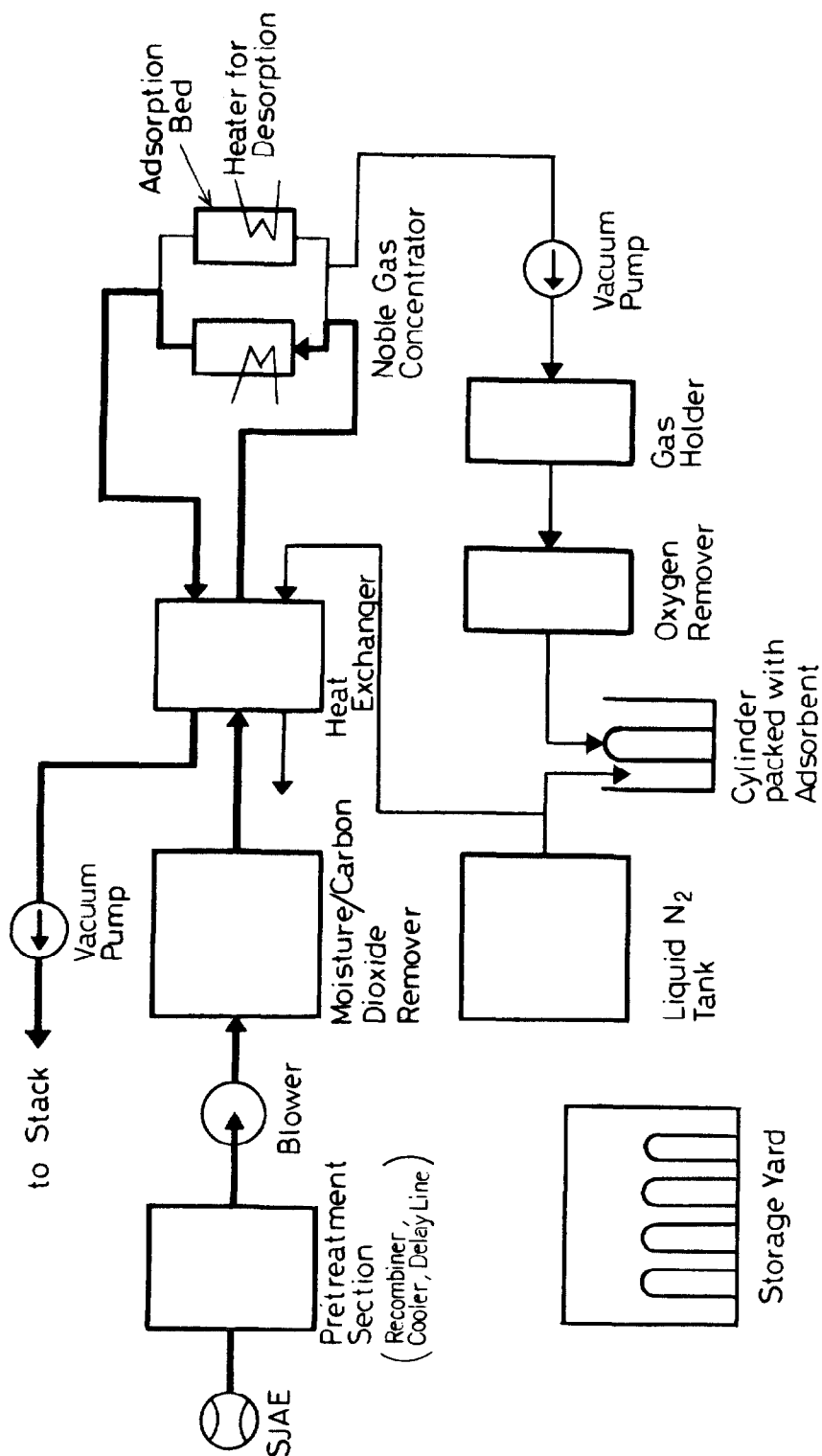
FIG. I   THE SCHEMATIC FLOW DIAGRAM OF THE PROPOSED OFF GAS
CLEAN UP SYSTEM FOR BWR PLANT

with a single stage enrichment system such as described above, and may require double or more stages to get the sufficient noble gas concentration for the purpose of the permanent storage. This was a significant dis-advantageous point of the noble gas enrichment system using the adsorption method. The authors believe this problem has been resolved by combining recycle technique with present selective adsorption-desorption method as mentioned above. Besides, the present noble gas concentrator is operated at subatmospheric pressure through all the processes, and this is another advantageous point of the present method.

Inlet flow to the storage system contains not only concentrated noble gases but also nitrogen, oxygen, ozone and other gaseous impurities. In order to store these concentrated gases safely for an extended period, it is required to remove not only ozone and other impurities but also oxygen which might have possibility to change to ozone during storage. So, the proposed system equips with oxygen (and other gaseous oxide impurities) remover. "Metal getter absorption method" is to remove oxygen and to decompose ozone and nitrogen oxide by letting them contact with some kinds of metals. For instance, zirconium metal does not absorb noble gases at all while it absorbs a large amount of oxygen at elevated temperature. It also absorbs nitrogen, but the absorption rate of nitrogen is so far less than that of oxygen that it can be regarded as a selective absorbent of oxygen. Inlet flow to the storage system first passes through the oxygen remover utilizing this Zr getter absorption method, and then enters the storage section.

The main part of the storage section consists of metallic cylinder in which a certain type of adsorbent is packed. The cylinder is cooled with liquid nitrogen when the gas from the noble gas concentrator is required to deliver for storage. With this cooling of the cylinder, the system requires no pumps or compressors for the transportation of the concentrated gas between the gas holder and the storage cylinder by the adsorption power of cooled adsorbent in the cylinder, and furthermore the system can be oper-ated at subatmospheric pressure. At the completion of the storage period, the cylinder is sealed, left to room temperature and transported to the storage yard. Internal pressure of the cylinder at room temperature is kept lower by the action of adsorbent packed in the cylinder than the case the cylinder contains no adsorbent.

3.   Cryogenic Adsorption-Desorption Process

3.1   General Description and Definition

The noble gas concentrator can be divided into two charcoal beds (A, B), valves and piping. A typical cycle of operation of the two charcoal beds, based on one day switching interval, is shown schematically in Fig. 2. The cyclic process, as shown in the figure, is fundamentally composed of four steps.

1) Selective Adsorption Step

The feed is passed through a cooled bed until the breakthrough of krypton is detected. Radioactive noble gases are removed from the feed by being adsorbed on adsorbents. Noble gases enriched on adsorbents are desorbed at regeneration step.

2) Regeneration Step (- recycle step or storage step)

The bed is evacuated with raising temperature to 50°C - 100°C following the selective adsorption step or selective desorption step. Desorbed gases are recycled to the feed at recycle step, and are transferred to the next oxygen removal process at storage step. In order to achieve greater DF by the cryogenic adsorption process, it would be necessary to purge the bed with clean gas at this step.

3) Selective Desorption Step

After selective adsorption step, the bed as being kept at low temperature is evacuated to a desired pressure with a vacuum pump. Since noble gases are not desorbed so easily as carrier gas, because of the difference of physical properties such as mass transfer resistance and adsorption potential between them, the ratio of noble gases content to the carrier gas becomes greater in the bed.

4) Cooling Step

After the regeneration step, the bed is cooled to a desired temperature and kept waiting for the next cycle.

The cryogenic adsorption-desorption process, as previously mentioned, plays the roles of both removing radioactive noble gases from off gas streams and enriching noble gases. The efficiency of the former or its DF could be estimated by using the breakthrough curve of noble gases, and the characteristics of the latter could be described with enrichment factors at the selective adsorption step, the recycle step or the selective desorption step. These outlines are described below.

FIG. 2   THE TYPICAL CYCLE OF TWO CHARCOAL
BEDS OPERATION

Definition of DF and Analytical Method of Breakthrough Curve

DF could be expressed by a breakthrough curve of non-active krypton and decay effect of radioactivity in the bed as follows,

$$DF \cong \frac{\sum_i A_i(Kr) + \sum_j A_j(Xe)}{t_B^{-1} \int_0^{t_B} \frac{C}{C_0} \sum_i A_i(Kr) e^{-\lambda_i \cdot t} dt} \quad ----- \quad (1)$$

where,

$A_i(Kr)$: release rate of radioactive krypton at an entrance of the bed ($\mu Ci/sec$)

$A_j(Xe)$: release rate of radioactive xenon at an entrace of the bed ($\mu Ci/sec$)

C/C_0 : breakthrough curve of non-active krypton ($-$)

t_B : breakthrough time (sec)

i, j : nuclide

λ_i, λ_j : decay constant (1/sec)

Since the adsorption coefficient of xenon is greater than that of krypton, it has been postulated that xenon does not appear in the effluent at the breakthrough of krypton ($\leq 10^{-2}$). In order to evaluate DF by the equation (1), it is necessary to establish an analytical method of the measured breakthrough curve and a method to calculate the breakthrough curve under given conditions. Although the various methods to analyze, and calculate the breakthrough curve had been proposed, the method proposed by Rosen[2] was adopted in this article. A material balance and linear-equilibrium relationship give

$$\varepsilon D \frac{\partial^2 c}{\partial x^2} = \gamma \frac{\partial q}{\partial t} + \varepsilon \frac{\partial c}{\partial t} + u \frac{\partial c}{\partial x} ,$$

$$\gamma \frac{\partial q}{\partial t} = K_F a_v (C - q/K)$$

$$\left. \right\} \quad ----- \quad (2)$$

using the boundary conditions q=0 for t=0, $x \geq 0$ and C=Co for $t \geq 0$, x=0, and neglecting the diffusion term, $\varepsilon D \frac{\partial^2 c}{\partial x^2}$, the approximate solution to the equations (2) is

973

$$C/Co = e^{-(\zeta+\theta)} Jo(Z_i\sqrt{\zeta+\theta})$$

$$+ \int_0^\zeta e^{-(\mu+\theta)} Jo(Z_i\sqrt{\mu\cdot\theta})\,d\mu \quad \text{-----} \quad (3)$$

$$\zeta = \frac{K_F a_v}{\gamma K}\left(t - \frac{x}{u/\epsilon}\right), \quad \theta = \frac{K_F a_v}{u}\cdot x$$

Under the condition $\theta \gg 1$, the equation (3) is able to be approximated with equations,

$$C/Co = \frac{1}{2}(1 + erf\ E) \qquad \text{---------} \quad (4)$$

$$E = \frac{\zeta-\theta}{2\sqrt{\theta}} = \frac{1}{2\gamma}\sqrt{\frac{u\cdot K_F a_v}{xK^2}}\,t - \frac{1}{2}\sqrt{\frac{x\cdot K_F a_v}{u}} \quad \text{-----} \quad (5)$$

where,

Co   : concentration of krypton in the feed (mol/cc)

C   : concentration of krypton in gas phase at distance along charcoal bed, x and time of adsorption process, t   (mol/cc)

D   : diffusion coefficient of krypton in air (cm^2/sec)

Jo   : Bessel function of zero order

K   : adsorption coefficient $(\frac{mol}{g} / \frac{mol}{cc})$

$K_F a_v$: total mass transfer coefficient (1/sec)

q   : amount of krypton adsorbed per unit mass of adsorbent (mol/g)

t   : time of adsorption process (sec)

u   : superficial velocity (cm/sec)

x   : distance along charcoal bed (cm)

ϵ : void fraction of charcoal bed ($-$)

γ : bulk density of charcoal (g/cm^3)

Adsorption coefficient K and total mass transfer coefficient $K_F a_v$ are calculated by applying the equations (4) and (5) to a measured breakthrough curve. Breakthrough curve under any conditions can be counter-calculated from the equations (4) and (5) for given values of K and $K_F a_v$.

Definition of Enrichment Factor

We have defined the enrichment factor of noble gases as the ratio of noble gases content in the bed to that in the feed. From the definition, total enrichment factor, Ψ , is described as follows,

$$\Psi \cong \frac{[\text{ noble gases/carrier gas (in the bed)}]_a}{[\text{ noble gases/carrier gas (in the feed)}]} \quad \text{---} \quad (6)$$

where, the suffix, a , shows that selective desorption step has been conducted.

The equation (6) can be described as follows.

$$\Psi = \Psi_1 \times \Psi_2 \quad \text{----------} \quad (7)$$

where,

$$\Psi_1 = \frac{[\text{noble gases/carrier gas (in the bed)}]_b}{[\text{noble gases/carrier gas (in the feed)}]} \text{----} \quad (8)$$

$$\Psi_2 = \frac{[\text{noble gases/carrier gas (in the bed)}]_a}{[\text{noble gases/carrier gas (in the bed)}]_b} \quad \text{---} \quad (9)$$

and the suffix, b, shows that selective adsorption step has been conducted.

The equation (9) can be transformed into the next equation.

$$\Psi_2 = \Psi_3 \times \eta \quad \text{------} \quad (10)$$

where,

$$\Psi_3 = \frac{[\text{ carrier gas (in the bed)}]_b}{[\text{ carrier gas (in the bed)}]^a} \quad \text{------} \quad (11)$$

$$\eta = \frac{[\text{ noble gases (in the bed)}]_a}{[\text{ noble gases (in the bed)}]^b} \quad \text{------} \quad (12)$$

From the equations (7) and (10), total enrichment factor is presented as follows,

$$\Psi = \Psi_1 \times \Psi_3 \times \eta \qquad -------- \quad (13)$$

The enrichment factor at selective adsorption step, Ψ_1, is transformed by taking account of recycle step as follows,

$$\Psi_1 = \Psi_0 \cdot (N + 1) \qquad ------- \quad (14)$$

where,

Ψ_0 : enrichment factor at selective adsorption step without recycle step

N : number of recycle

After all, total enrichment factor can be described as follows.

$$\Psi = \Psi_0 \cdot (N+1) \times \Psi_3 \times \eta \qquad -------- \quad (15)$$

In case breakthrough point is 10^{-2} for krypton, the enrichment factor, Ψ_0, of krypton can be approximately described from the equations (4) and (5) as follows.

$$\Psi_0 \cong \frac{u \cdot \frac{273}{T} \cdot P}{q_{carrier} \cdot \gamma \cdot L} \times t_B \cong \frac{273 \cdot P}{q_{carrier} \cdot T} \left[1 - 3.3 \sqrt{\frac{u}{L \cdot K_F a_v}} \right] \cdot K \quad ---- \quad (16)$$

where,

L : bed length (cm)

P : pressure in bed (atm)

$q_{carrier}$: amount of carrier gas adsorbed per unit mass of adsorbent (STP-cc/g)

T : bed temperature (K)

3.2 Laboratory Scale Experiment

Some breakthrough curves were measured with a laboratory scale apparatus to obtain adsorption coefficients and mass transfer coefficients, and to compare the measured breakthrough curves with the calculated breakthrough curves from the equations (4) and (5). Some basic data for enrichment factors shown in this paper were selected from the data which we had reported at 13th AEC Air Cleaning Conference[1].

Besides, based on these results, an engineering test plant has been constructed and experiments are being performed with the plant. Such engineering scale experimental results will be shown in the next chapter "Engineering Scale Experiment".

3.2.1 Experimental

Apparatus and Method

Although components of noble gases in the off gas stream were krypton and xenon, krypton was used as adsorbate in this work, because xenon was adsorbed easily and not desorbed easily in comparison with krypton.

The apparatus used in this work, shown schematically in Fig. 3, was designed to be able to perform adsorption experiment and desorption experiment, using krypton tagged with Kr-85 as adsorbate.
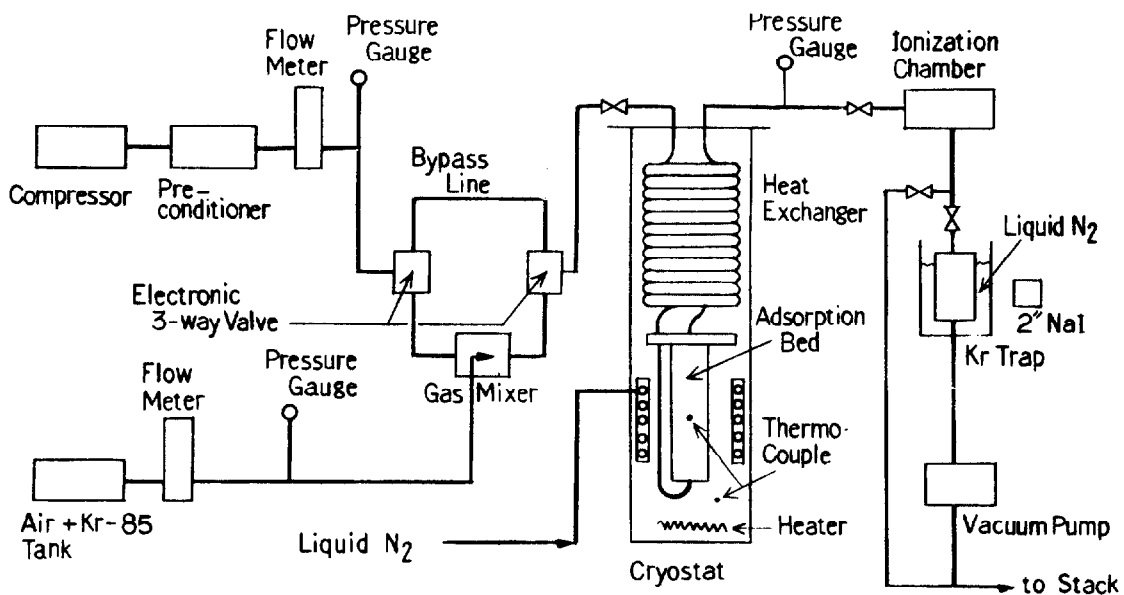
FIG.3   SCHEMATIC DIAGRAM OF LAB-SCALE
EXPERIMENTAL APPARATUS

The adsorption experiments were carried out by passing the feed through the adsorption bed cooled to a desired temperature. While the effluent was monitored with an ionization chamber to measure the breakthrough curve of krypton tagged with Kr-85. After adsorption experiments had been performed, the desorption experiments were conducted by evacuating the bed under low temperature through a Kr trap which was located in exhaust line, where Kr-85 was monitored with a NaI (Tl) scintillation detector to measure the amount of desorbed krypton.

An adsorption column which held the bed was placed in a cryostat, which was controlled over a range of temperature from -50°C to -150°C by using a heater and liquid nitrogen. The temperature of the cryostat was maintained within $\pm$ 1°C of the set point for the adsorption experiment and within $\pm$ 5°C of the set point for the desorption experiment. The adsorption column was a cylinder with a diameter of 2 inches filled with adsorbents.

Inlet and outlet lines from the column were of 1/2 in. outer dia. copper tubing, and were silver-soldered together in parallel for a length of 3.2 m to effect heat transfer from the incoming to the outgoing gas.

The Kr trap was a glass cylinder which was about 3 cm in diameter and 15 cm in effective length, filled with activated charcoal and immersed in liquid nitrogen. It was confirmed that the Kr trap was able to collect more than 90% of desorbed krypton.

The feed was made up by mixing air supplied by a compressor and krypton - dry air gas mixture tagged with Kr-85 which was stored at high pressure in an air - Kr-85 tank. Moisture and carbon dioxide in the air supplied by the compressor were removed with the preconditioner, which was composed of molecular sieves beds and cooler.

Breakthrough Curve, Adsorption Coefficient and Total Mass Transfer Coefficient

The adsorption coefficients and the total mass transfer coefficients were calculated by applying the equations (4) and (5) to the measured breakthrough curves. The theoretical breakthrough curves obtained by adopting these calculated coefficients are compared with the measured breakthrough curves.

Enrichment Factors

The enrichment factor, Ψ_O , at the selective adsorption step was calculated by the equation (16) using the coefficients K and $K_{F}a_v$ obtained in this work and the amount of carrier gas adsorbed per unit mass of adsorbent, q carrier, which was measured with a B.E.T. apparatus.

978

In order to determine the enrichment factor, Ψ_2 , at the selective desorption step, the factors Ψ_3 and η defined in the equations (11) and (12) were estimated by the methods shown below.

The counting rate of Kr-85 collected in the Kr trap was measured during the selective desorption experiment. After the selective desorption experiment, the bed was heated to 50°C and the amount of remained air in the bed was determined from the pressure and the volume of the column with the correction of the air amount adsorbed on adsorbents at the temperature of 50°C. Then, the column was evacuated to 10^{-2} Torr through the Kr trap and the counting rate of the Kr trap was measured at the Kr trap. Ψ_3 and η were estimated from these data by using the equations shown below.

$$\Psi_3 = q \text{ carrier} / q' \text{ carrier}$$

$$q' \text{ carrier} = 0.845 \text{ Vd P} + q'' \text{ carrier}$$

$$\eta = 1 - A/B$$

where,

A	:	counting rate at the Kr trap after the selective desorption experiment, but before the bed heating to 50°C
B	:	counting rate at the Kr trap after the bed was heated to 50°C and evacuated to 10^{-2} Torr
P	:	pressure in the column when the column was heated to 50°C (atm)
q' carrier	:	amount of remained carrier gas in the bed after the selective desorption process (STP-cc/g)
q'' carrier	:	amount of carrier gas adsorbed at the temperature of 50°C and the pressure of P, measured with the B. E. T. apparatus (STP-cc/g)
Vd	:	dead volume of the column (cm^3)

Experimental Condition

Some of the experimental conditions are summarized as follows,

Adsorbents	:	activated charcoal "Shirasagi G-A" (see Table 1)
Bed size	:	2 inches diameter and 11.7 to 19.4 cm in length

Carrier gas   :   air

Feed concentration
        :   1 ppm Kr. by volume, tagged with Kr-85

Temperature at the adsorption experiments
        :   -50°C to -150C

Pressure at the adsorption experiments
        :   1 atm

Air flow rate at the adsorption experiments
        :   1 cm/sec in superficial velocity

Pumping speed at the desorption experiments
        :   11 ℓ /min to 14 ℓ /min at the standard
        temperature of 30°C

Temperature at the desorption experiments
        :   fixed temperature at the adsorption experiments
        and raising temperature from -150°C to -100°C

Ultimate pressure at the desorption experiments
        :   10 Torr

Table 1   Properties of Adsorbents

	Charcoal			Molecular Sieves
	Kurale 4GA	Shirasagi G-A	VRG	MS 5A
Base	Coconut	Coconut	Coal	Zeolite
Shape	Cylindrical pellet	Cylindrical pellet	Granular	Granular
Size (Ave.) Dia.	3.8 mm	4.0 mm	1.0 mm	
Leng.	7.7 mm	4.1 mm	(14 mesh)	(60-80 mesh)
Apparent Density	0.78 g/cm^3	0.68 g/cm^3	0.82 g/cm^3	0.9 - 1.3 g/cm^3
Bulk Density	551 g/ℓ	459 g/ℓ·	529 g/ℓ	639 g/ℓ

3.2.2   Results and Discussion

Breakthrough Curve, Adsorption Coefficient and Total Mass Transfer
Coefficient

The measured breakthrough curve, taken from a typical run , is shown
in Fig. 4 together with representative experimental conditions. The solid
lines in the figure are the breakthrough curves calculated by the equations
(4) and (5).   The experimental data are fitted quite well by the theoretical
curves.

In Fig. 5, the obtained adsorption coefficients are plotted against
inverse temperature. The data for the temperature -15°C to 40°C in the
figure are the experimental values that we measured previously for the same
adsorbent. The data could be fitted by a straight line on a semilog paper at
a temperature above -100°C, and the fitting line becomes gradually curved
at the lower temperature by the reason of the interference effect which may
be due to the increase in the amount of adsorbed carrier gas on adsorbents.

The total mass transfer coefficient calculated from the measured
breakthrough curves was 2.1 ± 0.4 sec^{-1} at the temperature -150°C to -50°C.
According to our experiments performed previously for the same adsorbent,
values of the coefficient were 12 sec^{-1} at 40°C and 5 sec^{-1} at 0°C. Based on
these results, it is clear that the total mass transfer coefficient becomes
smaller at the lower temperature and the dependency of the coefficient on
the temperature is relatively small at the lower temperature. The coeffi-
cient might be affected considerably by the gas pressure in the bed and the
superficial velocity; the effect of these parameters was not investigated in
this work, however. The conditions in this work were as follows.

Pressure   :   1 atm

Superficial velocity   :   about 1 cm/sec

Enrichment Factor

The enrichment factor, Ψ_0 , shown in Fig. 6 was calculated by the
equation (16) using the experimental data which were obtained under the
conditions as follows.

Bed size   :   2 inches in diameter and 19.4 cm in
                               length (same as the bed size at the
                               selective desorption experiments)

Breakthrough point   : 10^{-2}

Pressure   :   1 atm

Superficial velocity   :   1 cm/sec

ADSORPTION COEFFICIENT K (mol/g/mol/cc)

BED TEMPERATURE (°C)

● : Values by lab-scale experiment (pressure : 1 atm)

○ : Values by engin-scale experiment
△ □   (see the chapter "Engineering scale experiment")

pressure
△ : 0.6 atm
○ : 0.93 atm
□ : 0.94 atm

FIG. 5   ADSORPTION COEFFICIENT

BREAKTHROUGH C/Co

ADSORPTION TIME (HR.)

Weight of adsorbent : 150 g
Temperature : -150°C
Pressure : 1 atm
Superficial velocity : about 1 cm/sec
Bed size : 2 inches in diameter, 176 mm in length

○ : Experimental values
— : Calculated

FIG. 4   BREAKTHROUGH CURVE
BY LAB-SCALE EXPERIMENT

Since properties of the factors, Ψ_2 , Ψ_3 and η at the selective desorption, defined in the equations (9), (11) and (12) were discussed previously in the 13th AEC Air Cleaning Conference, only the experimental values of the factors will be shown here. In Fig. 6, the factors Ψ_3 and Ψ_2 are shown with the factor Ψ_0 and the total enrichment factor, Ψ , calculated by the equation (7). The desorption rate of krypton at the selective desorption, 1- η , are shown in Fig. 7. The data labelled with a mark * in Fig. 6 and 7 are the experimental values which were obtained by evacuating the bed with increasing the temperature -150°C to -100°C. The other data in the figures are the experimental values obtained by evacuating the bed at the fix temperature.

It could be concluded from these results that the equations (4) and (5) proposed by Rosen were suitable to the breakthrough curve analysis and the enrichment factor was increased without noticeable increase of krypton desorption rate by evacuating the bed with increasing temperature. In order to confirm whether the above conclusions are applicable to an actual scale facility or not, an engineering test plant has been constructed and the experiments are being performed, which will be presented in the next chapter "Engineering Scale Experiment .
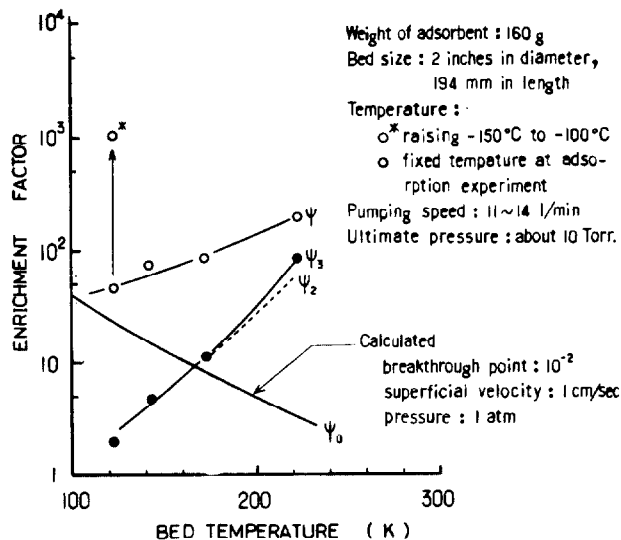
FIG.6   ENRICHMENT FACTORS
AT LAB - SCALE EXPERIMENT
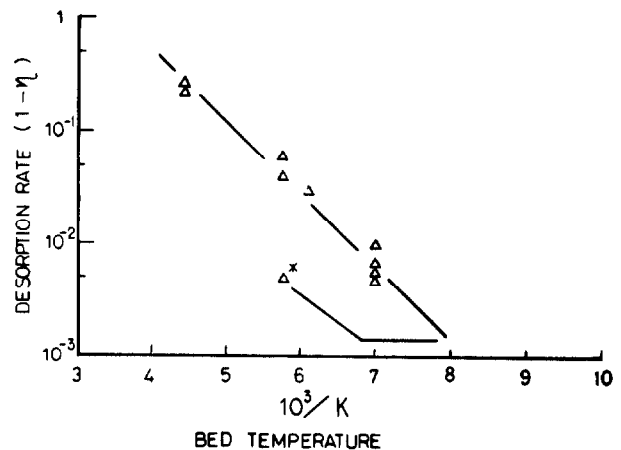
FIG.7   DESORPTION RATE OF ADSORBED
Kr AT SELECTIVE DESORPTION
LAB - SCALE EXPERIMENT

3.3   Engineering Scale Experiment

An engineering test plant for adsorption-desorption experiments has been designed and constructed utilizing the data of adsorption-desorption in laboratory scale experiment, and performance is now examined.   This report shows the interim results.

3.3.1   Test Plant

A process flow diagram of the test plant is shown in Fig. 8 and the photographs are shown in Fig. 9.
Experiments are performed by passing the air with about 1 ppm Kr tagged with Kr-85 in down flow through the adsorption bed of charcoal.   The air of 50 Nm^3/hr is intaked and pressurized to 1.2 kg/cm^2 Abs. by main blower and fed to one of the moisture/carbon dioxide remover towers after pre-cooled to 10°C.   Moisture and carbon dioxide are removed to the levels of less than 1 ppm and 2 ppm respectively in towers packed with adsorbent, "Zeorum F-9".
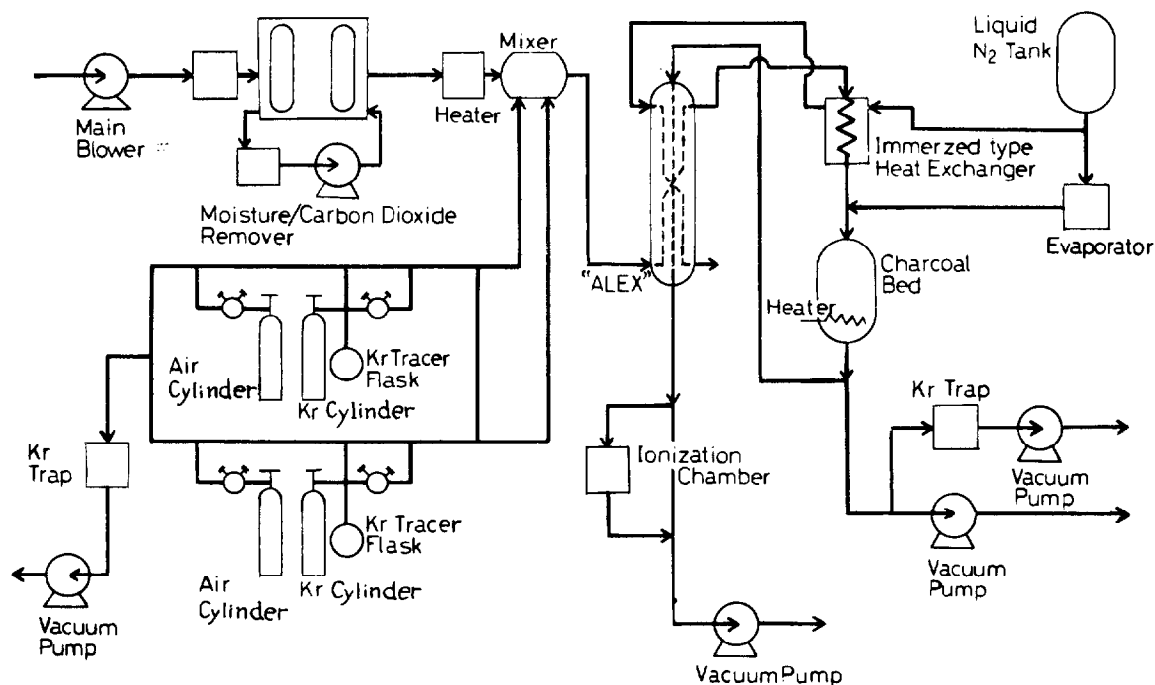
FIG. 8   PROCESS FLOW DIAGRAM OF ENGINEERING
SCALE TEST PLANT
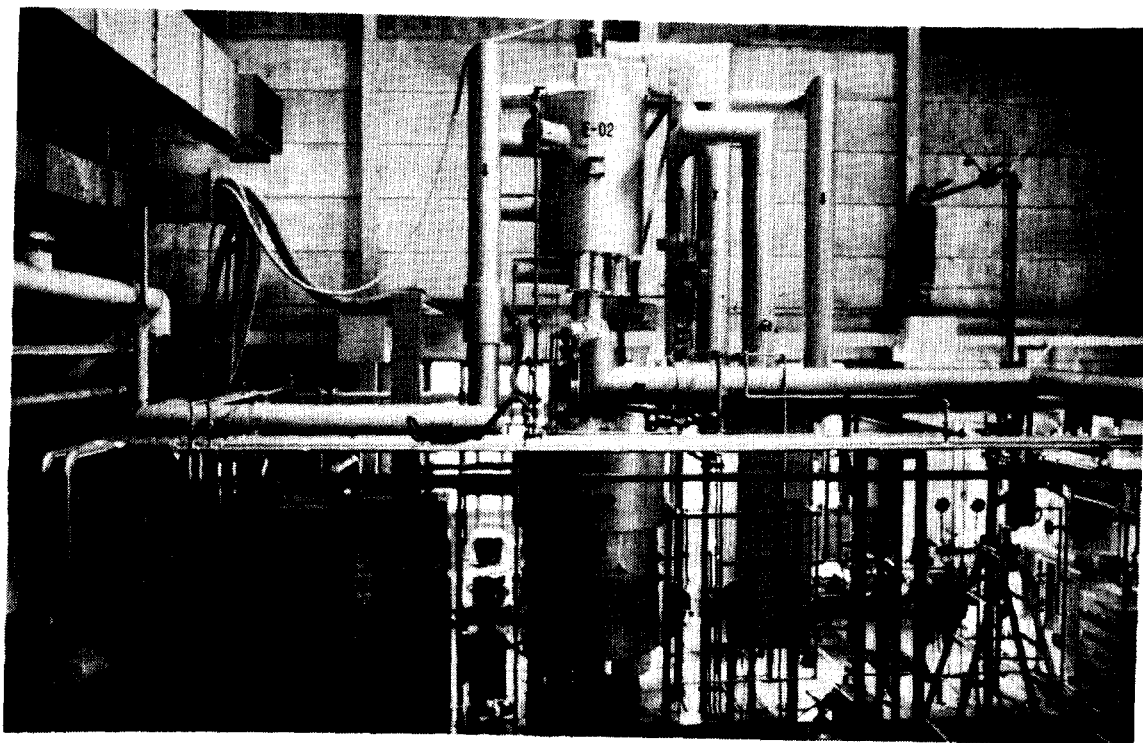
TOTAL VIEW OF TEST PLANT
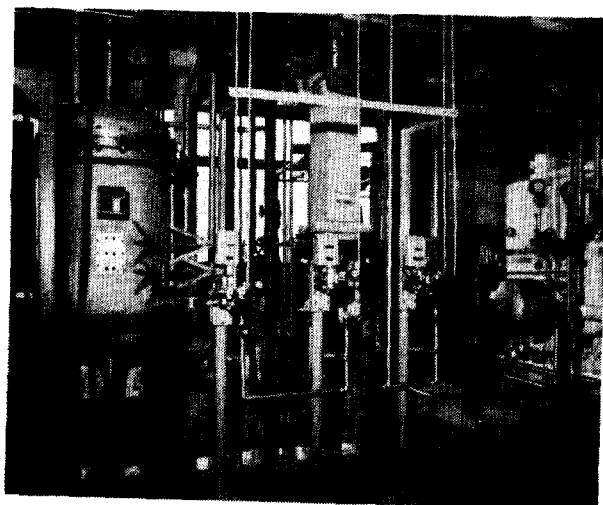
CONCENTRATOR AND
HEAT EXCHANGER
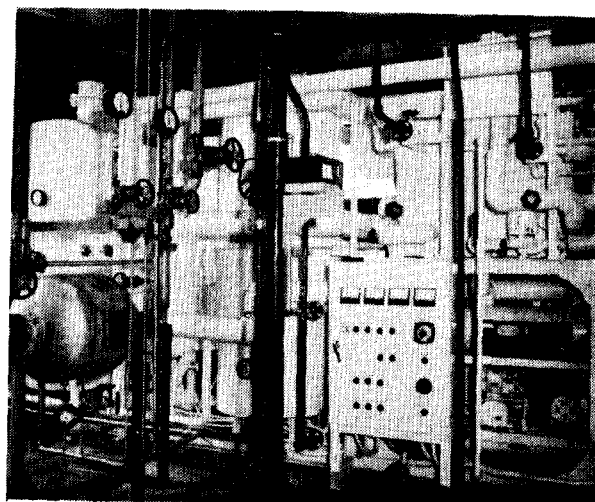
MOISTURE/CARBON DIOXIDE
REMOVER

FIG. 9 PHOTOGRAPHS OF ENGINEERING SCALE
TEST PLANT

985

When one of towers is ↗ adsorption step, the other is in regeneration step or in cooling step, and ↙e path of feed gas is automatically changed every 8 hours. After the tower in adsorption step is saturated with moisture and carbon dioxide, the adsorbents are heated up to about 300°C for regeneration, and are purged with purified gas of 10 Nm^3/hr from the other tower.

In this remover, both internal and external heatings are adopted to get the high removal efficiency of moisture and carbon dioxide for the prevention of blockage in small piping lines at the low temperature section.

Dried feed gas of 40 Nm^3/hr tagged with Kr-85 at the gas mixer goes into the "ALEX" heat exchanger. The feed gas is cooled down in this heat exchanger and is further cooled down in the next immersed type heat exchanger. The temperature of the effluent gas from the immersed type heat exchanger is controlled from about -185°C to -190°C by means of controlling the level and the pressure of liquid nitrogen in the heat exchanger.

Then the effluent gas is fed into the charcoal bed which has been sufficiently cooled down prior to the adsorption experiment by cold nitrogen gas, and the temperature of the charcoal bed is kept at -160°C to -170°C by the cold of the feed gas itself during the adsorption experiment. Krypton tagged with Kr-85 in the feed gas is adsorbed in the charcoal bed and the effluent gas from the bed is exhausted by a vacuum pump. A part of the effluent gas is passed through an ionization chamber which measures the breakthrough curve of krypton. The pressure in the charcoal bed is controlled at the range of 0.6 ata to 1.0 ata by regulating the valves at the suction of the vacuum pump and the outlet of the moisture and carbon dioxide remover. The charcoal bed is 750 mm in diameter and 300 mm in depth.

Raschig rings are packed at the upper and down sides of the bed and six semicircle heaters of total capacity of 30 kW are buried in the charcoal bed. In this experiment 46 kg of "Shirasagi G-A" charcoal was packed. The bed temperature is measured with the C-C thermocouples at nine locations. Cold nitrogen for the low temperature section is supplied from the liquid nitrogen tank, using a liquid nitrogen line for the immersed type heat exchanger and a cold nitrogen gas line for pre-cooling of the charcoal tower. Urethane foam is used to insulate the low temperature section for the convenience of various works such as changing of adsorbents.

For the selective desorption experiment, two vacuum pumps and a Kr trap are installed. One of the pumps of a pumping speed of 3 m^3/min is used for the evacuation of the bed. The other pump of a smaller pumping speed is used for sampling a portion of desorbed gas. The sampled gas is collected in the Kr trap and monitored by Na I (Tl) scintillation detector. The Kr trap is packed with charcoal and immersed in liquid nitrogen.

3.3.2   Experimental

Cooling

It is needed to pre-cool the charcoal bed prior to the adsorption experiment. In this plant, the bed is pre-cooled by feeding cold nitrogen gas directly to the bed to shorten cooling time and to reduce a consumption of liquid nitrogen. After passed through the bed, nitrogen gas is fed into the "ALEX"heat exchanger, cools the low temperature section and is exhausted. While this pre-cooling operation, liquid nitrogen is supplied to the immersed type heat exchanger. When the temperature of the charcoal bed reached to about -170°C, the supply of cold nitrogen gas was stopped, and a stabilizing operation was started. When the temperature was balanced in the "ALEX" heat exchanger a vacuum pump was started for the normal operation.

Adsorption Experiment

When the normal operating conditions were obtained, the adsorption experiment was started by injecting Kr-85 tracer into the feed gas. Kr-85 in the effluent gas from the charcoal bed was measured by the ionization chamber.

a)   Preparation of Kr-85 Tracer

The Kr-85 tracer supplying section was composed of two series of a Kr tracer flask, an air bombe, a Kr bombe, one charcoal trap and one vacuum pump. About 100 mCi of Kr-85 in a Kr tracer flask was sucked into a Kr bombe, well evacuated beforehand and was diluted with air to a certain concentration.

b)   Measurement of Breakthrough

The concentration of Kr-85 in the effluent gas from the charcoal bed, C, was measured by the ionization chamber. On the other hand, the concentration Kr-85 in the feed gas, C_o, was measured by passing the feed gas directly in the ionization chamber.

The breakthrough ratio (C/C_o) was calculated from C and C_o. The adsorption coefficient, K, and the total mass transfer coefficient, K_{Fa_v} , were calculated from the breakthrough curve with Rosen's equations (4) and (5).

Desorption Experiment

When the adsorption experiment was finished, the charcoal bed was isolated from the feed gas line. The selective desorption was performed by heating and evacuating the bed. A portion of krypton desorbed from the bed

during the selective desorption experiment was trapped in the Kr trap and was measured by the Na I (Tl) scintillation detector. When the selective desorption was finished, the bed was heated to about 100 °C. From the temperature and the pressure of the bed, the enrichment factor at the selective desorption step was calculated in the same way as the laboratory scale experiment.

After that, the bed was evacuated and the desorption rate of krypton in the effluent gas was measured by the Na I (Tl) scintillation detector in the same way as the selective desorption step. The experimental conditions were shown in Table 2.

Table 2   Experimental Condition

Charcoal Bed Size : 750 mm in diameter and 300 mm in length
Adsorbent   : Shirasagi G-A pelletized coconut base charcoal, 46. 3 kg

At the Adsorption Step

Pressure   : 0. 6 atm and 0. 94 atm
Temperature   : -160 °C to -170 °C
Feed Gas Flow Rate : 40 Nm^3/hr.
Conc. of Kr in the Feed Gas   : 1 ppm
Superficial Velocity : 1. 6 cm/sec (at 0. 6 atm) and
                         1. 0 cm/sec (at 0. 94 atm)

At the Selective Desorption Step

Increasing Rate of Bed Temperature : $\simeq$25 °C/hr
Pumping Speed   : $\simeq$80 m^3/hr
Temperature of Bed   :   -100 °C
Pressure in Bed   :   20 to 25 mmHg

3.3.3   Results and Discussion

Cooling

The charcoal bed and the "ALEX" heat exchanger were cooled down by cold nitrogen in a relatively short time of about 2 hours and 0.5 hour respectively. However, it took much more time to stabilize the bed temperature after setting the pressure and flow rate under the experimental conditions succeeding to the pre-cooling. The amount of liquid nitrogen consumed in pre-cooling was 700 Nm^3, for the fill-up of the immersed type heat exchanger and 100 Nm^3 for cooling down of the charcoal bed by cold nitrogen gas. Consumption of liquid nitrogen during the adsorption experiments was about 40 Nm^3/hr.

Breakthrough Curve

Breakthrough curve for the run No. 3 is shown in Fig. 10 with experimental conditions. And E-t curves for the run No. 1, No. 2 and No. 3 are shown in Fig. 11, 12 and 13 with the change of the bed temperature during the adsorption, where E was derived from the breakthrough ratio (C/C_0) using the equation (4). In the run No. 1 and No. 2, a small change of the bed temperature was observed.

Presumably owing to this fractuation of the temperature, E-t curves were not linear and the gradients of the curves were in correspondence with the change of the bed temperature. In the run No. 3, ten more hours than run No. 1 and No. 2 was devoted to the temperature stabilization for the confirmation of above mentioned problem. Even in this run, the change of the temperature could not be avoided. However, the influence on the curve was smaller and the curve became linear except the initial part. Calculating the adsorption coefficient, K, and the total mass transfer coefficient, $K_F a_v$, from the breakthrough curve of this run,

$$K = 7,300 \ \frac{mol}{g} \ / \ \frac{mol}{cc}$$

and,

$$K_F a_v = 1.0 \qquad 1/sec$$

for the adsorption pressure of 0.94 atm and temperature of -160°C.
This value of 1.0 1/sec for $K_F a_v$ seems too small for this experimental conditions. This might be attributed to the slight high temperature at the beginning of the adsorption. In the run No. 1 and No. 2, the method by Rosen is not effective for the calculation of K owing to the non-linearity of the E-t curves. So, the K values are derived approximately from the equation shown below using the time $t_{0.5}$ which gives the C/C_0 ratio of 0.5.

$$K = \frac{u \cdot t_{0.5}}{\gamma \cdot L}$$

This K value will be larger for the initial high temperature and smaller for the lower temperature in one test run and was shown in Table 3 and Fig. 5.

Fig. 5 shows the K value depends on the gas pressure and gets larger with the decrease of the gas pressure. This will be explained by the idea that the decrease of co-adsorbed carrier gas amount in low gas pressure raises the adsorption capacity of Kr, because the co-adsorbed carrier gas hinder the adsorption of Kr. We could not quantitatively evaluate the effect of the gas pressure on Kr adsorption owing to the scarcity of data and the change of temperature, however it will be said that the effect of gas pressure is greater at low temperature than at the ambient temperature.

At the ambient temperature, the decrease of pressure leads to the shortening of the hold up time of Kr because of the larger effects of gas velocity than the co-adsorption. On the contrary, pressure decrease raise the hold up time at the low temperature as in this experiment. In the following experiment, we exclude the temperature fractuation and make much more data to obtain the accurate K and K_{Fa_V} and the pressure dependence.

Enrichment Factor by Desorption

Enrichment factors by the selective desorption and the desorption ratio of Kr from the bed are shown in Table 3.

<div align="center">

Table 3   Enrichment Factor

</div>

Run	K	Enrichment factor	Kr desorption ratio
No. 1[*]	20,000	~ 25	0.5 %
No. 2[*]	7,600	25 ~ 30	0.7 %
No. 3	7,300	25 ~ 30	2.3 %

[*] K values were derived from the above equation.
These runs were stopped before 100% breakthrough.

Enrichment factors obtained in this engineering scale experiments are in conformity with the value of 40 in the laboratory scale experiments.
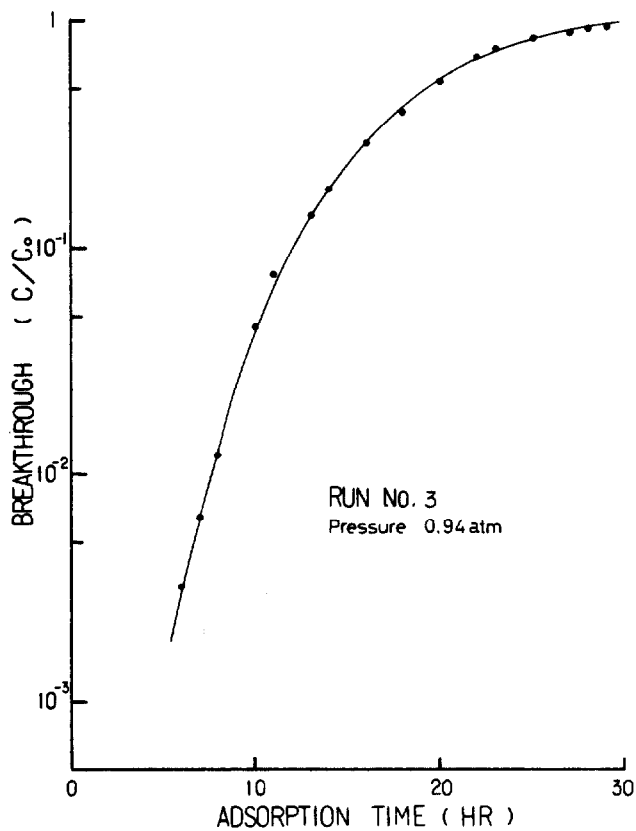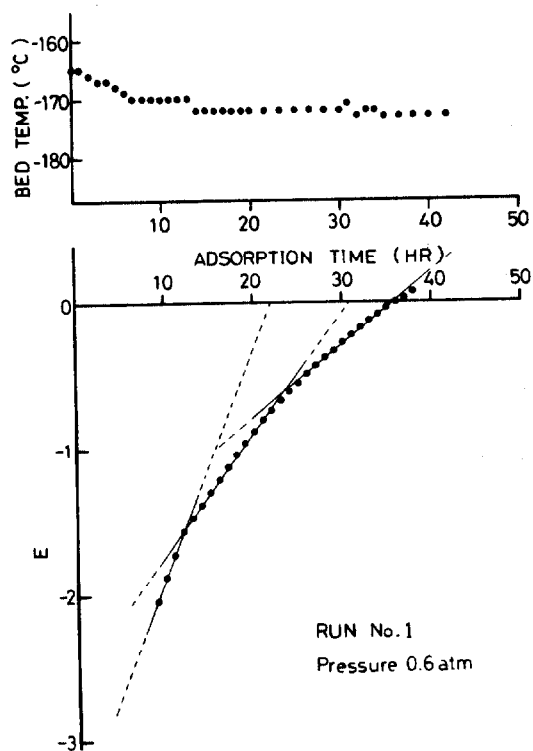
FIG. 10 BREAKTHROUGH CURVE

RUN NO. 3
Pressure 0.94 atm

FIG. 11 E-T CURVE & BED TEMP.

RUN No. 1
Pressure 0.6 atm

RUN No. 2
Pressure 0.93 atm
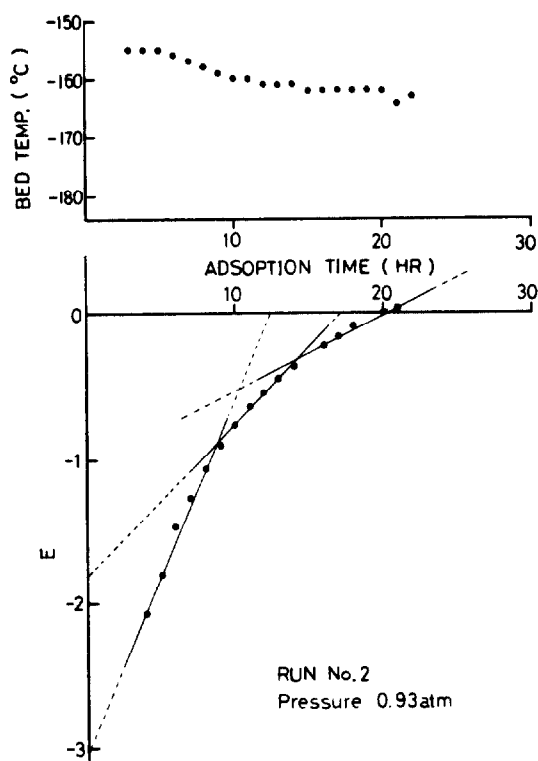
FIG. 12 E-T CURVE & BED TEMP.

RUN No. 3
Pressure 0.94 atm
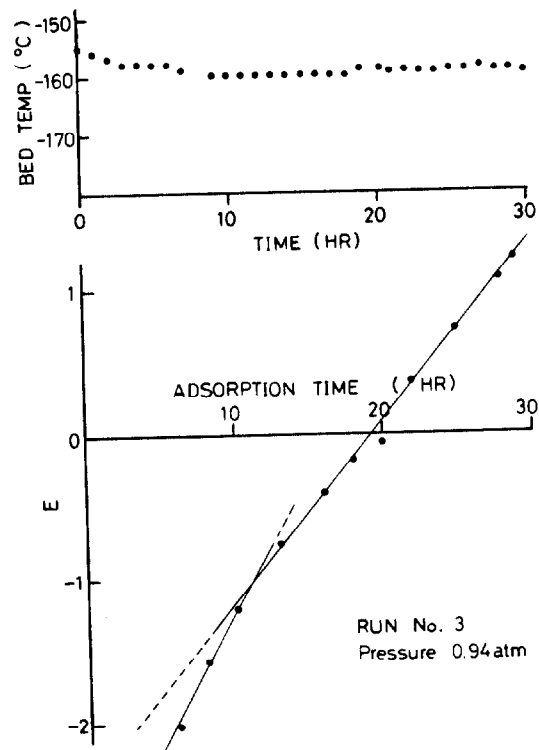
FIG. 13 E-T CURVE & BED TEMP.

4. Oxygen Removal Process

As described in Chapter 2, "metal getter absorption" method has been studied for the oxygen removal process, and the applicability of the method to the actual plant is experimentally being investigated. Two kinds of experiments were conducted. One was that sample gas was reacted with metal getter in a closed vessel during a constant time (static experiment), and the other was that sample gas was reacted with metal getter under a constant flow rate of the same magnitude as expected in the actual plant (dynamic experiment). In this report, results from the static experiments and the description of the dynamic experimental apparatus are presented.

Transition metals of the fourth group such as Zr, Ti and Hf and of the fifth group such as V, Nb and Ta are well known to have the characteristics to absorb nitrogen and oxygen and not to absorb noble gases in the field of vacuum technology[3] However most of the studies in this field have focused their concern on the studies of fundamental metal-gas reaction and reported data are limited to those obtained under high vacuum conditions and/or single component gas reaction. The data required for the discussion in the present study are those for the metal to multi-component gas reaction under atmospheric pressure.

Authors chose Zr metal as most promising gas absorbent or getter, and first have carried out the laboratory scale experiment to know its absorption capacity and absorption rate of concerned gases in air under atmospheric pressure. Air was chosen because its component is similar to that of enriched gases. Also, data for some pure gases were obtained.

4.1 Static Experiment

Apparatus and Method

The static experimental apparatus is shown in Fig. 14. Reaction tube made of quartz (80 cc) can be heated over a range of temperature from 100°C to 900°C by an electric furnace and controlled at a constant temperature within $\pm$ 5°C. Before the absorption experiments, a Zr sample washed in acetone and dried was put into the reaction tube and it was evacuated to a vacuum of 10^{-2} mmHg. Then, the specimen was heated to a predetermined temperature and the reaction tube was evacuated continuously for about two hours.

After that, sample gas was introduced into the reaction tube to a certain pressure from a gas cylinder. When the sample gas was a single component, reacting amount of sample gas was determined from the pressure change. And when the sample gas was a multi-component, reacting amount was determined by the volumetric method with mass spectrometry. The weight gain of the Zr sample was determined from these results.

Experimental Condition

The experimental conditions are summarized as follows.

Specimen	:	Zr foil (20μ m thick), weight 10 - 100 mg Zr sponge (5 - 8 mm$^\phi$ beads), weight 100 - 500 mg
Sample gas	:	N_2, O_2, Kr, Xe, NO_2 (each purity $\geq$ 99.5 vol.%) Air
Loading pressure	:	20 - 700 mmHg
Reaction temperature	:	400 - 800°C
Reaction time	:	5 - 300 min
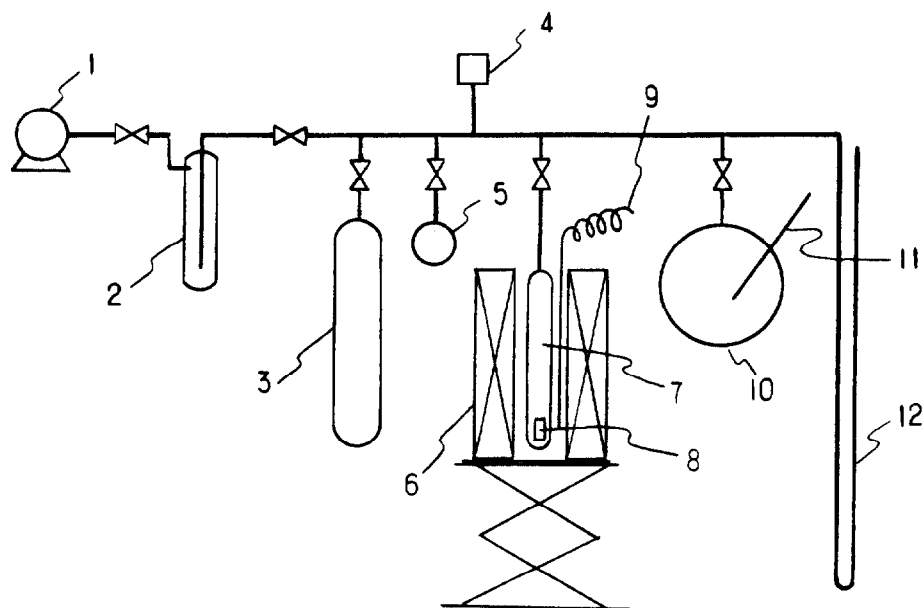
1. Vacuum Pump   2. LN₂ Trap   3. Gas Cylinder   4. Diaphragm Vacuum Gauge
5. Gas Sampler   6. Electric Furnace   7. Reaction Tube   8. Specimen
9. Thermocouple   10. Gas Holder   11. Thermometer   12. Manometer

FIG. 14 STATIC EXPERIMENTAL APPARATUS

Results and Discussion

Changes of the weight gain of Zr foil are plotted against time in Fig. 15 and 16 with temperature and loading pressure. From Fig. 15, it is realized that both $Zr-O_2$ and $Zr-N_2$ reactions follow the so-called parabolic law expressed by the following equation :

$$w^2 = kt \qquad \text{------- (17)}$$

where,   w : weight gain (g/cm^2)
            k : parabolic rate constant $(g^2/cm^4 \cdot min)$
            t : reaction time   (min)

Fig. 16 shows the weight gain for oxygen (or nitrogen) in air is not different from that for pure oxygen (or nitrogen). From this fact, it would be said that the absorption rate for oxygen was not affected by the existence of nitrogen. The same experiments were performed for Zr sponge and it was clarified that the parabolic law was also effective and absorption rate for oxygen was independent of the existence of nitrogen. From the experimental results, its reactive surface for oxygen was determined as about 50 cm^2/g. It was also found that the reaction rate constant or weight gain between Zr and oxygen (or nitrogen) were independent of the loading pressure and dependent on the temperature. These results well agree with several previous reports.

The temperature dependence on oxygen and nitrogen for the temperature range from 600°C to 800°C is described in the following equations (18) and (19) respectively.

$$k = 0.11 \exp \left(-\frac{32000}{RT} \right), \text{ for oxygen} \qquad \text{----- (18)}$$

$$k = 0.20 \exp \left(-\frac{48000}{RT} \right), \text{ for nitrogen} \qquad \text{----- (19)}$$

From Fig. 15 and 16, the weight gain of oxygen is found to be greater in one or two order than that of nitrogen. In experiments with pure krypton or pure xenon at 700°C, these gases were not absorbed in Zr at all as expected.

The consumption of metal getter should be taken into account from the economical point of view, and would be strongly dependent on the absorption capacity of Zr for oxygen. Oxygen was absorbed by Zr to 45 at.% in the experiments and so it may be thought its absorption capacity is at least 45 at.%.

As described before, enriched gas contains small amount of ozone and nitrogen dioxide besides oxygen, and these must also be removed before storage. Ozone can be expected to decompose thermally at high temperature.

Nitrogen dioxide also seemed to decompose, although no data were reported about it. In order to confirm this expectation, nitrogen dioxide was examined in the same manner as pure oxygen at 700°C and 100 Torr. As the result, nitrogen dioxide was found to decompose into oxygen and nitrogen as expected, and they were absorbed in the zirconium with each absorption rate.

FIG. 15 REACTION OF Zr FOIL
WITH O_2 AND N_2

FIG. 16 REACTION OF Zr FOIL
WITH AIR
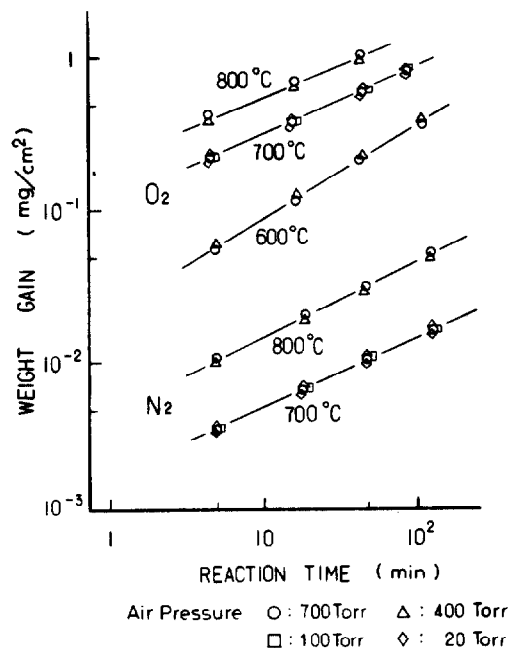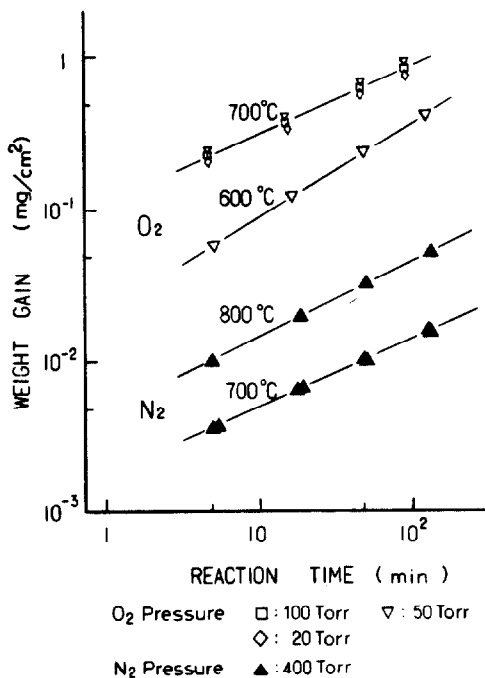
4.2 Study of Dynamic Experimental Apparatus

Based on the static experimental results, the dynamic experimental apparatus was designed as follows. In order that the oxygen concentration in the effluent gas from Zr bed is almost equal to zero, the following equation should be established.

$$t \geq \tau \qquad\qquad \text{----- (20)}$$

where, $\quad$ t : contact time (min)

τ : time required for oxygen removal (min)

and,

$$t = \frac{W/\rho}{F} \times \left(\frac{273}{T}\right) \qquad \text{----- (21)}$$

From the static experimental results,

$$\tau = \frac{(Wo/A)^2}{k} \qquad\qquad \text{----- (22)}$$

995

$$A = W \times 50 \times 10^3 \qquad \text{-----} \quad (23)$$

$$Wo \cong Ft \times \frac{1}{5} \times \frac{32}{22.4} \qquad \text{-----} \quad (24)$$

where, W : weight of Zr sponge (kg)
ρ : packed density of Zr sponge (=2.2) (kg/ℓ)
F : air flow rate (Nl/min)
T : reaction temperature (K)
k : Zr-O_2 reaction rate constant (g^2/cm^4.min)
A : surface area of Zr sponge (cm^2)
Wo: weight of oxygen (g)
R : gas constant (cal/mole·k)

Therefore,

$$k \geq 1.6 \times 10^{-11} \frac{F}{W} \times \left(\frac{273}{T}\right) \qquad \text{-----} \quad (25)$$

or

$$\frac{F}{W} \leq 6.5 \times 10^{10} k \times \left(\frac{T}{273}\right) \qquad \text{-----} \quad (26)$$

The equations (26) shown in Fig. 17 indicates that, if dynamic experiment is performed at reaction temperature of 500°C with 1 kg of Zr sponge, air flow rate should be less than 20 Nl/min. In order to confirm the expectation, a dynamic experimental apparatus has been constructed and dynamic experiment is being performed.
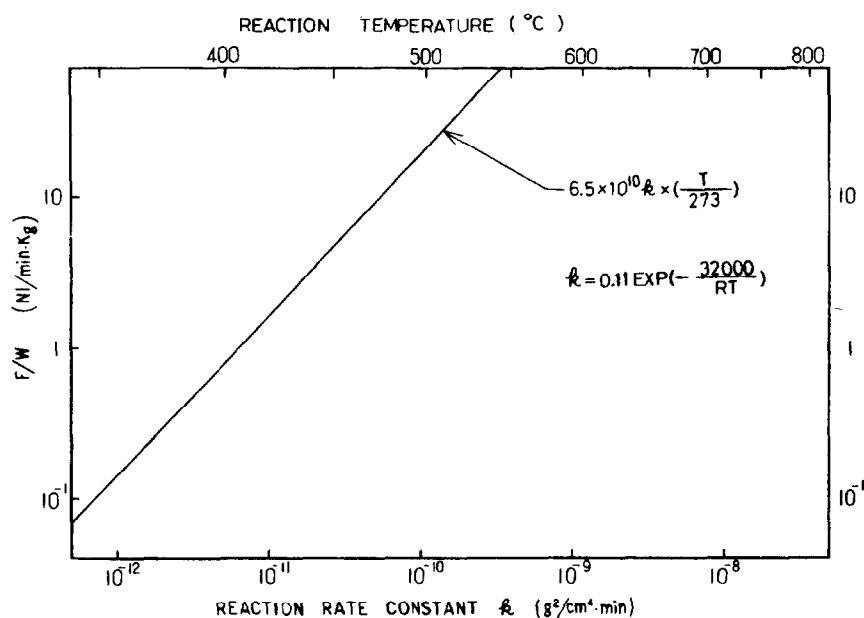
FIG. 17 ESTIMATION OF DINAMIC EXPERIMENT

5. Storage Process

As to the storage of the radioactive noble gases, various methods[4] are proposed and investigated. Among them, the method to compress the gas into a cylinder will be most promising at the present stage, thinking of the practicability, economy and safety. However, this method necessitates the use of compressors in the high radioactive lines and the operation at high pressure, and these demands cause the problems of the leakage of the compressed radioactive gas, the recovery of the residual gas in the connecting lines and overpressurization of a cylinder. As the storage process handles the most high radioactive gas in the total system, even a small leakage cannot be permitted, otherwise DF of the total system will be spoiled to a great extent. To eliminate these problems, a new storage process has been developed and examined. This process consists of a gas holder always operated at subatmospheric pressure, a cylinder packed with adsorbent and a cold bath.

The radioactive gas from the cryogenic adsorption process is once stored in the gas holder and then sucked into the cylinder by adsorption pump mechanism with cooling down the adsorbent in the cylinder. At this time, the cylinder is isolated, taken out of the cold bath and transferred to the pertinent storage yard. Pressure in the cylinder gradually becomes higher with the rise up of the adsorbent temperature. However, the equilibrium pressure at the ambient temperature is about one third of that of the conventional cylinder method. In our method, compressors and pumps are eliminated from the process and the gas is always handled at the pressure below one atmospheric. So, the above mentioned problems can not be expected.

5.1 Experimental

Apparatus and Method

A flow sheet of the experimental apparatus and equipment's sizes are shown in Fig. 18. Equipments are in about one hundredth scale of the assumed actual plant system. Before the experiments, adsorbent was heated to 85°C and evacuated to 0.1 mmHg to remove the adsorbed moisture and impurities. Pure nitrogen gas was used as the process gas, because the majority of the assumed radioactive gas is nitrogen (about 90%). The volume of the gas sucked into the cylinder was calculated using the volume and pressure of the gas holder. Adsorption was started simultaneously with cooling down by liquid nitrogen, and the pressure and adsorbent temperature were measured. After the completion of adsorption, the cylinder was isolated and warmed up to the ambient temperature from 25°C to 40°C. Adsorbents used are 3 charcoals, "Kurale 4GA", "Shirasagi G-A" and "VRG" and molecular sieves 5A. Their properties are shown in Table 1.
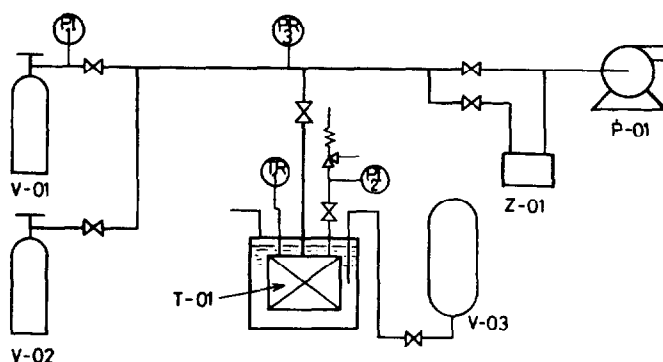
FIG.18 FLOW SHEET OF EXPERIMENTAL APPARATUS

EQUIPMENTS				INSTRUMENT		
No.				No.		
V-01	N₂ Cylinder	Volume	50 l	PI-1	Bourdon's Tube, Range 0~800mmHg	
V-02	Gas Holder	//	10 l	PI-2	// , // 0~25 kg/cm²	
V-03	Liq. N₂ Tank	//	20 l	PR-3	Pirani Gauge, Range 200~1×10⁻³mmHg	
T-01	Cylinder	//	0.3 l	TR-1	C-A Thermocouple	
Z-01	Cold Trap					
P-01	Oil Rotary Vacuum Pump					

5.2   Results and Discussion

Pressure obtained by Adsorption

The pressure and temperature of adsorbent were plotted against the adsorption time in Fig. 19. Pressure in the cylinder reached to 1×10^{-3} mmHg by every adsorbents as shown in the figure. Both cooling down and adsorption should be started up simultaneously to reduce the necessary time for the operation using the thermal conductivity of the process gas.

Cylinder Pressure during Storage

Results are shown in Fig. 20 and 21. Cylinder pressure was about one third of that of the conventional cylinder method as shown in Fig. 20, and was in the following order. "Kurale" < "Shirasagi" < "VRG" < MS 5A As Fig. 21 shows, there is no remarkable increase of the cylinder pressure at the temperature from 25°C to 40°C. Although the temperature rise due to decay heat is anticipated in the actual plant, the large part of radioactivity of the off gas from the nuclear power plant is attributed to short lived nuclides and so the decay heat shortly becomes negligible after the storage. By our calculations, the temperature rise at the center of a cylinder with charcoal is about 20°C just after the storage and becomes nearly zero in a week. Next items will be the future subjects to be examined.

1) Stability of adsorbent properties, especially adsorption capacity in long term storage.

2) Investigation as a whole system including handling, radiation shielding and remote control.
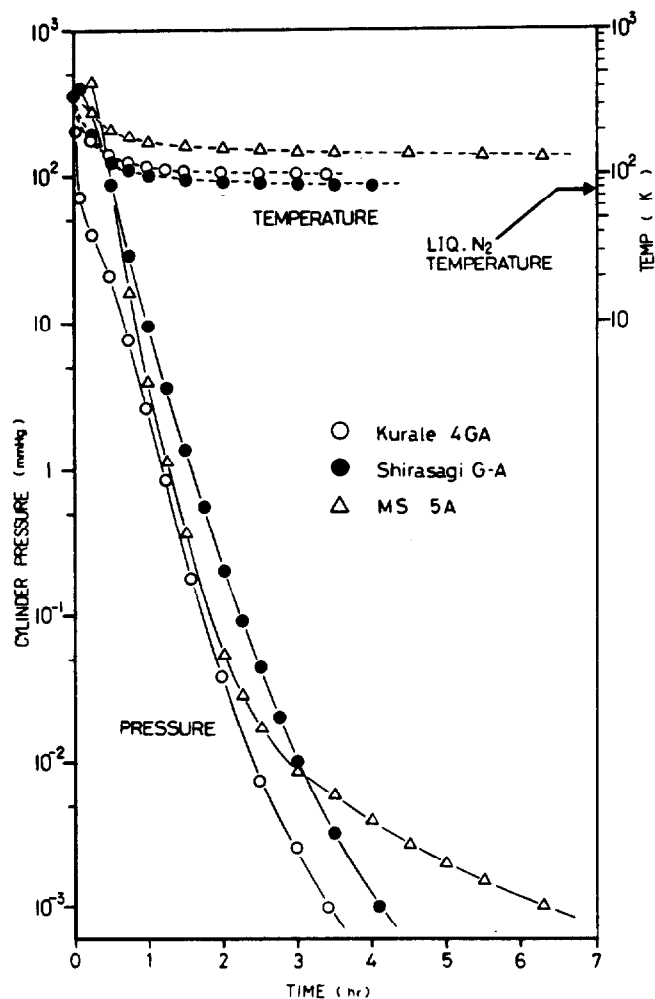
FIG. 19   PRESSURE AND TEMPERATURE
          AFTER START UP OF COOLING DOWN
          AND ADSORPTION
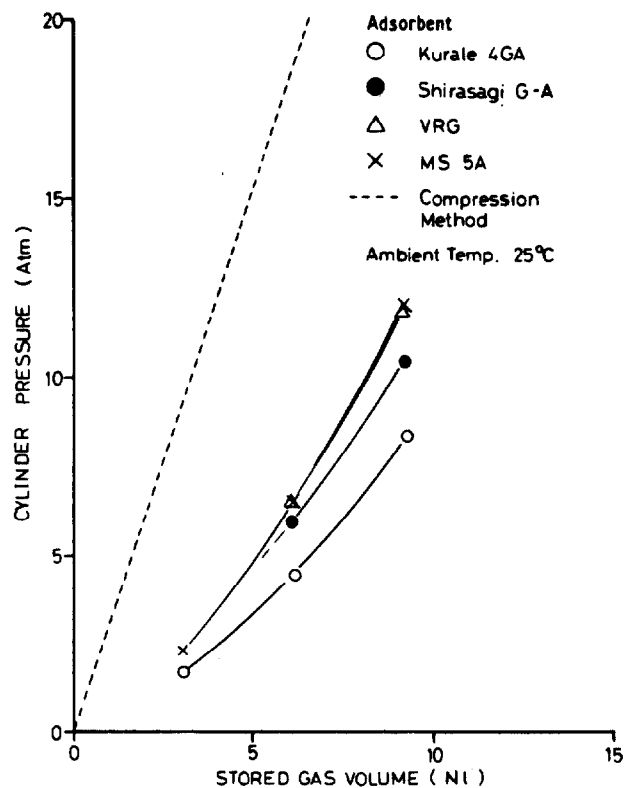
FIG. 20   CYLINDER PRESSURE vs.
           STORED GAS VOLUME
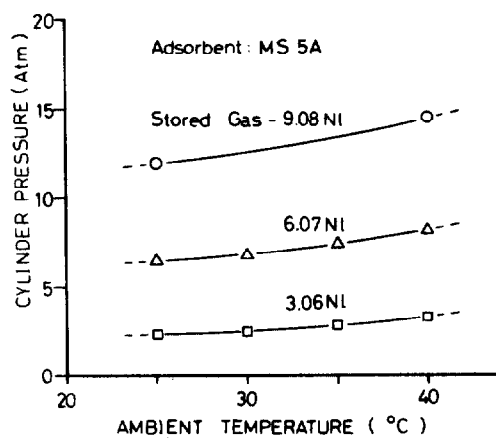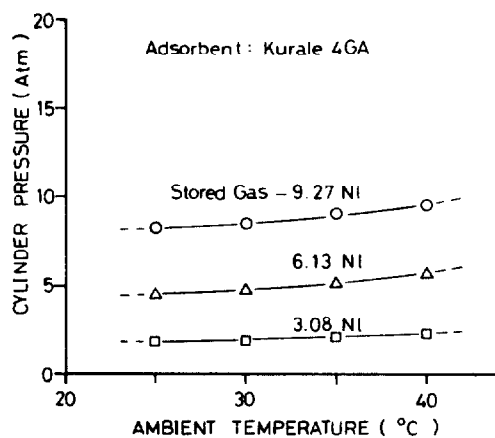
FIG. 21   EFFECT OF TEMPERATURE ON CYLINDER PRESSURE

999

6. Conclusion

It was proved that our proposed methods would be effective to recover radioactive noble gases from off gas streams of nuclear facilities. However, further investigation is necessary to settle some interesting problems obtained from a series of experiments.

References

1) Y. Yuasa, M. Ohta, A. Watanabe, A. Tani and N. Takashima, "Selective Adsorption-Desorption Method for the Enrichment of Kr", Presented at The 13th AEC Air Cleaning Conference (1974).

2) J. B. Rosen, Ind. Eng. Chem., Vol. 46, 1590 (1954)

3) M. Nagasaka, "Bulk Gettering Action of Titanium, Zirconium and Some Alloys Based on them", Shinku, Vol. 17, No. 7, 220-227, (1974).

4) B. A. Foster, et al., "Long Term Storage Techniques for Kr-85", Paper Presented at The 13th AEC Air Clearing Conference (1974).

DISCUSSION

STUART: We have built a similar system installed at Point Beach, a PWR with low oxygen content. For BWR's with high oxygen we recommend use of an inorganic adsorbent to avoid the potential problem of interaction of charcoal saturated with oxygen enriched air. Have you considered this safety issue?

TANABE: We have done a safety analysis involving ozone and oxygen. By the current analysis, we don't expect much difficulty with handling ozone in the charcoal bed. However, the actual behavior of ozone and oxygen has to be found out by future experimental work.

STUART: I think you may be right on ozone. We have a limited amount of data which indicates that it is formed. It may be simultaneously destroyed within the adsorbent bed. I think that additional data must be obtained.

KNECHT: Can this process be scaled up for 85 Kr removal from a commercial scale fuel reprocessing plant (1,400 ton per year scale)? If so, I would be interested in a comparison with other processes currently being considered such as cryogenic distillation and liquid fluorocarbon absorption.

TANABE: Engineering scale data will be obtained by future experiments.

SEPARATION OF THE FISSION PRODUCT NOBLE GASES KRYPTON AND XENON
FROM DISSOLVER OFF-GAS IN REPROCESSING HTGR-FUEL

J.Bohnenstingl, S.H. Djoa[+), M.Laser, St.Mastera, E.Merz, P.Morschl
Kernforschungsanlage Jülich GmbH
Institute for Chemical Technology
5170 Jülich / Germany

Abstract

This paper describes a process developed for the retainment and separation of volatile (^3H, $^{129+131}J$) and gaseous (^{85}Kr, Xe) fission products from the off-gas produced during dissolution of HTGR-fuel. To prevent unnecessary dilution of liberated noble gases by surrounding atmosphere, a helium purge-gas cycle is applied to enable a coarse fractionating of krypton and xenon by cold-trapping at about 80 K after precleaning the gas stream. The process consists of the following steps:
- deposition of droplets and solid aerosols
- chemisorption of iodine on silver impregnated silica gel
- catalytic removal of nitrogen oxides and oxygen
- drying of the process gas stream
- final filtering of abraded solids
- deposition of xenon in solid form at 80 K and low subpressure
- deposition of krypton in solid form at 80 K after compression to about 6 bar
- decontamination of ^{85}krypton-containing xenon by batch distillation for eventual industrial utilization
- removal of nitrogen and argon enrichment during continuous operation in the purge-gas stream by inleaking air with charcoal.

A continuously operating dissolver vessel, closed to the surrounding atmosphere, yields a very high content of noble gases, f.e. 0.35 vol % krypton and 2.0 vol % xenon. The presented off-gas treatment unit is operated in cold runs with 1/3 of the full capacity and can treat about 1 m^3 STP/h helium, corresponding to a quantity of about 10,000 MW_e HTGR-fuel reprocessing plant.

1. Introduction

The principle waste products from the nuclear power program resulting from the fission process are radioactive fission products. Whereas high-level radioactive wastes have been carefully stored under surveillance, it has been customary up to now either to discharge low-level streams directly to the environment or to give them the minimum treatment necessary to decrease the activity below specific levels.

Several gaseous (^{85}Kr, Xe) and volatile (^3H, $^{129+131}J$) radio-nuclides pose problems which are not already solved by the present state-of-the-art technology with the existing commercial reprocessing plants. Since the delaytime between fuel discharge from the nuclear power reactor and fuel reprocessing is usually more than 150 days,

[+) Kernforschungsanlage Jülich GmbH
Central Division for Advanced Technology

the short-lived products decay to insignificant low-levels during this cooling period. However, ^{85}Kr with a half-life of 10,76 years remains a potential hazard for many years. To avoid local release problems and long-term build-up in the atmosphere, ^{85}Kr must be separated at suitable points at a reprocessing plant and stored for a long period of about 100 years to allow a substantial decay. To keep the radiation dose to the population as low as possible the Commission for Radiation Protection of the Federal Republic of Germany recommends a limitation of the ^{85}Kr release for a reprocessing plant to a value of 10^6 Ci/year. This limitation requires a decontamination factor of $\geq$ 100 for any ^{85}Kr separation process being applied [1].

Although, at present, several cryogenic separation techniques for ^{85}Kr based upon the principle of liquefaction of air are under advanced development [2, 3, 4, 5, 6, 7] careful considerations of the costs and the risk analysis during hot operation as well as positive consequences of the dissolver vessel development encouraged us to initiate the development of a somewhat simpler but very effective equipment. The costs of the above mentioned techniques are very sensitive to the off-gas volume which have to be treated. Therefore, special precautions should be taken to prevent disadvantageous dilution of the liberated fission product noble gases by inleaking air or instrument air.

The main objective of the R&D program of the Kernforschungs-anlage Jülich GmbH is the development of the HTGR and the closing of the thorium fuel cycle. Therefore, also the noble gase separation techniques are specially designed for HTGR-fuel reprocessing.

2. HTGR-fuel reprocessing off-gas treatment

In the course of reprocessing spent HTGR-fuel elements, essentially all of the gaseous and volatile radioactive nuclides are released during the head-end treatment, which includes
- crushing and burning the graphite matrix of the fuel element with oxygen, air or oxygen enriched air and
- dissolution of the remaining oxide ash or particles, respectively, in Thorex-reagent.

For both head-end steps specific off-gas treatment units are under development in the KFA: The AKUT-process [8] for the burner off-gas and a helium purge-gas cycle for the dissolver off-gas resulting from an advanced type of continuously operating closed dissolver unit [9]. This type of dissolver has been developed in our institute [10] to simplify the arising off-gas problems. Its main component is a dissolver vessel closed to the surrounding atmosphere suited for the application of a helium purge-gas cycle. Therefore, the resulting off-gas is relatively rich in fission product noble gases.

In a reprocessing plant, serving for about 10,000 MW_e, approximately 240 kg/day heavy metal are dissolved yielding about 3.6 l STP/h krypton and 19.9 l STP/h xenon. The ^{85}Kr release will amount to about 350 Ci/h.

The other components of the helium-stream are nitrogen oxides, iodine, water vapor, droplets and solid aerosols as well as traces of inleaking air. No major alterations in the off-gas composition are

expected during continuous operation of the dissolver. The equipment has been designed for the treatment of the mentioned fission product noble gas rich helium carrier gas stream with a through-put of 3 m^3 STP/h helium. Flow-rate and composition of the gas stream leaving the dissolver unit are listed in <u>table 1</u>.

3.   Process description

Utilizing a carrier gas two advantages may be obtained: Firstly, an influx of relatively large quantities of air is prevented by taking constructive measures. Secondly, owing to the quantity of carrier gas supplied, the total partial pressure of krypton and xenon in the gas stream can be adjusted to such an extent that in the first succeeding cooling of the gas mixture by means of liquid nitrogen, xenon is deposited in solid form. In order to minimize the quantity of additionally frozen krypton as well as krypton dissolved in solid xenon, it is desirable to keep the partial pressure of krypton and xenon in the gas mixture as low as possible. It has been found advantageous to add to the liberated noble gases such a quantity of helium that the total partial pressure of krypton plus xenon is lowered to about 16 mbar or below. At such a partial pressure the precipitated solid xenon is contaminated with only about 0.1 vol % krypton.

3.1 <u>Separation of contaminants from the helium-stream</u>

In addition to helium and the fission product noble gases the gas mixture contains carbon dioxide, nitrogen oxides, iodine, water vapor, droplets and solid aerosols as well as small traces of air components (O_2, N_2, Ar).

To prevent freezing out and eventual plugging of piping and valves in the cryogenic part of the unit these contaminants must be removed by a gas clean-up system. To achieve this removal the following subsystems are applied:
- filtering of droplets aerosols
- filtering of solid aerosols
- chemisorption of iodine on silver impregnated silica gel (AC-6120)
- catalytic decomposition of the nitrogen oxides and simultaneous deposition of oxygen
- deposition of carbon dioxide and water vapor by adsorption on molecular sieve
- final filtering of abraded solids.

In order to obtain a higher deposition efficiency of iodine on the sorption material AC-6120 [11] the accompanying nitrogen oxides are advantageously removed after iodine filtering. At present the main experimental work is done on cryogenic separation of the noble gases. Therefore the preclean-up system provided for hot operation is only discussed concisely. A schematic block-diagram reviews the necessary processing steps <u>(Figure 1)</u>.

a.   <u>Filtering of droplet aerosols</u>

Before entering a droplet aerosol filter the temperature of the off-gas stream is lowered by a water-cooled radiator to about 20 $^\circ$C. Consequently, condensating water is deposited together with droplet aerosols in a suitable filter. A spraying system consisting of a spray pot and a spraying pump is additionally installed to improve

the self-purification of the filter from simultaneously deposited solid aerosols. By this equipment the off-gas stream is fogged. For this type of filter, f.e. in the case of a fibrous ring-layer filter, a deposition efficiency of 99.997 % for particles < 3 μ is guaranteed by the manufacturer. But up till now no utilization in nuclear technology has taken place.

b. Filtering of solid aerosols

For the removal of eventually present solid aerosols, a commercially available solid aerosol filter is put in line. Usual high-efficiency aerosol filters of the special class S result a deposition efficiency for solid aerosols of < 0.3 μ particle size to equal or better than 99.96 %. To avoid a watering of this filter the gas stream is heated to about 80 °C.

c. Chemisorption of iodine

Subsequently, the temperature of the gas stream is raised to about 150 °C to favour an optimal iodine sorption. This is achieved by fixation in two alternately operated filter cartridges, filled with the sorption material AC-6120 [11], a silver impregnated product on the basis of amorphous silicic acid. To measure and to check the efficiency of the iodine filtering device, a test filtering cartridge has been installed in the hot cells to be operated in connection with the continuous dissolver under hot conditions.

d. Catalytic separation of nitrogen oxides and inleaking oxygen

The catalytic reduction of the nitrogen oxides takes place by reaction with added hydrogen. The required temperature of about 600 °C is obtained applying an electric heater in connection with a temperature controller. The catalyst is used as bulk material laying on a conic sieve plate to enable a withdrawal to a material handling system by means of a vibrator after being spent. The function of the catalyst is controlled by measuring the oxygen and nitrogen oxide concentration before and after the catalyst bed. The outcoming hot gas mixture is than cooled down from about 700 °C to 20 °C and again condensed water is removed. Any condensed water resulting in the course of this treatment is withdrawn applying a special retainment device.

e. Process gas drying

The helium-stream will contain water vapor, corresponding to a dew-point of about 20 °C, the cooling water temperature, traces of carbon dioxide and ammonia. Prior of the low temperature separation, they will be removed by adsorption in a gas dryer filled with molecular sieve material. After a break-through of the humidity, adjusted to a limiting value of the dew-point of - 80 °C is reached, an automatical change-over to a stand-by dryer is initiated by a hygrometer, installed behind the dryer. Simultaneously, the water is withdrawn from the loaded dryer by means of a closed recovery cycle at a temperature of about 250 °C. Soon after the regeneration is finished the dryer is cooled down automatically to operating temperature.

f. Absolute filters

Before entering the cryogenic unit, the precleaned off-gas stream must pass alternately operated absolute filters of the HEPA type to guarantee complete removal of any abraded solid particles still present in the gas stream.

3.2 Cryogenic separation and concentration of the fission product noble gases and final purification of nonradioactive xenon

Separation of the crude krypton and xenon product obtained and further purification of the xenon fraction . achieved by a cryogenic system including
- two precoolers
- two pairs of alternately operated cold-traps for deposition of solid xenon and solid krypton at 80 K
- two high-pressure tanks for intermediate storage of liquid or gaseous noble gas fractions
- a low temperature distillation column for decontaminating ^{85}Kr containing xenon batches
- a charcoal adsorber bed
- a cooling tank for liquid nitrogen.

The components of the separation system are filled into a vacuum container (height: 3.6 m; diameter: 1 m) evacuated by a high-vacuum pumping station to 10^{-5} Torr. Figure 2 gives a full-view illustration of the complete plant. A schematic flow-sheet of the process is shown in figure 3.

The gas mixture arising from the preclean-up system consists mainly of helium, krypton and xenon. After entering the cryogenic part, the preconditioned gas passes a cold-trap for depositing xenon in solid form at the boiling temperature of liquid nitrogen ($\sim$ 80 K). In order to minimize thermal losses, a heat-exchanger is interconnected before the traps to precool the gas stream. The heat-exchanger is designed for lowering the temperature of the gas mixture to about 20 ° above the temperature at which freezing of xenon in the cold-trap starts so that a freezing out and eventual plugging of piping and valves is avoided with certainty. Then the deposition of xenon is carried out at a low subpressure of 0.7 bar to lower the krypton-content in solid xenon to about 0.1 vol %. Deposition efficiences of > 3 · 10^3 were achieved for xenon. In cold runs the capacity of the separators was determined to be 0.48 kg, corresponding to a loading period of 4 hours.

Then the xenon-free gas mixture is sucked from the Xe-separator by a pump (Figure 4) to be compressed by a compressor (Figure 5) to at least 6 bar. To regulate the through-put the high-pressure and low-pressure sides of the compressor are connected with a regulator valve. The compressed mixture flows to the second cold-trap to deposit krypton in the same way. At operation pressure the deposition efficiency is only about 80 %. After expansion to operation pressure of the dissolver vessel by a pressure reducing valve, remaining rest-krypton containing helium is recycled to the dissolver equipment to enable further loading with liberated fission product noble gases.

The separators are subdivided into individual chambers by radially extending thermal conducting copper sheets. Through those

the waste gas flows in axial direction, entering in the upper part of the container, called the precooling zone. It is precooled by residual gas mixture which leaves the cold-traps counter-currently. In order to provide optimal deposition areas of maximum size in the freezing zone, the number of copper sheets in the lower part is doubled in relation to the number in the precooling zone. The cooling of the deposition surfaces is effected by a tubular jacket filled with liquid nitrogen. During the regenerating period the liquid nitrogen for cooling the freezing zone is discharged to a collecting vessel. The deposited solids are rapidly thawed by a heating coil extending around the jacket.

When a sufficient quantity of xenon and krypton, respectively has been deposited, the pressure drop in the separator increases to a limiting value, so that the gas feeding is routed automatically to the second separator, while the loaded one is regenerated. To guarantee a continuous operation of the process in connection with the fuel dissolver the separating units are installed in parallel connection.

To recover deposited xenon from one of the cold-traps the container is heated to about 160-165 K to melt xenon, which is contaminated with small amounts of krypton, and to feed it through a flow metering device to a high-pressure bomb for intermediate collection or to introduce it directly to the still of the rectifying column.

The krypton deposited in the second separator in high-purity form is recovered by heating to about 120 K to enable the liquid flow to an intermediate collection tank from which it might be filled directly into steel cylinders for final storage. To remove ^{85}Kr to a content of 3 µCi ^{85}Kr/m^3 STP xenon and to get an extremely pure xenon for eventual industrial application, the previously deposited xenon-fraction must be refined. This is achieved by rectification. Therefore about 4.5 kg xenon-charges are transferred periodically to the still to be boiled under nearly total reflux. This takes place at a pressure of 2-3 bar and a temperature of about 162 K at the condenser of the rectifying unit. The cooling energy required is generated by a refrigerant which is circulated through four pipes between the condensator and the refrigerator. While ^{85}Kr-free, high-purified xenon is withdrawn from the bottom of the still to a high-pressure intermediate collection bomb by gravity feed and then to steel cylinders for further use, the Kr-fraction with some impurities of xenon is recycled from the top of the column to the helium purge-gas cycle.

In first runs unsatisfactory decontamination factors of $\sim 10^6$ were obtained. To obtain a decontamination factor of $> 10^9$, about 1 l STP of inactive krypton is added to the Xe-batch (~ 800 l STP xenon) to repeat rectification. Applying this technique, a ^{85}Kr-content of < 3 µCi ^{85}Kr/m^3 STP xenon is achievable.

To avoid an enrichment of inleaking air components (N_2, Ar) in the carrier gas stream, this must be purified from time to time by passing over a charcoal adsorber bed.

Cooling of the different components of the recovery system is achieved in all cases by liquid nitrogen from a 100 l storage tank located inside the vacuum container. The charging preferably takes

place in accordance with the principle of communicating tubes.

The complete cryogenic system is controlled automatically by a computer program.

Because the possibility of malfunction never can be excluded the cryogenic unit is connected with an additionally installed safety system including collection tanks for a total gas volume of 3 m^3 to take up the whole radioactive gas inventory of the several plant components. The connecting tubes are encapsulated by a second containment.

3.3 Bottling of the noble gas products

Pure fission product krypton and inactive xenon from the separators, respectively from the bottom of the rectifying column are transferred to the bottling system to be filled into steel cylinders and to be weighed. The piping and valves are inside of a second gas-proof containment to prevent outleaking of radioactivity. The bottling is operated automatically. Standard 50 l steel cylinders can be filled up to a pressure of 100 bar in the case of krypton and 200 bar in the case of xenon. A 50,000 MW$_e$ HTGR-reprocessing plant for example will produce approximately 30 cylinders/yr for krypton and 90 cylinders/yr for xenon. The radioactivity of ^{85}Kr per 50 l steel cylinder amounts up to about $5 \cdot 10^5$ Ci.

4. Conclusion and outlook

In summary the developed process is suitable to enable an economical separation of fission product krypton from the off-gas liberated during continuous dissolution of spent HTGR-fuel. The krypton-content of the deposited fraction in the Kr-separator is always 100 %. Furthermore, the process provides an economical method to produce high-purity and inactive xenon from nuclear fuel reprocessing for sale or further industrial application. However the most important incentive to initiate the development of this process is the small ^{85}Kr inventory arising during hot operation. In comparison to the principles of conventional air liquefaction processing, the ^{85}Kr inventory in the plant is lower by a factor of about 10^4.

The unit presented is operated with nonradioactive noble gas mixtures. At present and for the very next future experiments with nonradioactive noble gases will be continued to obtain optimal operation parameters. Then the behaviour of the unit will be tested with traces of ^{85}Kr. The result obtained from cold and tracer runs will give valuable information for the design of a dissolver off-gas clean-up system in a HTGR-fuel reprocessing prototype plant.

References

[1] Bundesanzeiger, Jahrgang 27, No. 132 vom 2. Juli 1975,
Empfehlungen der Strahlenschutzkommission auf ihrer 4. Sitzung
am 26. Juni 1975, Punkt 1:
"Abtrennung von Krypton-85 aus Abgasen von Wiederaufarbeitungs-
anlagen".

[2] Bohnenstingl, J., Heidendael, M., Laser, M., Mastera, St.,
Merz, E.:
"Cryogenic separation of krypton and xenon from dissolver
off-gas".
International Symposium on the Management of Radioactive Wastes
from the Nuclear Fuel Cycle, Vienna, Austria, 22-26 March 1976.
Paper IAEA-SM-207/20.

[3] Miquel, P., Chesne, A., LeBouhellec, J., Kroebel, R.,
Schneider, E.:
"Progress in areas of relevance to the treatment of gaseous
effluents from reprocessing plants".
International Symposium on the Management of Radioactive Wastes
from the Nuclear Fuel Cycle, Vienna, Austria, 22-26 March 1976.
Paper IAEA-SM-207/33.

[4] Collard, G., Broothaerts, J., Bruggemann, A., Goossens, W.R.A.,
Baetsle, L.H.:
"Treatment and control of gaseous effluents from light water
reactors and reprocessing plants".
International Symposium on the Management of Radioactive Wastes
from the Nuclear Fuel Cycle, Vienna, Austria, 22-26 March 1976.
Paper IAEA-SM-207/8.

[5] Takashima, Y., Segawa, T., Tsutsumi, K., Yusa, H., Nishizawa, Y.,
Ohno, M.:
"Research and development on removal of radioactive noble gases
in Japan".
International Symposium on the Management of Radioactive Wastes
from the Nuclear Fuel Cycle, Vienna, Austria, 22-26 March 1976.
Paper IAEA-SM-207/14.

[6] Bendixsen, C.L., Offutt, G.F., Wheeler, B.R.:
"Cryogenic rare gas recovery in nuclear fuel reprocessing".
Chemical Engineering, 4 Oct. 1971, p. 55-57.

[7] Hutter, E., Neffe, G., von Ammon, R., Weinländer, W.,
Leichsenring, C.H.:
"Krypton- und Xenon-Entfernung aus der Abluft kerntechnischer
Anlagen".
1. Halbjahresbericht 1975, KFK-2195.

[8] Laser, M., Barnert-Wiemer, H., Beaujean, H., Merz, E.,
       Vygen, H.:
       "AKUT - A process for the separation of aerosols, krypton and
       tritium from the burner off-gas in HTGR-fuel reprocessing".
       13th USAEC-Air Cleaning Conference, San Francisco, California,
       12-15 August 1974.

[9] Bohnenstingl, J., Koeppe, W., Mastera, St.:
       "Verfahren zum Abtrennen von Krypton aus einem radioaktiven
       Abgasgemisch und Gastrennanlage zum Durchführen des Verfahrens".
       Deutsches Patentamt, Auslegeschrift No. 2426764.

[10]   Bodewig, F.G., Johannisbauer, W., Kaiser, G., Sckuhr, P.:
       Reaktortagung des Deutschen Atomforums 1973, Karlsruhe.
       ZAED-Karlsruhe / Germany 1973.

[11]   Wilhelm, J.G., Deuber, H., Dillmann, H.G., Furrer, J.,
       Kaempfer, R., Weinert, A.:
       "Spaltjod-Abtrennung in Kernkraftwerken und Wiederaufarbeitungs-
       anlagen".
       1. Halbjahresbericht 1975, KFK-2195.

	l STP/h	Ci/h	g/h	vol %
helium	˜ 1000	–	–	97.14
xenon (stable)	19.9	–	–	2.0
krypton (stable)	3.36	–	–	0.34
krypton-85	0.24	˜ 350	–	0.024
iodine-129	–	$3.5 \cdot 10^{-5}$	0.22	–
tritium	–	$7.5 \cdot 10^{-2}$	–	–
water vapor	–	–	22.55	–
nitrogen oxides	˜ 5.0	–	–	˜ 0.5

Table 1:   Flow-rate and composition of the off-gas stream
          leaving the dissolver equipment

Figure 1: Block-diagram of the gas clean-up system
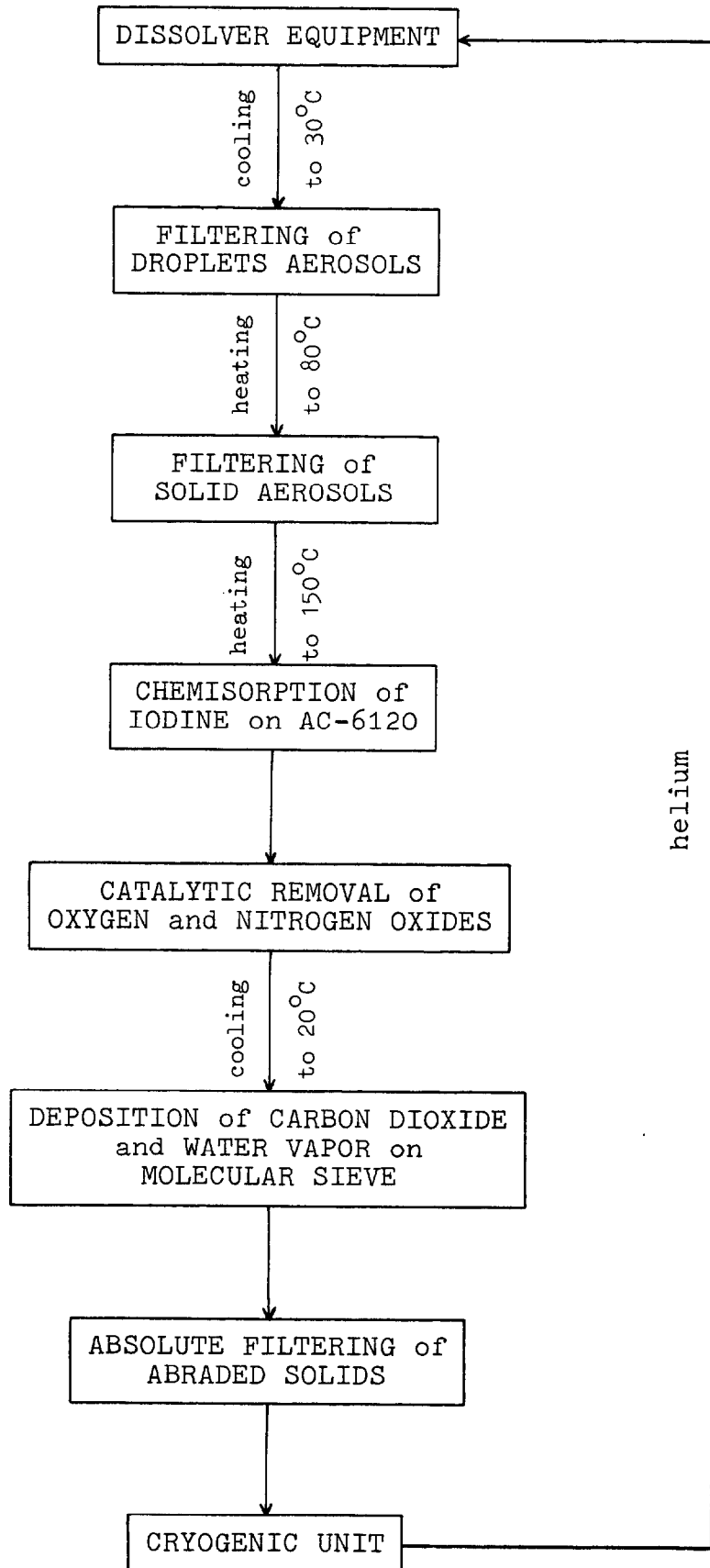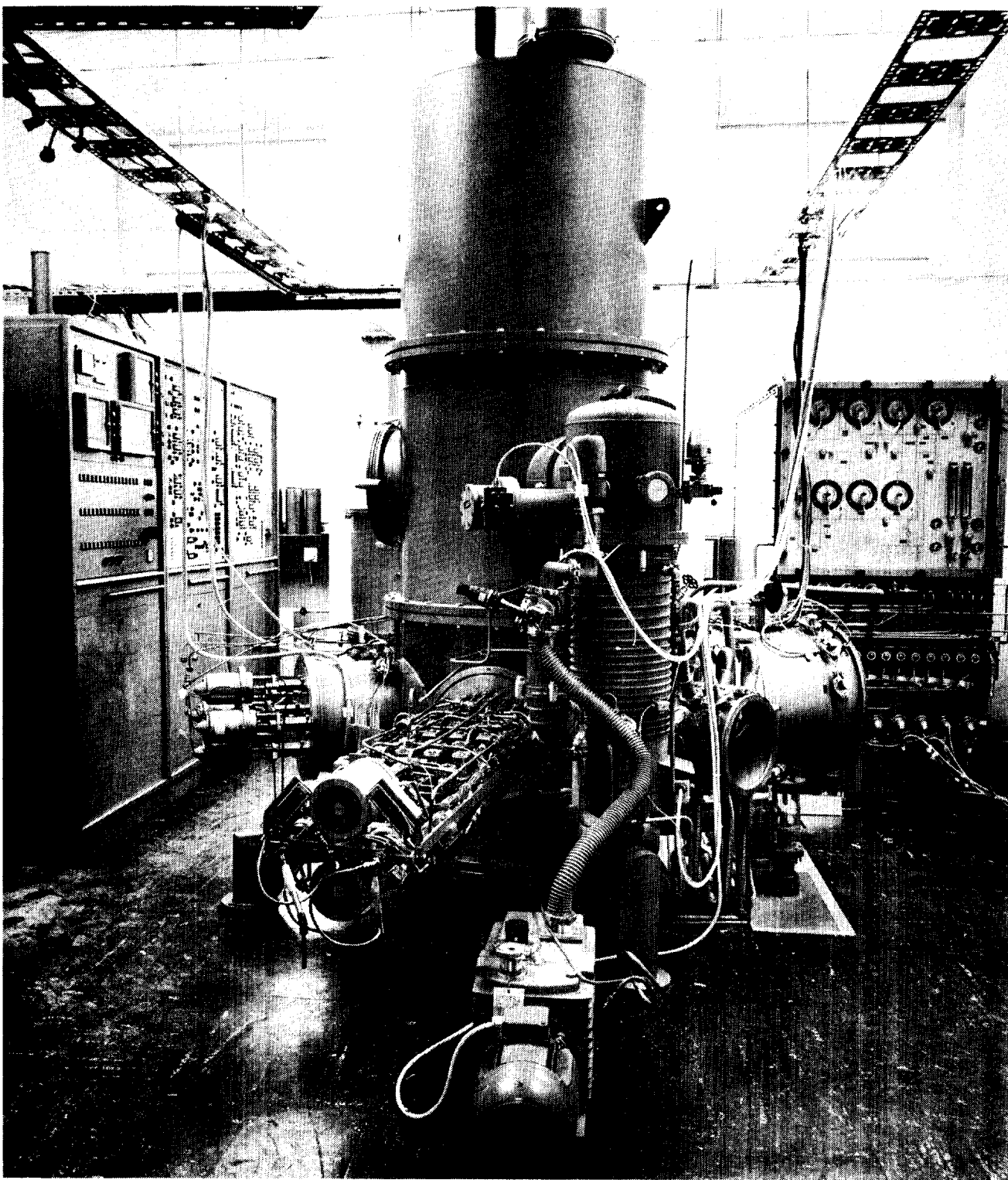
Figure 2:   Full-view illustration of the complete plant
             left: Instrument and control board
             central: Cryogenic unit
             right: Safety system

Figure 3: Flow-sheet of the cryogenic part of the helium purge-gas cycle
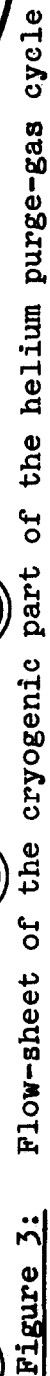
Figure 4:

Pumping station of the helium
purge-gas cycle
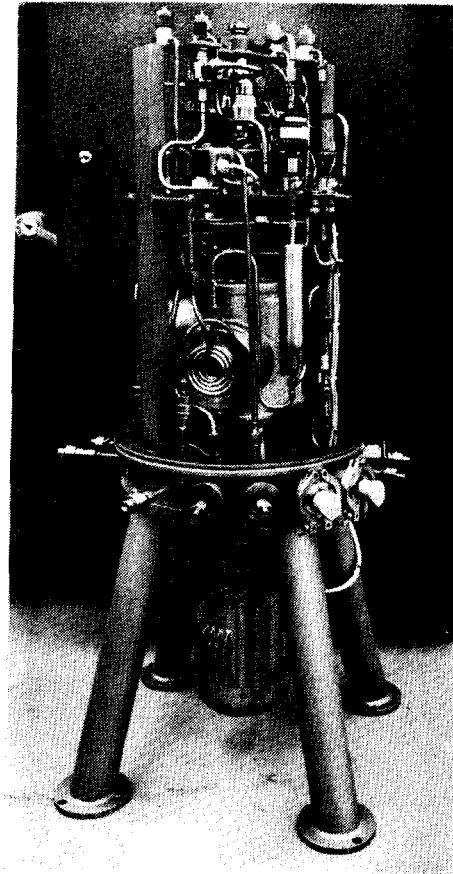
Figure 5:

Compressor station of the
helium purge-gas cycle

DEVELOPMENT OF THE FASTER PROCESS FOR
REMOVING KRYPTON-85, CARBON-14, AND OTHER CONTAMINANTS
FROM THE OFF-GAS OF FUEL REPROCESSING PLANTS*

M. J. Stephenson, R. S. Eby

Union Carbide Corporation
Nuclear Division
Oak Ridge Gaseous Diffusion Plant
Oak Ridge, Tennessee

Abstract

The Oak Ridge Gaseous Diffusion Plant has the primary responsibility for the development of the FASTER (Fluorocarbon Absorption System for Treating Effluents from Reprocessors) process for application to LMFBR and LWR fuel reprocessing plants. Krypton-85 removals in excess of 99.9% and carbon-14 as carbon dioxide removals greater than 99.99% have been obtained in a development pilot plant. So far, pilot plant tests show that the presence of other reprocessing plant off-gas components does not appreciably affect the general operability or removal efficiency of the process. Tests also indicate that the one process designed for krypton and carbon removal may be even more effective in removing other fission products and objectionable chemical contaminants such as nitrogen dioxide. Elemental and organic iodine removals in excess of 99.99% and nitrogen dioxide removals over 99% were recently achieved. Higher process decontaminations are possible. Trapping studies show that 13X molecular sieves are very effective in removing the fluorocarbon vapor from the process product stream.

I. Introduction

Stringent emission standards are being formulated to limit the release of various volatile fission products from nuclear fuel cycle facilities. At this time, the viability of the nuclear fuel cycle rests, in part, on how well the industry can effectively manage all the associated nuclear wastes. The long-lived isotopes of krypton and carbon are of particular concern because the control technology has not yet been adequately demonstrated for removing either of these two fission products from the off-gas of commercial nuclear fuel reprocessing plants. The generally straightforward problem of off-gas decontamination is greatly complicated in this case by the presence of other common reprocessing plant off-gas components such as nitrogen oxides (NO, N_2O, NO_2), carbon dioxide, water, iodine, various organics, ruthenium tetroxide, and particulates. In the case of carbon-14, it is generally assumed that the volatile form of carbon will be carbon dioxide, although admittedly, quantities of carbon monoxide and light organics such as methane could also be present.

Oak Ridge has the primary responsibility for the development of the FASTER (Fluorocarbon Absorption System for Treating Effluents from Reprocessors) process for removing krypton-85, carbon-14, nitrogen oxides, and possibly other contaminants from the off-gas of LMFBR and LWR fuel reprocessing plants. This work is being supported by the Division of Nuclear Fuel Cycle and Production of the United States Energy Research and Development Administration. The overall program is divided into four major areas: (1) process development, (2) process application, (3) solvent chemistry, and (4) reliability analysis. Process development is being done at the Oak Ridge Gaseous Diffusion Plant (ORGDP) in an existing pilot facility built specifically to study application of the FASTER process to reprocessing plants. Process application studies are being performed at both ORGDP and the Oak Ridge National Laboratory (ORNL), while the solvent chemistry work is being performed solely at ORNL. Kaman Sciences Corporation, Colorado Springs, Colorado, has been given a contract to perform the process reliability analysis. The main objective of the process development work is to generate all process technology required to completely define the fluorocarbon-based process for the reprocessing plant application. Process application studies will provide design models required for process optimization and conceptual plant design. This work will identify relative effects and importance of individual process elements and operating conditions on the overall system function. The solvent chemistry effort will establish and/or confirm component solubilities, phase relationships, component interactions, and corrosion characteristics of the fluorocarbon system. The process reliability studies proposed by Kaman will evaluate the FASTER process reliability and recommend necessary flow sheet redundancy and backup support systems to ensure a high process on-line efficiency. The overall program effort will culminate in the detailed design and economic evaluation of an off-gas decontamination facility applicable to commercial LMFBR and LWR reprocessing plants. ORGDP and ORNL share the responsibility for the LMFBR design, while the Savannah River Laboratory (SRL) has the responsibility for the LWR application.

Recent pilot plant data are presented and discussed in this report, along with the initial results obtained from the solvent chemistry program. The reliability analysis will be available later as an ORNL report. Process application work has only recently begun, and progress in this area will also be available later.

II. Pilot Plant Description

Figure 1 is a schematic of the ORGDP selective absorption pilot plant. Figure 2 is a photograph of the facility. Four packed columns comprise the main working sections of the process. The first three columns are designed to exploit certain gas-liquid solubility differences that exist between the solvent and the various volatile feed gas constituents. The solvent still, on the other hand, is designed to take advantage of vapor pressure differences between the solvent and the high boiling feed gas components. The main separation of contaminants is accomplished in the absorber. The other columns function in a variety of ways to separate and isolate the feed gas components dissolved in the solvent during the absorption step and ultimately purify the solvent for recycle. Other process equipment includes a process gas compressor, solvent pump, gas and solvent heat

DWG. NO. G-76-677

GAS
RECYCLE

CONTAMINATED
FEED GAS

N_2	NO_2	Kr
O_2	NO	Xe
Ar	N_2O	RuO_4
CO_2	I_2	CH_4
H_2O	CH_3I	H_2

SOLVENT
RECOVERY

DECONTAMINATED
VENT GAS

ABSORBER

STRIPPER I

STRIPPER II

SOLVENT STILL

VOLATILE SOLUBLE
COMPONENTS Kr, CO_2, Xe

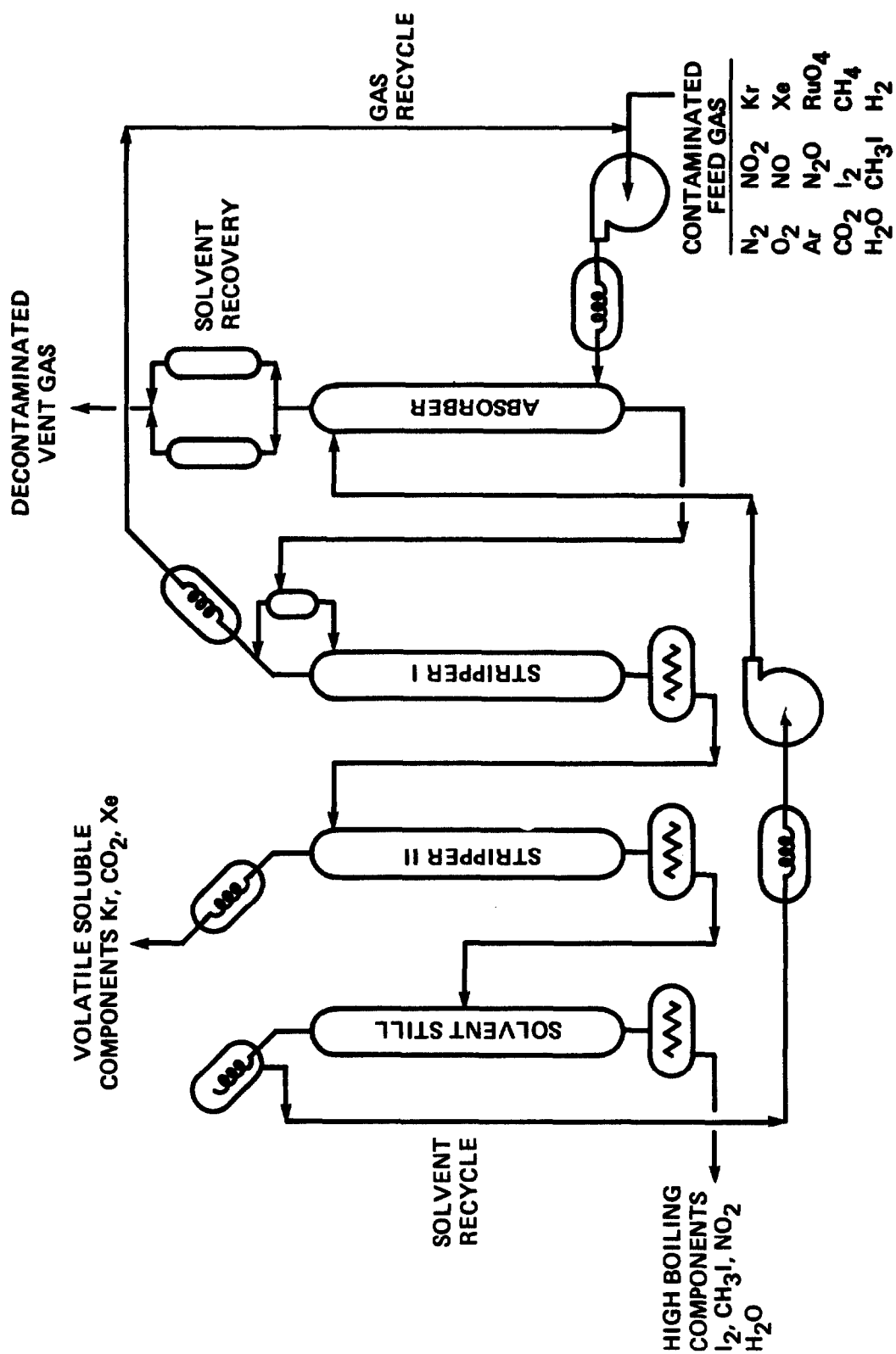SOLVENT
RECYCLE

HIGH BOILING
COMPONENTS
I_2, CH_3I, NO_2
H_2O

Figure 1. Schematic of the ORGDP Selective Absorption Pilot Plant

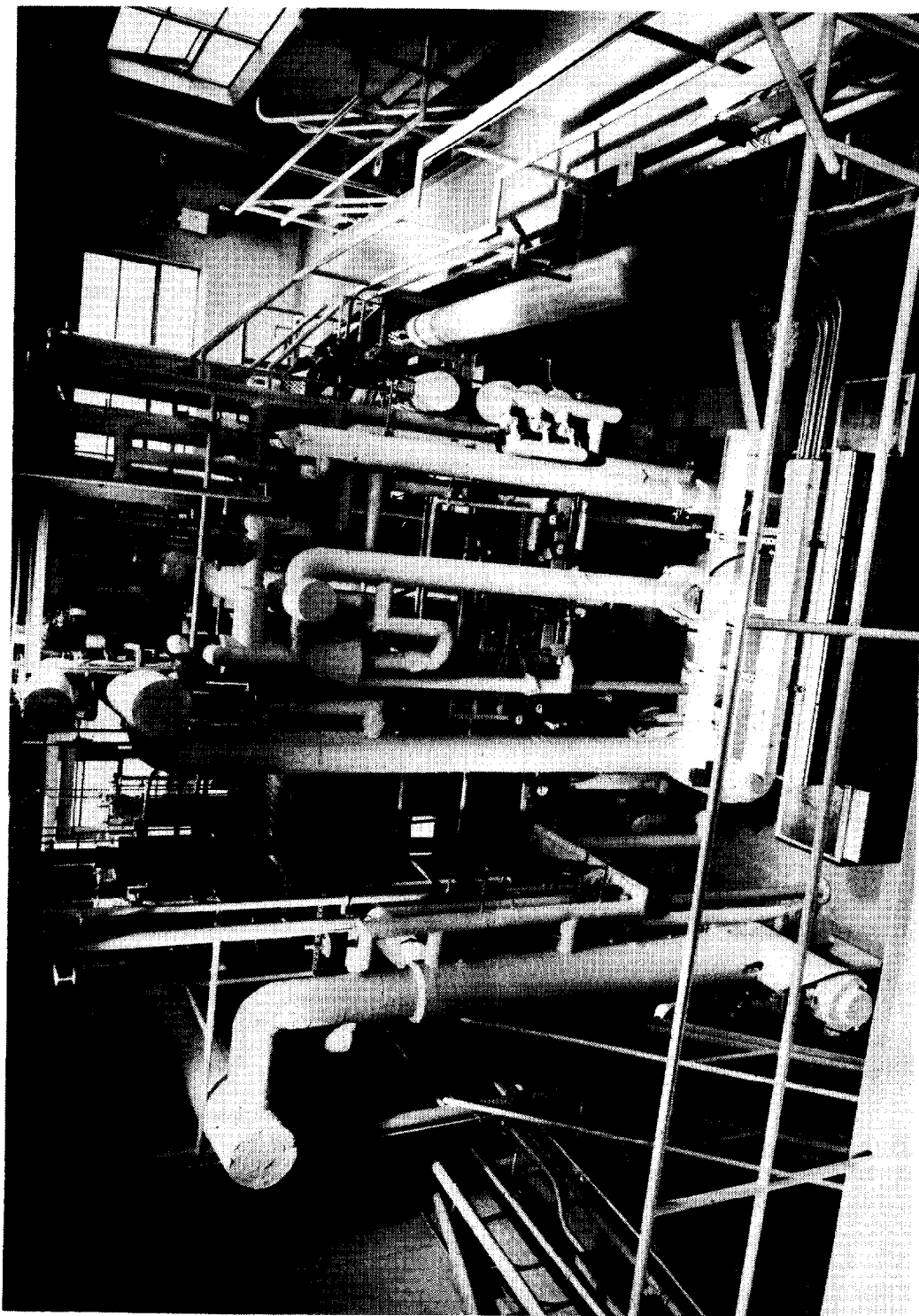Figure 2. Overall View of the ORGDP Selective Absorption Pilot Plant

exchangers, and several refrigeration compressors. Physical and chemical traps are also installed for solvent recovery and final product separation and purification. Details of the process and development pilot plant are available in several program reports[3,4,5].

III. Experimental Program Plan

As currently envisioned, the krypton-85/carbon-14 removal process will be the final step in an integrated chain of processes designed to collectively decontaminate fuel reprocessing plant off-gas. The integrity and reliability of any off-gas decontamination system will undoubtedly be the subject of much scrutiny. Legitimate concern will be expressed not so much about how well the off-gas train will function in a normal operation, but about the overall consequences of abnormal operation and the capability of the individual processes to meet the challenges imposed by irregular or otherwise uncontrolled feed conditions. In this context, several fundamental questions need to be answered: (1) what happens in the event the upstream primary removal equipment fails and large amounts of other fission products and chemical contaminants inadvertently pass downstream; (2) can the downstream process(es) be relied upon as a short-term backup system to remove the other radioactive components from the reprocessing plant off-gas in case of such a failure; and (3) how well can the fluorocarbon process function as the primary removal facility for iodine and other fission products, including ruthenium oxides, and chemical contaminants such as nitrogen dioxide. Pilot plant work is currently being directed toward exploring these points by establishing the general process behavior of feed gas components such as nitrogen oxides, iodine, methyl iodide, and water, and defining the effects of these components on the general operability and overall performance of a process designed for krypton-85 and carbon-14 removal.

Figure 3 gives the relative solubilities of various volatile feed gas components in the process solvent, refrigerant-12. Xenon and carbon dioxide are the most soluble of this group, while helium is the least. Figure 4 gives the predicted distribution coefficients of important feed gas components that are classified as high boiling components relative to the solvent. Those components more volatile than refrigerant-12 end up in either the process vent with the less soluble components, such as nitrogen and oxygen, or in the process product stream with the more soluble volatile components, such as krypton and carbon dioxide; while the less volatile components, i.e., iodine and nitrogen dioxide, collect in the solvent still reboiler. Water, not shown in figure 4, is more volatile than iodine but significantly less volatile than methyl iodide. Because krypton and xenon removals in excess of 10^3 were achieved previously, high process removals were projected for the even less volatile feed gas components.

DWG. NO. G-76-671

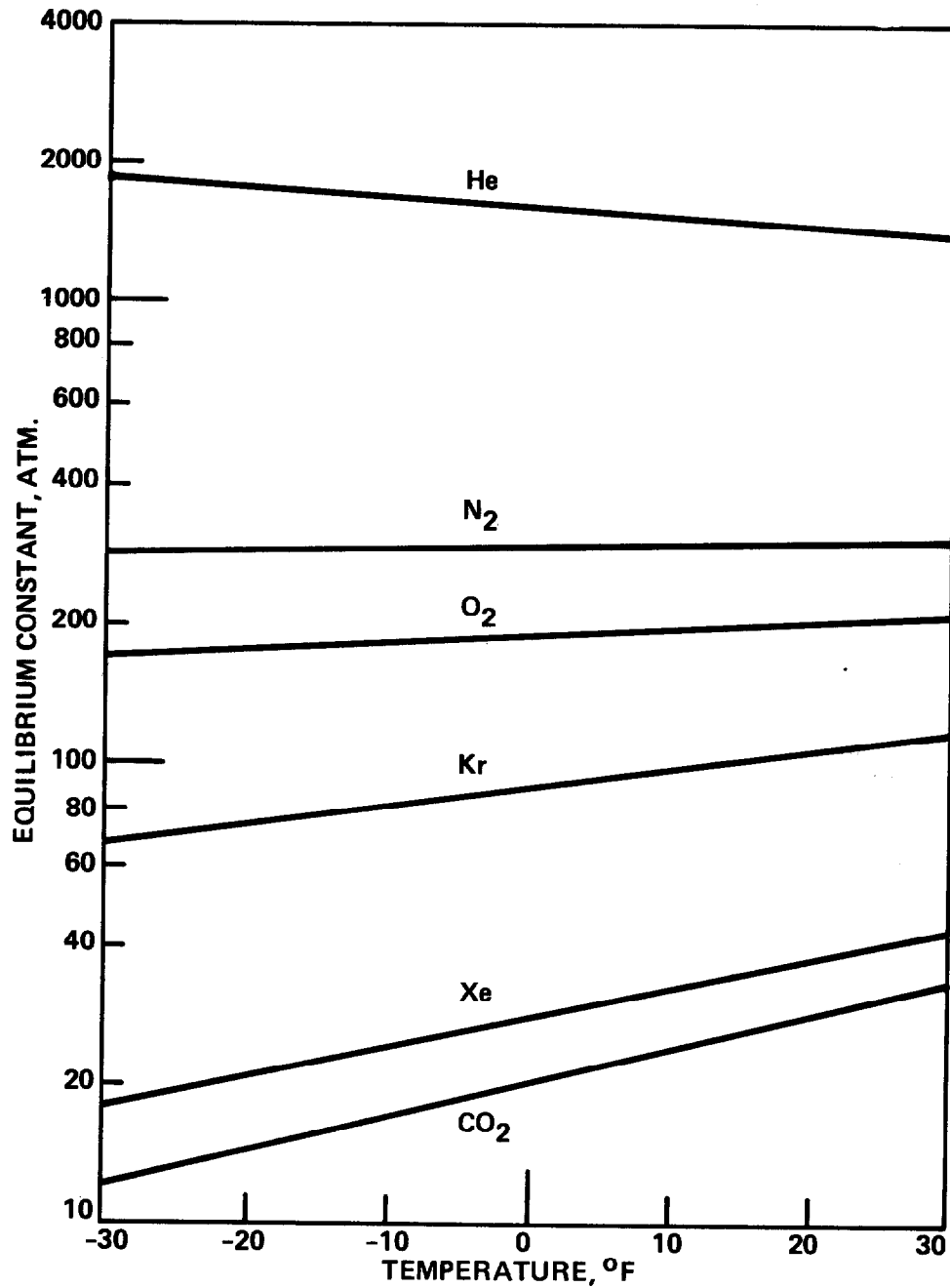Figure 3. Equilibrium Distribution Coefficients of Various
Feed Gas Components in Refrigerant-12 (CCl_2F_2).
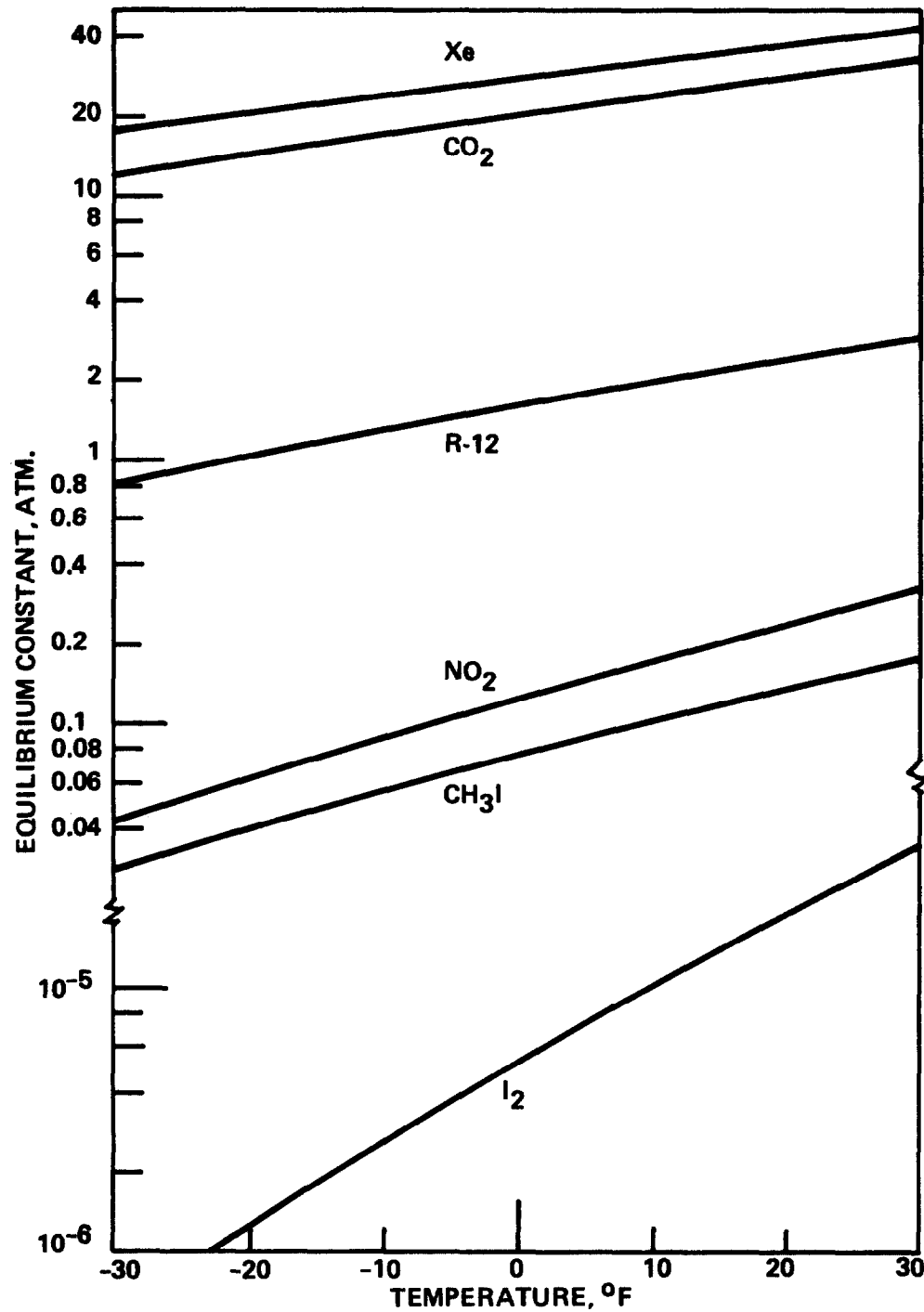
1022

DWG. NO. G-76-670

Figure 4.   Predicted Distribution Coefficients of High Boiling
Feed Gas Components in Refrigerant-12 (CCl_2F_2).

IV. Pilot Plant Test Results

Krypton absorption data were obtained several years ago and mass transfer correlations developed to describe the absorption phenomena[1,2]. Most of these tests, however, were conducted with a nitrogen feed gas containing only krypton. Recent pilot plant tests have been made with nitrogen feed gases containing (1) 0.1 ppm Kr, (2) 0.1 ppm Kr and, in addition, between 1000 and 3000 ppm CO_2 and between 6000 and 7000 ppm N_2O, (3) 0.1 ppm Kr and no feed gas cooler, (4) 0.1 ppm Xe, and (5) up to 6% carbon dioxide. The results of these tests are summarized in figure 5. Krypton tests were performed with 1 to 1.5 curies of Kr-85 and gamma scintillation techniques were used to analyze krypton process performance. Xenon tests were performed with 1 to 2 curies of Xe-133. Refrigerant-12, carbon dioxide, and nitrous oxide analyses were performed with an in-line infrared analyzer. Oxygen, nitrogen, and refrigerant-12 determinations were made with an in-line gas chromatograph and laboratory mass spectrometer. All tests were conducted at an absorber pressure of 300 psig, temperature between -25 and +10°F, solvent flow of 0.75 or 1.0 gpm, and feed gas flow between 7.5 and 22 scfm.

Pilot plant tests made with only krypton and nitrogen were repeated with high concentration of carbon dioxide and nitrous oxide (N_2O) to identify the effects of these very soluble feed gas components on krypton distribution in the system. The results of these tests suggest that, at least for the absorption step, the presence of other soluble feed gas components has no discernible effect on the process removal of krypton. Of course, the soluble components concentrate with the krypton and thereby dilute the krypton product. This problem, however, is not a very difficult one because the process product flow is only a small fraction of the reprocessing plant off-gas and can be handled in relatively small-scale equipment. Several product purification options are currently being evaluated to separate and isolate the krypton-85 and carbon-14[5].

Hot-gas feed is being considered as an alternative to desublimation of certain feed gas components such as iodine and water in the process gas cooler. In absence of the gas heat exchanger, the bottom of the absorber column will serve as the cooling section for the incoming feed gas and will allow the condensable and desublimable components to pass directly into solution. Comparison of plant tests with and without the feed gas cooler shows that the overall effect of the hot-gas feed on the process performance is small.

Xenon and carbon dioxide removals in excess of 99.99% were measured in pilot plant tests conducted at the same absorber conditions that yielded around 99% krypton removals. Carbon dioxide removals were a little higher than those measured for xenon. This is consistent with component solubilities given in figure 3. Based on pilot plant data, H_{OG} values for Xe and CO_2 were 6 to 10 inches. Significant amounts of carbon dioxide and xenon were found in the recycle solvent for those tests where final stripper molar L/V ratios above 2.0 existed. The absorber performance was noticeably affected by the recycle concentration in those cases where process removals exceeded 99.99%. Substantially better carbon dioxide removals were obtained in runs where higher stripper vapor upflows were maintained.
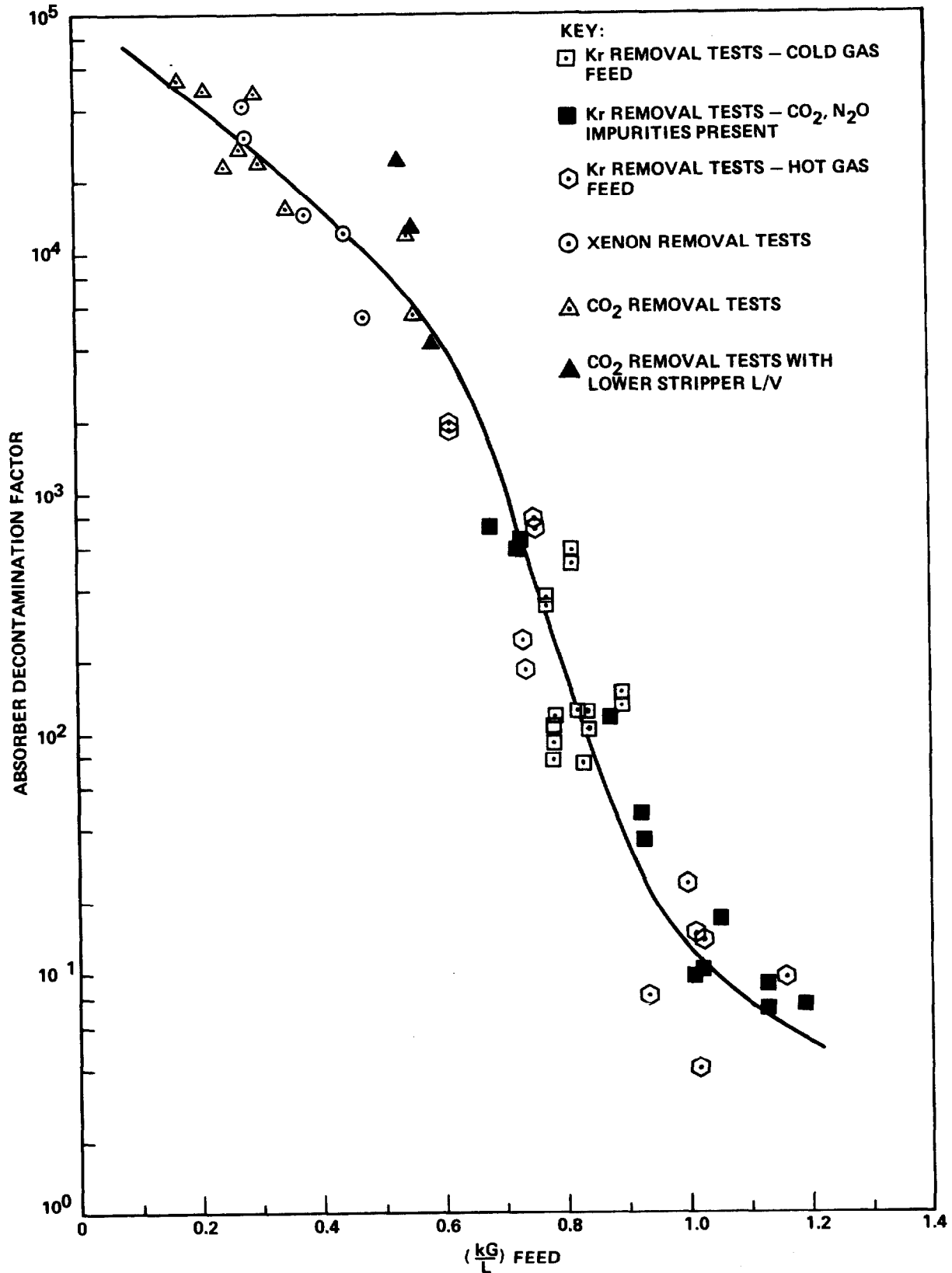
DWG. NO. G-76-753

Figure 5.   Summary of Pilot Plant Tests with
Krypton, Xenon, and Carbon Dioxide

In these cases, the stripper L/V ratio was near 1.8. At lower
stripper boilups, i.e., even when the L/V ratio was as high as 3.0,
krypton could not be detected in the recycle solvent. This observa-
tion is also consistent with component solubilities.

The results of the pilot plant tests with elemental and organic
iodine are summarized in table I. The methyl iodide tests were rela-
tively straightforward to perform and evaluate. A gas mixture was
prepared containing CH_3I traced with 5 mc of I-131 and subsequently
metered into the absorber feed gas line in the amount necessary to
give the desired feed gas composition. No transport problems were
evident. Elemental iodine, on the other hand, was difficult to feed
and reluctant to move through the feed gas circuit even though the gas
lines were heated. For these tests, solid iodine containing 5 mc of
I-131 was placed on a finely divided support screen inside a feed
cylinder and a pickup sweep gas flow was then diverted through the
cylinder and routed to the absorber. Upon contacting the solvent,
I_2 became mobile until collected in the solvent still reboiler.
Elemental and organic iodine removals in excess of 10^4 were achieved.
Gamma scintillation analytical techniques were again used to evaluate
process performance. The small amount of activity relative to the
plant size and long duration of the tests largely limited the quanti-
tative capability of the counting equipment, since process removals
were quite high and the off-gas in most cases contained an undectable
amount of iodine. In some cases, the absorber performance could be
calculated from the amount of activity in the recycle solvent by
assuming that the absorber off-gas was in equilibrium with the in-
coming solvent.

The test results clearly show that the efficiency of the process
to remove methyl iodide is definitely established by the performance
of the solvent purification still. Elemental iodine, on the other
hand, was much easier to remove from the recycle solvent. At the
conditions of the still, i.e., -10°F, the volatility of refrigerant-12
relative to methyl iodide is 24. This value is greater than 10^5 for
elemental iodine. Increasing the reflux ratio in the solvent still
from 0.13 to 0.34 (tests 7 and 8) resulted in a significant reduction
in the amount of methyl iodide in the recycle solvent and improved the
process removal efficiency by a factor of 4. The effect of any re-
cycled iodine on the process removal efficiency could not be deter-
mined because the iodine recycle concentrations were below the level
of detection. The test data clearly indicate that higher reflux
ratios and more rectifying stages will significantly improve the
recovery capability of the process. It is important to point out
that water and elemental iodine are significantly less volatile than
methyl iodide, and consequently, these two components are much easier
to remove from the solvent. Therefore, a process designed to achieve
a methyl iodide decontamination factor of 10^6 should be capable of
even higher elemental iodine and water removals.

The results of the nitrogen dioxide removal experiments are
summarized in figure 6. More than 2 months of the recent test series
was devoted to studying the long-term process behavior of NO_2. A
spectrophotometric analyzer having the capability of detecting from
1 to more than 6,000 ppm NO_2 was used for direct in-line concentration
determinations. Process removal efficiencies between 97 and 99.9%

Table I. Summary of Iodine Removal Tests*

Test Number	Iodine Form	Solvent Recycle	Still Reflux Ratio	Absorber Feed Gas Concentration, ppm	Measured Decontamination Factor†	Measured Decontamination Factor§
1	I_2	No	–	~ 0.01	$> 10^4$	–
2	I_2	Yes	**	~ 0.01	$> 10^3$	–
3	I_2	Yes	0.01	~ 0.01	$> 10^4$	–
4	CH_3I	No	–	136	$> 6 \times 10^4$	–
5	CH_3I	Yes	0.01	7	$> 2 \times 10^3$	1.5×10^4
6	CH_3I	Yes	0.34	248	$> 2 \times 10^4$	5.9×10^4
7	CH_3I	Yes	0.34	28	$> 2 \times 10^3$	4.0×10^4
8	CH_3I	Yes	0.13	28	$> 2 \times 10^3$	1.0×10^4

* General Test Conditions: Absorber Pressure, 300 psig; Absorber Temperature, -10°F; Solvent Flow, 1 gallon/minute.

† Based on absorber gas inlet and outlet stream I-131 analysis.

§ Based on absorber gas inlet and recycle solvent stream I-131 analysis and assumption that the absorber off-gas is in equilibrium with the recycle solvent.

** Solvent still partially by-passed.
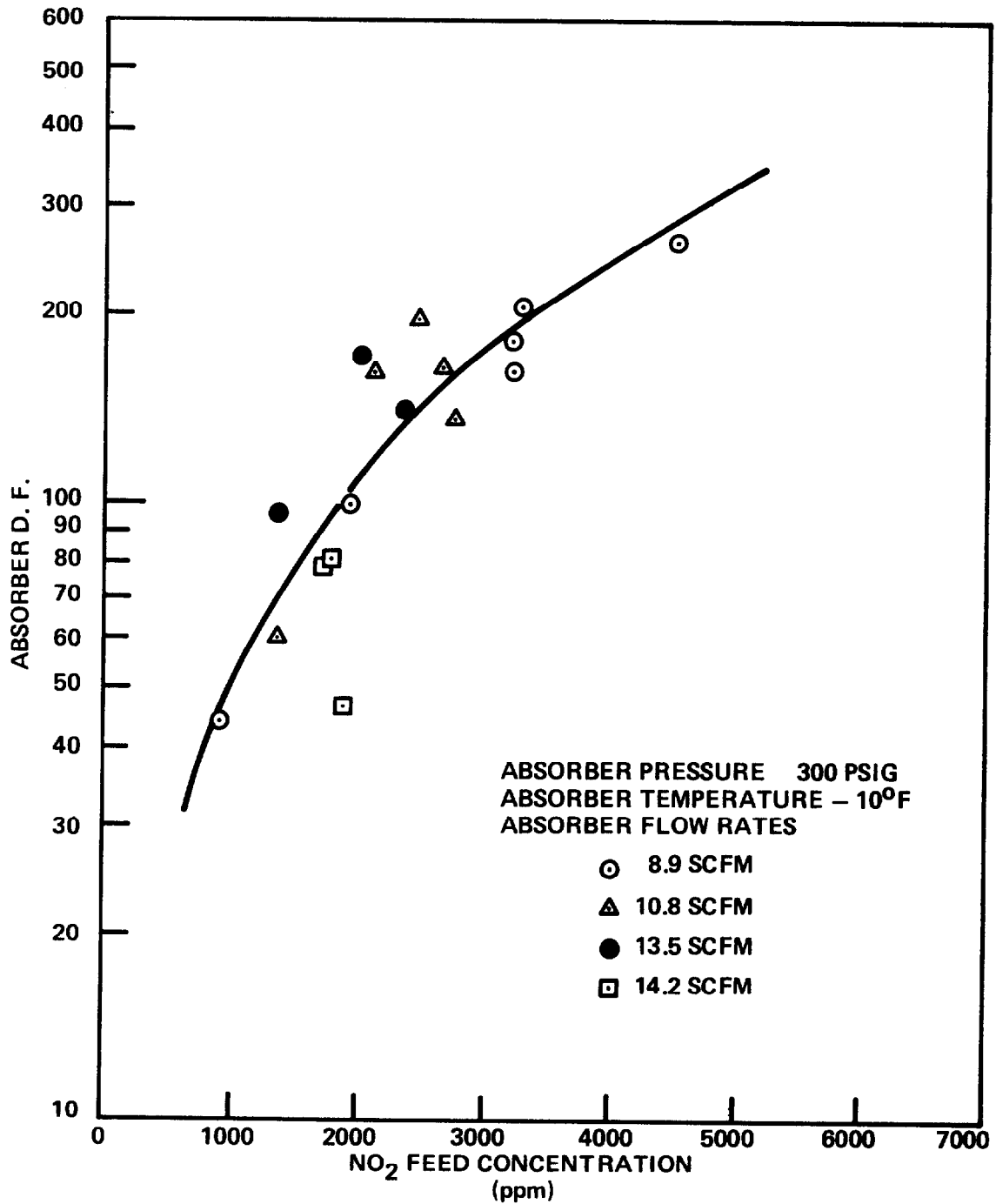
DWG. NO. G-76-668

Figure 6.   Fluorocarbon Process Removal of Nitrogen Dioxide
as a Function of Feed Gas Composition.

were achieved. No feed problems were encountered, and process effects due to the presence of the NO_2 in the feed gas and solvent lines were not observed. The data suggest that the removal of NO_2 is strongly dependent upon the feed concentration. This is contrary to previous experience with the less volatile components, I_2 and CH_3I, and the more volatile components, krypton and xenon. For one series of tests, the concentration of NO_2 in the absorber off-gas remained around 20 ppm regardless of the absorber feed gas flow or inlet concentration. This, of course, again indicates inadequate removal of high boiling components from the recycle solvent. The absorber off-gas concentration did decrease with an increase in the solvent still reflux but not to the extent that was found for the methyl iodide tests. This was not surprising since NO_2 is more volatile than CH_3I and thereby more difficult to remove from the solvent.

Another important part of the overall ORGDP development program is evaluation of process auxiliary subsystems. As part of this work, trapping studies were initiated to evaluate solid adsorbents for removing refrigerant-12 vapor from the process vent and krypton product. The results of these tests are given in table II. An ideal sorbent was identified as one that could reduce the refrigerant concentration in the process off-gas from a nominal 10% to less than 1 ppm. Three sorbent materials were initially considered: 5A molecular sieve, 13X molecular sieve, and H-151 alumina. Tests were conducted with 3-inch-diameter traps filled to a height of 4 feet with the test material. Initial bed temperatures were generally around 70 to 80°F. Tests were conducted with a total gas flow (R-12 and N_2) of 1934 sccm (0.02 ft/sec superficial velocity), 11,670 sccm (0.08 ft/sec), and 120,000 sccm (0.8 ft/sec). The 5A molecular sieve material proved to be unsatisfactory. Trap effluent contained 8.2 ppm before breakthrough, and the sorbent loading was only 0.5% at breakthrough. The alumina bed still could not achieve the desired refrigerant vapor removal. The trap effluent contained 10 ppm before breakthrough and refrigerant loading on the alumina varied between 2.2 and 2.9%. On the other hand, the 13X molecular sieve proved to be an excellent trapping material for the process solvent. The trap effluent contained less than 1 ppm R-12 and the 13X sieve loaded up to 30%. External cooling of the sorbent bed improved the loading capacity of the sieves. Regeneration studies showed that the loaded 13X sieves could be completely regenerated with a 350°F nitrogen sweep flow of 194 lpm in 6 to 7 hours.

V. Solvent Chemistry

The laboratory support work is being performed at ORNL by L. M. Toth, J. T. Bell, and D. W. Fuller. The initial program is designed to evaluate distribution coefficients of the various feed gas components in refrigerant-12, look at component interactions in a multicomponent system, and identify possible corrosion conditions that could develop. Undoubtedly, this important effort will be expanded as the program progresses. Work in this area was only initiated recently but a substantial amount of data has already been obtained. Several aspects of the physical and chemical behavior of I_2 in R-12 have been examined by absorption spectrophotometry in a high pressure optical cell. Iodine in R-12 has an electronic absorption band in the visible light region at 520 nm arising from a solvated I_2 molecular species.

Table II. Summary of R-12 Adsorption Studies for the Product
Purification and Solvent Recovery Subsystems

Test Number*	Adsorbent	Cycle	Total Feed Flow, sccm	Feed Composition†, % R-12	Bed Temp., °F Initial	Final	Breakthrough Time hr	% R-12§	R-12 in Effluent Before Break, ppm	Regeneration Scheme Temp., °F	Time, hr
1	5A Sieve	1	1,934	9.5	65	∿65	0.45	0.40	8.2	375	2.2
2	H-151 Alumina	1	1,934	9.5	75	∿75	2.50	2.3	10.1	440	3.6
3	H-151 Alumina	2	1,934	9.5	69	∿69	2.00	1.9	10.7	430	1.7
4	H-151 Alumina	3	11,670	10.0	77	88	0.30	1.7	19.0	420	1.5
5	13X Sieve	1	1,934	9.5	75	98	19.50	25.9	<1	375	4.0
6	13X Sieve	2	11,670	10.0	78	127	2.67	22.3	150**	330	6.0
7	13X Sieve	3	11,670	10.0	85	139	2.67	22.0	<1	350	7.7
8	13X Sieve	4	11,670	10.0	68	86††	2.92	24.8	<1	360	6.5
9	13X Sieve	5	1.2×10^5	3.1	73	85††	1.17	30.6	<1	350	6.0
10	13X Sieve	6	1.2×10^5	3.1	73	87††	1.12	29.5	<1	360	6.0
11	13X Sieve	7	1.6×10^5	2.3	88	145	0.5	13.3	<1	360	6.0
12	13X Sieve	8	1.6×10^5	2.3	75	113††	0.7	18.4	<1	340	6.0

* All tests except 11 and 12 conducted at 4.5 psig in a nominal 3-inch-diameter trap with 0.0513 ft² (47.6 cm²) cross section. Tests 11 and 12 were made at 21 psig.

† The bulk gas is nitrogen.

§ R-12 loading defined as [(lb R-12 adsorbed)/(lb adsorbent)] × 100.

** The previous regeneration of 375°F for 4 hours was not sufficient to regenerate the 13X sieve loaded during the previous test; hence, the high concentration of R-12 in the effluent.

†† These tests conducted using external bed cooling.

In the absence of any added water, dilute solutions of iodine in refrigerant-12 are not expected to chemically react with either the solvent or stainless steel containment. There is some indication, however, that refrigerant-12 solutions of iodine containing excessive amounts of free water might interact with stainless steel. The solubility and distribution coefficient of iodine is currently being measured as a function of temperature. Later, the solution effects of free water will be determined.

VI. Conclusions

Recent and more detailed pilot plant tests continue to support hypotheses drawn from earlier scoping tests and performance calculations[1]. In short, the fluorocarbon-based process is versatile, has a high tolerance for feed gas impurities, and can function in a multiplicity of ways to clean up reprocessing plant off-gas and isolate the many contaminants for long-term storage and disposal. Tests show that a process designed to remove krypton-85 and carbon-14 can also achieve high iodine, methyl iodide, water, and nitrogen dioxide decontaminations. A comprehensive pilot plant testing program and an exhaustive solvent chemistry laboratory effort are continuing to fully define the capability and limitations of the FASTER process. If the process development program proceeds according to schedule, sufficient information will be available within 3 years to begin final design of an LMFBR or LWR demonstration plant. So far, no detrimental effects due to the presence of the various feed gas components in the fluorocarbon process have been uncovered except maybe a possible corrosion problem that could develop in a stainless steel system if free water is present. Materials of construction will be selected after the solvent chemistry work has been completed and possible corrosion mechanisms identified. Substantially more testing is required at this point before the process can be fully evaluated.

VII. References

[1] J. R. Merriman, Analysis of a Multicomponent Gas Absorption System with Carrier Gas Coabsorption, U.S.E.R.D.A. Report KY-G-300, Paducah, Kentucky (1975).

[2] M. J. Stephenson, et al., "Experimental demonstration of the selective absorption process for Kr-Xe removal", Proceedings of the Twelfth AEC Air Cleaning Conference, 11-27 (1973).

[3] M. J. Stephenson, et al., "Absorption process for removing krypton from the off-gas of an LMFBR fuel reprocessing plant", Proceedings of the Thirteenth AEC Air Cleaning Conference, 263-275 (1975).

[4] M. J. Stephenson, et al., Fluorocarbon Absorption Process for the Recovery of Krypton from the Off-Gas of Fuel Reprocessing Plants, U.S.E.R.D.A. Report K-GD-1390, Oak Ridge, Tennessee (1976).

[5] M. J. Stephenson and R. S. Eby, ORGDP Selective Absorption Pilot Plant for Decontamination of Fuel Reprocessing Plant Off-Gas, U.S.E.R.D.A. Report K-1876, Oak Ridge, Tennessee (In Progress).

DISCUSSION

GRADY: How much additional research and development is required before the FASTER process will be sufficiently developed to design a commercial fuel reprocessing plant?

EBY: We feel that within three years, we will have sufficient design and application information to begin the design of a facility for a commercial fuel reprocessing plant.

STUART: What is the anticipated krypton content coming from the stripper?

EBY: The pilot plant is designed to achieve a krypton factor between 10^4 and 10^5.

STUART: What would that be in terms of what percentage of krypton in the total gas stream?

EBY: From 10-50%.

R. A. BROWN: You mentioned limitations. What do you consider to be the major limitations of a fluorocarbon absorption process?

EBY: That is what we are trying to find out right now.

R. A. BROWN: Do you now anticipate any serious limitations?

EBY: We are presently working on a solvent chemistry program and we are studying solubility limitations and possible corrosion effects. This may be a problem, but right now we don't know. We think it is a very versatile process.

MURBACH: What are you going to do with the absorbed NO_2?

EBY: The NO_2 collects in the solvent still reboiler, and then, depending on its concentration, can either be recycled back to the dissolver or disposed of.

VAN BRUNT: What is the rate of ratiolytic decomposition of the solvent?

EBY: G values have been measured from Refrigerant-12 and are around four. We don't consider this important as the quantities will be small and the principal decomposition products will be R-113, R-114, which will collect in the solvent still reboiler.

VAN BRUNT: Do you forsee any significant hydrochloric acid formation?

EBY: This may be possible. We don't consider this a problem though.

SKOLRUD: In regard to solvent cleanup applications of the FASTER process, what is proposed for recovery and final conversion

of absorbed iodine and organic iodides?

EBY: These components will collect in the solvent still reboiler along with the NO_2 and will be reacted to a suitable solid form for storage.

HTGR–REPROCESSING OFF–GAS CLEANING BY THE AKUT–PROCESS

H. Barnert-Wiemer, H. Beaujean, M. Laser, E. Merz, H. Vygen
Kernforschungsanlage Jülich   GmbH
Institute for Chemical Technology
5170 Jülich / GERMANY

Abstract

During reprocessing of HTGR-fuel the graphite matrix has to be removed in order to gain the heavy metal, which is accomplished by burning the crushed fuel elements. During the burning part of the krypton and tritium is released from the fuel. Since the combustion gas is a mixture of CO_2 and O_2, the burner off-gas consists mainly of CO_2 with a small amount of CO and fission products, mainly in gaseous form but also aerosols.

A facility, called AKUT II, which consists of the following process steps
- aerosol removal by electrostatic precipitators followed by HEPA-filters
- catalytic conversion of CO and O_2 to CO_2
- compression and liquefaction
- separation of krypton by distillation
- adsorption of tritiated water on molecular sieve
is now being installed in the KFA hot cells. The facility will be ready for cold operation early in 1977. After start-up of the HTGR-reprocessing pilot plant JUPITER the off-gas from the head-end will be treated in the AKUT facility.

Introduction

Hot tests with a smaller facility - AKUT I, throughput 1-3 m^3/h STP - were carried out in 1974. A review of those tests and of preliminary cold tests has been presented at the 13th USAEC Air Cleaning Conference [1]. Experience with the AKUT I facility has led to the construction of an improved and scaled-up AKUT II facility with a throughput of 10-20 m^3/h STP. Extensive tests with simulated off-gas are planned before the AKUT facility will be connected to the JUPITER pilot plant.

In the JUPITER head-end the AVR fuel elements, which contain (U/Th)O_2 fuel particles, will be crushed and burned in a fluidized bed burner, which will be operated with a CO_2-O_2-combustion gas. In steady state the off-gas will contain ~ 90 % CO_2, ~ 10 % CO, nil O_2, ~ 1 ppm Kr, and ~ 1 ppb T. Since the burner is operated at low pressure, inleakage of air from the cell atmosphere may result in small amounts of O_2 and N_2 in the off-gas. CO and O_2 are converted to CO_2 in a catalytic burner. The off-gas is then compressed, condensed and distilled to produce both a krypton-rich product stream and a purified liquid stream. The distillation will be operated at temperatures between 0 °C and 20 °C at the column inlet and pressures between 35 and 100 bar, depending on the amount of light gases whose behavior in the distillation column needs to be further investigated. According to MERZ et al. [2] it is expected that krypton is concen-

trated faster at the top then the light gases. The tritium - in the form of tritiated water - leaves the column with the bottom stream from which it is removed by molecular sieve.

Facility description

Simplified process flowsheet

The AKUT II flowsheet is shown schematically in Figure 1. The feed gas - from gas cylinders or, in a later phase, from the JUPITER facility - enters at room temperature. During cold tests the electrostatic precipitators (EF 1 and EF 2) are not needed and are bypassed. During hot tests one precipitator is in use while the other one is cleaned with water and afterwards dried by heating the outside and purging with CO_2. Figure 2 shows the electrode, the casing with the heating elements and a completely assembled precipitator. The precipitators and the tank for the wash water are placed in a shielded (50 mm lead) air tight box in which a low pressure of 10 mm H_2O is maintained. The box for the HEPA-filters FF 1 and FF 2 is also kept at low pressure but is not shielded, because in earlier hot tests [1] it was found that practically all aerosol activity was removed by the electrostatic precipitator.

After the filter step the off-gas is fed into the catalytic converter system, in which by means of the blower K 2 so much CO_2 is constantly recycled that even an off-gas consisting of 100 % CO is sufficiently diluted that it can be converted to CO_2 without damaging the catalyst CTK 1 or reaching the explosion limits of a CO_2-CO-O_2- system. The reaction heat is removed by water cooler WT 1. The recycle gas remains at the working temperature of the palladium catalyst, so that the electrical heating is only needed for start-up or to make up for heat losses of the gas to the environment. Behind the entrance point of the off-gas into the recycle stream the CO and O_2 contents of the recycle stream are measured. Utilyzing these data the control valves for additional CO or O_2 are operated. After the catalytic conversion the gas should not contain more than 0.1 % O_2 or CO.

When the gas leaves the converter it is cooled to ambient temperature in heat exchanger WT 2. It is then fed to the three stage piston compressor K 4. The compressed gas is cooled and condensed in the main compressor surge tank TK 1, which is water cooled, and the heat exchanger WT 4, which is cooled by refrigerant (a silicon oil) of - 30 $^\circ$C from the refrigeration unit. Tank TK 1 is designed to hold the entire liquid charge of the high pressure part of the facility without need for cooling.

The liquefied gas is fed into the distillation column. The column has an inner diameter of 40 mm and a height of 5.4 m without condenser and reboiler. The maximum height of the column was pre-determined by the space available in the hot cells. The column has 5 gas-liquid sampling points (Figure 3) and 4 sections of packing (wire spirals 4 x 4 mm, Figure 4) between the samplers. Column performance has been tested with air and water. Figure 5 shows generalized flooding curves: No. 1 for the wire spirals, determined with air/H_2O; No. 2 for Goodloe packing, determined with CO_2/CO_2 (according to ORNL data [4]); No. 4 for the samplers, determined with air/H_2O and No. 3 gives the calculated values for wire spirals and

Goodloe packing, where

u_m = superficial gas velocity — m/s

ρ_g and ρ_L = gas and liquid density — kg/m^3

μ_L = liquid viscosity — cP

L and G = liquid and gas mass — kg/h

g = gravitational constant — m/s^2

The samplers, except the ones at top and bottom, can also be used as feed points, so that the most advantageous feed point can be determined.

The reboiler has two capacitance type liquid level probes and is flanged with a 5 kW electrical immersion heater. The condenser is of annular shell-and-tube construction with the process fluid on the shell side. The internal volume is reduced by use of a displacement body. Refrigerant enters through the upper cap via three tubes. The three refrigerant coils are arranged in three coil banks. The three tubes leave the lower cap separately and exit on a common header. Should any O_2 or CO accumulate at the top of the condenser, it can be withdrawn and fed back into the surge tank NDB 1 before the catalytic converter.

The product from the top can be withdrawn in liquid or gaseous form. It is pumped into cylinders at a maximum pressure of 150 bar at ambient temperature.

The purified liquid from the bottom is heated in heat exchanger WT 6 and expanded to 20 bar. Before expansion to atmospheric pressure tritium absorbers (Figure 6) are intended to be put in. The gaseous CO_2 which contains traces of tritiated water is fed to absorber I while the second one is regenerated with hot CO_2. The hot regeneration gas is cooled to ambient temperature. The water condenses and flows into waste tank WTK. The regeneration gas is reintroduced into the burner off-gas. The purified off-gas from absorber I is then used to cool the regenerated absorber II and is then expanded to atmospheric pressure and, after passing a HEPA-filter, is released to the atmosphere. Laboratory tests have shown that at 20 bar and 0 $^{\circ}$C and a gas velocity of 0.05 m/s 1000 g 4 Å molecular sieve will absorb 160 g H_2O. For regeneration ~ 0.9 m^3 CO_2 per kg molecular sieve will suffice. This type of molecular sieve has already be tested for tritium removal in earlier hot tests [3].

The tritium absorption system is scheduled to be designed this year and to be put into the facility in the first half of 1977.

Sampling and analysis

System variables such as temperature, pressure, flowrate and concentrations at some points (e.g. in-line Kr-monitoring at column entrance, top, and bottom; O_2 and CO concentrations in the catalytic converter etc.) are necessary for process control and are routinely measured. Additional data, which are necessary for quantitative treatment of experimental results, are made available by drawing gas and liquid samples from the column, the top and bottom streams and several tanks. The concentration of ^{85}Kr is measured with beta scintillation cells. For nonradioactive components of the samples, a mass spectrometer will be used. This instrument is capable of

detecting atomic mass units in the range 2 to 300 and trace impurities in gases down to 2 ppm.

Facility control

The facility has a main control panel, a sampling station, which contains instruments and manually actuated solenoid valves needed for sampling, and a transmitter station. The refrigeration unit has its own small control panel.

Status of the facility installation

As was mentioned before the facility is now being installed in the KFA hot cells on the roof of the hot cell row in which the JUPITER facility is housed. The catalytic converter is the first unit to be tested. It was mounted in a rack and was transported to the hot cells as a complete unit. It is now being connected to the main control panel and as much piping as is necessary for the separate testing of this unit is being fitted. Function tests of the catalytic converter are scheduled for August 1976.

The condenser and reboiler will be welded to the column in August. The complete column will be placed in a rack in the machine shop. Into this rack the boxes with the electrostatic precipitators and the HEPA-filters will later on be mounted. They are not needed for the preliminary cold tests. All parts have been delivered and the final assembling is scheduled to begin in September 1976. Cold tests are expected to start in February 1977.

References

[1] M. Laser et al.:
"AKUT - A Process for the Separation of Aerosols, Krypton and Tritium from Burner Off-Gas in HTR Fuel Reprocessing".
13th AEC Air Cleaning Conference, San Francisco, California/USA, 12-15 August 1974.

[2] E. Merz et al.:
"Verfahren zum Abtrennen von Krypton aus einem bei der Verbrennung graphithaltiger Kernbrenn- und/oder -brutelemente anfallenden Abgas".
DP 24 37 810.

[3] H. Beaujean et al.:
"Reinigung der Verbrennungsabgase bei der Wiederaufarbeitung von HTR-Brennelementen".
JÜL-925-CT (1973).

[4] R. W. Glass et al.:
"Development of the Krypton Absorption in Liquid Carbon Dioxide (KALC) Process for HTGR Off-Gas Reprocessing".
13th AEC Air Cleaning Conference, San Francisco, California/USA, 12-15 August 1974.

Figure 1: Simplified flowsheet of the AKUT II facility
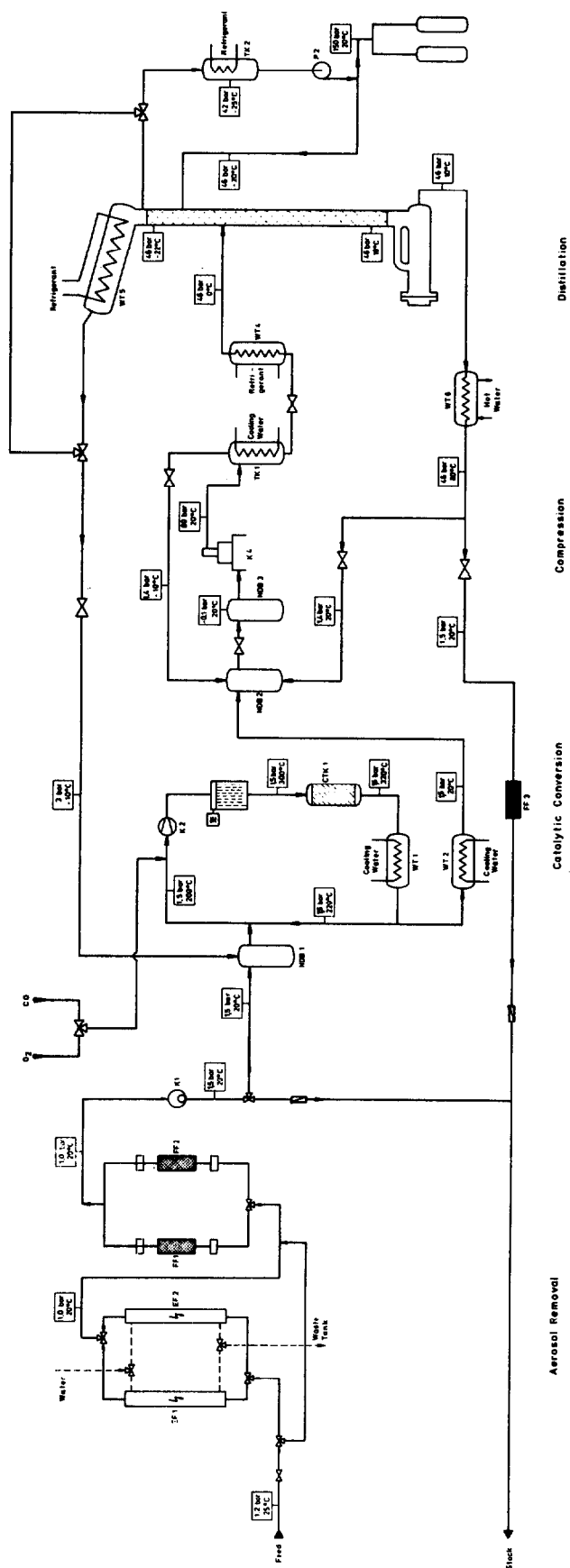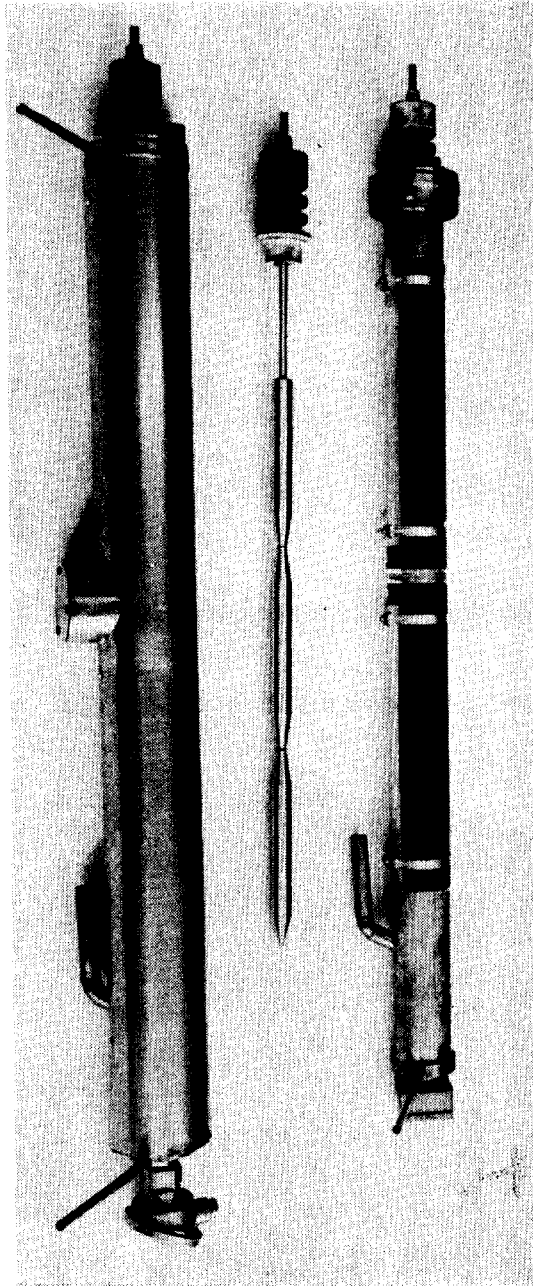
Figure 2:   Electrostatic precipitator
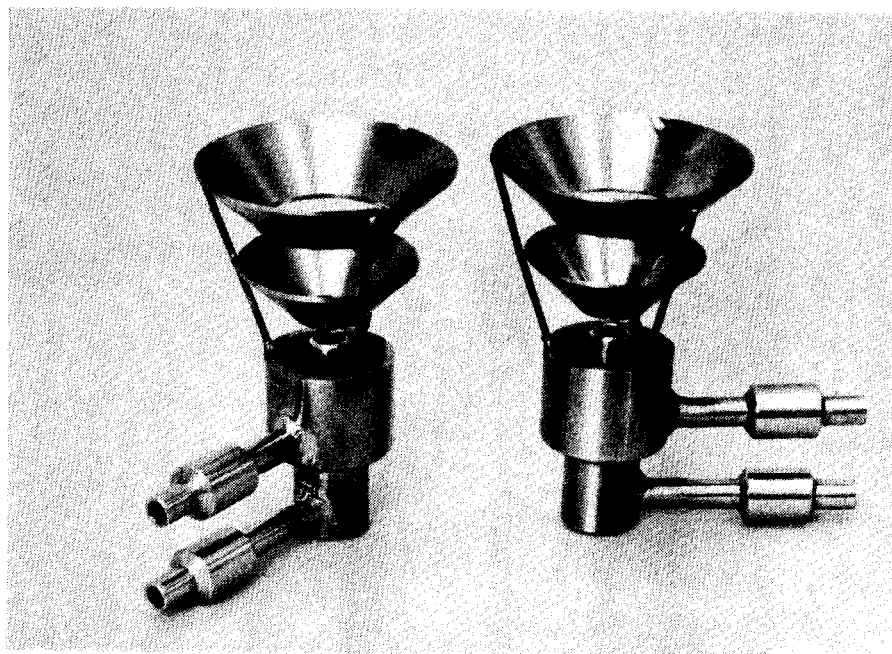
Figure 3:   Gas-liquid samplers in the distillation column
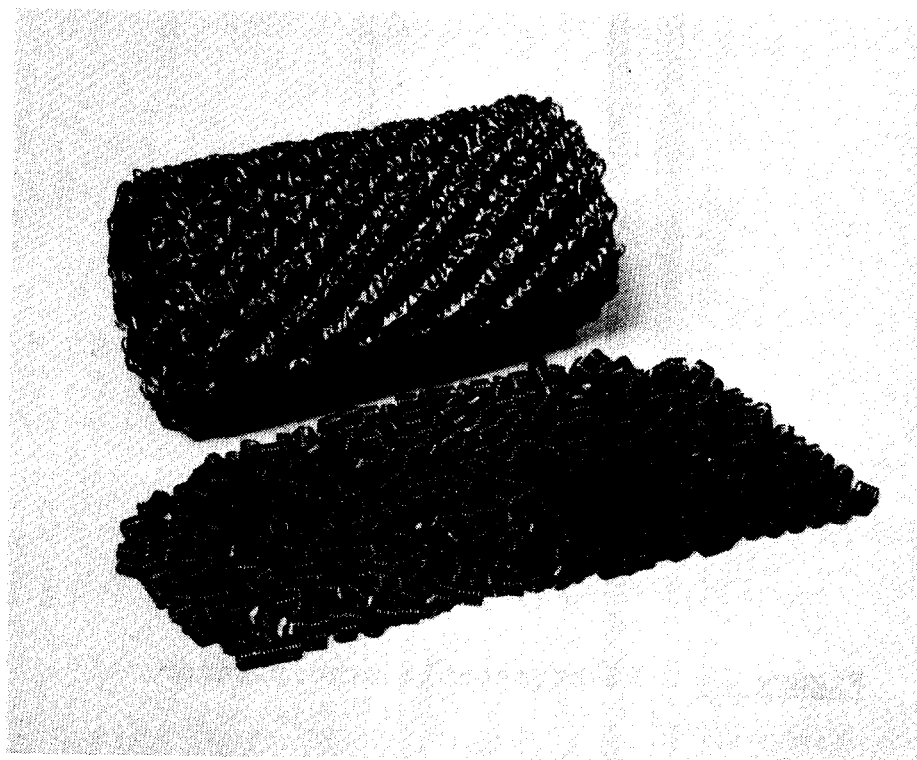
Figure 4:   Packings
            Goodloe packing   (top)
            wire spirals 4 x 4 (bottom)
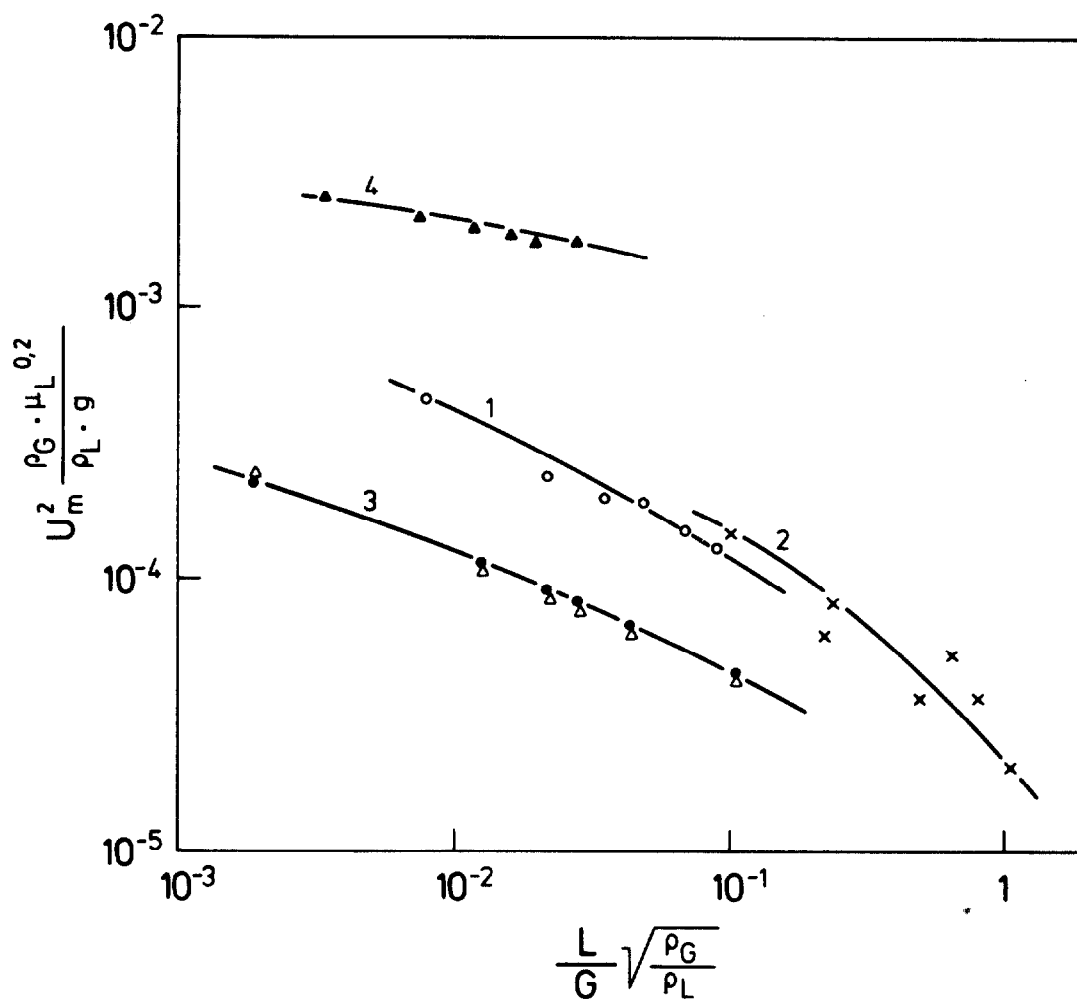
Figure 5:   Flooding curves for packed columns

1)   Braunschweiger Wendeln 4 x 4
      (wire spirals), system air/H_2O

2)   Goodloe packing, system CO_2/CO_2 (ORNL-data)

3)   Calculated values for 1) and 2)

4)   Gas and liquid samplers in the column,
      system air/H_2O
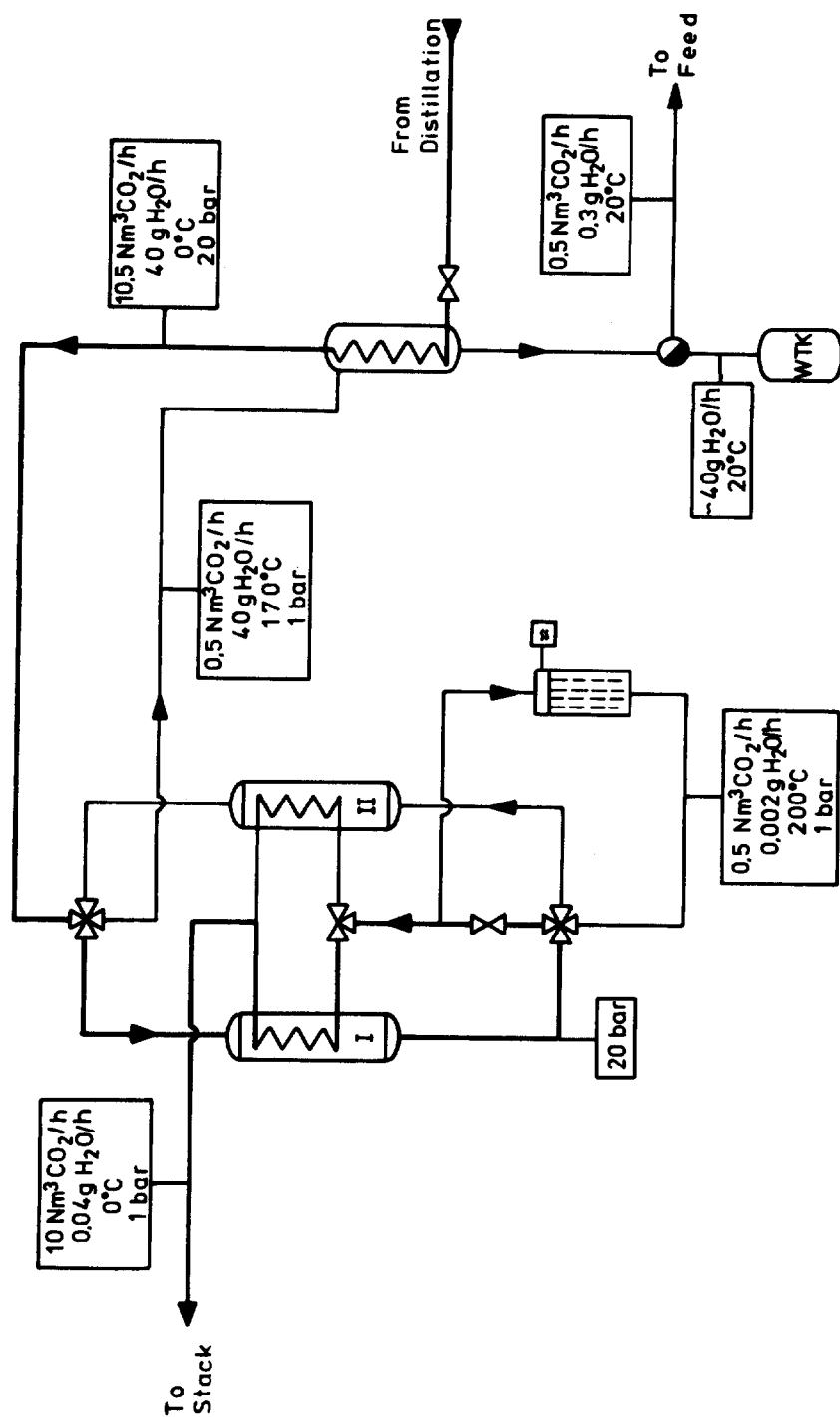
Figure 6: Schematic flowsheet of the tritium removal system for AKUT II

Absorber I: Loading
„ II: Regeneration

DISCUSSION

DEMPSEY:　　　　　The paper did not mention ^{14}C.　Will this radionuclide be removed by AKUT-2?

BOHNENSTINGL:　　　Carbon 14 is a problem in this process.　Some work must be done on a fuel fabrication program to remove or separate carbon 14 dioxide from other gases.

EXPERIMENTAL STUDIES ON THE KRYPTON ABSORPTION
IN LIQUID CO_2 (KALC) PROCESS*

R. W. Glass, H. W. R. Beaujean,** V. L. Fowler, T. M. Gilliam,
D. J. Inman, and D. M. Levins***

Oak Ridge National Laboratory
Oak Ridge, Tennessee

Abstract

Results are presented for a series of experiments to quantify krypton removal from simulated High-Temperature Gas-Cooled Reactor reprocessing off-gas by the KALC process. The Experimental Engineering Section Off-Gas Decontamination Facility used in the campaign provides engineering-scale experiments with nominal gas and liquid flows of 5 scfm and 0.5 gpm respectively.

Equilibrium and nonequilibrium mass transfer experiments for the CO_2-O_2-Kr system are described. Data analysis indicates values of HTU for krypton on the order of 0.5 ft for decontamination factors from 100 to 10,000. Recent flooding information for the packed columns is combined with previous data and is shown to be well represented by an empirical flooding equation.

Introduction

As part of the Thorium Utilization Program developmental work being carried out at the Oak Ridge National Laboratory, the Experimental Engineeering Section Off-Gas Decontamination Facility[1] (EES-ODF, see Fig. 1) has been operated to quantify the absorption of krypton by liquid CO_2. The work presented here comprises approximately 30 experiments involving the mass transfer of krypton into liquid CO_2 in the presence of O_2 and 10 experiments in which conditions within the packed absorption column were chosen such that CO_2-Kr equilibrium values were obtained as a check on values of equilibrium data reported in the literature.[2,3] Additional column flooding data are also presented and compared with previous values.[1]

**Guest scientist from West Germany. Present address: Institute for Chemische Technologie, der Kernforschungsanlage, Julich GmbH, 517 Julich, West Germany.

***Guest scientist from Australia. Present address: Chemical Technology Division, Australian Atomic Energy Commission, Research Establishment, Private Mailbag, Sutherland 2232, N.S.W. Australia.
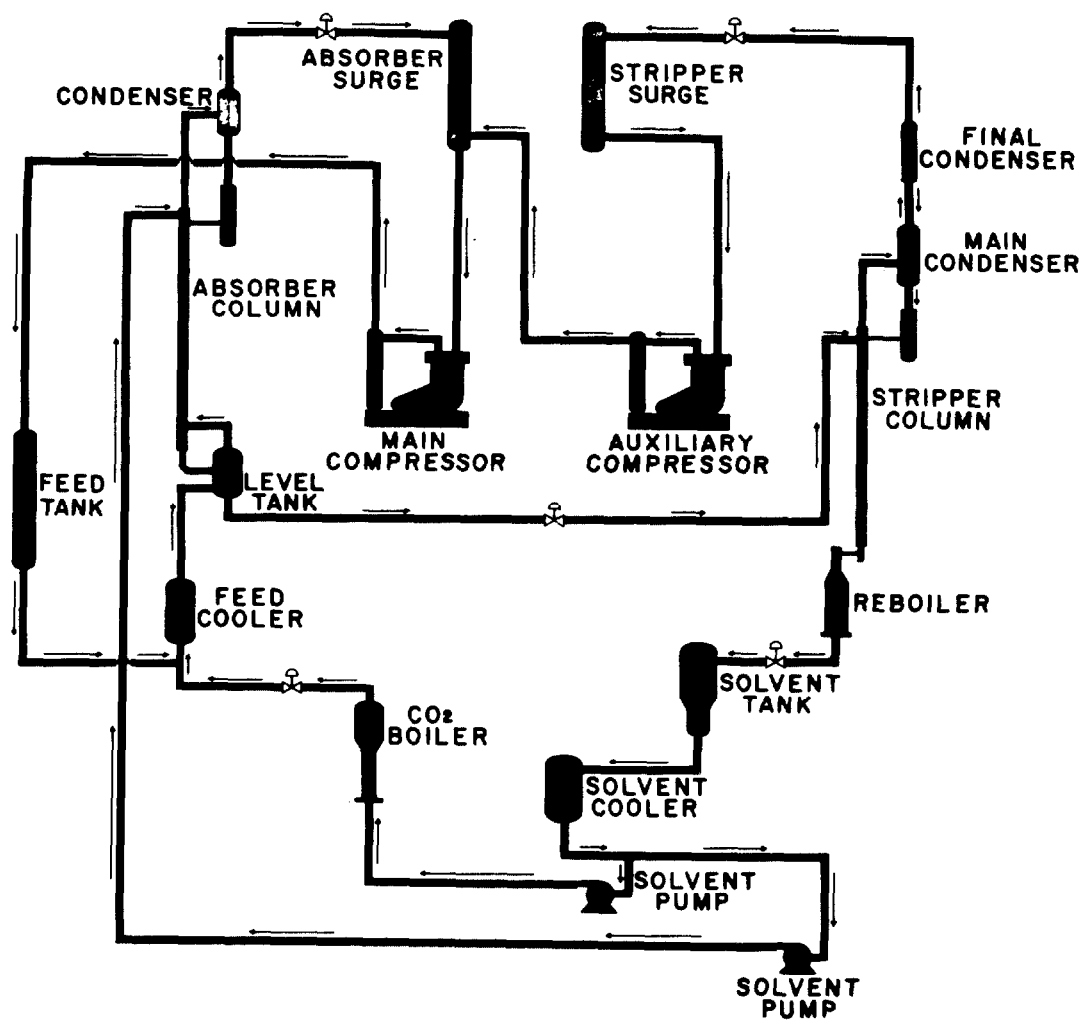
Fig. 1. Experimental Engineering Section Off-Gas Decontamination Facility.

Flooding Studies

Fluid dynamic data for the EES-ODF packed columns have been reported.[1] More recently, a few additional experiments with the liquid CO_2 system were conducted during a High-Temperature Gas-Cooled Reactor (HTGR) campaign in the Oak Ridge Gaseous Diffusion Plant (ORGDP) facility for off-gas decontamination studies.[4]

Figure 2 presents the collective flooding information obtained for the packed columns investigated. Included in the data shown in this figure are flooded conditions found for the 1-1/2-in. absorber column and the 3-in. stripper column in the EES-ODF, together with the more recent data (darkened points) acquired from operation of the 3-in. fractionator column in the ORGDP facility. All columns are packed with presized canisters (6 in. long) of Goodloe* wire mesh packing.

The flooding curve is presented in a standard form for the particular packing (i.e., no "packing factor" is included in the ordinate grouping). The following quantities are noted for Fig. 2:

$$L = \text{liquid flow rate, lb/ft}^2 \cdot \text{hr,}$$

$$G = \text{gas flow rate, lb/ft}^2. \text{ hr,}$$

$$\rho_G = \text{gas-phase density, lb/ft}^3,$$

$$\rho_L = \text{liquid-phase density, lb/ft}^3,$$

$$\mu_L = \text{liquid-phase viscosity, cP,}$$

$$U_M = \text{gas velocity at flooding, ft/sec,}$$

$$g = 32.2 \text{ ft/sec}^2.$$

With the addition of the four experimental points from the ORGDP fractionator, a curve has been fitted to all points shown. The results are as follows:

$$\bar{y} = a + b\bar{x} + c\bar{x}^2 = \log (y), \qquad (1)$$

where

$$\bar{x} = 2.0 + \log (x),$$

$$y = \text{ordinate values of } \frac{U_M^2 \, \rho_G \, \mu_L^{0.2}}{g \, \rho_L},$$

$$x = \text{abscissa values of } \frac{L}{G}\sqrt{\frac{\rho_G}{\rho_L}},$$

$$a = -3.44748,$$

$$b = 0.379889,$$

$$c = -0.315457.$$

---

*A product of the Packed Column Co., a Division of Metex Corp., Edison, N.J.

ORNL DWG 75-5186
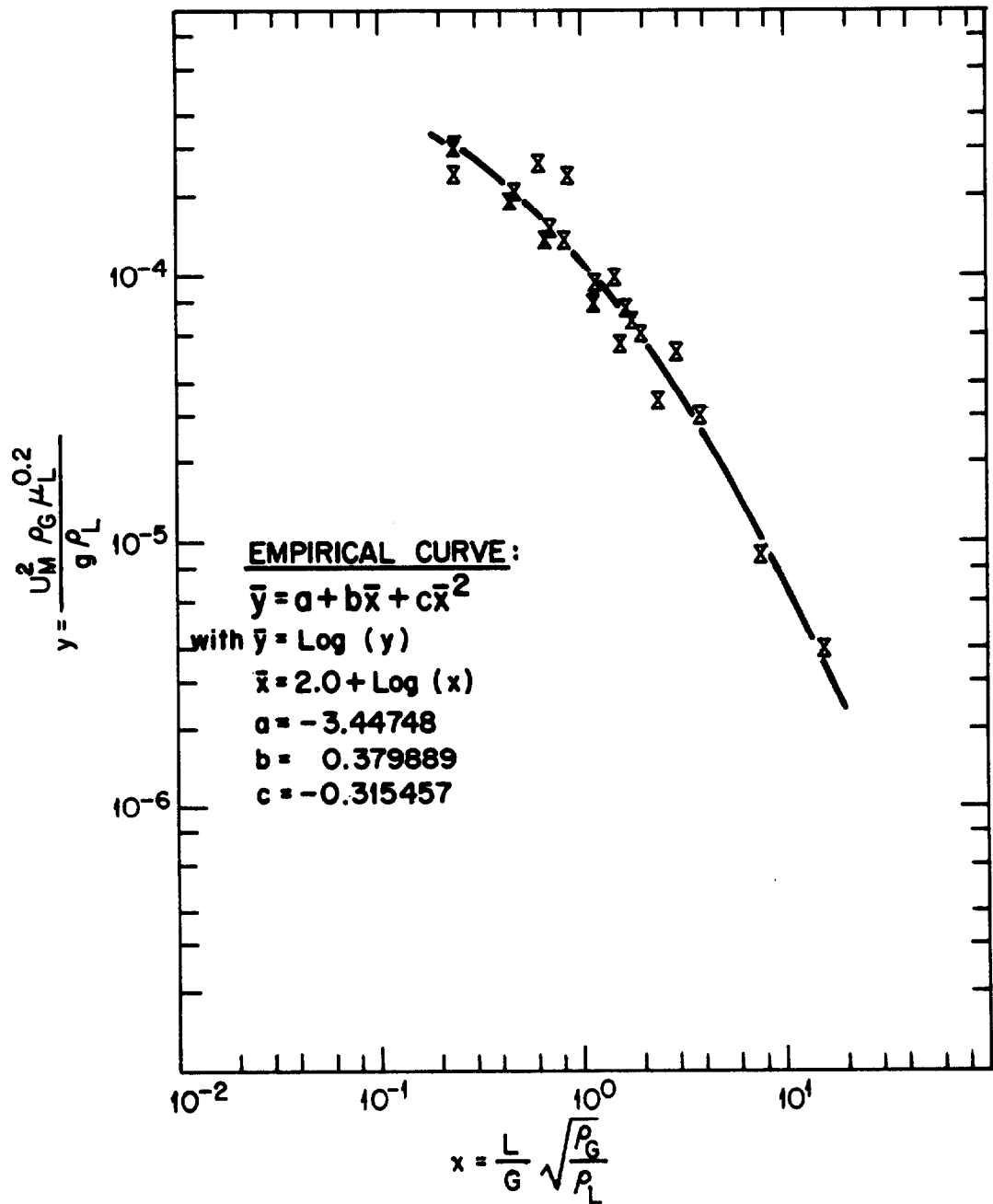
Fig. 2. Curve constructed by using collective flooding information.

Practically all of the fluid dynamic experiments represented by the flooding curve have involved CO_2 only (i.e., both gas and liquid phases are essentially pure CO_2). The effect of light gases such as O_2, N_2, etc., is not experimentally implicit. However, most of the areas of concern in the KALC process involve pure CO_2. The capacity or throughput of the packing at flooding is less than that suggested in literature supplied by the vendor (overall, by perhaps 50% depending on conditions). The pressure drop at flooding is approximately 0.5 in. H_2O per foot of packing.

Equilibrium Operations

At the beginning of the present work, it was recognized that a fundamental question concerning $Kr-CO_2$ equilibrium existed. The problem can be explained by referring to Fig. 3. Two independent sets of equilibrium data[2,3] for the same system were available, and these were not in agreement. The data are expressed as the equilibrium ratio y/x, where y and x denote krypton concentrations in the vapor and liquid CO_2 phases, respectively. Calculations based on each set of data produce widely varying results.[5] Moreover, decisions as to what experimental conditions to use for the present work depended on the value of the Kr-CO_2 equilibrium ratio. Thus a series of experiments was conducted early to determine whether the dilemma could be resolved.

Two important considerations are worth noting. First, the EES-ODF is not designed to provide equilibrium data per se. Since the facility involves equilibrium in an indirect manner, it is a question of precision regarding the worth of equilibrium observations. Second, the degree of accuracy relative to sampling and analysis is very difficult to establish, especially in limited-time operations. Consequently, the objective of the equilibrium studies was to present evidence as to which set of equilibrium data was more nearly accurate. The studies also allowed a pseudo-quantitative evaluation of sampling and analytical techniques for the EES-ODF. Details of the sampling, monitoring, and analytical techniques for the EES-ODF are presented elsewhere.[1,6]

Table 1 presents the basic data for the ten equilibrium experiments. The method of operation during these experiments was straightforward. The facility was operated with varying amounts of oxygen, at different pressures and temperatures, but always with the liquid-to-vapor flow ratio in the absorber column set to produce a "pinched" condition at the bottom of the packed section. A pinched condition results when the liquid-to-vapor ratio is less than the equilibrium ratio (y/x), given sufficient packed section length. The result of operating in a pinched mode is that the vapor entering and the liquid leaving the column will be essentially in equilibrium.

Table 2 summarizes the equilibrium experiments with regard to the facility method of operation. After sufficient time had been allowed for system transients to subside in each run, both the gas and the liquid at the bottom of the packed section were sampled and analyzed for krypton and O_2. Calculated values given in Table 1 are based on the CO_2-O_2-Kr equilibrium model described in ORNL/TM-4947.[7] The equilibrium model assumes the validity of the data of Notz et al.[3] for krypton. Figures 4 and 5 present the computer model results for the equilibrium ratio and Henry's constant for the various components.

Figure 6 presents summary results of the equilibrium studies. Values of y and x (mole fraction) for krypton were determined by sampling and analysis, and

ORNL-DWG 72-6887R5
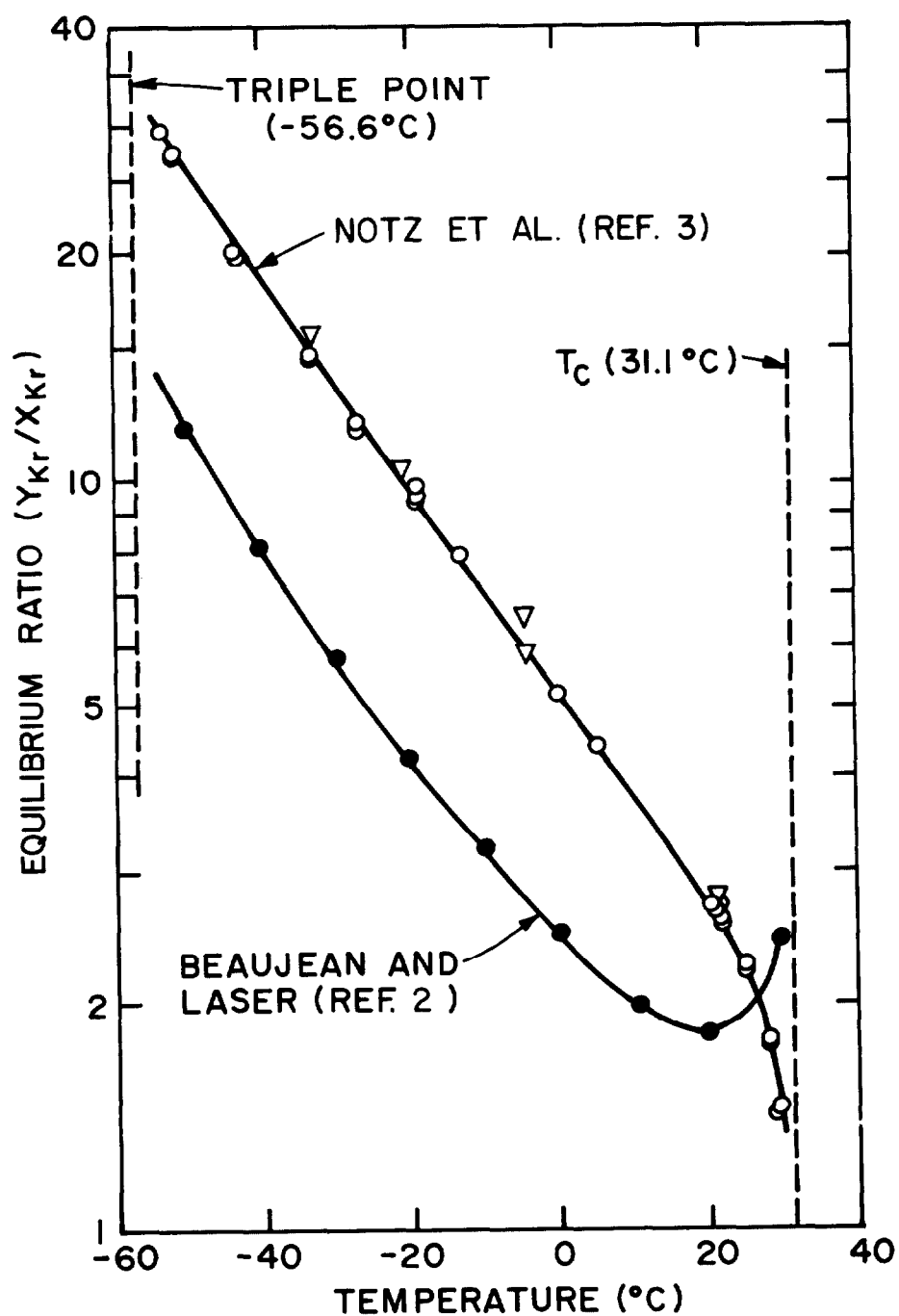
Fig. 3. Comparison of Kr-CO_2 equilibrium ratios from two independent sources.

Table 1. Summary of results obtained in ten equilibrium experiments in the EES-ODF

Experiment number	Pressure (psig)	Temperature (°C)	y_{O_2} Measured	y_{O_2} Calculated[a]	$(y/x)_{Kr}$ Measured	$(y/x)_{Kr}$ Calculated[a]
232	340	-17.5	0.0770	0.1005	6.94	7.74
241	254	-28.5	0.1510	0.1537	9.02	10.23
254	375	-12.1	0.0790	0.0534	6.90	7.00
268	309	-18.5	0.0338	0.0579	8.31	8.49
275-A	338	-13.5	~0	0.0103	7.17	7.75
275-B	280	-19.6	~0	0.0130	8.72	9.33
275-C	286	-19.4	~0	0.0238	9.75	9.14
275-D	218	-27.3	~0	0.0202	11.81	11.82
275-E	290	-19.0	~0	0.0245	7.90	9.02
296	290	-25.7	(0.1180)	0.1738	8.85	9.03

[a] Calculations were based on the CO_2-Kr-O_2 model presented in ORNL-TM-4947.[7] The $(y/x)_{Kr}$ ratio was calculated assuming the validity of the data of Notz et al.[3]

Table 2.   Summary of experimental equilibrium operations

Experiment number	Description of operation
232	Typical mass transfer experiment involving both gas and liquid countercurrent operation with a low value of liquid-to-vapor ratio
241	Similar to 232
254	Similar to 232
268	Similar to 232
275-A	Only liquid flow in operation; equilibrium with overgas achieved by long-term system operation
275-B	Similar to 275-A
275-C	Similar to 275-A
275-D	Similar to 275-A
275-E	Similar to 275-A
296	Similar to 232

ORNL DWG 75-796 R2

RATIOS SHOWN ARE FOR INFINITE
DILUTION IN LIQUID CARBON DIOXIDE

KRYPTON

XENON

NOTZ ET AL. (REF. 3)
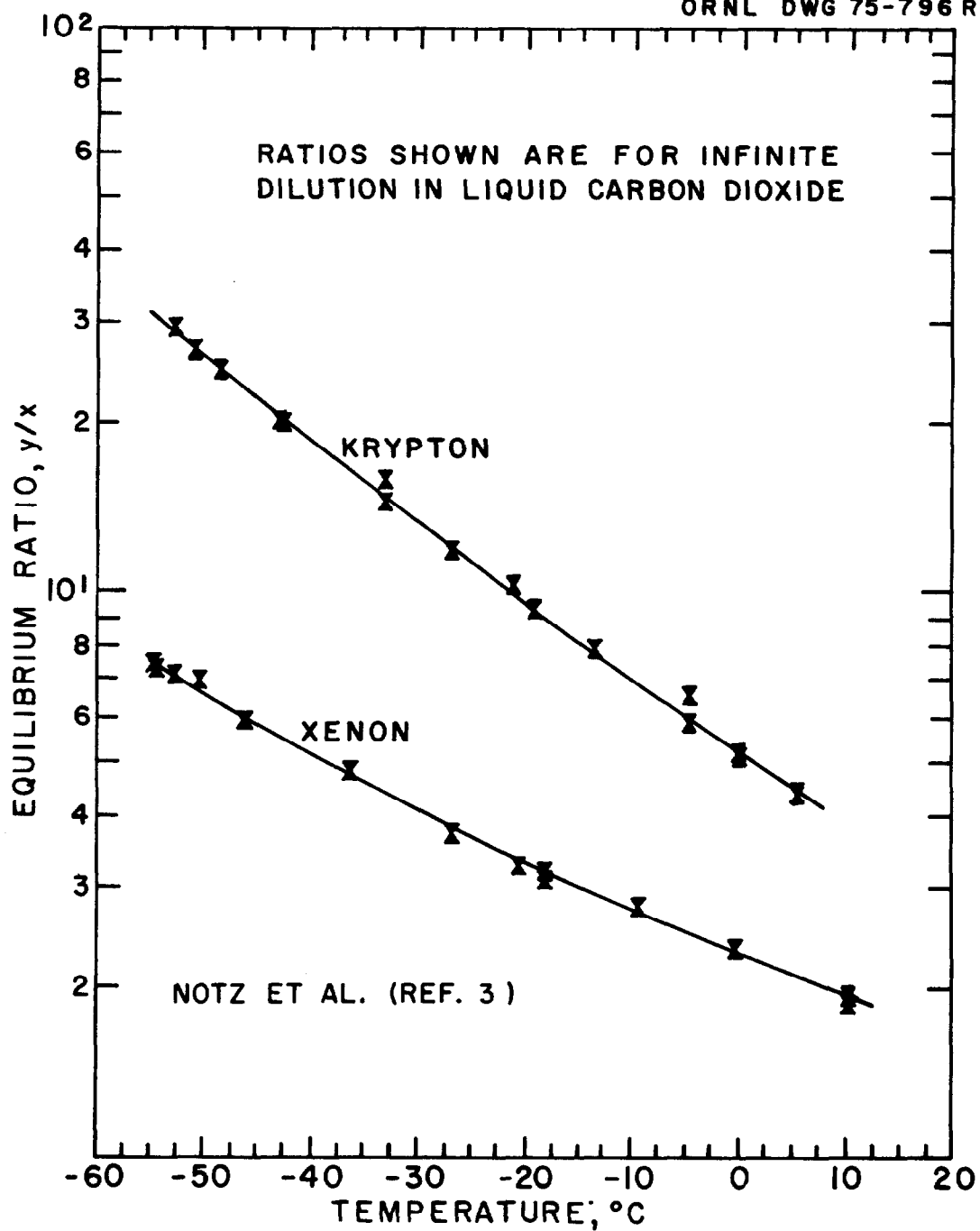
Fig. 4. Krypton and xenon equilibrium ratios as obtained by
the computer model.

ORNL DWG 75-976RI
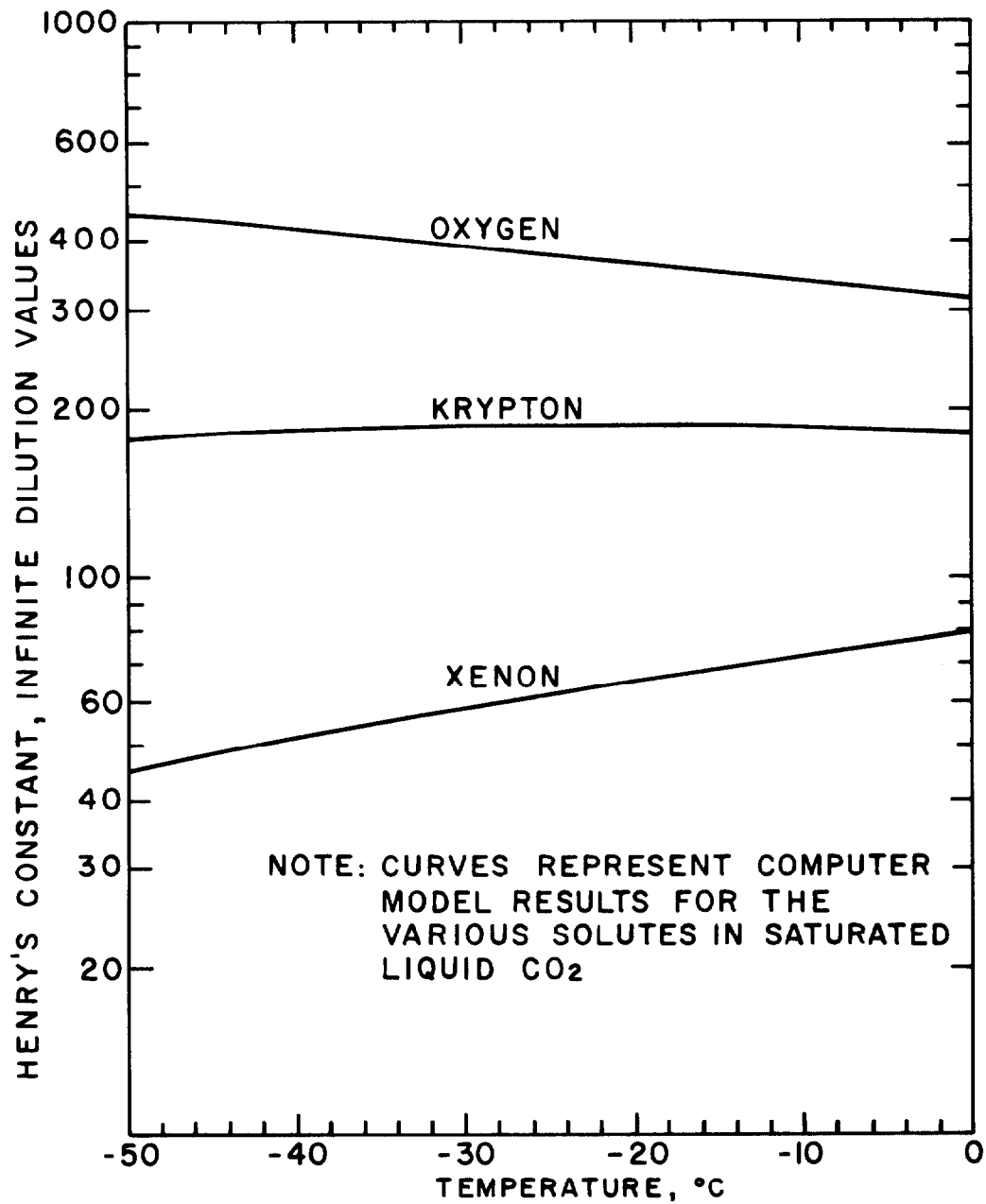
Fig. 5. Values of Henry's constant for selected solutes as
obtained by the computer model.

ORNL DWG 75-978R2

SYSTEM COMPONENTS
Kr-TRACER LEVEL
$O_2 - 1 - 15\%$
$CO_2 - $ BALANCE

DEVIATIONS INDICATE
VARIATIONS OF ± 5 psig
AND ± I °C BY CALCULATION

(Y/X) Kr CALCULATED

(Y/X) Kr EXPERIMENTAL

Fig. 6. Comparison of predicted and measured values of $(y/x)_{Kr}$ for the equilibrium experiments.

the value of $(y/x)_{Kr}$ experimental was obtained directly. For each experimental value of P (total pressure) and T (system temperature at the bottom of the absorber), the computer model for the CO_2-Kr-O_2 equilibrium provided a corresponding value of $(y/x)_{Kr}$ calculated. Additionally, the computer model provided a value of y_{O_2} at each P and T for comparison with the measured quantity.

Considering the range of concentrations involved (< 2 mole % O_2 in the liquid and tracer-level krypton), the agreement present in Fig. 6 is remarkably good and would tend to support the data of Notz et al.[3] Thus, for the remaining experiments, the data of Notz et al. are assumed to be valid.

Mass Transfer Experiments

During the mass transfer experiments the EES-ODF was operated in total re-cycle with approximately 10% light gas (O_2) and tracer-level krypton. The simulated reprocessing off-gas stream was compressed to slightly more than the desired absorption pressure and routed to the bottom of the absorber column. In the absorber, the gas (flowing upward) was contacted with essentially pure liquid CO_2 into which both O_2 and krypton were absorbed as the liquid flowed down the packed section. The solute-laden liquid was then routed to the stripper column where the dissolved gases were desorbed and released into the stripper off-gas stream. The stripper and absorber off-gases were subsequently combined to form feed gas and recycled to the compressor. Liquid leaving the stripper was recycled to the top of the absorber packed section as a continuous flow of solute-free solvent.

For each of the mass transfer experiments, an operating condition was chosen and the entire flow system was allowed time for transients to subside before sampling and data acquisition. Tables 3 and 4 present a portion of the data taken during the mass transfer experiments, and include data for four experiments (viz., 232, 241, 254, and 538) which were made under pinched conditions that do not reflect the nature of the other mass transfer experiments. These four experiments simply offer a lower bound to operational mass transfer. Some of the values listed in Table 3 were obviously not obtained directly by expe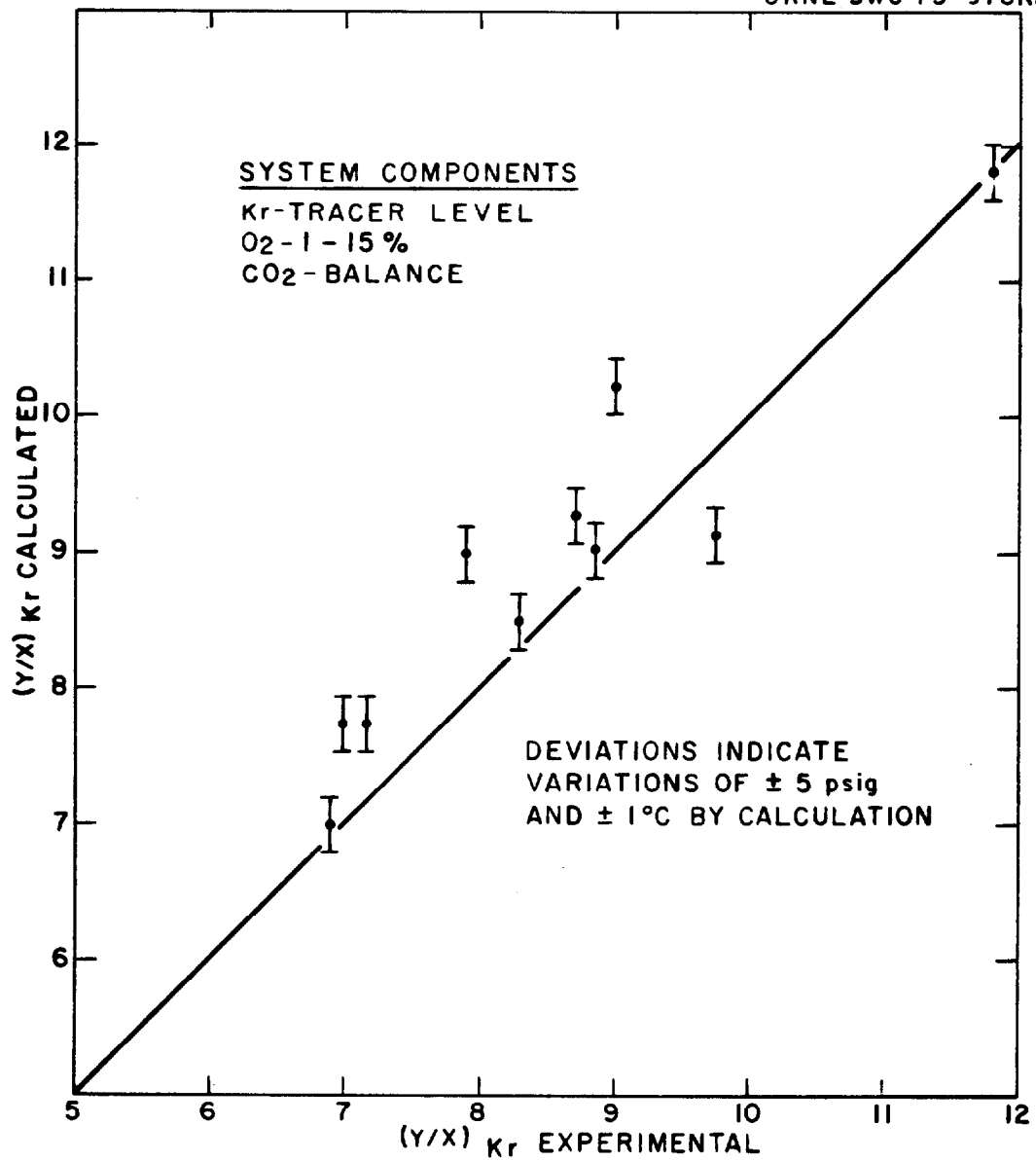riment but, instead, were calculated from more fundamental measurements. The absorber pressure, average absorber temperature, absorber ΔP, and liquid rate are shown as measured. Feed gas rates were dependent on rotameter calibrations, while the O_2 content of the feed gas and overall krypton decontamination factors (DF's) were based on sampling and monitoring.

Data Analysis

During operations only the feed gas stream could be identified with respect to both flow rate (via rotameter) and composition (sampling and analysis). Off-gas streams from the absorber and from the stripper were sampled and analyzed for composition, but their flow rates were not known accurately since flowmeters for these streams were unreliable. Knowledge of the compositions (O_2 and krypton) for these streams, together with the flow rate of the feed gas stream, allows calculation of flow rates for the off-gas streams by assumption of either O_2 or krypton material balances in conjunction with overall stream balances.

Operational experience provides more confidence in the determination of the ^{85}Kr content; therefore, the assumption of a complete krypton balance was made,

Table 3. Summary of absorber conditions during mass transfer experiments

Experiment number	Absorber pressure (psig)	Feed gas rate (scfm)[a]	Feed gas oxygen (%)	Average absorber temp. (°C)	Absorber ΔP (in. H_2O/ft)	Liquid flow rate (gpm)	Overall krypton DF[b]
222	324	5.44	10.35	-20.0	0.364	0.551	357.
232	340	7.09	7.08	-17.4	0.516	0.551	5.
241	254	6.19	9.42	-28.2	0.255	0.485	7.
254	375	7.22	7.79	-12.2	0.619	0.485	3.
309	302	4.65	7.13	-20.1	0.413	0.623	256.
320	308	4.56	6.82	-20.1	0.510	0.720	14039.
330	308	4.57	7.83	-20.4	0.449	0.693	4161.
340	313	4.27	8.99	-20.5	0.473	0.693	7000.
348	310	4.55	9.19	-20.3	0.668	0.748	9687.
358	313	4.73	9.28	-20.8	0.467	0.665	619.
368	321	4.81	12.60	-20.9	0.516	0.623	7206.
378	337	4.99	11.70	-20.0	0.437	0.582	3214.
388	337	4.97	11.64	-20.0	0.449	0.554	3043.
406	384	5.87	20.06	-18.8	0.461	0.485	1215.
416	387	6.21	15.14	-18.3	0.394	0.554	1013.
426	347	5.74	11.93	-20.5	0.443	0.554	153.
436	345	5.39	10.75	-19.3	0.419	0.554	539.
451	325	4.77	11.34	-20.9	0.319	0.416	590.
461	336	4.40	10.47	-19.2	0.328	0.416	2602.
470	333	3.78	8.88	-18.7	0.316	0.416	3075.
480	317	5.23	10.83	-22.2	0.307	0.416	87.
490	323	6.33	8.62	-21.9	0.327	0.416	10.
498	323	3.73	8.45	-18.9	0.303	0.416	5157.
518	405	4.50	7.57	-12.6	0.376	0.416	839.
528	402	3.63	10.05	-11.7	0.376	0.416	4038.
538	409	6.38	7.80	-11.6	0.425	0.416	5.
548	396	5.16	5.93	-12.7	0.399	0.416	17.
558	391	4.67	6.79	-13.2	0.387	0.416	100.
568	407	4.23	6.24	-11.9	0.388	0.416	1100.
578	392	3.49	6.01	-12.17	0.376	0.416	2908.

[a] scfm refers to real CO_2 gas at 70°F and 1 atm.
[b] DF = decontamination factor.

Table 4. Mass transfer values

Experiment number	Overall DF	Column[a] DF	Krypton HTU (ft)	O_2 balance factor	Absorption factor
222	357	227	0.561	0.93	1.29
232	5	5	1.329	0.94	0.81
241	7	7	0.700	0.94	0.90
254	3	3	3.220	0.97	0.72
309	256	219	0.355	0.94	1.15
320	14039	7757	0.383	0.84	1.43
330	4161	2750	0.339	1.06	1.32
340	7000	4139	0.385	1.02	1.43
348	9687	3866	0.348	1.02	1.45
358	619	471	0.380	1.02	1.23
368	7206	3350	0.374	1.10	1.41
378	3214	1927	0.405	1.02	1.42
388	3043	1887	0.400	0.97	1.40
406	1215	704	0.463	0.99	1.34
416	1013	621	0.464	1.05	1.30
426	153	115	0.506	0.97	1.19
436	539	343	0.493	0.99	1.33
451	590	354	0.430	0.93	1.27
461	2602	1267	0.418	0.94	1.42
470	3075	1358	0.482	0.95	1.55
480	87	72	0.345	0.99	1.07
490	10	10	0.588	0.92	0.92
498	5157	2119	0.441	1.08	1.58
518	839	642	0.400	0.98	1.26
528	4038	2455	0.378	0.92	1.40
538	5	6	1.720	0.98	0.87
548	17	18	0.816	0.99	1.02
558	100	96	0.479	0.96	1.13
568	1100	830	0.448	0.98	1.32
578	2908	1543	0.419	0.94	1.41

[a] Column DF's are calculated values which pertain to conditions at the top and bottom of the packing itself.

and the inaccuracies involved in flow rate, O_2 content, and krypton content have been combined into the oxygen balance factor noted in Table 4.

The overall krypton DF as presented in Table 3 is calculated from the krypton present in the feed gas and absorber off-gas streams as follows:

$$\text{Overall DF} = \frac{\text{Amount of Kr in feed gas}}{\text{Amount of Kr in absorber off-gas}} \ . \tag{2}$$

Calculations of HTU's for krypton are based on the following simple and classical equations:[8]

$$HTU = Z/NTU, \tag{3}$$

$$NTU = \frac{y_o - y_i}{(y^* - y)_{lm}} \ , \tag{4}$$

$$(y^* - y)_{lm} = \frac{(y_o^* - y_o) - (y_i^* - y_i)}{\ln \dfrac{y_o^* - y_o}{y_i^* - y_i}} \ , \tag{5}$$

where

HTU = height of transfer unit, ft,

Z = column packing height, ft,

NTU = number of transfer units,

y_i = inlet gas composition,

y_o = outlet gas composition.

Asterisked quantities (e.g., y_i^*) indicate phase compositions that are in equilibrium with corresponding compositions in the adjacent phase. All compositions refer to krypton; Z = 8.24 ft and y_o^* = 0. Values of HTU calculated by using Eq. (3) are presented in Table 4. Figure 7 illustrates the variation of the packing HTU with column DF. Figure 8 shows the variation of column DF with absorption factor.

<u>Discussion</u>

As necessary for clarity, certain details have been included with the experimental and analytical procedures already presented. A more complete discussion of the present work is presented in Reference 9. Earlier campaigns and reports concerning the EES-ODF have noted the experimental nature of the facility. The presentation of details indicate clearly one aspect of this facility. The facility, by design, is intended to provide development data as opposed to demonstration-type information. Development data collected relate specifically to krypton absorption by liquid CO_2. Subsequent work will be concerned with other operations of importance in the KALC process, such as fractionation of lighter gases that are coabsorbed with krypton or complete stripping of all
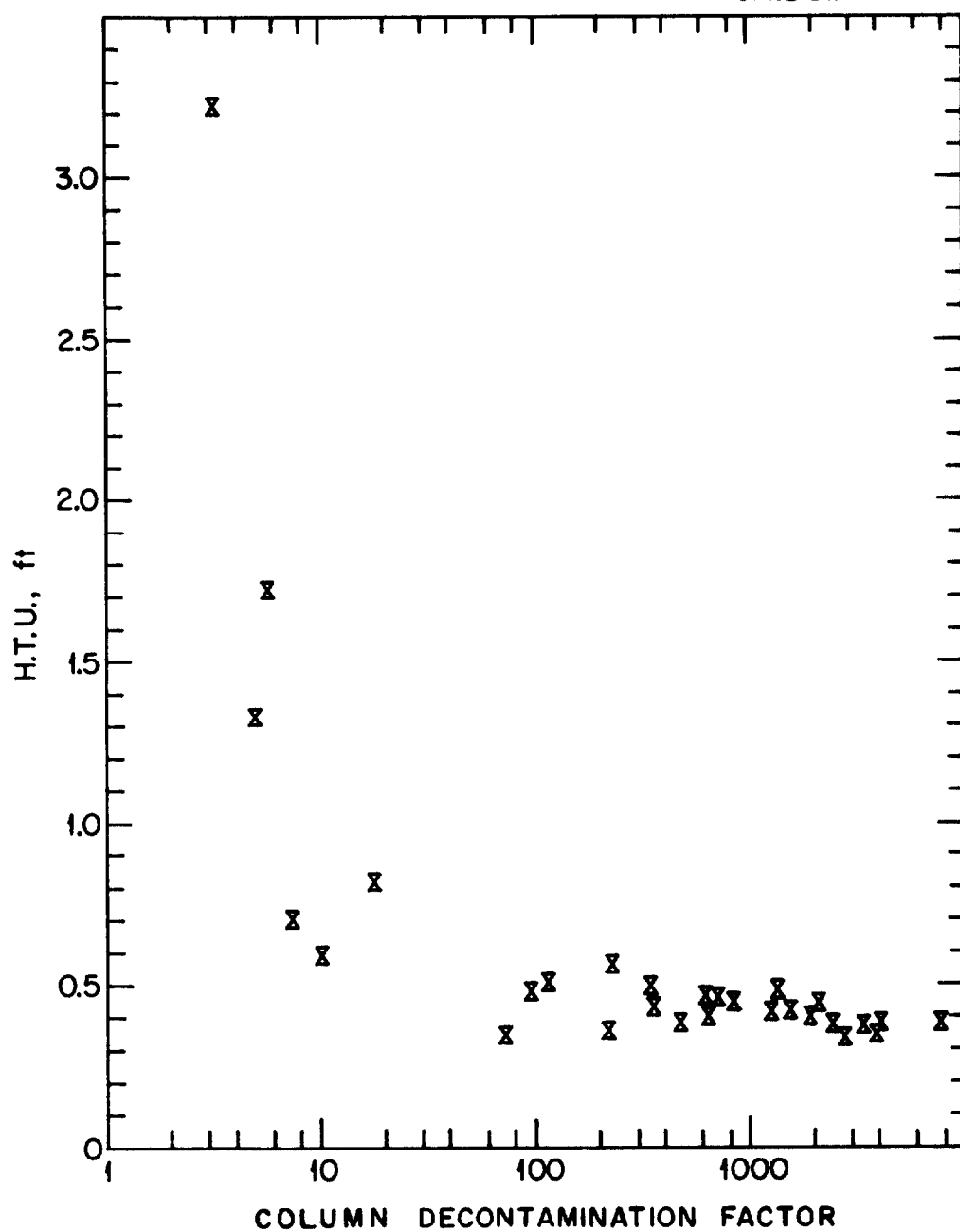
ORNL DWG 75-5351R2

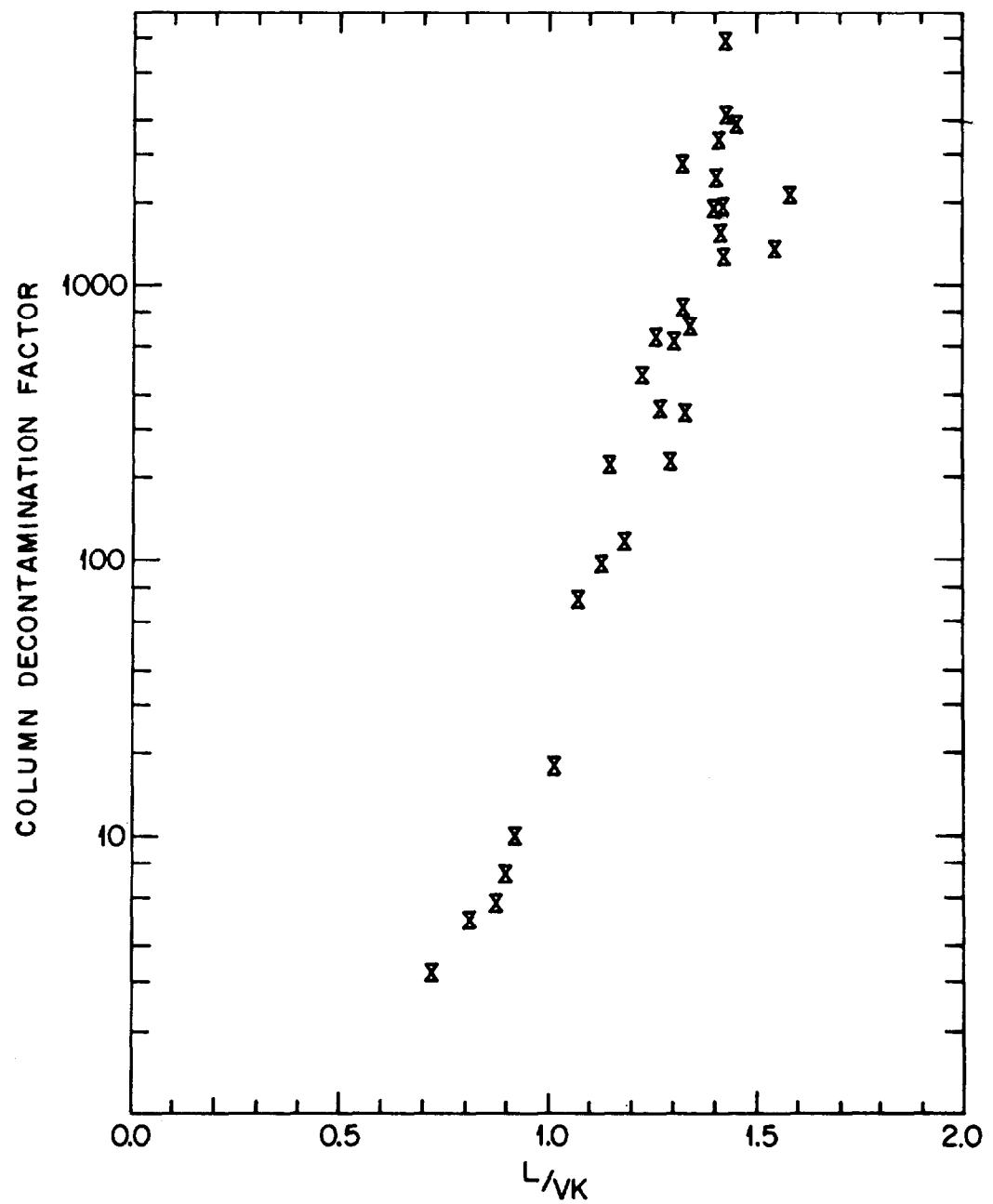Fig. 7. HTU values for mass transfer experiments.

ORNL DWG 75-5352 R2

Fig. 8. Decontamination factors vs absorption factors.

dissolved light gases. Each of these operations is important in the total development of the KALC process, but the EES-ODF is not designed to study all operations simultaneously. The facility is not a prototype KALC system. Rather, it represents an engineering-scale system designed to study individual operations of the KALC process under experimental conditions as closely similar to those expected in an overall process as possible.

Many features of the EES-ODF will undoubtedly have counterparts in a conceptual or subsequent design of the KALC system; however, such features will require technical review for operability, compatibility, and desirability before scale-up to the commercial or semicommercial system can occur.

The curve shown in Fig. 2 is of the form typically presented[10] as the "generalized" flooding curve except that the usual parameters, a_p/ϵ^3, in the ordinate grouping for the particular packing characteristics have been omitted. (Generally, a_p is the total area of packing (ft^2/ft^3 bed), and ϵ is the void fraction in dry packing.) Moreover, the curve in Fig. 2 only resembles the generalized curve and does not correspond exactly in shape. At any value of the abscissa grouping, the ratio a_p/ϵ^3 (i.e., the packing factor) can be evaluated by calculating the ratio of the generalized curve ordinate grouping to that of Fig. 2. For example, at a value of the abscissa grouping of unity (near the center of both flooding curves), the packing factor is calculated to be 215 by this method. Hence, in the instance described, the packing of Fig. 2 may be compared to other types as follows:

Packing type	a_p/ϵ^3	Relative factor
1/2-in. ceramic Raschig rings	428	1.99
5/8-in. polypropylene Pall rings	158	0.73
1/2-in. ceramic Berl saddles	596	2.77
1/2-in. ceramic Intalox saddles	400	1.86
Goodloe wire mesh packing	215	1.00

The relative factors presented above do not necessarily indicate a packing quality or utility higher or lower than the packing used. Two important performance considerations here are throughput (or capacity) and HTU.

Figure 2 presents evidence that the flooding characteristics of the packing for the 1-1/2-in.- and 3-in.-diam columns are essentially identical for the conditions investigated. Whether identical results will also be obtained in larger-diameter columns is not known. The effect of packing density has not really been determined for the wire mesh packing investigated.

It should be noted that in the event that diameter greatly influences the flooding (and therefore the capacity) in large columns, the use of other "dumped" packings would not circumvent this problem. In fact, the relative size of dumped packing to column diameter may be more difficult to handle for scale-up purposes than considerations of the density of mesh packing.

From the standpoint of capacity and within the available time for testing, it appears likely that the wire mesh will provide a reasonable basis for scale-up without undue compromise in mass transfer performance. Also, this material will probably be at least comparable, with regard to capacity, to other commercially available packings.

The question of mass transfer performance is another important consideration when selecting a packing material. The present work concerns only absorption in the 1-1/2-in. EES-ODF column. Figure 7 shows that for reasonable values of operational parameters a value of 0.4 to 0.5 ft for HTU results. A number of considerations relating to the accuracy of the calculational procedures will be discussed later. Of question here is whether the HTU value will vary appreciably with column diameter. Obviously, the question cannot be answered from the present absorption experiments alone.

Most of the important considerations in equilibrium operations have been discussed previously. At the time the experiments were performed, valid questions existed as to (1) the importance of the equilibrium data accuracy, and (2) the effect of uncertainties in the equilibrium ratios (y/x). Certainly, the data of Notz et al. do exhibit an internal consistency over a relatively large range of temperatures, and all of their data are reported at essentially infinite dilution. Correlation techniques were used by Mobley to test the apparent consistency with other solutes in liquid CO_2. The net result of the equilibrium operations, together with the finding of Mobley, is that, while the data of Notz et al.[3] are definitely more nearly accurate, a margin of uncertainty regarding absolute accuracy remains.

Just how important it is that the Kr-CO_2 equilibrium values are known to within a given range, say $\pm$ 10%, is not clear. Based on HTU values calculated with Eq. (3), a qualitative relation exists between HTU and K as follows:

$$HTU_2 = HTU_1 \left[\frac{K_2}{K_1} \right]^{-3} \qquad (6)$$

Consequently, a 10% variation in K (i.e., $\pm$ 5%) would result in a $\pm$ 15% uncertainty in HTU. Such an uncertainty in HTU would not be unacceptable per se; however, the true range of uncertainty would undoubtedly be larger since other factors are known to contribute.

Figure 6 indicates a slightly lower experimental value of $(y/x)_{Kr}$ than one would predict using the data of Notz et al. Mobley's findings via correlations also indicate a slightly lower value and thus tend to fall more in line with other solute behavior in liquid CO_2. Both the equilibrium operations considered here and elements of the correlation work exhibit uncertainties, so that it cannot be stated absolutely that the data of Notz et al. are in error. Finally, although the equilibrium experiments were tedious and time-consuming, perhaps more confidence could be placed in the results if additional experiments had been conducted. At the present time, however, there appears to be no compelling reason why the data of Notz et al. should not be accepted.

During the present mass transfer experiments, the independent variable of primary importance was the absorption column liquid-to-vapor flow ratio (L/V). Ranges for this and other important variables are summarized as follows:

Variable	Range
Pressure, psig	254 to 409
Temperature, °C	-28.2 to -11.6
Feed O_2 concentration, vol %	5.93 to 20.06
Liquid-to-vapor ratio	
Overall values	4.94 to 12.82
Column only	5.04 to 12.88

It should be recognized that a 1:1 correspondence does not exist for the above variables over their ranges. That is, the experiment with the highest pressure is not necessarily the experiment with the highest L/V, etc. However, the variables are not totally independent, and a careful review of all variables presented throughout this report is necessary for an appreciation of the nature of the absorption process.

An important experimental observation is that variables do behave relative to one another as would be expected based on thermodynamic and chemical engineering principles. In short, no surprises were found. Of equal importance was the considerable operational experience gained, which will be of use in subsequent campaigns and for scale-up design analyses. In some ways, the study of absorption may be the least difficult of the studies required (viz., absorption, fractionation, and stripping). However, there are certain similarities among the three studies, and the discussion presented in this report regarding absorption should be applied to future plans for fractionation and stripping experiments.

The few results that indicate appreciably higher values of HTU than 0.4 ft (see Fig. 7) were obtained in essentially pinched experiments, where the HTU equation is erroneously attributing all the mass transfer to the entire packing length instead of to the shorter, effective length. The result is a higher apparent HTU value, and this phenomenon is not unexpected. The fact that Fig. 8 shows a rather sharp increase in DF as the value of the "absorption factor," L/VK, exceeds unity is indicative of (1) more than just a "few" stages in the absorber, and (2) the "correct" choice of experimental $Kr-CO_2$ equilibrium data. If only a few stages were present, it would be expected that DF would not increase as rapidly with L/VK. If the data of Beaujean et al.[2] were correct (or if the data of Notz et al. were grossly in error), the "inflection" of the DF curve of Fig. 8 would not necessarily be at L/VK = 1. Of course, the value of L/V used in L/VK could be in error; nevertheless, it is doubtful that the general error associated with L/V would exactly compensate for a corresponding uncertainty in K. Further, since DF is essentially a measured quantity, the ordinate of Fig. 8 can be expected to be indicative of the true situation as far as curve shape is concerned.

Conclusions

The present work has provided a wealth of operating experience on which subsequent operations can realistically be based. Sampling and analytical techniques appear to be valid and provide a relatively quantitative measurement of composition. However, the absolute accuracy of composition measurements can be evaluated only with additional experimentation.

Flooding performance of the wire mesh packing is reasonably well correlated for the conditions and equipment studied. The krypton equilibrium data of Notz et al.[3] appear to be sufficiently accurate for experimental purposes of the EES-ODF. For process decontamination factors on the order of 1000, a value of 0.5 ft for the krypton absorption HTU seems realistic and, within the range of the experiments conducted, does not vary for reasonable absorption conditions.

References

1. R. W. Glass, H. W. R. Beaujean, H. D. Cochran, Jr., P. A. Haas, D. M. Levins, and W. M. Woods, "Development of the Krypton Absorption in Liquid Carbon Dioxide (KALC) Process for HTGR Off-Gas Reprocessing," Proceedings of the 13th AEC Air Cleaning Conference, August 12-15, 1974, pp. 232-245.

2. H. W. R. Beaujean et al., "Off-Gas Treatment and Krypton Disposal in HTGR-Fuel Element Reprocessing," presented at the Symposium on the Management of Radioactive Wastes from Fuel Reprocessing, Paris, France, November 27 - December 1, 1972.

3. K. J. Notz, A. B. Meservey, and R. D. Ackley, "The Solubility of Krypton and Xenon in Liquid CO_2," Trans. Am. Nucl. Soc. 17, 318-19 (1973).

4. M. J. Stephenson, et al., "Absorption Process for Removing Krypton from the Off-Gas of an LMFBR Fuel Reprocessing Plant," Proceedings of the 13th AEC Air Cleaning Conference, August 12-15, 1974, pp. 263-275.

5. R. M. Mobley, "Calculations for the Separation of Radioactive Krypton from the Off-Gas from the Reprocessing of High Temperature Gas-Cooled Reactor Fuel Elements," M.S. Thesis, Department of Chemical Engineering, Clemson University, Clemson, S.C., August 1973.

6. D. M. Levins, R. W. Glass, M. M. Chiles, and D. J. Inman, Monitoring and Analysis of Process Streams in a Krypton-85 Off-Gas Decontamination System, ORNL/TM-4923 (July 1975).

7. R. W. Glass, T. M. Gilliam, and V. L. Fowler, An Empirical Model for Calculating Vapor-Liquid Equilibrium and Associated Phase Enthalpy for the CO_2-O_2-Kr-Xe System for Application to the KALC Process, ORNL/TM-4947 (January 1976).

8. A. S. Faust et al., Principles of Unit Operations, p. 278, Wiley, New York, 1960.

9. R. W. Glass, et al., Krypton Absorption in Liquid CO_2 (KALC): Campaign II in the Experimental Engineering Section Off-Gas Decontamination Facility, ORNL/TM-5095 (February 1976).

10. R. H. Perry and C. H. Chilton (eds.), Chemical Engineers' Handbook, 5th ed., p. 18-22, McGraw-Hill, New York, 1973.

EXPERIMENTAL DETERMINATION OF REACTION RATES
OF WATER – HYDROGEN EXCHANGE OF TRITIUM
WITH HYDROPHOBIC CATALYSTS

J. C. Bixel, B. W. Hartzell, and W. K. Park
Monsanto Research Corporation
Mound Laboratory*
Miamisburg, Ohio
45342

Abstract

This study was undertaken to obtain data needed for further development of a process for the enrichment and removal of tritium from the water associated with light-water reactors, fuel-reprocessing plants, and tritium-handling laboratories. The approach is based on the use of antiwetting, hydrophobic catalysts which permit the chemical exchange reactions between liquid water and gaseous hydrogen in direct contact, thus eliminating problems of catalyst deactivation and the complexity of reactor design normally associated with current catalytic-detritiation techniques involving gas-phase catalysis. An apparatus and procedure were developed for measuring reaction rates of water-hydrogen chemical exchange with hydrophobic catalysts. Preliminary economic evaluations of the process were made as it might apply to the AGNS fuel reprocessing plant.

I. Introduction

There has been a rapid increase in both the size and number of nuclear reactors used in the generation of electrical energy. These reactors produce a large quantity of radioactivity primarily resulting from the fission process. The release of radioactivity from a light water reactor is very small, and most of the fission products, including tritium, are transported to the fuel reprocessing plants in the spent fuel elements. Here the fission products are separated from the fuel which is recycled, and nearly all these fission products, with the exception of krypton and tritium, are concentrated and stored. Current practice is to release all the tritium to the environment as HTO either via a stack to the atmosphere or by injecting it into surface or deep well waters. The existing ERDA fuel reprocessing plants discharge their tritium in a liquid waste stream to surface waters. The AGNS plant at Barnwell, N.C., is designed to discharge the HTO through a stack to the atmosphere. The NFS plant, now undergoing modifications to increase its capacity, discharges 90% of its tritium to surface waters and 10% through stack effluents. These discharges represent the largest release point for radioactive material in the entire fuel cycle.

Because of the expanding nuclear power industry and the increased emphasis on minimizing release of radioactive materials to the environment, there is an increasing need for the development of safe handling and disposal methods for the radioisotopes being produced. With the exception of tritium, all the radioisotopes produced in the operation of a light-water reactor are amenable to some form of chemical or physical separation process for removal from the effluent streams. Tritium, however, is generally encountered in the oxide form and therefore follows the natural water streams. The detritiation of these aqueous wastes requires isotopic separation processes.

The purpose of this study is to develop a tritium separation and concentration process based on a H_2/H_2O catalytic exchange technique which can be used to detritiate contaminated water from light-water reactors, fuel-reprocessing plants, and tritium-handling laboratory facilities.

II. Catalytic Exchange Separation of Hydrogen Isotopes

Work in progress is directed toward development of an improved version of the basic HT/H_2O catalytic exchange process and demonstration of the separation of tritium for the particular concentrations and types of low-level aqueous wastes (LLAW) obtained from light-water reactors and fuel-reprocessing plants. The process will also apply to the removal of tritium from heavy water (D_2O) used as the moderator and coolant in several research and all U.S. government production reactors.

The improved approach to HT/H_2O catalytic exchange is based on the use of antiwetting hydrophobic catalysts which permit the chemical exchange reactions between liquid water and gaseous hydrogen in direct contact, thus eliminating problems of catalyst deactivation and the complexity of reactor design normally associated with current catalytic exchange techniques [1-3] involving gas-phase catalysis. Use of hydrophobic catalysts was first reported [4] in relation to studies directed toward an improved heavy-water process. The catalyst consists of platinum on an alumina substrate with a coating of semipermeable, water-repellent material such as silicone or Teflon.

The highest isotopic separation factors for HT/H_2O exchange are obtained at low temperatures because of the nature of the chemical equilibrium,

$$HT + H_2O \rightleftharpoons HTO + H_2$$
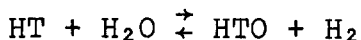
with a value of the isotopic separation factor of about 6 at 25°C. The processes involving steam-hydrogen reactions in the vapor state require higher temperatures to prevent water condensation and are faced with the resulting lower isotopic separation factors.

The hydrophobic low-temperature mixed-phase system potentially has many advantages over the gas-phase system; for example, higher isotopic separation factor, lower energy consumption, higher through-put rate, and simpler equipment.

There are two major alternative applications of the HT/H_2O catalytic exchange process to detritiation of LLAW. The first alter-native is to apply the process to the total waste stream and deplete the tritium to a degree that the resulting detritiated waste stream may be dispersed to the environment. This alternative has been referred to by Ribnikar and Pupezin[5] as the stripping scheme. The second alternative application would produce a similar enriched tri-tium stream, but the water is detritiated to a lesser degree and returned to the reactor (or plant), thus maintaining a desired steady tritium concentration in accord with applicable regulations for in-plant exposure of operating personnel. Ribnikar and Pupezin[5] have called this alternative the recycling scheme. Of course, a wide spectrum of options exists within either scheme when a design basis for the detritiation system is selected. For example, regula-tory factors and in-plant parameters such as LLAW throughput quan-tity and tritium concentration levels could affect the size of the system and the necessary degree of separation and enrichment of the tritium.

The throughput required for removal of tritium from LLAW could vary over a wide range depending on the application. Likewise, the degree of separation and recovery required could vary considerably. For example, the internal flow of water in a PWR cooling-water recycling detritiation application could be on the order of 10-50 liters/hr with an overall separation factor requirement of 100 to 1000. In comparison, application of the stripping scheme to the flow of LLAW from a fuel reprocessing plant could require a through-put of 500-2500 liters/hr with an overall separation requirement of 10^{11} to 10^{13}. Since the costs associated with detritiation of water increase with increased throughput and also increase with the in-creased overall separation factor, the application of the stripping scheme to the fuel reprocessing plant would be the most costly, as both throughput and separation requirements are a maximum for the fuel reprocessing LLAW stripping application.

The fuel reprocessing plant application of the waste water detritiation process was chosen for economic evaluation on the basis of being the most stringent, and most costly, application in the fuel cycle.

Preliminary Economics

A preliminary economic evaluation was made of the HT/H_2O cata-lytic exchange detritiation stripping process as it might apply to the Allied-Gulf Nuclear Services (AGNS), Barnwell, S.C., 5-metric ton/day nuclear-fuel-reprocessing plant. A schematic of the strip-ping process is given in Figure 1. This processing scheme would

H₂O H₂

472.95 l/hr (water)
$2 (10^{-8})$ Ci/l
0.075 Ci/yr
T/H = 6.25 x 10^{-15}

Catalytic Exchange Column

LLAW 473 l/hr
0.2 Ci/l
750,000 Ci/yr
T/H = 6.25 (10^{-8})

O₂

H₂

Hydride Fixation

Electrolysis Modules

0.0473 l/hr
2000 Ci/l
749,999.925 Ci/yr
T/H = 6.25 (10^{-4})
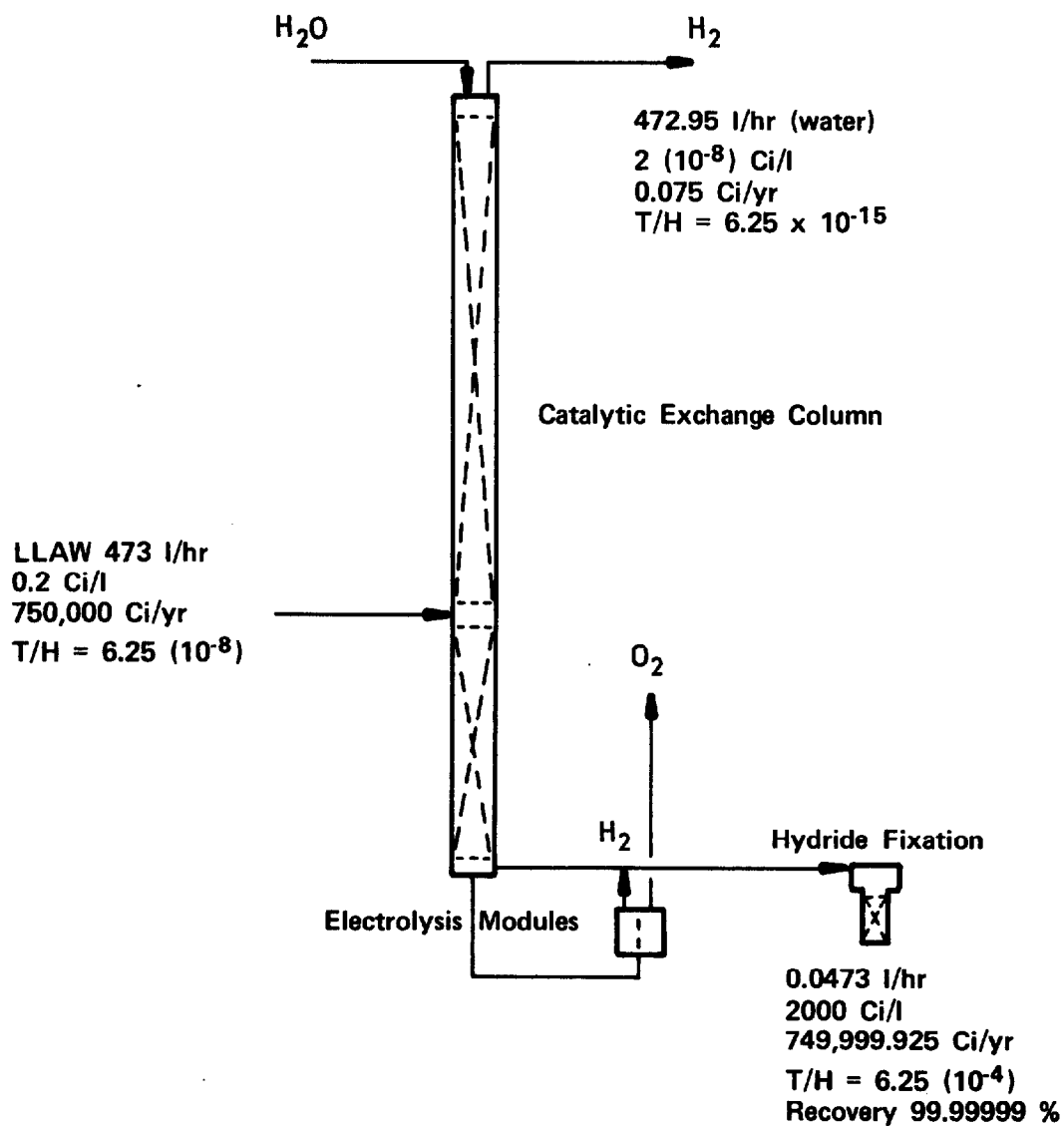Recovery 99.99999 %

FIGURE 1   AGNS LLAW detritiation.

detritiate approximately 500 liters/hr of LLAW containing 0.2 Ci/ liter of tritium to an extremely stringent degree. Of the tritium contained in the aqueous waste stream (750,000 Ci/yr), 749,999.925 Ci/yr would be concentrated in a quantity of water which would be only 47.3 cm^3/hr, or the equivalent quantity of gaseous hydrogen isotopic mixture, 5900 cm^3/hr of gas. The remainder of the 500 liters/hr feed stream would be detritiated to such a degree that it would be below the newly proposed EPA drinking water standard of 20,000 pCi/liter.[6]

Operation cost estimates are given in Table 1. The operating cost of $1,800,000 per year may be compared to the projected cost of biological damage due to released tritium from a 5 metric ton/day reprocessing plant. The recent tentative assignment of $1000 per total-body man-rem by the NRC and the whole body dose for tritium from a 5 metric ton/day fuel-reprocessing plant of 3,700 man-rem per year, as projected by the EPA,were used to obtain a cost for biological damage due to release of tritium of $3,700,000 per year. Thus the estimated operating cost of $1,800,000 per year is well below the cost-benefit balance point. Presumably, applications of the process in a recycling scheme or other less stringent applications than chosen for the above analysis would be even more economically favorable.

On the basis of the above preliminary economic evaluation, the HT/H$_2$O catalytic exchange detritiation process is judged worthy of further research and development effort.

Experimental

A bench-scale experimental apparatus was built for operation in a controlled glovebox under recirculating helium atmosphere. Figure 2 is a schematic of the experimental apparatus.

The experimental system is comprised of a low-temperature (20-70°C) reactor (3.8 cm i.d. x 28 cm), a high temperature (100-500°C) reactor (3.8 cm i.d. x 28 cm), support equipment, and analytical instruments. The low-temperature reactor packed with hydrophobic platinum-coated catalyst (0.48 cm diam.) was designed for a liquid gas countercurrent flow, and tritium is enriched in the liquid water (i.e., H$_2$O$_{(l)}$ + HT $\overset{\rightarrow}{\text{cold}}$ HTO$_{(l)}$ + H$_2$). The high-temperature reactor with regular nonhydrophobic platinum-coated catalyst (0.32 cm diam. x 0.32 cm) was built for a gas-gas cocurrent flow, and the tritium was depleted from the water vapor (i.e., H$_2$O$_{(g)}$ + HT $\overset{\rightarrow}{\text{hot}}$ HTO$_{(g)}$ + H$_2$). Hence, with these two reactors combined in a system consisting of an evaporator, condenser, phase separator, pumps, etc., a complete closed-loop experimental apparatus involving gas-phase and liquid-phase tritium exchange reactions is obtained. This apparatus is capable of continuous recycling of the enriched and depleted water and hydrogen streams. Operating parameters, such as flow rate and temperature, may be adjusted and steady state conditions may be obtained. Reaction rates are then measured.

TABLE 1 Operation cost estimate AGNS LLAW detritiation.

Detritiated Water - 3.75 (10^6) liter/yr
750,000 Ci/yr @ 0.2 Ci/liter
On Stream 330 days/yr
Recovered Tritium 749,999.925 Ci/yr
375 liter/yr @ 2000 Ci/liter

Unit Investment:
On Site $ 3,817,000
Off Site   1,336,000
Total $ 5,153,000

Item	Quantity, yr	Cost/unit	Cost/yr	Cost/Ci
Variable Costs:				
Cooling H_2O	60,300 kgal	$ 0.02	$ 1,000	
Electricity	4.17 (10^7) kWhr	0.025	1,043,000	
Catalyst	950 lb	20.00	19,000	
Total Variable Costs			$1,063,000	$ 1.417
Fixed Costs:				
Direct Labor 8,760 man hr @ $6.00			$ 53,000	
Supervision @ 20% DL			10,000	
Maintenance @ 4% PI			153,000	
Supplies @ 10% Maintenance			15,000	
Payroll Burden @ 30% DL			19,000	
Taxes and Insurance @ 3% PI			114,000	
Depreciation 10% Straight Line			382,000	
Total Fixed Costs			$ 746,000	$ 0.995
Total Operating Costs			$1,809,000	$ 2.412

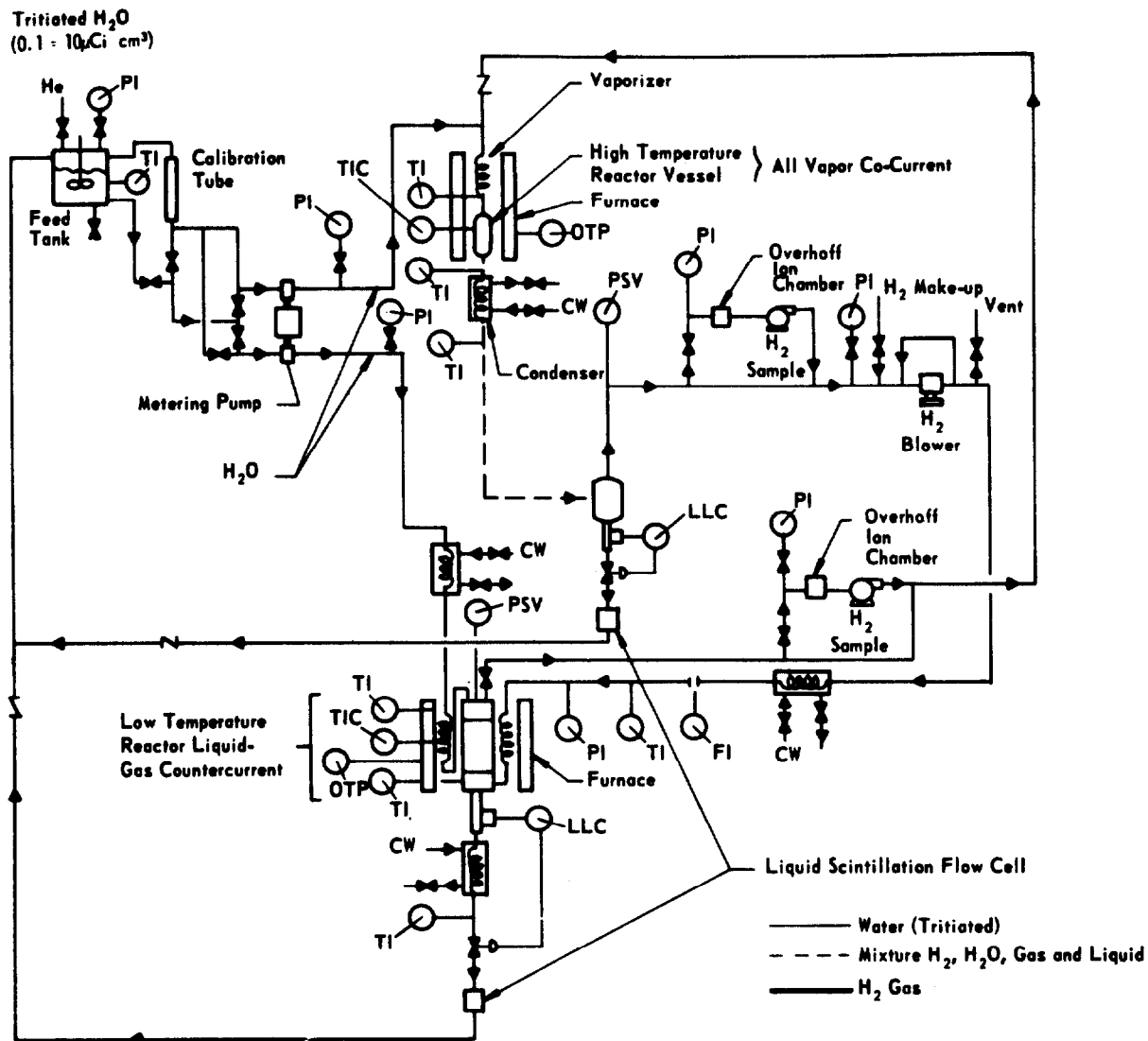FIGURE 2   Experimental system for measuring reaction rates of water-hydrogen chemical exchange.

This apparatus is being used for catalyst evaluation tests; the first catalyst to be evaluated is an Engelhard Minerals and Chemicals Company hydrophobic catalyst consisting of platinum on an alumina substrate with a semipermeable coating of a proprietary water-repellent material.

Experimental Results

The height of one equilibrium stage has been calculated from the data to be 18 ft. Since the preliminary economic evaluation (Table 1) was conducted with an assumed height of 20 ft, the 18-ft height calculated from the data would enhance the economic evaluation. The hydrophobic catalyst, therefore, appears to be propagating the liquid-gas chemical exchange effectively.

Discussion

The experimentation is continuing in order to generate data at different parameters of flow rate, temperature, and tritium concentration. The development of the mechanism of the exchange, as well as the optimum operational parameters, is to be completed. This information will be used to scale up to a pilot-plant exchange system.

Conclusion

Kinetic and thermodynamic performance data will be obtained and evaluated not only on the Engelhard catalyst, but also on a catalyst developed by Atomic Energy of Canada, Ltd., who have an interest in the catalytic exchange detritiation process for their heavy-water reactor program. In 1975, an agreement was initiated between ERDA and AECL for a cooperative program to share information concerning the catalytic exchange detritiation process. Work on the process will continue.

References

1. V. Mercea, N. Palibroda, T. Fudor, and L. Stoicovici, "Depletion column for the collection of protium oxide, ^1H_2O, by isotopic exchange between hydrogen and water," Isotopenpraxis, vol. 4, p. 328 (1968).

2. P. Savic, S. Ribnikar, and B. Pavlovic, "Efficiency of some catalysts in the exchange reaction between heavy water and hydrogen," Proc. Int. Conf. on the Peaceful Uses of Atomic Energy, Geneva, 1955, vol 8, p. 414, United Nations, New York (1956).

3. V. Mercea, Estimative Calculation of a Tritium Decontamination Unit for a Nuclear Power Plant, Institute for Atomic Physics of the Rumanian Academy of Sciences, Klug, Rumania (June 1974).

4. W. H. Stevens and F. P. Blackstein, "Heavy water production using hydrogen-water exchange," AECL Research and Development in Eng., Winter 1973, Atomic Energy of Canada, Ltd., AECL-4606, 1973.

5. S. V. Ribnikar and J. D. Pupezin, "Possibilities of tritium removal from waste waters of pressurized water reactors and fuel reprocessing plants", Proceedings of the Thirteenth AEC Air Cleaning Conference, San Francisco, California, Aug. 12-15, 1974, CONF-74087, pp. 929-945.

6. U. S. Nuclear Regulatory Commission, "Numerical Guides for Design Objectives and Limiting Conditions for Operation to Meet the Criterion 'as Low as Practicable' for Radioactive Material in Light-Water-Cooled Nuclear Power Reactor Effluents," Docket No. RM-50-2, p. 91.

DISCUSSION

R. A. BROWN: What will be the impact of the many contaminants in fuel reprocessing plant aqueous streams on performance?

BIXEL: We have considered it and it's probably going to be necessary to have pure water going into the catalytic exchange column. The water will probably have to be demineralized.

R.A. BROWN: That might be an important consideration in your design expansion.

BIXEL: This is something we will investigate in our experiments. I hope we will be able to determine the effect of trace elements.

RICHARDSON: I would like to make a brief comment on the drinking water standard that you referred to. That standard is not any longer proposed. It is effective July of this year, but I think we should put it in perspective. The standard applies to drinking water at the tap. I think it is fairly unlikely that people would be drinking effluents from your system.

BIXEL: I agree.

YARBRO: I was a little concerned about your presentation of cost benefits. Correct me if I am wrong, but I think the thousand dollar per man-rem you quoted as an NRC number applies to a 50 mile radius. The 3,000 plus man-rem EPA number, I believe, is a long-term worldwide integrated dose. I think you are multiplying apples times oranges and I believe this calculation is misleading.

BIXEL: It is my understanding that the thousand dollars per man-rem applies to world wide exposures.

YARBRO: I believe that it is specifically stated to be for a 50 mile radius.

BIXEL: I don't see the logic to applying it only to a 50 mile radius.

SKOLRUD: Have you investigated or determined the performance of this catalyst in pure gas phase applications rather than just for an aqueous gas mixture?

BIXEL: It appears that other catalysts are better in the gas phase. Our experimental system has two reactors, one, a gas phase reactor and the other, a countercurrent two-phase reactor, and we use different catalysts. The gas phase catalyst is better for gas phase exchange. We haven't tried the hydrophobic catalyst in the gas phase.

SKOLRUD: You stated that you were going to investigate the effect of contaminants in the aquaeous phase stream in this application. What contaminants do you anticipate will be included in the future tests of catalytic exchange?

BIXEL: We would have to get some information from the fuel
reprocessing people on what they expect in their water streams.

VAN BRUNT: Do you foresee any adverse interaction of deuterium
on your process?

BIXEL: Yes. That is a complicating factor in the isotopic
separation. Of course, deuterium is there to the extent of 150 parts
per million. This is a much higher level than tritium. In the pro-
cess of concentrating tritium, deuterium is also concentrated. Separat-
ing tritium from deuterium has a lower separation factor of about 1.5.

COLLINS: I would like to comment on the use of a thousand dol-
lars per man-rem. The statement is right, it is for a 50-mile radius.
I think your use of the thousand dollar figure in that sense is not
correct.

BIXEL: Apparently I stand corrected.

DEMPSEY: The other alternatives are also very costly. I
would just like to remind the audience that in the preprint envelope,
we included a copy of a portion of the TAD document which covers this
point and some others that will be discussed this afternoon.

SEPARATION OF KRYPTON FROM CARBON DIOXIDE AND OXYGEN WITH MOLECULAR SIEVES*

Charles W. Forsberg, Sc.D.
Oak Ridge National Laboratory
Oak Ridge, Tennessee 37830

Abstract

Molecular sieves were investigated to separate 1% mixtures of krypton in gas streams containing 90+% CO_2 and a few percent O_2. Such a system will be required to concentrate the krypton gas between radioactive off-gas cleanup systems such as KALC[1] (Krypton Absorption in Liquid Carbon Dioxide) and any krypton gas bottling station. Linde 5A molecular sieve was found to be capable of selectively removing the CO_2 from the gas stream while partially separating the oxygen from the krypton, i.e., effecting a three-component gas separation. This use of molecular sieves differs from standard practice in two respects: (1) bulk removal of the gas (>90%) is accomplished rather than the normal practice of removing trace impurities and (2) two separations, CO_2 from other gases and krypton from oxygen, occur simultaneously in a single bed. The use of molecular sieves for separating krypton and carbon dioxide is superior to alternatives such as CO_2 freezeout and chemical traps when there are only moderate gas flows and there is a need for very high reliability and ease of maintenance.

I. Introduction

The general approach in reprocessing HTGR nuclear fuels containing large amounts of carbon is to burn the fuel to release the fissile and fertile material. The burning process produces a CO_2-rich gas which contains all other gases in the fuel, including radioactive krypton. Since radioactive krypton cannot be released to the atmosphere, it must be removed. A process called KALC (Krypton Absorption in Liquid Carbon Dioxide)[1] has been developed to remove this radioactive krypton from the off-gas stream; however, KALC does not produce a pure product stream of krypton gas. (This is also true of several alternative processes.) Although 99+% of the krypton is removed from the off-gas by KALC and the isolated krypton may be concentrated by a factor of a 1000, the final krypton product stream contains less than 2% krypton, 0 to 5% O_2, 0 to 5% xenon, with the remainder being CO_2.

It is desirable for safety[2] and economic reasons to concentrate this krypton product further by removal of all CO_2 and most of the O_2 before bottling the krypton. The CO_2 and O_2 removed in this step, if contaminated with radioactive krypton, can be recycled back to the front end of the primary krypton removal system. The gas flows in this secondary system are so small, as compared with the primary system, that complete recycle of CO_2 and O_2 will not

significantly affect the primary system. Evaluation of many
alternatives, including chemical adsorbents and CO_2 freezeout,
indicate that molecular sieves would be preferred on the bases of
reliability, performance, and safety. Initially, the removal of
only CO_2 was planned; however, experiments also showed the
feasibility of removing most of the oxygen. Hence, it was decided
to take advantage of this additional capability.

II. Basic Process

The process for separating krypton from O_2 and CO_2 is based
on the gas adsorption characteristics of molecular sieves. Molecular
sieves are alumina-silicate crystals which have the ability to
adsorb certain gases, such as CO_2, up to 20% of their own weight. By
using molecular sieves in a manner similar to a frontal analysis gas
chromatograph[3], separation of a mixture of krypton, O_2, and CO_2
into relatively pure components in a single column is possible.

Column Behavior

If a gas mixture of krypton, O_2, and CO_2 flows through a bed
of 5A molecular sieve near atmospheric pressure at $0°C$, both CO_2
and krypton will be adsorbed. Carbon dioxide is, however, more
strongly adsorbed than krypton and thus will displace krypton gas
from the bed. In examining a long molecular sieve bed supplied with
a feed gas of O_2, krypton, and CO_2, one observes that the zone of
the molecular sieve bed nearest the feed point is saturated with
CO_2 while the gas phase contains the feed gas. At the end of this
zone, there is a transition region where CO_2 is being adsorbed onto
the bed and krypton is being displaced from the bed into the gas
phase. Beyond this first transition region is a zone where adsorbed
krypton is held by the bed and only oxygen and krypton exist in the
gas phase. At the end of this zone lies a second transition region
where krypton is being adsorbed onto the bed. Beyond the latter
region are found only oxygen and a molecular sieve bed which has
very little gas adsorbed on it.

If the gas mixture is continuously fed to the bed and the
gas exiting from the bed is analyzed, a bubble of oxygen is first
observed, followed and pushed out successively by a bubble of
krypton containing some oxygen and by the feed gas. At the end
of this process, the bed is saturated with adsorbed CO_2. Heat is
generated during the process, therefore, provisions for heat
dissipation must be included since the bed must be kept at constant
temperature to ensure good separations.

Plant Design

Two columns filled with molecular sieve and associated
equipment, as shown in Figure 1, are needed to effect the desired
gas separation on a continuous basis. The feed gas is introduced
into Bed I. When the bubble of oxygen departs from Bed I, it is
diverted to the oxygen product line. When the transition region
between the oxygen and krypton leaves Bed I, it is diverted to Bed
II. After this transition zone pases and concentrated krypton
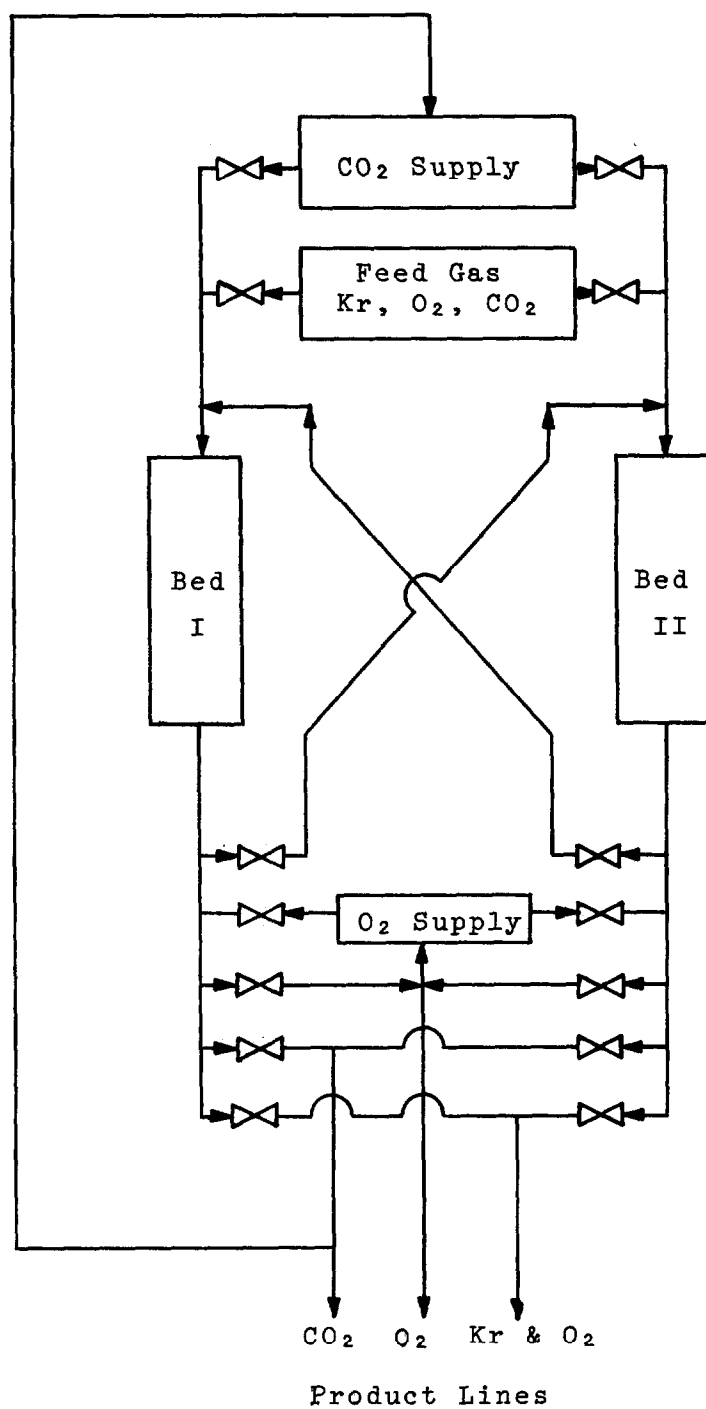begins to leave Bed I, the concentrated krypton is diverted to the

ORNL DWG 76-1020

Figure 1. Process Flowsheet

krypton product line. Finally, when the krypton-CO_2 interface exits Bed I, it is diverted to Bed II; after it reaches Bed II, the feed gas is cut from Bed I and sent to Bed II directly. At this point, Bed II undergoes the same steps that occurred in Bed I.

During the period that Bed II is adsorbing CO_2 and before the oxygen-krypton front leaves Bed II, Bed I undergoes the following steps. First, a small amount of pure CO_2 is fed to Bed I to displace the feed gas out of the void spaces and piping. This ensures that only CO_2 is present in Bed I. The small amount of gas leaving Bed I is mixed with the feed gas to Bed II. Second, Bed I is heated to at least +150°C and the pressure is decreased to near vacuum, which removes all adsorbed CO_2 from the bed. The CO_2 removed should contain little or no krypton. Third, the bed is cooled down and pressurized to system pressure with relatively nonadsorbing O_2. Bed I is now capable of handling gas from Bed II. This two-bed process, in which each bed experiences an identical cycle, can handle a constant feed gas flow and yield a highly concentrated krypton gas product. Depending upon system cycle times and economics, the process can use multiple molecular sieve beds, each bed being in a different part of the cycle. If any of the by-product O_2 or CO_2 is contaminated with radioactive krypton, it can be recycled to the front end of the primary krypton removal system, KALC.

III.   Theoretical Analysis

For design purposes, it is important to be able to predict the performance and characteristics of any proposed process. Because of the extensive work on molecular sieves, the only important characteristic of this system not found in the literature is the concentration of krypton in the krypton product stream as a function of feed gas composition, bed pressure, and bed temperature. A very simple model and computer program was developed to determine this concentration. The results of these calculations are in agreement with experimental data, as discussed in the "Experimental" section.

The model can best be described by example. The following information as input data is required: temperature of the molecular sieve, gas pressure over the bed, feed gas composition, and the amount of each gas adsorbed per gram of molecular sieve as a function of temperature and the partial pressure of that gas. Adsorption data are available in the literature in the form of graphs and equations for O_2[4,5], CO_2[6-8], and Kr[9-14]. The maximum capacity for a bed of any size can be calculated from adsorption curves for CO_2.

Assume that a bed of Linde 5A molecular sieve is to be used at a constant temperature of 0°C and 1 atm of pressure. A gas with the composition of 93.09% CO_2, 1.48% Kr, and 5.43% O_2 by volume is fed to the bed. This model is based on following a unit volume through the bed. For this example, 1 cm^3 of volume will be used. This volume enters the bed and is unaffected and unadsorbed until it reaches the CO_2 adsorption zone in the bed. At this time, 93.09% of the gas (the CO_2) is adsorbed onto the bed, leaving 0.0543 cm^3 of O_2 and 0.0148 cm^3 of krypton. Given that the CO_2 partial pressure
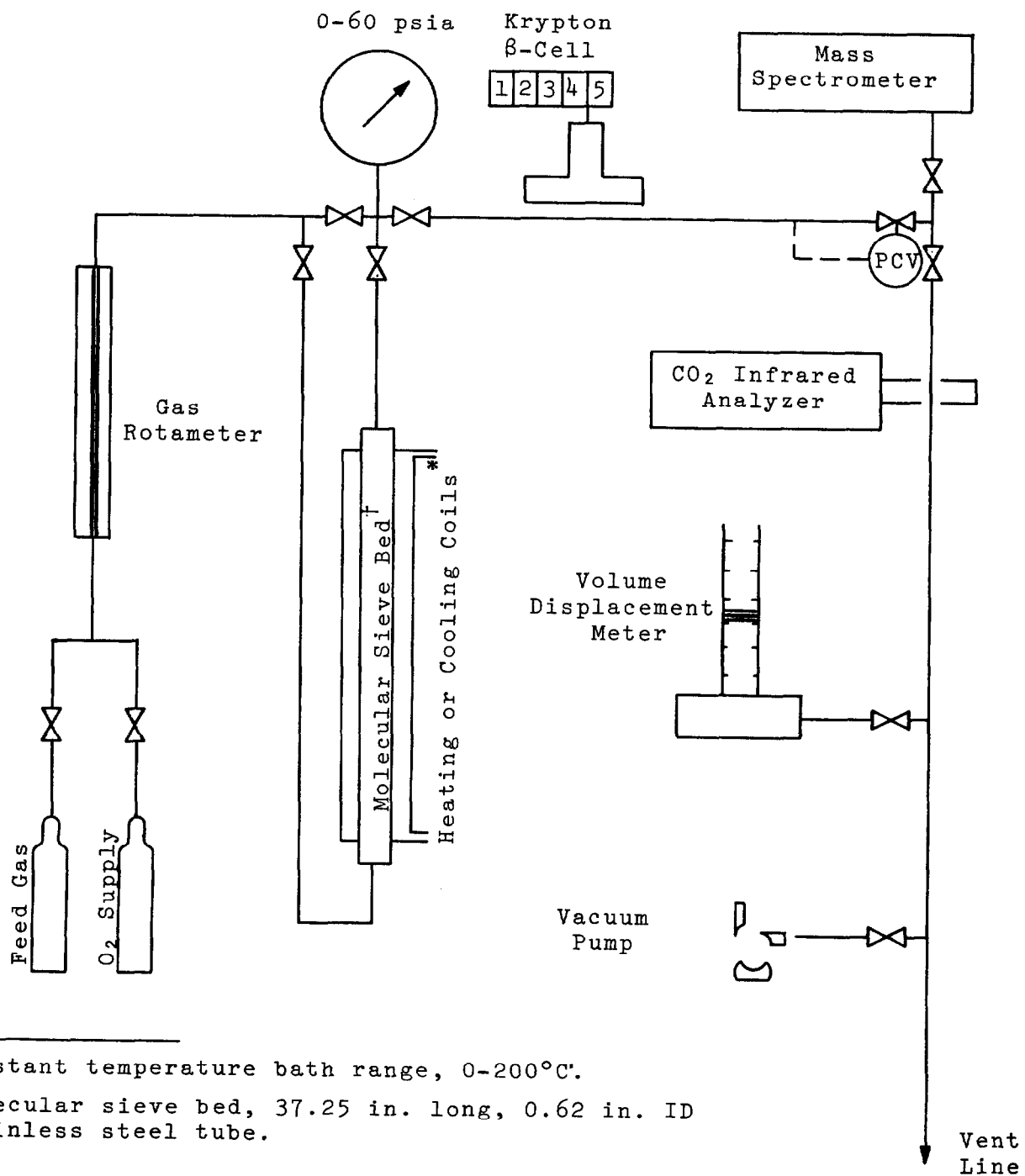
Figure 2.   Simplified diagram of experimental apparatus.

of the feed gas is 0.9309 atm, 0.9309 cm^3 of CO_2 can be adsorbed on 0.010442 g* of 5A molecular sieve at 0°C. An iterative procedure is required to determine how much krypton gas was pushed off this 0.010442 g by the CO_2. For an initial estimate of the krypton gas pressure in the zone with no CO_2, the total pressure is multiplied by 0.0148/(0.0148 + 0.0543), which is the ratio of krypton in the feed gas to the krypton and oxygen in the feed gas. Given this krypton gas pressure of 162.77 torr and 0.010442 g of Linde 5A molecular sieve saturated with krypton, the amount of krypton calculated to be on the molecular sieve is 0.0363573 cm^3 [9]. Past the adsorption front, the first calculated composition of the gas consists of 0.0148 + 0.0363573 cm^3 of krypton gas plus 0.0543 cm^3 of oxygen. This implies that 48.51% of the gas is krypton, or a krypton gas pressure of 368.68 torr. With this new krypton gas pressure, one recalculates the amount of krypton adsorbed on 0.010442 g of molecular sieve and recalculates a new gas composition. This iteration is continued until convergence on a final gas composition is achieved. For this example, the composition of the final gas is 71.49% krypton and 28.51% O_2. In theory, one expects some krypton to remain on the molecular sieve in the presence of CO_2; however, experiments showed that the equilibrium adsorption is so favorable toward CO_2 that this amount of krypton can be ignored.

There is a slight adsorption of oxygen on a clean bed; thus this method must be repeated for the oxygen-krypton transition region in order to determine the exact amount of oxygen desorbed per unit of feed gas introduced. If the bed is initially saturated with oxygen and feed with a low oxygen content is used, this slight correction becomes significant.

IV. Experimental Program

Equipment

Figure 2 shows a sketch of the experimental apparatus used to test and verify that the proposed process works. This apparatus can duplicate conditions in one column of the proposed process. Most experimental runs involve feeding a gas of known composition, flow rate, pressure, and temperature into a molecular sieve bed of known composition and observing the composition, flow rate, pressure, and temperature of the exit gas as a function of time. To ensure a feed gas of known and constant composition, the gas was premixed, analyzed by several techniques, and then stored in a standard gas cylinder. For accurate analysis, the krypton was spiked with radioactive [85]Kr, which allowed the use of accurate on-line beta radiation detection cells[15] to measure krypton concentration as a function of time. The CO_2 was analyzed by a Beckman 315A infrared analyzer. A mass spectrometer was used to verify the absence of any significant system contamination.

---

*This calculation assumes that commercial molecular sieve containing 20 wt % clay binder is used and that the equivalent of 0.02 g of CO_2 per gram of molecular sieve is already on the molecular sieve as a result of earlier incomplete bed desorption and/or bed degradation.

Choice of Molecular Sieve

Type 4A and 5A molecular sieves were tested experimentally. Screening tests showed that, while 4A was capable of removing CO_2, it did not adsorb significant amounts of krypton and its adsorption kinetics for CO_2 were slow as compared with 5A. Initial tests on molecular sieve 5A showed excellent performance characteristics; hence all major work was done with 5A molecular sieve. The following parameters characterize the 5A molecular sieve that was used:

Properties of 5A Molecular Sieve

Type: 5A (commercially produced form)
Manufacturer: Union Carbide Corporation, Linde Division
Form: 1/16-in. pellets, ~3/16 in. long
Composition: Calcium form of alumina-silicate crystals, Type A
Analysis[16]: ~80% active crystalline material, ~20% inert
    clay binder
Density (minimum): 40 lb/ft^3
Heat of Adsorption for CO_2: 12,500 cal/mole
Heat of Adsorption for Kr[9]: 3720 cal/mole
Heat of Adsorption for H_2O (max): 18,000 cal/mole

Experimental Variables

During all of the experimental runs, the molecular sieve was kept in a constant-temperature bath at $0°C$. The composition of the feed gas was 93.09% CO_2, 5.43% O_2, and 1.48% krypton with ^{85}Kr tracer. The system pressure was varied from 1 to 2.5 atm, while the feed gas flow was varied from 1.494×10^{-2} g per minute per square centimeter of molecular sieve bed cross section [7.62 cm^3(STP)/cm^2-min] to 29.964×10^{-2} g/cm^2-min (152.86 cm^3/cm^2-min). When it was desired to strip the molecular sieve of CO_2, the bed was heated to at least $150°C$ for 8 hr under vacuum provided by a mechanical vacuum pump and purged with oxygen several times during bakeout.

Experimental Results

Table I and Figure 3 present some of the experimental data collected. The following results were obtained:

(1) In all runs where the bed was carefully desorbed of CO_2, the concentrations of CO_2 in the oxygen bubble and the oxygen-krypton product were below the limit of CO_2 detection (10 ppm) by the instrumentation being used.
(2) No krypton has been detected in the oxygen bubbles expelled from the bed. This implies a krypton decontamination factor of at leat 1000, i.e., that the krypton concentration in the oxygen is not more than 1/1000 the krypton concentration in the feed gas.
(3) Mass transfer between CO_2, krypton, and the adsorbing surface is fast and does not limit the performance of a molecular sieve bed under reasonable operating conditions. Table 1 shows the length of the krypton-CO_2 mass transfer zone within the molecular sieve bed. Note that this length is only about three times that of the molecular sieve pellets (0.5 cm). The mass

1082

transfer length is defined as the minimum distance through the bed where the concentration of krypton changes by 90% of the difference between its peak values and its value in the feed. A mass transfer zone, at most a few centimeters long in a bed that is several meters long, does not limit bed performance or operation. Figure 3, which is a plot of the concentration of krypton exiting from the bed as a function of time for a single run, is nearly a discontinuous function between the krypton product wave and the feed gas coming through the bed. Unlike some other uses of molecular sieves, mass transfer is not a limiting factor in performance here.

(4) Starting with a feed gas containing 1.48% krypton, the concentrations of krypton in the product streams of all experiments exceeded 50%. This implies removal of all CO_2 and significant separation of O_2 from krypton since the maximum krypton concentration possible by removal of CO_2 is 21.4%. Table 1 shows the krypton product concentration. From theory, a krypton concentration of 71.5% would be expected at 0°C and 1 atm of pressure with the above feed gas. Note that the predicted krypton concentration is higher than the experimentally determined concentration. Adsorption of CO_2 releases large amounts of heat (12,500 cal/mole) which result in a decrease in the adsorption of krypton. This decrease, according to the model, results in a decrease in the maximum krypton concentration. It is believed that a rising internal bed temperature caused this difference between theory and experiment. The column labeled "Implied Temp. Difference" in Table 1 shows how much the bed temperature must be heated above 0°C in order for the model to fit experimental results. As a point of comparison, the heat of adsorption of the CO_2 on the molecular sieve would be sufficient to increase the temperature of the bed to 240°C if there was no cooling and if higher temperatures did not desorb CO_2 and thereby reverse the heat effects. This temperature effect indicates that the limiting design condition for a molecular sieve bed in the proposed process is the rate at which heat of adsorption can be removed from the bed.

(5) The capacity of the molecular sieve to adsorb CO_2, using the manufacturer's data[6], is 94.2 cm^3/g at 0°C, 1 atm of pressure, and a gas composed of 93.09% CO_2. This value agrees with the experimental results shown in Table 1. The experimental data show considerable scatter because the amounts of CO_2 entering and leaving the experimental apparatus are simply measured by rotameters over a period of several hours - a technique which is not designed to obtain accurate values. At these CO_2 partial pressures, the molecular sieve is approaching saturation and small changes in pressure have little effect on the amount of CO_2 adsorbed.

(6) Preliminary molecular sieve bed desorption runs have been made by heating the bed to 150°C. The results indicate that the CO_2 evolved from the bed has less than 1/50 of the krypton that the feed contained. This is an upper limit. Future work after equipment modifications should be able to more accurately measure this ratio.

Table I. Experimental results

Run number	Pressure (atm)	Flow rate $\frac{cm^3/min}{cm^2}$[a]	Length of mass transfer zone (cm)	Max. krypton concentration (%)	Implied temp. difference (°C)	CO_2 adsorbed (cm^3/g)[b]
1	1.0	7.6	1.0	52.3	30	89.8
2	1.0	34.1	2.3	55.6	25	93.9
3	1.0	49.9	1.0	58.0	21	103.5
4	1.0	76.2	1.4	56.2	24	93.5
5	1.0	91.7	1.5	55.5	25	99.6
6	1.14	48.0	1.1	58.6	–	87.9
7	1.14	48.9	1.1	58.2	–	93.8
8	2.36	50.3	2.1	51.6	–	94.6
9	2.36	96.4	3.1	61.8	–	96.6
10	2.36	152.9	2.3	57.4	–	93.1

[a]Gas at standard temperature and pressure.
[b]Gas at standard temperature and pressure adsorbed per gram of molecular sieve.

Time from Start of Experiment (min) $\propto$ Gas Flow into Bed
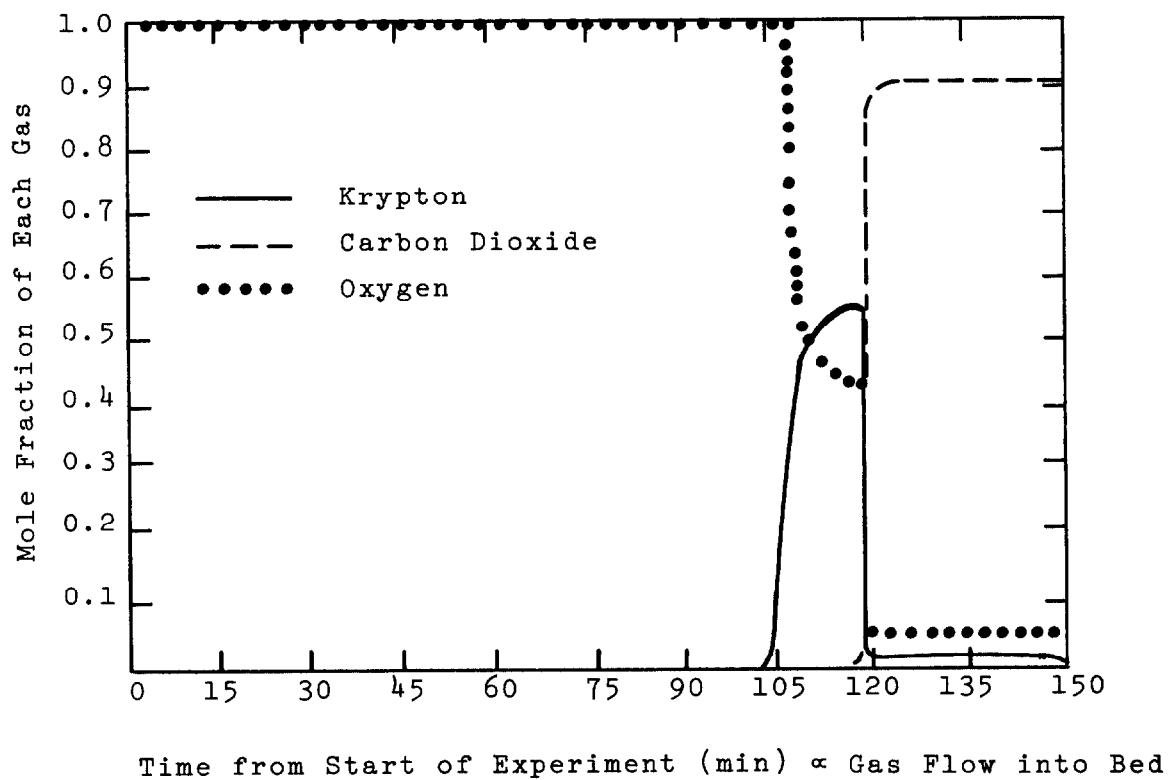
Molecular Sieve: Linde 5A
Feed Gas: 93.09% CO_2, 5.43% O_2, 1.48% Kr
Bed Conditions: 0°C, 1.14 atm
Feed Gas Flow: 48.9 $cm^3(STP)/cm^2$-min
Bed Length: 94.6 cm (37.25 in.)

Figure 3.   Gas composition from molecular sieve bed vs time.

V. Conclusions

Experiments have shown that 5A molecular sieve can separate krypton and oxygen from bulk amounts of CO_2 while partially separating the krypton from the oxygen. This process should be a reliable, economic way to separate bulk CO_2 from semiconcentrated radioactive krypton in a nuclear fuel reprocessing plant. Future experiments are planned to more accurately assess temperature transient effects in the system as well as in systems with xenon gas added.

VI. References

(1) R. W. Glass, V. L. Fowler, T. M. Gilliam, D. J, Inman, H. W. R. Beaujean, and D. M. Levins, "Experimental studies on the Krypton Absorption in Liquid CO_2 (KALC) Process," Proceedings of the 14th ERDA Air Cleaning Conference, August 2-4, 1976.

(2) M. Anbar and P. Perlstein, "Mechanism of radiolysis of carbon dioxide," Trans. Faraday Soc. 62, 1803 (1966).

(3) S. Claesson, "Studies on adsorption and adsorption analysis with special reference to homologous series," Arkiv For Kemi, Mineralogi och Geologi, Band 23A, No. 1 (1946).

(4) Union Carbide Corporation, "Oxygen Adsorption, Isotherm Data Sheet 51."

(5) D. Breck, Zeolite Molecular Sieves, John Wiley & Sons, Inc., New York, 1974.

(6) Union Carbide Corporation, "Carbon Dioxide Adsorption, Isotherm Data Sheet 22."

(7) C. J. Major, B. J. Sollami, and K. Kammermeyer, "Carbon dioxide removal from air by adsorbents," Ind. Eng. Chem. Process Design Develop. 4, No. 3, 327 (July 1965).

(8) Union Carbide Corporation "Carbon Dioxide Adsorption, Isotherm Data Sheet 24."

(9) S. Kitani and J. Takada, "Adsorption of krypton and xenon on various adsorbents," J. Nucl. Sci. Technol. 2, No. 2, 51 (Feb. 1965).

(10) M. H. Lloyd and R. A. McNees, "Adsorption of Krypton and Xenon by Various Materials," ORNL-3228, Nov. 16, 1961.

(11) C. L. Carnahan, "Gas-Chromatographic Separations of Rare Gases," USNRDL-TR-535, Nov. 2, 1961.

(12) R. D. Ackley and W. E. Browning, Jr., "Equilibrium adsorption of krypton and xenon on activated carbon and Linde molecular sieves," ORNL-CF-61-2-32, Feb. 14, 1961.

(13) L. C. Lewis, "Evaluation of Adsorbants for Purification of Noble Gases in Dissolver Off-gas, IN-1402, July 1970.

(14) K. Kawazoe and T. Kawai, "Investigation of effective diffusivities and equilibria of trace component in adsorption at elevated pressures," J. Kagaku Kogaka Issue 1, Series 36, 71, (1972).

(15) D. M. Levins, R. W. Glass, M. M. Chiles, and D. J. Inman, "Monitoring and Analysis of Process Streams in a Krypton-85 Off-Gas Decontamination System," ORNL-TM-4923, July 1975.

(16) C. K. Hersh, Molecular Sieves, Reinhold Publishing Corp. New York, 53-90 (1961).

DISCUSSION

COLLARD: Did you investigate the behavior of ozone due to krypton 85 radiation on the adsorption column?

FORSBERG: We have not investigated ozone yet. We don't think there should be a problem but we're going to be doing some more literature searches on that area. We have, of course, although it was done after I submitted this paper, investigated effects of xenon through one of these beds. You first get an oxygen peak, a krypton peak, a xenon peak, and then the feed gases. So there's no problem in that respect.

CLOSING REMARKS OF SESSION CHAIRMAN:

In this session you've heard a lot about krypton removal and very little about Carbon 14 or tritium removal. You have heard even less about what we're going to do with any of these removed species. I believe that the momentum of these conferences is going to continue and that there will be a 15th Air Cleaning Conference in two years. As a means of summarizing this session, I would like to see the 15th Air Cleaning Conference, address two major things; first, on the part of the rulemakers and policymakers, whether we have reached an international consensus on removal of these species or not. I think we should hear much more about that subject in two years.

Second, if we are going to remove them, then we should be hearing much more about finished processes for krypton removal and much more about what we're going to do about the other two isotopes and particularly, in all three cases, what are we going to do in the way of temporary storage or permanent disposal of all three of these isotopes.

With that as an intervening charge for the next two years, a lot of people are going to have to be pretty busy in this field.

SESSION XII

REGULATION

Wednesday, August 4, 1976
CHAIRMAN: J. T. Collins

USE OF ANSI N-509 IN DESIGN AND LICENSING OF NUCLEAR AIR CLEANING
SYSTEMS
C. A. Thompson

RECENT DEVELOPMENTS IN NRC GUIDLINES FOR ATMOSPHERE CLEANUP SYSTEMS
R. R. Bellamy

THE IMPACT OF APPENDIX 1 TO 10 CFR 50 ON ATMOSPHERE CLEANUP SYSTEMS
J. T. Collins

OPENING REMARKS OF SESSION CHAIRMAN:

On behalf of th eprogram committee, I would like to welcome you
to the 12th session entitled "Regulation." I venture to say that
it would be hard to attend any kind of a national meeting at which
we failed to hear something on regulation and I'm sure that we won't
disappoint you this afternoon. I think it's also safe to say that
there's a number of people at this conference and in industry who
feel that our nuclear industry is overregulated. On the other hand,
there are other people who are looking for additional guidance; who
are looking for more specific regulations. One could construe from
that that we are damned if we do and damned if we don't. We're not
going to discuss the merits of either.

The speakers this afternoon will take up the subject of implemen-
tation of standards used in the design of air cleaning systems. We
will then discuss with you some recent developments pertaining to
guides and regulations applicable to nuclear power reactors. Then
we'll talk about some of our experience in some recent regulations.

USE OF ANSI N-509 IN DESIGN AND LICENSING
OF NUCLEAR AIR CLEANING SYSTEMS

Charles A. Thompson, PE
Project Engineer
Bechtel Power Corporation
Gaithersburg, Maryland

Abstract

American National Standard N-509, "Nuclear Power Plant Air Cleaning Units and Components", has been prepared for ASME by an ad hoc committee* (N45-8.1) of the Subcommittee on Nuclear Power Plant Air and Gas Cleaning Systems (N45-8). After reviewing the background of N-509, the standard is described and its use in design and licensing of nuclear air cleaning systems is discussed.

Background

The American National Standards Subcommittee on Nuclear Power Plant Air and Gas Cleaning Systems (N45-8) was formed to develop standards for testing standby gas treatment systems. At its first meeting, on July 20 and 21, 1971, the charter of the N45-8 Subcommittee was expanded to cover air and gas cleaning systems for all types of nuclear power plants. The subcommittee was organized into four (4) working groups to prepare the following standards:

N45-8.1 - Requirement for Purge and Post-Accident Gas Treatment Systems External to Primary Containments.

N45-8.2 - Requirements for Recirculating Purge and Post-Accident Gas Treatment Systems (Inside Containment).

N45-8.3 - Testing Programs for Nuclear Gas Treatment Systems.

N45-8.4 - Requirements for Condenser Off-Gas Treatment Systems.

The initial organization of the N45-8 Subcommittee, its progress, and descriptions of the first two standards to be prepared by the N45-8.1 and N45-8.3 Ad Hoc Committees were presented at the 12th AEC Air Cleaning Conference[1]. Soon thereafter the titles of the four proposed standards were revised as shown in the forward of American National Standards N-509 (ANSI N-509).

Subsequently it was recognized that the basic requirements for the two types of air cleaning systems included in the N45-8.1 and N45-8.2 areas are the same in all but a few respects. The scope of the standard to be prepared by N45-8.1 was revised to incorporate requirements for both types of systems and N45-8.2 was deleted.

* Ad Hoc Committee on Nuclear Power Plant Air Cleaning Units and Components (N45-8.1), C. A. Thompson, Chairman

The N-509 Standard has been prepared for the American Society of Mechanical Engineers (ASME) under the American National Standard Nuclear Technical Advisory Board (NTAB). ANSI N-509, Draft 9, was approved by the N45-8.1 Ad Hoc Subcommittee and the N45-8 Subcommittee in December, 1975, and forwarded to ASME for approval and printing. The standard was approved by the ASME Committee on Nuclear Power Codes and Standards with minor comments to be incorporated in a future addendum. The standard was to be published by ASME in July, 1976, but has been delayed several months for final ANSI approval.

Description of Standard

The scope, basic concepts, organization, and special features of ANSI N-509 are described next.

Scope

The N-509 Standard includes requirements for the design, construction, and testing of the units and components which make up Engineering Safety Features (ESF) and other high efficiency air and gas cleaning systems used in nuclear power plants. The standard identifies and establishes minimum requirements for filters, adsorbers, moisture separators, air heaters, filter housings, dampers, fans, motors, ducts, and other components. It also establishes requirements for operability, maintainability, and testability. Testing provisions are specified to verify the adequacy of the unit and component design and to assure proper fabrication, installation, and system performance in accordance with specification requirements. This includes acceptance testing, including minimum acceptance criteria, in accordance with ANSI N-510, which was prepared by the companion N45-8.3 Ad Hoc Committee [2].

Limitations of the Standard. The standard does not cover functional design or sizing of complete air cleaning systems or include requirements for redundancy or integration of individual units into the complete air cleaning systems. It does not apply to Boiling Water Reactor condenser off-gas systems or cover requirements for containment isolation valves, recombiners, or ordinary heating, ventilating, and air conditioning.

Basic Concepts

The N45-8.1 Committee incorporated several basic concepts during the preparation of N-509. Included in these basic concepts are safety classification; requirements, recommendations, and options; and systems, units, and components.

ESF and Non-ESF Systems. The consensus of the committee was that the basic requirements for units and components which comprise both Engineered Safety Features and other high efficiency air and gas cleaning systems used in nuclear power plants require essentially the same level of quality. In addition, components and units for ESF systems have other requirements which are related to the safety function; for example, seismic requirements, electrical motor qualifications, and isolation requirements. In general, most portions of the standard apply to both ESF and non-ESF systems. Specific requirements for ESF units and components are identified and, where practical, appear in separate paragraphs of the standard.

Requirements, Recommendations and Options. The basic purpose of the standard is to provide minimum requirements which are mandatory for all units and components which meet the standard. In addition, the committee felt it desirable to include non-mandatory recommendations which, if followed, will further improve the quality of the units and components. For both mandatory minimum requirements and recommended practices, in a number of instances several options are available to the user of the standard.

Systems, Units and Components. One of the early decisions of the N45-8.1 Committee was that it was necessary to limit its scope in order to prepare a usable standard in a reasonable period of time. Since no comprehensive standard for air cleaning systems and components was available, it appeared to be a very large undertaking to provide as a first effort a standard having such comprehensive coverage. It was therefore decided to limit the scope of the inital standard to components, i.e., to exclude system requirements. Even though complete air cleaning systems were excluded from the scope of the standard, many of the components are normally assemblied into a single housing which comprises a major portion or subdivision of complete air cleaning system. This led to the definitions of air cleaning systems, air cleaning unit, and components as given in Section 3 of N-509. As defined therein, an air cleaning unit is an assembly of components which comprise a single subdivision of a complete air cleaning system, including all components necessary to achieve the air cleaning function of that subdivision. A unit includes the housing plus all internal components installed therein. An air cleaning system consists of one or more units and associated external components required to convey air from one or more intake points through any combination of filters and adsorbers to one or more points of discharge. The term air cleaning unit thus became a basic concept in the N-509 standard.

Organization

An outline of the N-509 Standard is presented in Table I. This table is essentially an abbreviated table of contents of the standard and shows its principal portions. The major sections of the standard are those covering functional design, component requirements, acceptance testing, and the appendix covering test canisters.

Functional Design. Section 4 of the standard, covering functional design, includes those functional requirements of a unit and the principal components comprising an air cleaning system. Since N-509 does not provide complete system requirements, Paragraph 4.2 requires that the user of the standard specify the values of a number of design parameters normally developed by the system designer. These parameters are referenced throughout the standard in the requirements for units and components. Other functional requirements include the size or installed capacity of the unit as determined by the HEPA filters and adsorbers, design pressure considerations, maintainability criteria, monitoring requirements, adsorber radioactive decay cooling requirements, testability criteria, and pressure boundary leakage criteria.

Components. The largest portion of the N-509 standard is made up of the requirements of the several types of components, which are listed in Table I. In addition to design and testing requirements for each type of component, the standard provides requirements for drawings and documentation for most components. The component requirements incorporate or invoke by reference existing standards wherever possible. New criteria have been added where suitable existing standards were not found to be available. In particular, the criteria for housings, dampers, ducts, and test canisters were found to be unavailable and were developed during the preparation of N-509.

Acceptance Testing. Paragraph 8.5 of the standard provides requirements for acceptance tests to be made in accordance with the procedures of ANSI N-510 and provides the miminum acceptance criteria which must be satisfied by each of the applicable tests of ANSI N-510.

Test Canisters. Paragraph 4.11 of the standard, covering testability requirements, requires sufficient test canisters as described in Appendix A of the standard or other means of obtaining samples of used adsorbent to be installed in the adsorber system to provide a representative determination of the response of the adsorbent to the service environment over the predicted life of the adsorbent. General requirements for the test canisters are covered in Paragraph 4.11. Appendix A provides specific requirements for several test canister installation types. These include individual test canisters which are installed in the adsorber mounting frame and test canisters which are installed in a modified flat bed or deep bed adsorber cell.

Special Features

Several of the special features of the N-509 Standard are highlighted next.

Definition of Batch and Lot. The terms batch and lot have been used with different meanings by different people in the air cleaning industry. Late in the development of the standard, it was found necessary to provide specific definitions of both lot and batch, particularly in reference to adsorbent, in order to properly specify the qualification requirements for adsorbents. It is anticipated that the definition of these terms in the N-509 standard will become the standard definitions of the nuclear air cleaning industry. This could resolve long-standing confusion in the exact meaning of these terms as used by different persons.

Pressure Boundary Leakage. The criteria for leakage across the pressure boundary of any portion of an air cleaning system includes three distinct types of requirements as listed in Paragraph 4.12 of the standard. These are air cleaning effectiveness requirements, health physics requirements, and duct and housing quality requirements. In any particular case, any one of these three requirements may determine the allowable leakage. Paragraph 4.12 requires that the lowest value as determined by each of these·three items shall be used as the allowable leakage. This, in turn, will determine the type of duct construction, for example, welded or non-weld However, ducts for ESF systems and all housings are to be welded.

The definition of and criteria for each of the three types of pressure boundary leakage requirements are given in Paragraph 4.12. As discussed therein, the ultimate measure of air cleaning effectiveness is the reduction in concentration of airborne radioactivity in the contained space or in the effluent released to the off-site atmosphere. Health physics requirements concern limiting plant personnel exposure due to contaminated out-leakage from ducts or housings to dose values established by codes, regulations, or other accepted standards. Duct and housing quality requirements provide a minimum acceptable level of workmanship. Examples providing methods of determining the allowable leakage for the requirements of Paragraph 4.12 are provided in Appendix B.

Dampers and Ducts. Due to lack of existing standards for these components, the committee developed completely new criteria and requirements for both dampers and ducts. These new requirements are given in Paragraphs 5.9 and 5.10 of the N-509 Standard, respectively. Dampers are classified by function, configuration, construction, and leakage class. Recommended damper configurations and minimum requirements for construction and leakage are given in Table 5-2 of the standard and maximum permissible damper leak rates are provided in Table 5-3.

In addition to the specific design requirements given for ducts in Paragraph 5.10 of the standard, the air leakage test requirements discussed above and given in Paragraph 4.12 of the standard were derived as a result of preparation of the criteria for ducts.

Use of N-509 in Design

When designing total air cleaning systems for nuclear power plants, it is intended that the requirements of ANSI N-509 be specified for the units and components which comprise the system. N-509 is intended to be used in all phases of design, manufacturing, storage, installation, erection, and in-place testing of units and components used in nuclear power plants to reduce and minimize concentrations of airborne radioactive materials in normally occupied portions of the plant and in airborne effluents from the plant.

In addition to application to systems handling radioactive contaminated air, N-509 is also intended for use in purging and cleanup systems handling contaminated atmospheres which are rich in nitrogen and/or hydrogen.

Specifications

The primary use of N-509 will be in preparing specifications for the design, purchase, manufacturing, storage, installation, erection, and in-place testing of units and components which comprise nuclear air cleaning systems for nuclear power plants. The distinction between standards and specifications should be carefully noted at this point. The N-509 Standard includes mandatory minimum requirements and recommendations. Design and procurement specifications, on the other hand, include additional specific information and requirements for particular applications.

Specifications include special requirements of the purchaser in addition to minimum requirements covered in the standard, specify those recommendations and options of the standard which are to be incorporated, and provide system design and size parameters for all equipment being specified. Normally, specifications also include detailed shipping information and data sheets, purchase terms, agreements, contract forms, and price information to be completed by the potential vendor. In addition, specifications for units and components of ESF systems include seismic and quality assurance requirements to be followed for equipment supplied.

Specifications which require the use of ANSI N-509 or portions thereof are normally prepared for complete nuclear air cleaning systems. Therefore, the values of the design parameters required by Paragraph 4.2 of N-509 are to be included in the specification along with other general system requirements. It is also not unusual for one design specification to provide requirements for a number of nuclear air cleaning systems.

ESF and Non-ESF Specifications. As discussed earlier, the same basic quality is required for both ESF and non-ESF nuclear air cleaning systems, units, and components. The majority of the mandatory minimum requirements and of the recommendations of N-509 apply to both types of design. However, due to the additional requirements normally imposed upon ESF systems, including seismic design and analysis, quality assurance, and other requirements peculiar to ESF systems, units, and components, it is normal practice to include only ESF or non-ESF equipment in any particular design or procurement specification. It is the intent of the N45-8 Subcommittee that N-509 requirements and recommendations be invoked in specifications for both ESF and non-ESF systems, units and components. Specifications for ESF equipment would invoke these requirements while specifications for non-ESF equipment would normally exclude these requirements.

Invoking N-509 Requirements. The use of N-509 can materially reduce specification writing and result in uniform, high quality, readily maintainable and testable systems. Long-range price reduction can be expected to result from the use of uniform requirements in specifications if N-509 requirements are utilized by the majority of purchasers of this type of equipment.

The specification or requisition for a system "in accordance with ANSI N-509" would be accepted by the suppliers and would produce a good system; however, since N-509 includes requirements specifically for ESF units and components, contains recommendations which are not mandatory requirements, and also contains various options which must be selected by the user, a proper specification or requistion should require conformance to specific paragraphs of N-509. Alternately, the specificaton could require conformance to all portions of ANSI N-509, including all recommendations contained therein. In either case, it would be necessary to delineate in the specification which options were to be followed for the equipment to be supplied.

The specification should also include quality assurance requirements, seismic design and analysis requirements, data sheets for each component to be supplied to be completed by the selected vendor, and the values of the system design parameters required by Paragraph 4.2 of the standard. Although either method of using N-509 could be utilized, it appears preferable for the specification to require conformance with a list of specific paragraphs of N-509 including delineation of recommendations and options which are to be followed for the equipment to be supplied to that specification.

It would also be possible to use material requsitions or other short forms or purchasing requests which required conformance to specific paragraphs of N-509 and provided data sheets, standard purchaser quality assurance and seismic design attachments or specifications, and the values of the design parameters required by Paragraph 4.2 of N-509; thereby eliminating entirely the use of a formal specification. However, in general, requirements beyond the minimum requirements and recommendations of N-509 will also be necessary. For example, additional requirements are imposed by NRC licensing documents such as Regulatory Guide 1.52 for ESF systems and Branch Technical Position ETSB No. 11-2 for non-ESF systems. Thus short specifications invoking specific paragraphs of N-509 are preferred.

N-509 can also be used by architect/engineers and utilities which design their own systems in preparing standard specifications for their company's use. Such standard specifications would then be used for all equipment purchased for all future projects of that entity. This would even further simplify and standardize the preparation of specifications and the manufacture of units and components for nuclear air cleaning systems.

Manufacturing

In the future, incorporation of the requirements of N-509 by most purchasers will result in product lines which meet standard minimum requirements by all manufacturers supplying this type of equipment. The use of standard specifications by major architect/engineers and utilities would provide further savings and opportunity for even broader standardization of product lines of the suppliers. Standardization of component testing requirements incorporated in N-509 and the requirements for standard design drawings and design reports included in the standard would provide further savings for the suppliers. Supplier quality control programs meeting the requirements of N-509 should be acceptable to the majority of purchasers. Minimum requirements for packing and shipping would also be standardized by the majority of suppliers of this type of equipment.

Storage, Installation and Erection

It is possible for high quality, properly specified, designed and manufactured equipment to be rendered ineffective by improper storage, installation and erection procedures during the construction or modification of a nuclear power plant. Therefore, design specifications should require that all units and components be handled in conformance with the Sections 6, 7, and 8 of ANSI N-509. This will further assure the proper performance of high quality equipment supplied and installed in accordance with N-509 and avoid rejection with associated delays and costly replacement of components damaged or otherwise rendered unuseful by improper storage, installation, and erection.

In-Place Testing

In-place acceptance testing as specified by Paragraph 8.5 of ANSI N-509 should be required by design specifications for installation of nuclear air cleaning systems, units, and components during construction or modification of nuclear power plants. Such equipment should meet the criteria for acceptance specified in Paragraph 8.5 of the standard in order to assure that the installation or modification of the system equipment is adequate to allow the system to perform its intended function. Systems and equipment which fail to meet the criteria specified in Paragraph 8.5 should be repaired and retested until the criteria are met prior to accepting the system for operation.

Use of N-509 in Licensing

The N-509 Standard, as well as the companion N-510 Standard, is intended to be referenced in specifying licensing committments and requirements. The participation of the Nuclear Regulatory Commission (NRC) in preparation of N-509 and limitations adopted to the scope of the standard assure compatability with the Commission's licensing requirements. The utilization of standards prepared by industry in licensing applications and their subsequent review and approval by the NRC should minimize the areas of potential disagreement between the applicant and the Commission. Reference to portions of these standards in Revision 1 to NRC Regulatory Guide 1.52 and in NRC Branch Technical Position ETSB No. 11-2, and committment to requirements of the standards in licensing application documents are described.

Compatibility with Licensing Requirements

From the beginning of the committee activity, it was the intent to develop standards which users, suppliers, and the NRC can utilize to assure the maintaining of high efficiency nuclear air and gas treatment systems. It was believed that the availability of such standards would simplify and expedite the licensing process for nuclear power plants. In order to assure that this objective was met, at all stages of the development of the N-509 Standard as well as the companion N-510 Standard, the NRC (formerly the Atomic Energy Commission - AEC) was represented on the committee. The participation of these members of the Commission in the standard development effort helped to identify and resolve conflicts between the resulting standard and regulatory recommendations and guidelines which otherwise might have existed.

The restriction of the scope of the N-509 Standard to units and components further aided in eliminating differences which might have resulted between industry and Commission members of the committee. The regulatory recommendations and guidelines contain many system requirements as well as component requirements. It was believed that by restricting the scope of this standard to units and components, an industry accepted standard could most quickly be prepared which would be compatible and consistent with the regulatory recommendations. Furthermore, other standards activities, such as those covered by the American Nuclear Society, already included nuclear air cleaning system requirements in their scope. It was decided

that a standard covering only units and components would be useful in meeting the licensing objectives and would serve as a useful standard for incorporation by reference in system standards produced by other committees. Subsequent revisions of the regulatory guides and establishment of branch technical positions have incorporated by reference certain portions of the requirements for units and components covered in the N-509 standard.

Revision 1 to Regulatory Guide 1.52

Revision 1 to NRC Regulatory Guide 1.52 was issued for comment in July, 1976[3]. In addition to incorporating requirements of the ANSI N-509 and N-510 standards, the revised Regulatory Guide contains a number of other revisions to the original issue of the guide. Among these other revisions are changes to the title and scope of Regulatory Guide 1.52 to limit its application to Engineered Safety Features (ESF) systems. In addition to general reference to the N-509 and N-510 standards, the major revisions to the Regulatory Guide making reference to portions of N-509 include qualification of new carbon, carbon sampling in accordance with Appendix A, leakage rate testing of system housings and duct work, and required documentation. Table II provides a summary of portions of ANSI N-509 and N-510 required by Revision 1 to Regulatory Guide 1.52.

ETSB No. 11-2

NRC Branch Technical Position No. 11-2, "Design, Testing and Maintenance Criteria for Normal Ventilation Exhaust System Air Filtration and Adsorption Units of Light Water - Cooled Nuclear Power Reactor Plants", dated 11/24/75, is the non-ESF counterpart of NRC Regulatory Guide 1.52[4] Many of the recommendations of ETSB No. 11-2 are very similar to those of Regulatory Guide 1.52, but several are somewhat less restrictive. Like Revision 1 to Regulatory Guide 1.52, this Branch Technical Position incorporates requirements of both ANSI N-509 and N-510.

The Branch Technical Position incorporates a large number of recommendations by reference to particular paragraphs of N-509. ETSB No. 11-2 recommends conformance to the criteria given in N-509 for the following items: instrumentation for monitoring and alarm; housing and duct leakage; quality of HEPA filters; heaters; component mounting frames; filter housings, including floors, doors, electrical conduits and drains; ductwork; adsorber cells, including arrangement and documentation; system fans, including mounting and ductwork connections; dampers; accessability and maintainability; provisions for test probes; and carbon samples meeting the requirements of Appendix A of the standard. A summary comparing sections of ESTB No. 11-2 with portions of ANSI N-509 and N-510 required by the Branch Technical Position is given in Table III.

Licensing Applications

It is intended that applicants preparing licensing documents such as Preliminary and Final Safety Analysis Reports (PSAR, FSAR) commit to meeting requirements given in N-509 and N-510. Revision 2 of the Standard Format and Content of Safety Analysis Reports for Nuclear Power Plants requires information for habitability systems for the control room, ESF filter systems for fission product removal and control systems,

and air conditioning, heating, cooling and ventilating systems used for normal operation (non-ESF) in Sections 6.4, 6.5.1 and 9.4, respectively. Implementation of the requirements and recommendations of ANSI N-509 and N-510 should be included in these sections of the SARs submitted to the NRC, both by direct reference to the standards (both general and particular paragraphs) and indirectly by incorporating the guidelines and recommendations of Regulatory Guide 1.52, Revision 1, and Branch Technical Position ETSB No. 11-2.

Use in Other Standards and Other Applications

The ANSI N-509 Standard is expected to be incorporated in standards prepared by other organizations having scopes which include nuclear air cleaning systems requirements for use in both nuclear power plants and other applications, e.g., research facilities, hot cells, fuel reprocessing plants, fuel fabrication plants, and radioactive waste facilities. The N-509 Standard, as well as its companion N-510 Standard, may be used directly in applications other than nuclear power plants by incorporating its requirements in the design and licensing of such facilities. In addition, regulatory guides and requirements for facilities other than nuclear power plants may incorporate the requirements of these standards.

An example of the use of ANSI N-509 in more general standards for air cleaning systems for nuclear power plants is the proposed ANSI N-276, "BWR Containment Ventilation Systems", which is being prepared by the ANS-50 Committee. This standard acknowledges and makes reference to ANSI N-509. It is expected that in the future, additional standards will be prepared by the American Nuclear Society and other organizations which incorporate N-509 requirements.

Updating of N-509

The ANSI/N45-8 Subcommittee has been reorganized under the ASME "Accredited Organization Method" for preparing American National Standards. This new ASME Committee on Air and Gas Treatment Equipment will be one of several committees under the recently reorganized ASME Committee on Nuclear Power Codes and Standards. This committee, in turn, reports to the ASME Policy Board on Codes and Standards. Other committees included under the Committee on Nuclear Power Codes and Standards are Operation and Maintenance, Quality Assurance, Qualification Testing, Sections III and XI of the Boiler and Pressure Vessel Code, and Mechanical Equipment. Organizational meetings of the Air and Gas Treatment Equipment Committee were held February 26 and May 6, 1976.

The ANSI N-509 and N-510 standards now fall under the custody of the ASME Committee on Air and Gas Treatment Equipment. This committee will prepare subsequent issues and revisions to the N-509 and N-510 Standards as appropriate, which will then be reissued by ASME.

References

1. F. D. Leckie and C. A. Thompson, "ANSI/N45-8 Nuclear Gas Systems Treatment Standards", Proceedings of the 12th AEC Air Cleaning Conference, CONF-720823, Vol. 2, pp. 848-856, (1972).

2. American National Standard - Reactor Plants and Their Maintenance, "Testing of Nuclear Air Cleaning Systems", ANSI N-510-1975, The American Society of Mechanical Engineers (1975).

3. Regulatory Guide 1.52, "Design, Testing and Maintenance Criteria for Engineered Safety Feature Atmosphere Cleanup System Air Filtration and Adsorption Units of Light-Water-Cooled Nuclear Power Plants", Revision 1, June, 1976, U. S. Nuclear Regulatory Commission (1976).

4. NRC Branch Technical Position ETSB No. 11-2, "Design, Testing and Maintenance Criteria for Normal Ventialation, Exhaust System Air Filtration and Adsorption Units of Light-Water-Cooled Nuclear Power Reactor Plants", U. S. Nuclear Regulatory Commission (1975).

Table I

Outline of standard ANSI N-509

1. SCOPE

2. APPLICABLE DOCUMENTS

3. TERMS AND DEFINITIONS

4. FUNCTIONAL DESIGN
4.1   General
4.2   Design Parameters
4.3   Size (Installed Capacity) of Unit
4.4   Environmental Design Conditions
4.5   Structural Load Requirements
4.6   Design Pressures
4.7   Maintainability Criteria
4.8   Monitoring of Operational Variables
4.9   Adsorbent Radioactive Decay Heat Cooling
4.10 Insulation
4.11 Testability
4.12 Pressure Boundary Leakage

5. COMPONENTS
5.1   HEPA Filters
5.2   Adsorbers
5.3   Prefilters
5.4   Moisture Separators
5.5   Heaters
5.6   Filter Housing
5.7   Fan
5.8   Fan Motors
5.9   Dampers
5.10 Ducts

6. PACKAGING, SHIPPING, AND STORAGE OF COMPONENTS

7. INSTALLATION AND ERECTION

8. QUALITY ASSURANCE INCLUDING ACCEPTANCE TESTING

APPENDIX A.   SAMPLING METHODS TO DETERMINE PERFORMANCE DEGRADATION RATES
OF ADSORBENTS

APPENDIX B.   PROCEDURE TO DETERMINE TEST UNIT LEAKAGE FOR DUCTS AND HOUSINGS

APPENDIX C.   FIELD OBSERVATION CHECKLIST

Table II

Summary of ANSI N-509 and N-510 sections required
by NRC Regulatory Guide 1.52, Revision 1

Reg. Guide 1.52 Position	Subject	N-509 Section(s)	N-510 Section(s)
C.2.1	Testing and acceptance criteria	4.11, 8.5	All
C.5	Visual inspection	-	5
C.5.a	Flow distribution test	-	8
C.5.b	DOP testing of HEPA filters	-	10
C.5.c	Freon testing of adsorbers	-	12
C.6.b	Carbon samples	Appendix A	-
C.6.c	Detailed test procedures	4.11, 8.5	All
Table I	New activated carbon tests	5.2.3	-

Table III

Summary of ANSI N-509 and N-510 sections required by
NRC Branch Technical Position ETSB No. 11-2

ETSB No. 11-2 Position	Subject	N-509 Section(s)	N-510 Section(s)
B.2.c	Local instrumentation	4.8.1	-
B.2.g	Housing and duct leakage rate	4.12	6
B.3.a	Heaters	5.5	-
B.3.b	HEPA filter design	5.1	-
B.3.c	Component mounting frames	5.6.3	-
B.3.e	Unit filter housings	5.6	-
B.3.f	Ductwork	5.10	-
B.3.h	Adsorber cells	5.2	-
B.3.i	Fan and motor	5.7, 5.8	-
B.3.l	Dampers	5.9	-
B.4.b	Accessibility and maintenance	4.7	-
B.4.d	Permanent test probe parts	4.11	-
B.5.a	Visual inspection	-	5
B.5.b	Air flow distribution	-	8
B.5.c	In-place HEPA DOP test	-	10
B.5.d	Refrigerent testing of adsorbers	-	12
B.6.b	Carbon samples	Appendix A	-

DISCUSSION

PALMER: Why was the standard (ANSI N-509) taken away from the ANSI organization for updating, etc.? I don't understand that.

THOMPSON: This is a reorganization of the entire ASME committee structure and I have some brief comments on it in my paper. Let me refer to it to list the other committees that are included. The ASME committee on Nuclear Power Codes and Standards has incorporated a number of standards areas from ANSI and other organizations relating to nuclear power plants. Included under this committee are a number of other committees, including the committee on Operation and Maintenance, Quality Assurance, which would be the old N-45-2, Qualification Testing, Sections III and XI of the Boiler and Pressure Vessel Code, Mechanical Equipment, and the Air and Gas Treatment Equipment Committee. Beyond that, I can't give you much additional information but I hope it gives a partial answer to your question.

COLLINS: Is Jim Fish in the audience? Perhaps he could further clarify this matter.

FISH: N-45 was a committee that functioned under the chairmanship of Saul Bernstein of Wisconsin Power. That committee was finally terminated about one week ago. Under the new "Accredited Organization Method", the Nuclear Power Code and Standards Committee, of which we are a part, has picked up the air and gas treatment activity.

R. A. BROWN: If the ANSI standard has been made compatible with the Regulatory Guide, why do we need both?

THOMPSON: Perhaps I should defer comment inasmuch as we have two Nuclear Regulatory Commission members who will speak after me, but I will attempt an answer. I believe it is correct that NRC likes to be able to reference acceptable industry standards when these provide an acceptable degree of conservative design, testing, and operation to meet safety requirements.

R. A. BROWN: Then perhaps in your paper you should have said that the Regulatory Guide was compatible with the standard you established rather than your standard being compatible with the Regulatory Guide.

THOMPSON: We have worked closely with the Regulatory Commission on this standard and we have made every attempt to make the two viewpoints compatible   I guess it is not really a question of which came first, the chicken or the egg, because Regulatory Guide 1.52 was there first. We didn't want to disagree in any areas without good reason. There were some recommendations for revisions to the Regulatory Guide that were made by the committee, and some of these are, indeed, reflected in Revision 1.

RECENT DEVELOPMENTS IN NRC GUIDELINES FOR ATMOSPHERE CLEANUP SYSTEMS

Ronald R. Bellamy
U. S. Nuclear Regulatory Commission
Office of Nuclear Reactor Regulation
Washington, D.C. 20555

Abstract

The Nuclear Regulatory Commission (NRC) maintains the policy of updating when necessary, its published guidance for the design of engineered safety feature (ESF) and normal ventilation systems. The guidance is disseminated by means of issuing new, or revisions to, existing Regulatory Guides, Standard Review Plans, Branch Technical Positions and Technical Specifications. NRC guidance is updated only when a strong technical basis exists, resulting from standards development, research developments, the determination of additional review areas that are found to be needed based on operating reactor experience, or the review of Safety Analysis Reports.

Since the 13th Air Cleaning Conference two years ago, NRC has added to and changed many of its guidelines for atmosphere cleanup systems. This paper will discuss a revised Regulatory Guide, new Technical Specifications and new Standard Review Plans with Branch Technical Positions for atmosphere cleanup systems.

Regulatory Guide 1.52, "Design, Testing and Maintenance Criteria for Atmosphere Cleanup System Air Filtration and Adsorption Units of Light-Water-Cooled Nuclear Power Plants," was issued in July 1973. Since that time, NRC has received numerous comments from industry on the regulatory positions contained in the guide. During this period, NRC has participated in numerous meetings with various segments of the nuclear industry (utilities, architect-engineers, filtration system vendors and private consultants) concerning the positions set forth in this guide. Revision 1 to Regulatory Guide 1.52 reflects comments received from the industry, latest state-of-the-art technology, operating experience and the requirements set forth in recently issued ANSI Standards N510-1975, "Testing of Nuclear Air Cleaning Systems," and ANSI N509 (draft), "Nuclear Power Plant Air Cleaning Units and Components".

Technical Specifications for ESF filter systems that require a variety of in-place tests for these systems have been issued to all operating reactors and those utilities receiving operating licenses. Standard Review Plan 11.3, "Gaseous Waste Systems," was issued December 22, 1975 and contains Branch Technical Position (BTP) Effluent Treatment Systems Branch (ETSB) No. 11-2, "Design, Testing and Maintenance Criteria for Normal Ventilation Exhaust System Air Filtration and Adsorption Units of Light-Water-Cooled Nuclear Power Reactor Plants". BTP ETSB 11-2 outlines NRC guidance for normal ventilation exhaust systems that are designed to meet the "as low as is reasonably achievable" guidelines of Appendix I to 10 CFR Part 50, and contains NRC positions with respect to review procedures for HEPA filters for particulate removal and charcoal adsorption units for low-concentration radioiodine removal.

This paper will discuss the major comments received from the nuclear industry since the guide was issued in July 1973, NRC's experience in implementing the guide in recent license applications, status of operating plants in meeting the guidelines and NRC's continuing assessment of operating data and laboratory tests to assure that the guide reflects the latest technology.

I. Introduction

New and revised guidance for the design of atmosphere cleanup systems to be installed in commercial nuclear power facilities have appeared from various sectors of the nuclear industry in the last two years. Industry standards, research accomplishments, developments in operating experience, and new regulations have all impacted on this occurrence. The Nuclear Regulatory Commission (NRC) has made its contributions in the form of a revised Regulatory Guide, Standard Review Plans, Branch Technical Positions and Technical Specifications. This paper will discuss (1) Revision 1 to Regulatory Guide 1.52, "Design, Testing, and Maintenance Criteria for Engineered Safety Feature Atmosphere Cleanup System Air Filtration and Adsorption Units of Light-Water-Cooled Nuclear Power Plants,"[1] (2) Technical Specifications for engineered safety feature (ESF) filter systems, and (3) Branch Technical Position (BTP) Effluent Treatment Systems Branch (ETSB) No. 11-2, "Design, Testing, and Maintenance Criteria for Normal Ventilation Exhaust System Air Filtration and Adsorption Units of Light-Water-Cooled Nuclear Power Plants."[2]

II. Revision 1 to Regulatory Guide 1.52

Since Regulatory Guide 1.52[3] was issued in July 1973, NRC has received numerous comments on its contents. These comments have been received in various forms, including official submittals to the Advisory Committee on Reactor Safeguards, informal conversations, and scheduled meetings, and have been received from consultants, utilities, architect-engineers, filtration system vendors and other governmental agencies. Revision 1 has considered every comment received.

Many of the changes to Regulatory Guide 1.52 are minor clarifications. These changes will not be discussed here, but will be available for your review in the near future when the revised Guide is issued for public comment. The issuance of the revised Guide will be noted in the Federal Register, and information will be included pertaining to its availability. A 60-day comment period will follow, after which the NRC staff will consider all comments received and incorporate any applicable comments into the final version of Revision 1. However, once the draft of Revision 1 is issued for public comment, it may be referenced in license applications.

One of the major proposed changes to the Guide pertains to provisions to preclude possible iodine desorption and adsorbent autoignition that may result from radioactivity induced heat and the associated temperature rise. Previously, water sprays were considered necessary to inhibit adsorber fires. The proposed change would allow a single-failure proof low flow air bleed system to prevent any temperature rise. This means of cooling has been shown acceptable by various analyses,[4] including computer simulation.[5]

Experience with water sprays has shown their susceptibility to inadvertent activation (thus inhibiting the carbon from further usefulness as an adsorbent), and the possibility of the spray resulting in re-volatilization of adsorbed iodine.[6] A suitable low flow airbleed system may be obtained by cross-connections or redundant fans. The single failure criterion applies to the fans, cross-connections and heaters (to assure that any air bleed is at a maximum relative humidity of 70%).

A second major change is concerned with bypassing of any cleanup components during testing. Previously, temporary bypassing of banks of components was needed to prevent the test agents from contaminating the high efficiency particulate air (HEPA) filters or carbon adsorbers. Laboratory tests have shown such precautions to be unnecessary.[7, 8]

The third major change concerns utilization of two industry standards that were issued since July 1973. ANSI N510-1975, "Testing of Nuclear Air-Cleaning Systems,"[9] describes methods for field-testing of nuclear air cleaning systems. Sections of ANSI N510-1975 incorporated in Revision 1 to Regulatory Guide 1.52 include a visual inspection of filter trains, air flow distribution testing, in-place dioctyl phthalate (DOP) leak testing of HEPA filter banks, in-place halogenated hydrocarbon refrigerant leak testing of adsorber banks, and laboratory testing of adsorbent. ANSI N509-Draft 9 (November 1975), "Nuclear Power Plant Air Cleaning Units and Components,"[10] covers requirements for the design, construction, and testing of units and components which make up high efficiency air and gas cleaning systems used in nuclear power plants. Sections of ANSI N509-Draft 9 incorporated in Revision 1 to Regulatory Guide 1.52 include guidance on how to obtain representative used carbon samples, qualification of new carbon to be installed in ESF filter systems, and documentation. Mr. Thompson has just completed a discussion of the use of this standard in the design and licensing of nuclear air cleaning systems.[11]

The fourth major change to the Guide is concerned with in-place testing frequency. The Guide as now issued recommends in-place testing simply on a calender frequency, with no consideration for how long the filter system might actually have been in operation and degrading. The proposed change recommends in-place testing (1) initially, (2) at least once per operating cycle if in a standby status or after every 720 hours of filter system operation, and (3) following painting, fire, or chemical release in any ventilation zone communicating with the system that could contaminate the HEPA filters or carbon adsorbers. This testing frequency verifies that the system has been installed properly, that undue aging or weathering has not occurred, and that contamination of the filter system components has not occurred after painting, fire or chemical release. A testing frequency of 720 hours may seem unduly restrictive for those systems used for any normal plant ventilation, but is considered necessary to verify that poisoning or weathering of the carbon adsorbent has not occurred. A review of the available degradation data for in-service carbon [12-22] supports this testing frequency, when the uncertainties in the reactor site, the filter system location, and the contaminants the filter system will experience, are considered.

Some of the minor changes proposed to Regulatory Guide 1.52 include (1) allowing 1500 cubic feet per minute HEPA filters, (2) deleting the recommendation for provisions to replace contaminated filter trains as an intact unit, (3) leak testing in accordance with ANSI N510-1975, with acceptance criteria as outlined in ANSI N509-Draft 9, and (4) elimination of any reference to non-ESF atmosphere cleanup systems.

III. ESF Atmosphere Cleanup System Technical Specifications

Regulatory Guide 1.52 contains a section entitled "In-Place Testing Criteria." Although a utility commits to this testing program when the plant is being designed, site-specific Technical Specifications are needed to ensure that an adequate in-place testing program is being followed. Thus, Technical Specifications to cover the in-place testing of ESF atmosphere cleanup systems have been developed. These specifications reflect the proposed changes to Regulatory Guide 1.52 and have been issued to approximately 75% of the 58 reactor units licensed to operate to date (the remainder of the operating reactors are in the process of revising their Technical Specifications accordingly). The Technical Specifications are also part of the Standard Technical Specifications being issued to applicants seeking an operating license.

As previously discussed, the Technical Specifications for ESF atmosphere cleanup systems require in-place testing (1) initially, (2) at least once per operating cycle if in a standby status or after every 720 hours of filter system operation, and (3) following painting, fire, or chemical release in any ventilation zone communicating with the system that could contaminate the HEPA filters or carbon adsorbers. This testing frequency is considered appropriate to assure that, if called upon after a design basis accident, the ESF atmosphere cleanup system could perform its intended function in reducing the release of gaseous radioactive materials to the environment or protecting the control room operator. The Technical Specifications contain Surveillance Requirements, which outline surveillance testing (with procedures and acceptance criteria), to demonstrate that a limiting condition of operation (which require that a system either be in an operable status or steps are taken to return the system to operable status or the reactor is shut down), are not violated. Bases are also included which supply the justification for and reasoning behind the Technical Specifications.

The Technical Specifications for ESF atmosphere cleanup systems contain requirements to periodically check (1) pressure drop across the HEPA filters and carbon adsorbers, (2) air distribution across the HEPA filters and carbon adsorbers, (3) automatic initiation of the filter trains, (4) operability of heaters, (5) fan capacity, (6) leak tightness of the HEPA filter bank, (7) leak tightness of the carbon adsorber bank, and (8) removal capability of the carbon adsorbent for radioiodine by laboratory testing. If these requirements are not satisfied, the Technical Specifications allow a period of time to return the filter train to operable status, or the reactor is to be shut down. Guidance is given in the bases for returning the filter train to operable status, by indicating that replacement HEPA filters and carbon adsorbent should be qualified according to Regulatory Guide 1.52.

IV. Branch Technical Position ETSB No. 11-2

Standard Review Plans (SRP) are prepared for the guidance of the staff reviewer of the Office of Nuclear Reactor Regulation, NRC, who performs the detailed safety review of applications to construct or operate a nuclear power plant. The application of the SRP should improve the quality and uniformity of staff reviews, and present a well-defined base for evaluation of proposed changes in the scope and requirements of reviews. The SRP also serve to implement Nuclear Reactor Regulation policy on making information about regulatory matters widely available and to improve communication and understanding of the staff review process by interested members of the public and the nuclear power industry. SRP 11.3 is entitled "Gaseous Waste Management Systems."[23] Attached to this SRP is Branch Technical Position (BTP) Effluent Treatment Systems Branch (ETSB) No. 11-2, "Design, Testing and Maintenance Criteria for Normal Ventilation Exhaust System Air Filtration and Adsorption Units of Light-Water-Cooled Nuclear Power Reactor Plants." This BTP offers design guidance for particulate filtration and radioiodine adsorption units included in ventilation exhaust systems to reduce the quantities of gaseous radioactivity released from building or containment atmospheres during normal operation. In some instances, these ventilation exhaust systems will be necessary to satisfy the "as low as is reasonably achievable" criterion as expressed in Appendix I to 10 CFR Part 50[24] issued May 1975. Mr. Collins will discuss this regulation and its impact shortly.[25] This paper will discuss the major positions set forth in BTP ETSB No. 11-2; copies of SRP 11.3 containing the entire position paper are available as NUREG-75/087 through the National Technical Information Service in Springfield, Virginia.

BTP ETSB No. 11-2 indicates that an atmosphere cleanup system installed in a normal ventilation exhaust system should consist of the following components: heater for humidity control, HEPA filters for particulate removal, iodine adsorbers, fans for air movement, and associated ducts, dampers and instrumentation. The system need not be redundant, nor seismic Category I, but should be limited to a volumetric flow rate of 30,000 cubic feet per minute per train. Instrumentation should be provided to monitor pressure drops and flow rates. Draft standard ANSI N509 is referenced for qualification of heaters and HEPA filters, and for the design of component mounting frames, filter housings (including floors and doors), electrical conduits, drains, ductwork, adsorber cells (including arrangement and documentation), the system fan (including mounting and ductwork connections), dampers, test probes, and samplers to obtain representative carbon samples for laboratory testing. Standard ANSI N510-1975 is referenced for in-place testing of the air flow distribution to the HEPA filters and carbon adsorbers, leak-tightness of the HEPA filter banks, and leak-tightness of the carbon adsorber banks. In-place testing is recommended initially and at intervals not to exceed 18 months thereafter (during scheduled shutdowns is acceptable). During each in-place test, a representative sample of carbon is removed for laboratory testing. Guidance for performing this laboratory testing is presented in the BTP, and physical properties for new activated carbon to be installed in the adsorber units whenever used carbon does not pass the laboratory test is outlined.

BTP ETSB No. 11-2 is written in the same format as Regulatory Guide 1.52: the first section of the document contains technical positions, or one acceptable method of designing the system, then the second section of the document indicates the removal credit for various radioactive species that will be assigned the filter system if the positions in the first section of the document are satisfied. Table 2 of BTP ETSB No. 11-2 indicates that normal ventilation exhaust systems operating outside of containment and controlling the relative humidity to 70% will be assigned removal efficiencies for radioiodine of 70%, 90% and 99% when the bed depth of activated carbon is 2, 4 and 6 inches, respectively. Radioactive particulate matter will be assumed to be removed at an efficiency of 99%. Naturally, these removal efficiencies are based on the premise that all of the positions in the first section of BTP ETSB No. 11-2 are satisfied, and the inplace test program is followed and all test results are acceptable. Also, these removal efficiencies are the expected average removal efficiencies for the 30-year operating life of the plant.

The NRC welcomes, and solicits, any comments or supporting data for any of the above positions. Comments on BTP ETSB No. 11-2 should be forwarded to Director, Office of Nuclear Reactor Regulation, U. S. Nuclear Regulatory Commission, Washington, D.C. 20555.

V. Conclusion

This paper has discussed three NRC documents published in the last two years that present the NRC positions on atmosphere cleanup systems. Revision 1 to Regulatory Guide 1.52 and the Technical Specifications that implement part of the Regulatory Guide are concerned with ESF atmosphere cleanup systems; Branch Technical Position ETSB No. 11-2 is concerned with normal ventilation exhaust systems. This new guidance has been issued due to the adoption of two industry standards, research accomplishments, developments in operating experience, and new regulations. Comments or data impacting on any of these documents are invited. These comments, together with future developments in the field of atmosphere cleanup at nuclear

power reactors will be considered, and, when necessary and a strong technical basis exists, NRC will revise existing guidance or publish additional guidance relating to atmosphere cleanup systems in commercial nuclear power reactors.

References

1. USNRC Regulatory Guide 1.52 (Rev. 1), "Design, Testing and Maintenance Criteria for Engineered-Safety-Feature Atmosphere Cleanup System Air Filtration and Adsorption Units of Light-Water-Cooled Nuclear Power Plants," (to be issued for comment).

2. Branch Technical Position Effluent Treatment Systems Branch No. 11-2, "Design, Testing and Maintenance Criteria for Normal Ventilation Exhaust System Air Filtration and Adsorption Units of Light-Water-Cooled Nuclear Power Plants," NUREG 75/087, "Standard Review Plan for the Review of Safety Analysis Reports for Nuclear Power Plants - LWR Edition," September 1975.

3. USNRC Regulatory Guide 1.52, "Design, Testing and Maintenance Criteria for Atmosphere Cleanup System Air Filtration and Adsorption Units of Light-Water-Cooled Nuclear Power Plants," June 1973.

4. Final Safety Analysis Report, Florida Power and Light Company, St. Lucie, Unit No. 1, Docket 50-355, pp. 6.2-117, 118.

5. E. A. Bernard and R. W. Zavadoski, "The Calculation of Charcoal Heating in Air Filtration Systems," 13th AEC Air Cleaning Conference, Conf-740807, August 12-15, 1974.

6. Letter, Director, Naval Research Laboratory to Director, Atomic Energy Commission, Division of Waste Management and Transportation, "Influence of Solvent Vapors and of Water Flooding on Methyl Iodide Trapping by Charcoal," January 8, 1975.

7. Letter, C. H. Ice, Director, Savannah River Laboratory, Atomic Energy Division, to N. Stetson, Manager, Savannah River Operations Office, U. S. Atomic Energy Commission, DPST-74-495-TL, October 10, 1974.

8. A. H. Dexter, A. G. Evans and L. R. Jones, "Confinement of Airborne Radioactivity Progress Report: January-December 1974, Savannah River Laboratory DP-1390, October 1975.

9. ANSI N510-1975, "Testing of Nuclear Air Cleaning Systems," American National Standard Institute.

10. Draft Standard ANSI N509 (Draft 9-November 1975), "Nuclear Power Plant Air Cleaning Units and Components," American National Standards Institute.

11. C. A. Thompson, "Use of ANSI N509 in Design and Licensing of Nuclear Air Cleaning Systems," 14th ERDA Air Cleaning Conference, August 2-4, 1976 (to be published).

12. Taylor, L. R. and Taylor, R., The Aging of Impregnated Charcoals, Seminar on Iodine Filter Testing, Karlsruhe, December 1973.

13. Clifton, J. J., Operating Experience of the SGHWR Iodine Sorption System, Seminar on Iodine Filter Testing, Karlsruhe, December 1973.

14. Akley, R. D., et al., Aging, Weathering, and Poisoning of Impregnated Charcoals Used for Trapping Radioiodine, ORNL-TM-2860, March 1970.

15. Davis, R. J., et al., Long-Term Effects on Radioiodine Trapping by Charcoals, 12th AEC Air Cleaning Conference, CONF-720823, August 28-31, 1972.

16. Hesbol, R., et al., Iodine Filter Testing in Sweden, Seminar on Iodine Filter Testing, Karlsruhe, December 1973.

17. Collins, D. A., et al., The Development of Impregnated Charcoals for Trapping Methyl Iodide at High Humidity, 9th AEC Air Cleaning Conference, CONF-660904, September 13-16, 1966.

18. Wilhelm, J. G., Testing of Iodine Filter Systems Under Normal and Post-Accident Conditions, 12th AEC Air Cleaning Conference, CONF-720823, August 28-31, 1972.

19. Letter, Ralph B. Sewell, Consumers Power Company Nuclear Licensing Administrator, to R. A. Purple, NRR, June 18, 1975, Palisades Plant In-Place Filter Systems, Docket No. 50-255, License DPR-20.

20. Bennett, E. C., et al., Evaluation of Weathered Impregnated Charcoals for Retention of Iodine and Methyl Iodide, DUN-7985, June 1972.

21. Bennett, E. C., et al., Evaluation of Weathered Impregnated Charcoals for Retention of Iodine and Methyl Iodide, UNI-39, July 1973.

22. Bennett, E. C., et al., Evaluation of Weathered Impregnated Charcoals for Retention of Iodine and Methyl Iodide, UNI-251, August 1974.

23. Standard Review Plan 11.3, "Gaseous Waste Management Systems," USNRC NUREG-75/087, September 1975.

24. Appendix I to Title 10 of the Code of Federal Regulations, Part 50, "Numerical Guides for Design Objectives and Limiting Conditions for Operation to Meet the Criterion 'As Low As Is Reasonably Achievable' for Radioactive Material in Light-Water-Cooled Nuclear Power Reactor Effluents."

25. J. T. Collins, "The Impact of Appendix I to 10 CFR Part 50 on Atmosphere Cleanup Systems," 14th ERDA Air Cleaning Conference, August 2-4, 1976 (to be published).

DISCUSSION

SHERMAN:　　　　　What, in your opinion, would constitute an acceptable indication of total integrated running time up to 720 hours?

BELLAMY:　　　　　If I understand the question correctly, my answer will be a timing device on the filter system. It should be initiated whenever the filter system is seeing air through the carbon and automatically stopped whenever the air flow through the carbon is eliminated.

DEMPSEY:　　　　　Every two years, the Europeans come to this Conference and tell us the advantages of their well-used in-place testing procedures using methyl iodide 131. Would this technique be accepted by NRC as an alternate to the sampling and laboratory test now required if we demonstrated its efficiency?

BELLAMY:　　　　　I would say, if the usefulness is demonstrated and knowledgeable health physicists on the NRC staff make a decision that it is not detrimental to the tests, or the filter system, or to any of the operating personnel, I would say we would seriously consider it.

THOMPSON:　　　　　I have noticed that the credit for removal efficiencies for radioiodine for non-ESF units given in Branch Technical Position ETSB No. 11-2 are lower than the comparable values for ESF filter units. Normally, operating units discharge effluents indicating performance in excess of values for ESF credit. Discharges from normally operating units are monitored and recorded. They also have alarms and activate closure of inlet dampers if the release exceeds preset values for any reason, including sudden changes in filter efficiency. Could you comment on this?

BELLAMY:　　　　　My first comment would be that the bottom line in the use of normal ventilation exhaust systems is conformance or nonconformance with the environmental technical specifications for the plant. The numbers in the branch technical position are based on a very limited number of laboratory tests on filters that are operating continuously. A realistic assessment of these data leads me to conclude that the efficiencies that I would use, and that are in the branch technical position, are the ones that would be expected over the 30-year operating life of a plant. I would like to indicate that we are available to review all other data that anybody might have to support these numbers and I would like to do so.

COLLINS:　　　　　Let me make a further comment. The purpose of the branch technical position was to permit the staff to make an evaluation for license processing. It was not intended as an operating guide, i.e., as to what we would expect from a plant under normal operating conditions once it had been licensed. The staff needed to set forth some criteria as to how we would base our source term calculations and what would be considered as expected releases from the plant. Therefore, we set forth these numbers and they are a little different from what we put forth in 1.52. We hope that additional data will come to us on the normal releases from ventilation

systems that we do not now have in our possession. As Ron Bellamy said, if anybody has better data than we have, we would be very happy to look at them.

WILHELM: From a first glance at the revision of the Regulatory Guide, I read that after some service in the nuclear power plant, the filter should be tested in-place again. Because I know that the in-place test is a Freon test, I just can't make up my mind what this test should show. In Europe, especially in Germany, we get an impression that in-place tests are very expensive and do not tell much. If you use methyl iodide, the numbers you get are questionable because you won't have the same humidity condition and so on. Would it not be wise to use the money to test more charcoal, the charcoal itself, than to test the whole filter system by the in-place test? Then you can detect the event which loaded the filter with water, or with solvent, or with some other stuff.

BELLAMY: We have received that comment from other sources and it will be included and considered before the final revision.

COLLINS: Let me add an additional comment to the one that Ron Bellamy alluded to. In the development of our revision of 1.52, as many of you in this room know, a subject that received more discussion than anything else was the 720 hours. Ron Bellamy and I spent a lot of time, together with some of our other people, analyzing all of the data that were available to us. At the conclusion of our evaluation, we convinced ourselves that the available information would not support a change in that number. In January or February of this year, we sent letters to 54 operating reactors asking for their test data. Up to today, we have received seven responses. Of the seven responses we have received, two of them contained sufficient data for us to continue our evaluation. If industry wants us to change the numbers, I think industry has to be a little more responsive to us. We can only set forth numbers based on available data. We can't make it up. So if you're operating a reactor and you haven't responded, we certainly encourage you to do so.

THE IMPACT OF APPENDIX I TO 10 CFR PART 50 ON ATMOSPHERE CLEANUP SYSTEMS*

John T. Collins
U.S. Nuclear Regulatory Commission
Office of Nuclear Reactor Regulation
Washington, D.C. 20555

Abstract

On December 3, 1970, the Atomic Energy Commission published new sections 50.34a and 50.36a of 10 CFR Part 50 specifying design and operating requirements for nuclear power reactors to keep levels of radioactivity in effluents "as low as is reasonably achievable". The amendments provided qualitative guidance but not numerical criteria for determining when design objectives and operations meet the specified requirements.

On April 30, 1975, the Nuclear Regulatory Commission announced its decision in the rulemaking proceedings concerning the numerical guides for design objectives and limiting conditions for operation to meet the criterion "as low as is reasonably achievable" for radioactive material in light-water-cooled nuclear power reactor effluents. The Commission noted in the Statement of Considerations that the new rule, if met, provided one acceptable method of establishing compliance with the "as low as is reasonably achievable" requirement of sections 50.34a and 50.36a.

In adopting the new rule, the Commissioners expressed the opinion that Appendix I should guide the NRC staff and other interested persons in the use of appropriate calculational procedures for applying the numerical guides for design objectives. The Commissioners further stated that compliance with the rule should be demonstrated by calculational procedures based on models and data that will not substantially underestimate the actual exposure of an individual through appropriate pathways all uncertainties being considered together.

In addition to the numerical design objectives, applicants are required to include in their radwaste systems all items of reasonably demonstrated technology that when added to the system sequentially and in order of diminishing cost-benefit return can with a favorable cost-benefit ratio effect reduction in dose to the population reasonably expected to be within 50 miles of the reactor.

On September 4, 1975, the Nuclear Regulatory Commission published in the Federal Register (Volume 40, Number 172) amendments to Appendix I to 10 CFR Part 50. The amendments provide persons who have filed applications for construction permits which were docketed on or after January 2, 1971 and prior to June 4, 1976 the option of dispensing with the cost-benefit analysis required by Section II.D of Appendix I if the proposed or installed radwaste systems and equipment satisfy the Guides on Design Objectives for Light-Water-Cooled Nuclear Power Reactors proposed in the Concluding Statement of Position of the Regulatory Staff in Docket Number RM-50-2, dated February 20, 1974. Because the criterion proposed by the staff in the rulemaking hearing; namely 5 curies/yr/reactor for liquid effluents, excluding tritium and dissolved gases, 1 curie/yr/reactor of radioiodine-131, and 5 mrem annual whole body dose to individuals at or beyond the site boundary from all pathways of exposure, has led to the proposed or actual installation of radwaste systems and equipment to reduce expected effluent releases to low levels, the

---

*Paper to be presented at the 14th ERDA Air Cleaning Conference, Sun Valley, Idaho, August 2-4, 1976.

application of the $1000 per man-rem criterion specified in Section II.D to plants designed to proposed Appendix I is unlikely to result in radwaste equipment augmentation.

This paper will discuss dose design objectives in Appendix I to 10 CFR Part 50 for gaseous effluents from light-water-cooled nuclear power plants, the need for a cost-benefit analysis for certain proposed facilities, one acceptable method for performing a cost-benefit analysis, and the cost of ventilation equipment considered by the staff in its evaluation. The cost-benefit analysis will be used to show when additional radwaste equipment will be required.

I. Introduction

Part 50.34a of Title 10 of the Code of Federal Regulations (10 CFR Part 50.34a) requires the release of radioactive materials in liquid and gaseous effluents from nuclear power reactors to be "as low as is reasonably achievable" (ALARA)*. The term "as low as is reasonably achievable" as used in this context means "as low as is reasonably achievable taking into account the state of technology, and the economics of improvements in relation to the benefits to the public health and safety, and in relation to the utilization of atomic energy in the public interest".

Until the publication of Appendix I to 10 CFR Part 50 on April 30, 1975, the means of achieving ALARA was based on criteria set forth in proposed Appendix I dated June 9, 1971, Regulatory Guide 1.42, dated June 1973, Revision 1 to Regulatory Guide 1.42 dated March 1974, and criteria contained in the Concluding Statement of the Regulatory Staff, RM-50-2, dated February 20, 1974. In adopting the new rule, the Commissioners expressed the opinion that Appendix I should guide the NRC staff and other interested persons in the use of appropriate calculational procedures for applying the numerical guides for design objectives. The Commissioners further stated that compliance with the rule should be demonstrated by calculational procedures based on models and data that will not substantially underestimate the actual exposure of an individual through appropriate pathways all uncertainties being considered together. To assist applicants and licensees in this regard, the NRC staff has recently issued five Regulatory Guides (1.109, 1.110, 1.111, 1.112 and 1.113). These guides provide calculational models and parameters acceptable to the staff for calculating average expected releases of radioactive materials in liquid and gaseous effluents from normal operation, dispersion of effluents in the atmosphere and different bodies of water, models and parameters for calculating associated radiation doses to man, and cost-benefit aspects of treating radwaste for purposes of implementing the guidance on design objectives and limiting conditions in Appendix I.

In addition to the individual dose design objectives specified in Section II.A, B and C of Appendix I, Section II.D requires applicants to include in the design of their radwaste systems all items of reasonably demonstrated technology that when added to the system sequentially and in order of diminishing cost-benefit return, can for a favorable cost-benefit ratio, effect reduction in dose to the population reasonably expected to be within 50 miles of the reactor. As an interim measure and until establishment and adoption of better values (or other appropriate criteria) the values of $1000 per total body man-rem and $1000 per man-thyroid-rem (or lesser values as may be demonstrated to be suitable in a particular case) shall be used in the cost-benefit analysis.

---

*The phrase "as low as practicable" was replaced by "as low as is reasonably achievable" by the Commission on December 19, 1975 (40 FR 58847).

On September 4, 1975, the Commission amended Appendix I to 10 CFR Part 50 to provide persons who have filed applications for construction permits on or after January 2, 1971 and prior to June 4, 1976, the option of dispensing with the cost-benefit analysis if the proposed or installed radwaste systems and equipment described in the preliminary or final safety analysis report and amendments thereto satisfy the Guides on Design Objectives for Light-Water-Cooled Nuclear Power Reactors proposed in the Concluding Statement of Position of the Regulatory Staff in Docket No. RM-50-2, dated February 20, 1974. Because the criterion proposed in RM-50-2 and used by the staff that each plant meet those design objectives has led to the proposed or actual installation of radwaste systems and equipment to reduce to low levels the total radioactivity in effluent releases or expected effluent releases from such plants, the application of the interim value of $1000 per man-rem and $1000 per man-thyroid-rem criterion specified in Section II.D of Appendix I to these or similarly designed plants is unlikely to result in radwaste equipment augmentation.

In support of this amendment, a cost-benefit analysis was performed by the NRC staff of applications filed and reviewed since 1971 in accordance with the criterion set forth in RM-50-2, which showed that for BWRs and PWRs additional radwaste equipment cannot be added for less than $1000/man-rem. Therefore, in general plants which meet these criterion will meet the requirements of Section II.D.

Applications for construction permits filed after June 4, 1976 are required to include in their reactor's radwaste treatment systems all equipment of reasonably demonstrated technology that could be installed to reduce the cumulative dose to the population within a 50 mile radius of the reactor at an interim cost of $1000 per man-rem or $1000 per man-thyroid-rem in addition to any equipment needed to meet the criteria for doses to individuals required by Sections II.A, B and C of Appendix I.

In the case of plants whose applications for construction permits were filed prior to January 2, 1971, Appendix I does not provide specific guidance concerning the need for these plants to perform a cost-benefit analysis to demonstrate that their releases are ALARA. However, Section V.B of Appendix I states that for applications filed prior to January 2, 1971, licensees/applicants shall file with the Commission within 12 months from June 4, 1975 the following:

a. Such information as is necessary to evaluate the means employed for keeping levels of radioactivity in effluents to unrestricted areas as low as practicable, including all such information as is required by paragraph 50.34a(b) and (c) not already contained in his application; and
b. Plans and proposed Technical Specifications developed for the purpose of keeping releases of radioactive materials in unrestricted areas during normal reactor operation, including expected operational occurrences as low as practicable.

In December 1975, some seven months after the Commission adopted Appendix I, the U. S. Court of Appeals in the matter of Peach Bottom, Unit 2, (York Committee for a Safe Environment vs. NRC) handed down a decision indicating that they could not find anywhere in the record a cost-benefit balance as required by Commission regulations 10 CFR Part 20.1 and 10 CFR Part 50.34a. The case has been remanded back to the Commission to perform the required cost-benefit analysis to demonstrate that Peach Bottom meets the ALARA criterion and that adequate consideration is given to the balancing of "health and safety effects, costs, the state of technology and utilization of atomic energy in the public interest", as required by the

above regulations. In response to the Court action, the NRC staff is currently performing a generic cost-benefit analysis of augmented radwaste systems for plants whose applications for construction permits were filed prior to January 2, 1971, which includes Peach Bottom, Unit No. 2. We hope to show by this analysis that if the radwaste systems presently installed or proposed for these facilities are capable of meeting the dose and curie design objectives set forth in RM-50-2 additional radwaste equipment cannot be added for less than $1000/man-rem. Plants not electing this option will be required to perform a detailed cost-benefit analysis in conformance with Section II.D of Appendix I.

Table 1 shows a comparison of the annual design objectives set forth in Appendix I adopted by the Commission on April 30, 1975 with those proposed by the staff in the Concluding Statement of Position of the Regulatory Staff in Docket RM-50-2.

II. Discussion

The requirements set forth in Section II.D of Appendix I to 10 CFR Part 50 placed upon both the NRC staff and applicants the task of determining the incremental effects of radwaste additions on a case-by-case basis. To provide a uniform means to determine whether or not additions are needed for individual reactors to satisfy the requirements of Section II.D of Appendix I, the NRC staff prepared and issued Regulatory Guide 1.110, "Cost-Benefit Analysis for Radwaste Systems for Light-Water-Cooled Nuclear Power Reactors". It is the objective of this guide to provide an acceptable method of performing the required cost-benefit analysis. The guide provides cost parameters for estimating the costs for the various radwaste treatment equipment items in use or proposed for use at LWRs and a methodology for performing the analysis. The costs presented consider the direct equipment cost and the costs of building space, supportive services, maintenance, interest and operating, as well as other costs generally considered in analyzing capital and operating costs in power plant estimating. The basis for the costs used by the staff are given in Appendix B to this guide. All costs are based on the assumption that the reactor is in design stage and that augmentation of a radwaste system will not involve backfitting of an existing plant. Backfitting costs are determined on a case-by-case basis. Because the Commission did not outline any procedures for including the effects of inflation in the analysis, the NRC staff's analysis is based on 1975 dollars; i.e., neither the costs nor the interim criteria are escalated for the predicted effects of inflation. Since the worth of a man-rem or man-thyroid-rem to the public is subject to the same fluctuations in value as the cost of equipment to reduce radioactive emissions, the staff believes this approach to be reasonable.

The first setp in a cost-benefit analysis of a proposed radwaste system is to calculate the expected releases of radioactive materials in gaseous and liquid effluents for normal operation including anticipated operational occurrences.

Using these release values, the individual doses at the nearest site boundary and the population dose within 50 mile radius are then calculated. For staff analyses, the estimated releases, aquatic and meteorological dispersion characteristics, and dose calculations are based on the methodologies and parameters outlined in Regulatory Guides 1.109, 1.111, 1.112 and 1.113.

Before the cost benefit analysis is initiated, the radwaste systems must be shown to be capable of meeting the individual dose design objectives set forth in Sections II.A, B and C of Appendix I. Population doses are then broken down by release point (i.e., main condenser air ejector in a BWR, waste gas decay tanks in

a PWR and building ventilation exhaust systems for both BWRs and PWRs), by principal isotopes (iodine, noble gases and particulates) and into man-rem and man-thyroid-rem.

The next step is to examine the proposed radwaste system and determine locations of potential augments. In the case of a PWR, one could consider the following augments:

a. An additional waste gas decay tank

b. The installation of a HEPA filter downstream of the waste gas decay tanks

c. The installation of charcoal adsorbers and HEPA filters in the containment purge exhaust system

d. The installation of charcoal adsorbers and HEPA filters in the various building ventilation exhaust systems (turbine, auxiliary, fuel storage and radwaste building).

The next step is to determine the overall total body cost assessment and overall thyroid cost assessment. This is accomplished by multiplying the population total body dose (man-rem/yr) by $1000/man-rem and multiplying the population thyroid dose by $1000/man-rem. For example, if the total body dose is 5 man-rem/yr and the population thyroid dose is 20 man-rem/yr, then the overall cost assessment would be $5,000/yr and $20,000/yr respectively. These overall cost assessments represent the maximum benefit that could result from augmenting the system.

If the augmented cost is greater than both of the overall cost assessments, the augment is not cost effective and there is no need to proceed further with the detailed evaluation. If the augmented cost is less than either of the overall cost assessments, the augment is further evaluated by comparing its cost against the specific monetary value of the reduction in dose caused by the augment. For example, if the addition of a charcoal adsorber in the containment purge exhaust system resulted in a reduction in the population thyroid dose of 3 man-rem/yr out of a total of 20 man-rem/yr, the monetary value of that reduction in dose would be 3 man-rem/yr x $1000 = $3000. If the cost of the charcoal adsorber is greater than the monetary value of the dose reduction, the augment is not cost beneficial and the charcoal adsorber is not added. However, if the cost of the charcoal adsorber is less than the monetary value of the dose reduction, the addition of the charcoal adsorber is cost beneficial and would have to be installed to staisfy the regulation.

Regulatory Guide 1.110 contains a number of tables which list the direct cost of gaseous system equipment (equipment cost, site labor and site materials), annual operating costs for each item, annual maintenance costs for each item, labor cost correction factors to adjust for geographical labor cost differential, indirect cost factors such as construction facilities, services and equipment, engineering and construction manpower costs, interest during construction, and an allowance for miscellaneous owner's cost during construction. The annual expenses for operation and maintenance consider a baseloaded plant operating at an 80% plant capacity factor. The capital recovery factors given in Regulatory Guide 1.110 are levelized annual changes which account for the cost of borrowed money and the depreciation of assets over a 30-year plant operating life.

III. Regulatory Experience

Following the adoption of the Annex to Appendix I, dated September 4, 1975, all utilities whose applications for construction permits were docketed between January 2, 1971 and the present time, were notified by letter from the NRC staff of the need to provide additional information concerning the means to be employed to meet the guidelines of Appendix I of 10 CFR Part 50. Of the forty-seven utilities (representing 91 reactors) in this category, twenty-eight utilities (55 reactors) have elected to comply with the option to the cost-benefit analysis provided by the September 4 Annex rather than to perform the individual cost-benefit analysis required by Section II.D of Appendix I. Of this number, the staff has completed their evaluation of twenty-one and has shown that all of these facilities have radwaste systems capable of meeting the criteria in RM-50-2, and therefore, meet the requirements of Section II.D of Appendix I.

To date, the utilities that have elected to perform the detailed cost-benefit analysis are Watts Bar, Unit Nos. 1 & 2, Hartsville, Unit Nos. 1 - 4, Phipps Bend, Unit Nos. 1 & 2, Pilgrim, Unit No. 2 and Washington Public Power Supply System (WPPSS), Unit Nos. 3 & 5. The remaining fourteen utilities have not yet decided which way they intend to show conformance with Appendix I. Of those electing the detailed cost-benefit analysis of Section II.D, only the WPPSS evaluation has been completed by the NRC staff.

Based on the staff's evaluation of WPPSS and using a value of $1000 as the worth of a man-rem to be cost effective, gaseous waste treatment system additions beyond those required to meet the individual dose design objectives of Appendix I would not result in an annual cost in excess of $6,800 per year. Similarly, using a value of $1000 as the worth of a man-thyroid-rem to be cost effective, iodine control systems for gaseous waste management systems would not result in an annual cost in excess of $8000 per year to the annual cost of the system required to meet Section II.C of Appendix I. Augmentations that were considered for the gaseous waste management systems for WPPSS were an additional waste gas decay tank for the waste gas processing system, the addition of a charcoal adsorber to the waste gas processing system and the addition of charcoal adsorbers for the turbine building ventilation exhaust system. Annual costs for these systems ranged from $8000/yr to $660,000/yr. No items were found that could be added to the system at an annual cost per unit of dose reduction less than $1000 per man-rem or $1000 per man-thyroid-rem.

Based on the limited experience we have had to date, it appears that in most cases the individual dose design objectives of Sections II.A, B and C of Appendix I will be more limiting than the cost-benefit analysis of Section II.D. From our experience, a number of utilities have been required to add iodine control systems and particulate filters to meet the individual dose design objectives and that any additional augments can be shown not to be cost beneficial.

We have briefly discussed the cost-benefit analysis described in Regulatory Guide 1.110, and we welcome any comments or suggestions you may have concerning the cost parameters or methodology as outlined in this guide.

References

1. Appendix I to Title 10 of the Code of Federal Regulations, Part 50, "Numerical Guides for Design Objectives and Limiting Conditions for Operation to Meet the Criterion 'As Low As Is Reasonably Achievable' for Radioactive Material in Light-Water-Cooled Nuclear Power Reactor Effluents".

2. Annex to Appendix I, September 4, 1975, "Application of Cost-Benefit Requirements of Appendix I to Certain Nuclear Power Plants."

3. Concluding Statement of Position of the Regulatory Staff (Docket RM-50-2), Public Rulemaking Hearing On: "Numerical Guides for Design Objectives and Limiting Conditions for Operation to Meet the Criterion "As Low As Practicable" for Radioactive Material In Light-Water-Cooled Nuclear Power Reactors," February 20, 1974.

4. Regulatory Guide 1.109, "Calculation of Annual Doses to Man from Routine Releases of Reactor Effluents for the Purpose of Evaluating Compliance with 10 CFR Part 50, Appendix I", March 1976.

5. Regulatory Guide 1.110, "Cost-Benefit Analysis for Radwaste Systems for Light-Water-Cooled Nuclear Power Reactors", March 1976.

6. Regulatory Guide 1.111, "Methods for Estimating Atmospheric Transport and Dispersion of Gaseous Effluents in Routine Releases from Light-Water-Cooled Reactors", March 1976.

7. Regulatory Guide 1.112, "Calculation of Releases of Radioactive Materials in Gaseous and Liquid Effluents from Light-Water-Cooled Power Reactors", April 1976.

8. Regulatory Guide 1.113, "Methods for Estimating Aquatic Dispersion of Liquid Effluents from Routine Reactor Releases for the Purpose of Implementing Appendix I".

9. NUREG-0017, "Calculation of Releases of Radioactive Materials in Gaseous and Liquid Effluents from Pressurized Water Reactors" (PWR-GALE Code), April 1976.

10. NUREG-0016, "Calculation of Releases of Radioactive Materials in Gaseous and Liquid Effluents from Boiling Water Reactors" (BWR-GALE Code), April 1976.

TABLE 1

ANNUAL DESIGN OBJECTIVES

COMPARISON OF APPENDIX I (MAY 5, 1976) AND
THE STAFF'S PROPOSED APPENDIX I (RM 50-2, FEBRUARY 1974)

		APPENDIX I	RM 50-2
Sec. II.A	Liquid Effluents (Total Body)	3 Mrem/Reactor	5 Mrem/Site (Total Body or Any Organ)
	(Any Organ)	10 Mrem/Reactor	5 Ci/Reactor[1]
Sec. 11.B.1	Gaseous Effluents (Air Dose)	10 Mrad γ/Reactor	10 Mrad γ/Site
	(Air Dose)	20 Mrad β/Reactor	20 Mrad β/Site
OR			
Sec. II.B.2	Gaseous Effluents[2] (Total Body)	5 Mrem/Reactor	5 Mrem/Site
	(Skin)	15 Mrem/Reactor	15 Mrem/Site
Sec. II.C	Iodine and Particulates (Any Organ)	15 Mrem/Reactor	15 Mrem/Site
			1 Ci/Reactor I-131
Sec. II.D	Cost-Benefit Analysis (Total Body)	$1000/Man-Rem	
	50 Mile Radius (Thyroid)	$1000/Man-Rem	

[1] Excluding Tritium and Dissolved Noble Gases.

[2] Higher quantities may be permitted if assured that doses to any individual in an unrestricted area will be less than these values.

DISCUSSION

LIPTON: Why was "as low as practicable" changed to "as low as reasonably achievable"?

COLLINS: I really don't know. I think it was a preferred terminology on the part of the commissioners and took in more of the societal factors, along with cost factors. They determined that the later designation more reasonably expressed the term. I think "as low as practicable" was being interpreted sometimes as being "as low as possible" and not "as low as practicable".

LIPTON: You mentioned one thousand dollars per person-rem for the whole body and for the thyroid. Do you think that this will be extended? For example, if you had something that only exposed the lungs, would it be a thousand dollars per lung-rem, and so forth?

COLLINS: In response to that, we met with the commissioners about a month ago to discuss the need to proceed with the thousand dollar per man-rem rulemaking hearing. The commissioners told the staff to expedite the rulemaking hearing and, in our consideration of the scope of that hearing, to consider the cost to all organs.

FORSBERG: You mentioned that the thousand dollar per man-rem had a 50-mile circumference circle. Do you think that this distance will be expanded globally?

COLLINS: Speaking for myself and not for the Nuclear Regulatory Commission, I believe that the number will stick within a 50-mile radius of the reactor.

WATT: In my reading of RN-50-2, I don't remember anything specified regarding a 50-mile limit. Moreover, it would seem that a man-rem, no matter where delivered, should have the same value. It dosen't matter whether you get a man-rem in Claifornia or New York. I would, therefore, like to understand a little bit more about the origin of the 50-mile limit that you have mentioned but I do not recall being in RN-50-2.

COLLINS: You are right. RN-50-2 did not have a 50-mile radius and did not have a population dose. RN-50-2 never had a thousand dollar man-rem cost. RN-50-2 had two specific criteria within it. One was a five curie release in liquid effluent and another was a curie of iodine 131 in gaseous effluent. Nowhere in the RN-50-2 concluding statement did the staff mention a thousand dollar man-rem. The reason we did not, in the rulemaking hearing, is because the staff could not come up with a dollar value that it felt was worth one man-rem.

ANON: I got from the NRC a copy of RN-50-2 which, in the summary in the front, I am sure, has one thousand dollar per man-rem as a number.

COLLINS: If you did, then you received a copy of the September 4 amendment to Appendix I which specified the RN-50-2 criteria and it said that if you met your system design, met those releases, that

would satisfy Paragraph 2-D which does contain a thousand dollar man-rem.

ANON: I am reasonably sure the document I have does not allude to any other kind of standards. I hope you have a copy here. I would like to straighten it out.

COLLINS: I don't happen to have RN-50-2 with me, but I don't remember seeing that. I am sure what you have is the September 4 amendment, which was published in the Federal Register.

RICHARDSON: The Environmental Protection Agency is also quite interested in this question of dollar value of a man-rem or some other measure for cost benefit balancing. We are also in the process of looking at the question of the appropriate assignment of dollar values to both health impact and measures like a man-rem. I think it is axiomatic that any final determination in this area is going to have to assign different values to different kinds of impacts. Certainly, a lung man-rem is not the same thing as a whole body man-rem.

SESSION XIII

INTERNATIONAL SYMPOSIUM ON THE MANAGEMENT OF WASTES FROM THE NUCLEAR FUEL CYCLE

Wednesday, August 4, 1976
CHAIRMAN: R. W. Ramsey

OVERVIEW OF SYMPOSIUM AND EXPLANATION OF TECHNICAL ALTERNATIVES DOCUMENT (TAD)

R. W. Ramsey

TECHNICAL OVERVIEW OF AIR CLEANING ASPECTS OF SYMPOSIUM AND TAD

R. A. Brown

SUMMARIES OF AVAILABLE TECHNOLOGY ON GASEOUS EFFLUENT CONTROL OF KRYPTON, IODINE, TRITIUM, ^{14}CARBON, RUTHENIUM, NOx, HCl, AND PARTICULATES

D. A. Knecht, T. R. Thomas,
L. L. Burger, C. M Slanky,
J. D. Christian, C. A. Burchsted,

OVERVIEW OF SYMPOSIUM AND EXPLANATION OF TECHNICAL
ALTERNATIVES DOCUMENT (TAD)

R. W. Ramsey, ERDA

I am serving as session chairman in place of Alex Perge. He
was unable to make this, although he made some preparation to do so.
I am going to try to give you his impressions and some other impres-
sions that I have gathered from discussions on the topics that are
on the agenda.

First, I would like to give you some overview of the Denver Sym-
posium and then an explanation of the Technical Alternatives Docu-
ment and its relationship to the Symposium and the environmental im-
pact statement.

Then, I would like to turn the program over to Russel Brown, who
will cover the air cleaning aspects of the TAD document as an intro-
duction to panel discussions we plan to have later. We will follow
this with excerpts from each of the items that were covered in the
TAD by those who contributed them.

Following that, we will set up this room in a colloquial arrangement
and we will make the several TAD authors available to you for ques-
tioning and to talk to you about specific aspects of their part of
the TAD documents. In that way, we hope to give everyone a chance
to get their questions answered or discussed. Some of you may find
it helpful to stand and listen to the questions of others. I think
this informal atmosphere of exchange will be very useful to close this
meeting. When we do break for the seminar discussion, you may con-
sider that the adjournment of the 14th Air Cleaning Conference.

The International Symposium on the Management of Wastes from
the Nuclear Fuel Cycle was held in Denver on July 11-16, 1976, and
many of you here attended that meeting. That meeting and the tech-
nical alternatives document, called TAD for short, is referred to
as ERDA 76-43, Volume I through IV. That document and the meeting
are related to the requirement for an environmental impact statement
discussing the generic programs for management of radioactive wastes.
The idea of a meeting and TAD came into being shortly after the with-
drawal of the initial environmental impact statment in April, 1975.
It was one of the first actions of the new administrator of ERDA,
who withdrew the initial waste management environmental impact state-
ment and promised the preparation of a replacement.

The TAD document was addressed to critical comments that had
been made about the initial environmental impact statement. First
of all, alternatives were not discussed in that initial EIS and we
did not address ultimate disposition adequately. In particular, not
enough information was made available to assess the feasibility of
the various plans that were proposed in that environmental impact
statement and not enough time was given for review and discussion or
for experts to interact and give advice on a selection of methods to
be used in the management of waste. Therefore, one of the purposes

of the Symposium was to provide a timely opportunity for open discussion of the technology. It was made an international meeting so that this discussion of technology could be put on a worldwide basis. Therefore, it covered all the things being developed throughout the world to address the waste management problem.

The Symposium was planned to follow the issuance of a major document [TAD, ERDA 76-43], but to convene well in advance of the issuance of a new generic environmental impact statement. It was to be held at a central location for convenient attendance and to be an open meeting with attendance made available to anyone who wanteq to come, with the program arranged to discuss all of the topics that relate to the technology of waste management and to provide people with an opportunity to ask questions.

The results of the conference are difficult to assess. Everyone has different observations about it. Many are critical. However, the important facts to me seem to be as follows: It was attended by about 800 people. Many of the attendees were not members of the so-called "nuclear club". ·The sessions were well attended by a broad group, including just interested people. There were many representatives of utilities, AE's, state and local health officials, university consultants, and, considering the Olympics and the democratic national convention that were being held in parallel, it got reasonable press coverage.

Some people were disappointed by the conference, however. The reasons I have heard are, first of all, it did not enunciate a solution that some people though should be enunciated at such a meeting. Instead, it illuminated alternatives. It did not become a confrontation of opposing and advocate forces: although there was some flavor of that type in specific discussions. It was not as widely publicized as had been hoped, and some of the coverage, as is normal, left distorted impressions; but these were not too serious. Probably the most universal criticism has been that it did not discuss the sociological issues of the question of waste management from the nuclear fuel cycle, which everybody seems to think ought to be discussed by experts. Maybe it is because we don't feel expert in the sociological issues that we don't discuss them. It was recognized that this was to be a purely technical meeting; as it was. But another meeting has now been arranged. It is to be held by the Congress of Environmental Quality on October 27th through the 29th, in Chicago. This should afford an excellent opportunity for discussion of the sociological aspects and be a supplement to the technical program discussed at Denver.

In summary, my observations are that the Denver meeting was ambitious in scope. It was timely to the need for public discussion. It was reasonably accessible to anyone interested. Unfortunately, it will probably be judged by others as another highly technical gathering of the fuel cycle fraternities, rather than a public meeting to eliminate the issues.

Now, to turn to the TAD document. I mentioned that it, the Denver meeting, and the environmental impact statement are closely related. Both TAD and the Denver meeting are key elements of the program to document the generic environmental impact associated with

waste from the postfission nuclear cycle. You will hear that title used many times during the discussion of these documents. The environmental impact statement is now planned for issuance in draft form about April, 1977. It is a formidable task to write it because of its volume and coverage, as well as the schedule. As many of the officers will tell you, the TAD was just the first milestone of the environmental impact statement plan. TAD's objective was to provide a comprehensive and authoritative technical document for public consumption in sufficient time to allow it to be digested and discussed. The second milestone is the several meetings and conferences that are following the issuance of TAD. The Denver meeting I mentioned, is, of course, a cardinal milestone, as is the CEQ conference, the 14th Air Cleaning Conference, the ANS-AIChE meeting after it, and the ANS meeting in Washington, this fall. All the various meetings with topics on waste management that will be discussed by experts, are regarded as a part of this illumination. I understand that the University of Arizona is planning a waste management meeting in Tucson this fall. It is evident that a number of the institutions that have sponsored discussion of this topic are getting in at this time in an effort to give us as much illumination as possible.

The next milestone is the issuance of the draft environmental impact statement itself. A review will also follow it at various meetings. I am not an expert on this part of the plan, however, so I can't give you an exact schedule for what happens after the EIS is issued.

In summary, then, the TAD has satisfied an important objective of making all the technology publicly available well in advance and of documenting the technology for reference in the environmental impact statement. It is hoped that it will give ample time and opportunity for all the experts to digest it and give their advice.

Now, one personal comment is necessary, I think. I believe that there has been an inordinate diversion of technical expertise and creativity from real technical work for the purpose of documentation. This is extremely costly, and we must realize the costs. I don't know whether we can afford it, frankly. I am impressed that we see the same names on papers on this subject and on our progress reports and on the attendance lists of meetings such as this. The authors and contributors to the TAD and to the environmental impact statement are a very select group of people dealing with this subject of radioactive waste. These people are productive and good managers of their time, but I can't help but consider the cost of their continuous documentation efforts to the degree that they take them away from creative productivity in their labs and test facilities. I hope that we, in the field, recognize this problem and that we can think of a way to avoid this cost. Our country really needs to get on with solving this problem instead of getting on with documenting it. I am concerned that we are spending too much effort writing it down instead of doing it right. If you agree, why not let your congressman know your feelings about this, just as environmentalists let theirs know about their feelings?

With these comments, I will now ask Russell Brown to take over and give you an overview of the air cleaning aspects of the document.

TECHNICAL OVERVIEW OF AIR CLEANING ASPECTS OF SYMPOSIUM AND TAD

R. A. Brown, Allied Chemical, INEL

I'm going to call upon each of the task leaders of TAD to present a short summary but first I will give you a quick overview of what TAD is supposed to accomplish in the context of the gaseous waste problem and my impression of the Denver meeting. It bears out Bob Ramsey's description of the Denver meeting in that the world is distinctly not interested in the characteristics or status of technology for waste management. There was public participation and public attendance, and there were questions asked, but technology is not what stimulates people's curiosity. Those who were specifically involved and, I believe, properly involved in advocacy positions in opposition to nuclear power are more interested in finding the problems than hearing about potential solutions. I think when we went to that meeting, we had to bear that in mind. That is a very subjective view.

TAD was subject to several constraints in its preparation. Those of you who had a chance to thumb through the report, (and I don't imagine too many people have done so other than those who were involved in putting it together and for this reason had the opportunity) can see that it's very limited, very constrained, in what it does.

I thought I'd touch upon the same things I did in the introductory remarks to give you the flavor of it. Then we can open it up to the individual task leaders and they can give you a quick summary of what they said. By the way, I gave a paper on one subsection of this report at the Denver meeting and it took me thirty minutes to cover 22 different technologies. I can't help but feel that I didn't even do a service to the listeners of that meeting. I think anyone who presents a paper that comes from, essentially, something like an encyclopedia, must have reservations about presenting papers. Those who attended the meeting had an opportunity to hear it all at one place. But for the speakers, I think it left many of us nervous about doing it.

The TAD document is really just an encyclopedia of technology. It lists and describes. It's very limited in what it evaluates. In fact, its mission was not to evaluate technologies except in a very narrow sense. Technologies were characterized in terms of their availability. The dividing line between those that were judged available and those requiring development was often, of necessity, fuzzy.

Environmental impact was not discussed. That will be discussed in the next stage, the preparation of the generic environmental statement. I view preparation of that statement as a monumental job and, I fear, especially since I'm going to be involved in one aspect of it, that we haven't been given enough time to do the job that should be done to write a generic statement.

Economic analyses were not presented. They will be presented

in, and used in, the generic environmental statement. Decisions
and plans were not presented. The choice of technologies that were,
and were not, included in the document is open to some debate and I
hope, in our small discussions today, that if you have questions
about what was or was not included, you will raise them.

I also view the next stage as a learning process to find out
where we slipped up or where we made erroneous statements. We need
to hear about them. We even discussed a few nonradioactive ways.
They will not be included in the generic statement, but we included
them just because we felt they were of interest and potentially signi-
ficant.

As you can see from the list I've just given you, the document
contains more proscriptions than prescriptions. The TAD can proba-
bly be criticzed for all of the things that it couldn't or didn't
do. Those who desired ultimate storage of waste, are going to be
disappointed. Those who wanted economic or environmental analysis,
will find the report unsatisfactory. Those who expect some clear
proof or demonstration that all of these management problems are
truly solved, once and for all, will be unhappy. The material in
TAD could not meet the expectations of all who read it, but the com-
plete report does provide a valuable resource for those who want to
know about the technologies of waste management. It provides a
simple description of the known methods for handling waste. Those
descriptions, combined with rather extensive references, give all
readers a chance to know and learn more about recovery and stroage
methods. The TAD provides, above all else, a starting point for
analysis, evaluation, and discussion, and an expansion of our know-
ledge of these technologies. I believe that a review by the parti-
cipants in this conference and by readers in both the national and
international technical community will provide the necessary feed-
back for future additions to and refinements of the document.

With that presented, I would like to call upon those people
who will lead the seminar groups. The first will be Dieter Knecht
who will give us a very brief review of krypton.

SUMMARIES OF AVAILABLE TECHNOLOGY ON GASEOUS EFFLUENT CONTROL OF KRYPTON, IODINE, TRITIUM, ^{14}CARBON, RUTHENIUM, NOx, HCl, AND PARTICULATES

D. A. Knecht, Allied Chemical, INEL - Of the several krypton 85 methods of collection and storage, the first to be considered is cryogenic distillation. There is available technology which requires a demonstration at a commercial fuel reprocessing plant. Liquid fluorocarbon absorption or, as it was called in the talk today, the FASTER Process, is one that requires additional development. I believe the time scale that was given this morning was around two or three years for commercialization. I think we're getting to the point where they could apply it to a commercial-scale plant. Maybe I'm wrong there. We didn't include other techniques such as solid bed adsorption. We didn't consider them developed enough at this time for fuel reprocessing plant scale. If there are other opinions on this, we would be very happy to hear about them at the later discussion.

In storage technologies, we considered pressurized cylinder storage as an available technology. It is one that requires demonstration. It needs design, but we felt everything was available to do this. Zeolite encapsulation is one of the techniques of immobilization of krypton we felt had promise, but required, again, additional development before it could be incorporated into commercial fuel reprocessing scale. There are other methods of entrapping krypton being investigated on a laboratory scale. But, again, we didn't include them at this point because they need a lot more work before decisions can be made on their applicability to a reprocssing plant.

R. A. Brown, Allied Chemical, INEL - We didn't mention that the cut-off date for technologies was supposed to be September 25th. Although we deviated by a few months here or there, that is roughly the time scale we operated on.

T. R. Thomas, Allied Chemical, INEL - The section on the separation and retention of iodine was co-authored by me and Dr. Yarbro of Oak Ridge National Laboratory. We treated scrubbing techniques and other technologies. In that category, we had caustic scrubbing, mercuric nitrate scrubbing, and the 22 boric nitric acid scrub which is called the iodox process. Of these three processes, caustic is essentially outdated and outmoded. There doesn't appear to be any further development or application of that technology. A mercuric nitrate scrubbing system is being installed at the Barnwell Nuclear Fuel Plant. They anticipate a decontamination factor above 100. However, they have no current plans for the waste other than storage. The mercuric nitrate scrub system will also be tested at the research center in Belgium. There, they anticipate getting more design criteria in a pilot plant study. In the adsorbent technologies, there is only one serious contender and that is the use of silver coated adsorbents. By this, I mean adsorbents such as silica gel, alumina, amorphorus silicic acid, and zeolites which have been exchanged with silver salts. Current plans are to use silver exchange zeolite as a back-up bed at the Barnwell Nuclear Fuel Plants, i.e., as a polishing bed

for the mercuric nitrate scrub system. They plan to. do this also at the nuclear research center in Belgium on a pilot plant scale; again, as a polishing bed.

At the WAD plant in Karlsruhe, Germany, plans are to use silver impregnated amorphorus silicic acid subtrate as a bulk item removal system. They hope to obtain design criteria for a full scale processing plant handling up to 1,500 tons per year. The direct application of other metal-loaded adsorbents does not look too promising in that the loading capacities are extremely low. However, research is being done to use lead exchange zeolites as a storage adsorbent for iodine which has been desorbed from silver loaded adsorbents after they have been used as the primary adsorbent for recovery of processing offgas. The silver adsorbent will be .regenerated and the lead exchange zeolite will be used as a final storage medium. I have also treated the subject of the abatement of oxides of nitrogen in the TAD report. There were three categories of technologies: (1) aqueous scrubbing, (2) catalytic reduction of NO_x with reducing agents such as hydrogen, carbon monoxide, propane, methane, and so forth, and finally (3) the very specific catalytic reduction of NO_x by ammonia over hydrogen mordenite. It is anticiapted that all of the nitric acid waste generated by a 1,500 ton per year plant will be converted to NO_x. This would be about 500 ton per year of NO_2.

<u>L. L. Burger, Battelle-Pacific Northwest Laboratory</u> - I'd like to acknowledge the contributions from Exxon Mound Laboratory and by Fieldson from Brookhaven and, of course, a lot of valuable help from Russ Brown.

Tritium is unique with respect to our problems here because quite a bit is produced outside the fuel itself. However, as far as the TAD document is concerned, we're interested in closing the fuel cycle, as you have heard. So we're only really concerned with the reprocessing part of tritium. As you know, tritium, for the most part, doesn't end up at the reprocessing plant. This morning, someone commented that the available technology is to release it and that's essentially what we have. It can be released to the atmosphere as vapor or, in certain cases, it can be released through streams or other bodies of water. This is not completely true since there are technologies which are at various stages of development. One of these is headend treatments following oxidation which isolates the tritium in a concentrated form instead of the very dilute form which comes out of the tailend of the Purex reprocessing plant. Another approach is isotopic enrichment and this is the second place for producing an unusual isotope. It's essentially the only way we can handle this radioactive material if we want to concentrate it from aquaeous or gas streams. There are a number of isotopic enrichment materials that were considered. I won't mention all of them now, but the three that were discussed to some extent in the document were (1) catalytic exchange, (2) electrolysis, including reversable electrolysis which takes advantage of the possibility of cascading electrolytic cells, and (3) a future device, if I can call it that, the application of lasers or, another description, selective molecular excitation to separate the tritium. Isotopic enrichment can be used simply to concentrate any type of stream or it can be applied to recycle within the processing plant.

Another approach that was considered in the TAD document was recycle of the aqueous streams. As far as storage is concerned, we have no available technology, but perhaps that's not quite true. There are techniques that are fairly well along in development, including the application of concrete and impregnated concrete for large volume storage.

The possible use of organic polymers to tie up tritium rather completely, or the use of metal hydrides, looks favorable and is also one of the choice recovery methods considered.

As far as engineering is concerned, tank storage was the only item discussed in the document. There is another way in which one can dispose of tritium; namely, deep well storage, which is not included in this part, but it does show up in other parts of the document.

C. M. Slansky, Allied Chemical - Carbon 14 has proven to be a sleeper. As you know, there was very little interest in this effluent until a few years ago. We're lucky, I think, with carbon 14 insofar as it comes out of several of the gas treatment systems that are fairly well developed. For instance, in the krypton cryogenic system in Idaho. It would come out quite rapidly in the caustic scrubbing and pump system. In the fluorocarbon system, it comes out, as you heard today, quite readily. Of course, the obvious disposal method is the release of carbon dioxide. The technique of atmospheric dispersion is pretty well developed.

I think it might be interesting to dwell a few minutes on final disposition and form. The trend, as you know, has been toward solid forms. I think we can dispose of the gaseous waste in storage cylinders for at least 5,000 years. Let's consider the solid phase. The most obvious is calcium carbonate. I think it's fairly stable and, in cannisters, could be stored quite readily. Quantitatively, it's a little difficult to give a definite number but the calcium carbonate from the carbon 14 content of one year's effluent from a 50 giga-watt process plant would be something like 1.6 kilograms. Let's mix this up with ten to a hundred per cent natural carbon dioxide. This would run you something between 16 and 160 kilograms of calcium carbonate per year. I think this is a reasonable quantity of a beta emitter which could be stored in a salt mine or geological depository.

J. D. Christian, Allied Chemical, INEL - When fission product wastes are evaporated or when they're solidified at a high temperature, a fraction volatilizes. During evaporation, up to 2 per cent can volatilize, but this can be easily suppressed by reducing agents such as nitrous acid. The quantity retained during volatilization processes depends on the specific process and the operating conditions. It can vary anywhere between two thousandths of a per cent up to 100 per cent in certain situations, depending on the process. Then, release to the atmosphere would be anywhere between a tenth of a curie and a hundred thousand curies of ruthenium-106 per day from a five ton per day plant which is processing one year of fuel. This assumes these gases will be condensed in the offgas system for other purposes and that the scrubber will remove 90 per cent and the condenser between 90 and 99 per cent of the ruthenium. Of the various high temperature

waste treatment processes that are being developed for commercial wastes, fluid bed calcination and spray calcination offer the best potential for retaining the ruthenium as a solidified product. When fluid bed calcination is used with the bed being heated directly by the burning of kerosene, the volatility of ruthenium from the bed would be approximately 2000ths of a percent.

In a spray calcinator, using the in-pot melting process, approximately 2 per cent of the ruthenium normally volatilizes. If the salt is denitrated before the calcination, as is done in the German process, the volatility is reduced to 100th of a per cent. In other processes, ruthenium volatility would be substantially higher, one to ten per cent at best. Offgas cleaning devices that are effective to varying degrees for removing ruthenium from the gas stream are the (1) Venturi scrubber, which can provide a decontamination factor of approximately 10, (2) condensers that provide decontamination factors of 10-100, and (3) adsorbing materials. The silica gels and ferric oxide are the two commonly used ones and either will provide a DF of 10^3.

C. A. Burchsted, Oak Ridge National Laboratory - Essentially, what I talked about at Denver was dividing the subject of particulate removal from offgases into three categories; pretreatment, prefiltration, and absolute filtration. Absolute filtration, as has been widely discussed in this session during the last couple days, is the final barrier. The main object is to protect the final filter to enable it to remain effective under the most adverse circumstances. Therefore, both pretreatment and prefiltration are intended not only for particulate collection, but also to protect the last element in the chain. Pretreatment equipment includes cyclones, spray towers, electrostatic precipitators, bag filters, and similar devices. Most of the technology is well understood and well established and most of it represents the adaptation of more or less standard items to this particular application. Much of the development work of pretreatment devices is being undertaken by EPA. Prefiltration has also been talked about at this meeting, and includes the enhancement of particle collection by various means. This is the type of development that is ongoing in prefiltration. Otherwise, the prefilters in use today are generally conventional filters that are commonly used in everything from furnaces and air conditioners up to building ventilation. Two special areas of prefiltration I mentioned were deep bed glass filters seen in Hanford, and the deep bed sand filters that Don Orth talked about yesterday. Usually, offgases are characterized by high temperature, high humidity, low flow rates, and very corrosive environments. Pretreatment collection devices are often combined in an effort to get temperature and humidity down to levels that the absolute filters can handle. This is essentially what it is all about. Developments that we will see in the future include packing and reducing the volume of filters, enhancement of prefilters, and material improvements. Unfortunately, many types of pretreatment devices tend to convert a gaseous waste problem into a liquid waste problem. Therefore, the more we can look to dry methods of collection, the better off we will be. We generally reduce gaseous wastes to solid wastes eventually. This was covered in many of the talks during the last few days; the first day in particular. These included papers on incineration, compacters, etc.

DISCUSSION

RAMSEY: We are just a little bit ahead of our schedule, so I would like to take this opportunity for some questions and some comments from the floor. If you have questions that you want to ask me or Russ about the TAD document, you may do so. These would be welcome at this time. I will give you a chance to say anything that you think hasn't been said here that might be helpful to the overview of the status of air cleaning. If you have any questions that you always wanted to ask somebody from ERDA, I will try to answer them.

DEMPSEY: Being part of ERDA and sponsoring some of the possibilities that were mentioned, we are very keen on getting opinions whether they are ready for practical application. One that comes to mind is the excellent work we did and described here for solidification of krypton. The question that comes to mind is: was it worth the effort?

ANON: This is directed either to Burchsted or to someone from ERDA. In storage of plutonium, we have been faced with the problem of coming up with a suitable decontamination factor for plutonium particulates generated by a fire. It seems there is no standard decontamination factor applied across the country. Some of the ERDA offices have applied one factor and some another. I am wondering why we can't have a standard for HEPA filter decontamination or for multiple HEPA's in series.

BURCHSTED: We have been trying to come up with some reasonable numbers for this. There are two aspects to it. First, what is reasonable decontamination?   And, second, what is a reasonable number you want to permit for safety analysis purposes under the postulated accident?   Under normal operating conditions, considering the excellent filters we have today and the confidence we have in the quality assurance program, we can figure 3×10^3 as the decontamination factor for each stage. This would be the multiplier. But when it comes to the accident condition, the first filter in the chain could very well be destroyed. So, the most I would allow would be a decontamination factor of 5×10^2 as it appears that even when there are some gaping holes in the filter, it is an effective device for collecting materials as long as it is protected. This is what I was talking about a few minutes ago. We are trying to arrive at some numbers that would be reasonable for safety analysis reports.
                   In the Nuclear Air Cleaning Handbook, I discussed the subject but I didn't give any numbers for one, two, and three stages. I had started out to do it, but couldn't get enough agreement among the experts to stick my neck out and put the numbers in the book. But we will have an addendum to the book one of these days in which we will put that in.

RAMSEY: I think this is especially the type of question that will be very useful for us to discuss in the Symposium that takes place right after this meeting.

INDEX OF AUTHORS AND SPEAKERS

INDEX OF AUTHORS AND SPEAKERS

INDEX OF AUTHORS AND SPEAKERS

INDES OF AUTHORS AND SPEAKERS

INDEX OF AUTHORS AND SPEAKERS

LIST OF ATTENDEES
14th ERDA AIR CLEANING CONFERENCE
Sun Valley, Idaho
August 2-4, 1976

Thomas G. Acierno
Fluor Pioneer Inc.
200 West Monroe Street
Chicago, IL 60606

R.E. Adams
Oak Ridge National Laboratory
P.O. Box X
Oak Ridge, TN 37830

A.R. Allan, Jr.
Flanders Filters, Inc.
P.O. Box 1219
Washington, N.C. 27889

Thomas T. Allan
Flanders Filters
825 Hinckley Road
Burlingame, CA 94010

C.R. Allen
Westinghouse--Hanford
P.O. Box 1970
Richland, WA 99352

Howard W. Altman
CVI Corporation/Pennwalt
14539 Blythe Street
Van Nuys, CA 91402

Fernando Alvarez
Hidroelectrica Espanola
3 Hermosilla
Madrid, Spain

Bunzai An
Kobe Steel
4-Iwayanaka-Machi Nada
Kobe, Japan

B.V. Andersen
Battelle Northwest
606 Jefferson
Richland, WA 99352

Wendell L. Anderson
Naval Surface Weapons System
Code DT
Dahlgren, VA 22448

R.W. Andrae
LASL
56 Navajo
Los Alamos, NM 87544

P. Arnold
Atlantic Richfield Hanford Company
Federal Building
Richland, WA 99352

Richard L. Baker
CTI-Nuclear, Inc.
Waltham, MA 02154

John E. Ballou
Battelle, Pacific Northwest Lab-
   oratories
Richland, WA 99352

David L. Balsmeyer
Monsanto Research Corporation
Mound Laboratory
P.O. Box 32
Miamisburg, Ohio 45342

Ronald R. Bellamy
U.S. Nuclear Regulatory Commission
Washington, D.C. 20555

Gloria Bennett
Los Alamos Scientific Laboratory
Group WX-4, MS 985
P.O. Box 1663
Los Alamos, NM 87545

Roland G. Bernier
C.H. Dexter Division, The Dexter
   Corporation
One Elm Street
Windsor Locks, Connecticut 06096

David Bibb
Bechtel Power Corporation
P.O. Box 607
Gaithersburg, MD   20760

M.B. Biles
U.S.E.R.D.A.
Washington, D.C.   20545

John C. Bixel
Monsanto Research Corp.
Mound. Lab.
P.O. Box 32
Miamisburg, OH   45342

R.E. Blanco
Oak Ridge National Laboratory
P. O. Box X
Argonne, IL   60439

Don E. Black
Allied Chemical Corporation
550 Second Street
Idaho Falls, ID   83401

Alfred S. Bocchino
United Engineers and Construction
30 South 17th Street
Philadelphia, PA   19101

Josef Bohnenstingl
Kernforschungsanlage GmbH
D 517 Julich, Germany

Leon C. Borduin
Los Alamos Scientific Laboratory
P.O. Box 1663
Los Alamos, NM   87545

T.S. Borek
C.H. Dexter Corporation
One Elm Street
Windsor Locks, CN   06096

Rodney Bowser
Mound Laboratory
Miamisburg, Ohio   45342

Fred P. Brauer
Battelle-Northwest
P.O. Box 999
Richland, WA   99352

Roger J. Breeding
Energy Incorporated
P.O. Box 736
Idaho Falls, ID   83401

James F. Bresson
U.S.E.R.D.A.
P.O. Box 5400
Albuquerque, NM   87115

Knud Brodersen
Research Establishment Riso
Roskilde, Denmark

Blake P. Brown
U.S.E.R.D.A.
Washington, D.C.   20545

Russell A. Brown
Allied Chemical Corporation
550 Second Street
Idaho Falls, ID   83401

R.H. Brown, Jr.
Bechtel Power Corporation
50 Beale Street
San Francisco, CA   94100

W. Curtis Brown
Fluor Corporation
8339 Calmosa Avenue
Whittier, CA   90602

Aycardo Buchelli
R.M. Parsons
225 Cherry Drive
Pasadena, CA   91105

James A. Buckham
Allied Chemical Corporation
550 Second Street
Idaho Falls, ID   83401

C.A. Burchsted
Oak Ridge National Laboratory
P.O. Box X
Oak Ridge, TN   37830

L.L. Burger
Battelle-Northwest
Battelle Boulevard
Richland, WA   99352

Peter Burn
Nuclear Fuel Services Inc.
Box 124
West Valley, NY 14171

H.B. Burress
Sandia Laboratory
Albuquerque, NM 87115

M.R. Busby
Tennessee State University
Nashville, TN 37200

O.I. Buttedahl
Atomics International
Rocky Flats
P.O. Box 464
Golden, CO 80401

George H. Cadwell, Jr.
Flanders Filters, Inc.
P.O. Box 1219
Washington, N.C. 27889

Clifford W. Cain, Jr.
Johns-Manville
2391 W. Caley Avenue
Littleton, CO 80120

Robert L. Campbell
Mine Safety Appliances
Evans City, PA 15038

C. Lyle Cheever
Argonne National Laboratory
Building 14
Argonne, IL 60439

Eric T. Choi
Ontario Hydro
700 University Avenue
Toronto, Ontario, Canada

Jerry D. Christian
Allied Chemical Corporation
550 Second Street
Idaho Falls, ID 83401

Howard D. Christiansen
Allied Chemical Corporation
550 Second Street
Idaho Falls, ID 83401

Alfredo Cifuentes
Empresarios Agrupadds
Magallanes, 3
Madrid, Spain

H. Clyde Claiborne
Union Carbide Nuclear Div. - OWI
P.O. Box Y
Oak Ridge, TN 37830

James E. Cline
Nuclear Environmental Services/
    Science App.
No. 3 Choke Cherry Rd. Suite #3
Rockville, MD 20850

G. Collard
C.E.N./S.C.K.
Boerentang 200/B-2400
Mol, Belgium

John T. Collins
U.S. Nuclear Regulatory Commission
Washington, D.C. 20555

James N. Conway
Tera Corporation
2118 Milvia Street
Berjeketm CA 94704

Frank T. Cunniff
Calgon Croproation
Box 1346
Pittsburgh, PA 15230

Gregory C. Cwalina
Bechtel Power Corporation
5435-5 Old Tucker Row
Gaithersburg, MD 20760

Bernard Deckers
Association Vincotte
1640 Rhode-Saint-Genese
Belgium

James DeField
Los Alamos Scientific Laboratory
P.O. Box 1663
Los Alamos, NM 87545

Victor R. Deitz
Naval Research Laboratory
Washington, D.C. 20375

John Dempsey
U.S.E.R.D.A.
Washington, D.C.   20545

James T. Denovan
Westinghouse Hanford
P.O. Box 1970
Richland, WA   99352

A.H. Dexter
E.I. du Pont de Nemours & Co.
Aiken, SC   29801

D.P. Dietrich
Electrowatt Engineering
   Services, LTD
25 Harcourt House
19 Cavendish Sq.
London W1, England

Weldon D. Dillow
Tennessee Valley Authority
River Oaks Building
Muscle Shoals, AL   35660

T.S. Drolet
Ontario Hydro H14
700 University Avenue
Toronto, Ontario, Canada

Kenneth Duerre
Group WX-8, MS 312
Los Alamos Scientific Laboratory
Los Alamos, NM   87545

Ms. Lelia Duncan
Bechtel, Inc.
P.O. Box 3965
San Francisco, CA   94119

R.S. Eby
Union Carbide Corporation,
Nuclear Division
P.O. Box P, M.S. 381
Oak Ridge, TN   37830

James R. Edwards
Flanders Filters, Inc.
P.O. Box 1219
Washington, NC   27889

David N. Enegess
Combustion Engineering
1000 Prospect Hill Road
Windsor, CT   06095

William A. Emel
Allied Chemical Corporation
550 Second Street
Idaho Falls, ID   83401

Paul J. Estreich
Ebasco Services
21 West Street
New York, NY   10006

E.L. Etheridge
United Nuclear Ind.
Box 490
Richland, WA   99352

Harry J. Ettinger
Los Alamos Scientific Laboratory
P.O. Box 1663
Los Alamos, NM   87545

A.G. Evans
E.I. du Pont de Nemours & Co.
Savannah River Laboratories
Aiken, SC   29801

Arthur Feibush
AIRCO
Murray Hill, NJ   07971

John H. Field
C.H. Dexter Div., The Dexter Corp.
One Elm Street
Windsor Locks, CT   06096

George H. Fielding
U.S. Naval Research Laboratory
Washington, D.C.   20375

Melvin W. First
Harvard Air Cleaning Laboratory
665 Huntington Avenue
Boston, MA   02115

William F. Fischer
Rohm and Haas Company
Spring House, PA   19477

James F. Fish
American Air Filter Company, Inc.
215 Central Avenue
Louisville, KY   40201

Frederick H. Flor, Jr.
Rohm and Haas Company
Independence Mall West
Philadelphia, PA 19105

Hans Flyger
Research Establishment
R150
DK 4000 Rockilde
Copenhagen, Denmark

W.T. Foreman
Environmental Product Sales, Inc.
Charlotte, NC

Richard Fox
Atlantic Richfield Company
660-A George Washington Way
Richland, WA 99352

Charles W. Forsberg
Union Carbide Corporation
Oak Ridge National Laboratory
P.O. Box X
Oak Ridge, TN 37830

Edward J. Frederick
Oak Ridge National Laboratory
P.O. Box X
Oak Ridge, TN 37830

Sam S. Freeman
Mound Laboratory
Miamisburg, Ohio 45342

James J. Fuquay
Battelle Pacific Northwest Labs.
P.O. Box 999
Richland, WA 99352

J.D. Galbraith
Atlantic Richfield Hanford Company
Federal Building
Richland, WA 99352

Dean L. Gano
Washington Public Power Supply
    System
3000 George Washington Way
Richland, WA 99352

James R. Gaskill
Lawrence Livermore Laboratory
P.O. Box 808
Livermore, CA 94550

John A. Geer
Rockwell International
Rocky Flats, CO 80401

Humphrey Gilbert
H. Gilbert
P.O. Box 704
McLean, VA 22101

Robert Girton
Allied Chemical Corporation
550 Second Street
Idaho Falls, ID 83401

Ronald W. Glass
Oak Ridge National Laboratory
Union Carbide Nuclear Division
P.O. Box X, Building 4505
Oak Ridge, TN 37830

John A. Glissmeyer
Battelle-Pacific Northwest Labs.
Batelle Blvd.
Richland, WA 99352

Edward Golankiewicz
Engelhard Industries
Murray Hill, NJ 07971

Roger T. Goulet
Cambridge Filter Corporation
Box 1255
Syracuse, NY 13021

Billy J. Grady
Exxon Nuclear Company, Inc.
2955 George Washington Way
Richland, WA 99352

Arnold J. Granger
Houston Light & Power
P.O. Box 1700
Houston, Texas 77001

LeRoy F. Grantham
Atomics International Div.
Rockwell International Corp.
8900 DeSota Avenue
Canoga Park, CA 91304

Eugene E. Grassel
Donaldson Company, Inc.
P.O. Box 1299
Minneapolis, MN 55440

William Gregory
Los Alamos Scientific Laboratory
P.O. Box 1663
Los Alamos, NM 87544

Borje Gustavsson
AB ASEA ATOM
Box 53, S-721 04
Vasteras, Sweden

Robert F. Guyre, Jr.
CTI Nuclear, Inc.
266 Second Avenue
Waltham, MA 02154

Karl W. Haff
Oak Ridge National Laboratory
P.O. Box X
Oak Ridge, TN 37830

John J. Halligan
Air Quality Testing & Design, Inc.
2691 McCollum Parkway
Kennesaw, GA 30144

Mark S. Hanson
Battelle-Pacific Northwest Labs.
Battelle Blvd.
Richland, WA 99352

William J. Harrie
U.S.E.R.D.A.
550 Second Street
Idaho Falls, ID 83401

Frank J.T. Harris
Evans, Adlard & Co., Ltd.
Postlip Mills
Winchcombe, Glos (UK) GL54 5BB

Michael Hauf
TERA Corp.
2118 Milvin St.
Berkeley, CA 94702

Louis L. Hegyi
Burns & Roe, Inc.
650 Winters Avenue
Paramus, NJ 07652

H. Hendrick
SRD
P.O. Box 2952
San Francisco, CA 94121

William T. Heyse
Dexter Corporation
One Elm Street
Windsor Locks, CT 06096

Robert E. Heryford
Garrettson Elmensorft Zinow Reibin
      Architects & Engineers
124 Spear Street
San Francisco, CA 94105

Rolf Hesbol
AB Atomenergi
Fack S-611 01
Nykoping, Sweden

H. Wayne Hibbitts
U.S.E.R.D.A.
Box E
Oak Ridge, TN 37830

Frank B. Hill
Brookhaven National Lab
Upton, L.I., NY 11973

William C. Hinds
Harvard School of Public Heatlh
665 Huntington Avenue
Boston, MA 02115

Detlef W. Holm
Institut fur Reaktorsicherheit
5 Koln 1
Glockengasse 2, Germany

Duane K. Holsten
Westinghouse Hanford
P.O. Box 1970
Richland, WA 99352

Harley B. Hooker
Bechtel Power Corporation
15740 Shady Grove Road
Gaithersburg, MD 20760

Harry E. Hootman
DuPont
Savannah River Laboratory
Savannah River, GA 29801

J. Haspers
N.V. VERTO,
's Gravenweg, 264
Rotterdam, Holland

Benno Huber
Commission of European Communities
200 rue delaloi
Brussels 1040, Belgium

Philip W. Hufnell
De Pont Company
Louviers Building
Wilmington, DE   19898

John R. Hunt
Nuclear Consulting Services, Inc.
P.O. Box 29151
Columbus, Ohio   43229

Russ Hunter
Atomics International
8900 De Sota Avenue
Canoga Park, CA   91304

Irwin M. Hutten
Dexter Corporation
Windsor Locks, CT   06096

Felipe Ibanez
Hidroelectrica Espanola
3 Hermosilla
Madrid, Spain

Carol Iceland
Burns & Roe, Inc.
633 Industrial Avenue
Paramus, NJ   07652

Herbert S. Isbin
Dept. Chemical Engineering
   and Materials Science
University of Minnesota
Minneapolis, MN   55455

Yasuhiko Itoh
Nitta Belting Company, Ltd.
8-2-1 Chuo-Ku
Ginza, Tokyo, Japan

Jack W. Jacox
Nuclear Consulting Services, Inc.
P.O. Box 29151
Columbus, Ohio   43229

Gary Jelich
Ontario Hydro
700 University Avenue
Toronto, Ontario, Canada

David W. Jeppson
ARHCO
1126 Oak
Richland, WA   99352

Leonard A. Jonas
Edgewood Arsenal, Chemical Lab.
Aberdeen Proving Group
APG MD   21010

M.J. Kabat
Ontario Hydro
P.O. Box 160
Pickering, Ontario, Canada

Thomas Kabele
Battelle-Northwest
Box 999
Richland, WA   99352

Judd Kahn
Union Carbide Nuclear Division
Box X, Bldg. 1000
Oak Ridge, TN   37830

Harvey Kaye
CTI Nuclear
266 Second Avenue
Waltham, MA   02154

Saif U. Khan
Omaha Public Power District
1623 Harvey Street
Omaha, Nebraska   68102

Leo J. Klaes
Tennessee Valley Authority
W 9 C 135 C-K
Knoxville, TN   37902

Dieter A. Knecht
Allied Chemical Corporation
550 Second Street
Idaho Falls, ID   83401

Margaret K. Knecht
Energy, Incorporated
Idaho Falls, ID   83401

Harold W. Knudson
Hollingsworth & Vose Company
East Walpole, MA   02032

Daniel P. Kopy
Johns-Manville
Greenwood Plaza
Denver, CO 80217

J. Louis Kovach
Nuclear Consulting Services, Inc.
P.O. Box 29151
Columbus, Ohio 43229

Rudi Kratel
1222 Geneva, Switzerland

Frank A. Kujawski
Flanders Filters, Inc.
P.O. Box 1219
Washington, NC 27889

Therese L. Kujawski
Flanders Filters, Inc.
P.O. Box 1219
Washington, NC 27889

Lewis Landon
E.I. dePont de Nemours
Savannah River Laboratory
Aiken, SC 29801

Ernest W. Landow
Argonne National Laboratory
9700 South Cass Avenue
Argonne, IL 60439

James R. Laskie
Sutcliffe Speakman & Co
17 Lawrence Road
Wellesley, MA 02181

Stephen Lawroski
Argonne National Laboratory
9700 S. Cass Avenue
Argonne, IL 60439

Fred D. Lecki
Nuclear Containment Systems, Inc.
P.O. Box 19827
Columbus, Ohio 43219

Fred D. Leckie, Jr.
Nuclear Containment Systems, Inc.
P.O. Box 19728
Columbua, Ohio 43219

Harry A. Lee
Atlantic Richfield Hanford Co.
Building 271-T
Richland, WA 99352

David Leith
Harvard Air Cleaning Lab.
665 Huntington Avenue
Boston, MA 02115

F.J. Leonard
Witco Chemical
277 Park Avenue
New York, NY 10017

John Linehan
U.S. Nuclear Regulatory Commission
Washington, D.C. 20555

William V. Lipton
Argonne National Laboratory
9700 S. Cass Avenue
Argonne, IL 60439

Peter S. Littlefield
Yankee Atomic Electric
20 Turnpike Road
Westboro, MA 01581

Earvin K. Loop
U.S.E.R.D.A.
Germantown, MD 20767.

R.A. Lorenz
Oak Ridge National Laboratory
P.O. Box X
Oak Ridge, TN 37830

Roy A. Lucht
Los Alamos Scientific Labs.
P.O. Box 1663
Los Alamos, NM 87545

G. Terry McAmish
Allied General Nuclear Services
P.O. Box 847
Barnwell, SC 29812

J.D. McCormack
Westinghouse-Hanford Co.
P.O. Box 1970, Building 321
Richland, WA 99352

John McDonough
Mine Safety Appliances
Evans City, PA 16033

W.J. McDowell
Oak Ridge National Laboratory
P.O. Box X
Oak Ridge, TN 37830

1146

John McFee
Energy Incorporated
P.O. Box 736
Idaho Falls, ID 83401

R.W. McIndoe
Johns-Manville Corp.
Greenwood Plaza - 2W2
Denver, CO 80217

Doug K. McLellan
Brown & Root, Inc.
P.O. Box 3
Houston, Texas 77000

R.E. McLin
Goodyear Atomic Corporation
P.O. Box 628
Piketon, Ohio 45661

Wilbur D. McNeese
Los Alamos Scientific Lab.
P.O. Box 1663
Los Alamos, NM 87544

Hugh O. McPherson
Bahnson Company
P.O. Box 10458
Winston-Salem, N.C. 27108

Paul Magno
Nuclear Regulatory Commission
Washington, D.C. 20555

Robert I. Marble
Farr Company
P.O. Box 92187
Los Angeles, CA 90009

John Meardon
Exxon Nuclear Company
2955 George Washington Way
Richland, WA 99352

J.R. Merriman
Union Carbide Corporation
P.O. Box 1410
Paducah, KY 42001

James H. Metcalf
Sandia Laboratories
Albuquerque, NM 87115

Werner Meyer-Jungnick
SYSTEC Systemplanung u.
  Industrieberatung GmbH
Wildenbruchstrabe 28, 4000
Dusseldorf 11 /FRG

Lloyd R. Michels
General Electric Company
175 Curtner Avenue
San Jose, CA 95125

William H. Miller,Jr.
Sargent and Lundy
55E Monroe
Chicago, IL 60606

Marshall F. Mills
U.S.E.R.D.A.
P.O. Box 550
Richland, WA 99352

J.E. Mirabella
ARHCO
535 Franklin, P.O. Box 1041
Richland, WA 99352

Dade W. Moeller
Harvard University
665 Huntington Avenue
Boston, MA 02115

L.R. Monson
Argonne National Laboratory
P.O. Box 2528
Idaho Falls, ID 83401

J.R. Montagnon
PICA
16, Rue Trezel
92300 Levallois, France

John Montiguy
Dexter Corporation
One Elm Street
Windsor Locks, CT 06096

John R. Moore
C.F. Braun
Alhambra, CA 91800

W.W. Morgan
Atomic Energy of Canda Limited
Whiteshell Nuclear Research
    Establishment
Pinawa, Manitoba ROE 1LO

George A. Morris
University of California
Lawrence Livermore Lab.
P.O. Box 808L
Livermore, CA 94550

Lewis D. Muhlestein
P.O. Box 1970
Westinghouse Hanford Co.
Richland, WA 99352

Morris G. Munson
General Electric Co. MC 754
275 Curtner Avenue
San Jose, CA 95125

Tohru Murano
Power Reactor & Nuclear Fuel
   Development Corporation
Tokai, Ibaraki, Japan

E.W. Murbach
Allied General Nuclear Services
P.O. Box 847
Barnwell, SC 29812

Jack L. Murrow
Bechtel Power Corporation
P.O. Box 3965
San Francisco, CA 94119

Larry G. Musen
Aerojet Nuclear Company
550 Second Street
Idaho Falls, ID 83401

Norio Nakahashi
Kobe Steel, Ltd.
1-8-2, Chiyoda-Ku
Tokyo, Japan

Richard N. Nassano
Offshore Power Systems
8000 Arlington Exp.
Jacksonville, Florida 32200

Max Negler
U.S. Army Edgewood Arsenal
Edgewood Arsenal, MD 21010

Carl T. Nelson
Rockwell International, AI
8900 DeSoto
Canoga Park, CA 91303

Gary O. Nelson
Lawrence Livermore Labs.
Box 808
Livermore, CA 94550

Allen S. Neuls
Los Alamos Scientific Lab.
P.O. Box 1663
Los Alamos, NM 87544

Carl Newton
U.S.E.R.D.A.
Mail Stop F309
Washington,DC 20545

Emil Nicolaysen
Gibbs & Hill, Inc.
393 Seventh Avenue
New York, NY 10001

Karl Notz
Oak Ridge National Lab.
P.O. Box 4
Oak Ridge, TN 37830

T.T. Odajima
Cosmodyne
2920 Columbia Street
Torrance, CA 90509

J.P. Olivier
DECD Nuclear Energy Agency
38 Bd Suchet
F5016 Paris, France

Robert E. Olson
Westinghouse Electric Co.
P.O. Box 355
Pittsburgh, PA 15230

Donald A. Orth
E.I. duPont de Nemours
Savannah River Plant
Aiken, SC 29801

Bernice E. Paige
Allied Chemical Corporation
550 Second Street
Idaho Falls, ID 83401

David M. Paige
Allied Chemical Corporation
550 Second Street
Idaho Falls, ID 83401

J.F. Palmer
Atomic Energy of Canada Ltd.
Chalk River, Ontario
Canada KOJ IJO

E.H. Pantel
Atomic Energy of Canada, Ltd.
Sheridan Park Research Center
Mississauga, Ontario, Canada

Graham B. Parker
Battelle-Northwest
P.O. Box 999
Richland, WA 99352

R.W. Passmore
Aerojet Nuclear Company
550 Second Street
Idaho Falls, ID 83401

Ned B. Pauling
United Engineers & Constructors,Inc.
30 South 17th St.
Philadelphia, PA 19101

Bob Paulson
Atomics International
8900 DeSoto
Canoga Park, CA 91304

Hal Parish
CVI Corporation
P.O. Box 2138
Columbus, Ohio 43216

Robert D. Parsons
Hollingsworth & Vose
East Walpole, MA 02032

John R. Pearson
Barnebey-Cheney Co.
835 N. Cassady
Columbus, Ohio 43219

Peter J. Pelto
Battelle-Northwest
P.O. Box 999
Richland, WA 99352

Dallas T. Pence
Science Applications, Inc.
P.O. Box 2351
LaJolla, CA 92138

David C. Perry
Johns-Manville
Greenwood Plaza
Denver, CO 80217

Leonard S. Peterson
Public Service Indiana
1000 E. Main
Plainfield, Ind. 46168

Hardy M. Philippi
Atomic Energy of Canada Limited
Chalk River, Ontario, Canada
 KOJ 1JO

Arthur R. Piccot
Sargent & Lundy
55 E. Monroe
Chicago, IL 60606

James G. Pierce
CVI Corporation
P.O. Box 2138
Columbus, Ohio 43216

Frank K. Pittman
Self-Employed
10223 Gainsborough Road
Potomac, MD 20854

Udo Pohl
SYSTEC Systemplanung u.
  Industrieberatung GmbII
Wildenbruchstrabe 28, 4000
Dusseldorf 11 / FRG

Rich Porco
MSA
Evans City, PA 16033

Howard Pulley
Union Carbide Corporation,
  Nuclear Division
P.O. Box 1410
Paducah, KY 42001

M. John Quante
Flanders Filters, Inc.
P.O. Box 1219
Washington, NC 27889

Robert W. Ramsey, Jr.
Nuclear Fuel Cycle and
    Production
Washington, D.C.   20545

Howard R. Reedquist, Jr.
CTI-Nuclear, Inc.
4955 Bannock St.
Denver, Colorado   80216

Donald L. Reid
Battelle Northwest
P.O. Box 999
Richland, WA   99352

J. Donald Reilly
Farr Co.
P.O. Box 571
Falls Church, VA   22046

Meyer M. Reiss
Atomic Products Corp.
P.O. Box 657
Center Moriches, NY   11934

Allan Richardson
U.S. - EPA
401 M Street
Washington, D.C.   20460

Richard D. Rivers
American Air Filter Co.
Box 1100
Louisville, KY   40201

Arthur P. Roeh
Allied Chemical Corp.
550 2nd St.
Idaho Falls, ID   83401

W.M. Rogers
Englehard Industries
1000, Elwell Court
Palo Alto, CA   94303

Eugene E. Routon
Mallinckrodt, Inc.
3600 W. Second St.
St. Louis, MO   63147

Paul E. Ruhter
Energy Research and Develop.
    Administration
Idaho Operations Office
550 2nd St.
Idaho Falls, ID   83401

Don E. Savage
Allied General Nuclear Services
P.O. Box 847
Barnwell, SC   29812

Norman B. Scheffel
Johns Manville Corp.
Greenwood Plaza 2W2
Denver, CO 80217

W.O. Schikarski
GFK Karlsruhe
P.O. Box 3640
Karlsruhe, Germany

W. Schoeck
Kernforschungszentrum Karlsruhre
Laboraotirum for Aerosolphysik und F.
    Filtertechnik
Karlsruhe, 35 Germany

Larry E. Schuerman
Detroit Edison
2000 Second Avenue
Detroit, Michigan   48200

Martin C. Schumacher
USNRC IE:III
799 Roosevelt Road
Glen Ellyn, IL   60137

George A. Schurr
E.I. duPont de Numerous
Wilmington, Del. 19848

Burton G. Schuster
Los Alamos Scientific Lab.
Los Alamos, NM   87554

Frank R. Schwartz, Jr.
North American Carbon, Inc.
P.O. Box 19737
Columbus, OH   43216

Richard W. Schweizer
ACS Industries, Inc.
9000 S.W. Freeway
Houston, TX   77074

R.D. Scott
HEPA Corp.
3071 E. Coronado
Anaheim, CA   92806

Mildred B. Sears
Oak Ridge National Lab.
P.O. Box X
Oak Ridge, TN 37830

Paul Sigli
Commissariat A L'Energie Atomic
Stepam, Cen/Far. B.P.6,92260
Fontenay Aux Roses, France

Avrum Silverman
Nuclear Consulting Services
24 Church St.
Watertown, MA 02172

C.D. Skaats
Rockwe-1 International
P.O. Box 464
Golden, CO 80401

Jerry Skolrud
Exxon Nuclear
2955 Geo. Wash. Way
Richland, WA 99352

C.M. Slansky
Allied Chemical - ICP
550 Second St.
Idaho Falls, ID 83401

Eugene H. Smith
Allied Chemical Corp.
502 Second St.
Idaho Falls, ID 83401

P.R. Smith
New Mexico State Univ.
Box 3450
Las Cruces, NM 88003

Robert C. Smith
P.O. Box 1970
Westinghouse Hanford
Richland, WA 99352

Wayne Smith
MSA
Evans City, PA 16033

Jim Snider
Oak Ridge Nat. Lab. (ORNL)
P.O. Box X
Oak Ridge, TN 37830

Melvin W. Snover
Hollingsworth & Vose Co.
East Walpole, MA 02032

Ron Stafford
Los Alamos Scientific Lab.
P.O. Box 1663 M.S. 336
Los Alamos, NM 87544

Bruce A. Staples
Allied Chemical Corp.
550 2nd St.
Idaho Falls, ID 83401

Samuel Steinberg
Air Techniques Inc.
1717 Whitehead Rd.
Baltimore, MD 21207

M.L. Steindler
Argonne National Lab.
9700 S. Cass Ave.
Argonne, IL 60439

M.J. Stephenson
Union Carbide Corp.
Nuclear Division, ORGDP
Oak Ridge, TN 37830

C.E. Stevenson
Argonne National Lab.
9700 S. Cass Ave.
Argonne, IL 60439

Hans Stiehl
Delbag Luftfilter
Schweidnitzer Str.
1000 Berlin, Germany

John A. Stone
E.I. DuPont de Nemours & Co.
Savannah River Lab.
Aiken, SC 29801

Dennis M. Sirachan
Atlantic Richfield Hanford Co.
P.O. Box 250 (222S-200W)
Richland, WA 99352

Hans-Jochen Strauss
Ceagfilter und Entstaubungstechnik
  GmbH
4600 Dortmund/W. Germany
Munsterstrasse 231

Robert Stuart
CTI Nuclear
266 Second Avenue
Waltham, MA   02154

Frank P. Stumpp
Aerojet Nuclear Co. INEL
550 2nd St.
Idaho Falls, ID   83401

Terrence J. Sullivan
Consumers Power Company
1945 West Parnall Road
Lansing, Michigan 48900

George H. Sykes
E.I. duPont de Nemours
Savannah River Plant
Aiken, South Carolina   29801

John G. Tafoya
Hanford Environmental Health
    Foundation
P.O. Box 100
Richland, WA   99352

Hiromi Tanabe
Kobe Steel, Ltd.
1-Chome,Wakinohama-Cho
Fukiai-ku
Kobe, Japan

Toshi Tanaka
Kobe Steel, Ltd.
299 Park Avenue
New York, NY   10017

M. Gene Thomas
Fiber Process Division
Lydall Inc.
P.O. Box 1713
Rochester, NH   03867

Thomas R. Thomas
Allied Chemical Corporatin
803 S. Skyline
Idaho Falls, IL   83401

W. Neill Thomasson
U.S. Environmental Protection
    Agency
401 M. Street, S.W.
Washington, D.C.   20460

Charles A. Thompson
Bechtel Power Corporation
15740 Shady Grove Rd.
Geithersburg, MD   20760

Garry Tidrick
Pacific Gas & Electric Co.
77 Beale St.
San Francisco, CA   94100

Nelson R. Tonet
Ouquesne Light Company
435 Sixth Avenue
Pittsburgh, PA   15219

Henry Till
Electric Power Research Inst.
3412 Hillview Ave.
Palo Alton, CA   94304

Donald Traut
CTS - Nuclear Inc.
4955 Bannock St.
Denver, CO   80216

Fevzi Ulu
Brown & Root, Inc.
P.O. Box 3
Houston, TX 77000

Dwight Underhill
Harvard University
665 Huntington Avenue
Boston, MA   02115

Vincent Van Brunt
College of Engineering
University of South Carolina
Comunbia, SC   29208

Barend Verkerk
Reactor Centrum Nederland
Westerduiweg 3, Petten (NH)
Netherlands

William W. Vogelhuber
CVI Corporation
P.O. Box 2138
Columbus, OH   43216

B.E. Watt
Los Alamos Scientific Lab.
P.O. Box 1663
Los Alamos, NM   87545

Annie J. Webb
Group WX-8, MS 312
LASL
P.O. Box 1-63
Los Alamos, NM   86545

C. Weber
Union Carbide
Oak Ridge Gaseous Diffusion Plant
P.O. Box P
Oak Ridge, TN   37830

George Wehmann
U.S.E.R.D.A.
Idaho Operations Office
550 Second St.
Idaho Falls, ID   8340J

Raymond R. Weidler
Duke Power Company
P.O. Box 2178
Charlotte, NC   28242

Alan John Weir
Sutcliffe Speakman & Co., LTD.
Guest Street Leigh
Lancashire, England

Bert R. Wheeler
Allied Chemical Corp.
550 Second St.
Idaho Falls, ID   83401

Dave Wilcox
Flanders Filters, Inc.
825 Hinckley Rd.
Washington, NC 27889

J.G. Wilhelm
gsf, Laboratory for Aerosol
   Physics & Filter Tech.
Nuclear Research Center
Karlsruhe, Germany

Donald H. Willard
Battelle-Northwest Laboratories
Battelle Boulevard
Richland, WA 99352

R.J. Williams
U.K.A.E.A.
Wigshaw La. Culcheth
Warrington, Lancashire,
WA3 ANE England

R.M. Williams
Duke Power Company
P.O. Box 2178
Charlotte, NC   28242

R.W. Woodard
Atomics International
Golden,CO 80401

Nancy H.P. Yeh
Gibbs & Hill, Inc.
393 Seventh Ave.
New York, NY   10001

Jack W. Youngblood
General Electric
P.O. Box 1072
Schenectady, NY   12301

Yuli Zabaluez
International Atomic Energy Agency
Karntnerring 11, A-1011
Vienna, Austria

Orlan O. Yarbro
Oak Ridge National Lab.
P.O. Box X
Oak Ridge, TN   37830

R.D. Zeidman
Ontario Hydro (414-F19)
700 University Avenue
Toronto, Ontario, Canada

Donald L. Zeigler
Rockwell International
Golden, CO 80401

Donald B. Zippler
E.I. duPont
Savannah River Plant
Aiken, SC 29801